Summer 8-5-2023

[3+2]-CYCLOADDITIONS OF TERTIARY AMINE N-OXIDES AND DIPOLAROPHILES PROVIDING AN EFFICIENT ROUTE TO HETEROCYCLICS AND 1,2-DIAMINES, AND NICKEL CATALAYZED TRANSFORMATIONS

Sarah Hejnosz

[3+2]-CYCLOADDITIONS OF TERTIARY AMINE *N*-OXIDES AND DIPOLAROPHILES PROVIDING AN EFFICIENT ROUTE TO HETEROCYCLICS AND 1,2-DIAMINES, AND NICKEL CATALYZED TRANSFORMATIONS

A Dissertation

Submitted to the School of Science and Engineering

Duquesne University

In partial fulfillment of the requirements for

the degree of Doctor of Philosophy

By

Sarah Lynn Hejnosz

August 2023

[3+2]-CYCLOADDITIONS OF TERTIARY AMINE *N*-OXIDES AND DIPOLAROPHILES PROVIDING AN EFFICIENT ROUTE TO HETEROCYCLICS AND 1,2-DIAMINES, AND NICKEL CATALYZED TRANSFORMATIONS

By

Sarah Lynn Hejnosz

Approved June 30, 2023

Dr. Thomas D. Montgomery Assistant Professor of Chemistry and Biochemistry (Committee Chair)	Dr. Jeffrey D. Evanseck Professor of Chemistry and Biochemistry (Committee Member)
Dr. Paul A. Lummis Assistant Professor of Chemistry and Biochemistry (Committee Member)	Dr. Patrick T. Flaherty Associate Professor of Medicinal Chemistry, (External Reviewer)
Dr. Ellen S. Gawalt Dean, School of Science and Engineering Professor of Chemistry and Biochemistry	Dr. Mihaela-Rita Mihailescu Chair, Department of Chemistry and Biochemistry Professor of Chemistry and Biochemistry

ABSTRACT

[3+2]-CYCLOADDITIONS OF TERTIARY AMINE *N*-OXIDES AND DIPOLAROPHILES PROVIDING AN EFFICIENT ROUTE TO HETEROCYCLICS AND 1,2-DIAMINES, AND NICKEL CATALYZED TRANSFORMATIONS

By

Sarah Lynn Hejnosz

August 2023

Dissertation supervised by Dr. Thomas Montgomery

Nitrogen containing compounds are ubiquitous in nature as well as pharmaceuticals. These structures exhibit rich bioactive and chemical properties boasting an array of practical applications. As a result, the synthetic methods of forming nitrogen containing compounds are highly sought after. More efficient syntheses of these structures could result in less expensive industrial processes, particularly in the pharmaceutical industry. Roussi and coworkers established a highly efficient synthetic route forming nitrogen containing heterocycles in a single step from commercially available reagents, however this chemistry has not be used since its discovery in the 1980. Herein, this work greatly expanded Roussi's method and developed a new route accessing vicinal diamines as well as nitrogen containing heterocycles.

Allenes are also important motifs present in natural products and some pharmaceuticals. Moreover these compounds are useful building blocks for synthetic scaffolds because they exhibit unique

reactivities forming complex products from one-step transformations. The synthetic methods of forming allenes typically suffer from multiple steps and harsh reagents. This work focused on developing a mild synthetic method of forming substituted allenes using a nickel catalyzed process.

DEDICATION

To my Grandma Posie, I hope I made you proud!

ACKNOWLEDGEMENT

I would like to express my gratitude to my dissertation committee members over the past five years:

Thank you to Dr. Rita Mihailescu for serving on my committee for my first few years. Having her in the room really challenged me to be able to convey why the sort of exploratory work that I was doing was important. Being able to clearly establish why your research is important is an essential skill for any chemist to have. I am very grateful that she always challenged me on that, and because of that I have become a much better communicator, especially for a more general audience. I attribute the awards I won at the PLU symposia and the GSRS to those vital communication skills that she helped me sharpen.

Thank you to Dr. Evanseck for taking time out of his crazy schedule to be on my committee. I would also like to thank him for teaching me computational chemistry during the summer of COVID. It was nice to learn something new, and it was even more appreciated at that time because it kept me busy while being stuck at home. I also have really enjoyed working on the cycloaddition project, it truly is remarkable what you can uncover when you use both computational and experimental results to direct a research project.

I am very grateful to have been able to work with Dr. Patrick Flaherty. If it was not for his valuable input, especially with the cycloaddition project, I do not think I would have gotten a first author publication in Organic Letters. His suggestion on using silyl imines in the [3+2]-cycloaddition, in my mind, is what caused my part of this project to really take off and become a useful transformation that people were surprisingly excited to talk about at the ACS conference!

I would like to also thank Dr. Paul Lummis for joining my committee for my last year or so at Duquesne. I am grateful for all of the useful feedback I have received from him during group meetings, as well as all of the challenging questions. I am most grateful, I think, for the coffee his lab has supplied which gave me the energy to work through some really long days!

I am happy to have had the opportunity to work closely with Dr. Aaron Bloomfield too for my first couple years at Duquesne. He was another mentor that always challenged me to think deeper and taught me how to work through synthetic challenges. As it turns out, brute force is not a great approach, there is always a rational and methodical way to work through whatever research problem arises. I also have him to thank for our publication because together we worked through the weird initial results I was getting, and he was the first person to suggest that the imidazolidines were decomposing into 1,2-diamines. From that we were able to run with it and develop it into a full synthetic method, so I am incredibly grateful for that.

Lastly for my committee members, I would like to express my gratitude to my research advisor, Dr. Thomas Montgomery. I cannot thank him enough for letting me join his lab in the first place, but also for not kicking me out after my first semester. I am sorry I took a while to catch on, but after having the opportunity to learn from you these past five years, I would like to think that I have grown into an adept synthetic chemist after all. It has truly been a pleasure to see how our lab has developed from an empty room riddled with broken glass and sand, to a full-fledged synthetic lab complete with publications!

I also want to thank Dr. Jeffrey Rohde for starting the [3+2]-project in the first place! I owe much of my success to him for this project that I was allowed to be a part of.

I want to thank my lab mates: Danielle Beres, Alexander Cocolas, Benjamin Musiak, Martin Neal, Aiden Lane, Lindsey Ocheltree, Katie Kaczynski, Malavika Satheesan Nair, Tyler Kiss, Serina

Tressler, and Paige Aley. Working with all of them made the days where none of my reactions worked and everything just seemed disastrous, still enjoyable. I am so lucky to have lab mates that make me laugh so hard that I cry on a daily basis! We have fostered a wonderfully chaotic yet productive work environment. I am grateful to them for always being willing to bounce ideas and help troubleshoot. Working with such great people also motivated me to become a better chemist, and a better researcher, and for that I am grateful.

I would like to thank Daniel Bodner, Lance Crosby and Chris Lawson for helping us set up our lab, then helping us move labs, and then for fixing everything I broke! I also want to thank Christina Vowcheck, Scott Boesch, Dr. Timothy Evans, and Dr. Nithya Vaidyanathan for keeping our department running smoothly and just for being fantastic people to work with!

Thank you to my other friends that I have made along the way in graduate school: Jordan Kelly, Caleb Frye, Samuel Lenze, Lauren Stubbert, Caylee Cunningham, Ramez Hallak, Anna Vietmeier, Victoria Hrach, Marisa Guido, Derek Bedillion, Dr. Ashley Ebert, Dr. Kayce Tomcho, Dr. Jennifer Luke, Dr. Alexander Rupprecht, Dr. Gabrielle Pros, Dr. Tell Lovelace Dr. AJ Craig. (I am sorry if I missed anyone I could fill a whole page with names I swear!) They all in some way shape or form helped me with my exams and defenses, listened to me practice for presentations and helped me with research as well with instrumentation and also by giving an outside perspective to help troubleshoot. I also want to thank them and for providing emotional support; we have a really nice community of graduate students at Duquesne with a strong sense of comradery that I am happy I got to be a part of.

I also want to thank my students over the years for giving me the motivation to get through graduate school and earn my doctorate so I can hopefully one day become a professor. I have been incredibly

lucky to be able to teach some incredibly bright people, who are so much smarter than I ever was, and that are going to go and accomplish amazing things!

I am also indebted to my friends and family, especially my parents Cheryl and Anthony Hejnosz, my sister Elizabeth Hejnosz, my husband Ryan Hejnosz. I want to thank them all for providing me with a comfortable place to live, and for providing me with transportation! There were many mornings where I ran out the door with half of my make-up with the intention of still getting ready on the way to school, and I would get in the car with one of my parents surprising me with coffee and donuts since they knew that I did not have time for breakfast. There were also countless late nights where one of them would pick me up and surprise me by having dinner ready for me in the car. Having that strong support system made it possible for me to put in the amount of work that I did, and without that, I would not have been able to complete this dissertation. I also want to thank my aunt Mary Jo Legg, my great-aunt Marcie Walls, and my uncle Gary Walls for always checking in on me and sending me words of encouragement, food, and gifts to make graduate school easier. A special thanks to my uncle David Legg who gave me the idea to use self-healing polymers for my candidacy exam! Lastly, I also want to thank my friends Nicholle and Jesse Johnson, Alanna and Scott Snyder, Tressa Holodnik, Tia Quairiere, Maria Beecher, Phil Montalbano and Brendan Werley. They gave me the solid support system I needed to order to be successful in graduate school. Without their encouragement and help, I would have accomplished nothing.

TABLE OF CONTENTS

Page

LIST OF TABLES

LIST OF FIGURES

LIST OF SCHEMES

LIST OF ABBREVIATIONS

AAK1	adaptor associated kinase 1
5-HT_{1A}	serotonin 1A receptor
Ac	acetyl
BMAA	l-β-methylaminoalanine
Bn	benzyl
Boc	tert-butylcarbonyl
BSA	bovine serum albumin
CCR5	chemokine receptor 5
CDI	carbonyl diimidazole
COSY	correlation spectroscopy
Cox	cyclooxygenase
DCM	dichloromethane
DEPT	distortion-less enhancement spectroscopy
DMF	dimethylformamide
DMAP	4-dimethylamionpyridine
DORA	duel orexin receptor antagonist
dppe	1,2-bis(diphenylphosphino)ethane
dppf	1,1′-ferrocenediyl-bis(diphenylphosphine)
DPP-IV	dipeptidyl peptidase IV
dppp	1,3-bis(diphenylphosphino)propane
ee	enantiomeric excess

equiv.	equivalents
ESI	electrospray ionization
Et	ethyl
ET-1	endothelin 1
ETAR	Endothelin receptor A
EtOAc	ethyl acetate
EtOH	ethanol
GABA-A	gamma-aminobutyric acid type-A
GLP-1	glucagon-like peptide-1
HCV	hepatitis C virus
IR	infrared
JAK	Janus Kinase
LDA	Lithium diisopropylamide
LiHMDS	Lithium bis(trimethylsilyl)amide
Me	methyl
MeCN	acetonitrile
MIC	minimum inhibitory concentration
MS	mass spectrometry
nAChRs	nicotinic acetylcholine receptors
NaHMDS	sodium hexamethyldisilazide
NOESY	Nuclear over Hauser effect spectroscopy
^{n}BuLi	*n*-butyl lithium
NMM	*N*-methyl morpholine

NMR	nuclear magnetic resonance
ORX	Orexin-X
OX1R	orexin-1
OX2R	orexin-2
PGE_2	prostaglandin E2
Ph	phenyl
PTSD	post-traumatic stress disorder
RT	room temperature
SAR	structure activity relationship
SSRIs	selective serotonin reuptake inhibitors
^{t}BuLi	*tert*-butyl lithium
THF	tetrahydrofuran
THF	tetrahydrofuran
TMAO	trimethylamine *N*-oxide
TMSOTf	Trimethylsilyl trifluoromethanesulfonate
WHO	World Health Organization

Chapter 1: Cycloadditions of Silyl Imines Forming 1,2-Diamines in a Three-step One-pot Synthesis

1.1 Introduction

1.1.1 Contextual Summary

1,2-Diamines, or vicinal diamines, are found in an array of bioactive compounds such as natural products and pharmaceuticals, and as a result, are considered to be privileged structural motifs.[1-8] Structures are termed "privileged" when they have versatile binding properties leading to potent biological activities with a range of different applications.[9] Moreover, 1,2-dimaines function as useful building blocks for complex synthetic targets due to the myriad of transformations they can undergo.[1,2,10-13] Beyond this, these molecules are commonly employed as ligands for transition metal catalyzed processes.[14-18] Given the versatility of this motif, the creation of efficient methods for synthesizing this scaffold from base starting materials are highly sought after. Most synthetic

Scheme 1 Summary of syntheses for 1,2-dimaines highlighting the key disconnections typical of those methods.

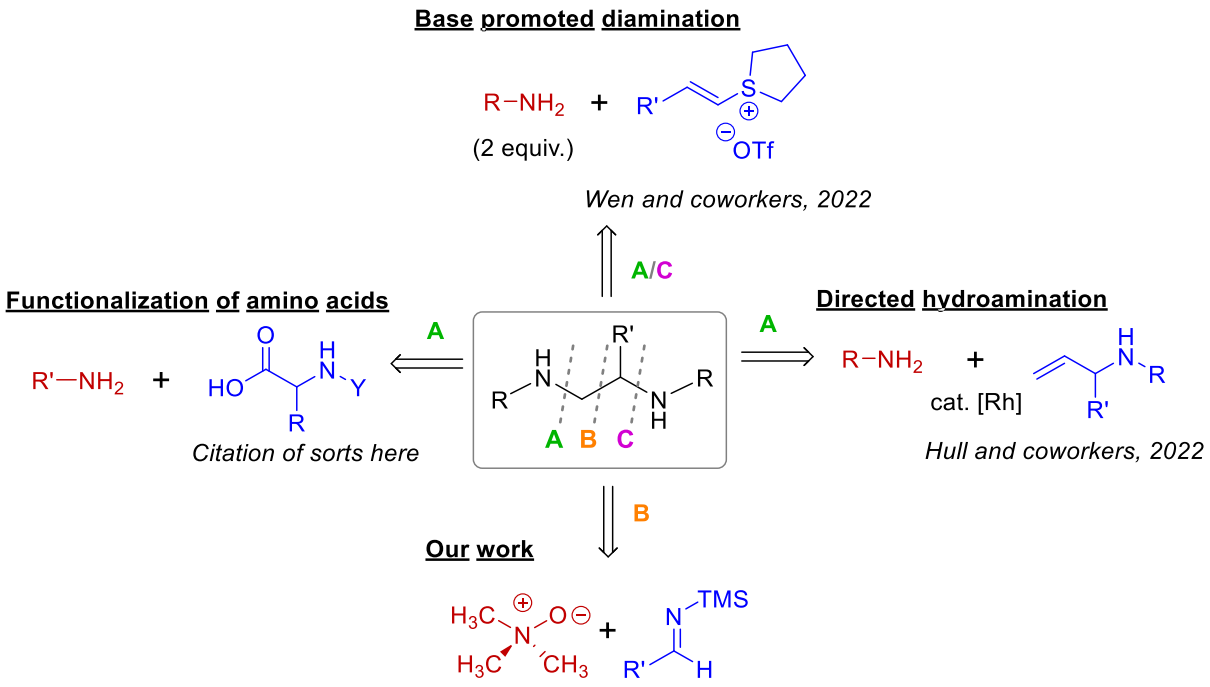

methods reported focus on the formation of carbon-nitrogen bonds (Scheme 1, disconnections **A** and **C**) which allows for the installation of diverse range of amines, but offer no way to functionalize the carbon backbone, with the substitutions on it remaining static. The method developed herein takes advantage of the unique disconnection **B** which allows for both functionalization of the amines as well as the carbon backbone just by changing the synthetic precursor providing rapid access to a more diverse library of vicinal diamines (Scheme 1).[19]

1.1.2 Natural Products and Pharmaceuticals Containing 1,2-Diamines

There are a wide range of bioactive compounds that exhibit the 1,2-diamine motif.[1-8] Bristol Myer Squibb filed a patent in 2016 on a class of 1,2-diamines that showed a range of inhibitory effects on adaptor associated kinase 1 (AAK1).[20] The inhibition of AAK1 is thought to be crucial in the discovery of new and effective treatments for a range of diseases[20] including: schizophrenia,[21,22] and Parkinson's disease.[23] Selected diamines **1-3** showed increasing IC_{50} values with **3** being the most active with an IC_{50}=1.3 nM (Figure 1).[20] Research with this class of diamines is presumably still ongoing, but it was surprising that the only non-amide in the patent was **1** (Figure 1). It would be interesting to see if the substitution of the primary amine or the amide is more effective for AAK1 inhibition. This is still an ongoing area of drug discovery research with other groups looking at it from different angles such as Acelot Inc (Figure 1b).

Acelot Inc. filed a patent in 2021 highlighting a plethora of nitrogen-rich small molecules that are effective in both disrupting and preventing TDP-43, alpha-synuclein, tau protein, and Huntingtin protein oligomers.[24] These oligomers, are associated with a number of neurological disorders such as Alzheimer's, Huntington's, and Parkinson's diseases.[24] Two highlights from this patent are diamines **4** and **5** which when administered to a subject, resulted in fewer tau protein oligomers

demonstrating significant promise in the search for more effective treatments for neurogenerative disorders (Figure 1b).[24]

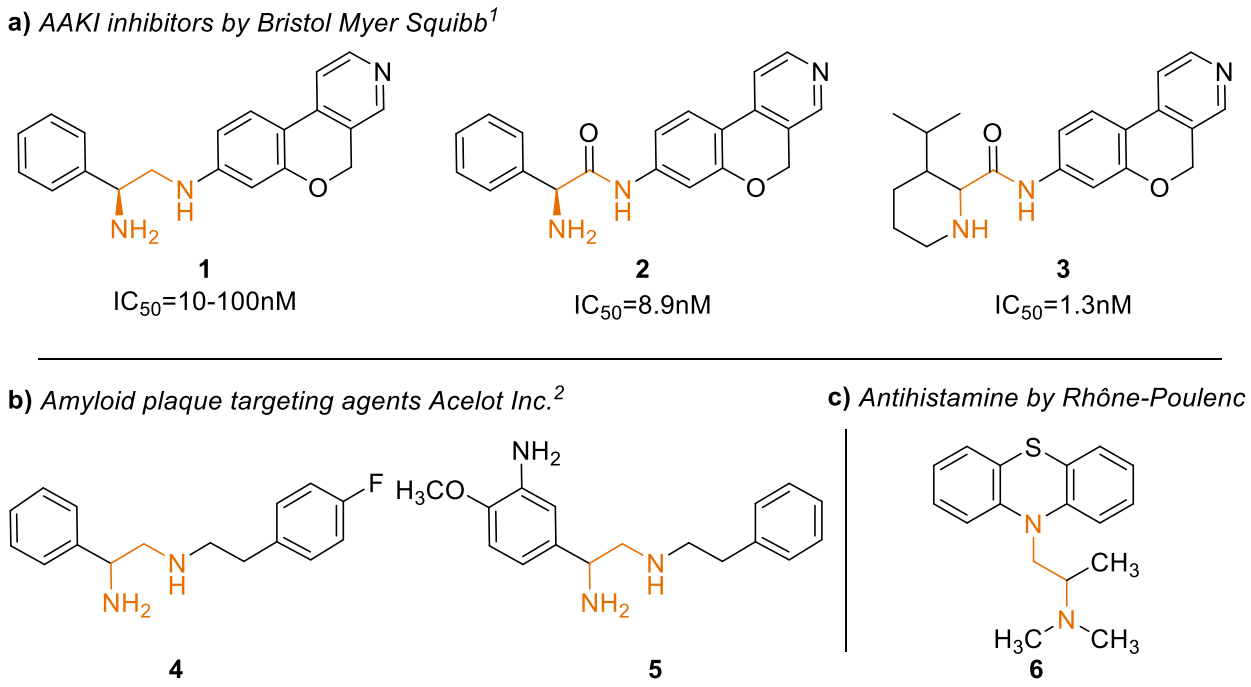

Figure 1. Drug Candidates Containing the 1,2-Diamine Motif

Promethazine was developed in 1944 by Rhône-Poulenc laboratories as part of their quest to discover better and safer antihistamines.[25] It exhibited mild antipsychotic properties as well as antidopaminergic, antihistamine, and anticholinergic properties.[25,26] It is a drowsy antihistamine, making it mild sedative, and it can be used to treat allergies as well as nausea, vomiting, and motion sickness.[26] Vicinal diamines of this sort are interesting synthetic targets due to the myriad of medical applications they might offer (Figure 1c).[27]

In addition to synthesized drug-like compounds, there are a wide variety of natural products exhibiting a 1,2-diamine moiety. Amoxicillin (**7**) has been used as an antibiotic to treat a variety of infections since 1972 (Figure 2),[28] and in 2020 it was the 40th most commonly prescribed medications in the United States.[29] While amoxicillin has been incredibly useful, the overprescription of antibiotics, such as this, has led to the rapid development of antibiotic resistant

pathogens, a situation which the World Health Organization (WHO) recognized as a global health threat in 2015.[30] Due to this developing crisis, discovering new and efficient methods forming functionalized 1,2-dimaines for antibiotic screenings is an active and important area of scientific research.

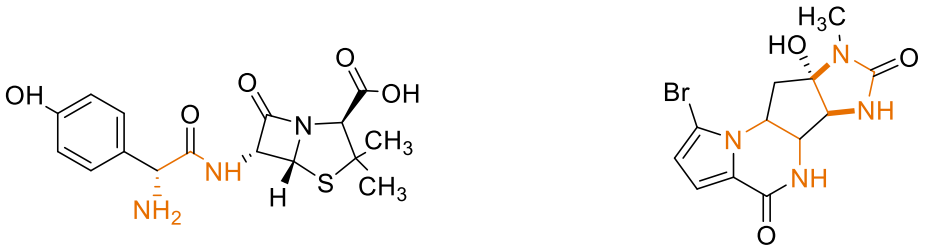

Figure 2. Naturally Occurring Vincinal Diamines: Amoxicillin and (-)-Agelastatin A

Agelastatin A (**8**) is natural product containing two sets of vicinal diamines; it was originally isolated in 1993 from a marine sponge *Agelas dendromorpha* found in the Coral Sea.[31] Agelastain A is a potent cytotoxic agent against leukemia and epithelial tumoural cells *in vitro*[32] as well as exhibiting high levels of OPN-mediated malignant transformation thus inhibiting cancer cell profileration.[33] In fact, it is generally 1.5 to 16 times more potent than cisplatin, an established chemotherapeutic benchmark, at inhibiting cancer cell growth.[33] Due to its potential to be an effective drug for cancer treatment, researchers have been looking into effective total synthetic pathways for this complex and remarkable target and its derivatives.[34-39] The most recent example was reported by Du Bois and When in 2009 requiring 11 steps from commercially available starting reagents.[34]

Another natural product containing a 1,2-diamine is Biotin (**9**), also called vitamin B_7 (Figure 3).[40] Biotin is a required nutrient in many different organisms ,including humans, where it is a key metabolic vitamin.[41] It serves as a coenzyme for carboxylase enzymes, these enzymes are responsible for breaking down amino and fatty acids into materials our body can use. Beyond this

biotin plays a key role in gluconeogenesis, the core mechanism behind converting stored energy into available energy.[41] The modification of this vitamin and the like are used in the biotechnology industry for assays in order to isolate proteins and non-proteins.[42]

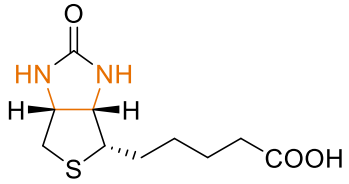

9

Biotin[4]

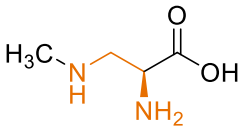

10

L-β-Methylaminoalanine[5]

Figure 3. Naturally Produced 1,2-Diamines: Biotin and L-β-Methylaminoalanine.

Non-proteinogenic amino acid (**10**), l-β-methylaminoalanine (BMAA), is a neurotoxin produced by cyanobacteria (Figure 3).[43,44] BMAA has been used to mimic the effects of Alzheimer's disease by generating the β-amyloid plaques of this disease in animal models, thus leading to the first *in-vivo* model of the disease.[45] The development of this *in-vivo* model has dramatically changed the research that can be done on such diseases because this reduces the reliance on human subjects as the only model organism.[45] Research in this subject with similar compounds might be able to further elucidate the reasons why and how these β-amyloid plaques form, thus gaining a better understanding of how to prevent their generation.

1.1.3 Vicinal Diamines as Ligands in Transition Metal Catalysis

Beyond their role as key components in biologically active systems, 1,2-diamines can function as ligands in transition metal catalyzed asymmetric transformations such as transfer hydrogenation,[14,16,46] conjugated additions,[47] and cross coupling reactions.[18] Both Wills and coworkers[48] and Alberico and coworkers[49] expanded on the Noyori catalyst[50] in the transfer hydrogenation of acetophenone (Scheme 2). This work highlights how small steric and electron changes significantly affect the catalytic activity.[14,48] We can see that substitution patterns which enforce the cisoid relationship between the diamines as shown favor higher conversions and faster

reaction times. Facile synthetic methods that can provide rapid access to a variety of ligands would greatly benefit this type of chemistry. The ligands could then be readily tuned to the catalysts needs with a more diverse library of ligands.

Scheme 2. Chiral 1,2-diamine ligands in Noyori asymmetric hydrogenation of acetophenone,

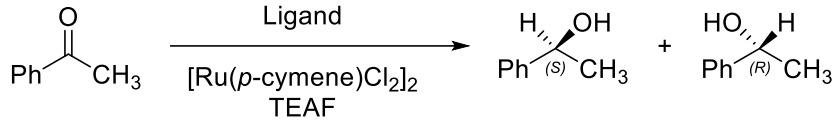

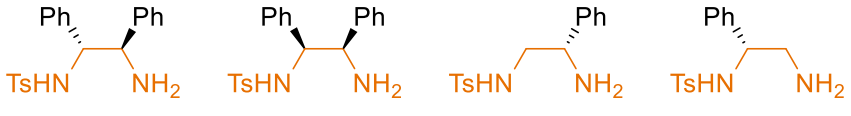

Ligand	(1*R*,2*R*)	(1*S*,2*R*)	(2*S*)	(1*R*)
Time	22h	220h	48h	13 days
Conv., %	100	32	95	46
Ee, %	98 (*R*)	70 (*S*)	69 (*S*)	33 (*R*)

Arguably 1,2-diamines are the reason why many copper catalyzed processes are still industrially relevant today because the implementation of these ligands made processes only attainable through harsh conditions possible with relatively mild reactions conditions, improving throughput and reducing energy needs.[15] These copper catalyzed transformations also have greater functional group compatibility than their predecessors and typically work well with simple and commercially available 1,2-diamine ligands (Figure 3).[15]

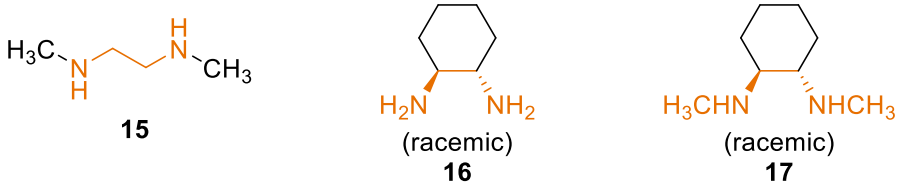

Figure 4. Commercially available 1,2-diamine ligands used in copper catalyzed processes.

Scheme 3. Original conditions for Ullmann (a) and Goldberg (b) reactions.[51,53]

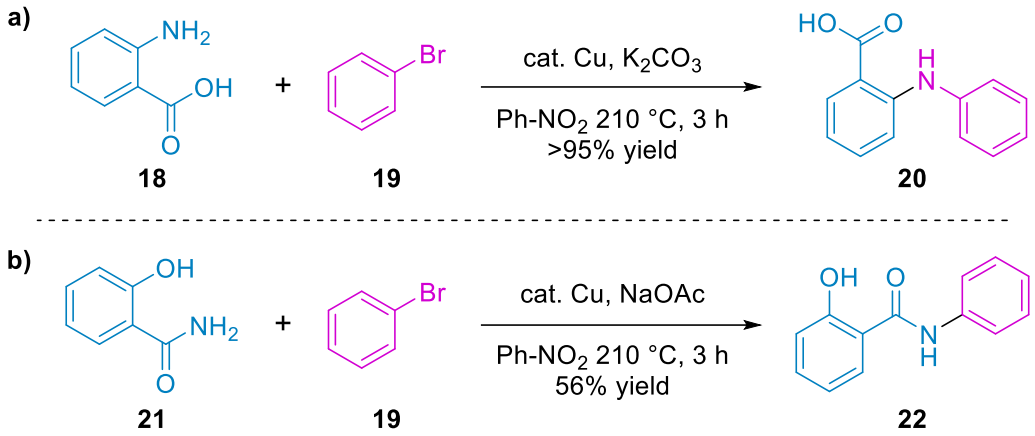

Copper catalysis is not a new area of chemistry, although it has seen a sort of renaissance in more recent years.[51] This field initially rose to prominence in 1901, when Fritz Ullmann reported the first example of a carbon-heteroatom bond forming reaction, which extended the scope of cross-coupling reaction beyond just carbon-carbon bond formation.[52] Ullmann and his student, Irma Goldberg, pioneered this method forming aryl-C-, aryl-N, and aryl-O bonds paving the way for other copper catalyzed transformations (Scheme 3a), and providing access to compounds that were not unachievable with other methods.[51] Moreover, Goldberg further expanded this work for amide-bond forming reactions where she successfully coupled a benzamide with bromobenzene in the presence of base and catalytic copper (Scheme 3b).[51,53] Consequently these transformation are the known as the Ullmann condensation[54-56] and the Goldberg reaction as a testament for their revolutionary work in this field.[53,57] These transformations serve as the basis for the current work still being done now in advancing this field.[51,58-63]

Researchers have further improved copper catalyzed amidations of aryl halides since their inception.[58-63] Buchwald and coworkers have been making significant advances in improving these reaction conditions, by implementing simple diamine ligands which facilitates this transformation under milder conditions, thereby extending the substrate scope.[58-63] Copper iodide and ligand **17**

were implemented to improve the typical Ullman-coupling conditions (Scheme 4b).[63] The reaction temperature was lowered from 132 °C to 110 °C by replacing *o*-bischlorobenzene with toluene, which is a less hazardous solvent.[63]

Scheme 4. a) Typical Ullman Coupling Reaction Conditions. b) Modified Ullman Coupling Conditions Improved by Buchwald and Coworkers.

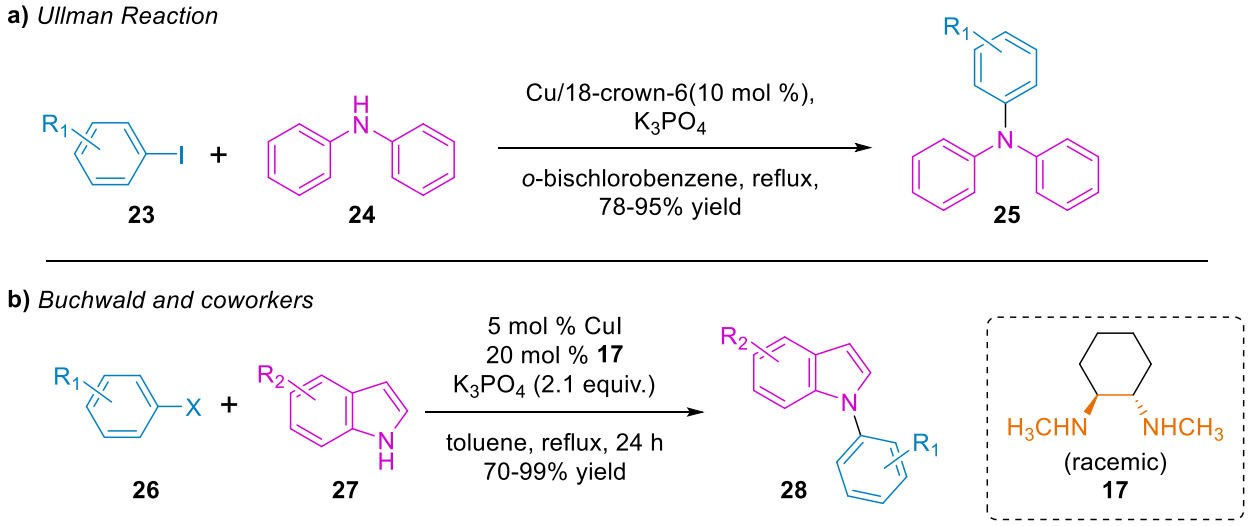

Scheme 5. a) Typical Goldberg Reaction Conditions. b) Modified Goldberg Reaction Improved by Buchwald and Coworkers.

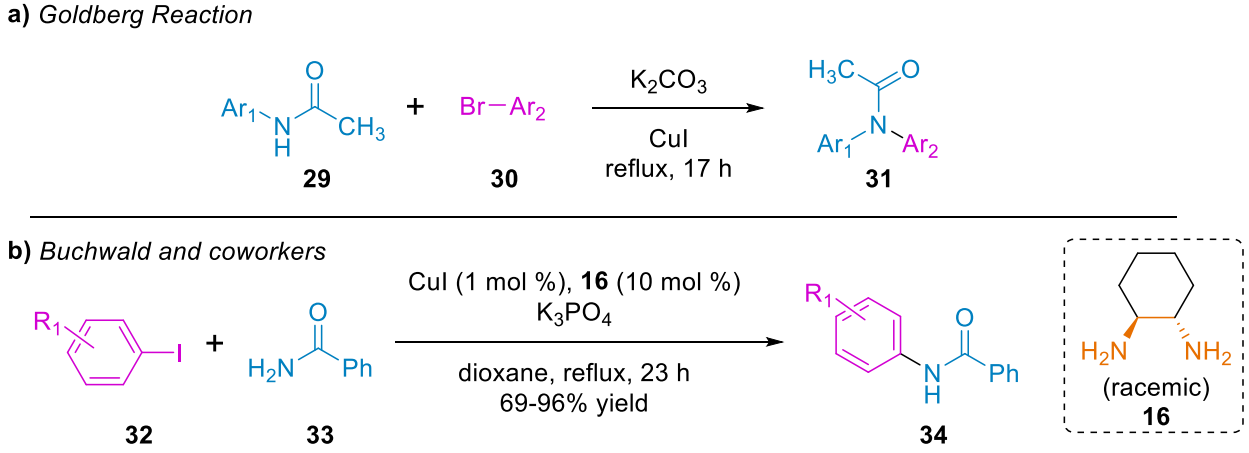

In a similar vein, copper iodide and ligand **16** were employed to improve the conditions of the Goldberg reaction by lowering the temperature to 101 °C (Scheme 5b).[60] By implementing this

ligand, the catalytic activity of copper was also improved so stoichiometric quantities were no longer necessary.

Scheme 6. a) Typical Goldberg Reaction Conditions. b) Modified Goldberg Reaction Improved by Buchwald and Coworkers.

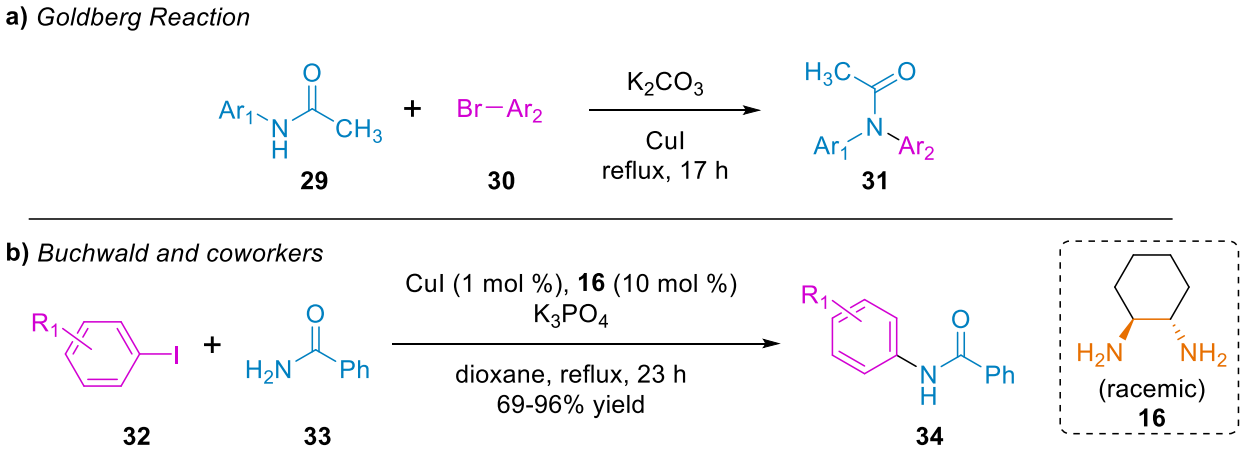

Scheme 7. Copper Catalyzed Imidazole Synthesis

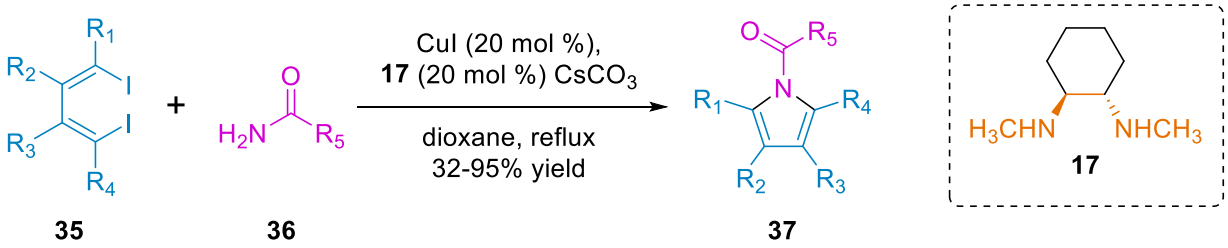

Surprisingly, simple alkyl 1,2-diamine ligands tend to perform the best in these copper catalyzed amidation reactions.[60,63] Li and coworkers used ligand **17** in a copper catalyzed transformation forming pyrrole derivatives **37** in yields up to 95% (Scheme 6).[64,65]

Indoline derivatives are another group of biologically important molecules, and they have been synthesized in high yields by implementing ligand **15** in copper catalyzed processes (Scheme 7).[60,66-68] The method developed by Klapars *et al*. uses an inexpensive catalysts and ligand system to generate indoline **39** through an intramolecular amidation of an aryl bromide **38** in >95% yield (Scheme 7a).[60] Miniatti *et al*. further developed this system for the intermolecular copper-catalyzed amidation/nucleophilic substitution reactions forming indoline derivatives **42** in good yields

(Scheme 3b).[67] These serve as just a few examples of the synthetic applications of these ligands with many more instances reported of ligands **15**,[69-71] **16**,[72-74] and **17**[75,76] being implemented in copper catalyzed arylation reactions to form complex bioactive scaffolds with medicinal applications.

Scheme 8. Copper Catalyzed Cross-Coupling Reactions forming Indolines[60,66-68]

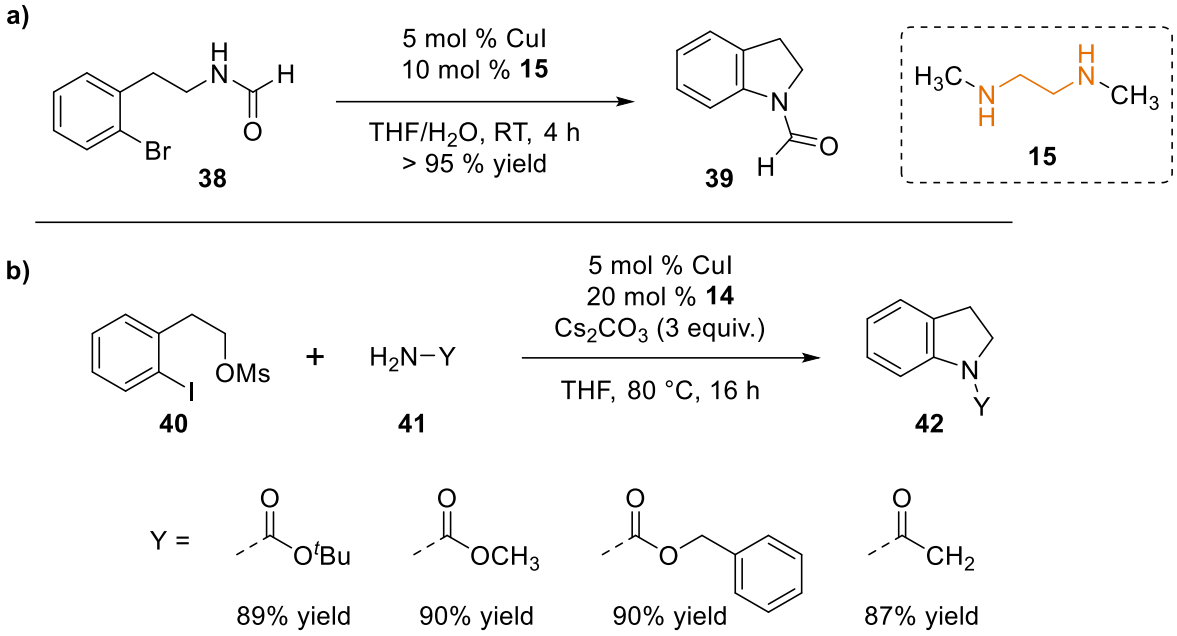

1.1.4 Transformations of 1,2-diamines

Naturally, 1,2-diamines have the same rich chemistry as other amine containing compounds; where 1,2-diamines can undergo sulfonylation, acetylation, cross coupling, nucleophilic aromatic substitution, and many other transformations. What makes vicinal diamines specifically advantageous in total synthesis is that they have access to a unique set of transformations beyond those available to mononuclear amines. This is due to the fact that they have two amines on the same carbon chain, they can form heterocycles under a variety of conditions. Unsurprisingly 1,2-diamines are widely used as synthetic building blocks for more complex scaffolds, including as potential drug targets.[11-13,77]

1.1.4.1 Cyclizations of 1,2-diamines

Imidazolidines

Scheme 9. Condensation of 1,2-Diamines and Aldehydes Forming Imidazolidines

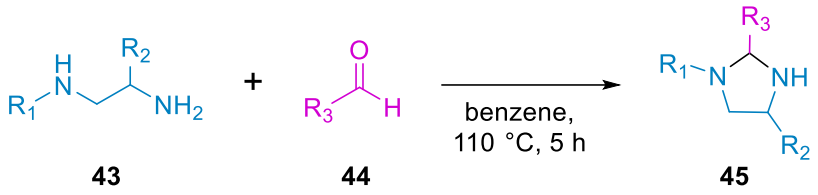

43 **44** **45**

The condensation of aldehydes **44** with 1,2-diamines **43** is the earliest and most common example of vicinal diamines being used to form imidazolidines **45** (Scheme 8).[78] There are numerous other examples of this method in the literature, and these will be discussed in depth in Chapter 2.[78-81]

Imidazolines

Scheme 10. Cyclization of 1,2-Diamine 40 with Iminoester Hydrochlorides[82]

46 **47** **48**

Another synthetic tactic dating back to the 1950s is the reaction of vicinal diamines and imidates to form various imidazolines.[82-84] Imidazolines are the partially unsaturated derivatives of imidazolidines also bearing the 1,2-dimaine motif. This transformation is highly facile and it forms these useful products in good yields and under mild reactions.[82-84] Karaali and coworkers used this method with **46** and iminoester hydrochloride **47** forming benzimidazolines **48** with >95% yields (Scheme 9).[82]

Imidazolidinones

There are some reagents that 1,2-diamines can react with to form imidazolidinones.[77,85-87]. Triphosgene, and other phosgene analogs, readily reacts with vicinal diamines to form

imidazolidinones via double addition to the carbonyl center. This transformation has been used in total synthetic routes to bioactive compounds **52** and **57**.[13,77] Fluoxetine (**52**), more commonly recognized as the brand name Prozac, is part of a class of antidepressants termed selective serotonin reuptake inhibitors (SSRIs)[88] Nair and coworkers synthesized this drug and other derivatives in 10 steps with diamine **49** as a key reaction intermediate (Scheme 10).[77]

Scheme 11. Total Synthesis of Prozac with Vicinal Diamine Precursor[77]

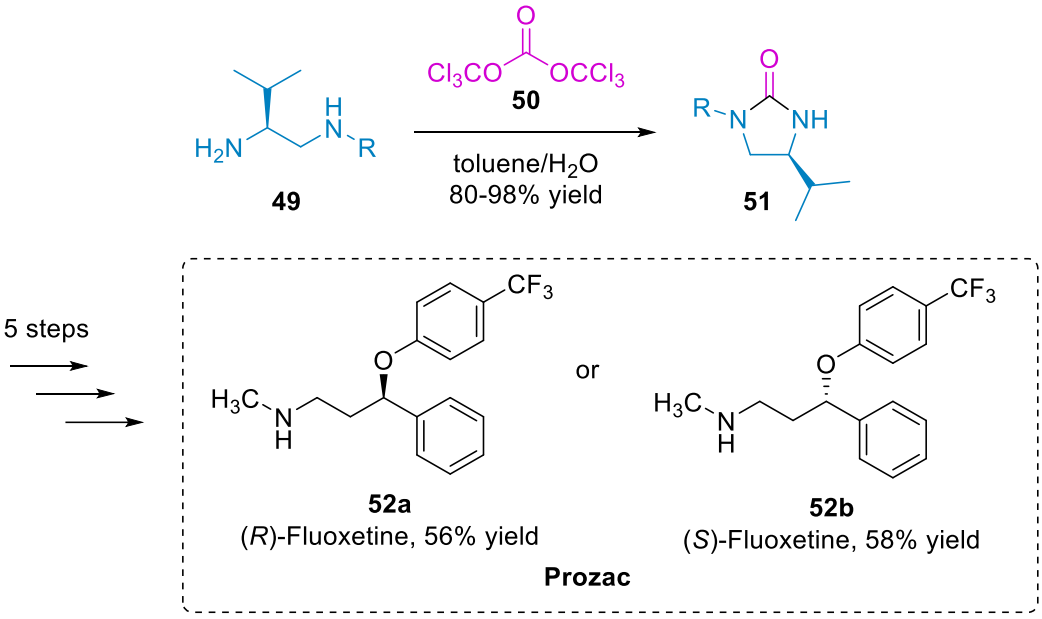

Skerlj and coworkers formed chemokine receptor 5 (CCR5) antagonists using this same transformation to form their final products (Scheme 11).[13] CCR5 antagonists are a synthetic priority because their pharmacological properties have made them a potential HIV therapeutic strategy.[89] Using a seven step synthetic method they were able to make and identify imidazolidinone **57** as a promising drug target.[13]

Scheme 12. Chemokine Receptor 5 Antagonist Synthesis[13]

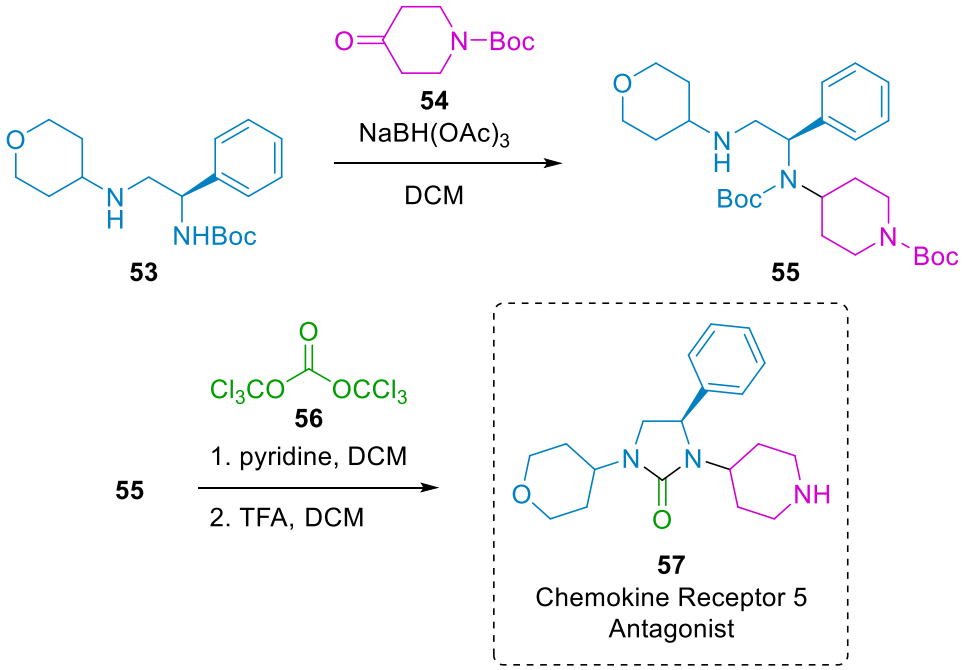

Imidazolidinones are also used as synthetic precursors in method development experiments such as the palladium-catalyzed N-H and C(sp^3)-H arylations established by Baudoin and Guyonnet to form tricyclic nitrogen containing heterocycles.[87] In lieu of triphosgene, they used a milder reagent, carbonyl diimidazole (CDI) with 1,2-diamines, to form their desired imidazolidinone synthetic precursors.[87]

1.1.4.2 Arylations and Aminations

Just the same as any amine, vicinal diamines can also undergo transition metal catalyzed arylations and aminations.[90-93] Under the right conditions, these transformations can be used on 1,2-dimaines to form piperazines, another class of privileged structures ubiquitous in nature. Wolfe and coworkers did exactly this using sequential palladium catalyzed transformation of 1,2-diamines.[92,94] Once the required diamines **58** were in hand, they could undergo palladium catalyzed arylation forming **60**, which could then be implemented in the palladium catalyzed alkene carboamination forming piperazines **62** in yields ranging from 50-73% (Scheme 12).[92,94]

Scheme 13. Palladium Catalyzed Arylation Followed by Alkene Carboamination as a Facile Approach to Piperazines.

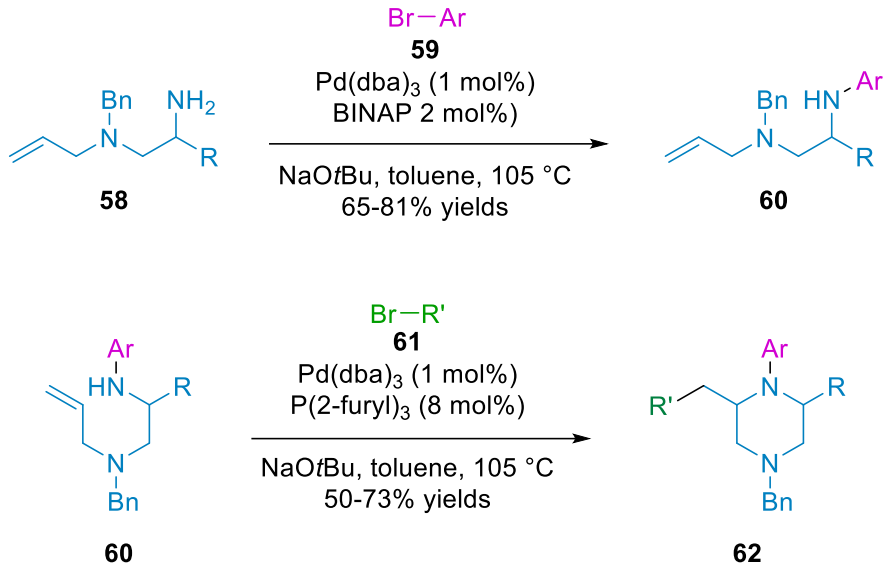

1.1.4.3 Nucleophillic Aromatic Substitution

Parker and Coburn used an intramolecular nucleophilic aromatic substitution (S_NAr) of **63** to form key reaction intermediate **64** for their synthesis of anti HIV-1 8-halo TIBO analogues **65** (Scheme 13).[95] They used this general method to form five different derivatives with potent antiviral properties in a total of five steps.[95]

Scheme 14. Synthesis of Potent Anti HIV-1 8-Halo TIBO Analogues from 1,2-Diamines via S_NAr[95]

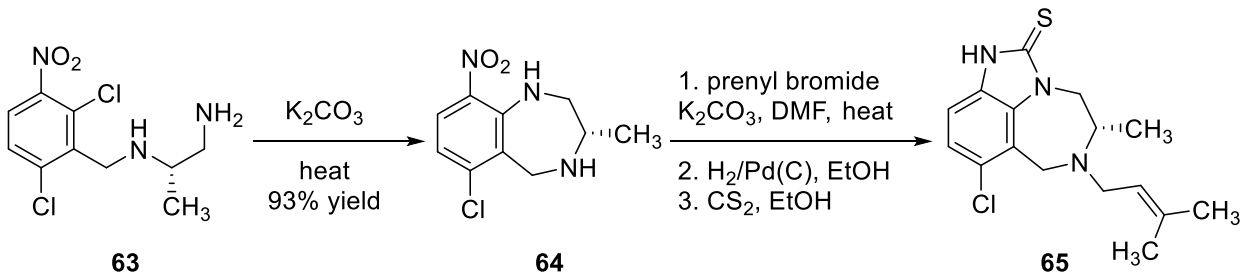

1.1.5 Synthetic Methods Forming 1,2-Diamines

The earliest and most common examples of 1,2 diamine formation originate from nucleophilic attack into *N*-protected amino acids.[10,92,96-102] Subsequent reduction and deprotection yields 1,2-

Scheme 15. Total Synthesis of AMBA[79]

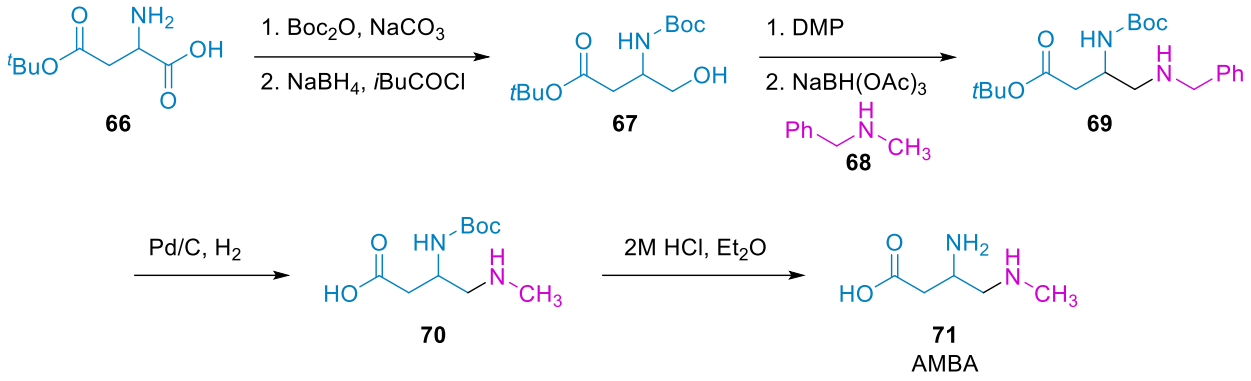

diamines bearing an amino acid side chain.[10,92,96-101] This method has been applied by Schofield and coworkers starting with amino acid derivative **66** (Scheme 14).[79] Once protected, the amine was Boc-protected, the carboxylic acid was reduced to form **67**. The alcohol was then converted into a better leaving group with DMP to then undergo nucleophilic attack of amine **68**. After reduction and deprotection, the final diamine **71** (AMBA) was produced.

Scheme 16. Total Synthesis of Chemokine Receptor Antagonist 50.[13]

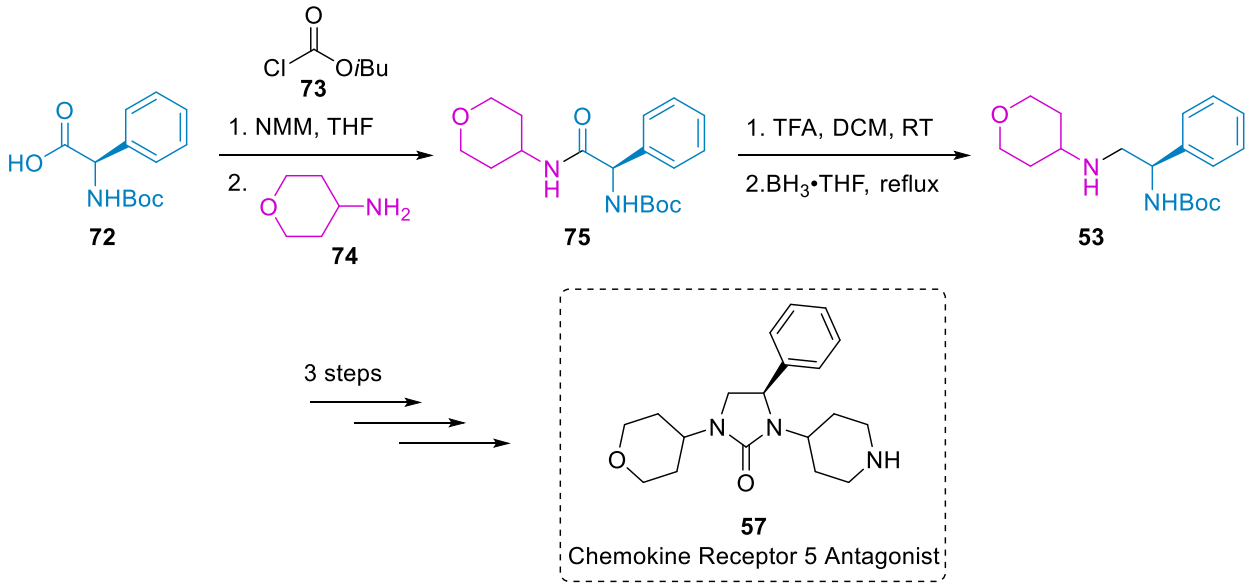

Skerlj and coworkers started with Boc-protected phenylalanine to produce a series of CCR5 antagonists in seven steps total with four steps dedicated to forming the necessary vicinal diamine (Scheme 15).[13] The carboxylic acid **72** was activated by converting it into the mixed carboxylic-

carbonic acid anhydride with **73** and *N*-methyl morpholine (NMM).[103] Once activated, it could undergo nucleophilic attack of amine **74** and form **75**, which is then used to form diamine **53** after subsequent deprotection and reduction.

The ten-step synthesis of Prozac **52** was carried out using the same basic steps as the previous examples (Scheme 16).[77] They started with valine **76** and protected the amine using Boc anhydride to form **77**. After activation of the carboxylic acid by ethylchloroformate, the carbonyl underwent nucleophilic attack to form **78** which afforded the desired diamine **49** after deprotection and reduction.

Scheme 17. Total Synthesis of Fluoextine Isomers (Prozac)[77]

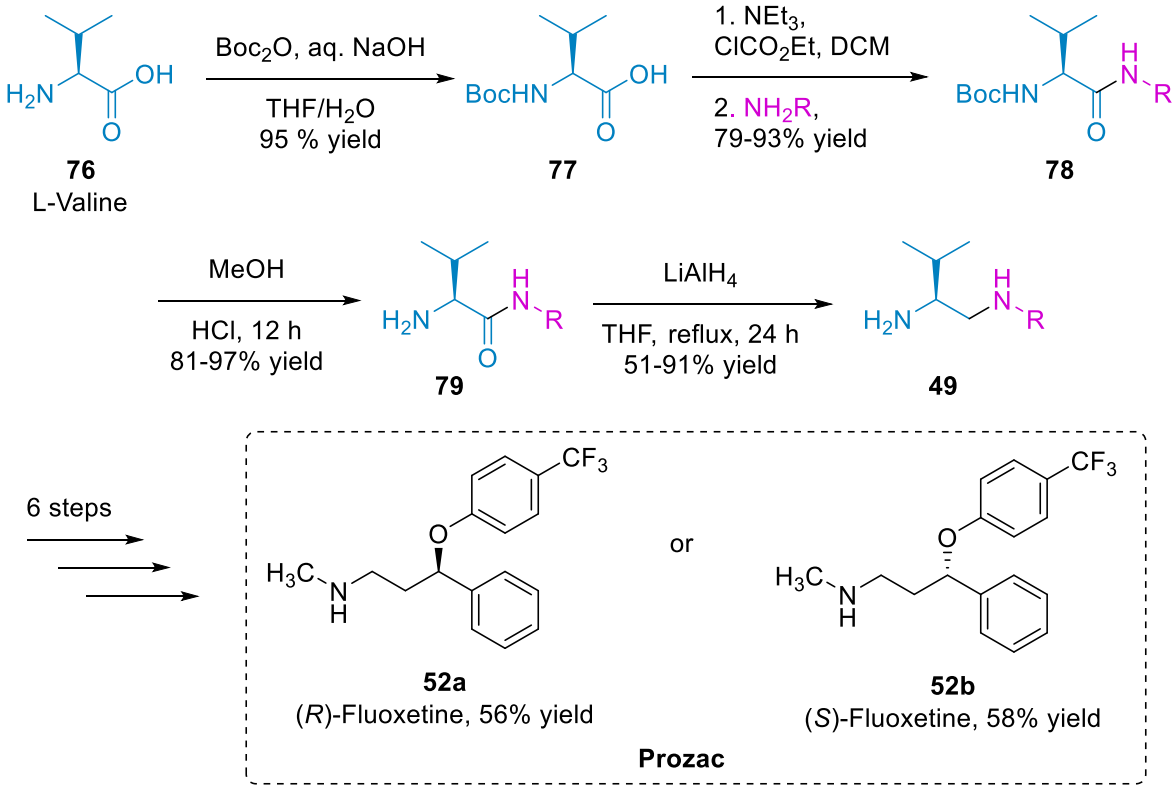

The functionalization of *N*-protected amino acids, although reliable and widely used, ultimately suffers from multiple steps (protection, deprotection, and reduction at least), and it is limited due to incompatibility with reduction sensitive functional groups. Moreover, the carbon backbone is

limited to what is available commercially with no option to further functionalize it under the synthetic reaction conditions; the only functionality installed is limited to the R-groups attached to the amine.

Other common methods of forming 1,2-diamines involve nucleophilic attack of aryl amines into electrophiles such as aziridines,[104,105] or by a transition metal catalyzed process.[106-110] The synthesis of diamines is a well established area of research, and consequently there are numerous synthetic protocols reported in the literature. However, there are also plenty of methods that have been developed in recent years making this still an active and relevant area of chemical research. Due to the wide range of bioactivities these privileged structures exhibit, there is a constant demand for novel and efficient syntheses producing novel varieties of this class of compounds.

As a more recent example, in 2022 Wen and coworkers reported a base promoted diamination of styrene sulfonium salts **82**, resulting in aryl 1,2-diamines **84** (Scheme 17).[111] This reaction tolerated a range of aryl amines (**83**) and sulfonium salts (**80**), but the transformation is limited to chemically indistinct amine functionalities since two equivalents of the same amine are added to the resulting carbon-carbon backbone.[111]

Scheme 18. Base-Promoted Diamination of Styrene Sulfonium Salts[111]

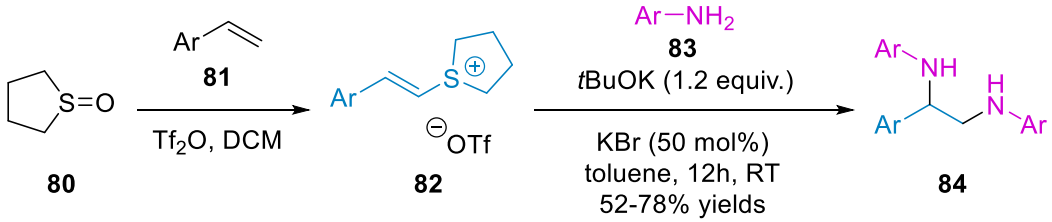

In another recent example, Hull and coworkers demonstrated a rhodium catalyzed synthesis of unsymmetrical vicinal diamines **87** (Scheme 18).[112] While they were able to access a wide range of 1,2-diamines **87** from unsubstituted olefins, the allyl amine substrates **85** are not commercially available and require a three-step synthesis to make.[43,112]

Scheme 19. Rhodium Catalyzed Directed Hydroamination[112]

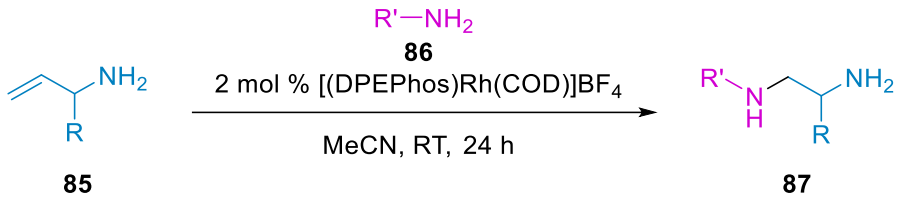

Scheme 20. Vicinal diamine syntheses forming carbon-carbon bonds

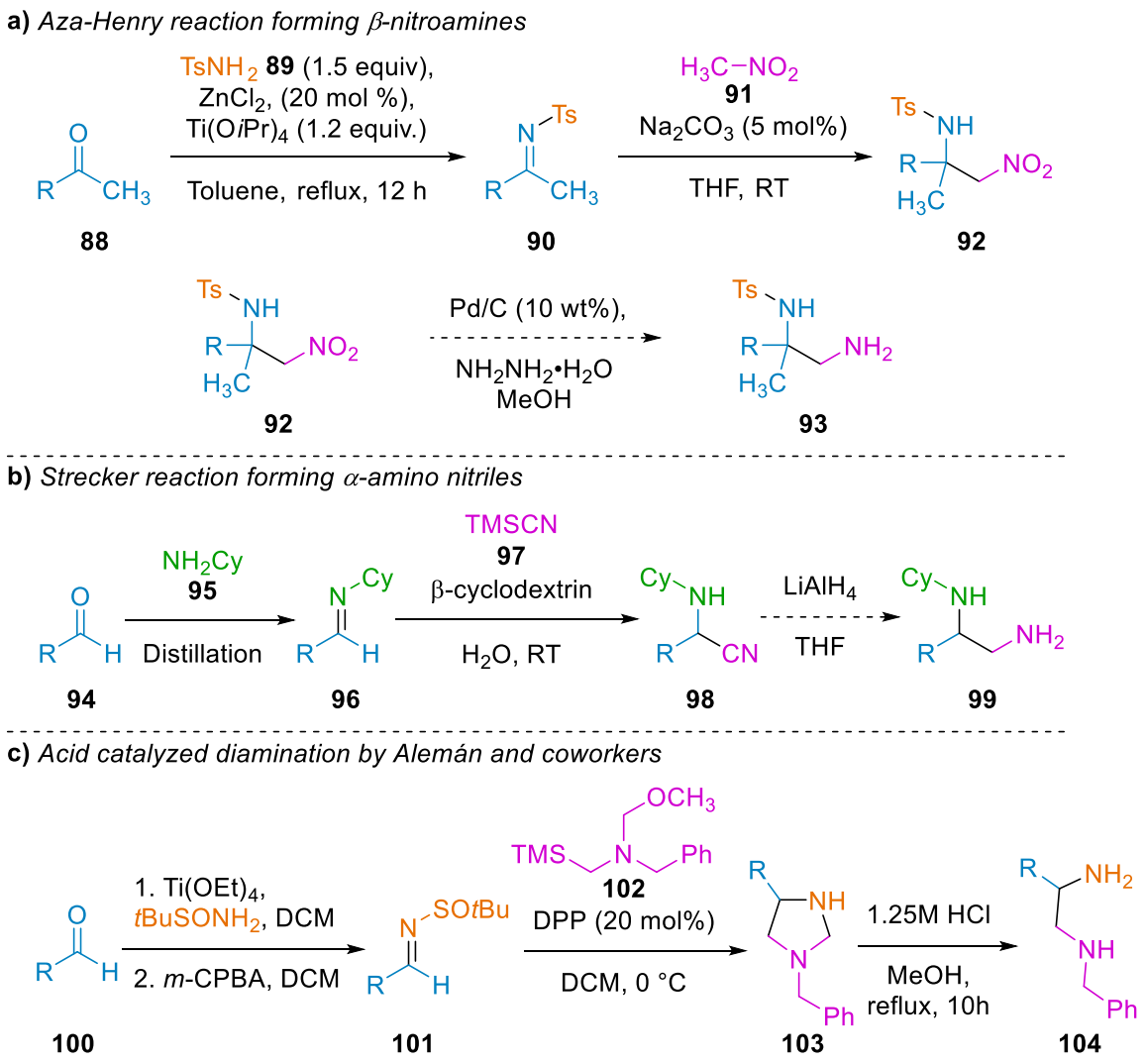

These are just a few representative examples where the synthetic precursors, or required ligands, to form vicinal diamines are not commercially available, requiring additional time and energy. This makes the method less attractive to other synthetic groups, since they offer few time benefits over

tried-and-true methods of converting amino acids into diamines. Moreover, another issue with most literature methods is that the carbon chain is static, with only C-N bond formation occurring. There are some methods that do form the C-C bond, such as with aza-Henry[113] and Strecker[114,115] reactions (Scheme 19a and 19b); however, these transformations suffer from both harsh conditions and multiple steps. Recent advances by Alemán have added to this area through their acid catalyzed imidazolidine formation reaction (Scheme 19c).[116] This method still requires an additional two steps with purification to form the *N*-sulfonyl aldimines **101** from commercially available starting reagents.

The method developed herein forms vicinal diamines through the formation of a C-C bond (Scheme 20), which is where our method differs from a vast majority of other methods. Moreover it has an inherent advantage from the aza-Henry, Strecker reactions, as well as the work from Alemán because the silyl imine is formed *in situ* and directly incorporated into the [3+2] cycloaddition. Additionally, we don't require the formation of complex precursors, making adoption of this method by other synthetic groups extremely facile. We were able to make use of an underutilized [3+2] cycloaddition[117-123] by investigating this system with silyl imines and tertiary amine *N*-oxides to form vicinal diamines in an innovative way (Scheme 20).

Scheme 21. Summary of [3+2]-Cycloadditions of Tertiary Amine *N*-oxides and Silyl Imines Resulting in Vicinal Diamines.

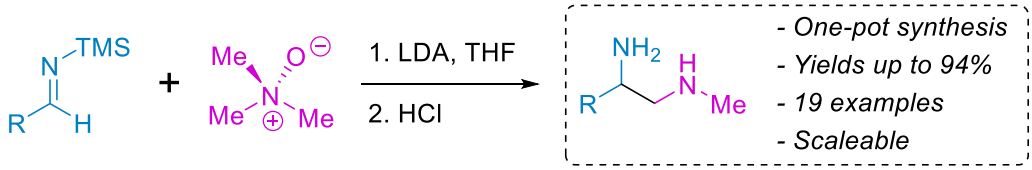

1.2 Results and Discussion

1.2.1 Reaction Optimization

The reaction between trimethylamine *N*-oxide (TMAO) **107** and silyl protected imine **106** was chosen because of the simplicity and the commercial availability of the *N*-oxide and aldehydes. Additionally, the regioselectivity issues Roussi and coworkers encountered were avoided by choosing TMAO **107** due to its symmetry.[120]

Scheme 22. Three-step One-pot Synthetic Method Forming 1,2-diamines

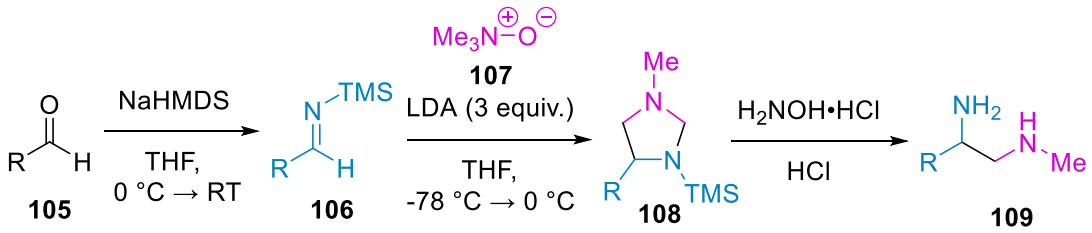

The three-step synthesis starts with the addition of sodium hexamethyldisilazide (NaHMDS) to an aldehyde **103**, forming silyl imine **106** via an aza-Brook rearrangement (Scheme 22).[124,125]

The mechanism works by **105** undergoing nucleophilic attack of HMDS, forming a tetrahedral intermediate **110**, with the negative charge on oxygen being stabilized by the sodium cation. A new silicon-oxygen bond is then formed, and the nitrogen-silicon bond is broken, which results in the

Scheme 23. Aza-Brook Rearrangement Mechanism

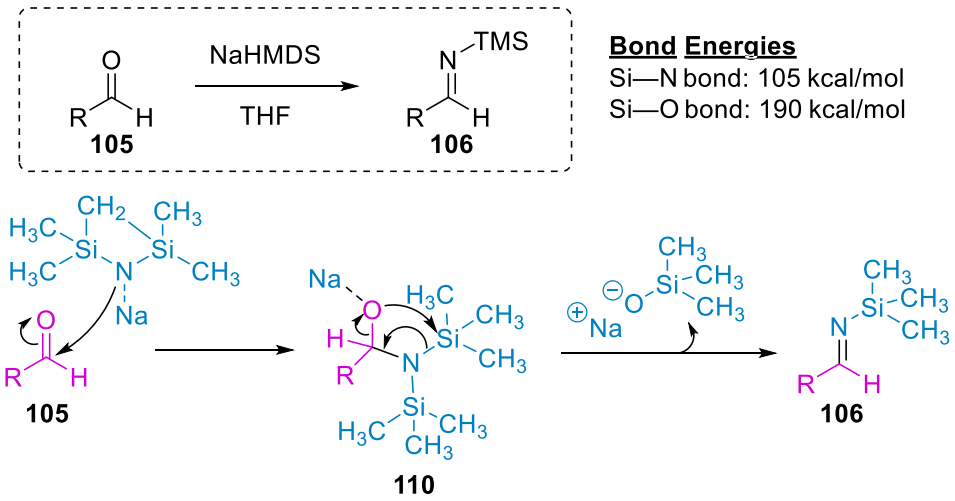

formation of imine **106**. The driving force for this transformation is the formation of the stronger silicon-oxygen bond and the breaking of the weaker silicon-nitrogen bond.[126,127]

Silyl imine **106** was then added to a solution of TMAO **107** and LDA in THF to undergo the [3+2] cycloaddition reaction, forming the imidazolidine intermediate **108**. Imidazolidine **108** was hydrolytically unstable, presumably due to the weak N-Si bond. We elected to trigger ring opening through addition of hydrochloric acid forming the resulting 1,2-diamine **109**. After observing a mixture of the imidazolidine, diamine, and other reaction products, hydroxylamine hydrochloride was added to the reaction to serve as a formaldehyde scavenger, presumably forming the aldoxime.[128] The addition of hydroxylamine hydrochloride with hydrochloric acid resulted in a cleaner conversion as shown by ^{1}H NMR, and thus our new method was ready for optimization.

Reaction optimization focused on the [3+2] cycloaddition because the aza-Brook rearrangement undergoes full conversion into the silyl protected imine, as determined by ^{1}H NMR, and the hydrolysis of the imidazolidine core is straightforward (Table 1). The initial conditions were a 1:1 ratio of 4-methyoxyphenyl silyl imine **106a** and TMAO in THF with three equivalents of base. Excitingly, following aqueous workup diamine **109a** was isolated in good (70%) yield after a three-hour reaction time on a 0.4 mmol scale (Table 1, Entry 1). Decreasing the reaction time to two hours gave a mild improvement in yield, (75% yield), while further decreasing the reaction time had a negative impact on the yield (Table 1, Entries 2-3).

Using less than three equivalents of LDA results in lower yields (Table 1, Entries 4-5), which satisfyingly agrees with our prior work on the mechanism of this transformation.[129] Computationally, we found it was most favorable to have two equivalents of LDA to doubly deprotonate the α-protons of the amine, with the third equivalent serving to complex and stabilize key transition states.[19,129]

Table 1. Optimization of reaction Conditions[a]

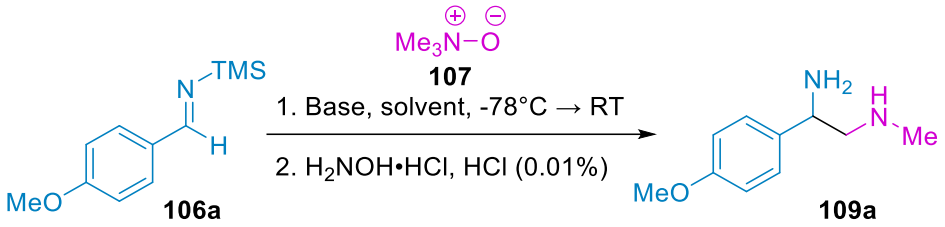

Entry	Base	Solvent	Time	Yield (%)[b]
1	LDA	THF	3h	70
2	**LDA**	**THF**	**2h**	**75 (90)**[c]
3	LDA	THF	1h	54
4	LDA (2 equiv.)	THF	2h	50
5	LDA (2.5 equiv)	THF	2h	67
6	LiHMDS	THF	2h	NR
7	NaHMDS	THF	2h	NR
10	LDA	Et_2O	2h	67
11	LDA	TBME	2h	45

[a]Reactions were conducted on a 0.4 mmol scale using **106a** (1 equiv.), TMAO (1 equiv.), and LDA (3 equiv.), in 0.1 M THF, followed by hydroxylamine hydrochloride (5 equiv.) and 1.2 M HCl (0.01M). [b]Isolated yields. [c]Reaction carried out on a 2 mmol scale.

Neither LiHMDS nor NaHMDS were compatible with the reaction, resulting in no reaction (Table 1, Entries 6-7), this provides some key insights into the basicity required for the reaction. The conjugate acids of LDA and LiHMDS have been reported in THF to be 35.7 and 25.8 respectively, indicating that the *N*-oxides have a pka in THF between 35 and 26,[130] likely trending towards the upper end of the scale since we see no reaction with LiHMDS. This was ultimately fortuitous because it meant that excess NaHMDS could be used to form the silyl imine without complicating

the later cycloaddition. This is also what really gave way to this being developed into a one-pot synthetic method. Finally, neither diethyl ether nor *tert*-butyl methyl ether offered any advantage over THF, again agreeing with prior mechanistic work by ourselves and others which indicates that solvent chelation plays a major role in polar reactions.[129,131-133]

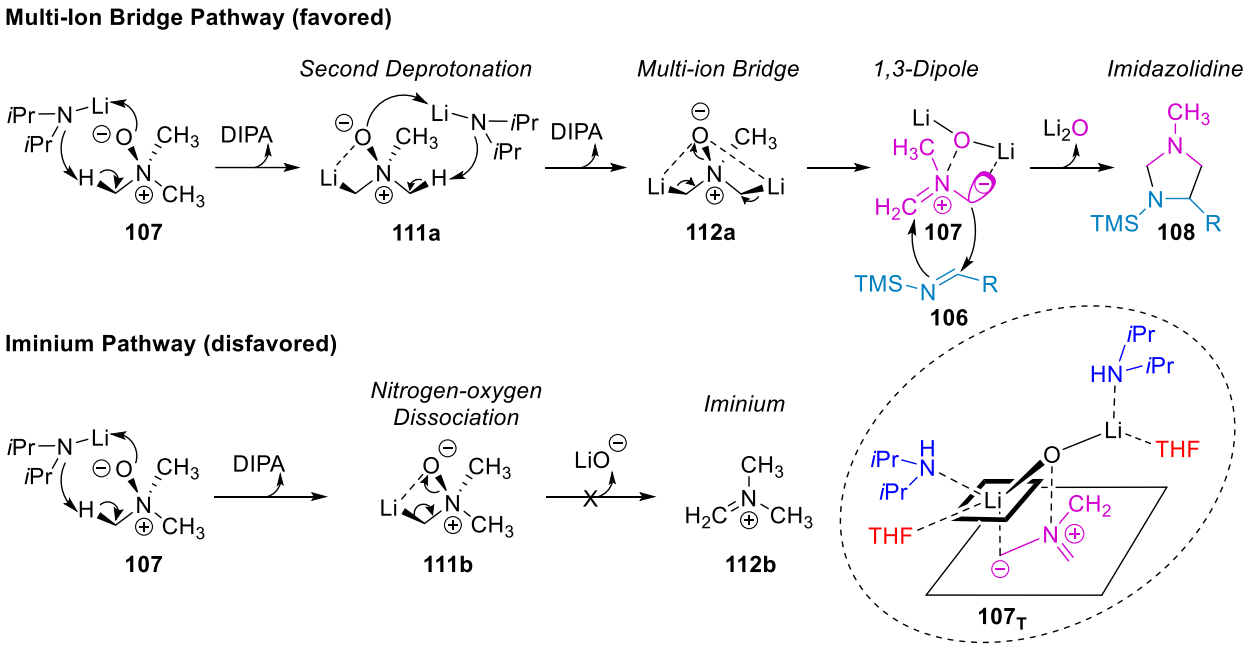

Figure 5. Proposed multi-ion bridge pathway forming the required 1,3-dipole for the [3+2] cycloaddition with stabilized key transition state. (Martin Neal)[19] Adapted from Hejnosz, S. L. *et al*. *Organic Letters* **2023**. Copyright 2023 American Chemical Society

The scalability of the method was then tested with optimized reaction conditions in hand. Surprisingly a 90% yield was achieved when the reaction was increased to a 2 mmol scale (Table 2, Entry 2). When the reaction scale was further increased to a 5 mmol scale the yield was about the same as it was on a 0.4 mmol scale (Table 2, Entry 3). This was advantageous because the reaction could be run on scale to generate sufficient diamine to then test different reactions further functionalizing the scaffold. This is another major limitation of many synthetic methods, they are not scalable which limits their utility for industrial chemists.

Table 2. Increasing the scale of the reaction.

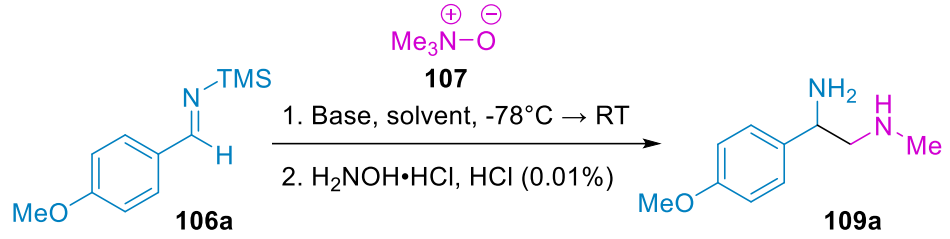

Entry	Scale	Yield[b] (%)
1	0.4 mmol	75
2	2.0 mmol	90
3	5.0 mmol	70

[a]Reactions were conducted on a 0.4 mmol scale using **106a** (1 equiv.), TMAO (1 equiv.), and LDA (3 equiv.), in 0.1 M THF, followed by hydroxylamine hydrochloride (5 equiv.) and 1.2 M HCl (0.01M). [b]Isolated yields.

1.2.2 Substrate Scope of Various Silyl Imines with TMAO

The substrate scope with various silyl imines was investigated (Scheme 23). Silyl imines with electron donating substituents on the *ortho* (**109a**) and *para* (**109c**) positions on the aryl ring worked well with the reaction, resulting in excellent yields of 94% and 93%. The lower yield for **109b** is most likely due to the low electronic contribution of the methoxy group at the *meta* position. Good yields were observed for electron donating **109d** and **109e** of 74% and 80%, respectively.

Relatively electronically neutral groups were well tolerated as well. Phenyl substituted silyl imine underwent the reaction to give **109f** in an 80% yield. Dimethyl substituted **109g** worked well and formed in a 77% yield. Biphenyl substituted **109h**, and the naphthyl derivative **109i** resulted in 88% and 71% yields respectively. Gratifyingly, this reaction tolerates alkyl substituents with non-enolizable protons demonstrated by **109j** and **109k** with yields of 60% and 72%.

Scheme 24. Substrate scope of silyl imines

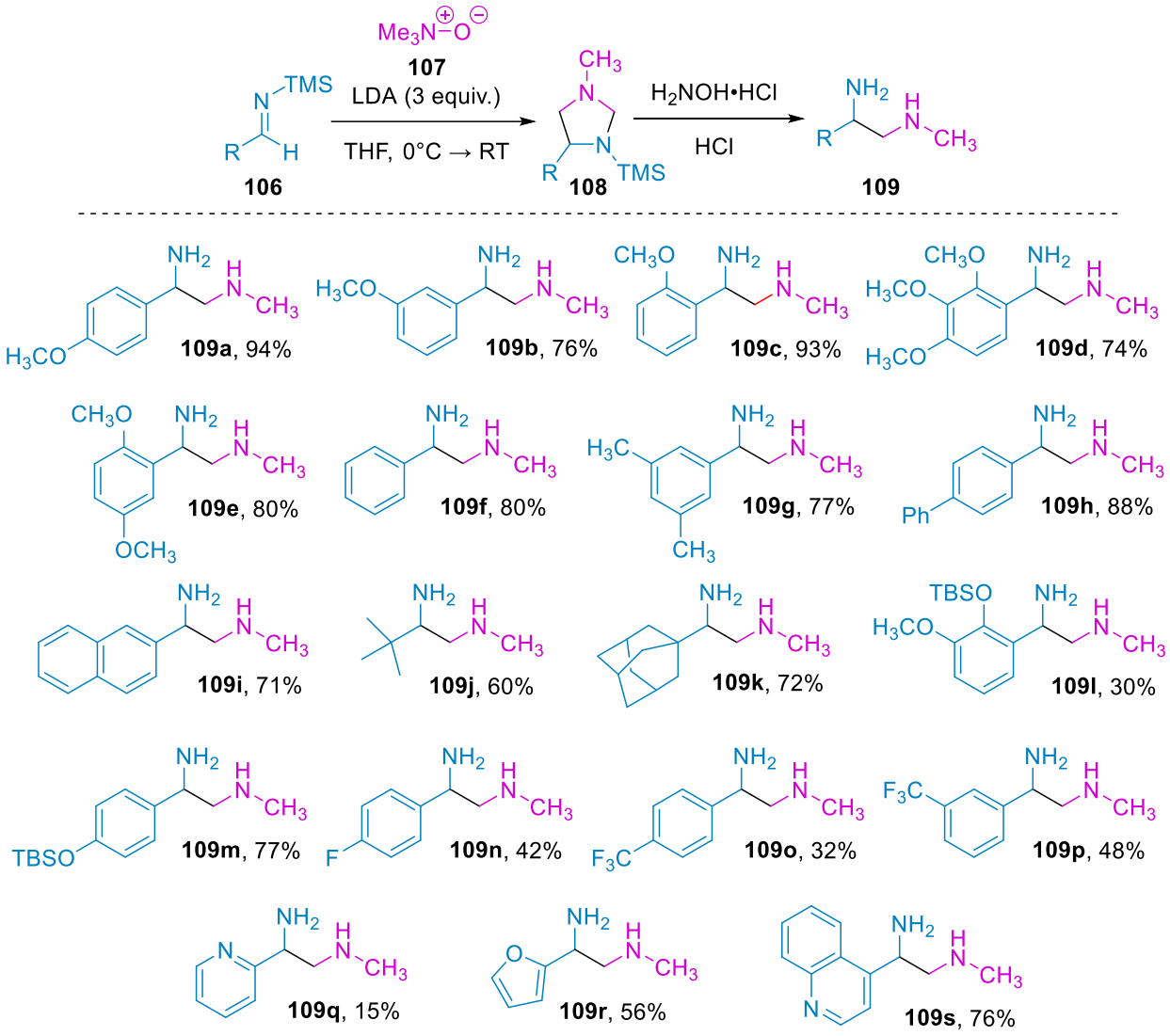

A silyl protecting group was introduced with **109l** which resulted in 30% yield, presumably due to the steric bulk of the *ortho* OTBS group. This reaction does tolerate silyl protected alcohols provided the steric bulk is farther away from the cycloaddition, demonstrated by **109m** giving a 77% yield. This is beneficial because the OTBS can be used as a functional group handle for future chemistry if needed. For instance, it can later be deprotected and converted into a triflate, which can used in cross coupling reactions to build a more complex molecular scaffold.

Strong electron withdrawing groups hindered this reaction. Fluoro-substituted **109o** demonstrated this reactions halide tolerance, although the reaction conditions had to be altered.[133,134] Careful temperature control as well as a quick water wash of the imidazolidine allowed us to afford **109o** in a 42% yield. Trifluoromethyl diamines **109o** and **109p** also resulted in lower yields of 32% and 48%. These also demonstrate the same effects seen in the methoxy derivatives with difference in the electronic contributions of substituents on the *para* and *meta* positions. Heteroaryl substituents were also implemented, though pyridyl substituted **109q** was not high yielding with a 15% overall yield. Furyl substituted **109r** was reasonably tolerated giving 56% yield, and quinoline-substituted **109s** resulted in a good yield of 76%. Intriguingly, it was found that the imidazolidines for the hetereocyclic substituents were more stable than their non-heterocyclic counterparts in some cases which will be discussed in chapter 2.

1.2.3. Substrate scope limitaions

Every method has its limitations, and in this case the reaction limitations arise from the use of LDA. Due to the nature of the lithium base, potential side reactions such as *ortho*-lithiation or lithium-halide exchange that may occur.[133,134] Evidence of such side reactions occurring were observed in the ^{1}H NMR of **109t** and **109u**. The aryl halides were transformed into the silyl imines with clean and full conversions, however in the presence of LDA the reaction mixture becomes an indiscernible mess with little indication that the desired products even formed. It has been reported that stilbenes bearing halide substituents formed pyrrolidines in low yields,[135] however there are inherent differences between the electronic characteristics of stilbene and imines. Imines have better potential of stabilizing the resulting anion of these lithiations, making this more likely to occur with aryl imines rather than stilbenes.[136]

Scheme 25. Substrate scope limitations

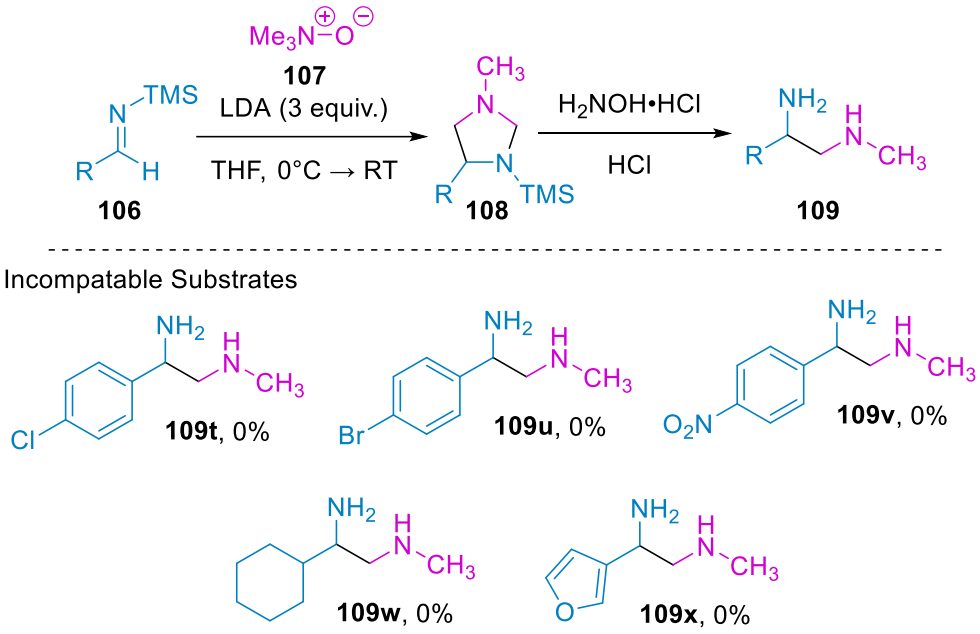

This reaction also does not tolerate nitro groups either due to the presence of LDA. The ^{1}H NMR for this reaction showed a clean conversion to the silyl imine **106v**, but had an abundance of new signals for the [3+2] cycloaddition, which suggests that other side reactions are occurring. This agrees with the literature where it has been reported that LDA can reduce nitro arenes,[137] causing off-target reactivity in this system.

Another scope limitation intrinsic to using LDA as a base is reaction sensitivity to α-protons since typically they have a pK_a around 20.[138] To overcome this incompatibility, cyclohexyl **109w** was implemented in this reaction to try including a substrate containing an α-proton that is fairly sterically hindered, making it less likely to undergo deprotonation by LDA. While the aza-Brook rearrangement provided a clean conversion, the cycloaddition transformation was extremely messy, including many different unidentified products; moreover, when the crude ^{1}H NMR was examined there were none of the indicative peaks for the desired imidazolidine.

Lastly, not an LDA issue neccessarly, but Interestingly enough for the reaction with 3-furyl **109x**, the desired imidazolidine intermediate did not form. This may be due to the difference of the electronic characteristics of the 2 and 3 position of the furyl, or it may be due to the chelation effects of base. This is discussed more in depth in Chapter 2.

1.2.4 Transformations of 1,2-Diamine 109a

1.2.4.1. Amine functionalization with protecting groups

To demonstrate the synthetic utility of these compounds, diamine **109a** was subjected to a variety of different transformations. Both amines can undergo tosylation forming **113** in > 95% yield (Scheme 25). Selective tosylation of the primary amine is observed when the reaction is cooled to -78 °C with slow addition of tosyl chloride, forming **114** in a 72% yield (Scheme 25). Moreover, selective protections of the primary amine are observed with nosyl **115** and pivaloyl **116**, giving 75% and 60% yields respectively (Scheme 26).

Scheme 26. Controlling the reaction conditions to either achieve functionalization of both amines, or just one selectively (Alexander Cocolas)

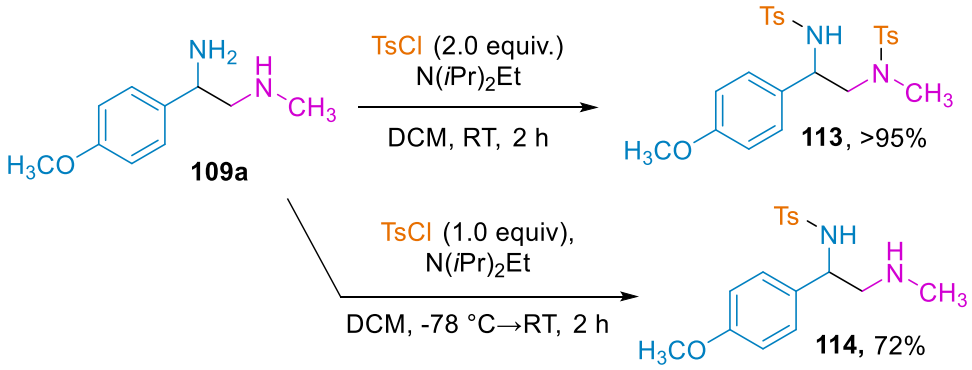

Scheme 27. Selective functionalization of the primary amine (Alexander Cocolas)

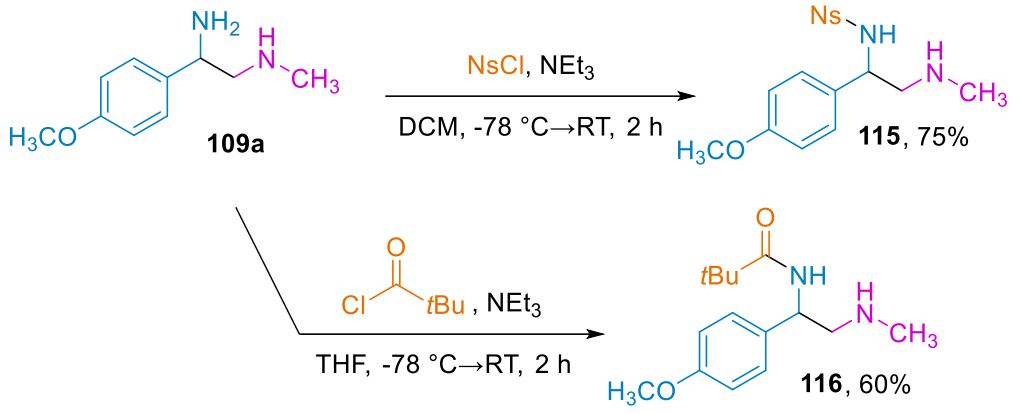

When contemplating mono-functionalization of one amine in the presence of the other there were two distinct possibilities; first chemical intuition suggests the more election rich secondary amine would be more nucleophilic, thereby resulting in selective functionalization of the secondary amine. On the other hand, the primary amine is less sterically hindered, which should favor reactions occurring at that nitrogen center. When we performed the experiments excitingly we achieved a single product as determined by ^{1}H NMR, however which amine had been functionalized was not immediately apparent. To solve this issue a 2D NOESY experiment was performed on the nosyl protected diamine **115** and it was confirmed that selective protection of the primary amine is occurred. Strong NOESY interactions are observed between H_a of the nosyl-group as well as H_b and H_c, which is possible if the nosyl group added to either position. What lead to the assignment that the primary amine is nosyl-protected was the strong interaction between H_a and the protons of the methyl group; the only possible way to have that nosyl-intereaction (H_a) with the methyl-group protons as well as H_b and H_c is if the nosyl group is on the primary amine. If the nosyl group was on the secondary amine, there could be special interactions of H_a with H_b and H_c, but not with the methyl-group, or vice-versa. Additionally, if the nosyl-group was on the

secondary amine, strong H_d and H_a interactions would be observed, however this interaction was not observed in the NOESY spectrum.

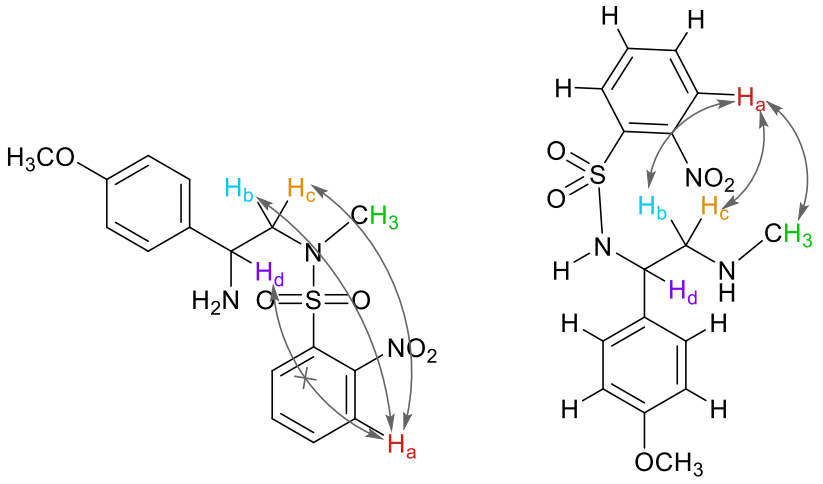

115

Secondary Amine Nosylation *Primary Amine Nosylation*

Figure 6. Observed NOESY interactions for nosylation of the primary amine

The synthetic utility of these 1,2-diamines as building blocks for heterocyclics was further examined, inspired by the presence of the diamine backbone present in bioactive compounds.[1] Vicinal diamine **109a** and ethyl benzimidate hydrochloride formed 4,5-dihydro imidazole **117** in 60% yield (Scheme 27). Additionally, diamine **109a** was reacted with triphosgene to afford imidazolidinone **118** in a modest 43% yield.

Scheme 28. Cyclization of diamine 109a forming imidazoline and imidazolidinone derivatives

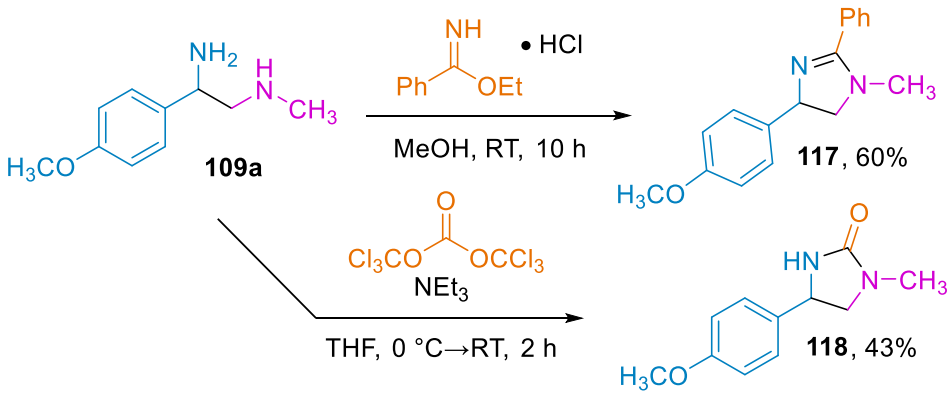

This clearly demonstrates that these 1,2-diamines can be used as synthetic building blocks for either selective functionalization of the amines or to form novel heterocycles. This is particularly exciting as structures containing similar cores exhibit bioactivities such as anti-inflammatory,[139] antihyperglycemic,[140] and NF-κB inhibition as previously discussed.[141]

1.3 Conclusions

We present here a straightforward, one-pot synthetic method for producing a wide range of 1,2-diamines in yields up to 93% in a three step one pot reaction. The lynchpin [3+2]-cycloaddition step works best for electron rich and neutral arenes, with electron deficient substrates giving lower yields. Moreover, these products can then undergo further transformation to produce more complex scaffolds, namely imidazolidines. Additionally, using DFT modeling we propose a reasonable mechanism which both agrees with our reported data and previous work. This approach allows for variable substitutions and flexibility that others methods do not offer; therefore, we further expanded the chemical space and constructed an array of bioactive targets.

1.4 References

(1) Lucet, D.; Le Gall, T.; Mioskowski, C. The Chemistry of Vicinal Diamines. *Angewandte Chemie International Edition* **1998**, *37* (19), 2580-2627. DOI: https://doi.org/10.1002/(SICI)1521-3773(19981016)37:19<2580::AID-ANIE2580>3.0.CO;2-L.

(2) Saibabu Kotti, S. R. S.; Timmons, C.; Li, G. Vicinal Diamino Functionalities as Privileged Structural Elements in Biologically Active Compounds and Exploitation of their Synthetic Chemistry. *Chemical Biology & Drug Design* **2006**, *67* (2), 101-114. DOI: 10.1111/j.1747-0285.2006.00347.x

(3) Michalson, E. T.; Szmuszkovicz, J. Medicinal agents incorporating the 1,2-diamine functionality. In *Progress in Drug Research*, Jucker, E. Ed.; Birkhäuser Basel, 1989; pp 135-149.

(4) Weerawarna, S. A.; Davis, R. D.; Nelson, W. L. Isothiocyanate-substituted kappa-selective opioid receptor ligands derived from *N*-methyl-*N*-[(1S)-1-phenyl-2-(1-pyrrolidinyl)ethyl] phenylacetamide. *J Med Chem* **1994**, *37* (18), 2856-2864. DOI: 10.1021/jm00044a006

(5) Chang, A. C.; Takemori, A. E.; Ojala, W. H.; Gleason, W. B.; Portoghese, P. S. kappa Opioid receptor selective affinity labels: electrophilic benzeneacetamides as kappa-selective opioid antagonists. *J Med Chem* **1994**, *37* (26), 4490-4498. DOI: 10.1021/jm00052a008

(6) Malcolmson, S. J.; Li, K.; Shao, X. 2-Azadienes as Enamine Umpolung Synthons for the Preparation of Chiral Amines. *Synlett* **2019**, *30* (11), 1253-1268.

(7) Magano, J. Synthetic Approaches to the Neuraminidase Inhibitors Zanamivir (Relenza) and Oseltamivir Phosphate (Tamiflu) for the Treatment of Influenza. *Chemical Reviews* **2009**, *109* (9), 4398-4438. DOI: 10.1021/cr800449m.

(8) Beke, F.; Meszaros, A.; Toth, A.; Botlik, B. B.; Novak, Z. Vicinal difunctionalization of carbon-carbon double bond for the platform synthesis of trifluoroalkyl amines. *Nat Commun* **2020**, *11* (1), 5924. DOI: 10.1038/s41467-020-19748-z

(9) DeSimone, R. W.; Currie, K. S.; Mitchell, S. A.; Darrow, J. W.; Pippin, D. A. Privileged structures: applications in drug discovery. *Comb Chem High Throughput Screen* **2004**, *7* (5), 473-494. DOI: 10.2174/1386207043328544

(10) Sheshenev, A. E.; Boltukhina, E. V.; White, A. J. P.; Hii, K. K. Methylene-Bridged Bis(imidazoline)-Derived 2-Oxopyrimidinium Salts as Catalysts for Asymmetric Michael Reactions. *Angewandte Chemie International Edition* **2013**, *52* (27), 6988-6991. DOI: https://doi.org/10.1002/anie.201300614.

(11) Sutton, A. E.; Richardson, T. E.; Huck, B. R.; Karra, S. R.; Chen, X.; Xiao, Y.; Goutopoulos, A.; Lan, R.; Perrey, D.; Vandeveer, H. G.; et al. Preparation of novel aminoazaheterocyclic carboxamides useful in the treatment of hyperproliferative diseases. WO2010093419, 2010.

(12) Synthesis of imidazolone derivatives as DYRK1, CLK1 and/or CLK4 protein kinases. EP3904354, 2021.

(13) Skerlj, R.; Bridger, G.; Zhou, Y.; Bourque, E.; McEachern, E.; Metz, M.; Harwig, C.; Li, T. S.; Yang, W.; Bogucki, D.; et al. Design of substituted imidazolidinylpiperidinylbenzoic acids as chemokine receptor 5 antagonists: potent inhibitors of R5 HIV-1 replication. *J Med Chem* **2013**, *56* (20), 8049-8065. DOI: 10.1021/jm401101p

(14) Gladiali, S.; Alberico, E. Asymmetric transfer hydrogenation: chiral ligands and applications. *Chemical Society Reviews* **2006**, *35* (3), 226-236, 10.1039/B513396C. DOI: 10.1039/B513396C.

(15) Surry, D. S.; Buchwald, S. L. Diamine Ligands in Copper-Catalyzed Reactions. *Chem Sci* **2010**, *1* (1), 13-31, 10.1039/C0SC00107D. DOI: 10.1039/C0SC00107D

(16) Ikariya, T.; Blacker, A. J. Asymmetric Transfer Hydrogenation of Ketones with Bifunctional Transition Metal-Based Molecular Catalysts. *Accounts of Chemical Research* **2007**, *40* (12), 1300-1308. DOI: 10.1021/ar700134q.

(17) Kizirian, J.-C. Chiral Tertiary Diamines in Asymmetric Synthesis. *Chemical Reviews* **2008**, *108* (1), 140-205. DOI: 10.1021/cr040107v.

(18) Chierchia, M.; Law, C.; Morken, J. P. Nickel-Catalyzed Enantioselective Conjunctive Cross-Coupling of 9-BBN Borates. *Angew Chem Int Ed Engl* **2017**, *56* (39), 11870-11874. DOI: 10.1002/anie.201706719

(19) Hejnosz, S. L.; Beres, D. R.; Cocolas, A. H.; Neal, M. J.; Musiak, B. S.; Hanna, M. M. B.; Bloomfield, A. J.; Montgomery, T. D. [3 + 2] Cycloadditions of Tertiary Amine *N*-Oxides and Silyl

Imines as an Innovative Route to 1,2-Diamines. *Organic Letters* **2023**. DOI: 10.1021/acs.orglett.3c01396.

(20) Vrudhula, V. M.; Dzierba, C. D.; Bronson, J. J.; Macor, J. E.; Nara, S. J.; Rajamani, R.; Karatholuvhu, M. S. Aryl amide-based kinase inhibitors. US20160016967, 2016.

(21) Kuai, L.; Ong, S. E.; Madison, J. M.; Wang, X.; Duvall, J. R.; Lewis, T. A.; Luce, C. J.; Conner, S. D.; Pearlman, D. A.; Wood, J. L.; et al. AAK1 identified as an inhibitor of neuregulin-1/ErbB4-dependent neurotrophic factor signaling using integrative chemical genomics and proteomics. *Chem Biol* **2011**, *18* (7), 891-906. DOI: 10.1016/j.chembiol.2011.03.017 From NLM.

(22) Greenwood, T. A.; Lazzeroni, L. C.; Murray, S. S.; Cadenhead, K. S.; Calkins, M. E.; Dobie, D. J.; Green, M. F.; Gur, R. E.; Gur, R. C.; Hardiman, G.; et al. Analysis of 94 candidate genes and 12 endophenotypes for schizophrenia from the Consortium on the Genetics of Schizophrenia. *Am J Psychiatry* **2011**, *168* (9), 930-946. DOI: 10.1176/appi.ajp.2011.10050723

(23) Latourelle, J. C.; Pankratz, N.; Dumitriu, A.; Wilk, J. B.; Goldwurm, S.; Pezzoli, G.; Mariani, C. B.; DeStefano, A. L.; Halter, C.; Gusella, J. F.; et al. Genomewide association study for onset age in Parkinson disease. *BMC Medical Genetics* **2009**, *10* (1), 98. DOI: 10.1186/1471-2350-10-98.

(24) Singh, A. K.; Lang, C. A. Small molecule drugs and related methods for treatment of diseases related to amyloid-β42 oligomer formation. WO2019089066, 2019.

(25) Li, J. J. *Laughing gas, Viagra, and Lipitor: The human stories behind the drugs we use*; Oxford University Press, 2006.

(26) BT., S.; Y, A. K. StatPearls [Internet]. StatPearls Publishing: Treasure Island (FL) 2022.

(27) Ban, T. A. Fifty years chlorpromazine: a historical perspective. *Neuropsychiatr Dis Treat* **2007**, *3* (4), 495-500.

(28) Roy, J. *An Introduction to Pharmaceutical Sciences: Production, Chemistry, Techniques and Technology*; Elsevier Science, 2011.

(29) SP, K. *Amoxicillin*. August 24, 2022. https://clincalc.com/DrugStats/Drugs/Amoxicillin (accessed 2023 May 2, 2023).

(30) Organization, W. H. Global action plan on antimicrobial resistance. **2015**.

(31) D'Ambrosio, M.; Guerriero, A.; Debitus, C. c.; Ribes, O.; Pusset, J.; Leroy, S.; Pietra, F. Agelastatin a, a new skeleton cytotoxic alkaloid of the oroidin family. Isolation from the axinellid sponge Agelas dendromorpha of the coral sea. *Journal of the Chemical Society, Chemical Communications* **1993**, (16), 1305-1306, 10.1039/C39930001305. DOI: 10.1039/c39930001305.

(32) D'Ambrosio, M.; Guerriero, A.; Pietra, F.; Ripamonti, M.; Debitus, C. c.; Waikedre, J. The Active Centres of Agelastatin A, a Strongly Cytotoxic Alkaloid of the Coral Sea Axinellid SpongeAgelas dendromorpha, as Determined by Comparative Bioassays with Semisynthetic Derivatives. *Helvetica Chimica Acta* **1996**, *79* (3), 727-735. DOI: 10.1002/hlca.19960790315.

(33) Mason, C. K.; McFarlane, S.; Johnston, P. G.; Crowe, P.; Erwin, P. J.; Domostoj, M. M.; Campbell, F. C.; Manaviazar, S.; Hale, K. J.; El-Tanani, M. Agelastatin A: a novel inhibitor of osteopontin-mediated adhesion, invasion, and colony formation. *Molecular Cancer Therapeutics* **2008**, *7* (3), 548-558. DOI: 10.1158/1535-7163.Mct-07-2251 (acccessed 5/15/2023).

(34) Wehn, P. M.; Du Bois, J. A stereoselective synthesis of the bromopyrrole natural product (-)-agelastatin A. *Angew Chem Int Ed Engl* **2009**, *48* (21), 3802-3805. DOI: 10.1002/anie.200806292

(35) Stien, D.; Anderson, G. T.; Chase, C. E.; Koh, Y.-h.; Weinreb, S. M. Total synthesis of the antitumor marine sponge alkaloid agelastatin A. *Journal of the American Chemical Society* **1999**, *121* (41), 9574-9579.

(36) Feldman, K. S.; Saunders, J. C. Alkynyliodonium salts in organic synthesis. Application to the total synthesis of (−)-agelastatin A and (−)-agelastatin B. *Journal of the American Chemical Society* **2002**, *124* (31), 9060-9061.

(37) Feldman, K. S.; Saunders, J. C.; Wrobleski, M. L. Alkynyliodonium salts in organic synthesis. Development of a unified strategy for the syntheses of (−)-agelastatin A and (−)-agelastatin B. *The Journal of Organic Chemistry* **2002**, *67* (20), 7096-7109.

(38) Yoshimitsu, T.; Ino, T.; Tanaka, T. Total synthesis of (−)-agelastatin A. *Organic Letters* **2008**, *10* (23), 5457-5460.

(39) Ichikawa, Y.; Yamaoka, T.; Nakano, K.; Kotsuki, H. Synthesis of (−)-agelastatin A by [3.3] sigmatropic rearrangement of allyl cyanate. *Organic Letters* **2007**, *9* (16), 2989-2992.

(40) Staggs, C. G.; Sealey, W. M.; McCabe, B. J.; Teague, A. M.; Mock, D. M. Determination of the biotin content of select foods using accurate and sensitive HPLC/avidin binding. *J Food Compost Anal* **2004**, *17* (6), 767-776. DOI: 10.1016/j.jfca.2003.09.015

(41) Marriott, B. P.; Birt, D. F.; Stalling, V. A.; Yates, A. A. *Present Knowledge in Nutrition: Basic Nutrition and Metabolism*; Elsevier Science, 2020.

(42) Green, N. M. AVIDIN. 3. THE NATURE OF THE BIOTIN-BINDING SITE. *Biochem J* **1963**, *89* (3), 599-609. DOI: 10.1042/bj0890599 From NLM.

(43) Viso, A.; Fernandez de la Pradilla, R.; Garcia, A.; Flores, A. Alpha,beta-diamino acids: biological significance and synthetic approaches. *Chem Rev* **2005**, *105* (8), 3167-3196. DOI: 10.1021/cr0406561

(44) Cox, P. A.; Banack, S. A.; Murch, S. J.; Rasmussen, U.; Tien, G.; Bidigare, R. R.; Metcalf, J. S.; Morrison, L. F.; Codd, G. A.; Bergman, B. Diverse taxa of cyanobacteria produce beta-*N*-

methylamino-L-alanine, a neurotoxic amino acid. *Proc Natl Acad Sci U S A* **2005**, *102* (14), 5074-5078. DOI: 10.1073/pnas.0501526102

(45) Cox, P. A.; Davis, D. A.; Mash, D. C.; Metcalf, J. S.; Banack, S. A. Dietary exposure to an environmental toxin triggers neurofibrillary tangles and amyloid deposits in the brain. *Proc Biol Sci* **2016**, *283* (1823), 20152397. DOI: 10.1098/rspb.2015.2397

(46) Wang, D.; Bruneau-Voisine, A.; Sortais, J.-B. Practical (asymmetric) transfer hydrogenation of ketones catalyzed by manganese with (chiral) diamines ligands. *Catalysis Communications* **2018**, *105*, 31-36.

(47) Wang, Y.; Hu, X.; Du, H. Vicinal-diamine-based chiral chain dienes as ligands for rhodium(I)-catalyzed highly enantioselective conjugated additions. *Org Lett* **2010**, *12* (23), 5482-5485. DOI: 10.1021/ol1023536

(48) Hayes, A.; Clarkson, G.; Wills, M. The importance of 1,2-anti-disubstitution in monotosylated diamine ligands for ruthenium(II)-catalysed asymmetric transfer hydrogenation. *Tetrahedron: Asymmetry* **2004**, *15* (13), 2079-2084. DOI: https://doi.org/10.1016/j.tetasy.2004.05.025.

(49) Brandt, P.; Roth, P.; Andersson, P. G. Origin of enantioselectivity in the Ru(arene)(amino alcohol)-catalyzed transfer hydrogenation of ketones. *J Org Chem* **2004**, *69* (15), 4885-4890. DOI: 10.1021/jo030378q

(50) Noyori, R.; Ohkuma, T.; Kitamura, M.; Takaya, H.; Sayo, N.; Kumobayashi, H.; Akutagawa, S. Asymmetric hydrogenation of .beta.-keto carboxylic esters. A practical, purely chemical access to .beta.-hydroxy esters in high enantiomeric purity. *Journal of the American Chemical Society* **1987**, *109* (19), 5856-5858. DOI: 10.1021/ja00253a051.

(51) Kunz, K.; Scholz, U.; Ganzer, D. Renaissance of Ullmann and Goldberg Reactions - Progress in Copper Catalyzed C-N-, C-O- and C-S-Coupling. *Synlett* **2003**, *2003* (15), 2428-2439. DOI: 10.1055/s-2003-42473.

(52) Ullmann, F.; Bielecki, J. Ueber synthesen in der biphenylreihe. *Berichte der deutschen chemischen Gesellschaft* **1901**, *34* (2), 2174-2185.

(53) Goldberg, I. Ueber Phenylirungen bei Gegenwart von Kupfer als Katalysator. *Berichte der deutschen chemischen Gesellschaft* **1906**, *39* (2), 1691-1692. DOI: https://doi.org/10.1002/cber.19060390298.

(54) Ullmann, F. Ueber eine neue Bildungsweise von Diphenylaminderivaten. *Berichte der deutschen chemischen Gesellschaft* **1903**, *36* (2), 2382-2384. DOI: https://doi.org/10.1002/cber.190303602174.

(55) Ma, D.; Zhang, Y.; Yao, J.; Wu, S.; Tao, F. Accelerating Effect Induced by the Structure of α-Amino Acid in the Copper-Catalyzed Coupling Reaction of Aryl Halides with α-Amino Acids. Synthesis of Benzolactam-V8. *Journal of the American Chemical Society* **1998**, *120* (48), 12459-12467. DOI: 10.1021/ja981662f.

(56) Gauthier, S.; Fréchet, J. M. J. Phase-Transfer Catalysis in the Ullmann Synthesis of Substituted Triphenylamines. *Synthesis* **1987**, *1987* (04), 383-385. DOI: 10.1055/s-1987-27953.

(57) Freeman, H. S.; Butler, J. R.; Freedman, L. D. Acetyldiarylamines by arylation of acetanilides. Some applications and limitations. *The Journal of Organic Chemistry* **1978**, *43* (26), 4975-4978. DOI: 10.1021/jo00420a018.

(58) Crawford, K. R.; Padwa, A. Copper-catalyzed amidations of bromo substituted furans and thiophenes. *Tetrahedron Letters* **2002**, *43* (41), 7365-7368. DOI: 10.1016/s0040-4039(02)01725-2.

(59) Liu, X.; Mao, D.; Wu, S.; Yu, J.; Hong, G.; Zhao, Q.; Wang, L. Copper-catalyzed direct oxidation and *N*-arylation of benzylamines with diaryliodonium salts. *Science China Chemistry* **2014**, *57* (8), 1132-1136. DOI: 10.1007/s11426-014-5140-9.

(60) Klapars, A.; Huang, X.; Buchwald, S. L. A General and Efficient Copper Catalyst for the Amidation of Aryl Halides. *Journal of the American Chemical Society* **2002**, *124* (25), 7421-7428. DOI: 10.1021/ja0260465.

(61) Kang, S.-K.; Kim, D.-H.; Park, J.-N. Copper-catalyzed N-Arylation of Aryl Iodides with Benzamides or Nitrogen Heterocycles in the Presence of Ethylenediamine. *Synlett* **2002**, *2002* (03), 0427-0430. DOI: 10.1055/s-2002-20457.

(62) Phillips, D. P.; Hudson, A. R.; Nguyen, B.; Lau, T. L.; McNeill, M. H.; Dalgard, J. E.; Chen, J.-H.; Penuliar, R. J.; Miller, T. A.; Zhi, L. Copper-catalyzed *N*-arylation of oxindoles. *Tetrahedron letters* **2006**, *47* (40), 7137-7138.

(63) Antilla, J. C.; Klapars, A.; Buchwald, S. L. The copper-catalyzed *N*-arylation of indoles. *J Am Chem Soc* **2002**, *124* (39), 11684-11688. DOI: 10.1021/ja027433h

(64) Yuan, X.; Xu, X.; Zhou, X.; Yuan, J.; Mai, L.; Li, Y. Copper-catalyzed double *N*-alkenylation of amides: an efficient synthesis of di- or trisubstituted *N*-acylpyrroles. *J Org Chem* **2007**, *72* (4), 1510-1513. DOI: 10.1021/jo062194s

(65) Li, E.; Xu, X.; Li, H.; Zhang, H.; Xu, X.; Yuan, X.; Li, Y. Copper-catalyzed synthesis of five-membered heterocycles via double C–N bond formation: an efficient synthesis of pyrroles, dihydropyrroles, and carbazoles. *Tetrahedron* **2009**, *65* (44), 8961-8968. DOI: https://doi.org/10.1016/j.tet.2009.08.075.

(66) Coste, A.; Toumi, M.; Wright, K.; Razafimahaléo, V.; Couty, F.; Marrot, J.; Evano, G. Copper-Catalyzed Cyclization of Iodo-tryptophans: A Straightforward Synthesis of Pyrroloindoles. *Organic Letters* **2008**, *10* (17), 3841-3844. DOI: 10.1021/ol8015513.

(67) Minatti, A.; Buchwald, S. L. Synthesis of Indolines via a Domino Cu-Catalyzed Amidation/Cyclization Reaction. *Organic Letters* **2008**, *10* (13), 2721-2724. DOI: 10.1021/ol8008792.

(68) Hodgkinson, R. C.; Schulz, J.; Willis, M. C. Tandem copper-catalysed aryl and alkenyl amination reactions: the synthesis of *N*-functionalised indoles. *Organic & Biomolecular Chemistry* **2009**, *7* (3), 432-434, 10.1039/B817254D. DOI: 10.1039/B817254D.

(69) Pei, Z.; Li, X.; von Geldern, T. W.; Longenecker, K.; Pireh, D.; Stewart, K. D.; Backes, B. J.; Lai, C.; Lubben, T. H.; Ballaron, S. J.; et al. Discovery and Structure−Activity Relationships of Piperidinone- and Piperidine-Constrained Phenethylamines as Novel, Potent, and Selective Dipeptidyl Peptidase IV Inhibitors. *Journal of Medicinal Chemistry* **2007**, *50* (8), 1983-1987. DOI: 10.1021/jm061436d.

(70) Procopiou, P. A.; Ancliff, R. A.; Bamford, M. J.; Browning, C.; Connor, H.; Davies, S.; Fogden, Y. C.; Hodgson, S. T.; Holmes, D. S.; Looker, B. E.; et al. 4-Acyl-1-(4-aminoalkoxyphenyl)-2-ketopiperazines as a Novel Class of Non-Brain-Penetrant Histamine H3 Receptor Antagonists. *Journal of Medicinal Chemistry* **2007**, *50* (26), 6706-6717. DOI: 10.1021/jm0708228.

(71) Lovering, F.; Kirincich, S.; Wang, W.; Combs, K.; Resnick, L.; Sabalski, J. E.; Butera, J.; Liu, J.; Parris, K.; Telliez, J. B. Identification and SAR of squarate inhibitors of mitogen activated protein kinase-activated protein kinase 2 (MK-2). *Bioorganic & Medicinal Chemistry* **2009**, *17* (9), 3342-3351. DOI: https://doi.org/10.1016/j.bmc.2009.03.041.

(72) Wu, B.; Kuhen, K.; Ngoc Nguyen, T.; Ellis, D.; Anaclerio, B.; He, X.; Yang, K.; Karanewsky, D.; Yin, H.; Wolff, K.; et al. Synthesis and evaluation of *N*-aryl pyrrolidinones as novel anti-HIV-1 agents. Part 1. *Bioorg Med Chem Lett* **2006**, *16* (13), 3430-3433. DOI: 10.1016/j.bmcl.2006.04.012

(73) Beghyn, T.; Hounsou, C.; Deprez, B. P. PDE5 inhibitors: An original access to novel potent arylated analogues of tadalafil. *Bioorg Med Chem Lett* **2007**, *17* (3), 789-792. DOI: 10.1016/j.bmcl.2006.10.069

(74) Beadle, C. D.; Boot, J.; Camp, N. P.; Dezutter, N.; Findlay, J.; Hayhurst, L.; Masters, J. J.; Penariol, R.; Walter, M. W. 1-Aryl-3,4-dihydro-1H-quinolin-2-one derivatives, novel and selective norepinephrine reuptake inhibitors. *Bioorg Med Chem Lett* **2005**, *15* (20), 4432-4437. DOI: 10.1016/j.bmcl.2005.07.038

(75) Schweinitz, A.; Dönnecke, D.; Ludwig, A.; Steinmetzer, P.; Schulze, A.; Kotthaus, J.; Wein, S.; Clement, B.; Steinmetzer, T. Incorporation of neutral C-terminal residues in 3-amidinophenylalanine-derived matriptase inhibitors. *Bioorganic & Medicinal Chemistry Letters* **2009**, *19* (7), 1960-1965. DOI: https://doi.org/10.1016/j.bmcl.2009.02.047.

(76) Dessole, G.; Branca, D.; Ferrigno, F.; Kinzel, O.; Muraglia, E.; Palumbi, M. C.; Rowley, M.; Serafini, S.; Steinkuhler, C.; Jones, P. Discovery of *N*-[(1-aryl-1H-indazol-5-yl)methyl]amides derivatives as smoothened antagonists for inhibition of the hedgehog pathway. *Bioorg Med Chem Lett* **2009**, *19* (15), 4191-4195. DOI: 10.1016/j.bmcl.2009.05.112

(77) Khatik, G. L.; Kumar, V.; Nair, V. A. Reversal of Selectivity in Acetate Aldol Reactions of *N*-Acetyl-(S)-4-isopropyl-1-[(R)-1-phenylethyl]imidazolidin-2-one. *Organic Letters* **2012**, *14* (10), 2442-2445. DOI: 10.1021/ol300949s.

(78) Riebsomer, J. L. A STUDY OF THE REACTION PRODUCTS OF 1,2-DIAMINES WITH ALDEHYDES. *The Journal of Organic Chemistry* **1950**, *15* (2), 237-240. DOI: 10.1021/jo01148a003.

(79) Henry, L.; Leung, I. K. H.; Claridge, T. D. W.; Schofield, C. J. γ-Butyrobetaine hydroxylase catalyses a Stevens type rearrangement. *Bioorganic & Medicinal Chemistry Letters* **2012**, *22* (15), 4975-4978. DOI: https://doi.org/10.1016/j.bmcl.2012.06.024.

(80) Chanu, L. G.; Singh, O. M.; Jang, S.-H.; Lee, S.-G. Regioselective Synthesis of Heterocyclic Ketene N,N-, N,O- and N,S-acetals in Aqueous Medium. *Bulletin of the Korean Chemical Society* **2010**, *31* (4), 859-862. DOI: 10.5012/bkcs.2010.31.04.859.

(81) Azzena, U.; Dettori, G.; Pisano, L.; Siotto, I. Reductive lithiation of 1,3-dimethyl-2-arylimidazolidines. *Tetrahedron* **2005**, *61* (13), 3177-3182. DOI: 10.1016/j.tet.2005.01.093.

(82) Karaali, N.; Aydin, S.; Baltas, N.; Mentese, E. Synthesis of novel tetra-substituted benzimidazole compounds containing certain heterostructures with antioxidant and anti-urease activities. *Journal of Heterocyclic Chemistry* **2020**, *57* (4), 1806-1815. DOI: https://doi.org/10.1002/jhet.3905.

(83) Campbell, A. S.; Oalmann, C. J.; Yamashita, D. S. Preparation of fused bicycles as inhibitors of microbially induced amyloid formation, methods for identifying such inhibitors and their use for treating Parkinson's disease. WO2021142333, 2021.

(84) Roger, R.; Neilson, D. G. The Chemistry of Imidates. *Chemical Reviews* **1961**, *61* (2), 179-211. DOI: 10.1021/cr60210a003.

(85) Alouane, N.; Boutier, A.; Baron, C.; Vrancken, E.; Mangeney, P. Remarkably Efficient Charcoal-Promoted Ring-Closing Carbonylations. *Synthesis* **2006**, *2006* (05), 885-889. DOI: 10.1055/s-2006-926340.

(86) Voronov, A.; Botla, V.; Montanari, L.; Carfagna, C.; Mancuso, R.; Gabriele, B.; Maestri, G.; Motti, E.; Della Ca, N. Pd-Catalysed oxidative carbonylation of alpha-amino amides to hydantoins under mild conditions. *Chem Commun (Camb)* **2021**, *58* (2), 294-297, 10.1039/D1CC04154A. DOI: 10.1039/d1cc04154a

(87) Guyonnet, M.; Baudoin, O. Synthesis of Tricyclic Nitrogen Heterocycles by a Sequence of Palladium-Catalyzed N–H and C(sp3)–H Arylations. *Organic Letters* **2012**, *14* (1), 398-401. DOI: 10.1021/ol2031763.

(88) Wong, D. T.; Perry, K. W.; Bymaster, F. P. Case history: the discovery of fluoxetine hydrochloride (Prozac). *Nat Rev Drug Discov* **2005**, *4* (9), 764-774. DOI: 10.1038/nrd1821

(89) Rao, P. K. CCR5 inhibitors: Emerging promising HIV therapeutic strategy. *Indian J Sex Transm Dis AIDS* **2009**, *30* (1), 1-9. DOI: 10.4103/0253-7184.55471

(90) Cabello-Sanchez, N.; Jean, L.; Maddaluno, J.; Lasne, M. C.; Rouden, J. Palladium-mediated *N*-arylation of heterocyclic diamines: insights into the origin of an unusual chemoselectivity. *J Org Chem* **2007**, *72* (6), 2030-2039. DOI: 10.1021/jo062301i

(91) Jean, L.; Rouden, J.; Maddaluno, J.; Lasne, M. C. Palladium-mediated arylation of 3-aminopiperidines and 3-aminopyrrolidines. *J Org Chem* **2004**, *69* (25), 8893-8902. DOI: 10.1021/jo0487193

(92) Nakhla, J. S.; Schultz, D. M.; Wolfe, J. P. Palladium-catalyzed alkene carboamination reactions for the synthesis of substituted piperazines. *Tetrahedron* **2009**, *65* (33), 6549-6570. DOI: 10.1016/j.tet.2009.04.017

(93) Sharma, K. K.; Sharma, S.; Kudwal, A.; Jain, R. Room temperature *N*-arylation of amino acids and peptides using copper(I) and beta-diketone. *Org Biomol Chem* **2015**, *13* (16), 4637-4641, 10.1039/C5OB00288E. DOI: 10.1039/c5ob00288e

(94) Nakhla, J. S.; Wolfe, J. P. A concise asymmetric synthesis of cis-2,6-disubstituted *N*-aryl piperazines via Pd-catalyzed carboamination reactions. *Org Lett* **2007**, *9* (17), 3279-3282. DOI: 10.1021/ol071241f

(95) Parker, K. A.; Coburn, C. A. Regioselectivity in intramolecular nucleophilic aromatic substitution. Synthesis of the potent anti HIV-I 8-halo TIBO analogs. *The Journal of Organic Chemistry* **2002**, *57* (1), 97-100. DOI: 10.1021/jo00027a019.

(96) Kondaparla, S.; Soni, A.; Manhas, A.; Srivastava, K.; Puri, S. K.; Katti, S. B. Synthesis and antimalarial activity of new 4-aminoquinolines active against drug resistant strains. *RSC Advances* **2016**, *6* (107), 105676-105689, 10.1039/C6RA14016E. DOI: 10.1039/C6RA14016E.

(97) Shen, P.-X.; Hu, L.; Shao, Q.; Hong, K.; Yu, J.-Q. Pd(II)-Catalyzed Enantioselective C(sp3)–H Arylation of Free Carboxylic Acids. *Journal of the American Chemical Society* **2018**, *140* (21), 6545-6549. DOI: 10.1021/jacs.8b03509.

(98) Vicker, N.; Burgess, L.; Chuckowree, I. S.; Dodd, R.; Folkes, A. J.; Hardick, D. J.; Hancox, T. C.; Miller, W.; Milton, J.; Sohal, S.; et al. Novel angular benzophenazines: dual topoisomerase I and topoisomerase II inhibitors as potential anticancer agents. *J Med Chem* **2002**, *45* (3), 721-739. DOI: 10.1021/jm010329a

(99) Wixey, J. S.; Ward, B. D. Chiral calcium catalysts for asymmetric hydroamination/cyclisation. *Chem Commun (Camb)* **2011**, *47* (19), 5449-5451, 10.1039/C1CC11229E. DOI: 10.1039/c1cc11229e

(100) Coldham, I.; O'Brien, P.; Patel, J. J.; Raimbault, S.; Sanderson, A. J.; Stead, D.; Whittaker, D. T. E. Asymmetric deprotonation of *N*-Boc-piperidines. *Tetrahedron: Asymmetry* **2007**, *18* (17), 2113-2119. DOI: 10.1016/j.tetasy.2007.09.001.

(101) Darensbourg, D. J.; Karroonnirun, O. Ring-opening polymerization of lactides catalyzed by natural amino-acid based zinc catalysts. *Inorg Chem* **2010**, *49* (5), 2360-2371. DOI: 10.1021/ic902271x

(102) Katritzky, A. R.; He, H.-Y.; Verma, A. K. Stereoselective syntheses of chiral (3S,9bS)-1,2,3,9b-tetrahydro-5H-imidazo[2,1-a]isoindol-5-ones. *Tetrahedron: Asymmetry* **2002**, *13* (9), 933-938. DOI: 10.1016/s0957-4166(02)00220-3.

(103) Chen, F. M. F.; Benoiton, N. L. The preparation and reactions of mixed anhydrides of *N*-alkoxycarbonylamino acids. *Canadian Journal of Chemistry* **1987**, *65* (3), 619-625. DOI: 10.1139/v87-106.

(104) S Yadav, J.; Reddy, B. V. S.; Rao, K. V.; Raj, K. S.; Prasad, A. R. Indium Tribromide Catalyzed Aminolysis of Aziridines: An Efficient Synthesis of vicinal-diamines. *Synthesis* **2002**, *2002* (08), 1061-1064.

(105) Peruncheralathan, S.; Henze, M.; Schneider, C. Scandium Triflate Catalyzed Aminolysis of meso-Aziridines. *Synlett* **2007**, *2007* (14), 2289-2291.

(106) Uraguchi, D.; Kinoshita, N.; Kizu, T.; Ooi, T. Synergistic Catalysis of Ionic Bronsted Acid and Photosensitizer for a Redox Neutral Asymmetric alpha-Coupling of *N*-Arylaminomethanes with Aldimines. *J Am Chem Soc* **2015**, *137* (43), 13768-13771. DOI: 10.1021/jacs.5b09329

(107) Cardona, F.; Goti, A. Metal-catalysed 1,2-diamination reactions. *Nat Chem* **2009**, *1* (4), 269-275. DOI: 10.1038/nchem.256

(108) Gan, X.-C.; Zhang, C.-Y.; Zhong, F.; Tian, P.; Yin, L. Synthesis of chiral anti-1,2-diamine derivatives through copper(I)-catalyzed asymmetric α-addition of ketimines to aldimines. *Nature Communications* **2020**, *11* (1), 4473. DOI: 10.1038/s41467-020-18235-9.

(109) Lee, S.; Jang, Y. J.; Phipps, E. J. T.; Lei, H.; Rovis, T. Rhodium(III)-Catalyzed Three-Component 1,2-Diamination of Unactivated Terminal Alkenes. *Synlett* **2021**, (Editorial Board), 1247-1252.

(110) Olson, D. E.; Su, J. Y.; Roberts, D. A.; Du Bois, J. Vicinal Diamination of Alkenes under Rh-Catalysis. *Journal of the American Chemical Society* **2014**, *136* (39), 13506-13509. DOI: 10.1021/ja506532h.

(111) Wang, C.; Liu, B.; Shao, Z.; Zhou, J.; Shao, A.; Zou, L. H.; Wen, J. Synthesis of 1,2-Diamines from Vinyl Sulfonium Salts and Arylamines. *Org Lett* **2022**, *24* (35), 6455-6459. DOI: 10.1021/acs.orglett.2c02604

(112) Lee, B. J.; Ickes, A. R.; Gupta, A. K.; Ensign, S. C.; Ho, T. D.; Tarasewicz, A.; Vanable, E. P.; Kortman, G. D.; Hull, K. L. Synthesis of Unsymmetrical Vicinal Diamines via Directed Hydroamination. *Organic Letters* **2022**, *24* (30), 5513-5518. DOI: 10.1021/acs.orglett.2c01911.

(113) Feng, X.; Wang, L.; Tan, C.; Liu, X. Aza-Henry Reaction of Ketoimines

Catalyzed by Na2CO3: An Efficient Way to β-Nitroamines. *Synlett* **2008**, *2008* (13), 2075-2077. DOI: 10.1055/s-2008-1077952.

(114) Kurti, L.; Czakó, B. *Strategic applications of named reactions in organic synthesis*; Elsevier, 2005.

(115) Surendra, K.; Krishnaveni, N. S.; Mahesh, A.; Rao, K. R. Supramolecular catalysis of Strecker reaction in water under neutral conditions in the presence of beta-cyclodextrin. *J Org Chem* **2006**, *71* (6), 2532-2534. DOI: 10.1021/jo052510n

(116) Izquierdo, C.; Esteban, F.; Ruano, J. L. G.; Fraile, A.; Alemán, J. Asymmetric Synthesis of 1,2-Diamines bearing Tetrasubstituted Centers from Nonstabilized Azomethine Ylides and *N*-

Sulfinylketimines under Brønsted Acid Catalysis. *Organic Letters* **2016**, *18* (1), 92-95. DOI: 10.1021/acs.orglett.5b03251.

(117) Beugelmans, R.; Benadjila-Iguertsira, L.; Chastanet, J.; Negron, G.; Roussi, G. Deprotonation de *N*-oxydes d'amines aliphatiques: schéma réactionnel général et nouvelle synthèse de pyrrolidines. *Canadian Journal of Chemistry* **1985**, *63* (3), 725-734. DOI: 10.1139/v85-120 (acccessed 2020/04/07).

(118) Roussi, G.; Beugelmans, R.; Chastanet, J.; Roussi, G. The [3+2] Cycloaddition Reaction of Nonstabilized Azomethine Ylide Generated from Trimetylmine *N*-Oxide to C=C, C=N, and C=S Bonds. *Heterocycles* **1987**, *26* (12), 3197-3202, Journal. DOI: 10.3987/r-1987-12-3197.

(119) Beugelmans, R.; Negron, G.; Roussi, G. Trimethylamine *N*-oxide as a precursor of azomethine ylides. *Journal of the Chemical Society, Chemical Communications* **1983**, (1), 31-32, 10.1039/C39830000031. DOI: 10.1039/c39830000031.

(120) Chastanet, J.; Roussi, G. Study of the regiochemistry and stereochemistry of the [3 + 2] cycloaddition between nonstabilized azomethine ylides generated from tertiary amine *N*-oxides and various dipolarophiles. *The Journal of Organic Chemistry* **1988**, *53* (16), 3808-3812. DOI: 10.1021/jo00251a026.

(121) Chastanet, J.; Roussi, G. *N*-Methylpiperidine *N*-oxide as a source of nonstabilized ylide: a new and efficient route to octahydroindolizine derivatives. *The Journal of Organic Chemistry* **1985**, *50* (16), 2910-2914. DOI: 10.1021/jo00216a020.

(122) Roussi, G.; Zhang, J. A 3+2 cycloaddition route to N-H pyrrolidines devoid of electron-withdrawing groups. *Tetrahedron Letters* **1988**, *29* (28), 3481-3482. DOI: https://doi.org/10.1016/0040-4039(88)85195-5.

(123) Roussi, G.; Zhang, J. The use of the β-amino-alcohol-n-oxide derivatives in the synthesis of 2,3 or 4-alkyl substituted nh pyrrolidines. *Tetrahedron* **1991**, *47* (28), 5161-5172. DOI: https://doi.org/10.1016/S0040-4020(01)87128-3.

(124) Gennari, C.; Vulpetti, A.; Pain, G. Highly enantio- and diastereoselective boron aldol reactions of α-heterosubstituted thioacetates with aldehydes and silyl imines. *Tetrahedron* **1997**, *53* (16), 5909-5924. DOI: https://doi.org/10.1016/S0040-4020(97)00251-2.

(125) Honda, T.; Mori, M. An Aza-Brook Rearrangement of (α-Silylallyl)amine. *The Journal of Organic Chemistry* **1996**, *61* (4), 1196-1197. DOI: 10.1021/jo952116x.

(126) Cottrell, T. L. *The strengths of chemical bonds*; Butterworths Scientific Publications, 1958.

(127) Kerr, J. A. Bond Dissociation Energies by Kinetic Methods. *Chemical Reviews* **1966**, *66* (5), 465-500. DOI: 10.1021/cr60243a001.

(128) Chaussoy, N.; Brandt, D.; Gérard, J.-F. Versatile Method To Reduce the Free Formaldehyde Content in Phenolic Resins for High-Temperature Applications. *ACS Applied Polymer Materials* **2022**, *4* (6), 4454-4463. DOI: 10.1021/acsapm.2c00148.

(129) Neal, M. J.; Hejnosz, S. L.; Rohde, J. J.; Evanseck, J. D.; Montgomery, T. D. Multi-Ion Bridged Pathway of *N*-Oxides to 1,3-Dipole Dilithium Oxide Complexes. *The Journal of Organic Chemistry* **2021**, *86* (17), 11502-11518. DOI: 10.1021/acs.joc.1c01047.

(130) Fraser, R. R.; Mansour, T. S.; Savard, S. Acidity measurements on pyridines in tetrahydrofuran using lithiated silylamines. *The Journal of Organic Chemistry* **1985**, *50* (17), 3232-3234. DOI: 10.1021/jo00217a050.

(131) Collum, D. B.; McNeil, A. J.; Ramirez, A. Lithium diisopropylamide: solution kinetics and implications for organic synthesis. *Angew Chem Int Ed Engl* **2007**, *46* (17), 3002-3017. DOI: 10.1002/anie.200603038

(132) Algera, R. F.; Gupta, L.; Hoepker, A. C.; Liang, J.; Ma, Y.; Singh, K. J.; Collum, D. B. Lithium Diisopropylamide: Nonequilibrium Kinetics and Lessons Learned about Rate Limitation. *J Org Chem* **2017**, *82* (9), 4513-4532. DOI: 10.1021/acs.joc.6b03083

(133) Mack, K. A.; Collum, D. B. Case for Lithium Tetramethylpiperidide-Mediated Ortholithiations: Reactivity and Mechanisms. *Journal of the American Chemical Society* **2018**, *140* (14), 4877-4883. DOI: 10.1021/jacs.8b00590.

(134) Tandel, S.; Wang, A.; Holdeman, T. C.; Zhang, H.; Biehl, E. R. The reaction of 2-chloro-4-nitrophenol and the isomeric chloronitrobenzenes with LDA under aryne-forming conditions. *Tetrahedron* **1998**, *54* (50), 15147-15154. DOI: 10.1016/s0040-4020(98)00971-5.

(135) Bao, L. L.; Liu, Z. Q. Tetrahydropyrrolization of Resveratrol and Other Stilbenes Improves Inhibitory Effects on DNA Oxidation. *ChemMedChem* **2016**, *11* (15), 1617-1625. DOI: 10.1002/cmdc.201600205

(136) Beak, P.; Brown, R. A. The tertiary amide as an effective director of ortho lithiation. *The Journal of Organic Chemistry* **1982**, *47* (1), 34-46. DOI: 10.1021/jo00340a008.

(137) Wang, A.; Biehl, E. Lithium diisopropylamide (LDA) reduction of nitroarenes. *Arkivoc* **2002**, *2002* (1), 71-75. DOI: 10.3998/ark.5550190.0003.111.

(138) Relative Acidity of alpha-Hydrogens https://chem.libretexts.org/@go/page/166396 (accessed Jul 6, 2023).

(139) Rainsford, K. D. Effects of Anti-inflammatory Drugs on Interleukin 1-induced Cartilage Proteoglycan Resorption In-vitro: Inhibition by Aurothiophosphines but no Influence from Perturbed Eicosanoid Metabolism. *Journal of Pharmacy and Pharmacology* **2011**, *41* (2), 112-117. DOI: 10.1111/j.2042-7158.1989.tb06404.x (acccessed 4/21/2023).

(140) Crane, L.; Anastassiadou, M.; El Hage, S.; Stigliani, J. L.; Baziard-Mouysset, G.; Payard, M.; Leger, J. M.; Bizot-Espiard, J. G.; Ktorza, A.; Caignard, D. H.; et al. Design and synthesis of novel imidazoline derivatives with potent antihyperglycemic activity in a rat model of type 2 diabetes. *Bioorg Med Chem* **2006**, *14* (22), 7419-7433. DOI: 10.1016/j.bmc.2006.07.026

(141) Kahlon, D. K.; Lansdell, T. A.; Fisk, J. S.; Tepe, J. J. Structural-activity relationship study of highly-functionalized imidazolines as potent inhibitors of nuclear transcription factor-kappaB mediated IL-6 production. *Bioorg Med Chem* **2009**, *17* (8), 3093-3103. DOI: 10.1016/j.bmc.2009.03.002 From NLM.

Chapter 2: Forming Imidazolidines Through [3+2] Cycloadditions of Trimethylamine *N*-Oxide and Imines

2.1 Introduction

2.1.1. Summary

Imidazolidines are a family of *N*-heterocycles which have captured the attention of researchers due to their applications for pharmaceutically relevant structures.[1,2] Typical synthetic methods to form this class of compounds include the condensation of 1,2-diamines with either aldehydes or ketones,[3-5] Lewis acid catalyzed aziridine ring openings with amine nucleophiles,[6,7] [3+2]-cycloadditions,[8-10] and multicomponent reactions.[11] Most of these methods are multistep and the synthetic precursors are not commercially available, requiring significant time and energy. In contrast, the base mediated [3+2]-cycloaddition of TMAO and benzylideneaniline established by Roussi and coworkers is a one-step transformation from base starting materials. This method has been underused with only one imidazolidine produced in the substrate scope.[12] Herein we have greatly expanded this highly efficient one-step transformation from commercially available precursors forming substituted imidazolidines.

2.1.2 Imidazolidines and Their Pharmacological Activities

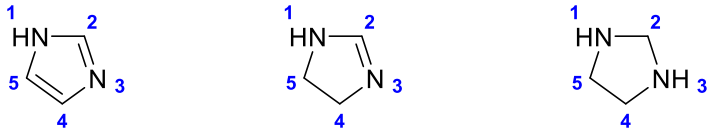

119 *Imidazole* **120** *Imidazoline* **121** *Imidazolidine*

Figure 7. Structures and numberings of imidazole, imidazoline and imidazolidine cores

Imidazolidines are privileged scaffolds, a term used by the pharmaceutical industry to describe motifs which typically display potent biological activity, that have been effective at treating a range of diseases.[13-16] In 2014, imidazoles, imidazolines, and imidazolidines were all within the top 25

most frequently occurring nitrogen containing heterocycles in FDA approved drugs (Figure 7).[16] The synthesis of these structures, and the examination of their bioactivities to be used as potential pharmaceuticals, is a prevalent area of synthetic and medicinal research due to the broad range of pharmacological activities these three related cores possess.

2.1.2.1.Anti-Inflamatories

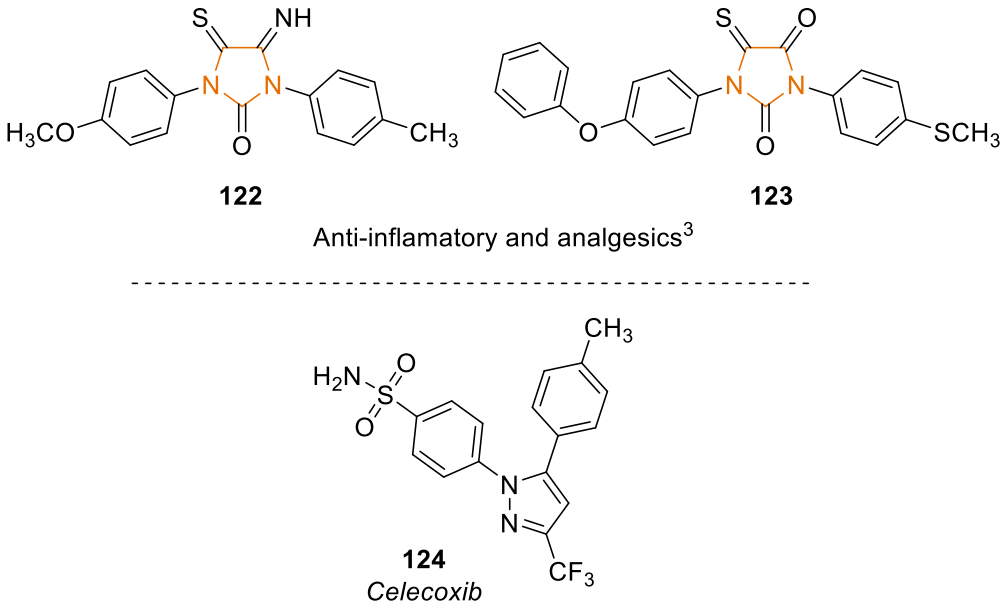

Figure 8. Structures of potential anti-inflammatory agents compared to Celecoxib[17]

Hassan and coworkers took an experimental and theoretical approach when investigating a series of 5-imino-4-thioxo-2-imidazolidinone derivatives (Figure 8) for their anti-inflammatory properties.[17] Eighteen derivatives of this class of compounds were synthesized and subjected to an *in vitro* cyclooxygenase (Cox) enzyme assay.[17] All of but one of their synthesized derivatives exhibited more potent COX-2 inhibition than that of the reference drug, celecoxib; compound **122** (Figure 8) demonstrated the strongest response with an $IC_{50} = 2.00 \times 10^{-6}\mu M$ for COX-2, which is four orders of magnitude more potent than celecoxib (**124**) ($IC_{50} = 4.0 \times 10^{-2}\mu M$).[17] It is anticipated that these scaffolds will be further investigated as drug candidates since all of the synthesized

compounds exhibited significantly higher activities than the reference drug, therefore a facile synthetic method with rapid access to this scaffold is ideal.

2.1.2.2. Antidiabetics

Baziard-Mouysset and coworkers synthesized and examined the antihyperglycemic activities of 36 different imidazoline derivatives.[18] They found that nine of their derivatives expressed good antidiabetic properties in normal and streptozotocin induced diabetic rats without any hypoglycemic affects, with imidazoline **125** demonstrating the most potent antihyperglycemic activity.[18] The imidazoline **7** was then replaced by benzimidazole **126**, tetrahydropyrimidine **127**, oxazoline **128**, thiazoline **129**, tetrazole **130**, amidine **131** for a structure-activity relationship study (Figure 9).[18] All of these replacements resulted in a total loss of activity thus demonstrating the necessity of the imidazoline moiety.[18]

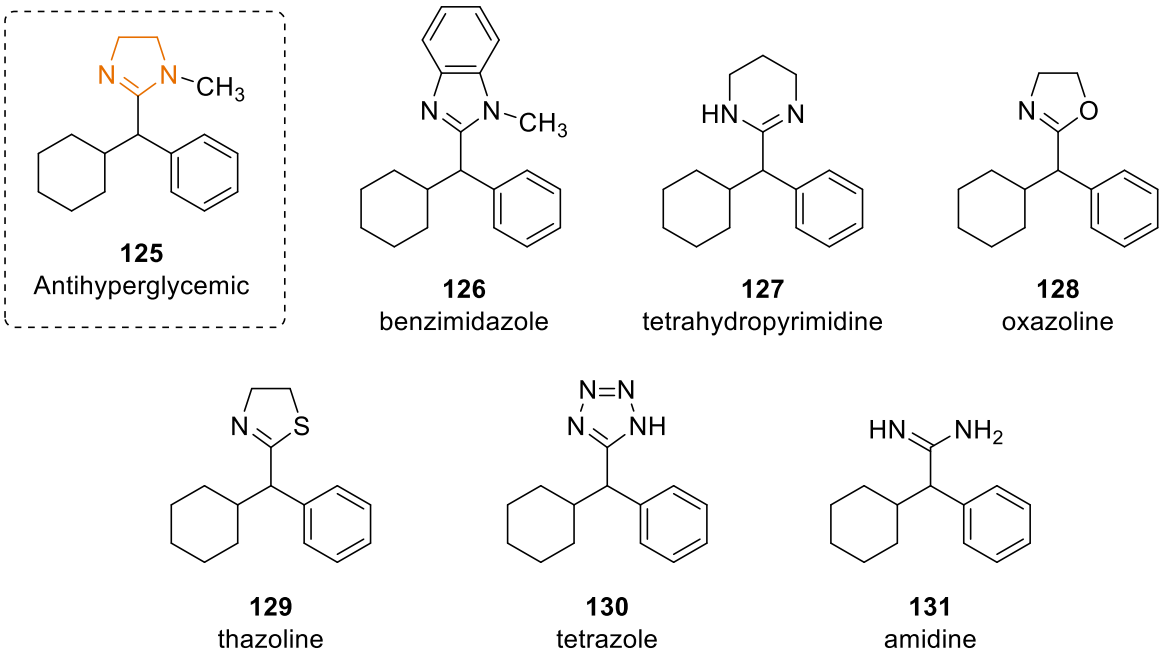

Figure 9. SAR study by Baziard-Mouysset and coworkers developing antidiabetic imidazolidine 125[18]

2.1.2.3. Anti-infective Agents

Schistosomiasis is the second most significant parasitic disease in the world effecting around 200 million people in 74 different countries.[19] This disease is caused by contact with water infected by the parasitic larvae, which once in the body, effect the liver, bladder, and urinary tract, and it is responsible for as high as 200,000 deaths per year.[19] As of now there is only one approved drug (praziquantel **133**) for the treatment of this disease, and unfortunately there have been increasing reports of parasitic resistance to it.[20,21] To combat this issue, Matos-Rocha and coworkers developed imidazolidine 130 and similar structures and analyzed their activities particularly against the parasites responsible for this disease (Figure 10).[20] Imidazolidine **132** showed good schistosomicidal activity *in vivo*, while not showing any cytotoxicity against white blood cells.[20] The promising results of this study demonstrate that this class of compounds have the potential to remedy this drug resistance thus improving the quality of life for the millions of people threatened by this illness.[20]

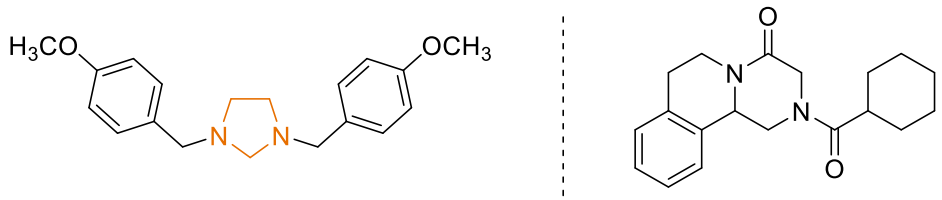

132
Anti-infective[1]

133
Praziquantel

Figure 10. Anti-infective agent with the corresponding reference drug praziquantel.

Leishmaniasis is another parasitic disease that effects an estimated 12 million people worldwide and poses high morbidity and mortality levels.[22] This disease is most prevalent in tropical and subtropical areas with 350 million people living in endemic areas.[22] Drugs such as Pentostam **134** (Figure 11), and Glucantime are used in the treatment of this disease, but they require lengthy treatments, and as a result, these treatments are being met with drug resistance.[4] Additionally, these

drugs inadvertently cause more problems due to their high toxicity resulting in many adverse side-effects, and consequently, many patients decide to refuse treatment.[22]

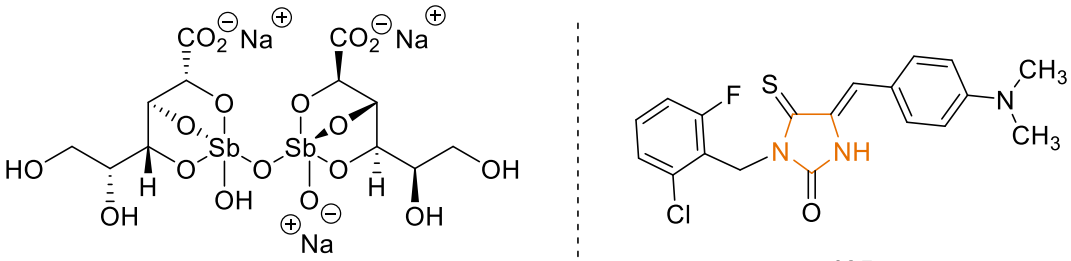

134
Pentostam

135
Antiparasitic[2]

Figure 11. Structures of reference anti-infective agent Pentostam and proposed new drug candidate by Da Silva and coworkers.[4]

To overcome this challenge, Da Silva and coworkers investigated imidazolidine derivatives and their cytotoxicity and anti-infective properties as potential treatments for leishmaniasis.[4] None of the nine compounds synthesized were cytotoxic to mammalian cells, and five of them showed good activity against *Leshmania*.[4] Imidazolidine **135** (Figure 11) demonstrated the best anti-infective activity on intracellular amastigotes, with an IC_{50} = 9.4 μg/mL.[4] Due to the promising biological properties of this scaffold, more drug candidates of the imidazolidine variety could prove beneficial for more effective treatments of this disease.

2.1.2.4. Antidepressants

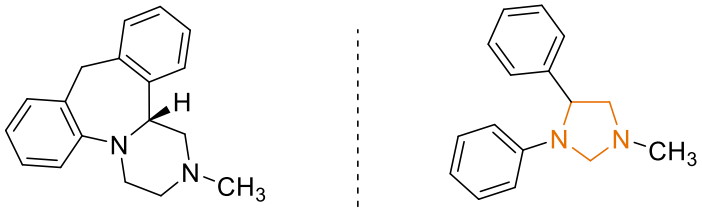

136
Mianserin

137
Antidepressant[5]

Figure 12. Structure of Mianserin and its analogue[23]

An SAR study on the tetracyclic antidepressant mianserin **136** and its analogues was conducted by Wieringa and coworkers to better connect structural properties and presynaptic α-blocking activity.[23] They determined that structures with a slightly bent geometry, such as six-membered fused rings, were better presynaptic α-blockers than flat-rigid or flexible compounds.[23] Among the analogues tested was imidazolidine **137**. Imidazolidine **137** demonstrates that even simple molecules are capable of having bioactive properties.[23]

2.1.2.5. Antibiotics

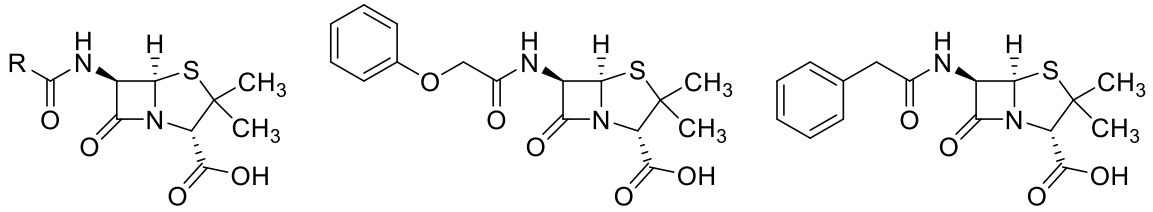

Figure 13. Structures of the penicillin family of antibiotics with commonly prescribed penicillin V and penicillin G.

It has been theorized that antibiotics have been used to treat infections for centuries or longer with references to the topical application of moldy bread dating back to ancient Egypt, China, Serbia, Greece and Rome.[24] Moving forward to the 20th century, penicillin **138** was extracted from a type of mold and exhibited remarkable antibiotic properties effective against many different bacterial strains.[25] Thus penicillin became a widely used treatment for infections,[25] ushering in the "Golden Age" of antibiotic discovery.[24] During this time, a wealth of new antibiotic families, like penicillin (Figure 13), were discovered.[24] This was a defining moment for modern medicine with many of these new drug families being effective in combating a broad range of bacterial infections.[26] Unfortunately, the discovery of new antibiotics did not continue with the same momentum as their prescriptions, thus leading to widespread antibiotic resistance.[27-29] Only three new drug families

have been approved for human use in the 21st century, with the most recent one put on the market in 2005, nearly two decades ago.[30] Penicillin is still prescribed today, but due to the growing resistance to these old antibiotic families, researchers have been actively seeking new antibiotic drug targets to address this issue.[30]

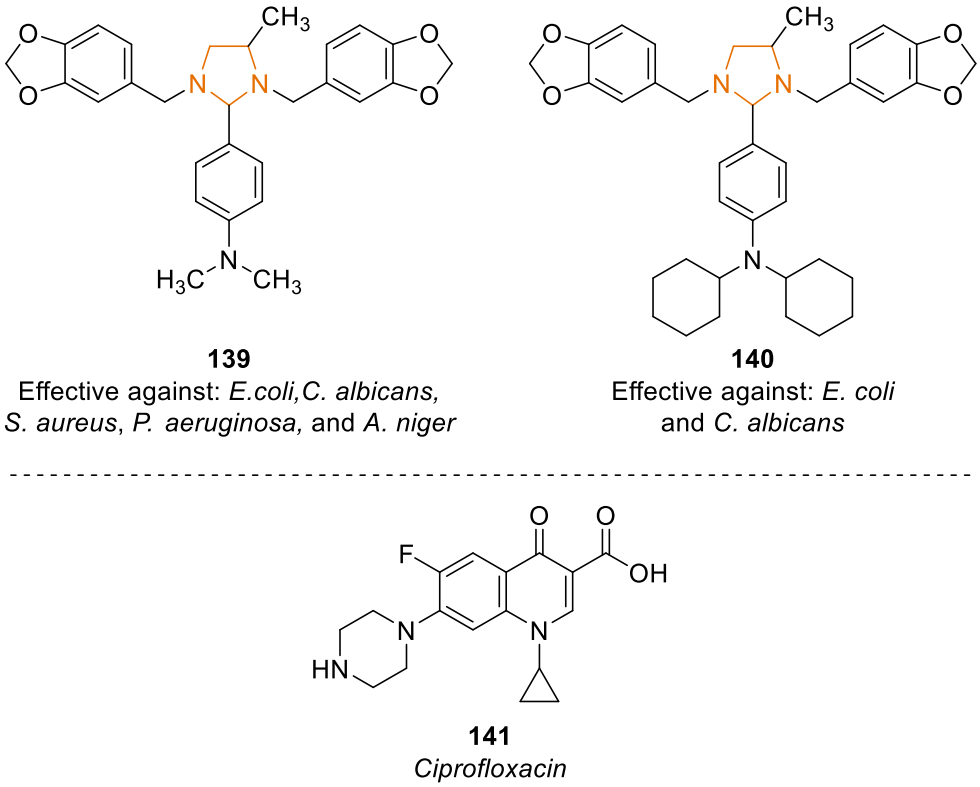

Figure 14. Antimicrobial agents developed by Husain and coworkers compared to the reference drug.[31]

A microbiological evaluation of 4-substituted-imidazoline derivatives was accomplished by Husain and coworkers.[31] All of the compounds exhibited at least moderate antimicrobical activities with imidazoline **139** being the lead compound (Figure 14).[31] Imidazoline **139** demonstrated good activity against *E. coli* and *C. albicans*, as well as *S. aureus*, and *P. aeruginosa*.[31] The efficacy of antibiotics are typically reported as the minimum inhibitory concentration (MIC) value, meaning the lowest concentration of an antibiotic at which bacterial growth is completely inhibited.[32] The

imidazolidines were compared against reference drug, ciprofloxacin **141** with MIC of 6.25 µg/mL (Figure 14).[31] Imidazolidine **139** exhibited a MIC of 12.5 µg/ml, and significant activity against *S. aureus, P. aeruginosa* and *A. niger* with MIC of 25 µg/ml.[31] These results demonstrate the utility of this compound as well as other synthetic derivatives as multipurpose antimicrobial agents to combat antibiotic resistance.

2.1.2.6 Anticancer

An SAR study carried out by Handzlik and coworkers screened a series of imidazolidinone derivatives as anticancer agents.[33] They synthesized a library of compounds with various substitutions around the ring in order to find a trend for what functionalities are beneficial for the action on the cancer ABCB1-efflux pump and vice versa in order to determine what moieties at which position deserve more synthetic attention.[33] ABCB1 is a part of the ABC family of ATP-dependent drug effluxers.[34-36] This effluxer promotes chemoresistance by actively expelling a broad range of substrates from tumor cells, including chemotherapeutic agents. This results in lower intracellular concentrations of the cytotoxic agents, with the end result being multidrug resistance.[37] Inhibition of this efflux pump is crucial to combat this issue, but so far drug targets focusing on this inhibition have failed due to low specificity, unsurprising given the ubiquitous nature of efflux pumps, and end up damaging healthy tissue to an unacceptable degree.[38]

Gratifyingly, imidazolinone **142** was more potent in ABCB1 efflux pump inhibition than verapamil, a commonly used anticancer drug; with imidazolidine **142** exhibiting 146% of the activity determined for verapamil **143**.[33] It also expressed lower cytotoxicity than doxorubicin **144**, a widely used chemotherapeutic, with 84 % HEK-293 cell viability.[33] Additionally, this study investigated the relationship between ABCB1 inhibition and the structure of the inhibitor via molecular docking of the drug candidates with a human Pgp (permeability-glycoprotein)

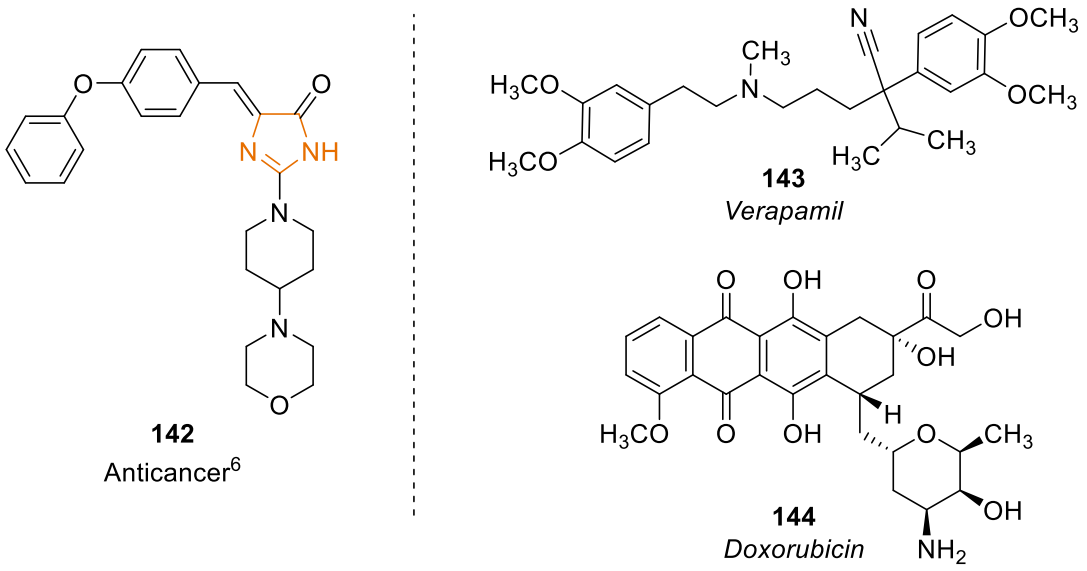

Figure 15. Imidazolidine anticancer agent developed by Handzlik and coworkers with reference drugs verapamil and doxorubicin

homology model.[33] Their study was able to display some trends in the position and functionalities of the substituents around the imidazolidine ring, and as a result a few potential drug candidates were discovered including imidazolinone **142**, exemplifying the importance of this class of compounds in cancer research.

2.1.2.7 Bioactivity Summary

The ubiquity of imidazolidines and derivatives in drug research is undeniable, and because of this, there is a consistently high demand for new methods forming this essential structural motif. Synthetic methods for generating imidazolidines have been around for over a century, however there is always a need for new ways to form these structures efficiently with even more diverse functionalities.

2.1.3 Synthetic Methods Forming 1,2-Diamines

2.1.3.1 Condensation of aldehydes and 1,2-Diamines

A reliable method of forming substituted imidazolidines through the condensation of 1,2-diamines and aldehydes has been around since the 1880s.[39] This is old chemistry indeed, but it is highly reliable and it has been further developed since then.[3,4,39,40] The synthetic and biological study previously mentioned by da Silva applied this chemistry to form their imidazolidine substrates **150** (Scheme 28).[4] The imidazolidines were produced in good yields over three-steps by starting with the condensation of vicinal diamine **146** and aldehyde **145** to form the diimine intermediate **147**. The diimine **147** then undergoes a mild reduction to form substituted diamine **148**, which is then cyclized by sequential nucleophilic attacks of the diamine into the carbonyl of aldehyde **149**, kicking off water and forming the desired imidazolidines **150**.

Scheme 29. Condensation of Aldehydes and 1,2-Diamines forming Symmetrical Imidazolidines[4]

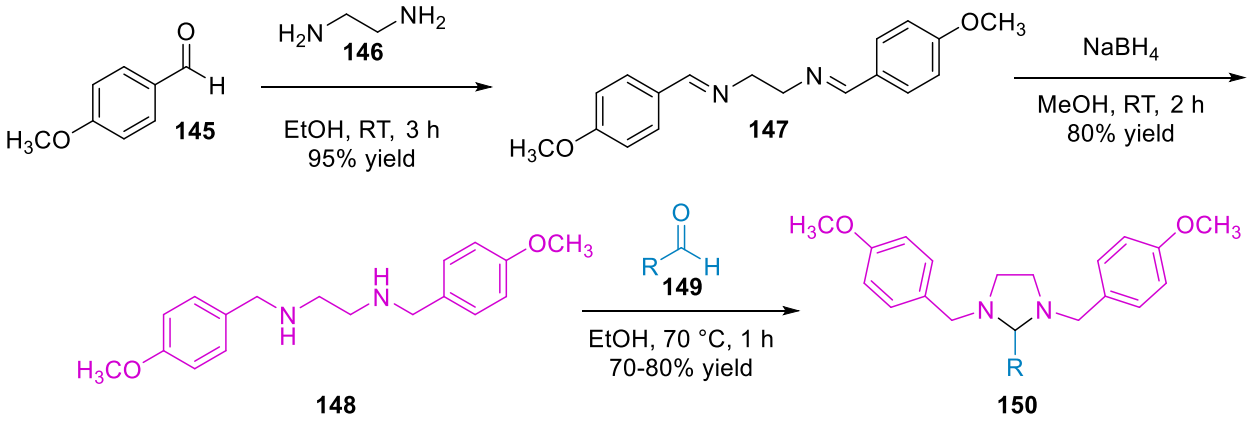

In a similar vein, Husain and coworkers used this chemistry as well to form various imidazolidines for their SAR study that was also mentioned in the previous section (Figure 14).[31] These are just a couple of modern-day examples and this is not an exhaustive list, but it does highlight that this

chemistry is still highly relevant particularly in the medicinal chemistry field due to its simplicity and effectiveness.

These facile condensation reactions are still being further developed and refined to broaden the substrate scopes. These examples are limited to symmetrical imidazolidines like **150** where the aldehyde is used to install a new functional group on the amine through the condensation reaction. Moreover this symmetry is echoed in the carbon backbone which lacks any distinctive functionality.

To overcome this limitation, Katritzky and workers developed a remarkable multicomponent condensation of aldehydes forming unsymmetrical imidazoldines **154** in good yields ranging from 85-95% (Scheme 29).[5] They went on to further capitalize on the unsymmetrical nature of these imidazolidines by selectively functionalizing them.[5] Moreover this method is highly efficient with good atom economy and mild reaction conditions aligning well with the principles of green chemistry.[41] The remaining limitation of this method, however though is the static carbon backbone limiting the structural diversity possible with these synthetic building blocks.

Scheme 30. Multicomponent Condensation Reaction Forming Asymmetrical Imidazolidines[5]

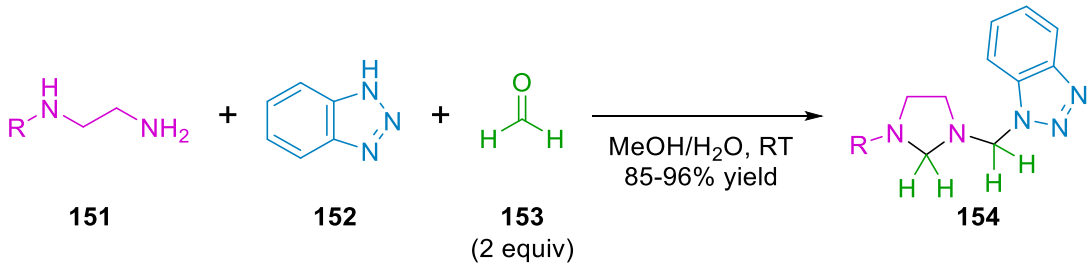

151 **152** **153** (2 equiv) **154**

2.1.3.2 Reactions with 1,3,5-Triazines

Liu and coworkers used reactions of 1,3,5-triazines **156** with aziridines **155** to form imidazolidines **157** in the presence of a zinc Lewis acid (Scheme 30). The reaction mechanism proceeds through a Lewis-acid mediated decomposition of triazine **155** into three equivalents of aryl imine, which

can react with the ring-opened aziridine. A variety of aryl amines **155** were tolerated with electron deficient anilines resulting in higher yields (82-92%), while electron rich and neutral anilines formed in lower yields (59-80%). They implemented one alkyl amine resulting in a 60% yield, so this is not strictly limited to aryl substituents. The 1,3,5-triazines **155** were readily synthesized from the condensation of paraformaldehyde and various anilines,[42] however, multiple steps are required to form the desired aziridines **156**.

Scheme 31. Reactions of 1,3,5-triazines with aziridines[6]

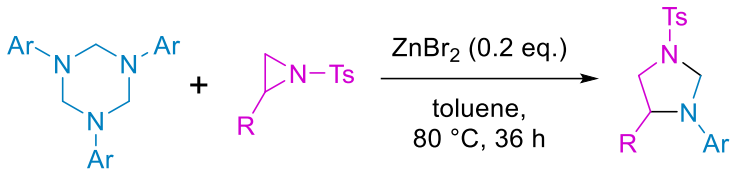

155 **156** **157**

Similar to Liu and coworkers, Sun and coworkers used 1,3,5-triazines **158** but instead of using aziridines, they expanded the scope and used tosylhydrazones **159** (Scheme 31). Since this method forms the aziridine *in situ*, there is no need for a Lewis acid to assist in ring opening, allowing this transformation to be purely base mediated. They observed yields ranging from 32-81% with electron rich substituents resulting in better yields. They observe the formation of two side products which explains why they only obtained moderate yields at best. Additionally, triazines **158** and tosylhydroazones **159** had to be prepared in-house.

Scheme 32. Reactions of 1,3,5-triazines and tosylhydrazones.[43]

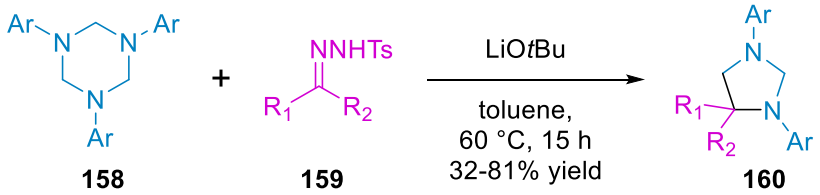

158 **159** **160**

2.1.3.3 [3+2]-Cycloadditions of Azomethine Ylides with Dipolarophiles

[3+2]-Cycloadditions of azomethine ylides with dipolarophiles are one of the most convenient methods used to access enantioenriched nitrogen containing heterocycles.[11,44-46] The application of imines as dipolarophiles in particular is still in development with limited progress thus far.[12] For clarity, this section will be broken up into different types of [3+2]-cycloadditions: metal catalyzed, acid catalyzed, and base promoted.

Metal Catalyzed [3+2] Cycloadditions

In 2018 Zhang and coworkers reported a rhodium catalyzed [3+2] cycloaddition of vinyl aziridines **161** with a range of alkyl and aryl oximes **162** under mild reaction conditions (Scheme 32).[8] This method is robust, achieving substituted imidazolidines **163** in yields ranging from 65-99%. While they report good enantioselectivity (83-99% ee), they have limited diastereoselectivity ranging from 4:1 to >20:1 dr.[8] Additionally, this synthetic route requires multiple steps to form the substrates as only the catalyst and cocatalyst are commercially avaiable.[47] Moreover, this method also requires the use of a rare-earth metal catalyst, which researchers have been devoting an enormous amount of time and resources to reduce the use of these, and to move onto common metals catalysts which are more sustainable.[48,49] While this transformation is effective, there have been improvements made in more recent years.

Scheme 33. Rhodium Catalyzed [3+2]-Cycloaddition of Vinyl Aziridines with Oximes[8]

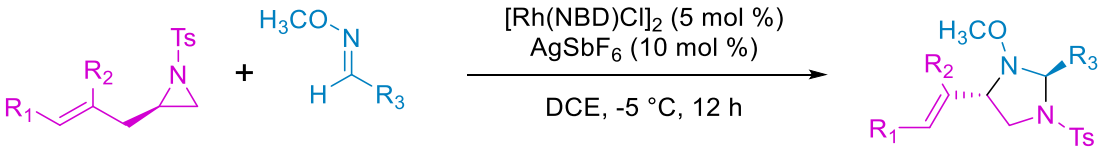

161 **162** **163**

A tandem [3+2]-cycloaddition/1,4-addition between aza-*o*-quinone precursors **164** and α-iminoesters **165** was reported by Gou and workers in 2017 (Scheme 33). The azomethine ylide is generated by deprotonation of the α-protons of the α-iminoesters **165** by KOH resulting in the

catalytically active metalloazomethine ylide.[10] They formed imidazolidines **167** in yields ranging from 28-90%, with enantioselectivities from 62-99% ee.[10] Electron deficient α-iminoesters **165** and aza-*o*-quinone precursors **164** resulted in higher yields and stereoselectivities whereas electronically neutral and donating substituents resulted in lower yields and selectivities.[10] This method still requires an expensive rhodium catalyst with a silver cocatalyst lowering its appeal for industrial use. Moreover, the synthetic precursors are not commercially available with the aza-*o*-quinone precursors along taking three steps and two purifications to make.

Scheme 34. Tandem [3+2]-Cycloaddition/1,4-Addition between α-Iminoesters and Aza-*o*-quinone Precursors[10]

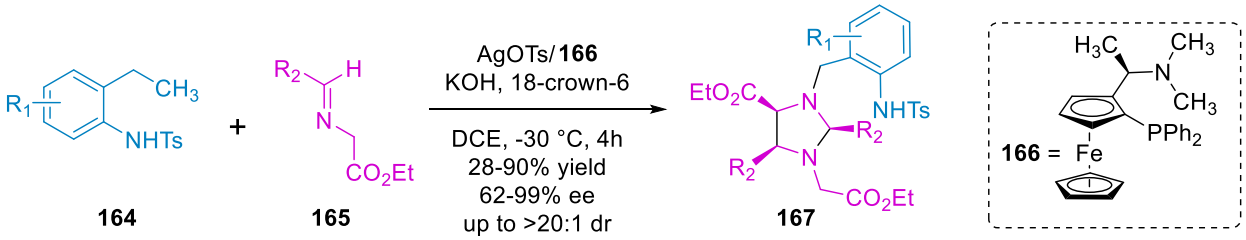

Scheme 35. Nickel Catalyzed [3+2]-Cycloaddition of Electron Deficient Aziridines and Aryl Amines[7]

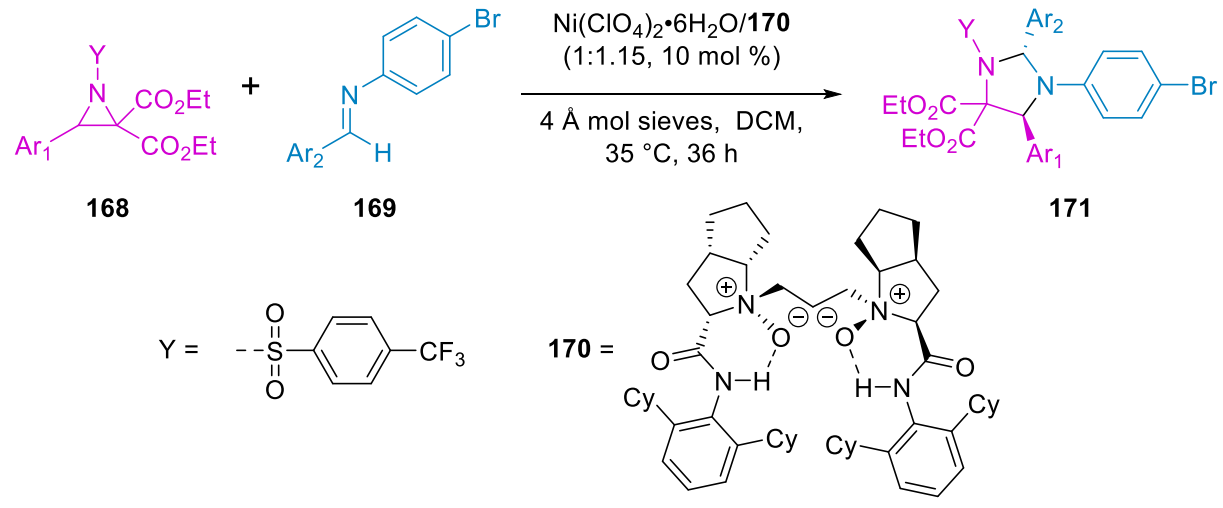

Just this year, Feng and coworkers reported a nickel catalyzed [3+2] cycloaddition of electron deficient aziridines **168** and aryl amines **169** (Scheme 34).[7] They were able to achieve imidazolidines **170** in yields ranging from 65-99% with reasonable stereocontrol (70-98% ee). An improvement from Zhang and coworkers is that a nickel catalyst is used in place of a rare-earth metal catalyst. This transformation, however, is strictly limited to aryl substituents both for the amine and the aziridine.[7]

Scheme 36. Synthesis of aziridine and imine precursors.[7]

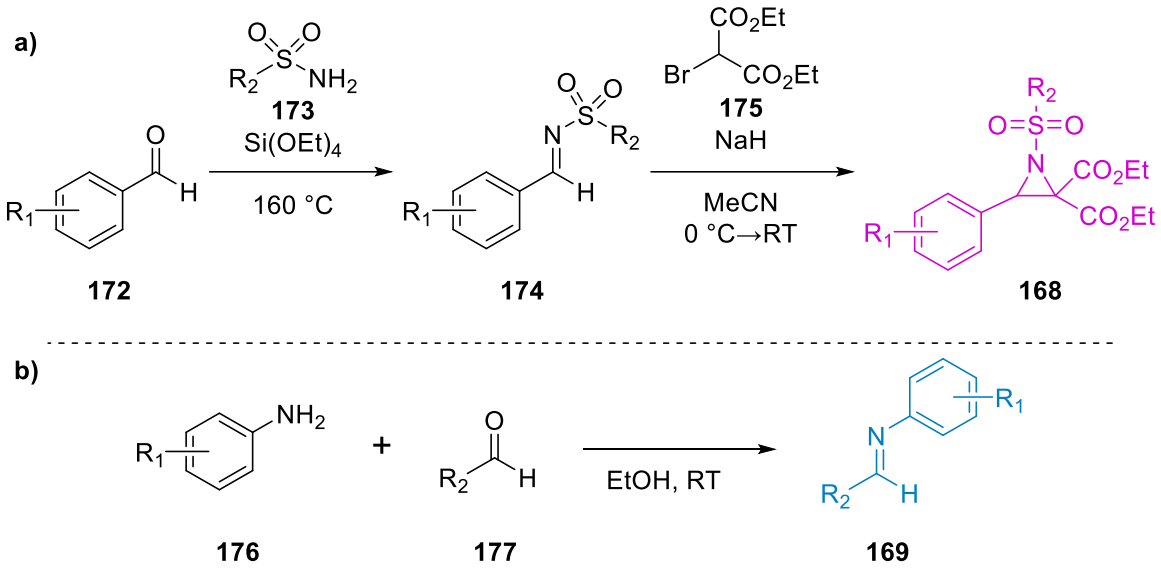

Moreover, the precursors as well as the required ligand are not commercially available. The aziridine **168** is formed in two steps from aldehydes **172**, while the imines **169** were produced in one step from the condensation of aldehydes **177** (Scheme 35).[7] The ligand **170** required for this transformation was prepared from Boc-protected proline in four steps, placing this transformation beyond the interest of most synthetic groups.[50]

Wang and coworkers reported a copper catalyzed [3+2]-cycloaddition between fluorinated imines **178** and azomethine ylides generated from α-iminoesters **177** (Scheme 36),[9] similar to Gou and coworkers. This reaction is tolerant to aryl and alkyl groups on the azomethine ylide generated

from **179** forming **181** with moderate yields (76-95%) and some stereo control.[9] They reported enantiomeric excess values from 89% to 98%, and diastereomeric ratios ranging from 10:1 to >20:1.[9] This method also employs a common metal copper catalyst, but it still requires additional steps to form the required synthetic precursors.[9] Moreover, this transformation is also strictly limited to electron-deficient imines.[9]

Scheme 37. Copper Catalyzed [3+2]-Cycloadditions between Fluorinated Imines and α-Iminoesters Esters[9]

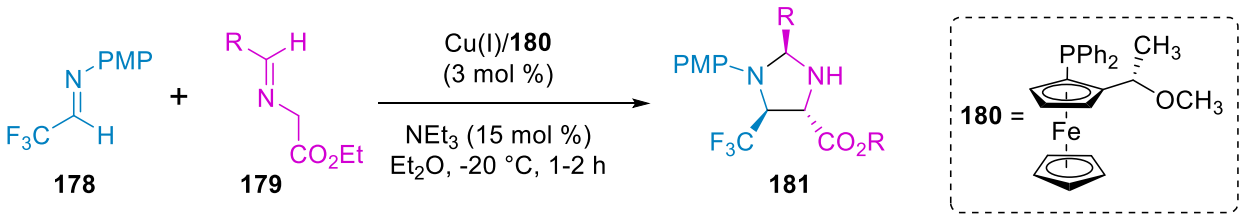

Acid Catalyzed [3+2] Cycloadditions

Multicomponent chiral Brönsted acid catalyzed [3+2]-cycloadditions were reported by Gong and coworkers, forming substituted imidazolidines **186** efficiently with yields ranging from 63-99% (Scheme 37a).[51] The azomethine ylides are formed *in situ* from aldehydes **184** and the amino-ester **182**.[51] Enantio- and diastereoselectivities were observed for anilines **183** bearing a nitro (91/9 dr, 98% ee), nitrile (90/10 dr, 98% ee), or methoxy group (91/9 dr, 98% ee) at the *para*-position.[51] This reaction is convenient with all reagents being commercially available, aside from the catalyst which is readily prepared in one step.[51]

Shi and coworkers further expanded the substrate scope using isatin-derived imines **187**, forming spiro[imidazolidine-2,3′-oxindole] frameworks **189** under similar reaction conditions (Scheme 37b).[52] This demonstrated one of only a few chemoselective examples of these transformations, as well as the first enantioselective formation of a spiro[imidazolidine-2,3′-oxindole] skeleton.[52] The

drawback to this methods is that it is cumbersome because the instatin-derived imines **187** and catalyst **185** are not commercially available, as is the case with many other methods.

Scheme 38. Chiral Bronsted Acid Catalyzed [3+2]-Cycloadditions

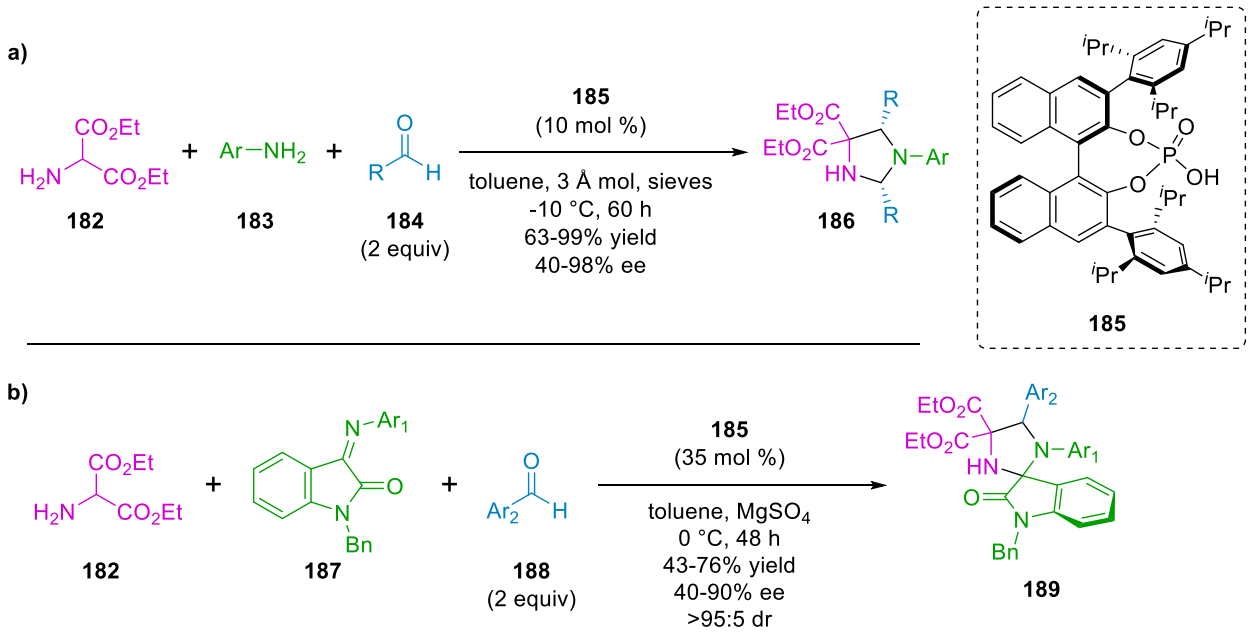

While there is a myriad of literature methods forming substituted imidazolidines with various levels of selectivity, most of these methods suffer from multiple steps, rely on the use of an expensive catalysts, or both. In this work, we were particularly interested in the method established by Roussi and coworkers in the 1980s. Their method is a one-step protocol making use of commercially available reagents to form imidazolidines, although they only reported one transformation of its kind. We thought that this transformation deserved more attention due to its simplicity and efficiency.

2.2 Results and Discussion

2.2.1 Replicating Roussi's Results

Before moving onto novel systems, the method established by Roussi and coworkers was investigated closely by carrying out their only reported [3+2] cycloaddition with an imine (Scheme

38). The reaction was modified from Roussi's original protocol as a reflection of results obtained from studying similar systems (Chapters 3-4). The modified protocol was a successful replication of the results reported in the literature producing imidazolidine **192** in a 72% yield (71% by Roussi and coworkers).[12] Given the utility and efficiency of this transformation from base starting materials, it was astounding that there has not been additional studies until now reported in the literature. We aimed to explore this chemistry deeper with the goal of expanding this method to potentially allow for rapid access of the imidazolidine scaffold which has become essential for drug development.

Scheme 39. [3+2] Cycloaddition of TMAO and Benzylideneaniline

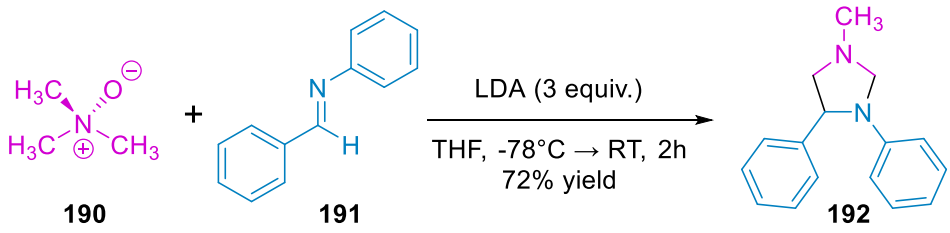

190 **191** **192**

2.2.2 Reaction of Trimethylamine *N*-oxide and Benzylidenebenzylamine

The work by Roussi and coworkers efficiently transforms commercially available starting materials into bioactive targets in a single step (Scheme 38). Interestly enough, as discussed in the previous section, imidazolidine **192** was examined for its antideppressive properties as a mianserin analogue (Figure 12). The limiation of using benzylideneaniline **191** is that the phenyl group is effectively reaction inert because the nitrogen-carbon bond is difficult to cleave, so further functionalization of the amine can not be readily achieved. The goal of our work was to further expand this chemistry with more labile protecting groups, resulting more sophisticated scaffolds being accessible from these simple reaction products. Initially the phenyl group was replaced with a benzyl group with benzylidenebenzylamine **193** (Scheme 39). The benzyl group is labile and is

easily removed with Pd/C and acid under a hydrogen atmosphere. The free amine could then undergo further transformations to build a more complex target.

Scheme 40. [3+2]-Cycloaddition of TMAO and Benzylidenebenzylamine

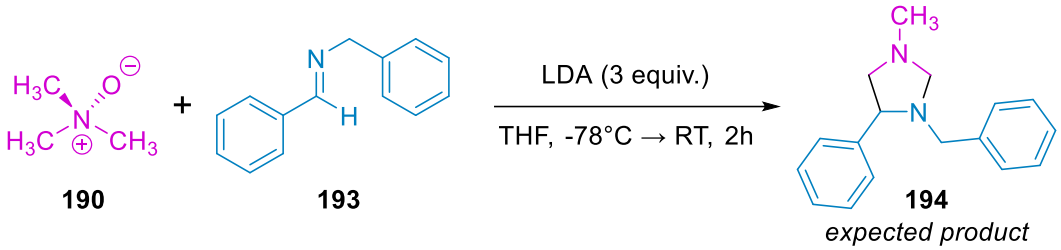

190 **193** **194**
expected product

The results of this transformation were that the expected imidazolidine **194** did not form. Upon warming to room temperature the reaction mixture was brilliantly colored bright fuchsia, unlike in the previous system. The crude reaction mixture was analyzed by ^{1}H NMR and it was difficult to discern if the imidazolidine was even present due to the amount of signals present. Imidazolidine **194** was by no means a major product if it even formed at all. It is likely that the acidic benzyl protons of **193** were deprotonated and that caused off-target reactivity.

2.2.3 Reactions of Trimethylamine *N*-oxide and Benzenesulfinamide

We wanted to see if this transformation was possible with sulfinyl imines because later applications of this research could include controlling enantioselectivity potentially through the use of Ellman's auxiliary.[53,54] The reaction between TMAO **190** and a less expensive sulfinyl imine **195** was investigated initially under standard reaction conditions as a proof of concept (Scheme 40). Benzenesulfinamide **195** was synthesized in a separate step following literature protocol, both product identity and purity were confirmed by ^{1}H NMR.

Scheme 41. [3+2] Cycloaddition of TMAO and Benzenesulfinamide

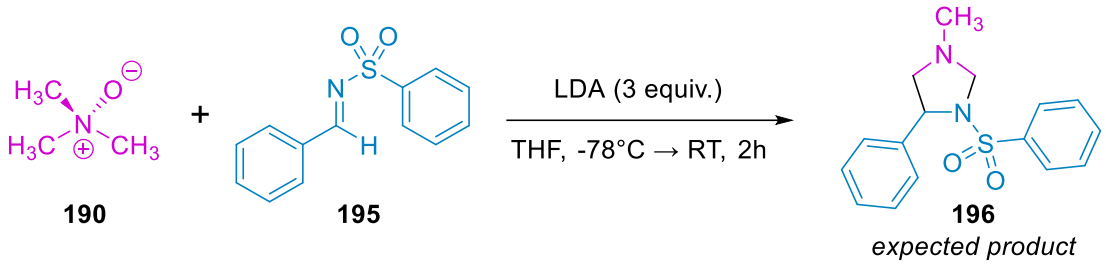

After attempting this reaction several times it became apparent that the desired imidazolidine **196** was not forming. A series of control experiments were conducted in order to distinguish what reagents were the cause of compound **196** failing to form. For example, the sulfinyl protecting group could be reacting with LDA and undergoing *ortho*-lithiation,[55] or the sulfinyl could be electrophilic enough for nucleophilic attack of the *N*-oxide to be favorable, and so on.

The control reaction with all components resulted in a 0% yield for the desired imidazolidine **196** (Table 3, entry 1). Imine **195** reacted with the LDA forming a wide array of side products which could not be readily identified (Table 3, entry 2). In our second control reaction we observed that sulfinyl **195** undergoes nucleophilic attack by the *N*-oxide without the presence of LDA, forming oxo-bridged compounds (Table 3, entry 3). The imine (**195**) is stable to the reaction conditions in the absence of base or N-oxide **190** (Table 3, entry 4). We tried to favor the [3+2] cycloaddition by combining TMAO and LDA at -78 °C and allowing that mixture to warm to RT in order to generate the azomethine ylide before introducing imine **195** (Table 3, entry 5). Once warmed to RT, imine **195** was added, and the reaction was carried out as normal (Table 1, entry 5). The rationale was the since the azomethine ylide was already formed, there should not be any *N*-oxide present to act as a nucleophile and preemptively react with the imine. The results, however, were the same as the control (Table 3, entry 1).

Table 3. Control reactions of benzenesulfinamide and various reaction conditions

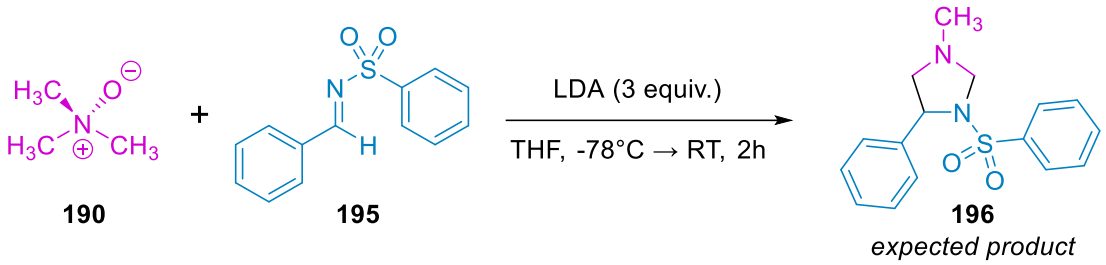

190 **195** **196**
expected product

Entry[a]	Imine	LDA	*N*-oxide	Result
1	0.2 mmol	0.6 mmol	0.2 mmol	0 % yield of **194**
2	0.2 mmol	0.6 mmol	---	Reaction occurred, no imine **193** present
3	0.2 mmol	---	0.2 mmol	Reaction occurred, no imine **193** present
4	0.2 mmol	---	---	No Reaction
5[b]	0.2 mmol	0.6 mmol	0.2 mmol	0% yield of **194**

[a]Reaction conditions: *N*-oxide **190** (1 equiv.) was dissolved in THF (0.1 M), and cooled to -78 °C. LDA (3 equiv.) was added dropwise followed by a 1 M solution of benzenesulfinamide **193** (1 equiv.) in THF. The reaction was removed from the cold bath and left to react for 2 h. Volatiles were removed and the residue was analyzed by ^{1}H NMR.

[b] *N*-oxide **190** (1 equiv.) was dissolved in THF (0.1 M), and cooled to -78 °C. LDA (3 equiv.) was added dropwise and the reaction was warmed to RT. Benzenesulfinamide **193** (1 equiv.) was added as a 1 M solution in THF and left to react for 2 h. Volatiles were removed and the residue was analyzed by ^{1}H NMR.

This could also be due to the fact that imine **195** also reacts with LDA, which might be able to be avoided if only two equivalents of LDA are used instead of three. Additionally, results from previous experiments in a similar system show that an additive such as triflic anhydride can be premixed with the *N*-oxide which would prevent it from acting as a nucleophile (See Chapter 3).

2.2.4 Reactions of Trimethylamine *N*-oxide and Silyl Imines

We next decided to implement the use of silyl imines **198** as dipolarophiles in [3+2] cycloadditions with TMAO **190** due to their ease of synthesis and functional group compatibility, being electronically similar to Roussi's system. Trimethylsilyl (TMS) is a labile nitrogen protecting group devoid of α-protons, and unlike the sulfonamide, TMS is fairly reaction inert so it was hypothesized that there would be no off-target reactivity. Silyl imines **198** are readily accessible through an aza-Brook rearrangement from commercially available aldehydes **197** and LiHMDS. While carrying out these reactions with arenes and alkyl groups, it became apparent that the resulting imidazolidines were unstable and readily hydrolyzed. This ended up turning into a three-step one-pot protocol forming 1,2-diamines in yields up to 94% as discussed at length in Chapter 1. To expand the substrate scope from arenes and quaternary alky groups, we implemented heterocyclics since many drug compounds contain more than one heterocyclic ring (Scheme 41). The implementation of the heterocyclic would also be interesting to investigate mechanistically since we have reported that the chelation effects of LDA and THF play a significant role in this transformations success.[56] The addition of heteroatoms could potentially aid in this chelation, or the additional heteroatoms could also hinder it.

Scheme 42. Three-step one-pot synthesis of imidazolidines using a [3+2] cycloaddition of TMAO and silyl imines.

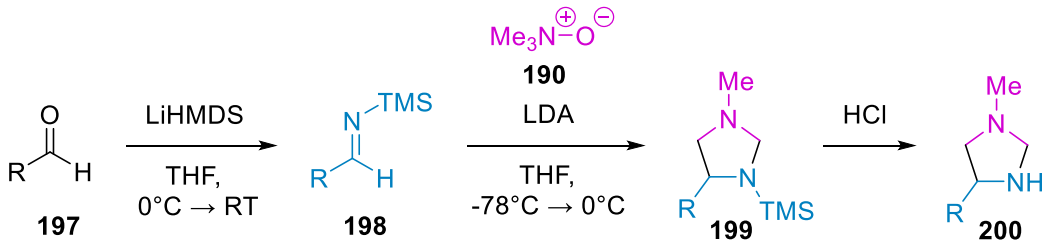

In implementing heteroarenes, it was discovered that they are more stable and easier to isolate as imidazolidines (**200**) than their 1,2-diamine (**109**) counterparts (Scheme 42). Additionally, the

implementation of heteroarenes required some slight changes to the reaction conditions: LiHMDS was used in place of NaHMDS for the aza-Brook rearrangement, the reaction temperature for the aza-Brook rearrangement was lowered to -78 °C, and the [3+2] cycloaddition reaction time was kept at -78 °C for 30 min and then stirred at RT for 2 h (Scheme 42). This three-step reaction route was carried out as an efficient one-pot synthesis.

Scheme 43. Substrate scope and limitation of [3+2] cycloadditions of TMAO and silyl imines.

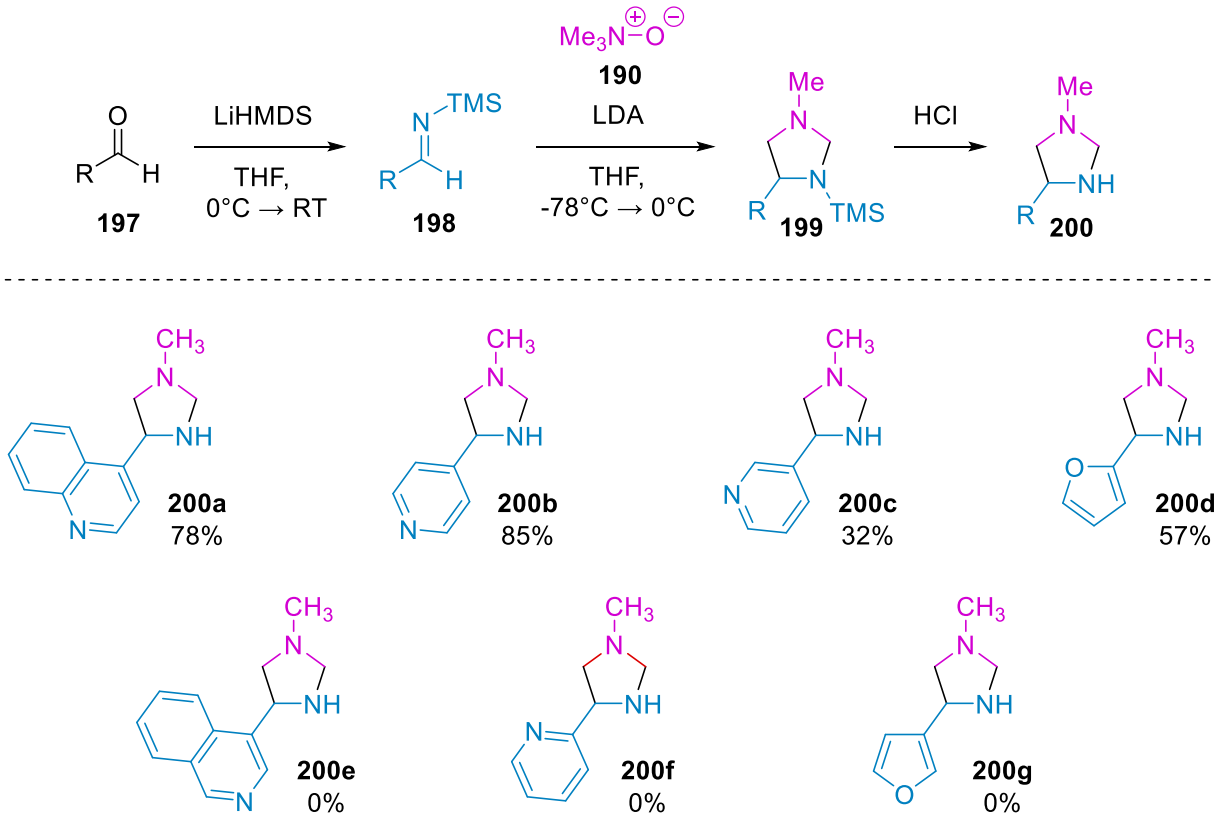

This reaction tolerated 4-quinoline and 4-pyridyl groups forming **200a** and **200b** in good yields of 78% and 85% respectively (Scheme 42). Interestingly incorporating a 3-pyridyl group resulted in a low 32% yield for **200c**. 2-Furanyl substituted **200d** was isolated in a 57% yield which was similar to its 1,2-diamine counterpart (56% yield). Substrates that were not tolerated by the reactions conditions were 3-quinoline, 2-pyridyl, and 3-furyl resulting in 0% yields for **200e-g**.

While a decreasing result, some trends were observed and it did allow us to gain some more insight into the reaction mechanism.

As the heteroatom moves closer to the 1-position, the yields decrease; 3-pyridyl produced **200c** in 32% yield, and then 2-pyridyl resulted in **200f** in a 0% yield. This same trend was observed with 3-quinoline also forming **200e** in a 0% yield as well as 3-furyl resulting in no imidazolidine **200g** formation (0% yield). This trend could be an electronic effect since 2-furaldehyde, like furan, exhibits a dipole moment away from the heteroatom, making the 2 and 3 positions more electron poor while the 4 and 5 positions are more electron rich (Figure 16).[57] Additionally, the α-protons on furan have a pK_a of 35.6, which is close to the pK_a of LDA (Figure 16). The aldehyde withdraws electron density from the furyl substituents, making those protons more acidic which increases the likelihood that deprotonation by LDA occurs. This could trigger side reactions in the [3+2]-cycloaddition which would account for the low yield of **200d** and the mix of products in the ^1H NMR for the reaction of **197g** and TMAO.

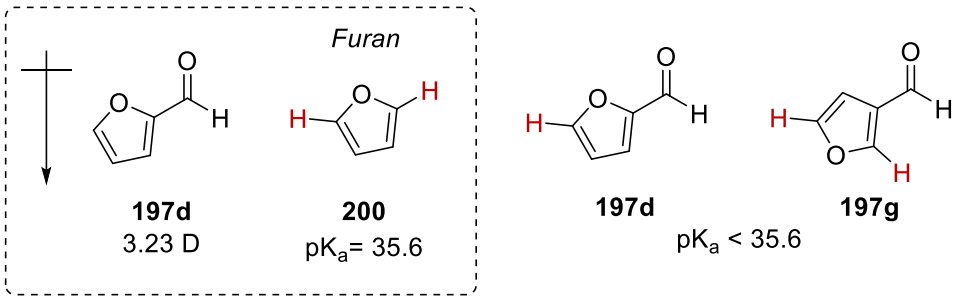

Figure 16. Dipole moment of 2-furaldehyde and pK_a of furan compared to 2- and 3-furaldehyde.

Pyridine is electropositive at positions 2, 4, and 6, and electronegative at positions 1, 3, and 5 which is explained by resonance (Figure 17a). This is a trend that quinolines also follow. Since **200a** and **200b** both formed in high yields, this could indicate that a partial positive charge at the α-position of the silyl imine is beneficial for the [3+2]-cycloaddition (Figure 17b). This is also in

agreement with the 2-furyl substituted **198d** where the α-position also has a slight positive character due to the net-dipole moment. Silyl imines **198c** and **198d** both have a partial negative charge at the α-position resulting in low yield of **200c** and no product formation for **200d**. The outlier for this trend is the case of **198f** where the ^{1}H NMR was indiscernible due to the amount of signals present. If the electronic nature of the silyl imine was the only trend, imidazolidine **200f** should have been formed in good yields.

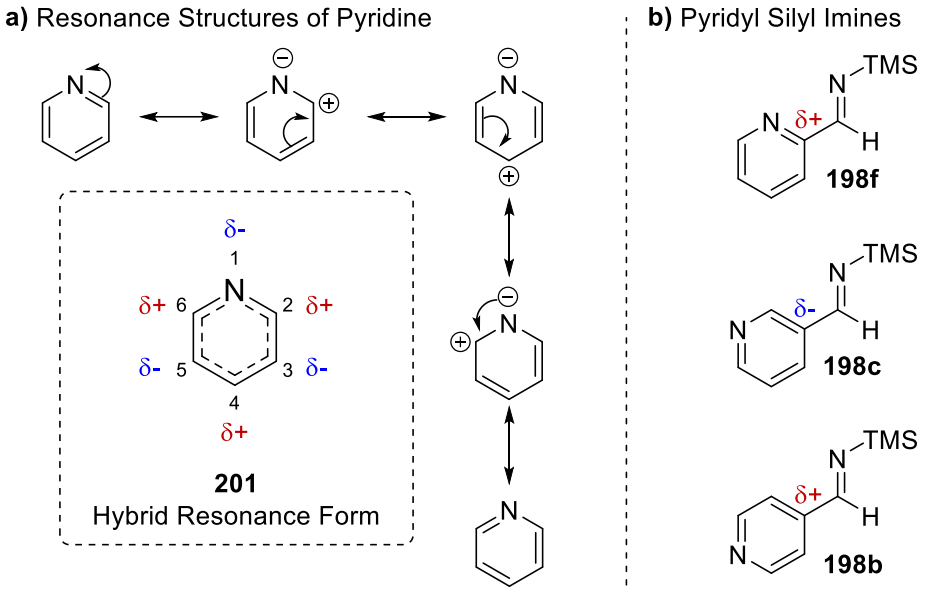

Figure 17. a) Resonance Structures of Pyridine; b) Electronic character of the α-positions of silyl imines

Another explanation to the low yields is that the introduction of these heteroatoms could be resulting in chelation of the lithium base (Figure 18). While this is reasonable for imines **198c** and **198f**, chelation is not likely with the 4-pyridyl **198b** and likewise the 4-quinoline **198a** imines because of the distances between the two nitrogen atoms. Additionally in the case of **198c**, there could be two equivalents of the imine that could sequester the lithium cation much like a porphyrin ring.

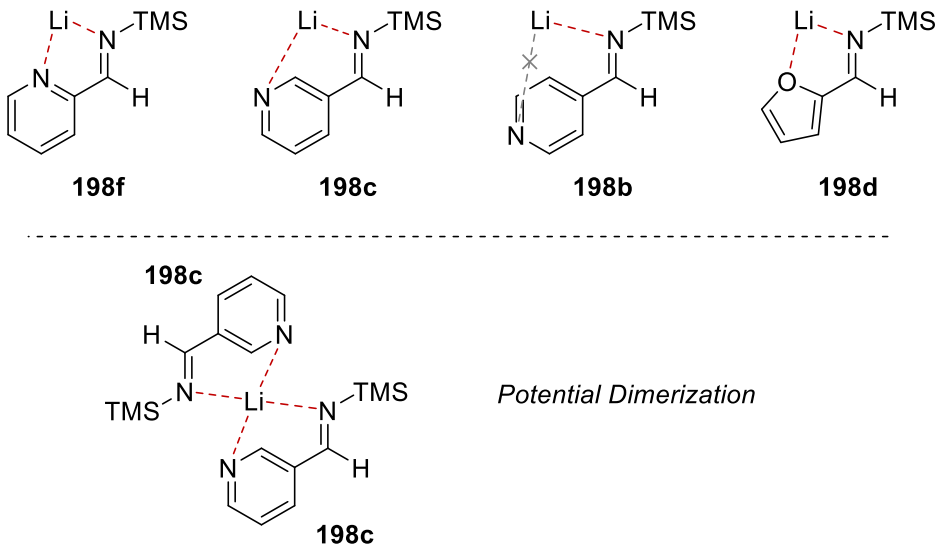

Figure 18. Proposed lithium chelation of heteroaryl silyl imines.

If the lithium of the LDA is chelated by the silyl imines, this could be problematic for the key intermediate **203** in our proposed reaction mechanism (Scheme 43). We reported that the multi-ion bridge **203** is essential to this this cycloaddition[56] so it might be reasonable to deduce that the placement of the heteroatoms could disrupt that multi-ion bridge formation, resulting in little to no imidazolidine formation.

Scheme 44. Proposed mechanism with blocked multi-ion bridge intermediate.[56]

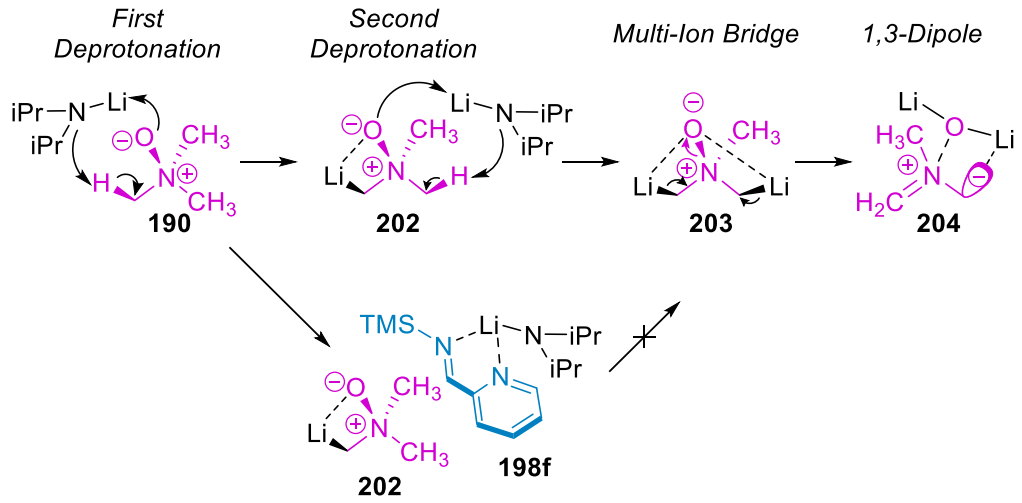

2.2.5 Transformations of 1,2-diamines forming imidazolidines and imidazolidines

Scheme 45. Condensation of 1,2-Diamine 109h and Benzaldehyde

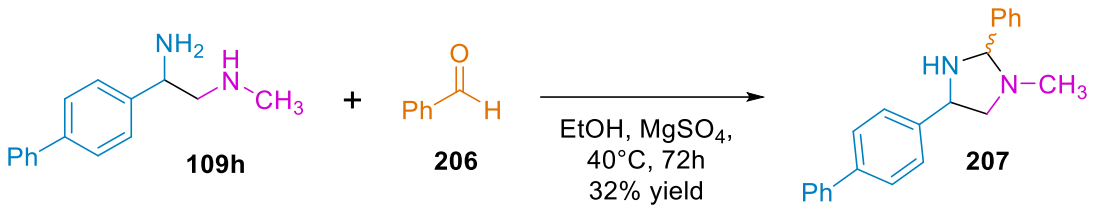

We wanted to demonstrate the synthetic utility of the 1,2-diamines synthesized in Chapter 1 in forming bioactive targets efficiently. This would also highlight how different functionalities could be installed for rapid access to a variety of heterocycles. Initially the simple condensation of 1,2-diamine **109h** and benzaldehyde **206** was carried out (Scheme 44). This resulted in a mixture of two diastereomers **207** which were isolated in 32% yield.

Scheme 46. a) Cyclization with ethyl benzimidate forming an imidazoline; b) Proposed hydrogenation forming imidazolidines as a single diastereomer.

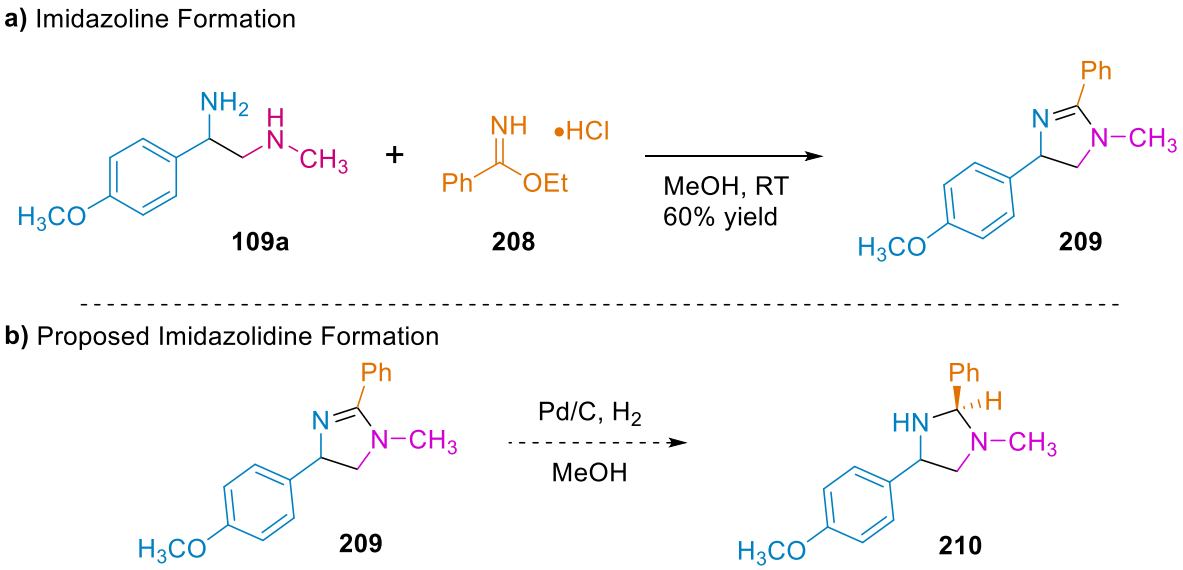

We then used another type of condensation reaction using ethyl benzimidate **206** with diamine **109a** to form the imidazoline instead of the imidazolidine (Scheme 45a). The imidazoline was formed as a single diastereomer in 60% yield. This could provide an efficient route to both imidazolines and imidazolines to be examined in SAR studies. The imidazolines **207** could

undergo hydrogenation to form their imidazolidine **208** counterparts (Scheme 45b). This would be of interest for a future direction with these products in particular.

2.3 Conclusions

The preliminary efforts by Roussi and coworkers were expanded by implementing a variety of imines. While [3+2] cycloadditions of TMAO with both benzyl and sulfonyl protected imines were wrought with off-target reactivity, reactions with silyl protected imines yielded several promising results. The [3+2]-cycloadditions of TMAO and silyl-protected heteroaryl-imines **198** achieved substituted imidazolidines **200a-g** with yields up to 85% in a three-step one-pot synthetic method. This could provide rapid access to drug-like targets from commercially available starting reagents, a stark difference to most methods reported in the medicinal chemistry literature.

2.4 References

(1) Sadarangani, I. R.; Bhatia, S.; Amarante, D.; Lengyel, I.; Stephani, R. A. Synthesis, resolution and anticonvulsant activity of chiral N-1′-ethyl,N-3′-(1-phenylethyl)-(R,S)-2′H,3H,5′H-spiro-(2-benzofuran-1,4′-imidazolidine)-2′,3,5′-trione diastereomers. *Bioorganic & Medicinal Chemistry Letters* **2012**, *22* (7), 2507-2509. DOI: https://doi.org/10.1016/j.bmcl.2012.02.005

(2) Unno, R.; Yamaguchi, T.; Usui, T.; Kakigami, T.; Fukushima, M.; Mizuno, K.; Baba, Y.; Kurono, M. Synthesis and Aldose Reductase Inhibitory Activity of 2-Substituted 6-Fluoro-2, 3-dihydrospiro[4H-1-benzopyran-4, 4'-imidazolidine]2', 5'-diones. *Chemical & Pharmaceutical Bulletin* **1994**, *42* (7), 1474-1478. DOI: 10.1248/cpb.42.1474.

(3) Riebsomer, J. L. A study of the reaction products of 1,2-diamines with aldehydes. *The Journal of Organic Chemistry* **1950**, *15* (2), 237-240. DOI: 10.1021/jo01148a003.

(4) de Carvalho, G. S.; Machado, P. A.; de Paula, D. T.; Coimbra, E. S.; da Silva, A. D. Synthesis, cytotoxicity, and antileishmanial activity of N,N'-disubstituted ethylenediamine and imidazolidine derivatives. *ScientificWorldJournal* **2010**, *10*, 1723-1730. DOI: 10.1100/tsw.2010.176

(5) Katritzky, A. R.; Suzuki, K.; He, H.-Y. Convenient Syntheses of Unsymmetrical Imidazolidines. *The Journal of Organic Chemistry* **2002**, *67* (9), 3109-3114. DOI: 10.1021/jo010868n.

(6) Tu, L.; Li, Z.; Feng, T.; Yu, S.; Huang, R.; Li, J.; Wang, W.; Zheng, Y.; Liu, J. Access to Imidazolidines via 1,3-Dipolar Cycloadditions of 1,3,5-Triazinanes with Aziridines. *The Journal of Organic Chemistry* **2019**, *84* (17), 11161-11169. DOI: 10.1021/acs.joc.9b01959.

(7) Qiao, J.; Wang, S.; Liu, X.; Feng, X. Enantioselective [3+2] Cycloaddition of Donor-Acceptor Aziridines and Imines to Construct 2,5-trans-Imidazolidines. *Chemistry – A European Journal* **2023**, *29* (18), e202203757. DOI: https://doi.org/10.1002/chem.202203757.

(8) Lin, T.-Y.; Wu, H.-H.; Feng, J.-J.; Zhang, J. Chirality Transfer in Rhodium(I)-Catalyzed [3 + 2]-Cycloaddition of Vinyl Aziridines and Oxime Ethers: Atom-Economical Synthesis of Chiral Imidazolidines. *Organic Letters* **2018**, *20* (12), 3587-3590. DOI: 10.1021/acs.orglett.8b01378.

(9) Li, Q.-H.; Wei, L.; Chen, X.; Wang, C.-J. Asymmetric construction of fluorinated imidazolidines via Cu(i)-catalyzed exo′-selective 1,3-dipolar cycloaddition of azomethine ylides with fluorinated imines. *Chemical Communications* **2013**, *49* (56), 6277-6279, 10.1039/C3CC43025A. DOI: 10.1039/C3CC43025A.

(10) Jia, H.; Liu, H.; Guo, Z.; Huang, J.; Guo, H. Tandem [3 + 2] Cycloaddition/1,4-Addition Reaction of Azomethine Ylides and Aza-o-quinone Methides for Asymmetric Synthesis of Imidazolidines. *Organic Letters* **2017**, *19* (19), 5236-5239. DOI: 10.1021/acs.orglett.7b02512.

(11) Yu, J.; Shi, F.; Gong, L.-Z. Brønsted-Acid-Catalyzed Asymmetric Multicomponent Reactions for the Facile Synthesis of Highly Enantioenriched Structurally Diverse Nitrogenous Heterocycles. *Accounts of Chemical Research* **2011**, *44* (11), 1156-1171. DOI: 10.1021/ar2000343.

(12) Roussi, G.; Beugelmans, R.; Chastanet, J.; Roussi, G. The [3+2] Cycloaddition Reaction of Nonstabilized Azomethine Ylide Generated from Trimetylmine N-Oxide to C=C, C=N, and C=S Bonds. *Heterocycles* **1987**, *26* (12), 3197-3202, Journal. DOI: 10.3987/r-1987-12-3197.

(13) Savjani, J. K.; Gajjar, A. K. Pharmaceutical Importance and Synthetic Strategies for Imidazolidine-2-thione and. *Pakistan Journal of Biological Sciences* **2011**, *14* (24), 1076-1089.

(14) Ferm, R. J.; Riebsomer, J. L. The Chemistry of the 2-Imidazolines and Imidazolidines. *Chemical Reviews* **1954**, *54* (4), 593-613. DOI: 10.1021/cr60170a002.

(15) Taylor, R. D.; MacCoss, M.; Lawson, A. D. G. Rings in Drugs. *Journal of Medicinal Chemistry* **2014**, *57* (14), 5845-5859. DOI: 10.1021/jm4017625

(16) Vitaku, E.; Smith, D. T.; Njardarson, J. T. Analysis of the Structural Diversity, Substitution Patterns, and Frequency of Nitrogen Heterocycles among U.S. FDA Approved Pharmaceuticals. *Journal of Medicinal Chemistry* **2014**, *57* (24), 10257-10274. DOI: 10.1021/jm501100b.

(17) El-Sharief, M.; Abbas, S. Y.; El-Sharief, A. M. S.; Sabry, N. M.; Moussa, Z.; El-Messery, S. M.; Elsheakh, A. R.; Hassan, G. S.; El Sayed, M. T. 5-Thioxoimidazolidine-2-one derivatives: Synthesis, anti-inflammatory activity, analgesic activity, COX inhibition assay and molecular modelling study. *Bioorg Chem* **2019**, *87*, 679-687. DOI: 10.1016/j.bioorg.2019.03.075

(18) Crane, L.; Anastassiadou, M.; El Hage, S.; Stigliani, J. L.; Baziard-Mouysset, G.; Payard, M.; Leger, J. M.; Bizot-Espiard, J. G.; Ktorza, A.; Caignard, D. H.; et al. Design and synthesis of novel imidazoline derivatives with potent antihyperglycemic activity in a rat model of type 2 diabetes. *Bioorg Med Chem* **2006**, *14* (22), 7419-7433. DOI: 10.1016/j.bmc.2006.07.026

(19) Chitsulo, L.; Loverde, P.; Engels, D. Focus: Schistosomiasis. *Nature Reviews Microbiology* **2004**, *2* (1), 12-12. DOI: 10.1038/nrmicro801.

(20) Matos-Rocha, T. J.; Lima, M. d. C. A. d.; Silva, A. L. d.; Oliveira, J. F. d.; Gouveia, A. L. A.; Silva, V. B. R. d.; Almeida Júnior, A. S. A. d.; Brayner, F. A.; Cardoso, P. R. G.; Pitta-Galdino, M. d. R.; et al. Synthesis and biological evaluation of novel imidazolidine derivatives as candidates to schistosomicidal agents. *Revista do Instituto de Medicina Tropical de São Paulo* **2017**, *59*.

(21) Melman, S. D.; Steinauer, M. L.; Cunningham, C.; Kubatko, L. S.; Mwangi, I. N.; Wynn, N. B.; Mutuku, M. W.; Karanja, D. M.; Colley, D. G.; Black, C. L. Reduced susceptibility to praziquantel among naturally occurring Kenyan isolates of Schistosoma mansoni. *PLoS neglected tropical diseases* **2009**, *3* (8), e504.

(22) Santos, D. O.; Coutinho, C. E. R.; Madeira, M. F.; Bottino, C. G.; Vieira, R. T.; Nascimento, S. B.; Bernardino, A.; Bourguignon, S. C.; Corte-Real, S.; Pinho, R. T.; et al. Leishmaniasis treatment—a challenge that remains: a review. *Parasitology Research* **2008**, *103* (1), 1-10. DOI: 10.1007/s00436-008-0943-2.

(23) Nickolson, V. J.; Wieringa, J. H. Presynaptic α-block and inhibition of noradrenaline and 5-hydroxytryptamine reuptake by a series of compounds related to mianserin. *Journal of Pharmacy and Pharmacology* **1981**, *33* (1), 760-766. DOI: 10.1111/j.2042-7158.1981.tb13927.x.

(24) Gould, K. Antibiotics: from prehistory to the present day. *J Antimicrob Chemother* **2016**, *71* (3), 572-575. DOI: 10.1093/jac/dkv484

(25) Lalchhandama, K. Reappraising Fleming's snot and mould. *Science Vision* **2020**, *20* (1), 29-42.

(26) Miller, E. L. The penicillins: a review and update. *J Midwifery Womens Health* **2002**, *47* (6), 426-434. DOI: 10.1016/s1526-9523(02)00330-6

(27) Zaman, S. B.; Hussain, M. A.; Nye, R.; Mehta, V.; Mamun, K. T.; Hossain, N. A Review on Antibiotic Resistance: Alarm Bells are Ringing. *Cureus* **2017**, *9* (6), e1403. DOI: 10.7759/cureus.1403

(28) Aslam, B.; Wang, W.; Arshad, M. I.; Khurshid, M.; Muzammil, S.; Rasool, M. H.; Nisar, M. A.; Alvi, R. F.; Aslam, M. A.; Qamar, M. U.; et al. Antibiotic resistance: a rundown of a global crisis. *Infect Drug Resist* **2018**, *11*, 1645-1658. DOI: 10.2147/IDR.S173867

(29) Iwu-Jaja, C. J.; Jaca, A.; Jaja, I. F.; Jordan, P.; Bhengu, P.; Iwu, C. D.; Okeibunor, J.; Karamagi, H.; Tumusiime, P.; Fuller, W.; et al. Preventing and managing antimicrobial resistance in the African region: A scoping review protocol. *PLoS One* **2021**, *16* (7), e0254737. DOI: 10.1371/journal.pone.0254737

(30) Lewis, K. The Science of Antibiotic Discovery. *Cell* **2020**, *181* (1), 29-45. DOI: 10.1016/j.cell.2020.02.056

(31) Khan, M. S.; Husain, A.; Sharma, S.; Rashid, M. Microbiological Evaluation of 4-substituted-imidazolidine Derivatives. *Indian J Pharm Sci* **2012**, *74* (1), 80-83. DOI: 10.4103/0250-474x.102549 From NLM.

(32) Kowalska-Krochmal, B.; Dudek-Wicher, R. The Minimum Inhibitory Concentration of Antibiotics: Methods, Interpretation, Clinical Relevance. *Pathogens* **2021**, *10* (2). DOI: 10.3390/pathogens10020165 From NLM.

(33) Kaczor, A.; Nové, M.; Kincses, A.; Spengler, G.; Szymańska, E.; Latacz, G.; Handzlik, J. Search for ABCB1 Modulators Among 2-Amine-5-Arylideneimidazolones as a New Perspective to Overcome Cancer Multidrug Resistance. *Molecules* **2020**, *25* (9), 2258.

(34) Ji, X.; Lu, Y.; Tian, H.; Meng, X.; Wei, M.; Cho, W. C. Chemoresistance mechanisms of breast cancer and their countermeasures. *Biomedicine & Pharmacotherapy* **2019**, *114*, 108800. DOI: https://doi.org/10.1016/j.biopha.2019.108800.

(35) Perez, E. A. Impact, mechanisms, and novel chemotherapy strategies for overcoming resistance to anthracyclines and taxanes in metastatic breast cancer. *Breast Cancer Res Treat* **2009**, *114* (2), 195-201. DOI: 10.1007/s10549-008-0005-6 From NLM.

(36) Sui, H.; Fan, Z. Z.; Li, Q. Signal transduction pathways and transcriptional mechanisms of ABCB1/Pgp-mediated multiple drug resistance in human cancer cells. *J Int Med Res* **2012**, *40* (2), 426-435. DOI: 10.1177/147323001204000204 From NLM.

(37) Yasuhisa, K.; Shin-ya, M.; Michinori, M.; Kazumitsu, U. Mechanism of multidrug recognition by MDR1/ABCB1. *Cancer Science* **2007**, *98* (9), 1303-1310. DOI: https://doi.org/10.1111/j.1349-7006.2007.00538.x.

(38) Chung, F. S.; Santiago, J. S.; Jesus, M. F.; Trinidad, C. V.; See, M. F. Disrupting P-glycoprotein function in clinical settings: what can we learn from the fundamental aspects of this transporter? *Am J Cancer Res* **2016**, *6* (8), 1583-1598.

(39) Moos, F. Ueber einige Condensationsproducte von Aethylenanilin mit Aldehyden. *Berichte der deutschen chemischen Gesellschaft* **1887**, *20* (1), 732-734.

(40) Riebsomer, J. The synthesis of imidazolines from 1, 2-diamines and carboxylic acids. *Journal of the American Chemical Society* **1948**, *70* (4), 1629-1632.

(41) Anastas, P. T.; Warner, J. C. Principles of green chemistry. *Green chemistry: Theory and practice* **1998**, *29*.

(42) Giumanini, A. G.; Verardo, G.; Zangrando, E.; Lassiani, L. Revisitation of Formaldehyde Aniline Condensation. VII. 1,3,5-Triarylhexahydro-sym-triazines and 1,3,5,7-Tetraaryl-1,3,5,7-

tetrazocines from Aromatic Amines and Paraformaldehyde. *Journal für Praktische Chemie* **1987**, *329* (6), 1087-1103. DOI: https://doi.org/10.1002/prac.19873290619.

(43) Liu, P.; Xu, G.; Sun, J. Metal-Free [2 + 1 + 2]-Cycloaddition of Tosylhydrazones with Hexahydro-1,3,5-triazines To Form Imidazolidines. *Organic Letters* **2017**, *19* (7), 1858-1861. DOI: 10.1021/acs.orglett.7b00600.

(44) Alvarez-Corral, M.; Munoz-Dorado, M.; Rodriguez-Garcia, I. Silver-mediated synthesis of heterocycles. *Chem Rev* **2008**, *108* (8), 3174-3198. DOI: 10.1021/cr0783611

(45) Stanley, L. M.; Sibi, M. P. Enantioselective Copper-Catalyzed 1,3-Dipolar Cycloadditions. *Chemical Reviews* **2008**, *108* (8), 2887-2902. DOI: 10.1021/cr078371m.

(46) Adrio, J.; Carretero, J. C. Novel dipolarophiles and dipoles in the metal-catalyzed enantioselective 1,3-dipolar cycloaddition of azomethine ylides. *Chem Commun (Camb)* **2011**, *47* (24), 6784-6794, 10.1039/C1CC10779H. DOI: 10.1039/c1cc10779h

(47) Feng, J.-J.; Lin, T.-Y.; Zhu, C.-Z.; Wang, H.; Wu, H.-H.; Zhang, J. The Divergent Synthesis of Nitrogen Heterocycles by Rhodium(I)-Catalyzed Intermolecular Cycloadditions of Vinyl Aziridines and Alkynes. *Journal of the American Chemical Society* **2016**, *138* (7), 2178-2181. DOI: 10.1021/jacs.6b00386.

(48) Philip Nuss; J. Eckelman, M. Life Cycle Assessment of Metals: A Scientific Synthesis. *PLoS ONE* **2014**, *9* (7), e101298. DOI: 10.1371/journal.pone.0101298 (acccessed 2020-08-27T01:38:42).

(49) Weng, Z.; Jowitt, S. M.; Mudd, G. M.; Haque, N. A Detailed Assessment of Global Rare Earth Element Resources: Opportunities and Challenges*. *Economic Geology* **2015**, *110* (8), 1925-1952. DOI: 10.2113/econgeo.110.8.1925 (acccessed 8/27/2020).

(50) Yu, Z.; Liu, X.; Dong, Z.; Xie, M.; Feng, X. An N,N′-Dioxide/In(OTf)3 Catalyst for the Asymmetric Hetero-Diels–Alder Reaction Between Danishefsky's Dienes and Aldehydes: Application in the Total Synthesis of Triketide. *Angewandte Chemie International Edition* **2008**, *47* (7), 1308-1311. DOI: https://doi.org/10.1002/anie.200704759.

(51) Liu, W.-J.; Chen, X.-H.; Gong, L.-Z. Direct Assembly of Aldehydes, Amino Esters, and Anilines into Chiral Imidazolidines via Brønsted Acid Catalyzed Asymmetric 1,3-Dipolar Cycloadditions. *Organic Letters* **2008**, *10* (23), 5357-5360. DOI: 10.1021/ol802177s.

(52) Wang, Y.-M.; Zhang, H.-H.; Li, C.; Fan, T.; Shi, F. Catalytic asymmetric chemoselective 1,3-dipolar cycloadditions of an azomethine ylide with isatin-derived imines: diastereo- and enantioselective construction of a spiro[imidazolidine-2,3′-oxindole] framework. *Chemical Communications* **2016**, *52* (9), 1804-1807, 10.1039/C5CC07924A. DOI: 10.1039/C5CC07924A.

(53) Ellman, J. A.; Owens, T. D.; Tang, T. P. N-tert-butanesulfinyl imines: versatile intermediates for the asymmetric synthesis of amines. *Acc Chem Res* **2002**, *35* (11), 984-995. DOI: 10.1021/ar020066u

(54) Liu, G.; Cogan, D. A.; Ellman, J. A. Catalytic Asymmetric Synthesis of tert-Butanesulfinamide. Application to the Asymmetric Synthesis of Amines. *Journal of the American Chemical Society* **1997**, *119* (41), 9913-9914. DOI: 10.1021/ja972012z.

(55) MacNeil, S. L.; Familoni, O. B.; Snieckus, V. Selective ortho and benzylic functionalization of secondary and tertiary p-tolylsulfonamides. Ipso-bromo desilylation and Suzuki cross-coupling reactions. *J Org Chem* **2001**, *66* (11), 3662-3670. DOI: 10.1021/jo001402s From NLM.

(56) Neal, M. J.; Hejnosz, S. L.; Rohde, J. J.; Evanseck, J. D.; Montgomery, T. D. Multi-Ion Bridged Pathway of *N*-Oxides to 1,3-Dipole Dilithium Oxide Complexes. *J. Org. Chem.* **2021**, *86* (17), 11502-11518.

(57) Baran, P.; Richter, J. Essentials of heterocyclic chemistry-I. *The Scripps Research Institute Heterocyclic Chemistry,* The Scripps Research Institute **2009**. https://www.scripps.edu/baran/heterocycles/Essentials1-2009.pdf (accessed 2023-07-06)

Chapter 3: Cycloadditions of Trimethylamine *N*-oxide and Dipolarophiles Forming Pyrrolidines

3.1 Introduction

3.1.1 Contextual Summary

Pyrrolidines are prevalent motifs in natural product and pharmaceuticals exhibiting rich bioactive properties.[1-4] Due to the ubiquity this family of compounds there is a constant demand for new and innovative synthetic methodologies taking advantage of unique disconnections to form substituted pyrrolidines. Moreover, the discovery of novel pyrroldines paves the way for new and more effective therapeutics. Efficient and robust synthetic methods are key in drug development for rapid bioactivity screenings and SAR studies. Most synthetic methods to form these privileged motifs are stunted by expensive catalysts, complex ligand systems, and multiple steps. Roussi and coworkers established a one-step protocol from commercially available tertiary amine *N*-oxides and alkenes forming substituted pyrrolidines in the 1980s, but since then it has seen little use. Convinced that this chemistry had more to offer, we elected to further study this transformation with new substrates.

3.1.2 Pharmaceuticals Containing Pyrrolidines

3.1.2.1 Antioxidants

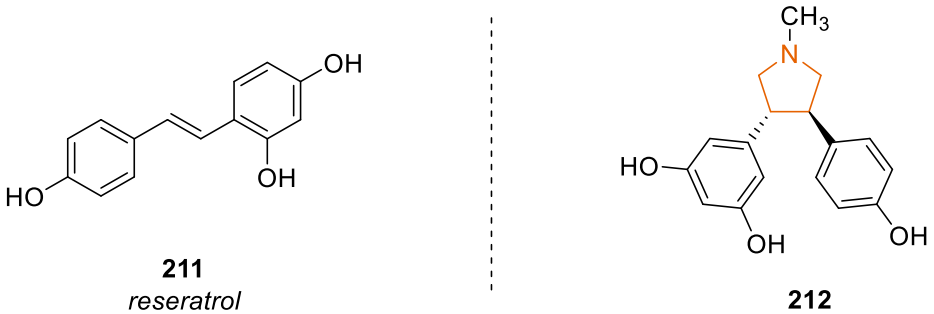

211
reseratrol

212

Figure 19. Structures of Antioxidants: Resveratrol and a Pyrrolidine Derivative[5]

The inhibitory effects of pyrrolidine derivative, resveratrol (**211**), on DNA oxidation has made it a drug target of interest for the treatment various diseases.[6] The antioxidant effects of resveratrol (**211**) were enhanced by adding a pyrrolidine moiety onto its backbone forming **212** (Figure 19).[5] This work by Liu and coworkers offers a new outlook on the search for novel antioxidants by simply enhancing the effects of alkene containing antioxidants by functionalizing them into pyrrolidine derivatives.[5]

3.1.2.2 Anti-inflammatory Agents

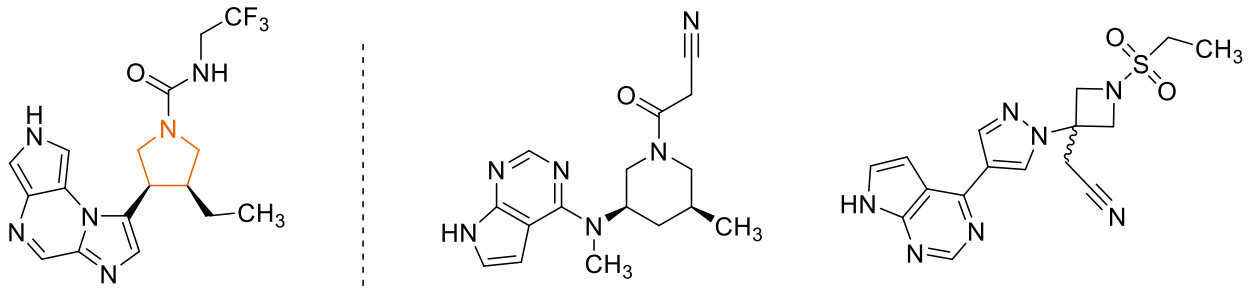

213
Upadacitinib

214
Tofactitinib

215
Baricitinib

Figure 20. Structures of Anti-inflamatory Agents: Upadacitinib,[7,8] Tofacitinib,[9,10] and Baricitinib.[11]

Upadacitinib (**213**), more commonly known as the brand name Rinvoq, is a Janus Kinase (JAK) inhibitor that is commonly prescribed to treat both rheumatoid and psoriatic arthritis.[7,8,12,13] JAKs are enzymes that are responsible for processes that result in inflammation, so blocking these enzymes blocks inflammation pathways and results in an anti-inflammatory effect. Upadacitinib (**213**) exhibits high selectivity for JAKI compared to JAK2 and JAK3, mostly due to strong hydrogen-bonding interactions combined with its structural geometry.[13] More concrete reasons for the observed strong affinity of **213** for JAK1 is something that researchers are still trying to elucidate through molecular modeling and SAR studies.[12,13] Tofacitinib (**214**) is a piperadine (six membered *N*-heterocyclic) that has a high affinity for both JAK1 and JAK3.[10] Similarly, baricitinib

(**215**) contains an azetidine (four membered *N*-heterocyclic), and has high affinities for both JAK1 and JAK2.[14] The high specificity of **213** for JAK1 could be linked to the ring size since they all bear very similar substituents (Figure 20). Not only is **213** used to treat rheumatoid arthritis, upadacitinib has also been approved for the treatment of Crohn's disease[15] as well as ulcerative colitis,[16] making it a versatile and effective anti-inflammatory agent.

3.1.2.3 Antiviral Agents

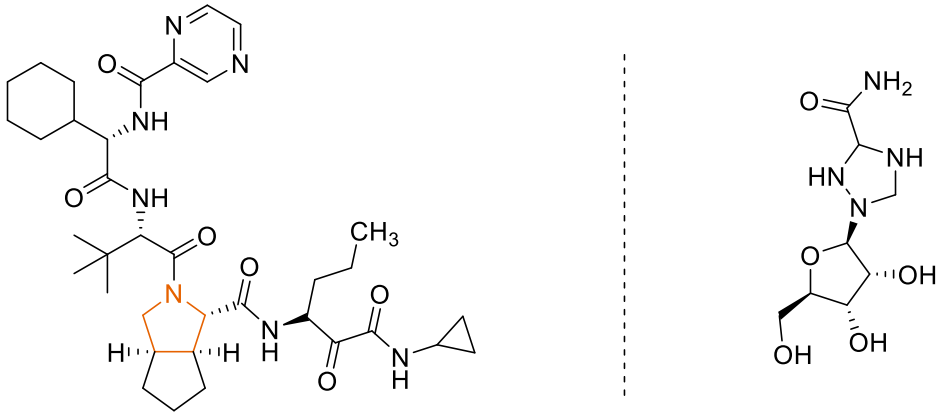

216
Telaprevir

217
Ribavirin

Figure 21. Structures of Antiviral Agents: Telaprevir and Ribavirin

The pyrrolidine derivative telaprevir **216** has been used in combination with antiviral ribavirin (**217**) to treat chronic hepatitis C virus (HCV).[17] This drug works by inhibiting NS3/4A, which is a serine protease encoded by HCV geneotype 1.[17] Surprisingly **216** also inhibits the SARS-CoV-2 3CL protease making it a potential treatment for this virus as well.[18]

3.1.2.4 Antipsychotics

Asenapine **218** is both a serotonin and dopamine receptor antagonist with a high affinity for the 5-HT_{2A} serotonin receptor, making it a useful antipsychotic agent.[19] An antagonist is a compound that blocks the action or effect of another substance, so in this case asenapine **218** binds to and

blocks serotonin and dopamine receptors.[20] Asenapine **218** is typically prescribed to treat patients with bipolar I disorder, it is also prescribed to treat schizophrenia.[21,22]

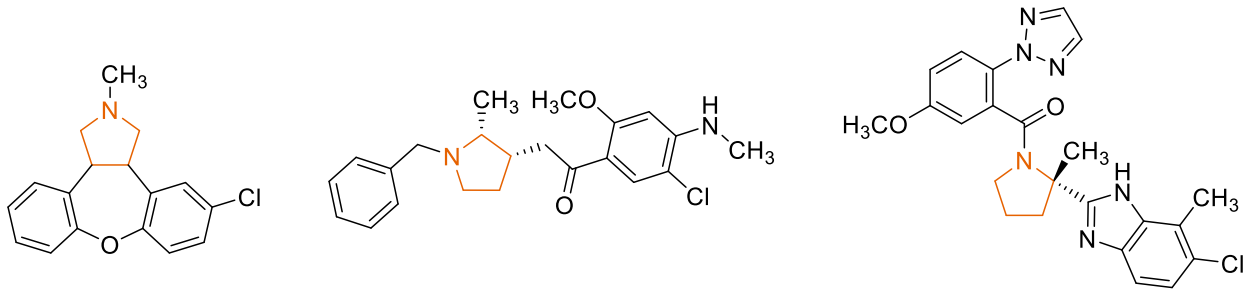

218
Asenapine

219
Nemonapride

220
Daridorexant

Figure 22. Structures of Antipsychotic Agents: Asenapine, Nemonapride, and Daridorexant

Nemonapride **219** is another pharmaceutical used to treat schizophrenia.[23] Unlike asenapine though, nemonaprode **220** is a serotonin 1A receptor (5-HT_{1A}) agonists, which is theorized to make it a more selective drug than the typically prescribed dopamine antagonists.[24] Interestingly, these agonists exhibit the same antipsychotic effects as the antagonists. However, by activating the 5-HT_{1A} receptor instead of turning off the dopamine D_2 receptor it is predicted that they have the potential to produce fewer side effects, ultimately making **219** an attractive drug candidate.[24]

In 2022, a new therapeutic, daridorexant **220**, became available in both the US and the EU to treat insomnia.[25] Daridoxrexant **220** is a duel orexin receptor antagonist (DORA) blocking OX1R and OX2R.[25-28] Blocking these receptors inhibits the binding of wake-promoting neuropeptides known as orexins, thereby allowing the subject to both fall asleep and stay asleep.[26-28] This drug is different from typical sleep aids because they commonly target gamma-aminobutyric acid type-A (GABA-A), serotonin, histamine, or melatonin receptors.[25] Daridoxrexant **220** offers an alternative for patients taking other medications that are incompatible with the traditional sleep aids.

3.1.2.5 Stimulants

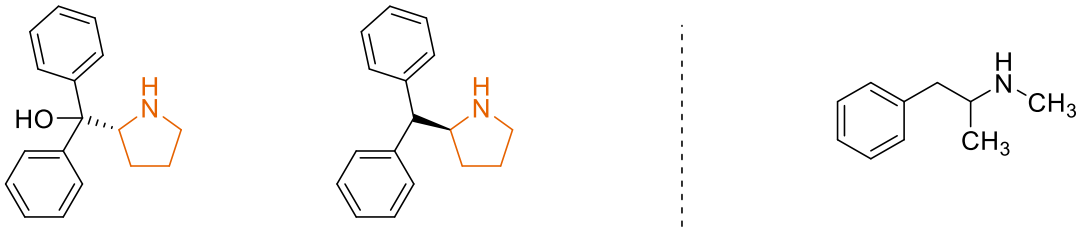

221
D2PM

222
Desoxy D2PM

223
Methamphetamine

Figure 23. Structures of Recreational Stimulants

Pyrrolidines **221** and **222** act as norepinephrine-dopamine reuptake inhibitors, producing amphetamine-like effects.[29,30] In a legal grey area, these are marketed as "legal highs" since they produce the same stimulating psychoactive effects as more widely known illicit drugs, such as methamphetamine (**223**), while circumventing the current drug controls in effect.[30] Additionally, since these compounds are not included in the analysis for standard drug tests, they will not result in a positive drug test result.[30] Researchers are working to stay up to date on what new designer drugs are being used in order to screen for their toxicologies as well as their potential pharmacological properties.[30] These are just a couple of examples of the rich psychoactive properties of pyrrolidine moieties.[31,32]

3.1.2.6 Antidiabetics

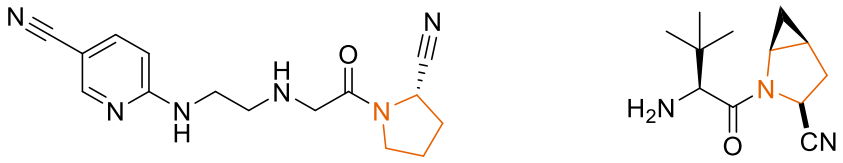

224 **225**

Figure 24. Structures of Antidiabetic Agents Synthesized by Villhauer and Coworkers (224),[33, 34] and Robl and Coworkers (225).[35]

Researchers have reported novel pyrrolidine derivatives **224** and **225** (Figure 24) with potent antihyperglycemic activities through inhibition of dipeptidyl peptidase IV (DPP-IV).[34,35] This is an emerging and valuable route to the treatment of type 2 diabetes through DPP-IV inhibition and its connection with the incretin glucagon-like peptide-1 (GLP-1).[36] Incretins are hormones found in our gut that regulate the amount of insulin that is secreted after eating, so low levels of GLP-1 result in lower insulin levels and higher glucose levels.[34] There are multiple mechanisms of action and it is difficult to fully elucidate direct trends, but Holst and Deacon have been able to directly link DPP-IV inhibition with increased active levels of GLP-1.[36] This is incredibly beneficial because GLP-1 serves many functions that contribute to normalizing glucose levels making this relationship important to the treatment of type 2 diabetis.[36]

3.1.2.7 Anticancer Agents

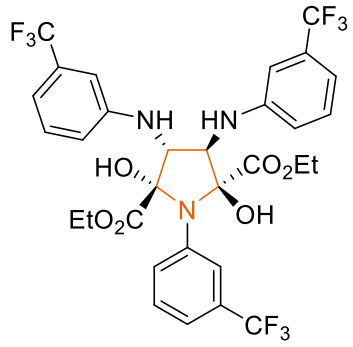

226

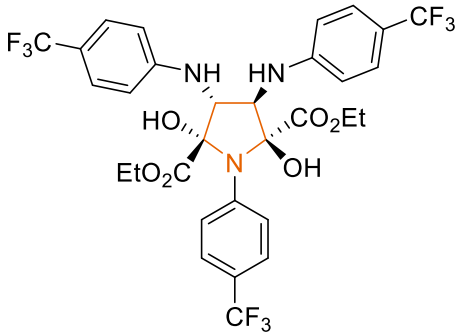

227

Figure 25. Structures of Anticancer Pyrrolidine Derivatives.[37]

Hu and coworkers studied a series of pyrrole and pyrrolidine analogues for their anticancer properties.[37] Pyrrolidines **226** and **227** exhibited IC_{50} values of 4.1 μM and 4.3 μM respectively against HCT116 (colon cancer) cell lines.[37] Moreover, both **226** and **227** showed potent cytotoxicity against nine other cancer cell lines making these pyrrolidine derivatives promising therapeutics in cancer research.[37]

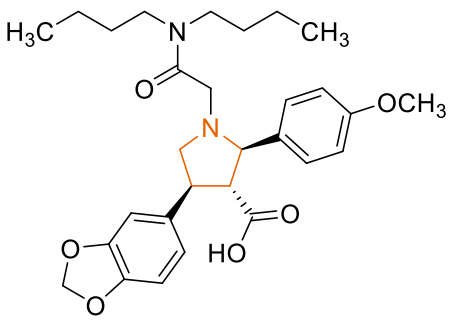

228
Atrasentan

Figure 26. Structure of Atrasentan[38]

Endothelin receptor A (ETAR) is a regulatory system of major relevance in human breast cancer. The study by Smollich and coworkers suggests that breast carcinoma invasiveness is triggered by the release of intracellularly stored endothein 1 (ET-1).[39] This signaling from tumor hyperlexia that causes carcinoma invasion may be inhibited by selective ETAR antagonism, thus paving the way to a new therapeutic target.[39] Atrasentan (**228**) is a selective ETAR antagonist that has promising potential in breast cancer treatment.[39] It also demonstrated direct effect on tumor proliferation, apoptosis, and angiogenesis in advanced non–small cell lung cancer.[38] Due to atrasentan's (**228**) promising anticancer properties, pyrrolidine derivatives of the like could potentially serve as a new generation of cancer therapeutics.

3.1.3. Naturally Occurring Pyrrolidines

Pyrrolidines are ubiquitous in natural products and are known to exhibit a diverse range of bioactive properties.[40] There are around 80 pyrrolidine alkaloids known, and many of these alkaloids are repeatedly found in different plant species.[40] For example. Hygrine is a common alkaloid that has been isolated from many different plant species including *Erythroxylum coca*.[41-45] Moreover, hygrine (**229**) is a biosynthetic precursor for both hyoscyamine and scopolamine, and it has been the subject of many different total synthesis projects dating back to as early as 1917.[46-

[48] Proline (**230**) is a naturally occurring amino acid that has been used as a catalyst in asymmetric synthesis for decades.[49,50]

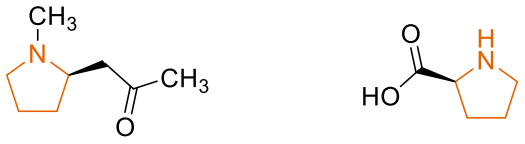

229
Hygrine

230
Proline

Figure 27. Small and Simple Naturally Occurring Pyrrolidines: Hygrine, Proline

Arisarum vulgare, or friar's cowl, is a flowering perennial that is widespread along the Mediterranean coast. Historically in Morocco, the tubers of this plant were consumed during periods of food scarcity which is problematic because it contains several toxic alkaloids. Among these alkaloids are pyrrolidine derivatives **231** (irniine) and **232** (bgugaine). Specifically, both **231** and **232** are hepatotoxins, which means that they causes liver damage in humans, and can cause other problems in live-stock.[51]

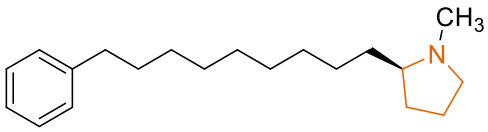

231
Irniine

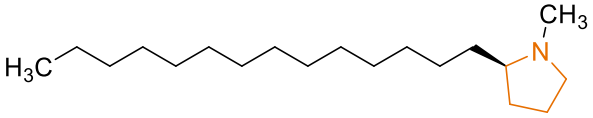

232
Bgugaine

Figure 28. Structures of Heptatotoxins Irniine[52] and Bgugaine[53] Isolated from *Arisarum vulgare*.

Liu and coworkers isolated alkaloid **233** from the root bark of *o. japonica* and found that this showed potential in serving as both a larvicide and nematicide. This natural remedy would be

beneficial particularly in underprivileged areas that are still ravaged by diseases carried by mosquitos such as malaria, dengue fever, wuchereriasis, and epidemic encephalitis B.[54] Many pesticides are toxic to other organisms, including people, so researchers are actively searching for more natural and more targeted alternatives.[54] Surprisingly enough, nicotine **234** is one of the botanical pesticides currently in use as of 2006.[55]

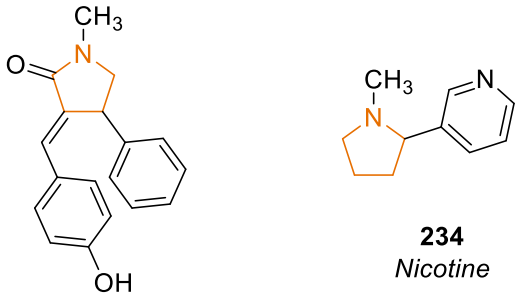

233 **234** *Nicotine*

Figure 29. Pyrrolidine Alkaloid Isolated from *O. Japonica* Root Barks and nicotine

Hyacinthoides non-scripta[56] (blue bells) and *Hyacinthus orientalis* (*Hyacinth*)[57] are not just simply beautiful flowers; they contain pyrrolidines that could lead to a new type of therapeutic for type-2 diabeteis.[56,57] Pyrrolidines **235-236** inhibit glycogen phosphorylase (GP) through an orthogonal mechanism of action that is entirely distinct from other known inhibitors.[58] Pyrrolidine **237** was further studied and it exhibited anti-hyperglycemic effects predominantly in obese mice, leading to the theory of inhibition of GP as a promising treatment in type 2 diabetes.[58]

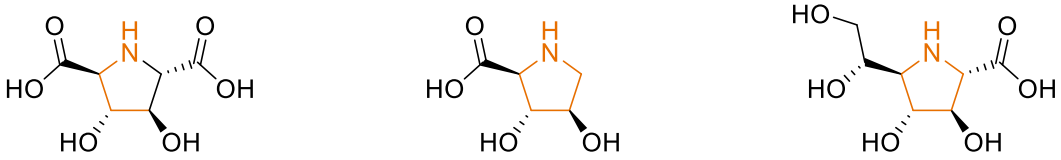

235 **236** **237**

Figure 30. Isolated from *Hyacinthoides non-scripta*[56] and *Hyacinthus orientalis*[57]

3.1.4 Synthetic Methods Forming Pyrrolidines

Researchers have extensively studied the synthesis of pyrrolidines developing a vast array of methods to achieve these privileged cores dating back to the 1920s.[59-62] The goal of this section is to highlight the most relevant synthetic methods currently in use to form pyrrolidines since an exhaustive review would be a thesis in itself. Among the methods highlighted are ones used to synthesize some of the pyrrolidine containing therapeutics discussed previously.

3.1.4.1 From Sulfinamides[63-66]

Chiral pyrrolidines are vital to medicinal research and drug discovery due to their diverse bioactivity profiles, therefore efficient and stereoselective methods of forming these compounds are essential due to the chiral nature of biology. One way to efficiently achieve chiral compounds is by installing and enantioenriched species, namely a chiral auxiliary. The Ellman auxiliary is widely used synthetic precursor in asymmetric syntheses to form enantioenriched products.[67] The *tert*-butyl group of Ellman's auxiliary acts as a directing group by providing sufficient steric bulk to block nucleophilic attack from one face of the molecule.

Scheme 47. Palladium-catalyzed nucleophilic functionalization of alkenes.[63]

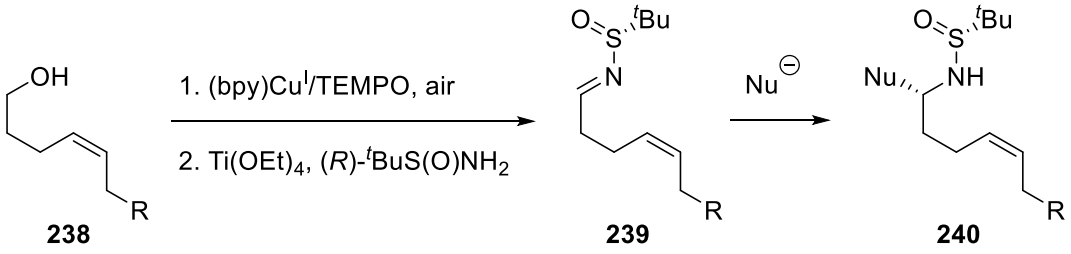

Stahl and coworkers used Ellman's auxiliary to their advantage to form pyrrolidines **241** in yields ranging from 54-85% all with diastereomeric ratios >20:1 (Scheme 46).[63] While effective in achieving good diastereoselectivity, the necessary precursor **240** to form the desired pyrrolidines **241** requires a three-step synthesis. First the alcohol was oxidized with TEMPO converting it into an aldehyde. The aldehyde undergoes a Lewis acid mediated amidation forming **239**, which is then subjected to nucleophilic attack forming the precursor **240** for the palladium catalyzed cycloamination.

The Ellman auxiliary was also used in another palladium catalyzed transformation by Stockman and coworkers where they formed a series of pyrrolidines from sulfinimines **242** and trimethylenemethane generated *in situ* from **244**.[64] Pyrrolidines **245** formed with modest diasteroselectivities (2:1 – 7:1 dr), and up to >95% yields (Scheme 47). The implementation of sulfinyl ketimines resulted in lower yields, while sulfinyl aldimines resulted in higher yields overall. An improvement to the previous palladium catalyzed example is the efficiency of this synthesis where pyrrolidines **245** can be produced in just two steps from commercially available reagents. Additionally, this system is bimolecular which increases the variability possible with this chemistry as opposed to a unimolecular system.

Scheme 48. [3+3]-Cycloaddition of Chiral Sulfinimines with Trimethylenemethane Generated *in situ*.[64]

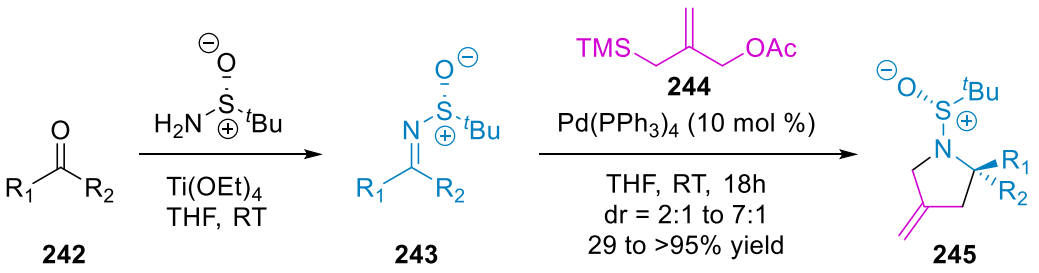

Chemla and coworkers reported a tandem 1,4-addition/carbozincation forming substituted pyrrolidines **251** in yields up to 83% with diastereomeric ratios ranging from 9:1 to >95:5 dr.[65] They were able to deduce that the interactions of $Sm(OTf)_3$ with the radical intermediate from **250** being primarily responsible for the observed diasteroselectivity.[65,68] While this method does afford chiral pyrrolidines in a selective manner, it suffers from multiple steps to render the desired pyrrolidines.[65] Intermediate **248** is formed in three steps starting with the condensation of Ellman's auxiliary and silylacetylenic aldehyde under Lewis acidic conditions resulting in *N*-propargyl sulfinimines.[65] After reduction, the sulfinamides were treated with *n*BuLi to form their respective lithium salts to then undergo allylation resulting in intermediates **250**.[65] The resulting pyrrolidines **251** were produced by a zinc-radical-transfer based 1,4-addition/cyclization of **250**.[65]

Scheme 49. Zinc Radical Transfer Based Modular Approach to Enantiopure Alkylidene-β-prolines from *N*-(*tert*-Butylsulfinyl)-α-(aminomethyl)acrylates[65]

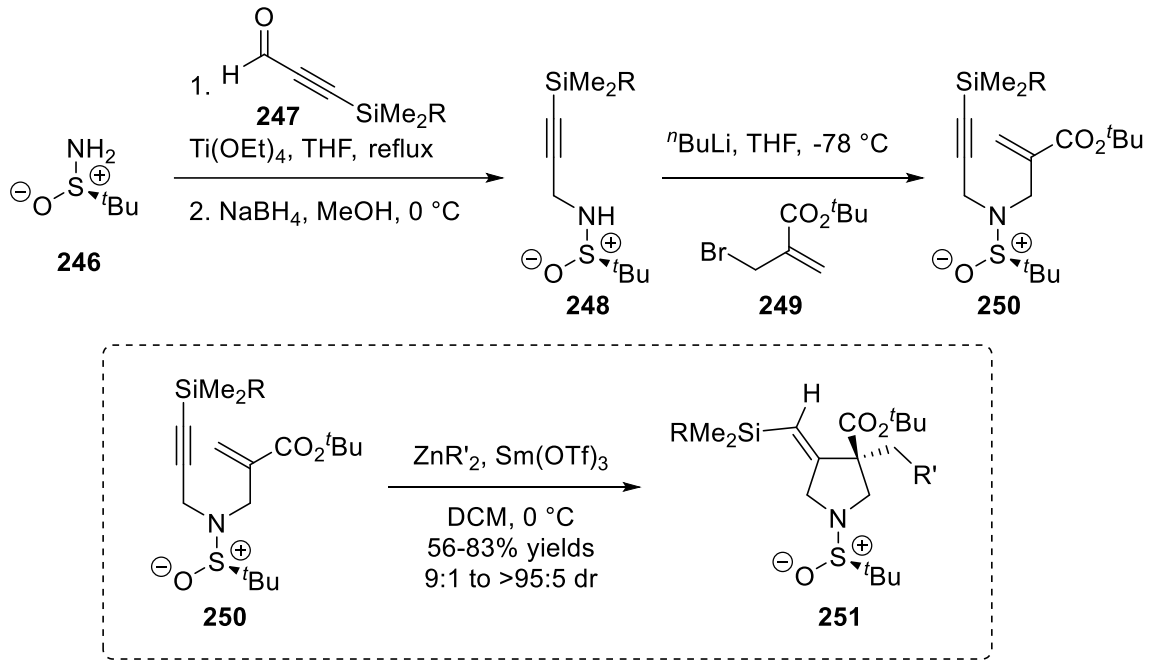

Kudale and coworkers reported the synthesis of nitrogen containing heterocycles in a single diastereomer by a modified Mitsunobu reaction with Tsunoda's reagent **256**.[69] Among the

heterocycles synthesized from this method were pyrrolidines **257** that formed in moderate yields (Scheme 49).[69] Kudale and coworkers also made use of Ellman's auxiliary to produce **257** in four steps by first forming the sulfinimine through a simple condensation reaction of a commercially available aldehyde.[69] Sulfininimine **252** was then reduced and alkylated forming **254** which then was used in a selective hydroboration method developed by Xu and Lin forming **255**.[70] The pyrrolidine formation step starts with activating the alcohol functional group using Tsunoda's reagent by converting it into a better leaving group while also producing acetonitrile as a biproduct.[69] The activated alcohol then undergoes nucleophilic attack by the sulfinamine forming the pyrrolidine ring **257** and eliminating trialkyl phosphine oxide. This is a very selective transformation, but the necessary precursor for the pyrrolidine synthesis requires four steps to make from commercially available reagents.[69]

Scheme 50. Synthesis of Chiral Pyrrolidines with Ellman's Auxilary and Tsunoda's Reagent.[69]

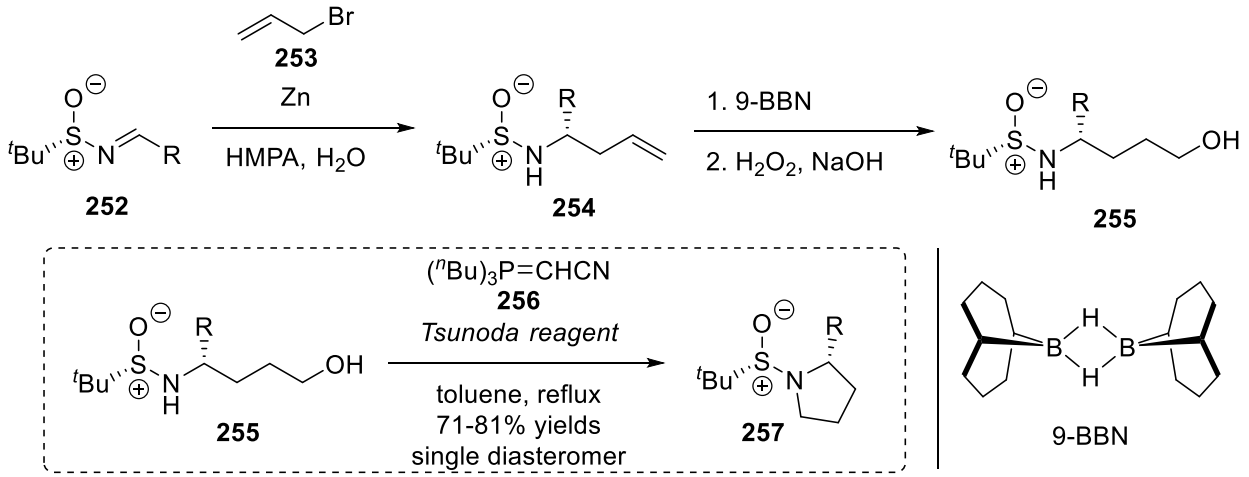

3.1.4.2 Subsequent Amination Reactions

A simple an efficient method of forming this valuable motif has been implemented as early as 1949, and it involves subsequent S_N2 reactions of an amine into a carbon chain with two leaving

groups (Scheme 50a-b).[71-73] The early examples use an amine, such as aniline or an alkyl amine, reacting with either 1,4-dicholorobutane (**259**) or 1,4-dibromobutane, while more modern examples used different leaving groups such as mesylates (**262**).[71-76] Elderfield and Hagemam refluxed butylamine (**258**) with 1,4-dichlorobutane (**259**) in ethanol to form pyrrolidine **290** in a 52% yield in 1949 (Scheme 50a).[71] Nearly 70 years later, Smith and coworkers used this same methodology with chiral precursors **261** and **262** to form enantiopure pyrrolidines **263** in up to 87% yield (Scheme 50b).[75] These pyrrolidines (**263**) were then used as building blocks for a new potential therapeutic targeting tamoxifen-resistant breast cancer.[75]

Scheme 51. Amination Cyclizations.[71,75]

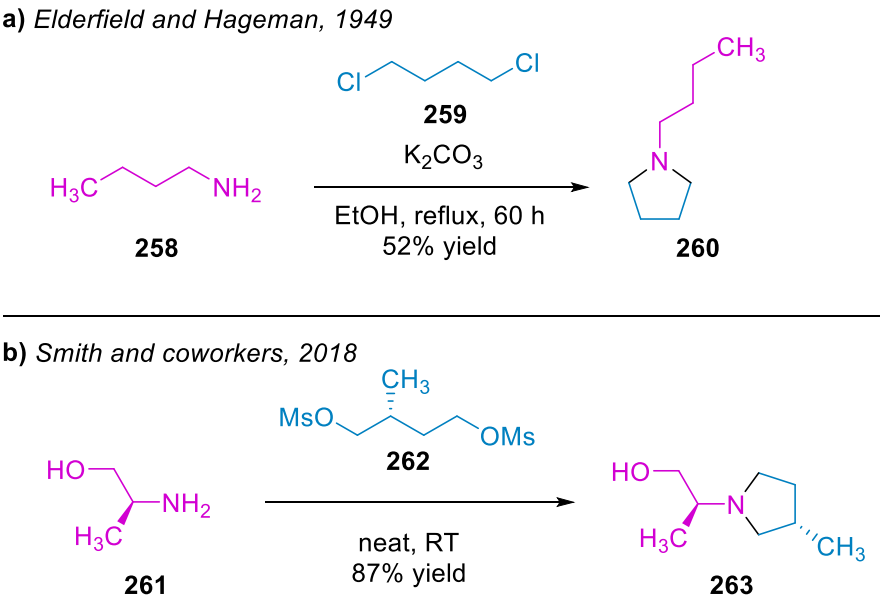

3.1.4.3 Microwave-Assisted Aminations

Microwave technology has aided in propelling this chemistry into the modern age by greatly expanding the substrate scope and improving the reaction times as well as yields.[77-79] Ju and Varma did a comparative study on traditional vs microwave methods for pyrrolidine synthesis using aniline derivative **264** and 1,4-dibromo butane (**265**).[78] They found that microwave heating not

only decreased the reaction time from 480 min to 20 min, but it also improved the reaction yield of **266** by 35% (Table 4).[78]

Table 4. Comparison of traditional and microwave methods producing pyrrolidines

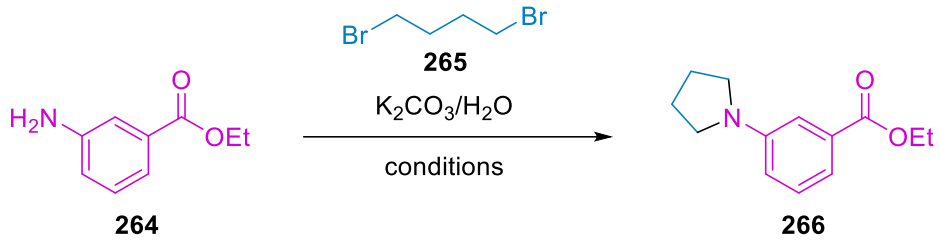

264 **266**

Method	**Time (min)**	**Yield (%)**
Conventional heating to reflux	480 min	58
Microwave (120 °C, 80-100 W)	20 min	93

The aminations of dimesylate **267** by microwave irradiation forming protected iminosugars **269** was established by Wu and coworkers (Scheme 51).[79] When attempting this transformation without microwave irradiation, incredibly low or no yields were obtained for the desired pyrrolidines, however with microwave assistance pyrrolidines **269** were achieved in excellent yields.[79] Moreover several of these transformations were done under solvent-free conditions, morphing this method into a greener approach to this chemistry.[79] This work is an effective demonstration of the advantage microwave assistance provides to further innovate and expand established tranformations.[79]

Scheme 52. Microwave Assisted Amination Forming Protected Iminosugars.[79]

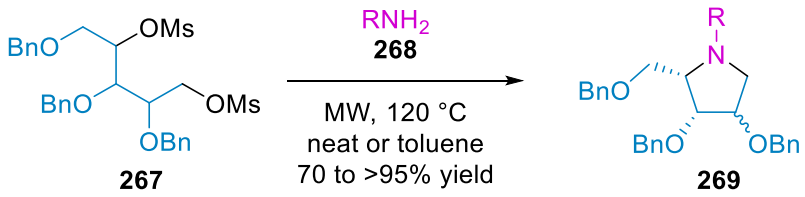

267 **269**

3.1.4.4 Transition Metal Catalyzed Hydroamination

Intramolecular hydroamination of unactivated alkenes is of interest as an atom economical synthetic strategy of to form nitrogen containing heterocycles. This has typically been done as a transition metal catalyzed C-N bond forming reaction with numerous examples in the literature using various transition metals, lanthanides, actinides, and alkali earth metals.[80] Within the last couple decades the main focus in this field has been on improving this transformation by implementing late transition metal catalysts, such as palladium,[81] platinum,[82,83] gold,[84] iridium,[85-87] rhodium,[88] and iron.[89] Many of these methods suffer from complex ligand systems that are not commercially available as well as substrates that require additional steps to make.

Hesp and Stradiotto have developed an intramolecular hydroamination reaction protocol to form pyrroidines **272** using a commercially available iridium precatalyst **271** with the active catalytic species forming *in situ* (Scheme 52). They demonstrated 15 examples from unactivated alkenes (**270**) with yields ranging from 52-89%. While the substrate requires a multistep synthesis, the advantage of their method over similar ones is that the catalyst is commercially available and it does not require an additional ligand to be synthesized.

Scheme 53. Iridium Catalyzed Hydroamination[87]

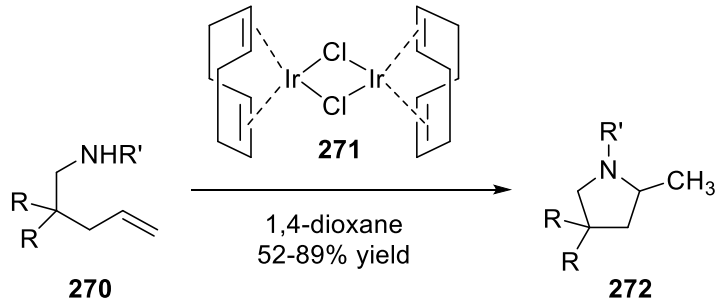

3.1.4.5 Cyclization of γ-Aminocarbonyl Compounds

γ-Aminocarbonyl derivatives have been used as intramolecular precursors to form substituted pyrrolidines in complex synthetic targets.[90] King and coworkers used this method to form simple

pyrrolidine motifs **274**-**275** from γ-aminoacetals **273** in good yields (Scheme 53a).[91,92] This protocol was then modified to form more complex structures with fused rings **277** from a similar starting material **276** (Scheme 53b). King and coworkers proposed that this occurs due to an unprecedented 1,2-phenyl shift which results in the formation of the final fused structure of **277**. The substrate is not commercially available, however it can be readily synthesized in one step. Due to this being a unimolecular system, there is an inherent limitation in the substrate scope availability, which hinders the synthetic utility of this transformation.

Scheme 54. Cyclization of γ-Aminoacetals Forming Pyrrolidines[91,92]

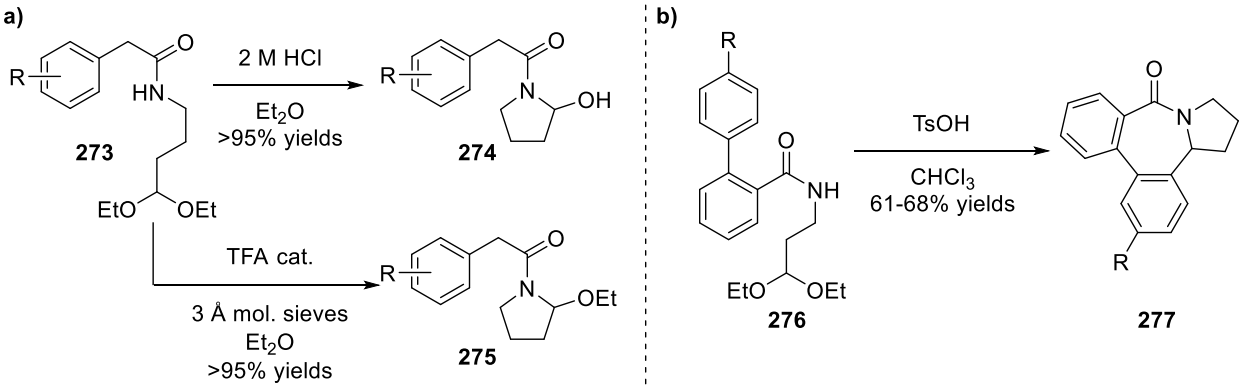

Blachert and Stragies used a similar strategy to form the final fused-ring system **280** in their total synthesis of tetraponerines natural products.[93] They were able to accomplish the total synthesis of **280** in eight total steps (Scheme 54).[93] The acid mediated cyclization was versatile enough to form all eight of the pyrrolidine containing natural products **280** from their respective intermediates, which demonstrates the synthetic utility and convenience of this cyclization method for late stage complex ring formations.[90,93]

Scheme 55. Total Synthesis of Tetraponerines Isolated from the venom of the New Guinean ant *Tetraponerasp*.

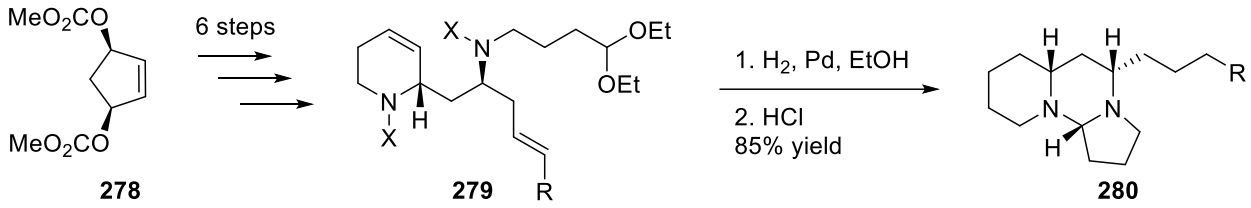

278 279 280

3.1.4.6 [3+2]-Cycloadditions

1,3-dipolar cycloadditions have been a long time and prominent method of forming pyrrolidines utilizing the generation of the 1,3-dipole, also referred as the azomethine ylide.[94] There are numerous ways to generate the azomethine ylide with the simplest being from commercially

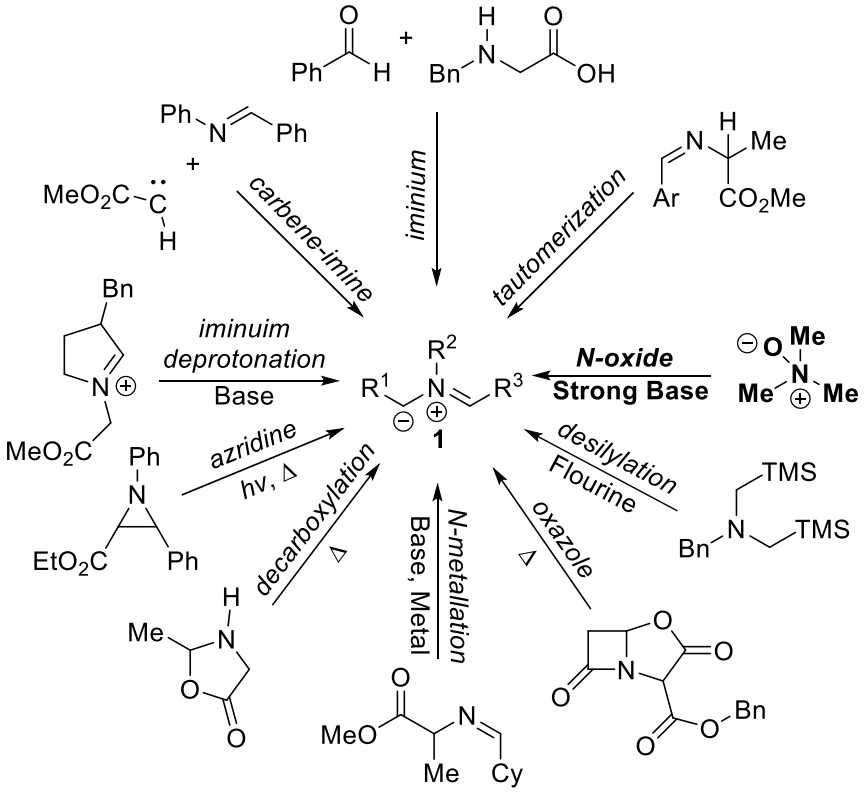

Figure 31. Common Methods of Azomethine Ylide Formation.[95] Reprinted with permission from Neal, M. J.; Hejnosz, S. L.; Rohde, J. J.; Evanseck, J. D.; Montgomery, T. D. Multi-Ion Bridged Pathway of *N*-Oxides to 1,3-Dipole Dilithium Oxide Complexes. *J. Org. Chem.* **2021**, *86* (17), 11502–11518. https://doi.org/10.1021/acs.joc.1c01047. Copyright 2021 American Chemical Society.

available *N*-oxides and base (Figure 31).[95] [3+2]-cycloadditions are an advantageous method of forming pyrrolidines with more substrate scope variability than most of the methods previously described. Many of those methods focused on a long carbon chain and an amine as synthons, limiting diverse functionalization. Moreover, those synthetic precursors are typically not commercially available and require multiple steps to form, limiting their transferability to other synthetic groups. Whereas, the synthons in [3+2]-cycloadditions are generally comparable in size, with each piece being able to change the overall shape of the final compound greatly. Additionally, just by going from a unimolecular system to a bimolecular system there is an inherent increase in the substrate scope variability.

Scheme 56. [3+2]-Cycloadditions of TMAO and Alkynes.[96]

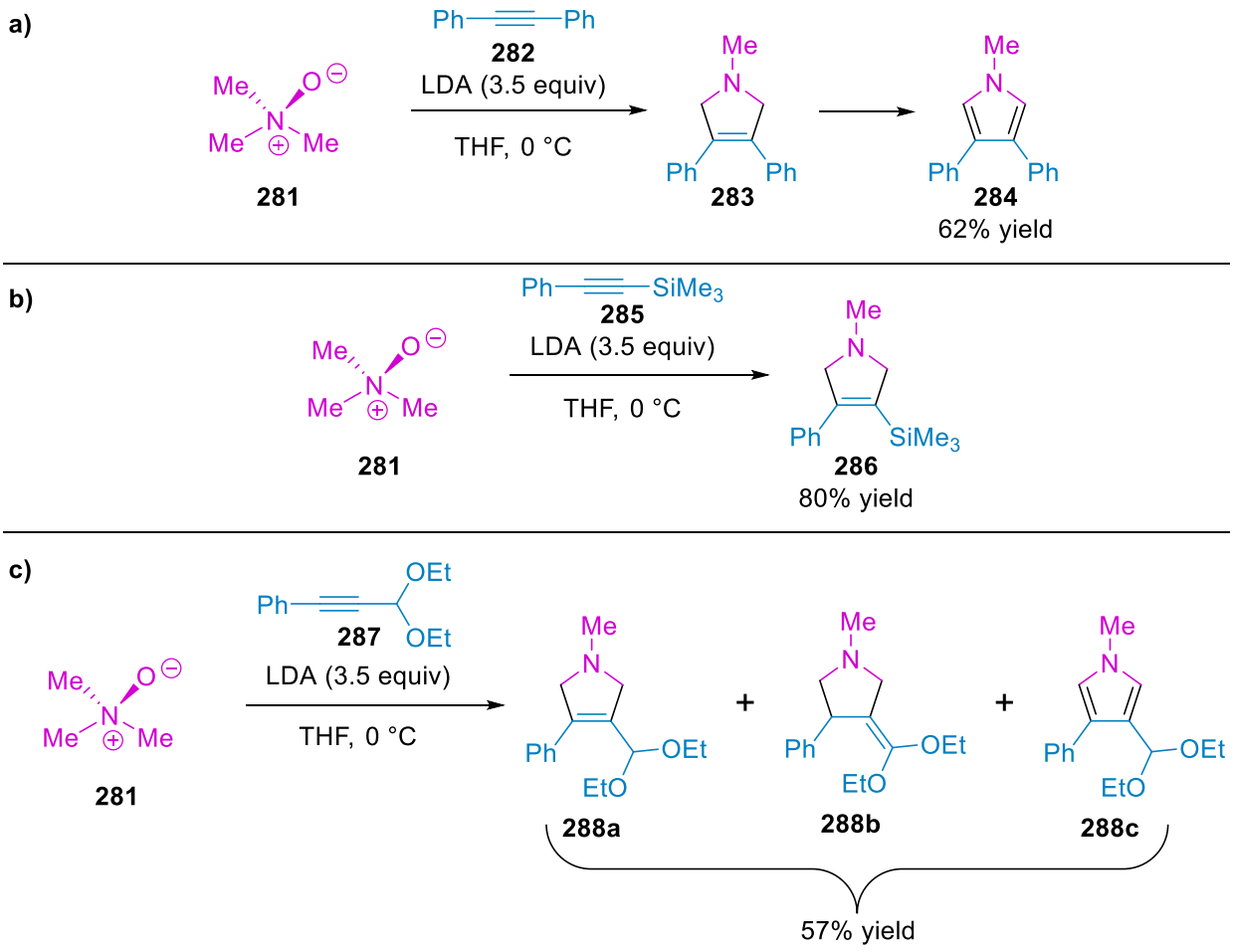

Roussi and coworkers developed an efficient [3+2]-cycloaddition of trimethylamine *N*-oxide (TMAO) **281** and various dipolarophiles providing rapid access to various nitrogen containing heterocycles such as pyrroles **284**, pyrrolines **286** and **288** (Scheme 55), and their fully saturated pyrrolidine derivatives (Scheme 56). The reactions forming pyrroles and pyrrolines achieved moderate yields (Scheme 55a-b), but some products were subject to tautomerization (Scheme 55). Gratifyingly this transformation is not just limited to aryl substituted dipolarophiles **282**, it is tolerant of silanes **285** and ethers **287** (acetals) as well.

A limitation of this method is that it is not regioselective as demonstrated by implementing *N*-oxide **289** into the reaction and a mixture of isomers formed **281a-c** (Scheme 56).[97] This selectivity issue can be mitigated by the use of a symmetrical *N*-oxide like TMAO **281**, or an *N*-oxide with only two positions bearing α-protons, limiting the possibilities to a single constitutional isomer.

Scheme 57. Regioselectivity of the [3+2]-Cycloaddition of Roussi and Coworkers[97]

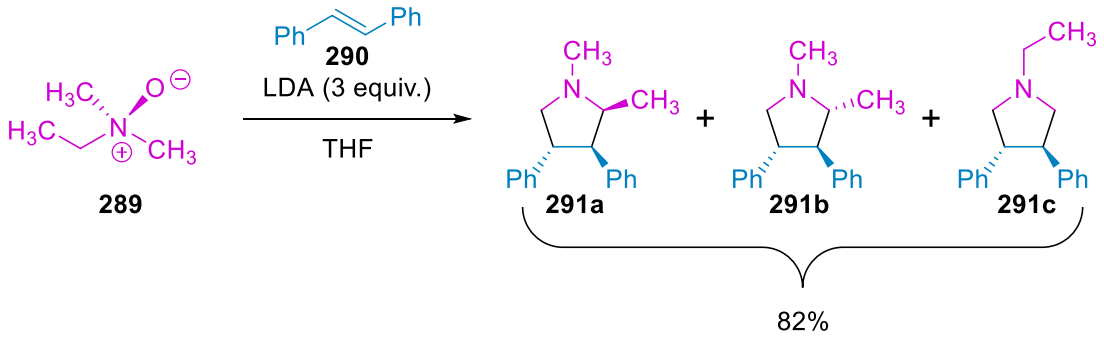

The [3+2] cycloaddition of TMAO **281** and *trans*-stilbene **290** was originally reported by Roussi and coworkers in 1983,[99] but it was revisited by Davoren and coworkers at Pfizer in 2010 noting that this method provided them with access to pyrroldines **293a-e** that are otherwise inaccessible by other synthetic methods (Scheme 57).[98] Moreover in 2016, Liu and Bao used this chemistry for rapid access to a series of pyrrolidine derivatives **293f-m** that were anticipated to mimic the antioxidant effects of resveratrol (Scheme 57).[5] This method allowed researchers to form

privileged motifs for drug research in one step from base starting materials making this an attractive synthetic route.

Scheme 58. Base Mediated Cycloaddition of TMAO and Aryl-Alkenes[5,98]

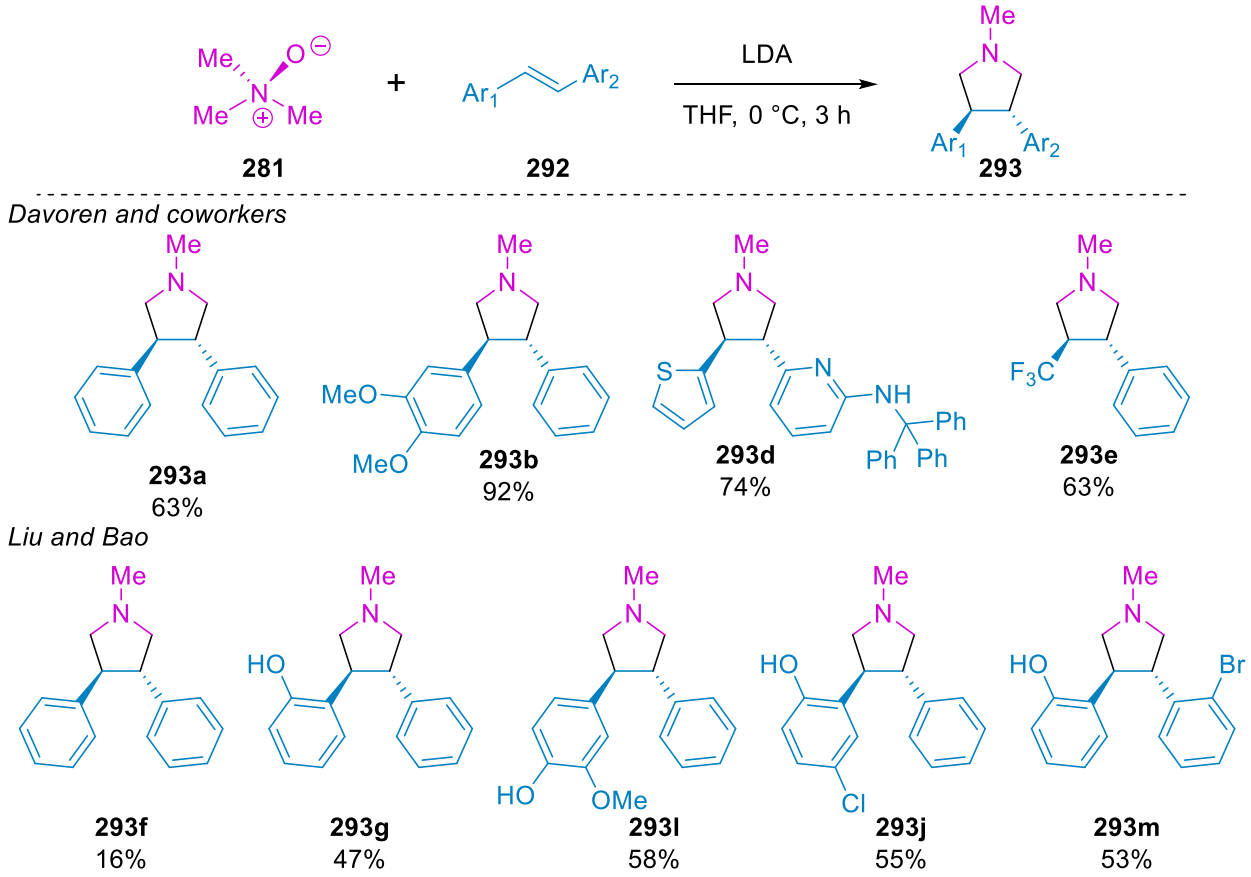

Acid mediated cycloadditions make use of 293, a different azomethine ylide precursor, with alkenes to form 3,4-substitited pyrroldines 295 (Scheme 58).[5] This method is tolerant of electron deficient alkenes only, making it a complementary approach for the base mediated transformation as that works best with electron rich olefins.

The disadvantage with the acid mediate conditions, however, is that the azomethine ylide precursor 293 is not widely commercially available nor is it cost effective to purchase ($1,600/gram);[100] this precursor required a two-step synthesis to make from base starting reagents. Another limitation of this method is that it is only tolerant of deficient olefins.[5]Both the acid and base mediated

conditions have pros and cons, but overall, the base mediated cycloaddition has the inherent advantage of commercially available synthetic precursors and a broader substrate scope.

Scheme 59. Acid Mediated Cycloaddition of Aryl-Alkenes.[5]

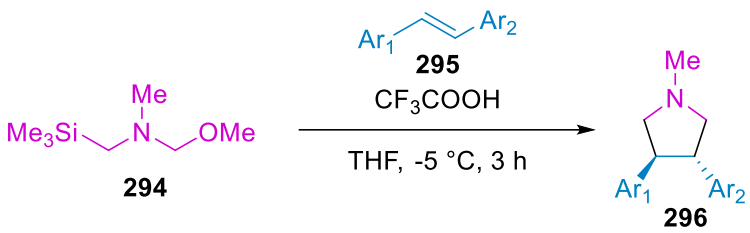

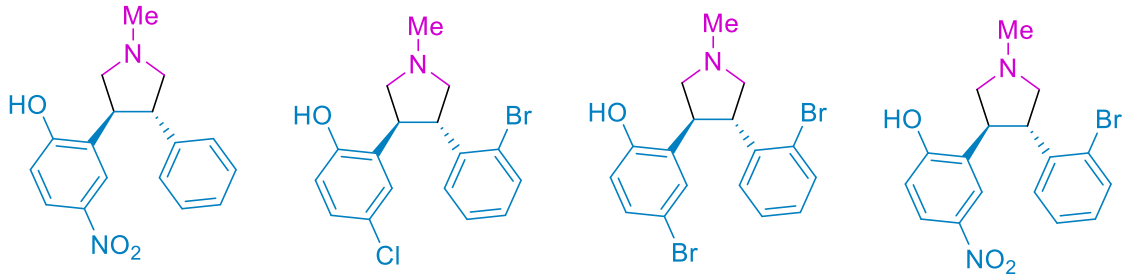

296a 92%

296b 66%

296c 76%

296d 76%

3.2 Results and Discussion

3.2.1 Reaction Optimization

The [3+2] cycloadditions of tertiary amine *N*-oxides and dipolarophiles, mainly alkenes, was established by Roussi and coworkers as a simple and powerful method of forming nitrogen rich heterocycles.[96,97,99] This chemistry was then repeated by Davoren and coworkers about two decades later in 2010, and the substrate scope was further expanded by Liu and coworkers in 2016.[5,98,99] Looking at these results, however, there is an interesting discrepancy with the reaction of trimethylamine *N*-oxide (**281**) and *trans*-stilbene (**290**) where the yield reported by Roussi and coworkers was 72%,[99] while the yield reported by Davoren and coworkers was 63% yield,[98] and then the yield by Liu and Bao was 16% (Scheme 60).[5] We decided a good start to our work with

expanding this substrate scope was to replicate this transformation to use both literature results as benchmarks.

Scheme 60. [3+2]-Cycloaddition of TMAO and *Trans*-Stilbene.

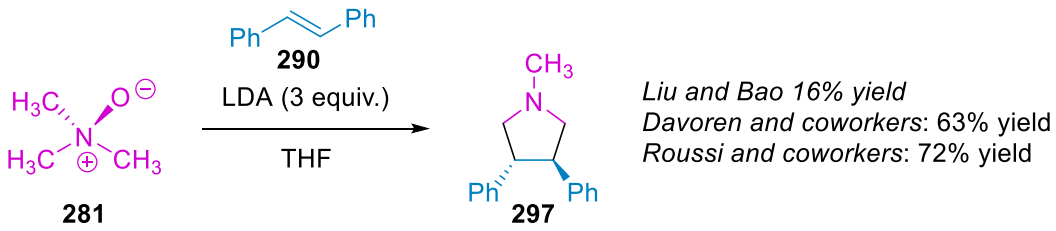

Table 5. Examining work-up conditions

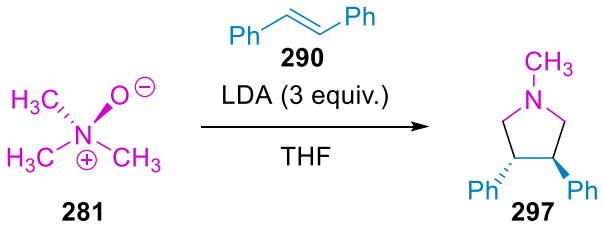

Entry	Aqueous Work-Up Method	Yield[c] (%)
1	quench with sat. NH_4Cl solution	81
2	quenched w/ pH 7 buffer	35
3	quenched w/ NH_4Cl soln and washed w/ bicarb	78
4	quenched w/ water	81

[a]Standard reaction conditions: 1 equiv. *N*-oxide, 1 equiv. trans stilbene, 3 equiv LDA, 0.1 M THF. [b]Standard aqueous work-up: quench with sat. NH_4Cl solution and extract with EtOAc (3X's), dry over $MgSO_4$ and concentrate. Purify by FCC. [c]Isolated yields

The specific aqueous work-up method conditions from Roussi's reports were slightly ambiguous i.e., "acid-base extraction". To try and replicate their results, several different standard aqueous

work-up conditions were tested (Table 5). Intriguingly, the isolated yields of pyrrolidine **297** were already higher than those reported in the literature (Table 5). This result was encouraging as this suggest that this transformation needed some more optimization to really uncover its full potential (Table 5). Quenching the reaction with saturated ammonium chloride solution and carrying out the aqueous work-up resulted in 81% yield (Table 5, entry 1). When ammonium chloride solution was replaced with a pH 7 buffer solution the yield decreased to 35% (Table 5, entry 2). Quenching the reaction with ammonium chloride solution and then basifying the aqueous layer with saturated sodium bicarbonate solution also resulted in a lower 78% yield (Table 5, entry 3). The simplest solution of just quenching the reaction with water and working it up resulted in the same yield as quenching with ammonium chloride solution (Table 5, entry 4).

Table 6. Time of addition of *trans*-stilbene into reaction mixture

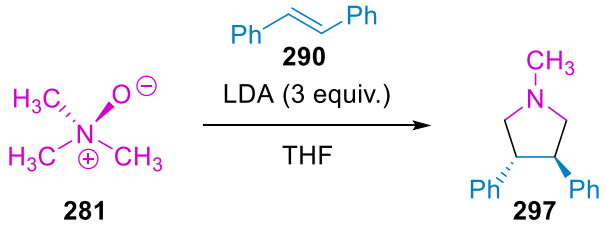

Entry	Time of Addition of 11	NMR Yield (%)[a,d]
1	Control[b]	86 (95)[c]
2	0 h	82
3	1 h	34
4	2 h	15
5	3 h	3

[a]NMR calculated using 1,3,5-trimethoxybenzene standard.[101] [b]Stilbene was added as a solution for the control. Average NMR yield of five reactions. [c]Isolated yield. [d]Average of three reactions.

We next wanted to determine the optimal time for the addition of the dipolarophile **290**. For the initial reaction conditions, *trans*-stilbene (**290**) and TMAO (**281**) were added to the reaction flask, dissolved in THF, and cooled to -78 °C, etc. This could be counterintuitive because per the proposed mechanism, the azomethine ylide must first form for the cycloaddition with the dipolarophile to even occur, so later additions of *trans*-stilbene (**290**) were examined (Table 6). Since *trans*-stilbene (**290**) is a solid, it was added as a solution for this reaction set (including the control reaction) in order to reduce the potential of air breaching the reaction vessel. This resulted in no change in yield from the control, which resulted in a 95% isolated yield for **297** (Table 6, Entry 1). Changing the order of addition by adding *trans*-stilbene (**290**) after LDA resulted in very little change in yield (Table 6, Entry 2). The yield decreased with later additions of *trans*-stilbene (Table 6, Entries 3-4), proving that the optimal time to add the dipolarophile is either with the *N*-oxide before the LDA, or just after the LDA addition (Table 6, Entries 1-2).

Table 7. Rate of addition of *trans*-stilbene into reaction mixture

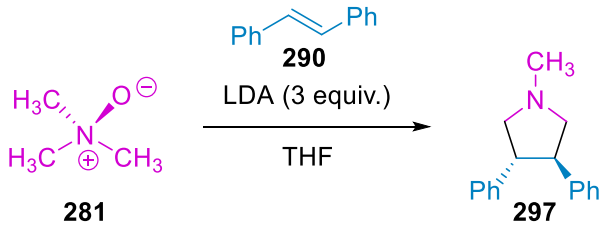

Entry	Comments	NMR yield (%)[a]
1	Control	83
2	One Aliquot	83
3	Drop-wise	69
4	Drop-wise over 30 min	15

[a]NMR yield determined from 1,3,5-trimethoxybenzene standard.[102] Reported as the average of two experiments.

Table 8. Cycloaddition reaction time

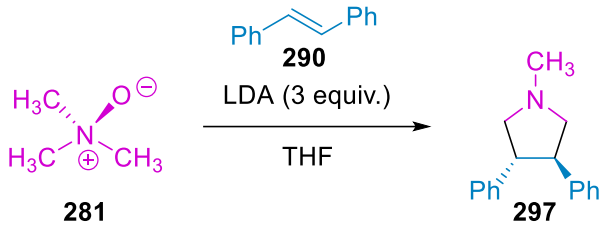

Entry	Reaction Time	NMR Yield[a]
1	5 min	48[b]
2	15 min	57[b]
3	30 min	75[c]
4	1 h	78[b]
5	2 h	83[c]
6	3 h	82[b]

[a]NMR yield determined from 1,3,5-trimethoxybenzene standard. [b]Reported as the average of two experiments. [c]Reported as the average of four experiments.

The rate of addition of *trans*-stilbene (**290**) was then investigated in order to see if there is any change in the yield of reaction. Again, since the azomethine ylide must form first for the cycloaddition to occur, it was hypothesized that slower additions of the dipolarophile could be beneficial for this transformation. Adding *trans*-stilbene (**290**) at the same time as TMAO (Table 7, Entry 1) resulted in the same yield as adding *trans*-stilbene (**290**) in one aliquot as a solution in THF just after the addition of LDA (Table 7, Entry 2). This is consistent with the results from the time of *trans*-stilbene experiments in Table 6. Dropwise addition of *trans*-stilbene resulted in a slightly lower yield (Table 7, Entry 3), and dropwise addition over 30 min resulted in only a 15%

yield, however this result is likely unreliable since the solution kept freezing on the needle resulting in uneven addition over the time period (Table 7, Entry 4).

Next, we varied the reaction time to find the optimal timeframe for the reaction to occur. The reaction progress was monitored by ^{1}H NMR and surprisingly after just five minutes, 48% yield was achieved (Table 8, Entry 1). The NMR yield increases with increasing reaction time (Table 8, Entries 1-5), until the two- and three-hour marks are reached where the reaction yield stays consistent (Entries 5-6). Moving forward, two hours was used as the optimal reaction time.

3.2.2 Substrate Scope

Mostly aryl alkenes have been used where Roussi and coworkers have demonstrated that this chemistry is tolerant of other functional groups such as ethers and silanes (Scheme 55). While they have implemented these functional groups with alkynes, it is curious why they neglected to report any of these functional groups with alkenes.

Scheme 61. Reactions of TMAO and Alkenes[a]

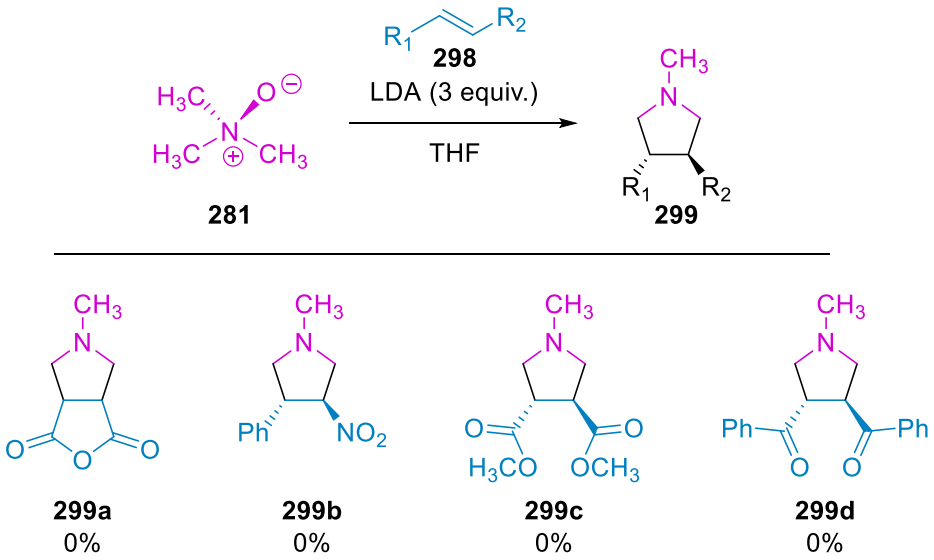

In order to further expand the substrate scope we investigated a series of alkenes that have not been reported for this transformation (Scheme 61). Maleic anhydride **298a**, a standard dipolarophile,

was implemented into this transformation but the desired product did not form after several attempts. In each case the reaction turned dark purple in color, and neither staring material nor pyrrolidine **299** were present in the crude ^{1}H NMR.

When an electron withdrawing nitro group was implemented **298b**, pyrrolidine **299b** did not form in an appreciable amount. The crude ^{1}H NMR showed a complex mixture of products which we were not able to successfully isolate nor identify. Electron-withdrawing groups being incompatible with these reaction conditions does have literature precedent; this was reflected in the work by Lui and Bao where they had to switch the azomethine precursor from an *N*-oxide to **294**, along with the reaction conditions to an acid mediated transformation, rather than the [3+2] cycloaddition under strongly basic conditions.

Additionally, when esters **298c** and ketones **298d** were introduced to the substrate scope, neither reagent was tolerated. Both reactions resulted in a complex mixture of products that were indiscernible by ^{1}H NMR. This does align with observations in Chapter 2 where the *N*-oxide and sulfinamide formed side products. Similar to the sulfinamide, the ketone and esters are both electrophilic which could undergo nucleophilic attack by the *N*-oxide (**281**) causing side products. Another reason for the complex mixture could be that the addition of two carbonyls (**298c-d**) could interfere with the multi-ion bridge intermediate that is necessary for pyrrolidine formation. The carbonyls could effectively chelate lithium which could in turn block the multi-ion bridge from forming.

As a proof of concept a control reaction was run with the addition of **300**, and it was anticipated that the *N*-oxide **281** would react with triflate **300** to form intermediate **301** (Scheme 61). Unlike the *N*-oxide **281**, the intermediate **301** is not nucleophilic so this would make it possible to now implement dipolarophiles that have electrophilic substituents without that side nucleophilic attack

of the *N*-oxide occurring. This was carried out and pyrrolidine **297** was formed in 24% NMR yield. While not as high as the base reaction (95% yield), it still demonstrates that it is possibly to use some additive to block the nucleophilicity of the *N*-oxide. This can still be improved with further optimization experiments.

Scheme 62. [3+2] cycloaddition of TMAO and *trans*-stilbene with the addition of TMS-triflate (299).

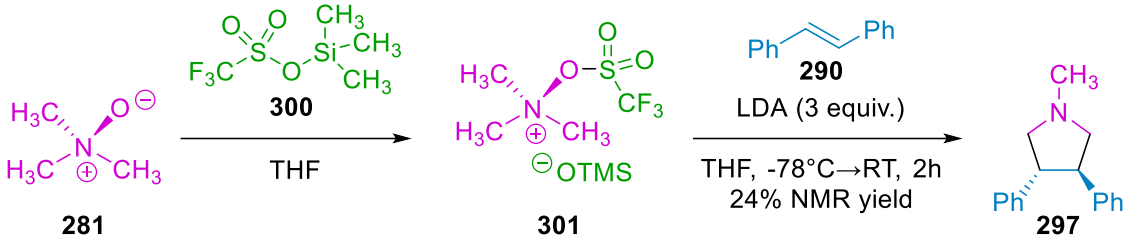

3.3 Conclusions

The reaction of TMAO and trans stilbene was studied in greater depth than reported in the literature examining various reaction conditions, and, as a result, the yield was improved from the 72% yield reported by Roussi, to 95% yield. New dipolarophiles such as maleic anhydride, *trans*-β-nitrostyrene, dimethylfumarate, and *trans*-Dibenzoylethene were implemented into the [3+2] cycloaddition with TMAO; however, after repeated attempts no pyrrolidines were formed from these substrates. Although these results were negative, they did allow us to gain insight into the substrate scope compatibility with electron-withdrawing groups such as carbonyls and nitro-groups being problematic. These observations also aligned with those from the literature and from previous experiments. Additionally, an additive such as triflate **299**, can be used for substrates that are sensitive to nucleophilic attack by the *N*-oxide. Although the yield was lower with the additive, there is still room to improve these specific reaction conditions.

3.4 References

(1) Taylor, A. P.; Robinson, R. P.; Fobian, Y. M.; Blakemore, D. C.; Jones, L. H.; Fadeyi, O. Modern advances in heterocyclic chemistry in drug discovery. *Organic & Biomolecular Chemistry* **2016**, *14* (28), 6611-6637, 10.1039/C6OB00936K. DOI: 10.1039/C6OB00936K.

(2) Bhat, A. A.; Tandon, N.; Singh, I.; Tandon, R. Structure-activity relationship (SAR) and antibacterial activity of pyrrolidine based hybrids: A review. *Journal of Molecular Structure* **2023**, *1283*, 135175. DOI: https://doi.org/10.1016/j.molstruc.2023.135175.

(3) Li Petri, G.; Raimondi, M. V.; Spanò, V.; Holl, R.; Barraja, P.; Montalbano, A. Pyrrolidine in Drug Discovery: A Versatile Scaffold for Novel Biologically Active Compounds. *Topics in Current Chemistry* **2021**, *379* (5), 34. DOI: 10.1007/s41061-021-00347-5.

(4) Bonifazi, A.; Del Bello, F.; Giorgioni, G.; Piergentili, A.; Saab, E.; Botticelli, L.; Cifani, C.; Micioni Di Bonaventura, E.; Micioni Di Bonaventura, M. V.; Quaglia, W. Targeting orexin receptors: Recent advances in the development of subtype selective or dual ligands for the treatment of neuropsychiatric disorders. *Med Res Rev* **2023**, *n/a* (n/a), https://doi.org/10.1002/med.21959. DOI: 10.1002/med.21959 (acccessed 2023/05/07). From NLM Publisher.

(5) Bao, L. L.; Liu, Z. Q. Tetrahydropyrrolization of Resveratrol and Other Stilbenes Improves Inhibitory Effects on DNA Oxidation. *ChemMedChem* **2016**, *11* (15), 1617-1625. DOI: 10.1002/cmdc.201600205

(6) Chrząścik, I. Analysis of Biologically Active Stilbene Derivatives. *Critical Reviews in Analytical Chemistry* **2009**, *39* (2), 70-80. DOI: 10.1080/15389580802570184.

(7) Kremer, J. M.; Emery, P.; Camp, H. S.; Friedman, A.; Wang, L.; Othman, A. A.; Khan, N.; Pangan, A. L.; Jungerwirth, S.; Keystone, E. C. A Phase IIb Study of ABT-494, a Selective JAK-1 Inhibitor, in Patients With Rheumatoid Arthritis and an Inadequate Response to Anti–Tumor Necrosis Factor Therapy. *Arthritis & Rheumatology* **2016**, *68* (12), 2867-2877. DOI: https://doi.org/10.1002/art.39801.

(8) Semerano, L.; Decker, P.; Clavel, G.; Boissier, M.-C. Developments with investigational Janus kinase inhibitors for rheumatoid arthritis. *Expert Opinion on Investigational Drugs* **2016**, *25* (12), 1355-1359. DOI: 10.1080/13543784.2016.1249565.

(9) Padda, I. S.; Bhatt, R.; Parmar, M. Tofacitinib. In *StatPearls [Internet]*, StatPearls Publishing, 2022.

(10) Dhillon, S. Tofacitinib: A Review in Rheumatoid Arthritis. *Drugs* **2017**, *77* (18), 1987-2001. DOI: 10.1007/s40265-017-0835-9 From NLM.

(11) Weston, G.; Strober, B. 18 - Phosphodiesterase-4 and Janus Kinase Inhibitors. In *Comprehensive Dermatologic Drug Therapy (Fourth Edition)*, Wolverton, S. E. Ed.; Elsevier, 2021; pp 199-208.e193.

(12) Wang, F.; Sun, L.; Wang, S.; Davis, J. M.; Matteson, E. L.; Murad, M. H.; Luo, F.; Vassallo, R. Efficacy and Safety of Tofacitinib, Baricitinib, and Upadacitinib for Rheumatoid Arthritis: A Systematic Review and Meta-Analysis. *Mayo Clinic Proceedings* **2020**, *95* (7), 1404-1419. DOI: https://doi.org/10.1016/j.mayocp.2020.01.039.

(13) Taldaev, A.; Rudnev, V. R.; Nikolsky, K. S.; Kulikova, L. I.; Kaysheva, A. L. Molecular Modeling Insights into Upadacitinib Selectivity upon Binding to JAK Protein Family. *Pharmaceuticals (Basel)* **2021**, *15* (1). DOI: 10.3390/ph15010030 From NLM.

(14) Ahmad, A.; Zaheer, M.; Balis, F. J. Baricitinib. In *StatPearls [Internet]*, StatPearls Publishing, 2021.

(15) Rosenmayr-Templeton, L. Industry update for May 2022. *Therapeutic Delivery* **2022**, (0).

(16) Park, B. Rinvoq Approved for Moderately to Severely Active Ulcerative Colitis. *MPR Monthly Prescribing Reference* **2022**.

(17) Loo, N.; Lawitz, E.; Alkhouri, N.; Wells, J.; Landaverde, C.; Coste, A.; Salcido, R.; Scott, M.; Poordad, F. Ombitasvir/paritaprevir/ritonavir + dasabuvir +/- ribavirin in real world hepatitis C patients. *World J Gastroenterol* **2019**, *25* (18), 2229-2239. DOI: 10.3748/wjg.v25.i18.2229

(18) Pathak, N.; Chen, Y.-T.; Hsu, Y.-C.; Hsu, N.-Y.; Kuo, C.-J.; Tsai, H. P.; Kang, J.-J.; Huang, C.-H.; Chang, S.-Y.; Chang, Y.-H.; et al. Uncovering Flexible Active Site Conformations of SARS-CoV-2 3CL Proteases through Protease Pharmacophore Clusters and COVID-19 Drug Repurposing. *ACS Nano* **2021**, *15* (1), 857-872. DOI: 10.1021/acsnano.0c07383

(19) Balaraman, R.; Gandhi, H. Asenapine, a new sublingual atypical antipsychotic. *J Pharmacol Pharmacother* **2010**, *1* (1), 60-61. DOI: 10.4103/0976-500x.64538 From NLM.

(20) National Cancer Institute, Dictionary of Cancer Terms, *Antagonist*. National Cancer Institute https://www.cancer.gov/publications/dictionaries/cancer-terms/def/antagonist (accessed 2023/05/24).

(21) Vieta, E.; Montes, J. M. A Review of Asenapine in the Treatment of Bipolar Disorder. *Clinical Drug Investigation* **2018**, *38* (2), 87-99. DOI: 10.1007/s40261-017-0592-2.

(22) Room, P.; Tielemans, A. J. P. C.; De Boer, T.; Van Delft, A. M. L.; Tonnaer, J. A. D. M. The effect of the potential antipsychotic ORG 5222 on local cerebral glucose utilization in freely moving rats. *European Journal of Pharmacology* **1991**, *205* (3), 233-240. DOI: https://doi.org/10.1016/0014-2999(91)90903-4.

(23) Miyamoto, S. Nemonapride. In *Encyclopedia of Psychopharmacology*, Stolerman, I. P. Ed.; Springer Berlin Heidelberg, 2010; pp 823-823.

(24) Assié, M.-B.; Cosi, C.; Koek, W. 5-HT1A receptor agonist properties of the antipsychotic, nemonapride: comparison with bromerguride and clozapine. *European Journal of Pharmacology* **1997**, *334* (2), 141-147. DOI: https://doi.org/10.1016/S0014-2999(97)01207-7.

(25) Peitl, V.; Vlahović, D. Daridorexant. *Archives of Psychiatry Research: An International Journal of Psychiatry and Related Sciences* **2022**, *58* (2), 297-298.

(26) Dauvilliers, Y.; Zammit, G.; Fietze, I.; Mayleben, D.; Seboek Kinter, D.; Pain, S.; Hedner, J. Daridorexant, a New Dual Orexin Receptor Antagonist to Treat Insomnia Disorder. *Annals of Neurology* **2020**, *87* (3), 347-356. DOI: https://doi.org/10.1002/ana.25680.

(27) Roch, C.; Bergamini, G.; Steiner, M. A.; Clozel, M. Nonclinical pharmacology of daridorexant: a new dual orexin receptor antagonist for the treatment of insomnia. *Psychopharmacology* **2021**, *238* (10), 2693-2708. DOI: 10.1007/s00213-021-05954-0.

(28) Park, J.; Render, P., Kandon P.; Cates, P., Drew W. Daridorexant: Comprehensive Review of A New Oral Agent for the Treatment of Insomnia. *Annals of Pharmacotherapy 0* (0), 10600280221143794. DOI: 10.1177/10600280221143794.

(29) Henary, M.; Kananda, C.; Rotolo, L.; Savino, B.; Owens, E. A.; Cravotto, G. Benefits and applications of microwave-assisted synthesis of nitrogen containing heterocycles in medicinal chemistry. *RSC Advances* **2020**, *10* (24), 14170-14197, 10.1039/D0RA01378A. DOI: 10.1039/D0RA01378A.

(30) Coppola, M.; Mondola, R. Research chemicals marketed as legal highs: The case of pipradrol derivatives. *Toxicology Letters* **2012**, *212* (1), 57-60. DOI: https://doi.org/10.1016/j.toxlet.2012.04.019.

(31) Banister, S. D.; Kevin, R. C.; Martin, L.; Adams, A.; Macdonald, C.; Manning, J. J.; Boyd, R.; Cunningham, M.; Stevens, M. Y.; McGregor, I. S.; et al. The chemistry and pharmacology of putative synthetic cannabinoid receptor agonist (SCRA) new psychoactive substances (NPS) 5F-PY-PICA, 5F-PY-PINACA, and their analogs. *Drug Testing and Analysis* **2019**, *11* (7), 976-989. DOI: https://doi.org/10.1002/dta.2583.

(32) Ratni, H.; Ballard, T. M.; Bissantz, C.; Hoffmann, T.; Jablonski, P.; Knoflach, F.; Knust, H.; Malherbe, P.; Nettekoven, M.; Patiny-Adam, A.; et al. Rational design of novel pyrrolidine derivatives as orally active neurokinin-3 receptor antagonists. *Bioorganic & Medicinal Chemistry Letters* **2010**, *20* (22), 6735-6738. DOI: https://doi.org/10.1016/j.bmcl.2010.08.138.

(33) Bhat, A. A.; Tandon, N.; Tandon, R. Pyrrolidine Derivatives as Anti-diabetic Agents: Current Status and Future Prospects. *ChemistrySelect* **2022**, *7* (6), e202103757. DOI: https://doi.org/10.1002/slct.202103757.

(34) Villhauer, E. B.; Brinkman, J. A.; Naderi, G. B.; Dunning, B. E.; Mangold, B. L.; Mone, M. D.; Russell, M. E.; Weldon, S. C.; Hughes, T. E. 1-[2-[(5-Cyanopyridin-2-yl)amino]ethylamino]acetyl-2-(S)-pyrrolidinecarbonitrile: A Potent, Selective, and Orally Bioavailable Dipeptidyl Peptidase IV Inhibitor with Antihyperglycemic Properties. *Journal of Medicinal Chemistry* **2002**, *45* (12), 2362-2365. DOI: 10.1021/jm025522z.

(35) Magnin, D. R.; Robl, J. A.; Sulsky, R. B.; Augeri, D. J.; Huang, Y.; Simpkins, L. M.; Taunk, P. C.; Betebenner, D. A.; Robertson, J. G.; Abboa-Offei, B. E.; et al. Synthesis of Novel Potent Dipeptidyl Peptidase IV Inhibitors with Enhanced Chemical Stability: Interplay between the N-Terminal Amino Acid Alkyl Side Chain and the Cyclopropyl Group of α-Aminoacyl-l-cis-4,5-methanoprolinenitrile-Based Inhibitors. *Journal of Medicinal Chemistry* **2004**, *47* (10), 2587-2598. DOI: 10.1021/jm049924d.

(36) Holst, J. J.; Deacon, C. F. Inhibition of the activity of dipeptidyl-peptidase IV as a treatment for type 2 diabetes. *Diabetes* **1998**, *47* (11), 1663-1670. DOI: 10.2337/diabetes.47.11.1663 (acccessed 5/25/2023).

(37) Ji, J.; Sajjad, F.; You, Q.; Xing, D.; Fan, H.; Reddy, A. G. K.; Hu, W.; Dong, S. Synthesis and biological evaluation of substituted pyrrolidines and pyrroles as potential anticancer agents. *Archiv der Pharmazie* **2020**, *353* (12), 2000136. DOI: https://doi.org/10.1002/ardp.202000136

(38) Chiappori, A. A.; Haura, E.; Rodriguez, F. A.; Boulware, D.; Kapoor, R.; Neuger, A. M.; Lush, R.; Padilla, B.; Burton, M.; Williams, C.; et al. Phase I/II Study of Atrasentan, an Endothelin A Receptor Antagonist, in Combination with Paclitaxel and Carboplatin as First-Line Therapy in Advanced Non–Small Cell Lung Cancer. *Clinical Cancer Research* **2008**, *14* (5), 1464-1469. DOI: 10.1158/1078-0432.Ccr-07-1508 (acccessed 5/24/2023).

(39) Smollich, M.; Götte, M.; Kersting, C.; Fischgräbe, J.; Kiesel, L.; Wülfing, P. Selective ETAR antagonist atrasentan inhibits hypoxia-induced breast cancer cell invasion. *Breast Cancer Res Treat* **2008**, *108* (2), 175-182. DOI: 10.1007/s10549-007-9589-5 From NLM.

(40) Bhat, C.; Tilve, S. G. Recent advances in the synthesis of naturally occurring pyrrolidines, pyrrolizidines and indolizidine alkaloids using proline as a unique chiral synthon. *RSC Advances* **2014**, *4* (11), 5405-5452, 10.1039/C3RA44193H. DOI: 10.1039/C3RA44193H.

(41) Witte, L.; Müller, K.; Arfmann, H. A. Investigation of the Alkaloid Pattern of Datura innoxia Plants by Capillary Gas-Liquid-Chromatography-Mass Spectrometry. *Planta Med* **1987**, *53* (02), 192-197. DOI: 10.1055/s-2006-962670.

(42) Leete, E. Biosynthesis and Metabolism of the Tropane Alkaloids. *Planta Med* **1979**, *36* (06), 97-112. DOI: 10.1055/s-0028-1097249.

(43) Parr, A. J. Alternative metabolic fates of hygrine in transformed root cultures of Nicandra physaloides. *Plant cell reports* **1992**, *11* (5-6), 270-273. DOI: 10.1007/BF00235080

(44) Zárate, R.; Hermosin, B.; Cantos, M.; Troncoso, A. Tropane Alkaloid Distribution in Atropa baetica Plants. *Journal of Chemical Ecology* **1997**, *23* (8), 2059-2066. DOI: 10.1023/B:JOEC.0000006489.76006.cb.

(45) Johnson, E. L.; Emche, S. D. Variation of Alkaloid Content in Erythroxylum coca Leaves from Leaf Bud to Leaf Drop. *Annals of Botany* **1994**, *73* (6), 645-650. DOI: https://doi.org/10.1006/anbo.1994.1081.

(46) Arévalo-García, E. B.; Colmenares, J. C. Q. A short synthesis of (+)-hygrine. *Tetrahedron Letters* **2008**, *49* (25), 3995-3996. DOI: https://doi.org/10.1016/j.tetlet.2008.04.098.

(47) Anet, E.; Hughes, G. K.; Ritchie, E. Syntheses of Hygrine and Cuscohygrine. *Nature* **1949**, *163* (4138), 289-289. DOI: 10.1038/163289a0.

(48) Lee, J.-H.; Jeong, B.-S.; Ku, J.-M.; Jew, S.-s.; Park, H.-g. Total Synthesis of (+)-Hygrine via Asymmetric Phase-Transfer Catalytic Alkylation. *The Journal of Organic Chemistry* **2006**, *71* (17), 6690-6692. DOI: 10.1021/jo061108l.

(49) List, B. Proline-catalyzed asymmetric reactions. *Tetrahedron* **2002**, *58* (28), 5573-5590.

(50) Panday, S. K. Advances in the chemistry of proline and its derivatives: an excellent amino acid with versatile applications in asymmetric synthesis. *Tetrahedron: Asymmetry* **2011**, *22* (20-22), 1817-1847.

(51) Rakba, N.; Melhaoui, A.; Loyer, P.; Guy Delcros, J.; Morel, I.; Lescoat, G. Bgugaine, a pyrrolidine alkaloid from Arisarum vulgare, is a strong hepatotoxin in rat and human liver cell cultures. *Toxicol Lett* **1999**, *104* (3), 239-248. DOI: 10.1016/s0378-4274(98)00375-0 From NLM.

(52) Rakba, N.; Melhaoui, A.; Rissel, M.; Morel, I.; Loyer, P.; Lescoat, G. Irniine, a pyrrolidine alkaloid, isolated from Arisarum vulgare can induce apoptosis and/or necrosis in rat hepatocyte cultures. *Toxicon* **2000**, *38* (10), 1389-1402. DOI: 10.1016/s0041-0101(99)00232-9 From NLM.

(53) Majik, S. M. Bgugaine: An Account of Isolation, Biological Perspective and Synthetic Aspects. *Letters in Organic Chemistry* **2017**, *14* (3), 147-152. DOI: http://dx.doi.org/10.2174/1570178614666170221141900.

(54) Liu, X. C.; Lai, D.; Liu, Q. Z.; Zhou, L.; Liu, Q.; Liu, Z. L. Bioactivities of a New Pyrrolidine Alkaloid from the Root Barks of Orixa japonica. *Molecules* **2016**, *21* (12), 1665. DOI: 10.3390/molecules21121665

(55) Isman, M. B. Botanical insecticides, deterrents, and repellents in modern agriculture and an increasingly regulated world. *Annual Review of Entomology* **2006**, *51* (1), 45-66. DOI: 10.1146/annurev.ento.51.110104.151146.

(56) Watson, A. A.; Nash, R. J.; Wormald, M. R.; Harvey, D. J.; Dealler, S.; Lees, E.; Asano, N.; Kizu, H.; Kato, A.; Griffiths, R. C.; et al. Glycosidase-inhibiting pyrrolidine alkaloids from Hyacinthoides non-scripta. *Phytochemistry* **1997**, *46* (2), 255-259. DOI: https://doi.org/10.1016/S0031-9422(97)00282-3.

(57) Asano, N.; Kato, A.; Miyauchi, M.; Kizu, H.; Kameda, Y.; Watson, A. A.; Nash, R. J.; Fleet, G. W. J. Nitrogen-Containing Furanose and Pyranose Analogues from Hyacinthus orientalis. *Journal of Natural Products* **1998**, *61* (5), 625-628. DOI: 10.1021/np9705726.

(58) Fosgerau, K.; Westergaard, N.; Quistorff, B.; Grunnet, N.; Kristiansen, M.; Lundgren, K. Kinetic and Functional Characterization of 1,4-Dideoxy-1,4-imino-d-arabinitol: A Potent Inhibitor of Glycogen Phosphorylase with Anti-hyperglyceamic Effect in ob/ob Mice. *Archives of*

Biochemistry and Biophysics **2000**, *380* (2), 274-284. DOI: https://doi.org/10.1006/abbi.2000.1930.

(59) Pichon, M.; Figadère, B. Synthesis of 2,5-disubstituted pyrrolidines. *Tetrahedron: Asymmetry* **1996**, *7* (4), 927-964. DOI: https://doi.org/10.1016/0957-4166(96)00091-2.

(60) Mitchinson, A.; Nadin, A. Saturated nitrogen heterocycles. *Journal of the Chemical Society, Perkin Transactions 1* **2000**, (17), 2862-2892, 10.1039/A908537H. DOI: 10.1039/A908537H.

(61) Husinec, S.; Savic, V. Chiral catalysts in the stereoselective synthesis of pyrrolidine derivatives via metallo-azomethine ylides. *Tetrahedron: Asymmetry* **2005**, *16* (12), 2047-2061. DOI: https://doi.org/10.1016/j.tetasy.2005.05.020.

(62) Bellina, F.; Rossi, R. Synthesis and biological activity of pyrrole, pyrroline and pyrrolidine derivatives with two aryl groups on adjacent positions. *Tetrahedron* **2006**, *62* (31), 7213-7256.

(63) Redford, J. E.; McDonald, R. I.; Rigsby, M. L.; Wiensch, J. D.; Stahl, S. S. Stereoselective Synthesis of cis-2,5-Disubstituted Pyrrolidines via Wacker-Type Aerobic Oxidative Cyclization of Alkenes with tert-Butanesulfinamide Nucleophiles. *Organic Letters* **2012**, *14* (5), 1242-1245. DOI: 10.1021/ol3000519.

(64) Procopiou, G.; Lewis, W.; Harbottle, G.; Stockman, R. A. Cycloaddition of Chiral tert-Butanesulfinimines with Trimethylenemethane. *Organic Letters* **2013**, *15* (8), 2030-2033. DOI: 10.1021/ol400720b.

(65) Beniazza, R.; Romain, E.; Chemla, F.; Ferreira, F.; Jackowski, O.; Perez-Luna, A. Zinc Radical Transfer Based Modular Approach to Enantiopure Alkylidene-β-prol-ines from *N*-(tert-Butylsulfinyl)-α-(aminomethyl)acrylates. *European Journal of Organic Chemistry* **2015**, *2015* (35), 7661-7665. DOI: https://doi.org/10.1002/ejoc.201501173.

(66) Philip, R. M.; Radhika, S.; Saranya, P. V.; Anilkumar, G. Applications of tert-butanesulfinamide in the synthesis of *N*-heterocycles via sulfinimines. *RSC Advances* **2020**, *10* (69), 42441-42456, 10.1039/D0RA08819F. DOI: 10.1039/D0RA08819F.

(67) Brinner, K. M.; Ellman, J. A. A rapid and general method for the asymmetric synthesis of 2-substituted pyrrolidines using tert-butanesulfinamide. *Organic & Biomolecular Chemistry* **2005**, *3* (11), 2109-2113, 10.1039/B502080H. DOI: 10.1039/B502080H.

(68) Lewiński, J.; Śliwiński, W.; Dranka, M.; Justyniak, I.; Lipkowski, J. Reactions of [ZnR2(L)] Complexes with Dioxygen: A New Look at an Old Problem. *Angewandte Chemie International Edition* **2006**, *45* (29), 4826-4829. DOI: https://doi.org/10.1002/anie.200601001.

(69) Kudale, A. A.; Anaspure, P.; Goswami, F.; Voss, M. Asymmetric synthesis of 2-substituted cyclic amines. *Tetrahedron Letters* **2014**, *55* (52), 7219-7221. DOI: https://doi.org/10.1016/j.tetlet.2014.11.022.

(70) Sun, X.-W.; Xu, M.-H.; Lin, G.-Q. Room-Temperature Highly Diastereoselective Zn-Mediated Allylation of Chiral *N*-tert-Butanesulfinyl Imines: Remarkable Reaction Condition Controlled Stereoselectivity Reversal. *Organic Letters* **2006**, *8* (21), 4979-4982. DOI: 10.1021/ol062216x.

(71) Elderfield, R. C.; Hageman, H. A. THE VON BRAUN CYANOGEN BROMIDE REACTION I. APPLICATION TO PYRROLIDINES AND ETHYLENIMINES (1). *The Journal of Organic Chemistry* **1949**, *14* (4), 605-637. DOI: 10.1021/jo01156a015.

(72) Elderfield, R. C.; Green, M. SYNTHESIS OF SOME GUANIDINO AMINO ACIDS FROM CYANOGEN BROMIDE1, 2. *The Journal of Organic Chemistry* **1952**, *17* (3), 442-452. DOI: 10.1021/jo01137a017.

(73) Duprè, D. J.; Elks, J.; Hems, B. A.; Speyer, K. N.; Evans, R. M. 113. Analgesics. Part I. Esters and ketones derived from α-amino-ω-cyano-ωωdiarylalkanes. *Journal of the Chemical Society (Resumed)* **1949**, (0), 500-510, 10.1039/JR9490000500. DOI: 10.1039/JR9490000500.

(74) Lin, J.; Chan, W. H.; Lee, A. W. M.; Wong, W. Y.; Huang, P. Q. Asymmetric synthesis of 1,3- and 1,3,4-substituted pyrrolidines. *Tetrahedron Letters* **2000**, *41* (16), 2949-2951. DOI: https://doi.org/10.1016/S0040-4039(00)00278-1.

(75) Nagasawa, J.; Govek, S.; Kahraman, M.; Lai, A.; Bonnefous, C.; Douglas, K.; Sensintaffar, J.; Lu, N.; Lee, K.; Aparicio, A.; et al. Identification of an Orally Bioavailable Chromene-Based Selective Estrogen Receptor Degrader (SERD) That Demonstrates Robust Activity in a Model of Tamoxifen-Resistant Breast Cancer. *Journal of Medicinal Chemistry* **2018**, *61* (17), 7917-7928. DOI: 10.1021/acs.jmedchem.8b00921.

(76) Feng, E.; Wang, M.; Jin, Z.; Li, Y.; Shen, X.; Lou, J. Preparation of fused-ring pyridone derivatives as histamine H3 receptor antagonists and its application. CN115448877, 2022.

(77) Li, H. B.; Liang, W.; Liu, L.; Chen, K.; Wu, Y. Microwave-assisted convenient synthesis of *N*-arylpyrrolidines in water. *Chinese Chemical Letters* **2011**, *22* (3), 276-279. DOI: https://doi.org/10.1016/j.cclet.2010.09.034.

(78) Ju, Y.; Varma, R. S. An Efficient and Simple Aqueous *N*-Heterocyclization of Aniline Derivatives: Microwave-Assisted Synthesis of *N*-Aryl Azacycloalkanes. *Organic Letters* **2005**, *7* (12), 2409-2411. DOI: 10.1021/ol050683t.

(79) Chang, Y.-C.; Chir, J.-L.; Tsai, S.-Y.; Juang, W.-F.; Wu, A.-T. Microwave-assisted synthesis of pyrrolidine derivatives. *Tetrahedron Letters* **2009**, *50* (34), 4925-4929. DOI: https://doi.org/10.1016/j.tetlet.2009.06.062.

(80) Müller, T. E.; Hultzsch, K. C.; Yus, M.; Foubelo, F.; Tada, M. Hydroamination: Direct Addition of Amines to Alkenes and Alkynes. *Chemical Reviews* **2008**, *108* (9), 3795-3892. DOI: 10.1021/cr0306788.

(81) Cochran, B. M.; Michael, F. E. Mechanistic Studies of a Palladium-Catalyzed Intramolecular Hydroamination of Unactivated Alkenes: Protonolysis of a Stable Palladium Alkyl Complex Is the Turnover-Limiting Step. *Journal of the American Chemical Society* **2008**, *130* (9), 2786-2792. DOI: 10.1021/ja0734997.

(82) Bender, C. F.; Widenhoefer, R. A. Platinum-Catalyzed Intramolecular Hydroamination of Unactivated Olefins with Secondary Alkylamines. *Journal of the American Chemical Society* **2005**, *127* (4), 1070-1071. DOI: 10.1021/ja043278q.

(83) Bender, C. F.; Hudson, W. B.; Widenhoefer, R. A. Sterically Hindered Mono(phosphines) as Supporting Ligands for the Platinum-Catalyzed Hydroamination of Amino Alkenes. *Organometallics* **2008**, *27* (10), 2356-2358. DOI: 10.1021/om8000982.

(84) Hamilton, G. L.; Kang, E. J.; Mba, M.; Toste, F. D. A Powerful Chiral Counterion Strategy for Asymmetric Transition Metal Catalysis. *Science* **2007**, *317* (5837), 496-499. DOI: doi:10.1126/science.1145229.

(85) Bauer, E. B.; Andavan, G. T. S.; Hollis, T. K.; Rubio, R. J.; Cho, J.; Kuchenbeiser, G. R.; Helgert, T. R.; Letko, C. S.; Tham, F. S. Air- and Water-Stable Catalysts for Hydroamination/Cyclization. Synthesis and Application of CCC−NHC Pincer Complexes of Rh and Ir. *Organic Letters* **2008**, *10* (6), 1175-1178. DOI: 10.1021/ol8000766.

(86) Sipos, G.; Ou, A.; Skelton, B. W.; Falivene, L.; Cavallo, L.; Dorta, R. Unusual NHC–Iridium(I) Complexes and Their Use in the Intramolecular Hydroamination of Unactivated

Aminoalkenes. *Chemistry – A European Journal* **2016**, *22* (20), 6939-6946. DOI: https://doi.org/10.1002/chem.201600378.

(87) Hesp, K. D.; Stradiotto, M. Intramolecular Hydroamination of Unactivated Alkenes with Secondary Alkyl- and Arylamines Employing [Ir(COD)Cl]2 as a Catalyst Precursor. *Organic Letters* **2009**, *11* (6), 1449-1452. DOI: 10.1021/ol900174f.

(88) Liu, Z.; Hartwig, J. F. Mild, Rhodium-Catalyzed Intramolecular Hydroamination of Unactivated Terminal and Internal Alkenes with Primary and Secondary Amines. *Journal of the American Chemical Society* **2008**, *130* (5), 1570-1571. DOI: 10.1021/ja710126x.

(89) Komeyama, K.; Morimoto, T.; Takaki, K. A Simple and Efficient Iron-Catalyzed Intramolecular Hydroamination of Unactivated Olefins. *Angewandte Chemie International Edition* **2006**, *45* (18), 2938-2941. DOI: https://doi.org/10.1002/anie.200503789.

(90) Smolobochkin, A. V.; Gazizov, A. S.; Burilov, A. R.; Pudovik, M. A. Nitrogen-containing acetals and ketals in the synthesis of pyrrolidine derivatives. *Chemistry of Heterocyclic Compounds* **2016**, *52* (10), 753-765. DOI: 10.1007/s10593-016-1960-1.

(91) King, F. D. A facile three-step synthesis of (±)-crispine A via an acyliminium ion cyclisation. *Tetrahedron* **2007**, *63* (9), 2053-2056. DOI: https://doi.org/10.1016/j.tet.2006.12.041.

(92) King, F. D.; Aliev, A. E.; Caddick, S.; Copley, R. C. B. An investigation into the electrophilic cyclisation of *N*-acyl-pyrrolidinium ions: a facile synthesis of pyrrolo-tetrahydroisoquinolones and pyrrolo-benzazepinones. *Organic & Biomolecular Chemistry* **2009**, *7* (17), 3561-3571, 10.1039/B907400G. DOI: 10.1039/B907400G.

(93) Stragies, R.; Blechert, S. Enantioselective Synthesis of Tetraponerines by Pd- and Ru-Catalyzed Domino Reactions. *Journal of the American Chemical Society* **2000**, *122* (40), 9584-9591. DOI: 10.1021/ja001688i.

(94) Adrio, J.; Carretero, J. C. Stereochemical diversity in pyrrolidine synthesis by catalytic asymmetric 1,3-dipolar cycloaddition of azomethine ylides. *Chemical Communications* **2019**, *55* (80), 11979-11991, 10.1039/C9CC05238K. DOI: 10.1039/C9CC05238K.

(95) Neal, M. J.; Hejnosz, S. L.; Rohde, J. J.; Evanseck, J. D.; Montgomery, T. D. Multi-Ion Bridged Pathway of *N*-Oxides to 1,3-Dipole Dilithium Oxide Complexes. *J. Org. Chem.* **2021**, *86* (17), 11502-11518.

(96) Roussi, G.; Beugelmans, R.; Chastanet, J.; Roussi, G. The [3+2] Cycloaddition Reaction of Nonstabilized Azomethine Ylide Generated from Trimetylmine *N*-Oxide to C=C, C=N, and C=S Bonds. *Heterocycles* **1987**, *26* (12), 3197-3202, Journal. DOI: 10.3987/r-1987-12-3197.

(97) Chastanet, J.; Roussi, G. Study of the regiochemistry and stereochemistry of the [3 + 2] cycloaddition between nonstabilized azomethine ylides generated from tertiary amine *N*-oxides and various dipolarophiles. *The Journal of Organic Chemistry* **1988**, *53* (16), 3808-3812. DOI: 10.1021/jo00251a026.

(98) Gray, D.; Davoren, J.; Harris, A.; Nason, D.; Xu, W. Remarkable [3+2] Annulations of Electron-Rich Olefins with Unstabilized Azomethine Ylides. *Synlett* **2010**, *2010* (16), 2490-2492. DOI: 10.1055/s-0030-1258026 (acccessed 2020-10-22T21:18:58).

(99) Beugelmans, R.; Negron, G.; Roussi, G. Trimethylamine *N*-oxide as a precursor of azomethine ylides. *Journal of the Chemical Society, Chemical Communications* **1983**, (1), 31-32, 10.1039/C39830000031. DOI: 10.1039/c39830000031.

(100) MilliporeSigma. *1-methoxy-n-methyl-n-(trimethylsilylmethyl)methanamine*. https://www.sigmaaldrich.com/US/en/product/astatechinc/ateh98066267?context=bbe (accessed 2023/05/24).

(101) Chauthe, S. K.; Sharma, R. J.; Aqil, F.; Gupta, R. C.; Singh, I. P. Quantitative NMR: An Applicable Method for Quantitative Analysis of Medicinal Plant Extracts and Herbal Products. *Phytochemical Analysis* **2012**, *23* (6), 689-696. DOI: https://doi.org/10.1002/pca.2375.

(102) Borovika, A.; Tang, P.-I.; Klapman, S.; Nagorny, P. Thiophosphoramide-Based Cooperative Catalysts for Brønsted Acid Promoted Ionic Diels–Alder Reactions. *Angewandte Chemie International Edition* **2013**, *52* (50), 13424-13428. DOI: https://doi.org/10.1002/anie.201307133.

Chapter 4: Development of a [3+2]-Cycloaddition Forming a Novel Azabicyclo[2.2.1]heptane

4.1 Introduction

4.1.1 Contextual Summary

Epibatidine is natural product secreted from a poison dart frog that has captured the attention of researchers for decades due to its analgesic properties being 200 times that of morphine.[1,2] Unfortunately, while it has incredible pain-relieving properties, it also has acutely toxic side effects making it unsuitable for use as pharmeceutical.[1,2] To overcome this limitation, researchers have developed numerous synthetic routes for this important class of products in an effort to make derivatives that exhibit similar analgesic properties of epibatidine without the undesired toxicity.[3,4] Most of these method use azabicyclic synthetic precursors,[5-14] which inherently limits the products accessible with these methods. A more attractive synthetic route would include the creation of the azabicyclic core, thereby expanding the potential of the chosen pathway and making it a more efficient method for rapid drug screening. Herein we developed a three-step synthetic protocol for forming a similar azabicyclic core in a [3+2]-cycloaddition. This [3+2]-cycloaddition originally developed by Roussi and coworkers takes advantage of readily available dipolarophiles and *N*-oxides to form cycloadducts.[15-17] Since this chemistry has been compatible with a variety of dipolarophiles, it seemed logical to take advantage of it for forming novel azabicyclo[2.2.1]heptane cores.

4.1.2. Epibatidine and Derivatives in Medicinal Chemistry

The most prominent natural product containing an azabicyclo[2.2.1]heptane core is epibatidine (**301**) (Figure 32a). Trace amounts of it were originally isolated 1974 by John Daly and Charles Myers from an Ecuadorian poison frog *Epipedobates anthonyi* (Figure 32b).[2,18] This alkaloid is secreted from the skin of *Epipedobates anthonyi* as well as other poison dart frogs from the

Ameerega genus and while it was isolated in 1974, its structure was not fully elucidated until 1992[18]. The incredible attribute of this natural product was that it exhibited analgesic properties 200 times that of morphine.[18] It is a potent agonist for the nicotinic receptors, specifically nicotinic acetylcholine recpetors (nAChRs).[1,2] This means that when epibatidine is bound, it activates nAChRs, thus resulting in pain-relieving properties.[1,2] Morphine on the other hand is an opioid-receptor agonist which activates opioid-receptors, also resulting in a potent analgesic effect.[19] Nicotinic receptor activation, however, results in a less addictive analgesic effect when compared to the opioid receptors because it is not paired with the euphoric effects that occur with opioid receptor activation, making epibatidine a potential target for new pain-relieving therapeutics that are less addicting.[4,20,21]

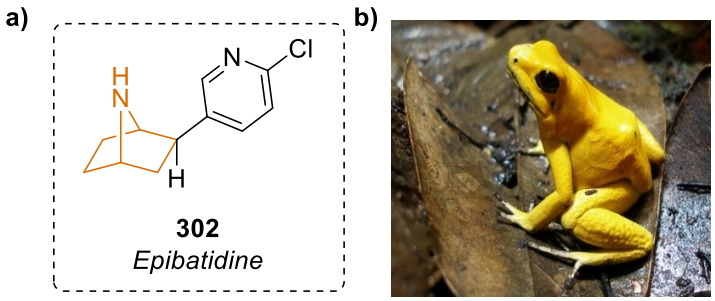

Figure 32a. Structure of Epibatidine. 32b. Poison Dart Frog from the *Ameerega* Genus (Licensed under CC BY)

The problem with epibatidine is that the lethal dose is too close to the therapeutic dosage.[1,2] This could be potentially overcome by the synthesis of different analogs in order to determine what structural properties are needed for the nicotinic agonism, and what aspects are responsible for its toxicity. Researchers have tried elucidating this through structure activity relationship (SAR) studies in order to find new pain-relievers as well as even discovering new treatments for nicotine addiction.

Liu and coworkers modified the skeleton of epibatidine by the addition of aminoesters at the 3-position forming derivatives **303-308** (Figure 33).[4] They tested these compounds for their analgesic properties as well as their toxicities.[4] Overall, the ammonium salts **306-308** exhibited more potent analgesic activities than the hydrochloride counterparts **303-305**, with **308** being the strongest.[4] While these compounds are not as effective analgesics as epibatidine, they do not have the same toxic properties as epibatidine making them potential candidates for pain-killers.[4]

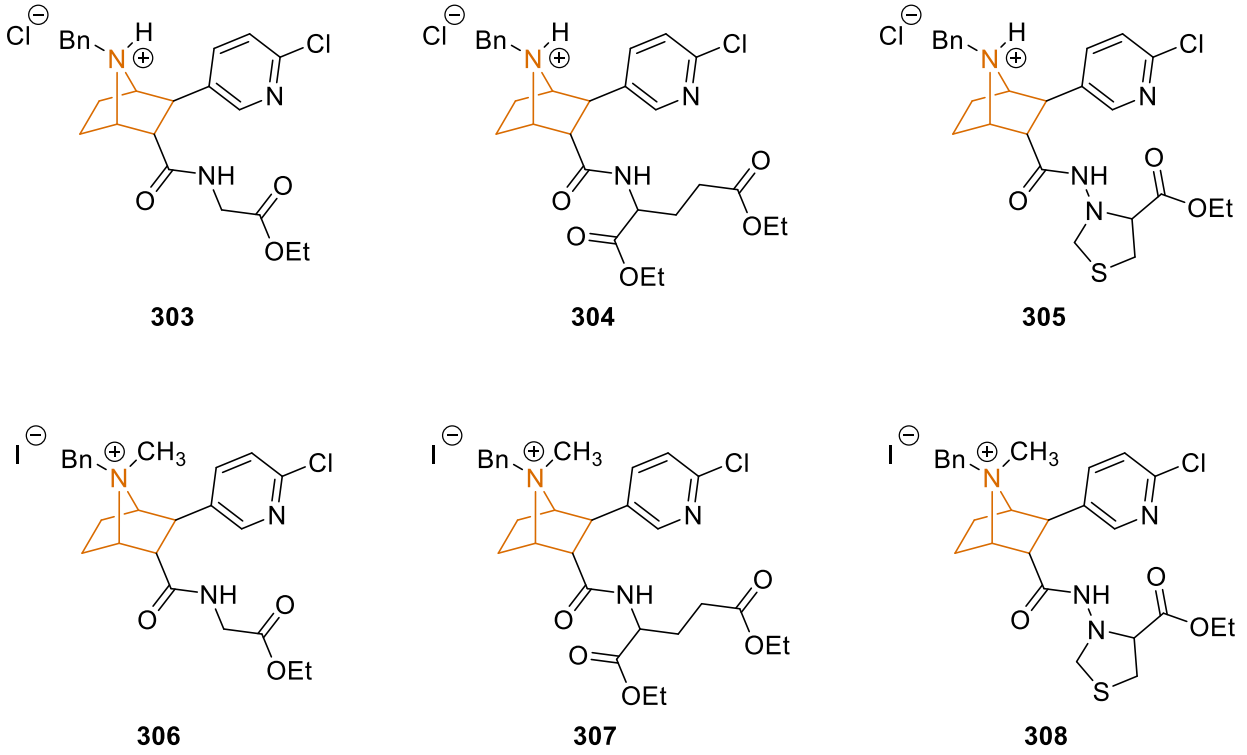

Figure 33. Analgesic Aminoester Epibatidine Derivatives

In addition to analgesics, epibatidine derivatives are of interest for potential therapeutics for central nervous system disorders such as Alzheimer's and Parkinson's disease as well as schizophrenia, anxiety, depression and Tourette's syndrome.[10,22] Carroll and coworkers synthesized 13 different azabicyclo[2.2.1]heptane analogues for a SAR study with the goal of elucidating nAChR subtypes, and while they were not able to differentiate between the subtypes, they did unveil novel

antagonists for this receptor (Figure 34).[10] In contrast to epibatidine which is an agonist (turns on the receptor), these derivatives are effective antagonists, meaning they turn off nAChR, with the most potent being **310**.[10] Moreover, derivatives similar to **310** (Figure 35),[3,10,23] did not exhibit any analgesic properties, but **309** did, suggesting that this biphenyl functionality had greater affinity for certain subtypes of nAChR, while those without (epibatidine and **309**) lack that directed affinity.[10]

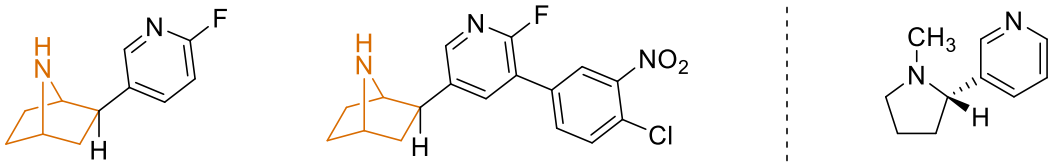

309 **310** **311**
Nicotine

Figure 34. Epibatidine Analogues Synthesized by Carroll and Coworkers Compared to Nicotine[10]

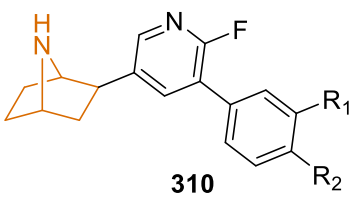

310

310a, $R_1 = NO_2$, $R_2 = Cl$
b, $R_1 = H$, $R_2 = H$
c, $R_1 = H$, $R_2 = F$
d, $R_1 = F$, $R_2 = H$
e, $R_1 = H$, $R_2 = Cl$
f, $R_1 = Cl$, $R_2 = H$
310g, $R_1 = H$, $R_2 = NO_2$
h, $R_1 = NO_2$, $R_2 = H$
i, $R_1 = H$, $R_2 = NH_2$
j, $R_1 = NH_2$, $R_2 = H$
k, $R_1 = H$, $R_2 = MeO$
k, $R_1 = MeO$, $R_1 = H$

Figure 35. Scope of Epibatidine Derivatives

Researchers only focused on derivatizing the phenyl ring, which is true for similar studies such as this (Figure 35)[3,6-8,10]. It would be interesting to see the effects of adding substituents to the 3-position of the ring rather than further functionalizing that of the two. Potentially having an additional aryl group on the 3-position could mimic the same effects of the biaryl system of **310**. The scope was somewhat limited, likely dictated by the chemistry used to build the core, but this

work demonstrated the potential for these derivatives can serve as therapies for nicotine addiction.[10]

4.1.3 Other Bioactive Compounds Containing Azabicyclo[2.2.1]heptane Cores

Orexin-A and -B (ORX) are excitatory neuropeptides that are responsible for the regulation of neuropathways such as sleep/wake cycles, circadian rhythms, anxiety, and stress responses to name a few. These oxerins, located in the hypothalamus, stimulate two distinct G-protein coupled receptors, orexin-1 (OX1R) and orexin-2 (OX2R). OX1R specifically is associated with triggering panic or anxious states.[24-27] Higher levels of ORX are directly associated to feelings of panic anxiety that are associated with post-traumatic stress disorder (PTSD) and other anxiety and panic disorders.[24-27] As a result, ORX antagonists have been a target for new treatments of panic disorders.[14,27] These ORX antagonists work faster than the typical selective serotonin reuptake inhibitors (SSRIs) that are typically prescribed, which can take 2-3 weeks after daily use in order to take effect.[28] Moreover, traditional SSRIs and benzodiazapines can also increase feelings of anxiety when prescribed.[29] OX1R antagonists also have the added benefit of preventing panic responses without the sedation effects that are typical of OX2R antagonists or panicolytic benzodiazepines.[30-32]

Shireman and coworkers at Janssen synthesized a range of azabicyclo[2.2.1]heptanes to conduct a structure-activity relationship (SAR) study in order to determine what factors are key for potent OX1R antagonism.[14] Compounds **312**-**314** had strong affinities for OX1R with **313** being the highest (Figure 36).[14,25] X-ray crystallography revealed that overall shape of **313** is a U, likely due to the intramolecular π/π stacking and hydrogen bonding (Figure 37),[14] which is characteristic of other single orexin receptor antagonists (SORAs) and dual orexin receptor antagonists (DORAs)

.[33,34] Due to these promising preliminary results, drug target **313** is being further developed by Janssen pharmaceuticals for the treatment of panic and anxiety disorders.[14]

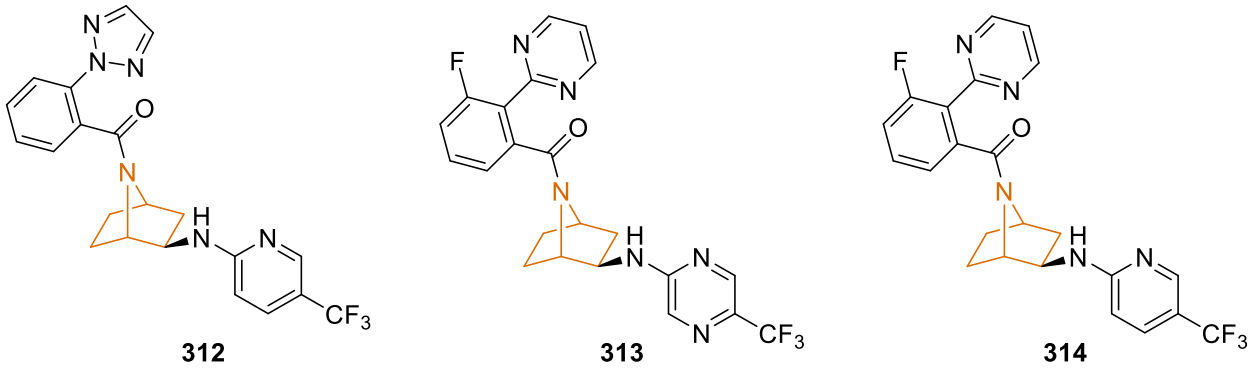

Figure 36. Azabicyclo[2.2.1]heptane Dual ORX Antagonists Developed by Janssen Pharmaceuticals.[14]

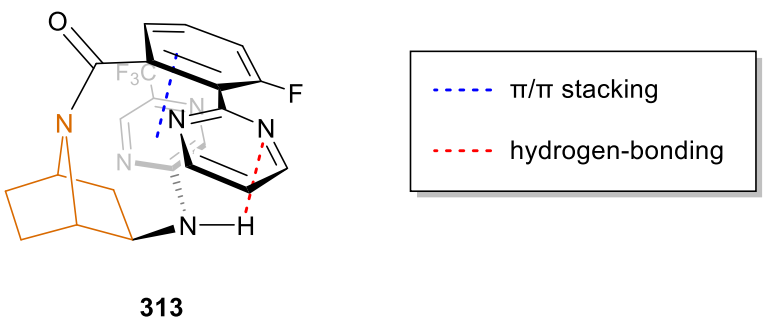

Figure 37. Conformational U-Shape of OX1R Inhibitor 12 by Janssen Pharmaceuticals[14]

Nitrosamines **315** in general are potent carcinogens and toxins in non-human animals such as rats.[35] They are regarded as potential genotoxins in humans, however not much is known about this particular mechanism of action as far as the structure of the nitrosamines goes.[36] Mochizuki and coworkers evaluated the mutagenicity of 7-azabicyclo[2.2.1]heptane *N*-nitrosamines as well as related monocyclic derivatives (Figure 38).[36]

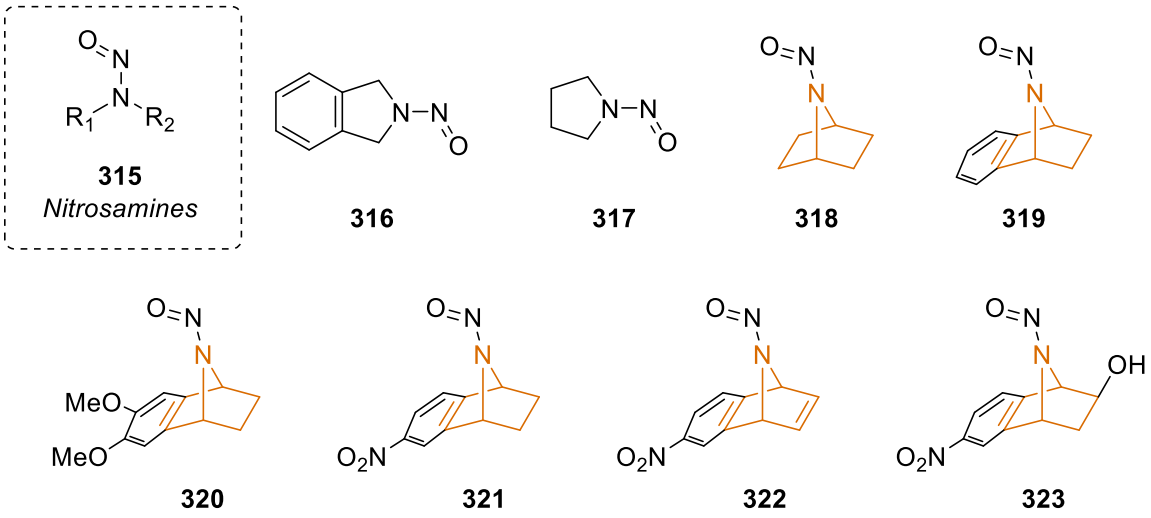

Figure 38. Nitrosamines Synthesized by Mochizuki and Coworkers.[36]

Compounds **316-323** were subjected to Ames assays, which are standard test used to determine whether a given substance can cause DNA mutations.[36] Their results indicate that the azabicyclics **318-323** have no mutagenic properties while **316-317** do, suggesting that the genotoxicity of nitrosamines are independent of the functional group itself.[36] These results offer an opportunity to further evaluate the bioactivities of these structure which could lead to the incorporation of this functionality into pharmaceuticals.[36]

4.1.4 Synthetic Methods Forming Epibatidine and Derivatives

There are numerous reported total synthetic methods forming epibatidine and derivatives.[3] Most synthetic methods reported of compounds containing the azabicyclo[2.2.1]heptane core do not actually form it; these methods merely functionalize an already existing azabicyclic core,[3,5-14] with very few building this motif from precursors.[4,9,37-39] This poses an inherent challenge when implementing these total synthetic methods for forming a library of derivatives for rapid drug screening. This section will mainly focus on total synthetic methods for epibatidine and derivatives that form the azabicyclic core rather than functionalizing a preexisting one.

Scheme 63. Clayton and Regan Epibatidine Synthesis.[40]

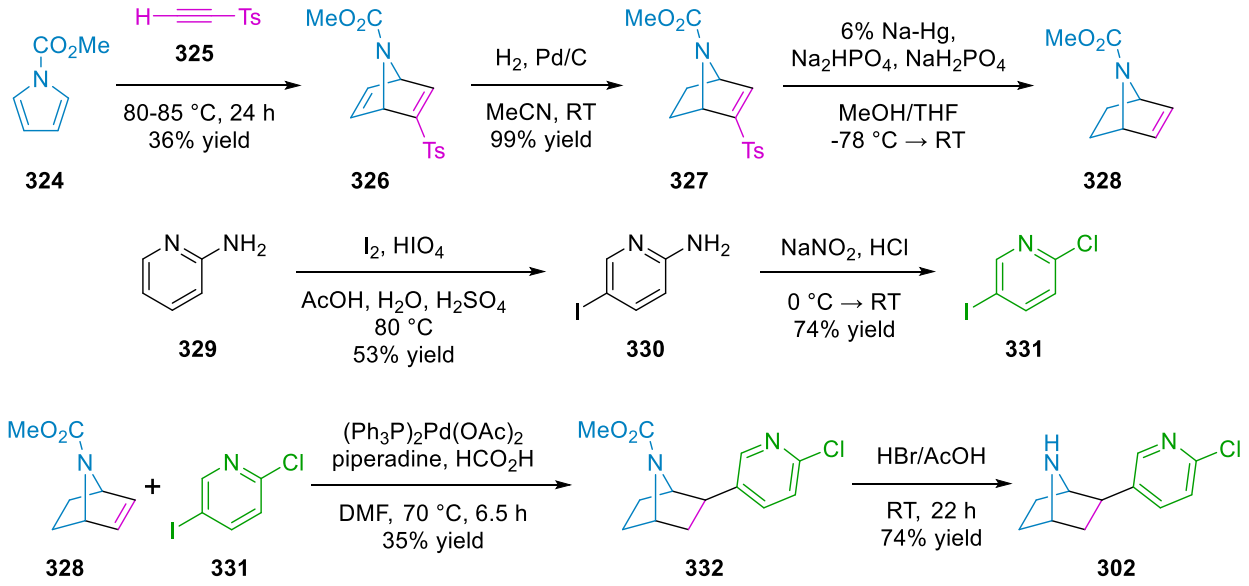

The first reported synthesis of epibatidine was in 1993 by Clayton and Regan (Scheme 62).[40] They formed (±)-epibatidine in a five step convergent synthesis using a Diels-Alder reaction forming the azabicyclic core **326**. This was then followed by a palladium-catalyzed Heck-type coupling to form the *exo*-isomer **332** selectively which affords (±)-epibatidine after deprotection of the bridging amine.[40] While relatively concise, this method lacks the stereoselectivity necessary for forming drug targets.

Huang and Shen improved this method by isolating both enantiomers of epibatidine (Scheme 63).[38] They were able to achieve the substituted azabicyclic core **335** in fewer steps by efficient use of a Diels Alder reaction installing the pyridyl substituent while simultaneously forming the core.[38] Hydrogenation and desulfonylation afforded (±)-epibatidine, and then they were able to use chiral resolution to successfully isolate both *R* and *S* enantiomers.[38] While this is an improvement from Clayton and Regan's total synthesis, the limitation of this method is the selectivity with the Diels Alder reaction forming both the *endo* and *exo* products, and each of those also form their respective *R* and *S* enantiomers limiting their yield to a maximum of 50% for the final step.[38]

Scheme 64.Huang and Shen Epibatidine Synthesis[38]

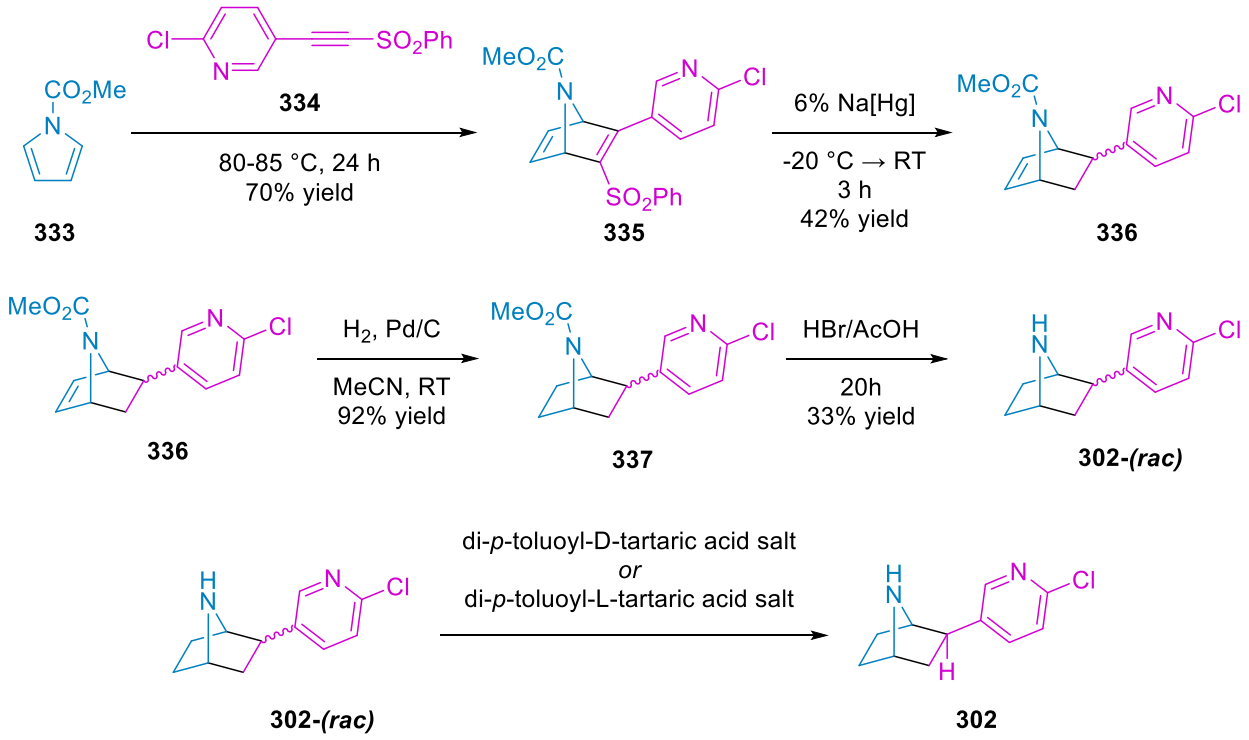

Researchers worked to improve this method further but were unsuccessful in achieving enantiopure epibatidine in reasonable yields.[39] In 2002, however, E. J. Corey and coworkers successfully carried out the total synthesis of enantiopure epibatidine in eleven steps.[37] The azabicyclic core **344** was formed in 46% overall yield from **338** in eight steps. Their method takes advantage of a Diels-Alder reaction with butadiene (**341**) to install the 6-membered ring base that will later become the aza-bicylic core **344**. This intermediate **343** then undergoes cyclization, forming a new carbon-nitrogen bond to afford azabicyclic 344.[37] After radical debromination and deprotection, optically pure epibatidine was formed in 42% yield overall which is an immense improvement from previous methods.[37]

Scheme 65. Total Synthesis of Epibatidine by Corey and Coworkers.[37]

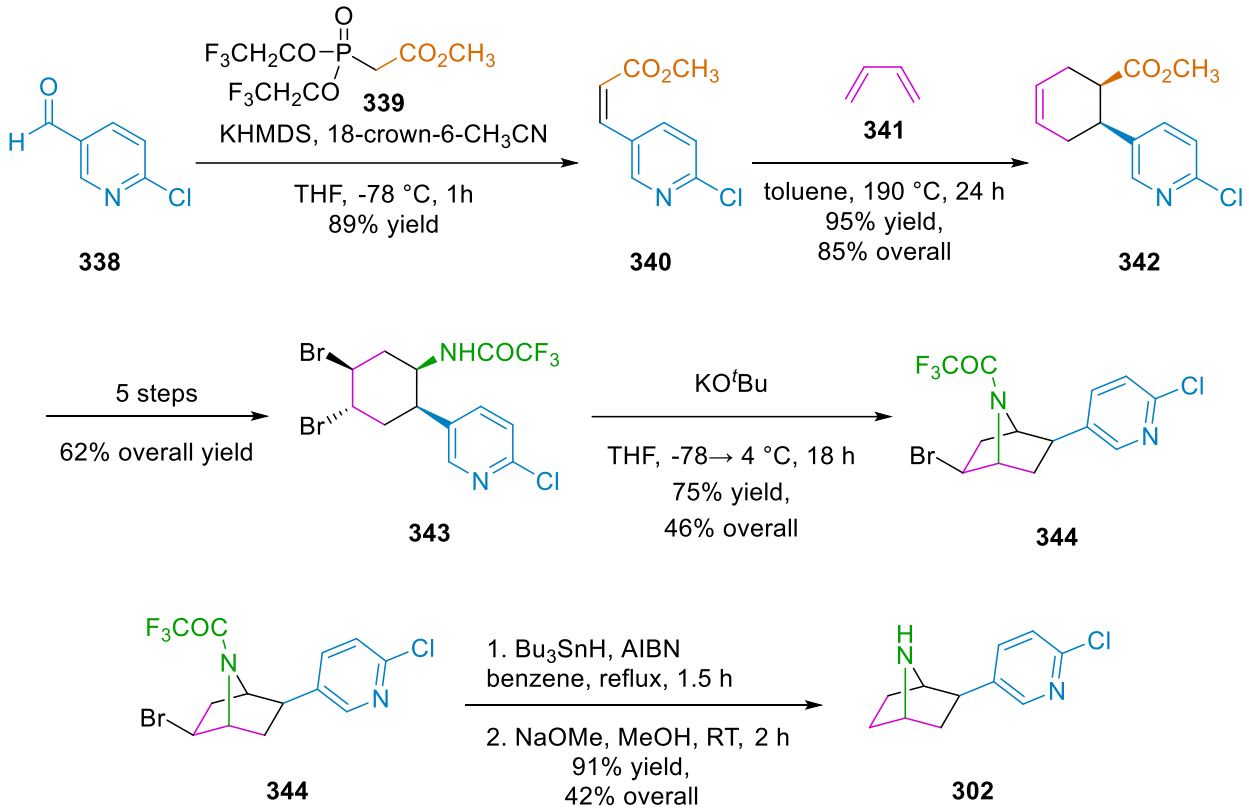

A year later in 2003, Liu and coworkers established a synthetic protocol forming aminoester derivatives of epibatidine **351** (Scheme 65).[4] Intermediate **346** was formed from Boc-protected pyrrolidine in four steps with 71% yield.[4] This intermediate is converted to the azomethine ylide *in situ*, which then undergoes a silver catalyzed [3+2] cycloaddition with **347** to form **348**.[4] The ester of **348** was saponified into a carboxylic acid **349**, which was then condensed with an amine to afford amide **350**.[4] These were then used to form two types of ammonium salts **351a** and **351b** which are potent analgesics.[4] This protocol formed the desired products total of 8 steps with enough flexibility to form six different epibatidine derivatives making this a useful approach for forming similar potential drug candidates.[4]

Scheme 66. Synthesis of Aminoester Epibatidine Derivatives by Li and Coworkers.[4]

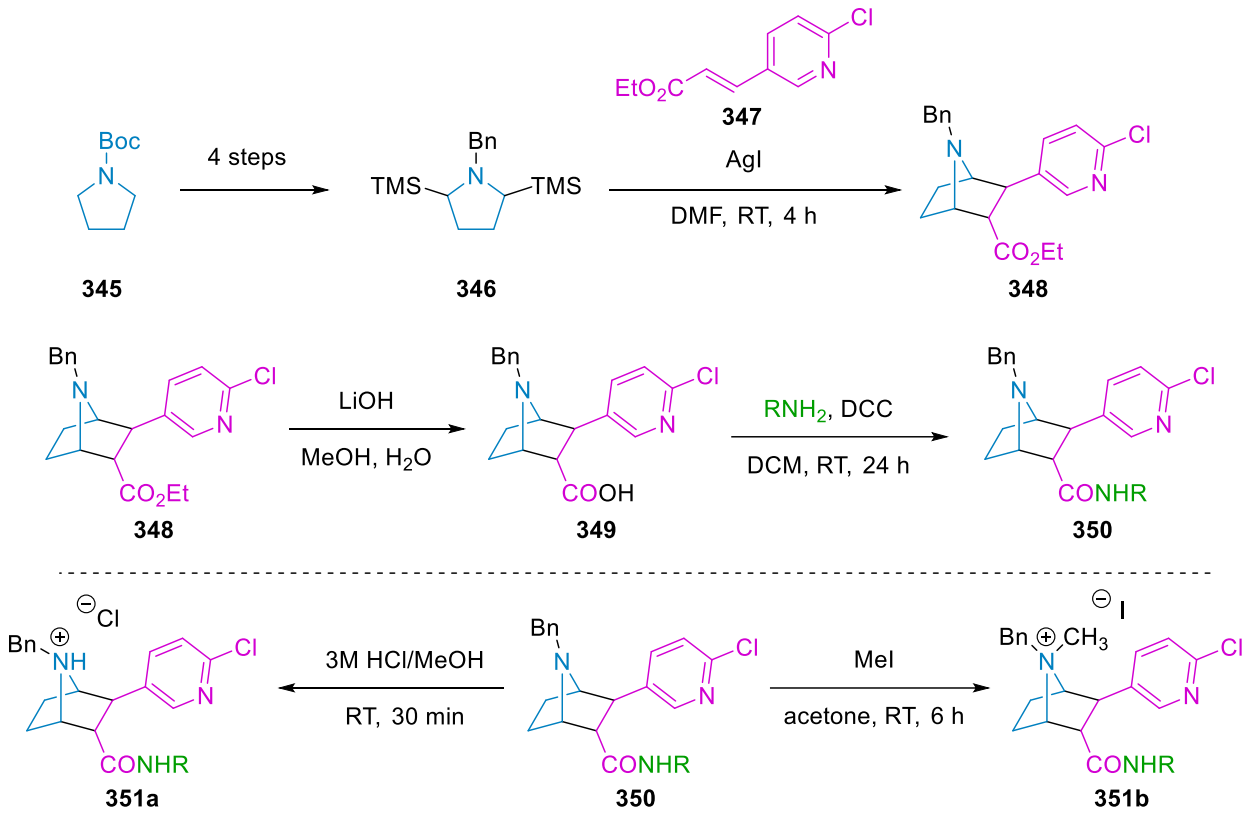

Most recently in 2020, Shireman and coworkers formed a library of azabicyclo[2.2.1]heptane OX1R antagonists **313** (Scheme 66).[14] Their most potent antagonist was **313** and it was produced in five steps from commercially available substrates **352** and **357** (Scheme 66).[14] This method was versatile enough to achieve a library of 20 different azabicyclo[2.2.1]heptane OX1R antagonists with minimal deviations from it.[14] This is an effective demonstration of a practical synthetic method that will hold up if the drug target is successful in being put to market, the limitation is that the azabicyclic core is restricted to those that are commercially available.

Scheme 67. Synthesis of Azabicyclo[2.2.1]heptane OX1R Antagonist.[14]

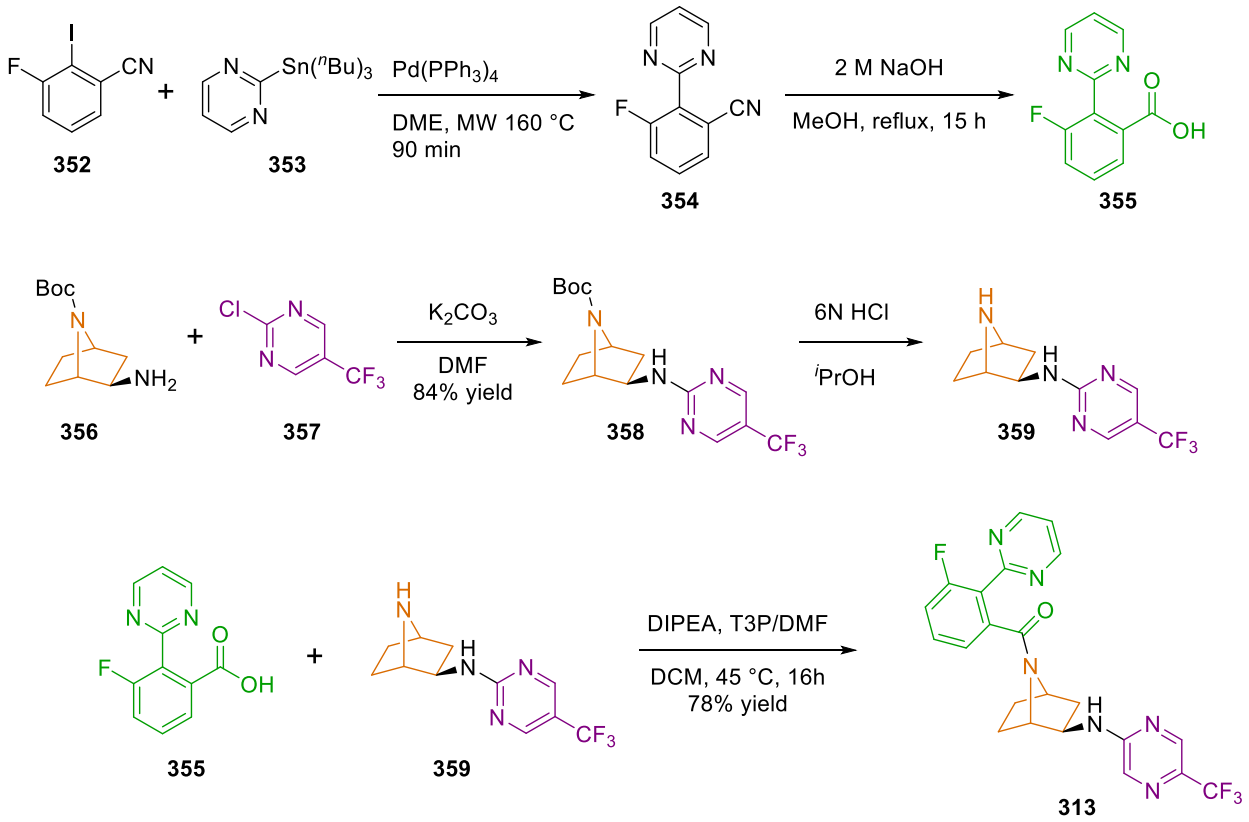

4.2 Results and Discussion

There are a number of different approaches to forming the azabicyclo[2.2.1]heptane core such as Diels Alder reactions,[38,40] substitution reactions,[37] and [3+2] cycloadditions.[4] Our focus was on implementing a [3+2]-cycloaddition of a tertiary amine *N*-oxide **360** and stilbene **361** to form a novel azabicylic core **362**. This method of using a tertiary amine *N*-oxides as a precursor was originally developed by Roussi and coworkers in the 1980s,[15-17] but has not yet been implemented to form this specific heterocycle. We decided that it had potential for providing rapid access to epibatidine-like derivatives, so we started with *tert*-butylamine *N*-oxide **360** and *trans*-stilbene (**361**) to gain preliminary results with this system (Scheme 67).

Scheme 68. Proposed [3+2] Cycloaddition Forming an Azabicyclic Core.

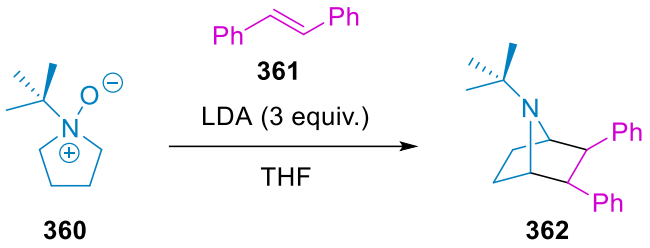

4.2.1 Reaction Optimization

The synthesis of the *N*-oxo pyrrolidine **360** requires two steps, the first being pyrrolidine formation from subsequent S_N2 reactions of **363** and **364**, and the second being oxidation forming **360**. The original protocol required three days to make the pyrrolidine, which once oxidized the necessary *N*-oxide **360** was formed (Scheme 68a).

Scheme 69. Synthesis of *tert*-butyl pyrrolidine *N*-oxide

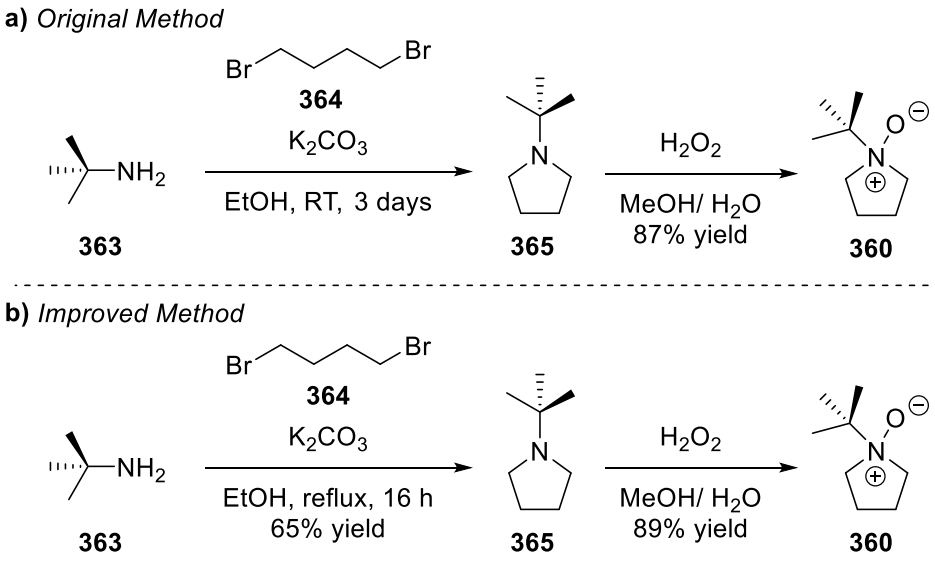

This was not conducive for quick reaction screening so the protocol for forming pyrrolidine **365** was modified (Scheme 68b); instead of stirring it for three days at room temperature (RT), the reaction was heated to reflux and was completed after 16 h. The oxidation conditions remained the same, shortening the overall reaction time for *N*-oxide **360** from about four days to effectively two

days. It is also important to note that these reactions were carried out on multigram scales (40 mmol) (Scheme 68).

Once enough *N*-oxide **360** was acquired, the [3+2] cycloaddition of **360** and *trans*-stilbene (**361**) was carried out. The azabicyclic **362** was isolated in a 56% yield, a significant improvement from the original studies carried out by other members of our research consortia. With our initial results in hand, we set out to optimize the reaction conditions to further improve the yield, and to also gain fundamental insights into the mechanism of this transformation.

Scheme 70. [3+2]-Cycloaddition of *trans*-stilbene and *tert*-butyl pyrrolidine *N*-oxide

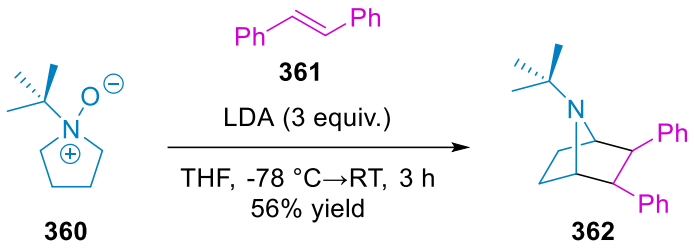

The first set of conditions examined was the base (LDA) used for the reaction. In order to confirm that the base is necessary for this cycloaddition to even occur, the reaction conditions were carried out without any base (Table 9, Entry 1). The result was that no reaction occurred, confirming that base is necessary for this cycloaddition to occur. A range of different lithium bases were then tested, each with varying properties.

Lithium bis(trimethylsilyl)amide (LiHMDS) was implemented into this reaction as a weaker lithium base with a pK_a around 30,[41] and no reaction occurred (Table 9, Entry 2). Lithium diisopropylamide (LDA, $pK_a = 36$) was the standard base used when the 56% isolated yield was achieved (Table 9, Entry 3). Lithium tetramethylpiperidide (LiTMP, $pK_a = 37$), a less sterically hindered base with a similar pK_a to LDA, was then implemented into the reaction conditions, and only 28% NMR yield of **362** was obtained (Table 9, Entry 4). Initially the hypothesis was that a

more sterically hindered base would improve the yield, but according to this result that turned out not to be the case.

Table 9. Summary of base screening for [3+2] cycloaddition

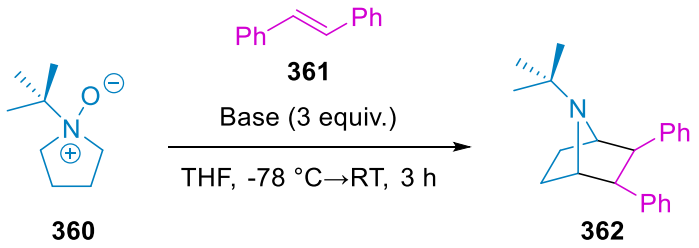

Entry	Base	NMR Yield (%)[a]
1	N/A	No Reaction
2	LiHMDS	No Reaction
3	LDA	50[b]
4	LiTMP	28[b]
5	BuLi	26
6	^{t}BuLi	28[b]

[a]NMR yield calculated using 1,3,5-trimethoxybenzene as the standard. [b]Reported as the average of two experiments.

Stronger bases were then implemented in order to discern if more basic species are required. The incorporation of *n*-butyl lithium (^{n}BuLi) resulted in a 26% yield with more signals in the ^{1}H NMR spectrum than with the reaction with LDA, indicating that more side reactions occurred with this base than LDA (Table 9, Entry 5). This could be due to ^{n}BuLi being much more basic than LDA with a pK_a of around 50, but it could also be attributed to the nucleophilic nature of ^{n}BuLi. This was further tested with *tert*-butyl lithium (^{t}BuLi), which is a slightly stronger base than ^{n}BuLi with a pK_a of 53, but it has less-nucleophilic character than ^{n}BuLi due to its steric bulk. When ^{t}BuLi

was implemented into the reaction, **362** formed in 28% yield (Table 9, Entry 6). Additionally, as observed previously with ^{n}BuLi, various side seemed to have occurred, making this base of limited use for this reaction. These results indicate that the basic character of the organolithium species is key for this reaction to work optimally. LDA lies within that "goldilocks" region of being basic enough, but not too basic.

Table 10. Summary of temperature screening for [3+2] cycloaddition

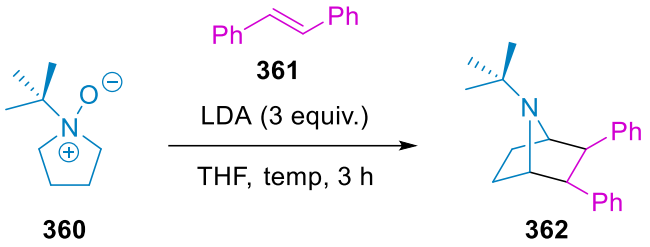

360 362

Entry	Temperature (°C)	NMR Yield (%)[a]
1	0	19
2	-10	26
3	-15	28
4	-40	37
5	-78→RT	44
6	-78	7

[a]NMR yield calculated using 1,3,5-trimethoxybenzene as the standard.

A crude ReactIR experiment suggested that the cycloaddition does not occur until the temperature warms up to at least -40 °C. We wanted to further test this initial observation with a series of temperature screenings. It should be first noted that all reaction temperatures were held constant over the course of three hours with the exception of the control experiment (Table 10, Entry 5).

Initially the reaction was held at a constant 0 °C (Table 10, Entry 1) resulting in a lower 19% yield. As the temperature decreased, the yield increased with -10 °C resulting in a 26% yield (Table 10, Entry 2), and -15 °C with a 28% yield (Table 10, Entry 3). The reaction held at -40 °C (Table 10, Entry 4) resulted in a 37% yield, which was the closest of any of the variables to the control experiment with a 44% yield (Table 10, Entry 5). Consistent with our ReactIR experiment, when the reaction was held at -78 °C, only 7% of the product **362** formed. It was concluded that the optimal temperature conditions for the [3+2]-cycloaddition was starting -78 °C and then warming up to room temperature.

According to Le Châtelier's principle, when stress is applied to a system in equilibrium, the system will shift in order to counteract that change. This is a fundamental concept we teach in General Chemistry I, when a reaction in equilibrium is disrupted by a change, such as with the reaction conditions, the equilibrium will shift to counteract that change. In accordance with this principle, we next examined the stoichiometric amount of *trans*-stilbene added. Our thought process was that if we added more of a particular reagent we could drive the reaction forward to product formation. *Trans*-stilbene **361** was chosen over *N*-oxide **360** since it was the less costly reagent. In regards to the reaction mechanism and previous observations, three equivalents of LDA are required for a single equivalent of *N*-oxide to form the azomethine ylide species.[42] So, in addition to cost and time efficiency, the stoichiometric equivalents of *trans*-stilbene were also the simplest to vary. Additional equivalents of *trans*-stilbene **361** had no effect on the yield of the reaction (Table 11, Entries 1-3), so moving forward, only one equivalent of dipolarophile **361** was used in the [3+2]-cycloaddition reactions.

Table 11. Summary of stoichiometric screening for [3+2] cycloaddition

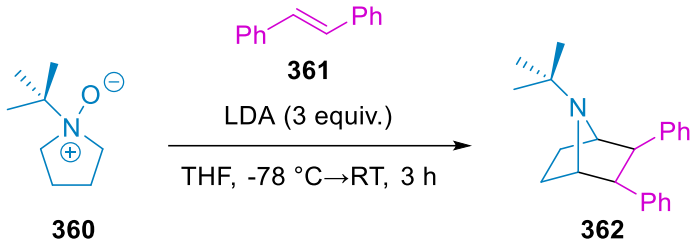

Entry	Equivalents of *Trans*-Stilbene	NMR Yield (%)[a]
1	1	51
2	1.5	51
3	2	52

[a]NMR yield calculated using 1,3,5-trimethoxybenzene as the standard. [b]Isolated yield. [c]Reported as the average of two experiments.

Scheme 71. Implementing an *N*-oxide salt into the [3+2] cycloaddition

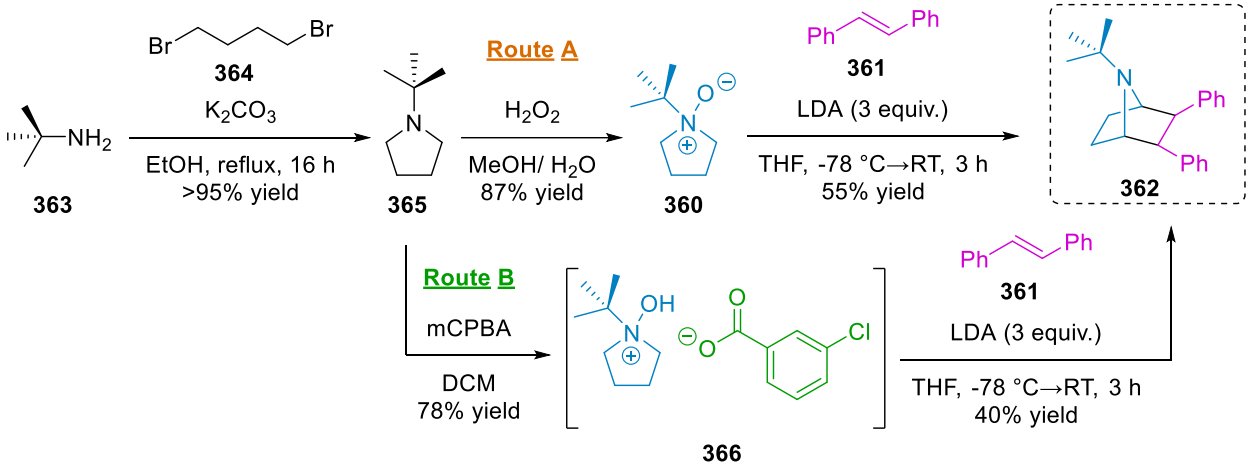

The hydroscopic nature of *N*-oxide **360** was problematic for the [3+2]-cycloaddition because of the moisture sensitivity of LDA, and of the potential intermediates required to form the cycloadduct **362**. In an attempt to combat this hygroscopicity, instead of using the discrete *N*-oxide

362, the *N*-oxide/mCPBA salt **366** was implemented (Scheme 70). While this lowered the yield from 55% to 40%, it could offer a long-term storage solution for the *N*-oxide. In order to avoid the *N*-oxide getting saturated with water, it could be stored as the salt **366**, and then converted back to the discrete *N*-oxide **366** just before it is implemented into a cycloaddition reaction.

4.2.2 Reactions with *Cis*-stilbene

The reactions of *N*-oxide **360** and *trans*-stilbene (**361**) to form **362** seemed to be diastereoselective since no diastereomeric protons were present in any crude ^{1}H NMR spectrum obtained. To further probe this observation, reactions with *cis*-stilbene (**367**) were carried out (Scheme 71).

Scheme 72. Reaction of *tert*-butyl pyrroldine *N*-oxide and *Cis*-stilbene

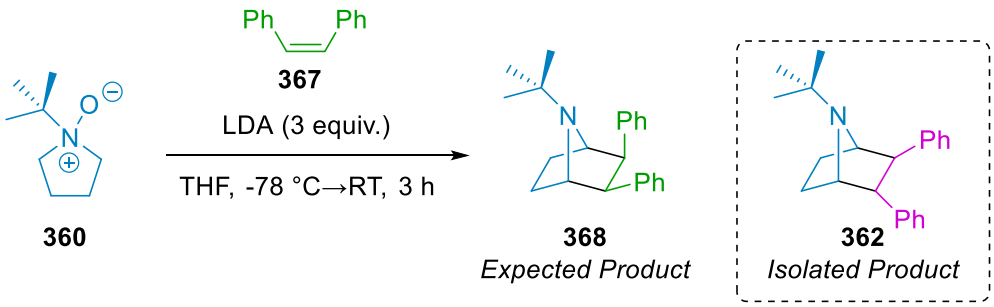

The crude reaction mixture had a significant amount of unreacted *cis*-stilbene (**367**) and a product present that had similar signals to **362**. Surprisingly only the *trans*-bicyclic **362** was isolated which could mean that this reaction undergoes a step-wise mechanism rather than the asynchronous concerted mechanism we had figured out computationally.[42]

A series of control experiments were carried out in order to determine if *trans*-stilbene was isomerizing into *cis*-stilbene under the reaction conditions (Table 4). Indeed, in the presence of LDA *cis*-stilbene isomerized into *trans*-stilbene under the reaction conditions with 11% NMR conversion (Table 12, Entry 3). The isomerization of *cis*-stilbene to *trans*-stilbene in the presence of lithium bases has also been documented by O'Shea and coworkers.[43] These results also suggest

that the [3+2]-cycloaddition with *trans*-stilbene is more favorable than with *cis*-stilbene since the *N*-oxide readily reacted with the *trans*-stilbene that was present forming **362** and leaving much of the *cis*-stilbene unreacted.

Table 12. Control experiments with *cis*-stilbene

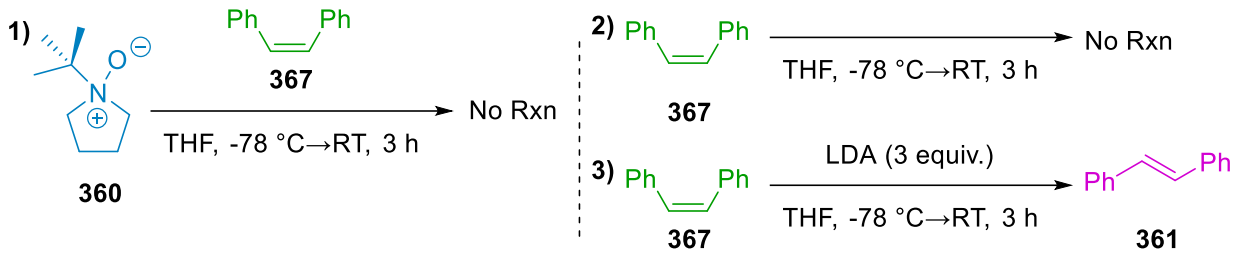

Entry	*N*-oxide	*Cis*-stilbene	LDA	NMR Conversion (%)[a]
1	0.2 mmol	0.2 mmol	--	No Reaction
2	--	0.2 mmol	--	No Reaction
3	--	0.2 mmol	0.6 mmol	11

[a]NMR conversion was calculated from the *cis*-stilbene signal at 6.5 ppm, and the *trans*-stilbene signal at 7.15 ppm

4.3 Conclusions

A new and relatively simple method of forming a substituted azabicyclo[2.2.1]heptane **362** was developed. Previous methods to form similar motifs were limited to commercially available azabicyclic cores, or suffered from multiple steps with limited opportunities to easily introduce new substrates into the reaction scope. This method offers an advantage over established methods by offering more substrate scope variability in a single step from simple starting reagents to form a substituted azabicyclic core. The observations and experimental evidence acquired from all of these reactions and tests aided in the computational determination of the mechanism for this [3+2]-cycloaddition reaction.[42] While only a 56% yield was achieved for **362** from this transformation,

in context it really is not that low considering the yields of the total synthetic methods used to achieve similar structures resulted in a 42% yield at most for the azabicyclic core. This methodology could serve as a powerful tool in the discovery of new therapeutics ranging from pain-killers to nicotine patches, and more.

4.4 References

(1) Traynor, J. Epibatidine and pain. *British journal of anaesthesia* **1998**, *81* (1), 69-76.

(2) Williams, M.; Martin Garraffo, H.; F. Spande, T. Epibatidine: From Frog Alkaloid to Analgesic Clinical Candidates. A Testimonial to "True Grit"! *Heterocycles* **2009**, *79* (1). DOI: 10.3987/REV-08-SR(D)5.

(3) Carroll, F. I. Epibatidine analogs synthesized for characterization of nicotinic pharmacophores-a review. *Heterocycles* **2009**, *79*, 99-120. DOI: 10.3987/rev-08-sr(d)1 From NLM.

(4) Dong, J. C.; Wang, X.; Li, R. T.; Zhang, H. M.; Cheng, T. M.; Li, C. L. Synthesis and analgesic activity of hydrochlorides and quaternary ammoniums of epibatidine incorporated with amino acid ester. *Bioorg Med Chem Lett* **2003**, *13* (24), 4327-4329. DOI: 10.1016/j.bmcl.2003.09.047

(5) Carroll, F. I.; Brieaddy, L. E.; Navarro, H. A.; Damaj, M. I.; Martin, B. R. Synthesis and pharmacological characterization of exo-2-(2'-chloro-5-pyridinyl)-7-(endo and exo)-aminobicyclo[2.2.1]heptanes as novel epibatidine analogues. *J Med Chem* **2005**, *48* (23), 7491-7495. DOI: 10.1021/jm058243v From NLM.

(6) Carroll, F. I.; Lee, J. R.; Navarro, H. A.; Ma, W.; Brieaddy, L. E.; Abraham, P.; Damaj, M. I.; Martin, B. R. Synthesis, nicotinic acetylcholine receptor binding, and antinociceptive properties of 2-exo-2-(2',3'-disubstituted 5'-pyridinyl)-7-azabicyclo[2.2.1]heptanes: epibatidine analogues. *J Med Chem* **2002**, *45* (21), 4755-4761. DOI: 10.1021/jm0202268 From NLM.

(7) Carroll, F. I.; Liang, F.; Navarro, H. A.; Brieaddy, L. E.; Abraham, P.; Damaj, M. I.; Martin, B. R. Synthesis, nicotinic acetylcholine receptor binding, and antinociceptive properties of 2-exo-2-(2'-substituted 5'-pyridinyl)-7-azabicyclo[2.2.1]heptanes. Epibatidine analogues. *J Med Chem* **2001**, *44* (13), 2229-2237. DOI: 10.1021/jm0100178 From NLM.

(8) Carroll, F. I.; Ma, W.; Yokota, Y.; Lee, J. R.; Brieaddy, L. E.; Navarro, H. A.; Damaj, M. I.; Martin, B. R. Synthesis, nicotinic acetylcholine receptor binding, and antinociceptive properties of 3'-substituted deschloroepibatidine analogues. Novel nicotinic antagonists. *J Med Chem* **2005**, *48* (4), 1221-1228. DOI: 10.1021/jm040160b From NLM.

(9) Carroll, F. I.; Robinson, T. P.; Brieaddy, L. E.; Atkinson, R. N.; Mascarella, S. W.; Damaj, M. I.; Martin, B. R.; Navarro, H. A. Synthesis and nicotinic acetylcholine receptor binding properties of bridged and fused ring analogues of epibatidine. *J Med Chem* **2007**, *50* (25), 6383-6391. DOI: 10.1021/jm0704696 From NLM.

(10) Carroll, F. I.; Ware, R.; Brieaddy, L. E.; Navarro, H. A.; Damaj, M. I.; Martin, B. R. Synthesis, nicotinic acetylcholine receptor binding, and antinociceptive properties of 2'-fluoro-3'-(substituted phenyl)deschloroepibatidine analogues. Novel nicotinic antagonist. *J Med Chem* **2004**, *47* (18), 4588-4594. DOI: 10.1021/jm040078g From NLM.

(11) Ivy Carroll, F.; Yokota, Y.; Ma, W.; Lee, J. R.; Brieaddy, L. E.; Burgess, J. P.; Navarro, H. A.; Damaj, M. I.; Martin, B. R. Synthesis, nicotinic acetylcholine receptor binding, and pharmacological properties of 3'-(substituted phenyl)deschloroepibatidine analogs. *Bioorg Med Chem* **2008**, *16* (2), 746-754. DOI: 10.1016/j.bmc.2007.10.027 From NLM.

(12) Okabe, K.; Natsume, M. Total Synthesis of a Frog Poison, (±)-Epibatidine, a Potent Non-opioid Analgesic. *Chemical & Pharmaceutical Bulletin* **1994**, *42* (7), 1432-1436. DOI: 10.1248/cpb.42.1432.

(13) Badio, B.; Garraffo, H. M.; Plummer, C. V.; Padgett, W. L.; Daly, J. W. Synthesis and nicotinic activity of epiboxidine: an isoxazole analogue of epibatidine. *Eur J Pharmacol* **1997**, *321* (2), 189-194. DOI: 10.1016/s0014-2999(96)00939-9

(14) Préville, C.; Bonaventure, P.; Koudriakova, T.; Lord, B.; Nepomuceno, D.; Rizzolio, M.; Mani, N.; Coe, K. J.; Ndifor, A.; Dugovic, C.; et al. Substituted Azabicyclo[2.2.1]heptanes as Selective Orexin-1 Antagonists: Discovery of JNJ-54717793. *ACS Medicinal Chemistry Letters* **2020**, *11* (10), 2002-2009. DOI: 10.1021/acsmedchemlett.0c00085.

(15) Roussi, G.; Beugelmans, R.; Chastanet, J.; Roussi, G. The [3+2] Cycloaddition Reaction of Nonstabilized Azomethine Ylide Generated from Trimetylmine *N*-oxide to C=C, C=N, and C=S Bonds. *Heterocycles* **1987**, *26* (12), 3197-3202, Journal. DOI: 10.3987/r-1987-12-3197.

(16) Roussi, G.; Zhang, J. A 3+2 cycloaddition route to *N*-H pyrrolidines devoid of electron-withdrawing groups. *Tetrahedron Letters* **1988**, *29* (28), 3481-3482. DOI: https://doi.org/10.1016/0040-4039(88)85195-5.

(17) Roussi, G.; Zhang, J. The use of the β-amino-alcohol-*N*-oxide derivatives in the synthesis of 2,3 or 4-alkyl substituted nh pyrrolidines. *Tetrahedron* **1991**, *47* (28), 5161-5172. DOI: https://doi.org/10.1016/S0040-4020(01)87128-3.

(18) Spande, T. F.; Garraffo, H. M.; Edwards, M. W.; Yeh, H. J. C.; Pannell, L.; Daly, J. W. Epibatidine: a novel (chloropyridyl)azabicycloheptane with potent analgesic activity from an Ecuadoran poison frog. *Journal of the American Chemical Society* **1992**, *114* (9), 3475-3478. DOI: 10.1021/ja00035a048.

(19) Ricarte, A.; Dalton, J. A. R.; Giraldo, J. Structural Assessment of Agonist Efficacy in the μ-Opioid Receptor: Morphine and Fentanyl Elicit Different Activation Patterns. *Journal of Chemical Information and Modeling* **2021**, *61* (3), 1251-1274. DOI: 10.1021/acs.jcim.0c00890.

(20) Wightman, R.; Perrone, J.; Portelli, I.; Nelson, L. Likeability and Abuse Liability of Commonly Prescribed Opioids. *Journal of Medical Toxicology* **2012**, *8* (4), 335-340. DOI: 10.1007/s13181-012-0263-x.

(21) Abril Ochoa, L.; Naeem, F.; White, D. J.; Bijur, P. E.; Friedman, B. W. Opioid-induced Euphoria Among Emergency Department Patients With Acute Severe Pain: An Analysis of Data From a Randomized Trial. *Academic Emergency Medicine* **2020**, *27* (11), 1100-1105. DOI: https://doi.org/10.1111/acem.13946.

(22) Lloyd, G. K.; Williams, M. Neuronal nicotinic acetylcholine receptors as novel drug targets. *Journal of Pharmacology and Experimental Therapeutics* **2000**, *292* (2), 461-467.

(23) Carroll, F. I.; Lee, J. R.; Navarro, H. A.; Brieaddy, L. E.; Abraham, P.; Damaj, M. I.; Martin, B. R. Synthesis, nicotinic acetylcholine receptor binding, and antinociceptive properties of 2-exo-2-(2'-substituted-3'-phenyl-5'-pyridinyl)-7-azabicyclo[2.2.1]heptanes. Novel nicotinic antagonist. *J Med Chem* **2001**, *44* (24), 4039-4041. DOI: 10.1021/jm015561v From NLM.

(24) Flores, Á.; Valls-Comamala, V.; Costa, G.; Saravia, R.; Maldonado, R.; Berrendero, F. The Hypocretin/Orexin System Mediates the Extinction of Fear Memories. *Neuropsychopharmacology* **2014**, *39* (12), 2732-2741. DOI: 10.1038/npp.2014.146.

(25) Bonaventure, P.; Dugovic, C.; Shireman, B.; Preville, C.; Yun, S.; Lord, B.; Nepomuceno, D.; Wennerholm, M.; Lovenberg, T.; Carruthers, N.; et al. Evaluation of JNJ-54717793 a Novel Brain Penetrant Selective Orexin 1 Receptor Antagonist in Two Rat Models of Panic Attack Provocation. *Frontiers in Pharmacology* **2017**, *8*, Original Research. DOI: 10.3389/fphar.2017.00357.

(26) Bonaventure, P.; Yun, S.; Johnson, P. L.; Shekhar, A.; Fitz, S. D.; Shireman, B. T.; Lebold, T. P.; Nepomuceno, D.; Lord, B.; Wennerholm, M.; et al. A Selective Orexin-1 Receptor Antagonist

Attenuates Stress-Induced Hyperarousal without Hypnotic Effects. *Journal of Pharmacology and Experimental Therapeutics* **2015**, *352* (3), 590-601. DOI: 10.1124/jpet.114.220392.

(27) Johnson, P. L.; Truitt, W.; Fitz, S. D.; Minick, P. E.; Dietrich, A.; Sanghani, S.; Träskman-Bendz, L.; Goddard, A. W.; Brundin, L.; Shekhar, A. A key role for orexin in panic anxiety. *Nature Medicine* **2010**, *16* (1), 111-115. DOI: 10.1038/nm.2075.

(28) Pollack, M. H.; Lepola, U.; Koponen, H.; Simon, N. M.; Worthington, J. J.; Emilien, G.; Tzanis, E.; Salinas, E.; Whitaker, T.; Gao, B. A double-blind study of the efficacy of venlafaxine extended-release, paroxetine, and placebo in the treatment of panic disorder. *Depression and Anxiety* **2007**, *24* (1), 1-14. DOI: https://doi.org/10.1002/da.20218.

(29) Goddard, A. W.; Brouette, T.; Almai, A.; Jetty, P.; Woods, S. W.; Charney, D. Early Coadministration of Clonazepam With Sertraline for Panic Disorder. *Archives of General Psychiatry* **2001**, *58* (7), 681-686. DOI: 10.1001/archpsyc.58.7.681 (acccessed 6/4/2023).

(30) Nutt, D. J.; Ballenger, J. C.; Sheehan, D.; Wittchen, H.-U. Generalized anxiety disorder: comorbidity, comparative biology and treatment. *International Journal of Neuropsychopharmacology* **2002**, *5* (4), 315-325. DOI: 10.1017/s1461145702003048 (acccessed 6/4/2023).

(31) Baldwin, D. S.; Anderson, I. M.; Nutt, D. J.; Bandelow, B.; Bond, A.; Davidson, J. R. T.; den Boer, J. A.; Fineberg, N. A.; Knapp, M.; Scott, J.; et al. Evidence-based guidelines for the pharmacological treatment of anxiety disorders: recommendations from the British Association for Psychopharmacology. *Journal of Psychopharmacology* **2005**, *19* (6), 567-596. DOI: 10.1177/0269881105059253.

(32) Cloos, J.-M.; Ferreira, V. Current use of benzodiazepines in anxiety disorders. *Current Opinion in Psychiatry* **2009**, *22* (1).

(33) Cox, C. D.; McGaughey, G. B.; Bogusky, M. J.; Whitman, D. B.; Ball, R. G.; Winrow, C. J.; Renger, J. J.; Coleman, P. J. Conformational analysis of N,*N*-disubstituted-1,4-diazepane orexin receptor antagonists and implications for receptor binding. *Bioorganic & Medicinal Chemistry Letters* **2009**, *19* (11), 2997-3001. DOI: https://doi.org/10.1016/j.bmcl.2009.04.026.

(34) Rappas, M.; Ali, A. A. E.; Bennett, K. A.; Brown, J. D.; Bucknell, S. J.; Congreve, M.; Cooke, R. M.; Cseke, G.; de Graaf, C.; Doré, A. S.; et al. Comparison of Orexin 1 and Orexin 2 Ligand Binding Modes Using X-ray Crystallography and Computational Analysis. *Journal of Medicinal Chemistry* **2020**, *63* (4), 1528-1543. DOI: 10.1021/acs.jmedchem.9b01787.

(35) Yang, C. S.; Yoo, J.-S. H.; Ishizaki, H.; Hong, J. Cytochrome P450IIe1: Roles in Nitrosamine Metabolism and Mechanisms of Regulation. *Drug Metabolism Reviews* **1990**, *22* (2-3), 147-159. DOI: 10.3109/03602539009041082.

(36) Ohwada, T.; Ishikawa, S.; Mine, Y.; Inami, K.; Yanagimoto, T.; Karaki, F.; Kabasawa, Y.; Otani, Y.; Mochizuki, M. 7-Azabicyclo[2.2.1]heptane as a structural motif to block mutagenicity of nitrosamines. *Bioorganic & Medicinal Chemistry* **2011**, *19* (8), 2726-2741. DOI: 10.1016/j.bmc.2011.02.049 (acccessed 2021-02-25T01:58:31).

(37) Corey, E. J.; Loh, T. P.; AchyuthaRao, S.; Daley, D. C.; Sarshar, S. Stereocontrolled total synthesis of (+)- and (-)-epibatidine. *The Journal of Organic Chemistry* **2002**, *58* (21), 5600-5602. DOI: 10.1021/jo00073a013.

(38) Huang, D. F.; Shen, T. Y. A versatile total synthesis of epibatidine and analogs. *Tetrahedron Letters* **1993**, *34* (28), 4477-4480. DOI: https://doi.org/10.1016/0040-4039(93)88063-O.

(39) Lynch, J. K.; Holladay, M. W.; Ryther, K. B.; Bai, H.; Hsiao, C.-N.; Morton, H. E.; Dickman, D. A.; Arnold, W.; King, S. A. Efficient asymmetric synthesis of ABT-594; a potent, orally

effective analgesic. *Tetrahedron: Asymmetry* **1998**, *9* (16), 2791-2794. DOI: 10.1016/s0957-4166(98)00291-2.

(40) Clayton, S. C.; Regan, A. C. A total synthesis of (±)-epibatidine. *Tetrahedron Letters* **1993**, *34* (46), 7493-7496. DOI: 10.1016/s0040-4039(00)60162-4.

(41) Reich, H. J. *Lithium Amide Bases--A Primer*. ACS Division of Organic Chemistry, **2002**. https://organicchemistrydata.org/hansreich/resources/organolithium/organolithium_data/amidebases.pdf

(42) Neal, M. J.; Hejnosz, S. L.; Rohde, J. J.; Evanseck, J. D.; Montgomery, T. D. Multi-Ion Bridged Pathway of *N*-Oxides to 1,3-Dipole Dilithium Oxide Complexes. *J. Org. Chem.* **2021**, *86* (17), 11502-11518.

(43) Tricotet, T.; Fleming, P.; Cotter, J.; Hogan, A.-M. L.; Strohmann, C.; Gessner, V. H.; O'Shea, D. F. Selective Vinyl C−H Lithiation of cis-Stilbenes. *Journal of the American Chemical Society* **2009**, *131* (9), 3142-3143. DOI: 10.1021/ja809941n.

Chapter 5: Development of a Nickel Catalyzed Route to Allenes

5.1 Introduction

5.1.1 Contextual Summary

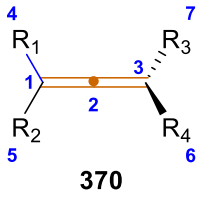

370

Figure 39. Structure of an Allene

Allenes (**370**) have continuously attracted the attention of researchers for decades due to their unique geometry (Figure 39).[1,2] These motifs are present in about 150 natural products, and they exhibit biological properties unlike other simple alkenes.[3,4] Moreover, allenes serve as simple building blocks for complex synthetic targets due to their axial chirality, and ability to transfer this chirality to stereo-enriched products.[5-7] Most of the reported methods for forming substituted allenes involve precious metal catalyzed processes, typically using palladium, iridium, or silver.[8-16] Due to cost and sustainability concerns surrounding precious metal catalysts there has been a concerted push to investigate the use of first-row transition metals as viable alternatives with the goal of developing new methods which mimic the chemistry of their second and third row counterparts. It is well established that both palladium and nickel catalyze the addition of "hard"[17] nucleophiles (i.e. organometallics) to propargylic species to generate substituted allenes.[18-20] What remains to be thoroughly investigated are nickel catalyzed reactions of "soft"[17] nucleophiles (i.e. enolates or alkoxides) and propargyl compounds. For palladium catalyzed reactions, soft nucleophiles and propargyl species undergo double-addition and/or cyclization.[19,21,22] Only one constrained example has been reported of a nickel catalyzed reaction of a soft nucleophile with a propargyl compounds, and instead of double-addition or cyclization products, a substituted allene was formed (Scheme 72a).[23] Focusing on this one example, we looked to expand this into an intermolecular reaction and develop a less

constrained nickel catalyzed method forming allenes from propargyl compounds and "soft" enolate based nucleophiles (Scheme 72b).

Scheme 73. a) Nickel Catalyzed Intramolecular Synthesis of Allenes. b) Proposed Nickel Catalyzed Bimolecular Synthesis of Allenes.

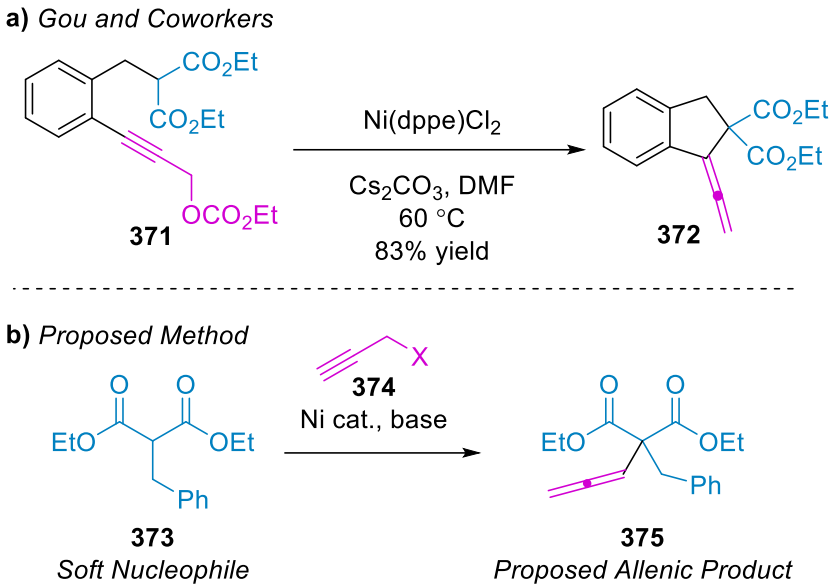

5.1.2. Bioactive Allenes

Allenes are a chemical curiosity dating back to 1875 when Vant Hoff originally proposed this unique structure (Figure 39),[2] which was then followed by the first synthetic method for the generation of allenes reported by Burton and von Pechmann in 1887.[24] Since their discovery, they have gained considerable attention within the past few decades due to their unique geometry, surprising stability, and orthogonal chemistry to other dienes.[1,3,7] Research in allene chemistry was initially hindered due to the assumption that the motif was fairly unstable, but in reality this structure is quite stable and provides access to a wealth of intermediates due to the variety of transformations it can undergo.[1,7,25] Moreover, this motif is remarkably ubiquitous in nature with around 150 allenic natural products that have been isolated so far, with **376** and **377** (Figure 39) being good examples.[3]

Allene **5** was first isolated by Horler in 1970 from the dried bean beetle *Acanthoscelides obtectus*.[26] This compound is postulated to be a pheromone secreted from males of this species.[26] Additionally, the aptly named grasshopper ketone **377** was isolated from the large flightless grasshopper *Romalea microptera*.[27,28] This product was extracted from the defense mechanism secretion of this grasshopper in 1968,[27,28] and then this same product **377** was later isolated from the brown algae *Sargassum fulvellum*, which is an edible seaweed native to South Korea.[29] Researchers have found that grasshopper ketone **377** exhibits anti-inflammatory properties, potentially through inhibition of kappa-B (NF-κB) and mitogen-activated protein kinases (MAPKs).[29]

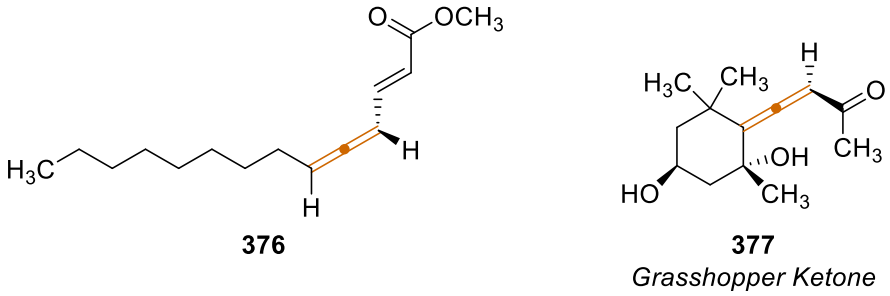

Figure 40. General Allene Structure with Naturally Occurring Allenic Compounds.[26-28]

Allenic alkaloids **378**[30,31] and **379**[32] were isolated from the skin of a Columbian poison dart frog from the *Dendrobates* family (Figure 41). Interestingly, frogs raised in captivity do not secrete **378** suggesting that this toxin is either a product or metabolite derived from their environment.[30,31] Alkaloid **379**, like epibatidine which was also isolated from a poison dart frog, demonstrated strong interactions with the nicotinic acetylcholine receptor (nAChR). Specifically, terminal allene **379** blocks the sodium ion channel of the nAChR, retarding hyperpolarization, which in turn results in an overall inhibitory effect.[33]

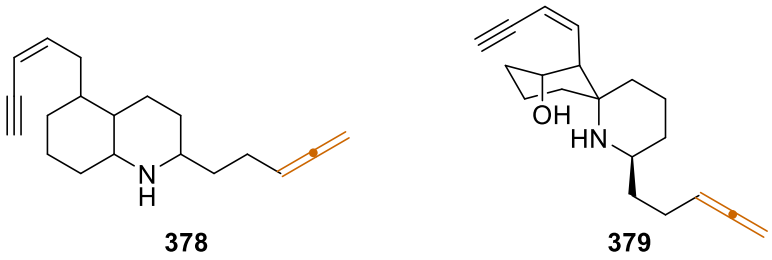

378 **379**

Figure 41. Allenic Alkaloids Isolated from Columbian Poison Dart Frogs from the *Dendrobatiodae* Family.

Not only are allenes abundant in nature, they have also been incorporated into pharmaceuticals and test treatments due to their unique bioactivities. In 1992, Zemlicka and coworkers synthesized both cytallene **380** and adenallene **381** (Figure 42) as enantiomeric pairs and reported their ability to treat human immunodeficiency viruses HIV-1 and HIV-2 through direct inhibition of viral replication and blocking cytopathic mechanisms.[34-36] This same group also reported antiviral activity of (*R*)-cytallene **380** against hepatitis B virus in 1997.[36]

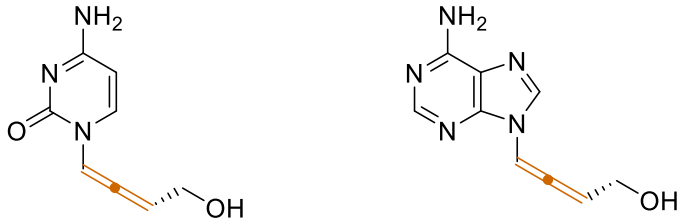

380 (*R*)-cytallene **381** (*R*)-adenallene

Figure 42. Prototype Nucleoside Agents (*R*)-cytallene and (*R*)-adenallene.[34-36]

One of the most noted examples of enhanced pharmacological activity from the incorporation of an allenic moiety is the case of enprostil (**382**) (Figure 43).[37] Enprostil (**382**) is a prostaglandin E_2 (PGE_2) analogue, and though the allenic and phenoxy modification seem minor, they render enprostil (**382**) over 600 times more potent than PEG_2 (**383**).[38]

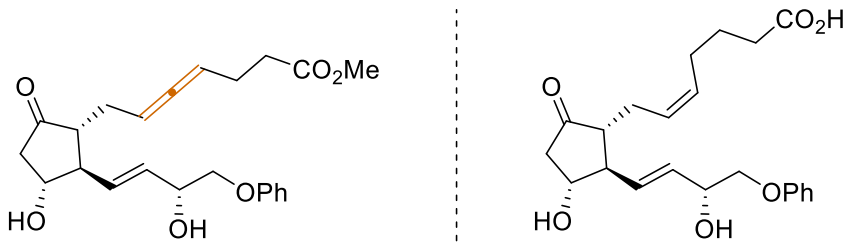

Figure 43. Allenic PEG$_2$ Analogue in Comparison to PEG$_2$[37]

5.1.3. Allenic Building Blocks

While allenes are stable enough to exist in a variety of natural and bioactive compounds, under the right conditions, their structures enable them to act as reactive precursors in the synthesis of complex target molecules of industrial and biological importance.[1,6,7,39] Such transformations include: electrophilic addition, nucleophilic addition, rearrangements, and cycloaddition reactions.[6,40] Their intrinsic chirality promotes stereoselective transformations from their unique ability to transfer axial chirality to one or more stereocenters.[5] Overall, allenes are interesting and high value products serving as effective building blocks for complex organic frameworks in an array of applications.

5.1.3.1 Cycloadditions of Allenes

The cycloadditions of allenes are common tactics to form heterocycles efficiently and stereoselectivity in some cases; the axial chirality of the allene allows it to transfer that chirality to the resulting products.[5] VanBrunt and Standaert took advantage of this ability in their short total synthesis of (+)-furanomycin **386** using a silver catalyzed [3+2]-cycloaddition to form the key intermediate **385** enantioselectively from an allenic precursor **384** (Scheme 73).[41]

Scheme 74. Silver Catalyzed Cyclization to Form Key Intermediate in Total Synthesis of (+)-Furanomycin.[41]

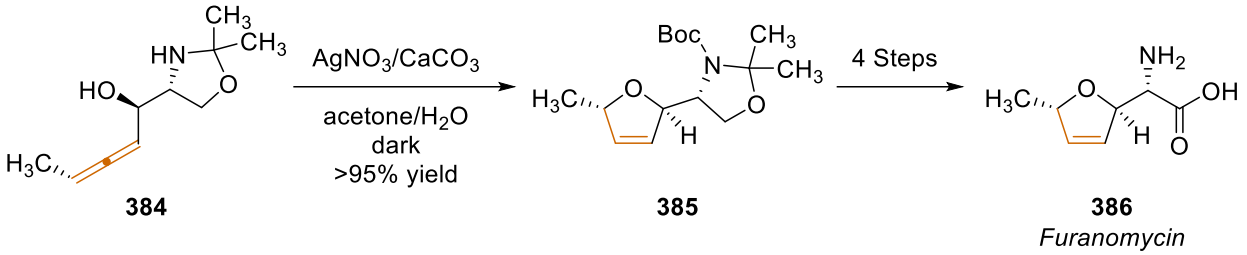

[2+2]-cycloaddition are a less common class of cycloadditions, however in 1989, Shima and coworkers reported a facile synthesis for bicyclic compounds using this transformation.[24] Allenes **387** and α,β-unsaturated cyclohexenones **388** undergo [2+2]-cycloadditions when irradiated to form **389** in yields ranging from 7-95% (Scheme 74a).[24] Similarly, Dauben and coworkers reported the light mediated intramolecular [2+2]-cycloaddition of **390** forming tricyclic compound **391** in 80% yield (Scheme 74b).[42]

Scheme 75. [2+2]-Cycloadditions Forming Bicyclic Products.[24,42]

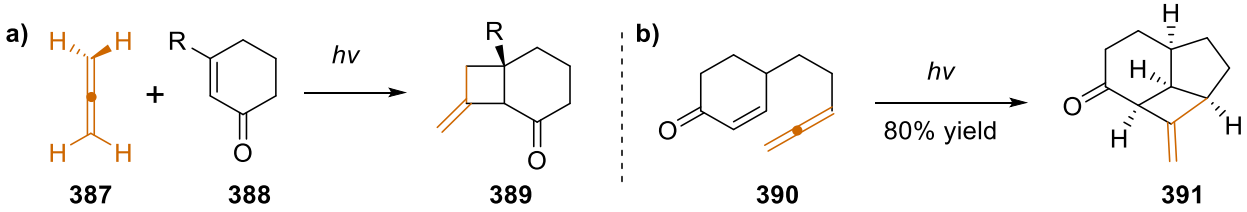

5.1.3.2 Electrophilic Additions of Allenes

The electrophilic addition of allenes is a useful approach for installing two separate functionalities in one step because the electrophilic addition is then followed by the addition of a nucleophile. Ma and coworkers implemented iodine as the electrophile, and in doing so, were able to overcome the regioselectivity challenges most electrophilic additions of this kind face.[43] With iodine serving as

the electrophile, the mechanism proceeds through the halonium intermediate **394,** only allowing S_N2 displacement at the sp^3 hybridized carbon (Scheme 75).[43]

Scheme 76. Electrophilic Addition of Iodine into Substituted Allenes.[43,44]

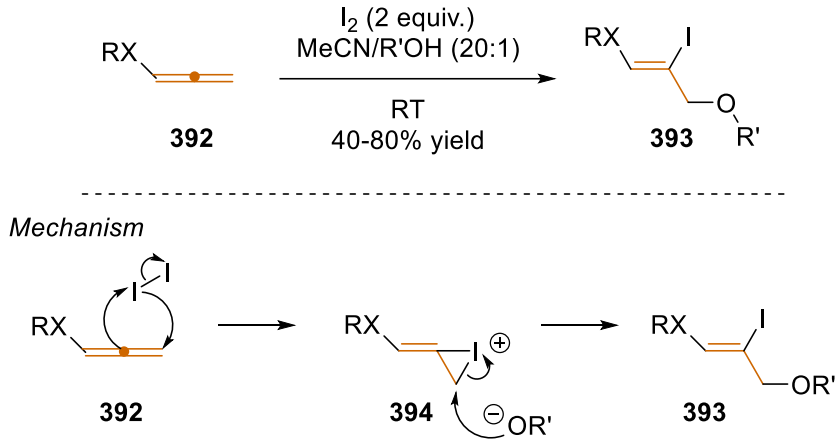

5.1.3.3 Nucleophilic Additions of Allenes

Like electrophilic addition, nucleophilic addition of allenes is a useful tool for installing two distinct functionalities in a single step. After undergoing nucleophilic attack, the electrons from the π-bond then are added into an electrophile. Tamaru and coworkers reported an interesting nucleophilic addition of vinylic species **395** into allene **394** forming bicyclic **396** (Scheme 76). After nucleophilic attack of **395** into allene **394**, the electrons from the π-bond of the allene then attack the electrophilic sulfur of the tosyl protecting group ultimately resulting in the formation of presumed zwitterionic intermediate **394** (Scheme 76). After nucleophilic attack by the nitrogen, bicyclic compound **396** is formed. They were able to achieve bicyclic compounds **396** in yields up to 92%.

Scheme 77. Nucleophilic Addition and Cyclization by Tamaru and Coworkers [45]

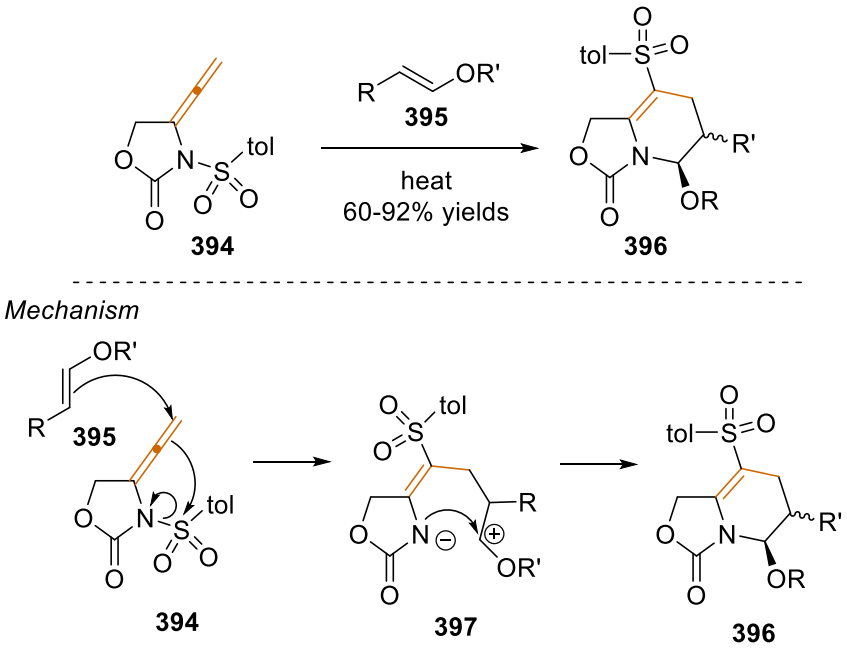

5.1.3.4 Rearrangements with Allenes

Ring expansions are efficient transformations that have led to the construction of various synthetic targets such as pharmaceuticals and natural products.[46] Shiro and coworkers palladium (0) catalyzed ring expansion of allenic benzannulated compounds **398** producing biologically relevant scaffolds **399** (Scheme 77).[47] This tactic formed isoquinolones, naphthoquinones, and isochromanones **399** efficiently in up to 98% yield.[47]

Scheme 78. Palladium Catalyzed Ring Expansion by Shio and coworkers.[47]

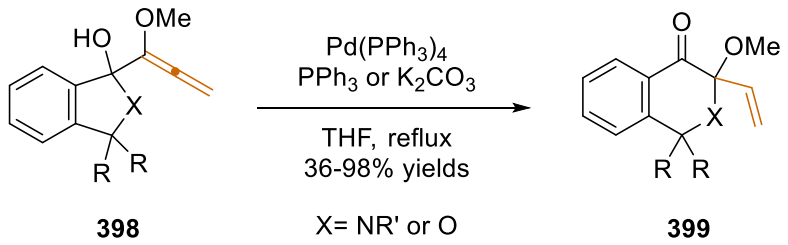

5.1.4. Allenes as Orthogonal Functional Group Handles

There is also increasing interest in utilizing allenes as orthogonal functional groups handles to selectively modify certain amino acid residues in peptides and proteins.[48,49] For example, Loh and coworkers used alleneamide **401** to selectively modify cysteine residues in peptide chains and proteins such as bovine serum albumin (BSA) proteins.[49] The allenamide **401** undergo selective addition to the nucleophilic thiol of cysteine **400** without bonding with any other reactive functionalities in the protein backbone (Scheme 78).[49] This work provides a new functional group handle to add to the repertoire of cysteine modifiers for selective peptide functionalization.

Scheme 79. Selective Modification of Cysteine Residues in Bovine Insulin

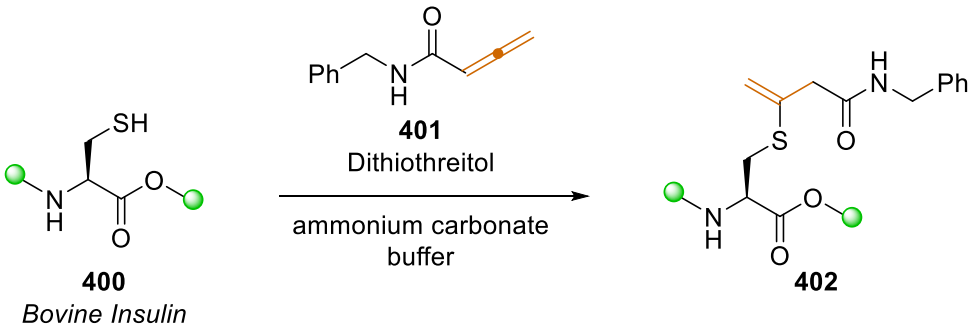

5.1.5 Synthesis of Allenes

Alleneamide **401** was synthesized via a three-step process; first 3-butynoic acid **404** was produced using harsh oxidizing agents, and then they formed desired alleneamide **401** via an esterification and amidation two step protocol (Scheme 79).[49] This method, although effective, has limited functional group compatibility due to the use of harsh oxidizing agents, which is true for many synthetic methods forming this class of compounds.

Scheme 80. Synthesis of Allenamide Cysteine Modifiers by Loh and Coworkers

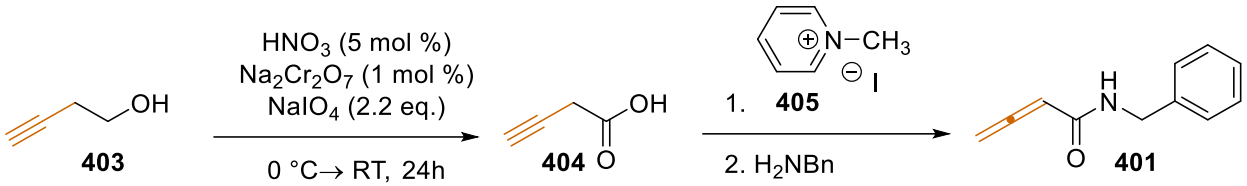

Scheme 81. Synthetic Methods Forming Substituted Allenes

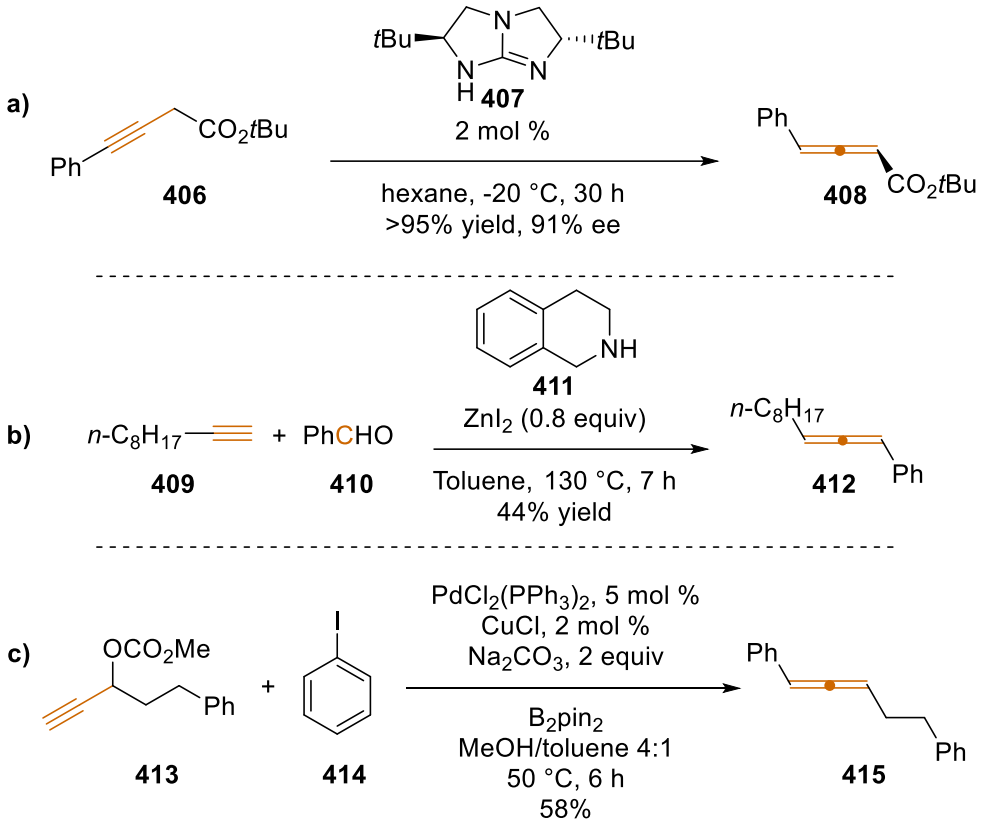

Generally, synthetic methods for forming substituted allenes include elimination reactions of allylic compounds, isomerization of alkynes (Scheme 80a) to more conjugated species,[50] reactions of aldehydes with terminal alkynes (Scheme 80b),[51] and metal catalyzed reactions of propargylic compounds (Scheme 80c).[9,52-54] Similar to Loh and coworker's method, often these methods require high temperatures, multiple steps, or harsh conditions which are incompatible with sensitive functionalities.

Metal catalyzed reactions of propargylic species are a commonly used tactic for substituted allene formation. [9,52-54] The catalysts used in this transformation are predominantly palladium,[55,56] with copper,[57,58] nickel,[59,60] and iron complexes also seeing limited use.[20] The scope of propargylic compounds that have been studied includes propargyl halides,[12,59,60] carbonates,[9,16,54,61] alcohols,[58,62] ethers,[63] and esters.[64]

Recently, Lee and coworkers reported regioselective synthetic methods to form allenes **419** from propargyl chlorides **416** and diisobutylaluminium hydride (DIBAL-H) **417** catalyzed by an *N*-heterocyclic carbene-copper complex **418** in high yield.[57] They reported a broad substrate scope, but the disadvantage of this method was that the reaction is air and moisture sensitive (Scheme 81).[57]

Scheme 82. Copper Catalyzed Regioselective Allene Synthesis from Propargyl Chlorides and DIBAL-H

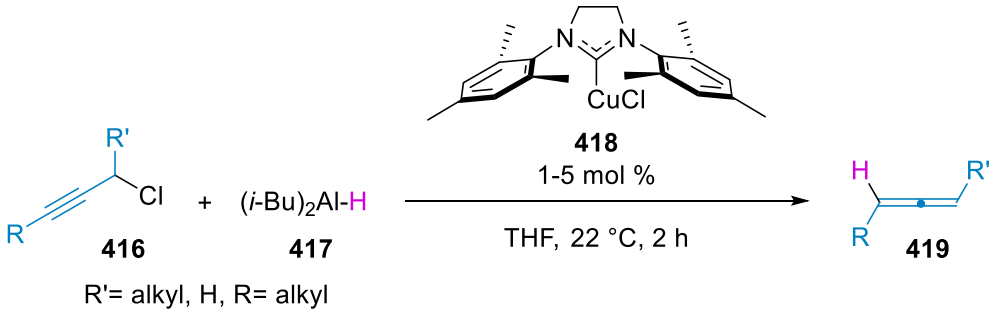

Gau and coworkers formed substituted allenes **422** from propargyl bromide **420** and organotitanium **421** in the presence of a nickel catalyst (Scheme 82).[60] They obtained yields up to 95%, the substrate scope was limited to unhindered aryl organotitanium species along with requiring air and moisture free environments.

Scheme 83. Nickel Catalyzed Substituted Allene Synthesis from Propargyl Halides and Organiotitanium

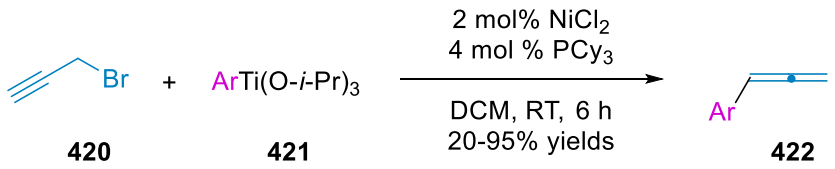

This group also reported allene synthesis from palladium catalyzed reactions of propargyl acetates **423** with trimethylaluminum **424** at ambient temperatures (Scheme 83).[9] Excitingly the substrate scope for this method was not as limited as that of the methods previously mentioned, but these reactions still are sensitive to air and moisture and, like many others, it requires the use of a precious metal catalyst.

While the work from these researchers has improved synthetic methods for forming allenes, there is still a void in the literature for an air stable broadly applicable reaction using common earth metals.

Scheme 84. Palladium Catalyzed Allene Synthesis from Propargyl Acetates with Treiethylaluminum

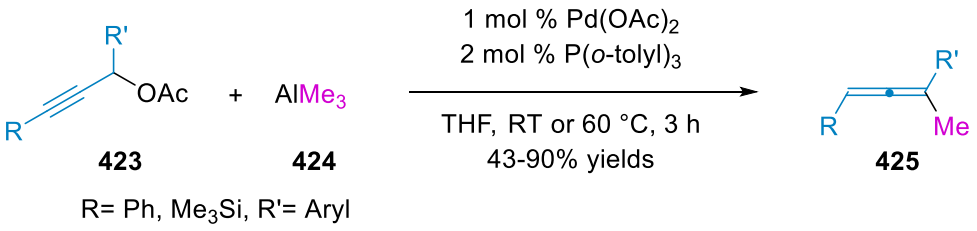

5.1.6 Palladium and Nickel Comparison in Catalysis

As in other aspects of transition metal catalysis, palladium is heavily utilized because of its well-tuned chemical properties and the wealth of knowledge about its mechanism.[65] It is well understood that palladium consistently undergoes two electron reduction-oxidation (redox) cycles (Figure 44).[18] Its reliable redox cycles have been utilized in a wide range of applications including

Suzuki-Miyaura[66] and Sonogashira cross-coupling,[67] Buchwald Hartwig amination,[25] C-H activation, reduction, oxidation, and olefin functionalization just to name a few.[18]

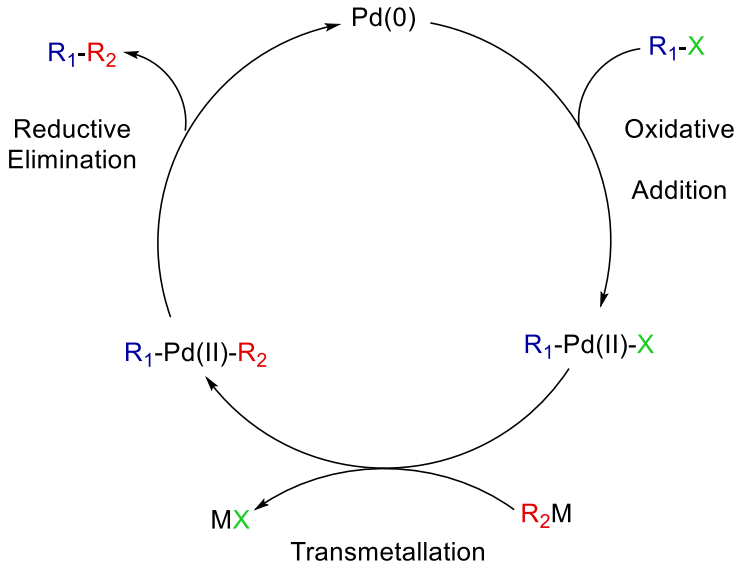

Figure 44. Typical Two Electron Redox Cycle for Palladium

Though palladium is well suited for catalysis, it is a precious metal with an abundance of $5x10^{-5}$ weight percent in the earth's crust.[68] This has led to a push to investigate nickel, a more commonly found first-row metal with a natural abundance of $1.0x10^{-2}$ weight percent in the earth's crust,[68] and is about 2,000 times less expensive than palladium.[69,70] Moreover nickel lies just above palladium on the periodic table, so they share many chemical properties, but there are also some pertinent differences. One major difference is that nickel is intrinsically more reactive than palladium since it has more readily accessible oxidation states and forms weaker carbon metal bonds.[69] This enhanced reactivity allows nickel to undergo the same two electron redox cycles as palladium (Figure 44), as well as participating in many one-electron redox cycles (Figure 45), and any combination of the two types of redox cycles, thus allowing for a myriad of other reaction pathways.[69,71] This difference is primarily attributed to the valence electron configuration with palladium having a filled $4d^{10}$ shell and nickel having a $3d^9$ $4s^1$ configuration. However, given its

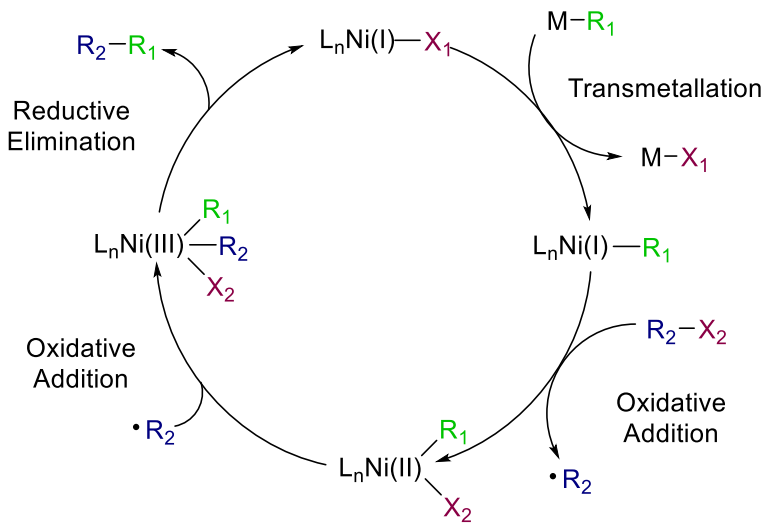

Figure 45. Typical One Electron Redox Cycle for Nickel

advantages many groups have studied this problem, uncovering new reaction mechanisms and methods for forming novel products.[72]

Nickel's high reactivity has historically rendered it difficult to control and nearly unpredictable. As a result, nickel was deemed the "spirited horse" in catalysis, but with modern advances in ligand design, this high reactivity can be harnessed to perform the same reactions completed by palladium's catalytic cycle while offering an opportunity to explore orthogonal pathways.[69,71,72] This is where the basis of our research interest lies: in studying the similarities and differences within the context of nickel's ability to facilitate the formation of substituted allenes in the presence of propargyl compounds and nucleophiles.

5.1.7 Palladium Catalysis in Allene Synthesis

It is well understood in the literature that palladium[18,19] and nickel[20] both catalyze the formation of substituted allenes by way of propargyl species with hard[17] nucleophiles.[18] A plausible mechanism for the formation of metallo-allene **427** is afforded by oxidative addition to the propargyl species in an S_N2' fashion.[73] This palladium allene can then transmetallate with a organomagnesium, organozinc, organostanane, or other organometallic species (M-R) to give

intermediate **430**. This can finally generate allene **431** following reductive elimination, regenerating the palladium catalyst (Figure 46).[18,73] To date this mechanism has not been rigorously studied and is simply one plausible pathway of several, the nickel pathways are even less understood and no mechanism is widely accepted.

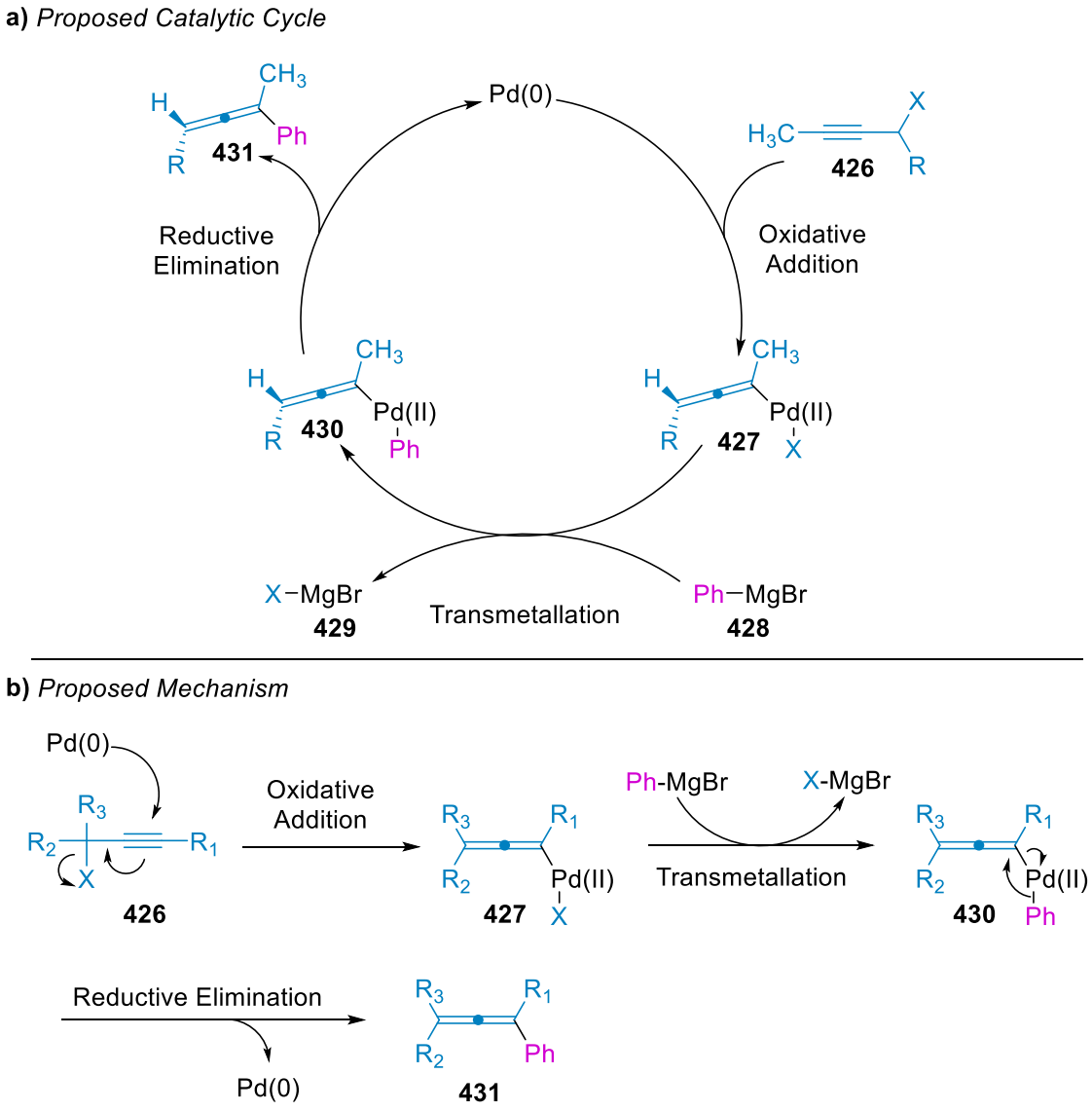

Figure 46. Catalytic Cycle for Palladium Catalyzed Allene Formation from Propargyl Compounds and Soft Nucleophiles

Scheme 85. Palladium catalyzed transformations of soft nucleophiles and propargyl carbonates: a) double addition, b) cyclization.

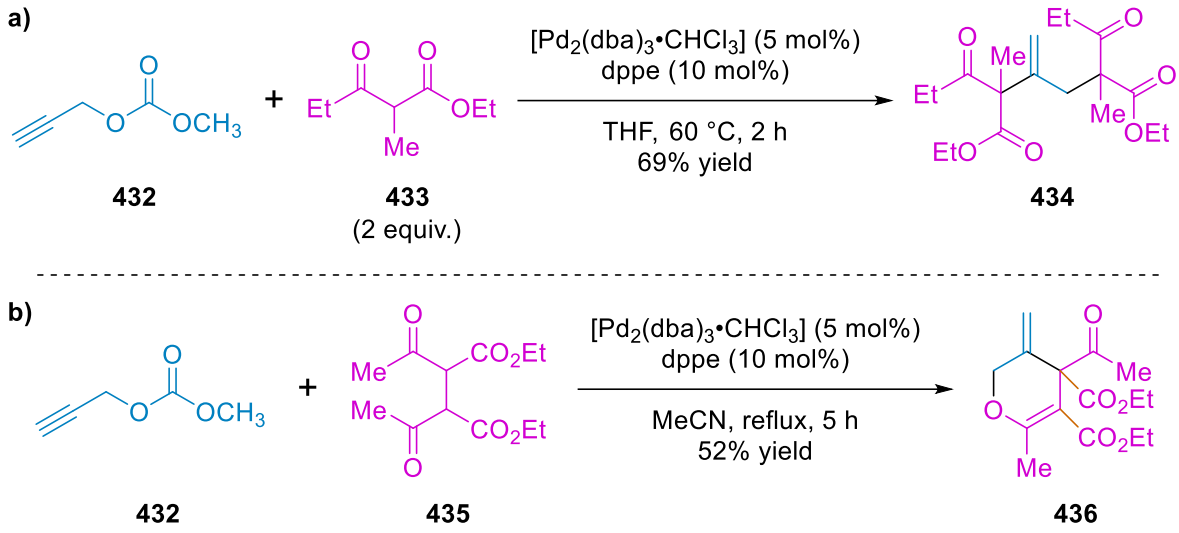

Interestingly, if a soft[17] nucleophile is implemented with palladium, the propargyl species undergoes double addition in the presence of two equivalents of the nucleophile **433** (Scheme 84a),[74] or it can undergo a cyclization if a single bidentate nucleophile **435** is used (Scheme 84b).[19,21,22,75] These palladium catalyzed cyclization have been used to form intriguing and complex fused ring systems.[19,22]

Most recently in 2021, Lin and coworkers used palladium catalysis to synthesize a variety of aryl allenes using an unusual β-hydride elimination.[76] Initially, their proof of concept used an α/β-unsaturated ketone **437** in the presence of a palladium catalyst and trace amounts of allene **438** was formed (Scheme 85a).[76] This was surprising since the presumed intermediate, the palladium η^3 complex, is typically viewed as being stable to β-hydride elimination. They elected to change the starting material to using vinyl bromide **439**, and diazoacetate **440** and formed allene **441** in 80% yield (Scheme 85b).[76] These conditions were then used to achieve a library of 42 different aryl allenes in 40-91% yields.[76] This reaction tolerates both electron rich and electron deficient substituents, but this reaction does require careful considerations of the steric environment.[76]

Scheme 86. Palladium Catalyzed Allene Formation via β-Hydride Elimination

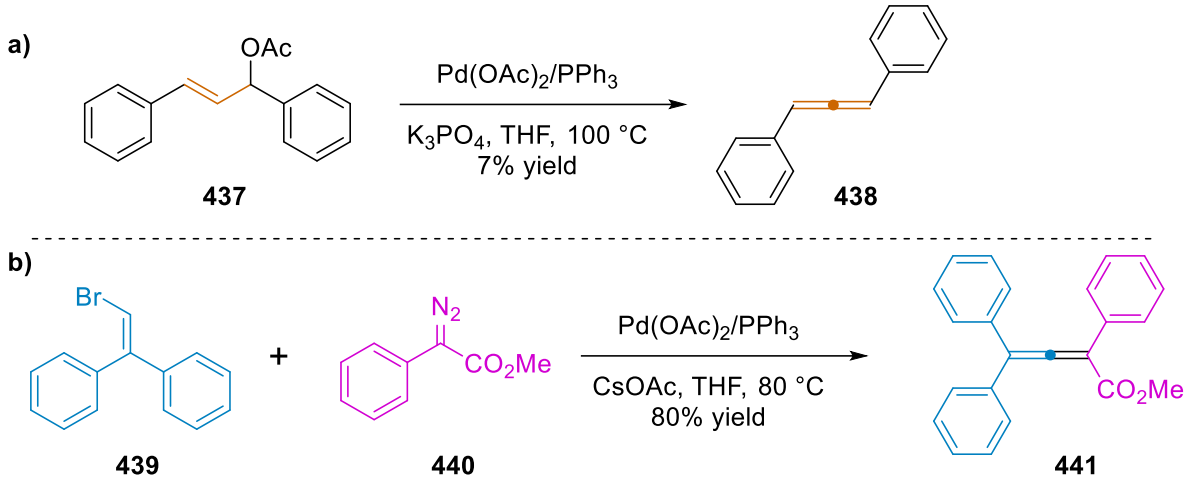

5.1.8 Nickel Catalysis in Allene Synthesis

In 2018, Li and coworkers reported the synthesis of multi-substituted allenes via a palladium catalyzed S_N2' substitution of organoaluminum with propargyl acetates.[13] They later expanded this research performing similar reactions with a nickel catalyst, which as discussed previously is a more sustainable alternative.[64] This system produces multi-substituted allenes from propargyl esters with aryls bearing electron-donating or electron-withdrawing groups and organoaluminium reagents.[64]

The proposed mechanism for this system starts with a ligand exchange switching the chloride ions with two methyl groups from trimethylaluminum which are then reductively eliminated forming the active catalyst $Ni(PPh_3)_2$ (Figure 47).[64] This then coordinates to the π system of the propargyl species forming **443**, followed by $Ni(PPh_3)_2$ undergoing an oxidative addition forming metaloallene **444**. Next a transmetallation step occurs exchanging acetate with a methyl group resulting in **445**, this then undergoes reductive elimination forming the substituted allene **446**. This work demonstrates that a nickel catalyst can promote the S_N2' reaction of a propargyl compound

with a hard[17] organometallic nucleophile, therefore this same system could potentially be incorporated with a soft nucleophile instead.

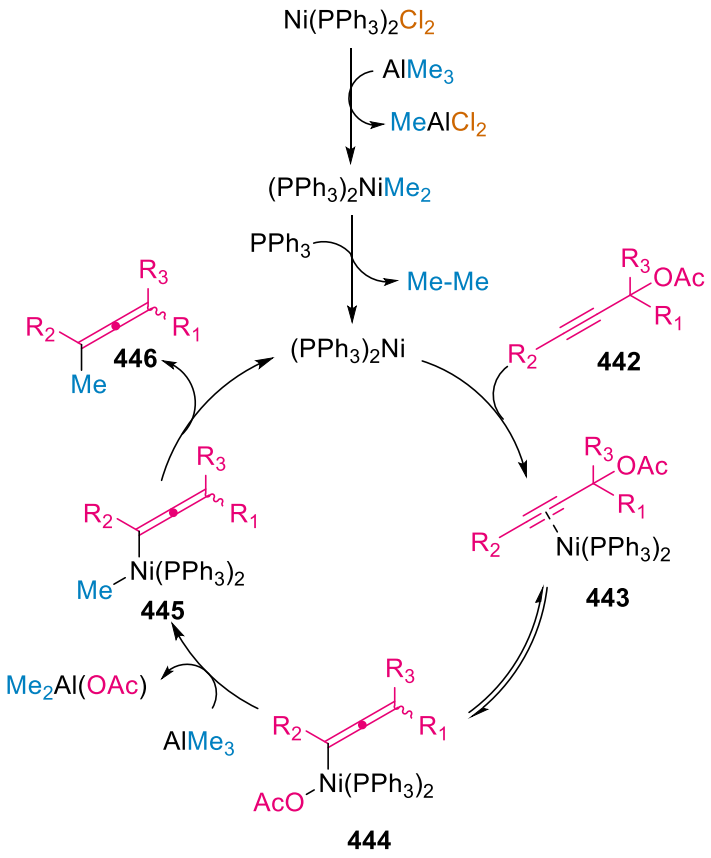

Figure 47. Proposed Catalytic Cycle for Nickel Catalyzed S_N2' Substitution Forming Allenes

Scheme 87. Intramolecular Nickel Catalyzed Allene Formation[23]

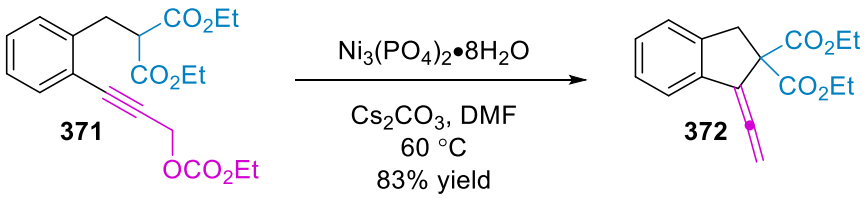

In 2008 Liang and coworkers reported a remarkable nickel catalyzed carboannulation of a propargylic species **371** forming an allene **372** under ambient conditions (Scheme 86).[23] This is a stark difference to the reaction pathway with palladium because under the same conditions, a cyclization would occur as did in Scheme 84b. This leads into the possibility of methods accessible

with nickel catalysis that have capabilities beyond what is possible with palladium chemistry. While innovative, this work by Liang and coworkers[23] is limited to an intramolecular reaction which is highly contrived and intrinsically limited in scope. We hypothesized that this reaction pathway would behave similarly in a bimolecular system as in a unimolecular system, thereby expanding the scope of this useful transformation.

5.2 Results and Discussion

5.2.1. Replication of a Literature Protocol

Our initial aim before investigating novel systems was to gain familiarity with this type of chemistry, so the multistep synthesis of a substituted allene reported by Liang and coworkers was replicated to ensure that: 1) we could successfully repeat these results and 2) we could verify that our technique was sound (Scheme 87). The first step is a S_N2 reaction where sodium hydride is used to deprotonate diethyl benzylmalonate **448**, and the resulting anion then displaced the bromine on the 2-iodobenzylbromide **447**. This reaction was carried out on a 1.0 mmol scale resulting in a 62% yield of **449**. The second step involved a Sonogoshira cross-coupling of **449**

Scheme 88. Control Multistep Synthesis Replicating Results Reported by Liang and Coworkers

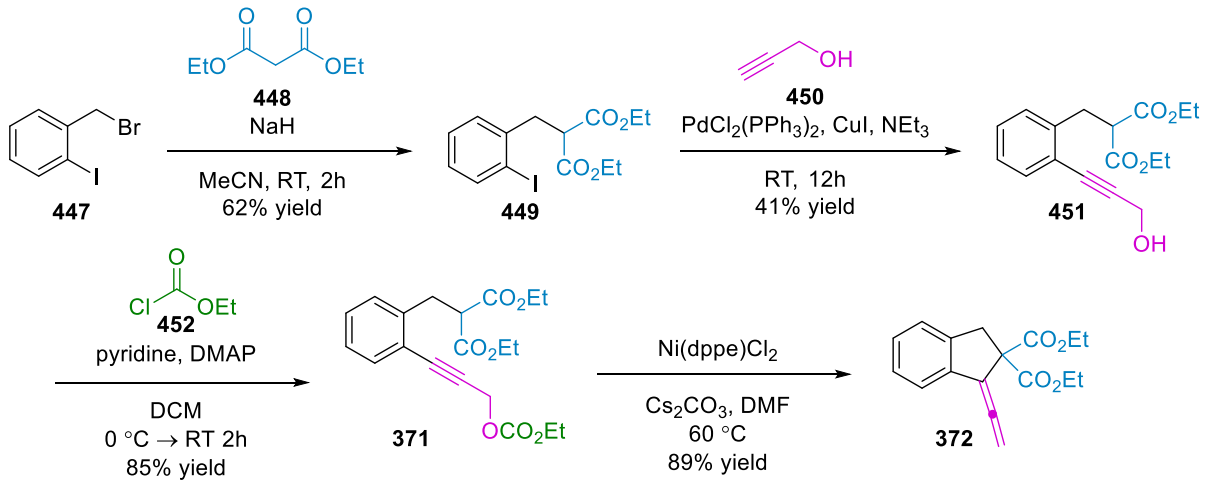

and **450** which converted the iodide of **449** into the propargylic **451** in 47% yield. The third step converts the alcohol into ethyl carbonate, a good leaving group which is essential for the formation of the allene. In this reaction, ethyl chloroformate **452** is activated by DMAP, and the propargyl alcohol is deprotonated by pyridine; the activated carbonyl is then attacked by the deprotonated alcohol forming an ethyl carbonate **371** in 85% yield. The last step forms allene **372** by a nickel catalyzed reaction in the presence of base, and a new bond forms between the diethylmalonate moiety and the propargylic portion. In our hands we achieved a 89% yield, which was higher than the 83% reported in the literature, so in carrying out this control experiment, we gained familiarity with this system which enabled us to move forward to examining novel reaction pathways with a high degree of confidence.

5.2.2. Synthesis of Propargyl Compounds

Scheme 89. Synthesis of Propargyl Compounds to be Incorporated into Nickel Catalyzed Reactions

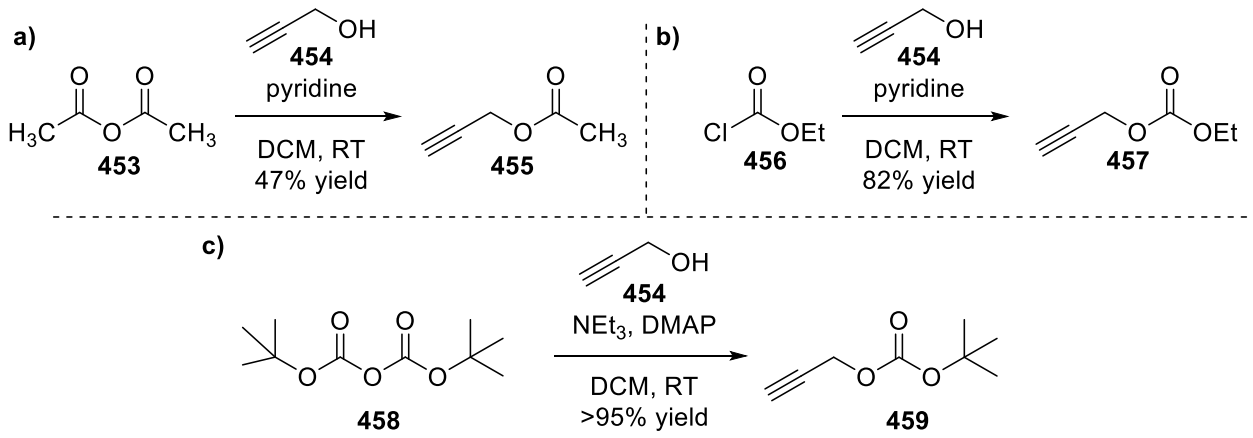

Propargyl compounds for the nickel catalyzed reaction screenings were readily synthesized using simple methods (Scheme 88). Nucleophilic attack of propargyl alcohol **454** into electrophiles **453** and **456** afforded propargyls **455** and **457**, respectively (Scheme 88a-b). Propargyl **459** was formed

under similar conditions, but Boc-anhydride **458** had to first be activated by DMAP in order to then undergo nucleophilic attack of **454** (Scheme 88c).

5.2.3. Synthesis of Soft Nucleophiles

The synthesis of the soft nucleophiles for nickel catalyzed reactions were also formed using facile methods (Scheme 89). Nucleophilic attack of malononitrile **460** into benzaldehyde, followed by reduction formed **461** in 60% yield (Scheme 89a). Deprotonation of **462** by sodium hydride (NaH) followed by nucleophilic substitution of benzyl bromide afforded **463** in 64% yield (Scheme 89b).

Scheme 90. Synthesis of Soft Nucleophiles to be Incorporated into Nickel Catalyzed Reactions

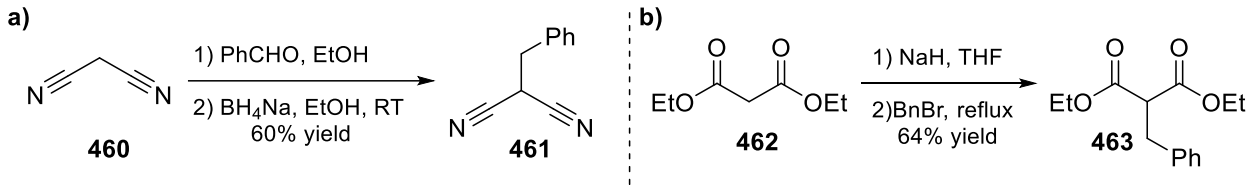

With a series of newly synthesized propargyl compounds and soft nucleophiles in hand, we could then conduct reaction screenings with nickel catalyzed to test if substituted allenes form under these reaction conditions.

5.2.4. Initial Reaction with Ethyl Propargyl Carbonate and Diethyl Benzyl Malonate

Ethyl propargyl carbonate **465** and diethyl benzyl malonate **464** were used in the initial reaction screening because of their similarity to the substrate in the intramolecular control experiment. The reaction conditions from method reported by Liang and coworkers[23] were used a starting point for this new system (Scheme 90). The initial screening of this system at 60 °C resulted in no reaction, so the temperature was increased to 80 °C, and then to 100 °C where there was an array of new signals present in the crude ^{1}H NMR. The most interesting signal from the crude ^{1}H NMR was a doublet of doublets around 5.10 ppm. The allenic protons for the final product of the control

experiment appeared around 5.42 ppm, therefore it seemed reasonable to deduce that the signal around 5.10 ppm would correspond to an allenic proton in predicted product **466**. The product responsible for this signal was isolated via flash column chromatography and characterized by ^{1}H NMR, ^{13}C NMR, COSY, NOESY, HSQC, IR, and ESI-MS.

Scheme 91. Reaction Screening of Nickel Catalyzed Reaction of Ethyl Propargyl Carbonate and Diethyl Benzyl Malonate

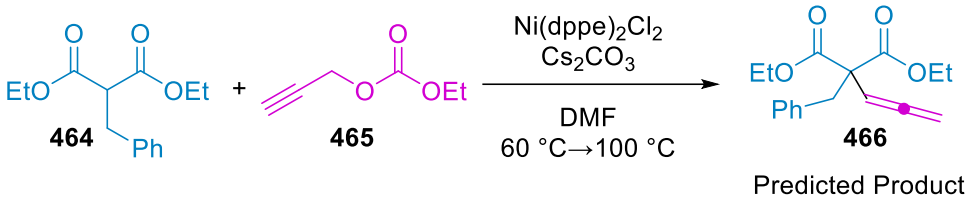

The ^{1}H NMR spectrum was similar to that expected for **466**, however there were only 18 protons present in the ^{1}H NMR spectrum as opposed to the 20 protons of **466**. The ^{13}C NMR also showed a deviation from the predicted product displaying only 14 carbons instead of the 17 carbons of **466**. Distortionless enhancement by polarization transfer (DEPT) provided more information about the ^{13}C NMR spectrum; DEPT 90 displays carbons bound to only one hydrogen, and DEPT 135 differentiates between CH/CH_3, and CH_2 carbons. DEPT was utilized in conjunction with ^{13}C NMR to determine which type of carbon is associated with each signal. These were the initial indications that another product formed.

Additionally, the IR spectrum definitively showed a strong ester stretch at 1746 cm^{-1}, but the allene stretch around 1900-2200 cm^{-1} was absent, thereby confirming the predicted product did not form. Electrospray ionization mass spectroscopy (ESI-MS) corroborated with the ^{13}C NMR in that the starting material, diethyl benzylmalonate, and the product contain the same amount of carbons and protons, suggesting the addition of an oxygen. This led us to the proposed structure **467** for the product (Figure 48), but more information was needed to confirm this structure.

Correlation spectroscopy (COSY) and nuclear overhauser effect spectroscopy (NOESY) were used to probe the structure of the product. COSY provided information on which protons are close through bonds (highlighted in blue, Figure 48), and NOESY exhibited which protons are nearby spatially (highlighted in red, Figure 48).

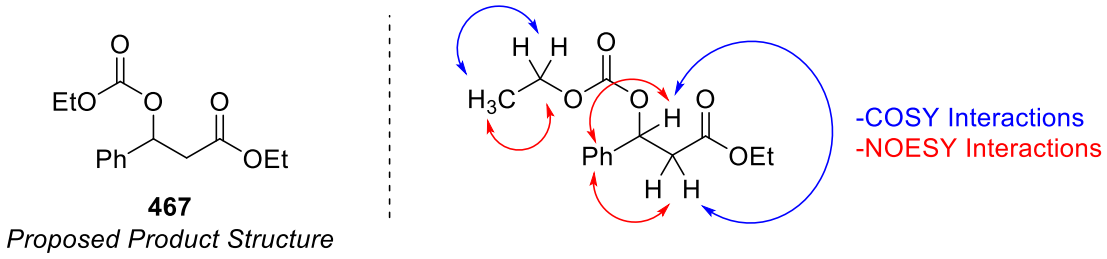

Figure 48. Proposed Structure of Product from Nickel Catalyzed Reaction with Corresponding COSY and NOESY Interations.

The COSY and NOESY support the proposed structure in conjunction with the NMR spectra previously mentioned. Furthermore, heteronuclear single-quantum correlation spectroscopy (HSQC) indicated which protons and carbons are bound by sigma bonds and was consistent with the proposed structure.

5.2.5. Studying the Formation of a Serendipitous Product

This reaction was replicated three times on different reaction scales (Table 13). The results of these experiments demonstrated a trend that as the reaction scale increased, the formation of the product decreased (Table 13, Entries 1-3). Additionally, these entries also verified that the unexpected results are in fact reproducible.

Table 13. Replication of reaction conditions

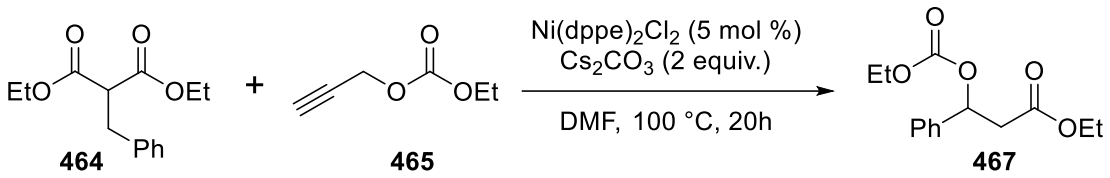

Entry	Nucleophile 464	Propargyl 465	Cs_2CO_3	$Ni(dppe)Cl_2$	NMR Yield (%)
1	0.5 mmol	0.5 mmol	1 mmol	5 mol %	7.2[a]
2	0.8 mmol	0.8 mmol	1.6 mmol	5 mol %	3.8[b]
3	2 mmol	2 mmol	4 mmol	5 mol %	Trace amount

[a]NMR yield calculated using 1,3,5-trimethoxybenzene as a standard. [b]NMR conversion was used instead of yield.

Once we were able to confirm that this reaction outcome was reproducible, a series of control experiments were performed to gain a better understanding of what was involved in the formation of this serendipitous product (Table 14). Entries 1 and 2 suggests that the product forms without the presence of the catalysts, however this result could be due to contamination of glassware or stir bars with nickel from previous experiments. Metal catalysts can linger on the surfaces of stir bars, spatulas, and glassware unless they are rigorously cleaned. These reactions were then repeated using a new test tube, stir bar, and spatula to ensure the reaction mixture is in a nickel free environment, and the same product formed (Table 14, Entries 1-2). Due to the high temperature of reaction necessary for the product to form, it is not an unfathomable result that this transformation is not catalyzed. If it is in fact a nickel catalyzed process, and it requires this high of a temperature, it must have to go through some high energy intermediates or transition states. We wanted to determine what reagents are needed to achieve the product so reactions were conducted in the absence of the propargyl compound, and then in the absence of the nucleophile.

Table 14. Control experiments for nickel catalyzed reaction

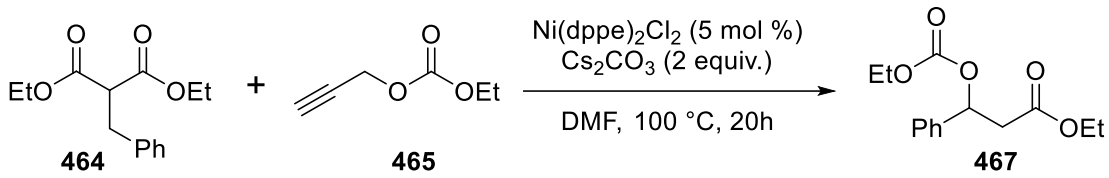

Entry	Malonate 464	Propargyl 465	Cs_2CO_3	$Ni(dppe)Cl_2$	NMR Yield (%)
1	0.2 mmol	0.2 mmol	0.4 mmol	N/A	3[a]
2	2 mmol	2 mmol	4 mmol	N/A	Trace amount
3	0.2 mmol	N/A	0.4 mmol	5 mol %	Trace amount
4	N/A	0.2 mmol	0.4 mmol	5 mol %	No Reaction

[a]NMR yield calculated using 1,3,5-trimethoxybenzene as a standard.

No reaction occurs without the nucleophile (Table 14, Entry 3), which makes sense from the structure of the product which is basically **464** rearranged and esterified. Trace amounts of the product still form without the propargylic species (Table 14, Entry 4) thereby suggesting that product does not form via a unimolecular process.

The problematic aspect of these results from Table 1 and Table 2 are that the baseline yield is so low that it makes it incredibly difficult to discern any trends with a strong degree of confidence. In an effort to simply increase the reaction yield, a series of optimization experiments were conducted.

5.2.6. Optimization of Reaction Conditions for the Transformation of Ethyl Propargyl Carbonate and Diethyl Benzyl Malonate

We initially wanted to determine solvent conditions because that could aid in understanding the intermediates involved for this product to form. A range of coordinating, non-coodinating, polar aprotic, polar protic, and non-polar solvents were incorporated into the reaction conditions (Table

Table 15. Solvent screening for nickel catalyzed reaction

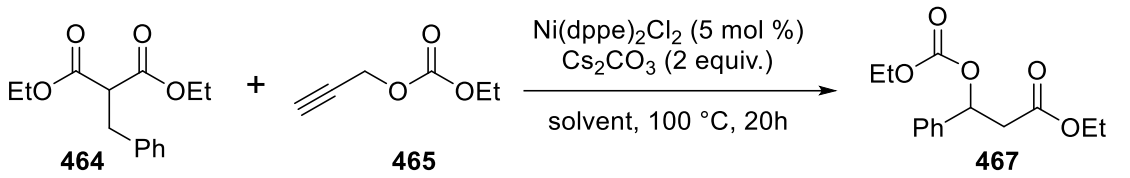

Entry	Solvent	Temperature	NMR yield (%)
1	DMF (Control)	80 °C	No Reaction
2	MeCN	80 °C	No Reaction
3	DME	80 °C	No Reaction
4	DMF	100 °C	15
5	Nitromethane	100 °C	6
6	NMP	100 °C	0.1
7	DMSO	100 °C	No reaction
8	CPME	100 °C	No reaction
9	1,4 Dioxane	100 °C	No Reaction
10	n-propanol	100 °C	No Reaction
11	Diglyme	100 °C	No Reaction
12	Toluene	100 °C	No Reaction

[a]NMR yield calculated using 1,3,5-trimethoxybenzene as a standard.

15). Careful considerations were made in terms of solvent boiling points due to the high temperature of the reaction. Acetonitrile (MeCN) was incorporated as a polar aprotic solvent, and dimethoxyethane (DME) served as a nonpolar coordinating solvent. Due to their lower boiling points, the reaction temperature was lowered to 80 °C, and a control experiment was run in DMF in order to determine if the reaction yield was a result of the solvent or the temperature. No reaction

occurred at 80 °C for DMF, MeCN, DME so the only takeaway from this set of reactions is that the temperature must be higher than 80 °C in order for the product to form regardless of the solvent used (Table 15, Entries 1-3). This is consistent with the original test reaction carried out when this product initially formed where no reaction occurred until 100 °C.

DMF is a polar aprotic solvent, so nitromethane, *N*-methyl-2-pyrrolidone (NMP), dimethyl sulfoxide (DMSO), and cyclopentyl methyl ether (CPME) were then incorporated into the reaction conditions. Of these solvents, only nitromethane and NMP resulted in any reaction at all with low yields of 6 and 0.1%, respectively (Table 15, Entries 4-5). All of the other polar aprotic solvents, aside from DMF (Table 15, Entry 4), resulted in no reaction (Table 3, Entries 7-9). Next, n-propanol served as a polar protic solvent, and it also resulted in no reaction (Table 15, Entry 10). A high-boiling point coordinating solvent, diglyme, was then used in this reaction, and it also resulted in no reaction (Table 15, Entry 11). Lastly, toluene was used as a nonpolar and noncoordinating solvent and again, no reaction occurred (Table 15, Entry 12).

DMF was determined to be the best solvent, with similar solvents resulting in no reaction or low yield. Additionally no reaction occurred with any other solvents. These results in conjunction suggest that this reaction is specific to DMF, or at least suggest that this reaction is specific to solvents containing either nitro groups or amides (Figure 49).

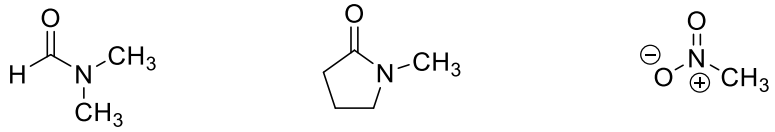

DMF *NMP* *nitromethane*

Figure 49. Structures of dimethylformamide (DMF), *N*-methyl-2-pyrrolidone (NMP), and nitromethane

Base screenings were initially conducted with other carbonate bases: sodium carbonate (Table 16, Entry 2) and potassium carbonate (Table 16, Entry3). When implemented into the reaction, neither resulted in a yield higher than that with cesium carbonate (Table 16, Entry 1). Bicarbonates were then used and sodium bicarbonate resulted in no reaction (Table 16, Entry 4), while potassium bicarbonate only resulted in trace amounts of product (Table 16, Entry 5).

Table 16. Base screening for nickel catalyzed reaction

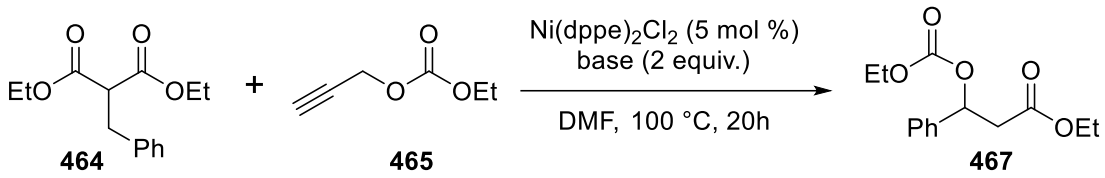

Entry	Base	NMR yield (%)[b]
1	Cesium Carbonate	12
2	Sodium carbonate	4
3	Potassium carbonate	7
4	Sodium bicarbonate	No reaction
5	Potassium bicarbonate	0.2
6	potassium phosphate monobasic	No Reaction
7	potassium phosphate dibasic	No Reaction
8	potassium phosphate tribasic	12
9	potassium *tert*-butoxide	1
10	pyridine	No Reaction
11	triethyl amine	No Reaction

[a]NMR yield calculated using 1,3,5-trimethoxybenzene as a standard.

Potassium phosphates were then examined and only potassium phosphate tribasic resulted in product formation with 12% yield (Table 16, Entry 8) which was the same as the control reaction with cesium carbonate (Table 16, Entry 1). It became apparent that only inorganic bases result in product formation because organic bases triethylamine and pyridine rendered no reaction (Table 16, Entries 10-11).

While cesium carbonate and potassium phosphate tribasic resulted in the same yield, later experiments demonstrated that reaction yields with potassium phosphate tribasic were more consistent than those with cesium carbonate. Because of this, potassium phosphate tribasic was then used as the standard base for further reaction screenings.

Table 17. Temperature screening for nickel catalyzed reaction

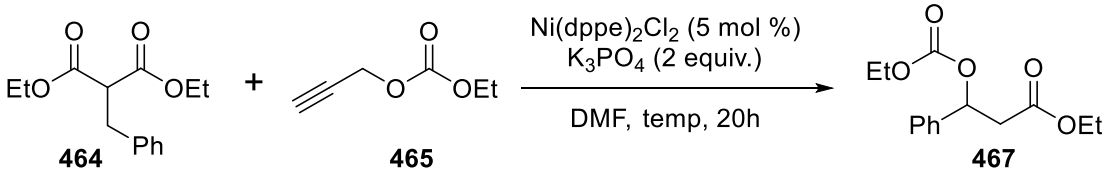

Entry	Temperature	NMR Yield (%)[a,b]
1	90 °C	14[c]
2	95 °C	17
3	100 °C	17
4	105 °C	5[d]
5	110 °C	11

[a]NMR yield calculated using 1,3,5-trimethoxybenzene as a standard. [b]Average of three experiments. [c]Average of six experiments. [d]Average of four experiments.

In previous experiments we found that temperatures of 80 °C and below result in no reaction, so our temperature screening started at 90 °C which resulted in an average of 14% yield (Table 17,

Entry 1). The same yield of 17% was achieved when the reaction was run at 95 °C and at 100 °C (Table 17, Entries 2-3). Reactions run at 105 °C and 110 °C both resulted in lower yield, with Entry 4 being an outlier (Table 17, Entry 4-5). Since the same results were achieved at a slightly lower temperature, we elected to change the reaction temperature to 95 °C for further experiments.

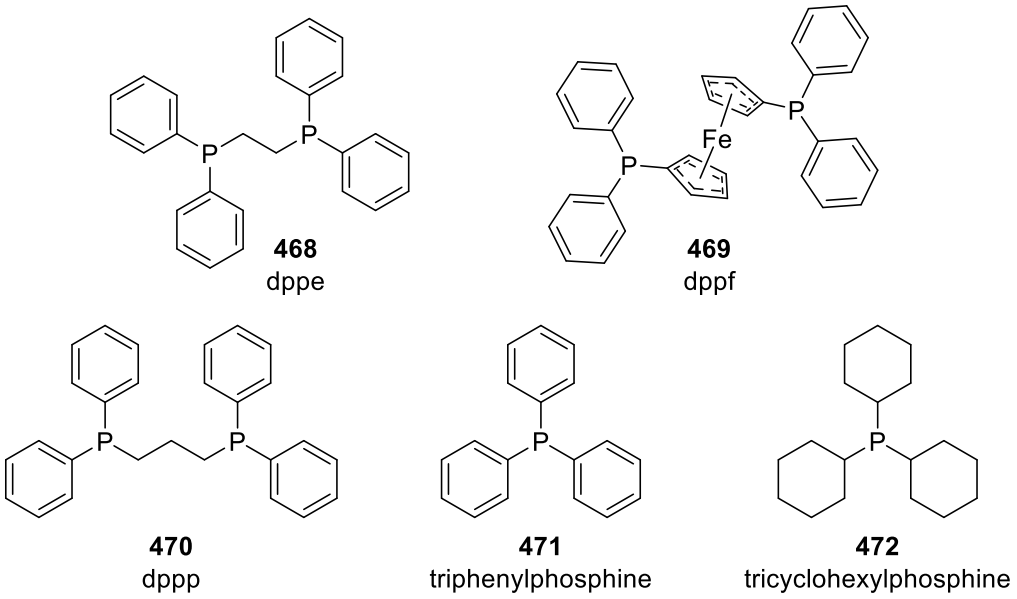

Figure 50. Phosphine ligands used in the nickel catalyst screening

While our initial control tests with this reaction suggest that the catalyst is not required, it might be that the catalyst just aids in product formation by a more favorable reaction pathway. Different nickel (II) catalysts with phosphine ligands were incorporated into the reaction conditions (Table 18). Initially bidentate phosphine ligands were chosen since our initial reaction screening was done with Ni(dppe)Cl_2. A slight decreases in yield was observed with Ni(dppf)Cl_2 (Table 6, Entry 2), and then the yield for Ni(dppp)Cl_2 was about the same as Ni(dppe)Cl_2 (Table 18, Entries 3 and 1). Monodentate triphenyl phosphine resulted in 20% yield which was the highest recorded thus far (Table 18, Entry 4). Lastly PCy_3 was used but resulted in a lower yield than PPh_3, likely due to the steric hinderance of the cyclohexyl groups (Table 18, Entry 5).

Table 18. Catalyst screening for rearrangement product

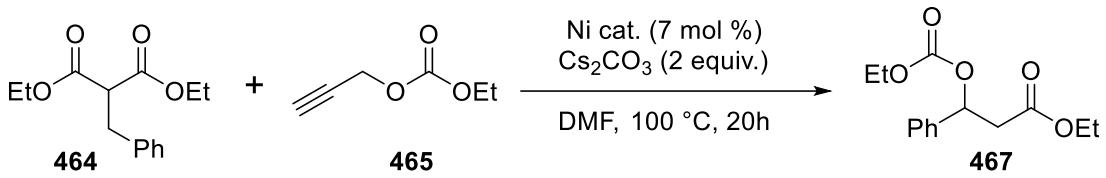

Entry	Ni cat. (7 mol %)	NMR yield (%)[a]
1	$Ni(dppe)Cl_2$	16
2	$Ni(dppf)Cl_2$	13
3	$Ni(dppp)Cl_2$	17
4	$Ni(PPh_3)_2Cl_2$	20
5	$Ni(PCy_3)_2Cl_2$	15

[a]NMR yield calculated using 1,3,5-trimethoxybenzene as a standard.

Table 19. Catalyst loading experiments

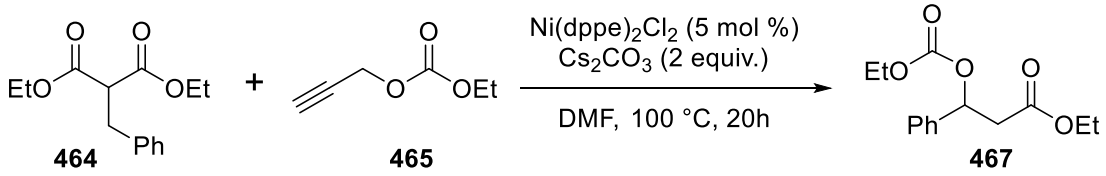

Entry	$Ni(PPh_3)_2Cl_2$	NMR yield (%)[a]
1	20 mol %	11
2	15 mol %	10
3	10 mol %	12
4	7.5 mol %	12
5	5 mol %	11
6	2.5 mol%	16
7	0 mol %	15

[a]NMR yield calculated using 1,3,5-trimethoxybenzene as a standard.

Since $NiPPh_3Cl_2$ resulted in the highest reaction yield out of the catalysts tested, the catalyst loading was then examined (Table 19). Interestingly, the yield was decreased by half to 11% yield when 20 mol% of catalyst was uses (Table 19, Entry 1). Moreover, the yield generally increased as catalyst loading decreased. The reaction yield for when 2.5 mol % catalyst was used (Table 19, Entry 6) was only a 1% difference in yield for when no catalyst was used (Table 19, Entry 7). From these results, it was concluded that the catalyst is not required for this transformation.

Table 20. Reaction time experiments

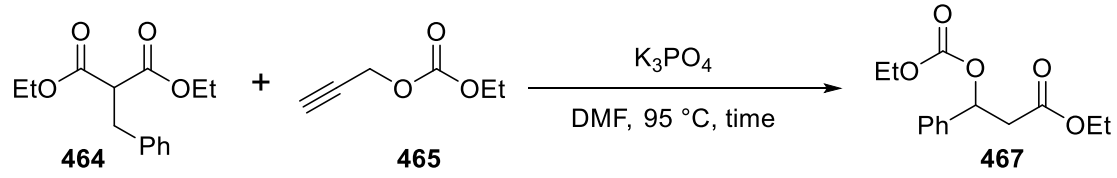

Entry	Time (h)	NMR Yield (%)[a]
1	4	0
2	7	3
3	10	4
4	20	17

[a]NMR yield calculated using 1,3,5-trimethoxybenzene as a standard.

We were interested to see if the reaction could potentially benefit from a shorter reaction time. It was possible that the low reaction yields could be contributed to the product decomposing under reaction conditions after a certain amount of time. In order to test this theory, shorter reaction times were then used and the results were that the yield only increased with increasing reaction times. At four hours no product was generated yet (Table 20, Entry 1), it was only at seven hours that a minimal amount of product was present in the ^1H NMR (Table 20, Entry 2). By the ten hour mark, the product yield only increased by 4% (Table 20, Entry 3), and then after 20 h 17% yield was

achieved. Looking back longer reaction times should have been implemented, but for the remaining reaction screenings, 20 h was used for the optimal reaction time.

Optimization Summary

Scheme 92. Optimized Reaction Conditions

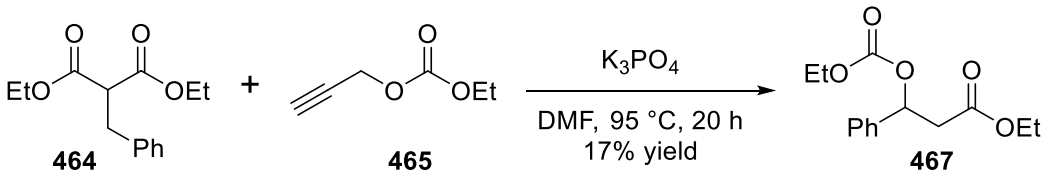

After examining every parameter of this reaction, the optimal reaction conditions were determined to be malonate **464**, propargyl **465**, with potassium phosphate tribasic, dissolved in DMF at 95 °C, and stirred for 20 h (Scheme 91). The highest yield obtained for **467** overall was 20% NMR yield.

5.2.7. Probing the Reaction Mechanism for the Unexpected Product.

Table 21. Control experiments revisited

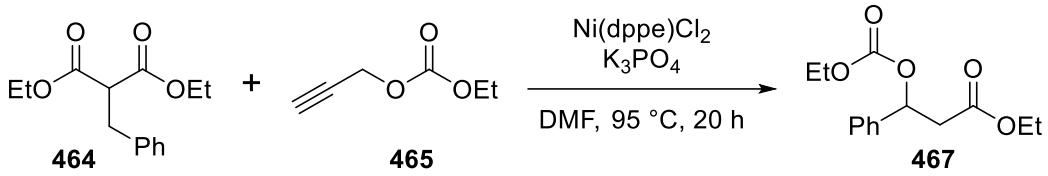

Entry	Malonate 464	Propargyl 465	K_3PO_4	$Ni(dppe)Cl_2$	NMR Yield[a,b]
1	0.2 mmol	0.2 mmol	0.4 mmol	5 mol %	11%
2	0.2 mmol	0.2 mmol	0.4 mmol	N/A	15%
3	0.2 mmol	0.2 mmol	N/A	N/A	No Reaction
4	0.2 mmol	N/A	0.4 mmol	N/A	No Reaction
5	N/A	0.2 mmol	0.4 mmol	N/A	0 %

[a]NMR yield calculated using 1,3,5-trimethoxybenzene as a standard. [b]NMR yield is the average of reactions performed in triplicate.

With better reaction conditions in hand, control experiments were revisited to gain a better understanding the process behind product formation. The role of the catalyst was of particular interest because the catalyst loading experiments showed no trend in the amount of catalyst versus product yield. The results of the control experiment are summarized in Table 21. The product does not form without both the nucleophile and the propargyl carbonate present as shown by Entries 4 and 5 respectively, thereby confirming that the product does not form via a unimolecular process. After all of the optimization reactions, the mechanism of the reaction was still unclear, and trying to determine both how the product forms, and what atoms from which substrate make up the product, was vexing. One idea of how the product forms was that it relied on moisture that could breach the reaction vessel. The thought process was that the propargylic species **465** was actually not participating in the reaction, which is why the product still formed in the absence of the propargyl compound (Table 21). Instead, the small amount of moisture due to humid lab conditions could breach the reaction vessel and result in this rearrangement product (Scheme 92a). To probe this, a drop of water was added to the normal reaction conditions and it only resulted in a 5% average yield for three replicates (Scheme 92b).

Scheme 93. Addition of Water to Reaction Conditions

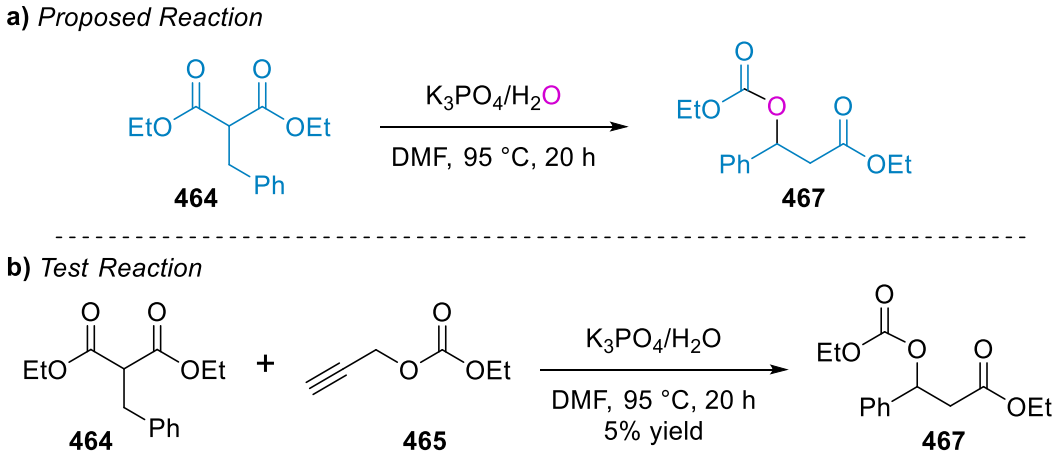

It was then postulated that if this product is the result of the reaction between propargyl **465** and malonate **464**, then the ester portion of product **467** could originate from propargyl **465** (Scheme 93a). If this assumption is correct, when propargyl **465** is replaced with **473**, product **474** should form (Scheme 93b). We then ran a set of parallel reactions with malonate **464**; the control reaction used propargyl **465**, and the other implemented propargyl **473** (Table 22).

Scheme 94. Reaction of Diethyl Benzylmalonate and Propargyl Boc.

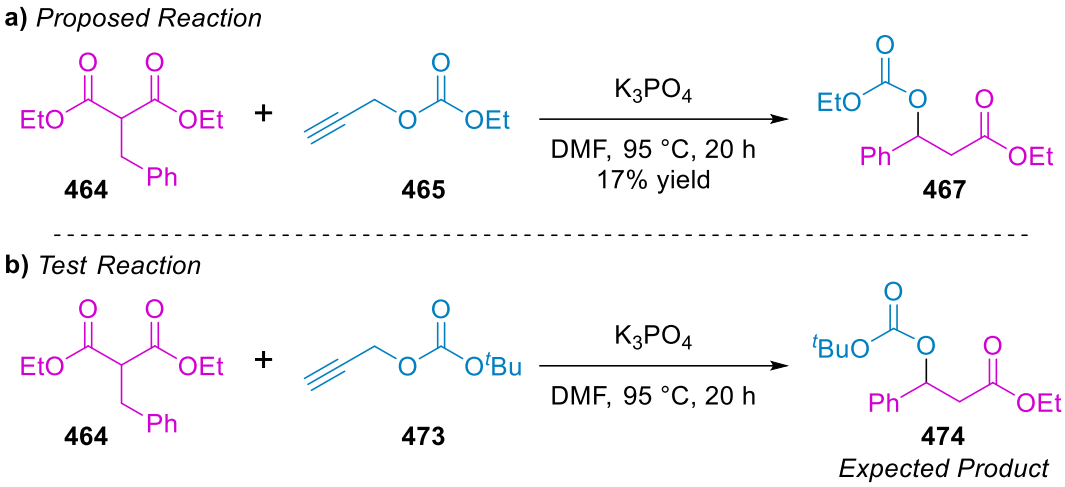

Table 22. Summary of results from propargyl screening

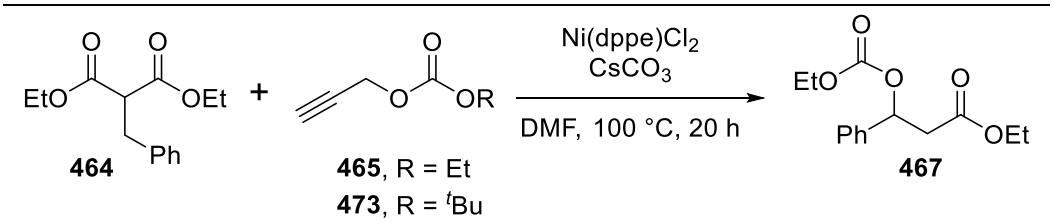

Entry	Propargyl	Product
1	R = Et	**467**
2	R = ^{t}Bu	**467**

Surprisingly, when propargyl **465**, is replaced with propargyl **473**, compound **467** still forms. After work-up there were no signals in the ^{1}H NMR characteristic of *tert*-butyl, and the spectra matched

that of **467**. Any theories that we had about the mechanism were thoroughly disproven by these results, so we elected to move onto another transformation. In the future, perhaps computational modelling could help shed some light on this vexing transformation.

5.1.8. Reactions with Propargyl Bromide

It is well understood in the literature that propargyl bromide and malonic nucleophiles undergo S_N2 reactions.[77] Moreover it has been reported that nickel catalysts can promote S_N2' reactions with propargyl species and trimethyl aluminum to form substituted allenes, but this transformation does have two competing reaction pathways (Figure 51).[64] With initial oxidative addition with the catalyst and propargyl species, there are two ways it can add. If the catalyst adds in between the carbon chain and OAc group, the catalytic cycle follows a formal S_N2-type process. However, if the catalyst adds in between R_2 and the alkyne, a metalloallene is formed and the cycles proceeds through an S_N2' process (Figure 52).

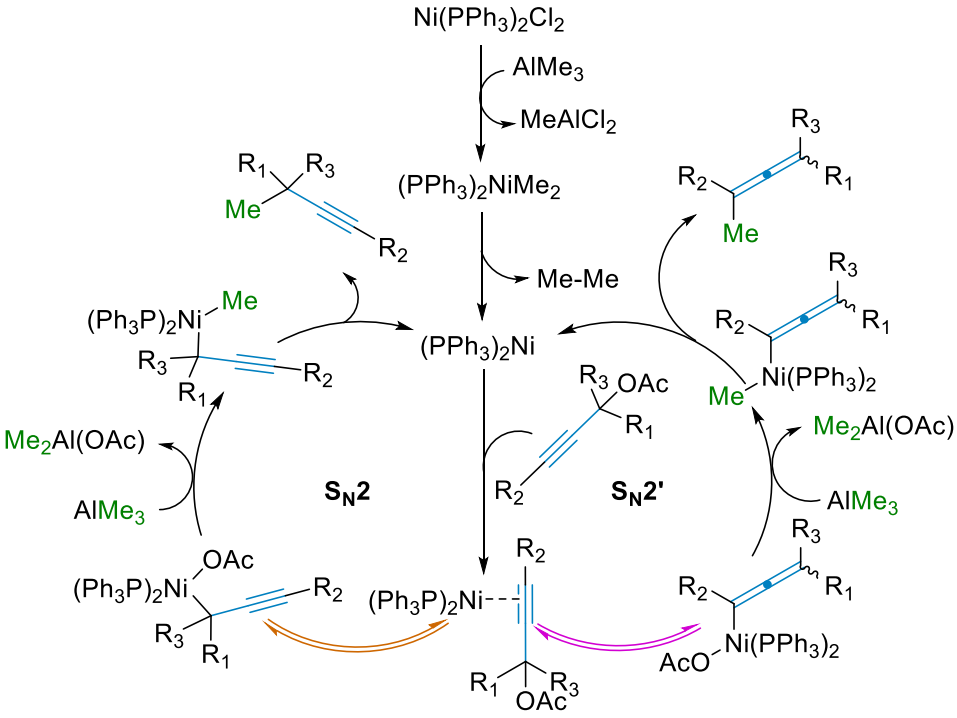

Figure 51. Competing Nickel Catalyzed Cycles for S_N2 and S_N2' Reactions

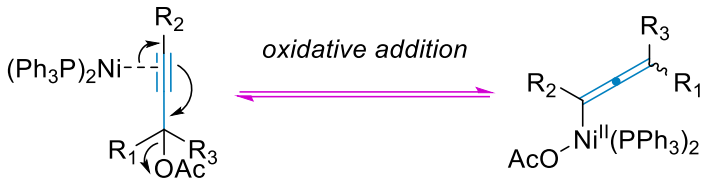

Figure 52. Mechanism of Metaloallene Formation via Oxidative Addition into a Propargylic Species

With this in mind, the next logical step was to incorporate a nickel catalyst into the S_N2 reaction of propargyl bromide (**420**) and diethylbenzyl malonate (**464**) to test if the S_N2' product **466** forms at all (Scheme 94). It should be noted that a nickel catalyst in this system has not yet been reported so if successful, this reaction could unveil a novel reaction pathway to form allenes through a nickel catalyzed process with less hazardous reagents than trimethylaluminum.

Scheme 95. a) Adapted S_N2 Conditions; b) Proposed Nickel Catalyzed S_N2' Reaction

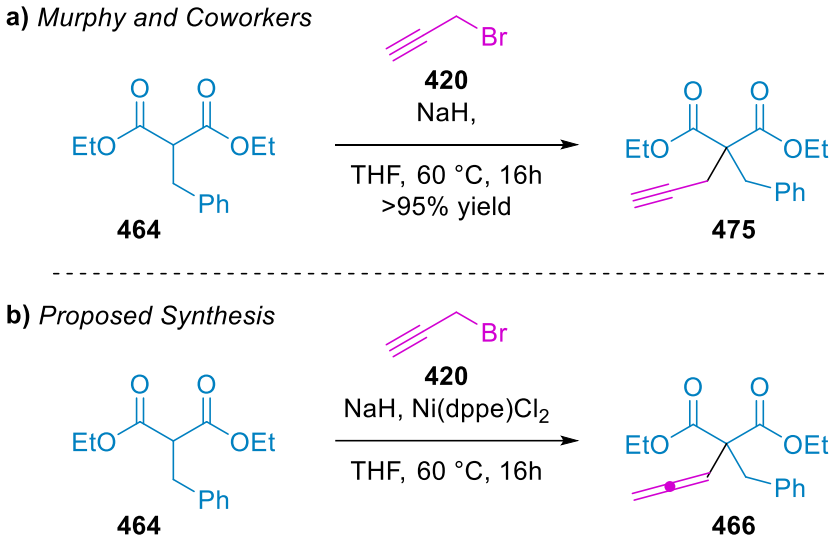

Initially we were able to discern by ^{1}H NMR that three species were present in the crude reaction mixture: the starting malonate **464**, the S_N2 product **475**, and the S_N2' product **466**. The S_N2 product **475** was able to easily be identified from the crude reaction mixture because it was previously isolated following the reaction conditions by Murphy and coworkers (Scheme 94a). The reaction

mixture was subjected to flash column chromatography (FCC) and the malonate **464** was easily separated, while **475** and **466** were nontrivial to isolate.

A range of TLC conditions were tested, but still the **475** and **466** had very similar R_f values (within 0.05 of eachother). To overcome this challenge, the S_N2 product **466** was chemically modified via click chemistry (Scheme 95). The mix of products was subjected to click reaction conditions in which only the disappearance on the alkyne of **475** was observed (Scheme 95). Once the alkyne was fully reacted into **477**, the mixture was purified by FCC to afford pure allene product **466** in 13% yield.

Scheme 96. Selective Copper Catalyzed "Click" Reaction

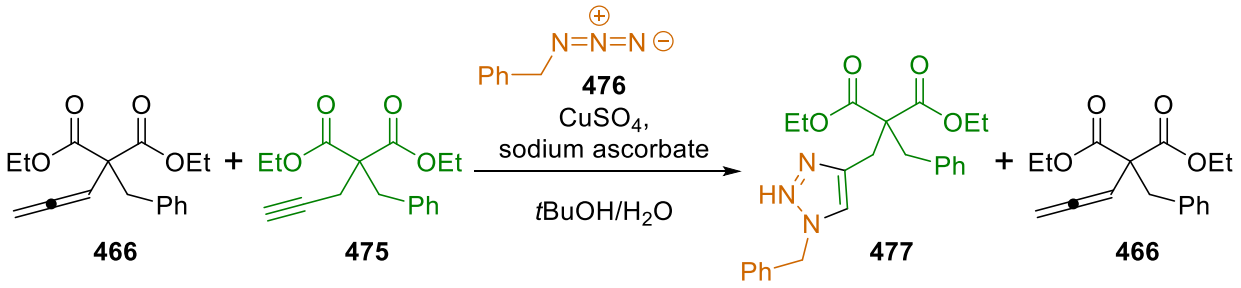

The poor yield of the alleneic product **466** is due to low reaction conversion overall, as well as the competing S_N2 and S_N2' pathways. To favor the S_N2' pathway, propargyl chloride was used in place of the propargyl bromide because chloride is a poorer leaving group, making the rate of S_N2 slower, thereby favoring the S_N2' pathway. Additionally the rate of addition was significantly reduced by using a syringe pump in order to further promote the S_N2' reaction. These changes did result in more S_N2' product **466** forming, but they were still in a 3:1 ratio of S_N2: S_N2' (Table 23, Entry 2). Morevover there was still starting malonate **464** leftover anyway (Table 23, Entry 2). We then tried an even slower addition of the malonate and while the ratio of S_N2:S_N2' improved from 3:1 to 2:1, there was still malonate leftover suggesting a longer reaction time would be more beneficial (Table 23, Entry 3). The reaction was then left over the weekend and the ratio between

the S_N2 product and the S_N2' product remained the same, and there was still the same amount of starting malonate present.

It was at this time that other projects really started to show significantly more success than this one, so my attention was then shifted to new projects focusing on [3+2] cycloadditions of tertiary amine *N*-oxides and dipolarophiles forming various heterocyclic compounds.

Table 23. Reaction conditions screening

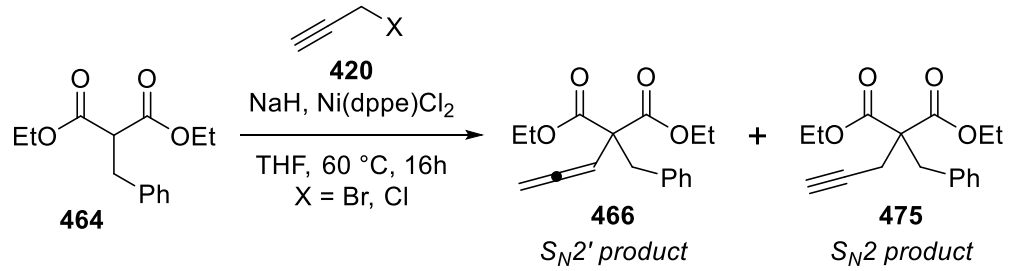

Propargyl	**NaH (equiv)**	**Rate of addition**[a]	**Reaction Time**	**Ratio**[b] **Nuc: S_N2: S_N2'**
R=Br[b]	1.4	15 min	Overnight	1: 2.08: 0.68
R=Cl	1	0.8 mL/h	Overnight	1: 1.58: 0.71
R=Cl	1	0.5 mL/h	Overnight	1: 0.88: 0.37
R=Cl	1	0.1 mL/h	Over the weekend	1: 0.83: 0.38

[a]Rate of addition of propargyl compounds. [b]Ratios were determined by ^{1}H NMR with the malonate proton resonance at 3.63 ppm set to an integration of 1.

5.3 Conclusion

In the search for a potential new nickel catalyzed reaction scope that is beyond that of palladium, we uncovered an unanticipated and unusual carbonylation/rearrangement product **474**. This

product arose through the reaction of ethyl propargyl carbonate and diethyl benzyl malonate presumably catalyzed by nickel, but it was later discovered that this particular transformation was not even catalyzed by nickel. After a valiant effort to optimize the reaction conditions, only a maximum of 20% NMR was achieved. Our attention was then turned toward a more promising reaction with propargyl bromide and diethyl benzyl malonate catalyzed by nickel instead. This reaction worked via nickel catalyzed S_N2' reaction forming a novel substituted allene **466**. While an exciting result, only a 13% isolated yield was achieved because of low overall conversion and competing reaction pathways.

5.4 References

(1) Taylor, D. R. The Chemistry of Allenes. *Chemical Reviews* **1967**, *67* (3), 317-359. DOI: 10.1021/cr60247a004.

(2) Hoff, J. H. *La chimie dans l'espace*; Bazendijk, 1875.

(3) Hoffmann-Röder, A.; Krause, N. Synthesis and Properties of Allenic Natural Products and Pharmaceuticals. *Angewandte Chemie International Edition* **2004**, *43* (10), 1196-1216. DOI: doi:10.1002/anie.200300628.

(4) Yu, S.; Ma, S. Allenes in Catalytic Asymmetric Synthesis and Natural Product Syntheses. *Angewandte Chemie International Edition* **2012**, *51* (13), 3074-3112. DOI: 10.1002/anie.201101460.

(5) Hoffmann-Röder, A.; Krause, N. Enantioselective Synthesis of and with Allenes. *Angewandte Chemie International Edition* **2002**, *41* (16), 2933-2935. DOI: doi:10.1002/1521-3773(20020816)41:16<2933::AID-ANIE2933>3.0.CO;2-6.

(6) Zimmer, R.; Reissig, H.-U. Alkoxyallenes as building blocks for organic synthesis. *Chemical Society Reviews* **2014**, *43* (9), 2888-2903, 10.1039/C3CS60429B. DOI: 10.1039/C3CS60429B.

(7) Ma, S. Some Typical Advances in the Synthetic Applications of Allenes. *Chemical Reviews* **2005**, *105* (7), 2829-2872. DOI: 10.1021/cr020024j.

(8) Lee, K.; Seomoon, D.; Lee, P. H. Highly Efficient Catalytic Synthesis of Substituted Allenes Using Indium. *Angewandte Chemie International Edition* **2002**, *41* (20), 3901-3903. DOI: 10.1002/1521-3773(20021018)41:20<3901::Aid-anie3901>3.0.Co;2-s.

(9) Li, Q.-H.; Jeng, J.-Y.; Gau, H.-M. Highly Efficient Synthesis of Allenes from Trimethylaluminum Reagent and Propargyl Acetates Mediated by a Palladium Catalyst. *European Journal of Organic Chemistry* **2014**, *2014* (35), 7916-7923. DOI: doi:10.1002/ejoc.201403008.

(10) Lo, V. K.-Y.; Zhou, C.-Y.; Wong, M.-K.; Che, C.-M. Silver(i)-mediated highly enantioselective synthesis of axially chiral allenes under thermal and microwave-assisted conditions. *Chemical Communications* **2010**, *46* (2), 213-215, 10.1039/B914516H. DOI: 10.1039/B914516H.

(11) Molander, G. A.; Sommers, E. M.; Baker, S. R. Palladium(0)-Catalyzed Synthesis of Chiral Ene-allenes Using Alkenyl Trifluoroborates. *The Journal of Organic Chemistry* **2006**, *71* (4), 1563-1568. DOI: 10.1021/jo052201x.

(12) Pasto, D. J. C., S.-K.; Waterhouse, A.; Shults, R. H.; Hennion, G. F. Transition Metal Catalysis in Allene Formation from Grignard Reagents and Propargyl Chlorides. *The Journal of Organic Chemistry* **1978**, (43), 1385-1388.

(13) Shao, X.; Wen, C.; Zhang, G.; Cao, K.; Wu, L.; Li, Q. Palladium-catalyzed, ligand-free SN2' substitution reactions of organoaluminum with propargyl acetates for the synthesis of multi-substituted allenes. *Journal of Organometallic Chemistry* **2018**, *870*, 68-75. DOI: https://doi.org/10.1016/j.jorganchem.2018.06.020.

(14) Wu, Z.; Berhal, F.; Zhao, M.; Zhang, Z.; Ayad, T.; Ratovelomanana-Vidal, V. Palladium-Catalyzed Efficient Enantioselective Synthesis of Chiral Allenes: Steric and Electronic Effects of Ligands. *ACS Catalysis* **2014**, *4* (1), 44-48. DOI: 10.1021/cs4007827.

(15) Yamamoto, Y.; Al-Masum, M.; Asao, N. Palladium-Catalyzed Addition of Activated Methylene and Methyne Compounds to Allenes. *Journal of the American Chemical Society* **1994**, *116* (13), 6019-6020. DOI: 10.1021/ja00092a083.

(16) Yoshida, M.; Okada, T.; Shishido, K. Enantiospecific synthesis of 1,3-disubstituted allenes by palladium-catalyzed coupling of propargylic compounds with arylboronic acids. *Tetrahedron* **2007**, *63* (30), 6996-7002. DOI: https://doi.org/10.1016/j.tet.2007.05.035.

(17) Ho, T.-l. The Hard Soft Acids Bases (HSAB) Principle and Organic Chemistry. *Chemical Reviews* **1975**, *75* (1), 1-20.

(18) Tsuji, J. *Palladium Reagents and Catalysis: New Reagents and Perspectives for the 21st Century*; John Wiley and Sons Ltd, 2004.

(19) Yoshida, M. Development of Palladium-Catalyzed Transformations Using Propargylic Compounds. *Chemical and Pharmaceutical Bulletin* **2012**, *60* (3), 285-299. DOI: 10.1248/cpb.60.285.

(20) Pasto, D. J.; Hennion, G. F.; Shults, R. H.; Waterhouse, A.; Chou, S.-K. Reaction of propargyl halides with Grignard reagents. Iron trichloride catalysis in allene formation. *The Journal of Organic Chemistry* **1976**, *41* (21), 3496-3496. DOI: 10.1021/jo00883a047.

(21) Guo, L.-N.; Duan, X.-H.; Liang, Y.-M. Palladium-Catalyzed Cyclization of Propargylic Compounds. *Accounts of Chemical Research* **2011**, *44* (2), 111-122. DOI: 10.1021/ar100109m.

(22) Franckevičius, V. Palladium-catalyzed construction of quaternary carbon centers with propargylic electrophiles. *Tetrahedron Letters* **2016**, *57* (32), 3586-3595. DOI: https://doi.org/10.1016/j.tetlet.2016.06.131.

(23) Gou, F.-R.; Bi, H.-P.; Guo, L.-N.; Guan, Z.-H.; Liu, X.-Y.; Liang, Y.-M. New Insight into Ni(II)-Catalyzed Cyclization Reactions of Propargylic Compounds with Soft Nucleophiles: Novel Indenes Formation. *The Journal of Organic Chemistry* **2008**, *73* (10), 3837-3841. DOI: 10.1021/jo800155a.

(24) Burton, B. S.; von Pechmann, H. Ueber die Einwirkung von Chlorphosphor auf Acetondicarbonsäureäther. *Berichte der deutschen chemischen Gesellschaft* **1887**, *20* (1), 145-149. DOI: https://doi.org/10.1002/cber.18870200136.

(25) Ruiz-Castillo, P.; Buchwald, S. L. Applications of Palladium-Catalyzed C–N Cross-Coupling Reactions. *Chemical Reviews* **2016**, *116* (19), 12564-12649. DOI: 10.1021/acs.chemrev.6b00512.

(26) Horler, D. F. (–) Methyl n-tetradeca-trans-2,4,5-trienoate, an allenic ester produced by the male Dried Bean beetle, Acanthoscelides obtectus(Say). *Journal of the Chemical Society C: Organic* **1970**, (6), 859-862, 10.1039/J39700000859. DOI: 10.1039/J39700000859.

(27) Meinwald, J.; Erickson, K.; Hartshorn, M.; Meinwald, Y. C.; Eisner, T. Defensive mechanisms of arthropods. XXIII. An allenic sesquiterpenoid from the grasshopper romalea microptera. *Tetrahedron Letters* **1968**, *9* (25), 2959-2962. DOI: https://doi.org/10.1016/S0040-4039(00)89622-7.

(28) DeVille, T. E.; Hursthouse, M. B.; Russell, S. W.; Weedon, B. C. L. Stereochemistry of allenes. *Journal of the Chemical Society D: Chemical Communications* **1969**, (13), 754-755, 10.1039/C29690000754. DOI: 10.1039/C29690000754.

(29) Kim, M. J.; Jeong, S. M.; Kang, B. K.; Kim, K. B.; Ahn, D. H. Anti-Inflammatory Effects of Grasshopper Ketone from Sargassum fulvellum Ethanol Extract on Lipopolysaccharide-Induced Inflammatory Responses in RAW 264.7 Cells. *J Microbiol Biotechnol* **2019**, *29* (5), 820-826. DOI: 10.4014/jmb.1901.01027 From NLM.

(30) Daly, J. W.; Witkop, B.; Tokuyama, T.; Nishikawa, T.; Karle, I. L. Gephyrotoxins, Histrionicotoxins and Pumiliotoxins from the Neotropical Frog Dendrobates histrionicus. *Helvetica Chimica Acta* **1977**, *60* (3), 1128-1140. DOI: https://doi.org/10.1002/hlca.19770600336.

(31) Spande, T. F.; Jain, P.; Garraffo, H. M.; Pannell, L. K.; Yeh, H. J. C.; Daly, J. W.; Fukumoto, S.; Imamura, K.; Tokuyama, T.; Torres, J. A.; et al. Occurrence and Significance of Decahydroquinolines from Dendrobatid Poison Frogs and a Myrmicine Ant: Use of 1H and 13C NMR in Their Conformational Analysis. *Journal of Natural Products* **1999**, *62* (1), 5-21. DOI: 10.1021/np980298v.

(32) Tokuyama, T.; Uenoyama, K.; Brown, G.; Daly, J. W.; Witkop, B. Allenic and Acetylenic Spiropiperidine Alkaloids from the Neotropical Forg, Dendrobates histrionicus. *Helvetica Chimica Acta* **1974**, *57* (8), 2597-2604. DOI: https://doi.org/10.1002/hlca.19740570835.

(33) Burgermeister, W.; Catterall, W. A.; Witkop, B. Histrionicotoxin enhances agonist-induced desensitization of acetylcholine receptor. *Proceedings of the National Academy of Sciences* **1977**, *74* (12), 5754-5758. DOI: doi:10.1073/pnas.74.12.5754.

(34) Hayashi, S.; Phadtare, S.; Zemlicka, J.; Matsukura, M.; Mitsuya, H.; Broder, S. Adenallene and cytallene: acyclic-nucleoside analogues that inhibit replication and cytopathic effect of human immunodeficiency virus in vitro. *Proceedings of the National Academy of Sciences of the United States of America* **1988**, *85* (16), 6127-6131. PubMed.

(35) Megati, S.; Goren, Z.; Silverton, J. V.; Orlina, J.; Nishimura, H.; Shirasaki, T.; Mitsuya, H.; Zemlicka, J. (R)-(-)- and (S)-(+)-Adenallene: synthesis, absolute configuration, enantioselectivity of antiretroviral effect, and enzymic deamination. *Journal of Medicinal Chemistry* **1992**, *35* (22), 4098-4104. DOI: 10.1021/jm00100a016.

(36) Zhu, Y. L.; Pai, S. B.; Liu, S. H.; Grove, K. L.; Jones, B. C.; Simons, C.; Zemlicka, J.; Cheng, Y. C. Inhibition of replication of hepatitis B virus by cytallene in vitro. *Antimicrobial Agents and Chemotherapy* **1997**, *41* (8), 1755-1760. DOI: 10.1128/aac.41.8.1755.

(37) Collins, P. W.; Djuric, S. W. Synthesis of therapeutically useful prostaglandin and prostacyclin analogs. *Chemical Reviews* **1993**, *93* (4), 1533-1564. DOI: 10.1021/cr00020a007.

(38) Carpio, H.; Cooper, G. F.; Edwards, J. A.; Fried, J. H.; Garay, G. L.; Guzman, A.; Mendez, J. A.; Muchowski, J. M.; Roszkowski, A. P.; Van Horn, A. R.; et al. Synthesis and gastric antisecretory properties of allenic 16-phenoxy-omega-tetranor prostaglandin E analogs. *Prostaglandins* **1987**, *33* (2), 169-180. DOI: https://doi.org/10.1016/0090-6980(87)90004-9.

(39) Chisato Mukai, T. H., Satoshi Teramoto, Shinji Kitagaki. Rh(I)-catalyzed allenic Pauson–Khand reaction: first construction of the bicyclo 6.3.0 undecadienone ring system. *Tetrahedron* **2005**, *61* (46), 10983 - 10994. DOI: https://doi.org/10.1016/j.tet.2005.08.088.

(40) Ma, S. Electrophilic Addition and Cyclization Reactions of Allenes. *Accounts of Chemical Research* **2009**, *42* (10), 1679-1688. DOI: 10.1021/ar900153r.

(41) VanBrunt, M. P.; Standaert, R. F. A Short Total Synthesis of (+)-Furanomycin. *Organic Letters* **2000**, *2* (5), 705-708. DOI: 10.1021/ol005569j.

(42) Dauben, W. G.; Shapiro, G.; Luders, L. Intramolecular [2+2] photocycloaddition of 4-(allenic-substituted)-2-cycloalken-1-ones. Ring size, length of sidechain and temperature effects.

Tetrahedron Letters **1985**, *26* (11), 1429-1432. DOI: https://doi.org/10.1016/S0040-4039(00)99063-4.

(43) Fu, C.; Chen, G.; Liu, X.; Ma, S. Stereoselective Z-iodoalkoxylation of 1,2-allenyl sulfides or selenides. *Tetrahedron* **2005**, *61* (32), 7768-7773. DOI: https://doi.org/10.1016/j.tet.2005.05.077.

(44) Ma, S.; Hao, X.; Huang, X. Highly regio- and stereoselective four-component iodoamination of Se-substituted allenes. an efficient synthesis of *N*-(3-organoseleno-2-iodo-2(Z)-propenyl) acetamides. *Chemical Communications* **2003**, (9), 1082-1083, 10.1039/B300879G. DOI: 10.1039/B300879G.

(45) Horino, Y.; Kimura, M.; Wakamiya, Y.; Okajima, T.; Tamaru, Y. Efficient Entry to Tetrahydropyridines: Addition of Enol Ethers to Allenesulfonamides Involving a Novel 1,3-Sulfonyl Shift. *Angewandte Chemie International Edition* **1999**, *38* (1-2), 121-124. DOI: https://doi.org/10.1002/(SICI)1521-3773(19990115)38:1/2<121::AID-ANIE121>3.0.CO;2-D.

(46) Hesse, M. *Ring enlargement in organic chemistry*; VCH Weinheim, 1991.

(47) Nagao, Y.; Ueki, A.; Asano, K.; Tanaka, S.; Sano, S.; Shiro, M. Facile Palladium(0)-Catalyzed Ring Expansion Reactions of Hydroxy Methoxyallenyl Cyclic Compounds via Hydropalladation. *Organic Letters* **2002**, *4* (3), 455-457. DOI: 10.1021/ol010287k.

(48) Jafari, M. R.; Lakusta, J.; Lundgren, R. J.; Derda, R. Allene Functionalized Azobenzene Linker Enables Rapid and Light-Responsive Peptide Macrocyclization. *Bioconjugate Chemistry* **2016**, *27* (3), 509-514. DOI: 10.1021/acs.bioconjchem.6b00026.

(49) Abbas, A.; Xing, B.; Loh, T.-P. Allenamides as Orthogonal Handles for Selective Modification of Cysteine in Peptides and Proteins. *Angewandte Chemie International Edition* **2014**, *53* (29), 7491-7494. DOI: 10.1002/anie.201403121.

(50) Liu, H.; Leow, D.; Huang, K.-W.; Tan, C.-H. Enantioselective Synthesis of Chiral Allenoates by Guanidine-Catalyzed Isomerization of 3-Alkynoates. *Journal of the American Chemical Society* **2009**, *131* (21), 7212-7213. DOI: 10.1021/ja901528b.

(51) Jiang, G.-J.; Zheng, Q.-H.; Dou, M.; Zhuo, L.-G.; Meng, W.; Yu, Z.-X. Mild-Condition Synthesis of Allenes from Alkynes and Aldehydes Mediated by Tetrahydroisoquinoline (THIQ). *The Journal of Organic Chemistry* **2013**, *78* (23), 11783-11793. DOI: 10.1021/jo4018183.

(52) Yokota, M.; Fuchibe, K.; Ueda, M.; Mayumi, Y.; Ichikawa, J. Facile Synthesis of 1,1-Difluoroallenes via the Difluorovinylidenation of Aldehydes and Ketones. *Organic Letters* **2009**, *11* (17), 3994-3997. DOI: 10.1021/ol9016673.

(53) Yu, S.; Ma, S. How easy are the syntheses of allenes? *Chemical Communications* **2011**, *47* (19), 5384-5418, 10.1039/C0CC05640E. DOI: 10.1039/C0CC05640E.

(54) Yang, Y.; Szabó, K. J. Synthesis of Allenes by Catalytic Coupling of Propargyl Carbonates with Aryl Iodides in the Presence of Diboron Species. *The Journal of Organic Chemistry* **2016**, *81* (1), 250-255. DOI: 10.1021/acs.joc.5b01842.

(55) Ma, S. Pd-Catalyzed Coupling Reactions Involving Propargylic/Allenylic Species. *European Journal of Organic Chemistry* **2004**, *2004* (6), 1175-1183. DOI: 10.1002/ejoc.200300352.

(56) Girard, D.; Broussous, S.; Provot, O.; Brion, J.-D.; Alami, M. Palladium mediated direct coupling of silylated arylalkynes with propargylic chlorides: an efficient access to functionalized conjugated allenynes. *Tetrahedron Letters* **2007**, *48* (34), 6022-6026. DOI: https://doi.org/10.1016/j.tetlet.2007.06.079.

(57) Kim, Y.; Lee, H.; Park, S.; Lee, Y. Copper-Catalyzed Propargylic Reduction with Diisobutylaluminum Hydride. *Organic Letters* **2018**, *20* (17), 5478-5481. DOI: 10.1021/acs.orglett.8b02413.

(58) Hu, G.; Shan, C.; Chen, W.; Xu, P.; Gao, Y.; Zhao, Y. Copper-Catalyzed Direct Coupling of Unprotected Propargylic Alcohols with P(O)H Compounds: Access to Allenylphosphoryl Compounds under Ligand- and Base-Free Conditions. *Organic Letters* **2016**, *18* (23), 6066-6069. DOI: 10.1021/acs.orglett.6b03028.

(59) Soler-Yanes, R.; Arribas-Álvarez, I.; Guisán-Ceinos, M.; Buñuel, E.; Cárdenas, D. J. NiI Catalyzes the Regioselective Cross-Coupling of Alkylzinc Halides and Propargyl Bromides to Allenes. *Chemistry – A European Journal* **2017**, *23* (7), 1584-1590. DOI: doi:10.1002/chem.201603758.

(60) Li, Q.-H.; Liao, J.-W.; Huang, Y.-L.; Chiang, R.-T.; Gau, H.-M. Nickel-catalyzed substitution reactions of propargyl halides with organotitanium reagents. *Organic & Biomolecular Chemistry* **2014**, *12* (38), 7634-7642, 10.1039/C4OB00677A. DOI: 10.1039/C4OB00677A.

(61) Wang, Y.; Zhang, W.; Ma, S. A Room-Temperature Catalytic Asymmetric Synthesis of Allenes with ECNU-Phos. *Journal of the American Chemical Society* **2013**, *135* (31), 11517-11520. DOI: 10.1021/ja406135t.

(62) Yoshida, M.; Gotou, T.; Ihara, M. Palladium-catalyzed direct coupling reaction of propargylic alcohols with arylboronic acids. *Tetrahedron Letters* **2004**, *45* (29), 5573-5575. DOI: https://doi.org/10.1016/j.tetlet.2004.05.147.

(63) Alexakis, A. M., I.; Mangeney, P.; Normant, J. F. Mechanistic aspects of the formation of chiral allenes from propargylic ethers and organocopper reagents. *Journal of the American Chemical Society* **1990**, *112* (22).

(64) Shao, X. B.; Zhang, Z.; Li, Q. H.; Zhao, Z. G. Synthesis of multi-substituted allenes from organoalane reagents and propargyl esters by using a nickel catalyst. *Organic & Biomolecular Chemistry* **2018**, *16* (26), 4797-4806, 10.1039/C8OB00781K. DOI: 10.1039/C8OB00781K.

(65) Zimmer, R.; Dinesh, C. U.; Nandanan, E.; Khan, F. A. Palladium-Catalyzed Reactions of Allenes. *Chemical Reviews* **2000**, *100* (8), 3067-3126. DOI: 10.1021/cr9902796.

(66) Suzuki, N. M. a. A. Palladium-Catalyzed Cross-Coupling Reactions of Organoboron Compounds. *Chem. Rev.* **1995**, (95).

(67) Chinchilla, R.; Nájera, C. The Sonogashira Reaction: A Booming Methodology in Synthetic Organic Chemistry. *Chemical Reviews* **2007**, *107* (3), 874-922. DOI: 10.1021/cr050992x.

(68) Fleischer, M. The abundance and distribution of the chemical elements in the earth's crust. *Journal of Chemical Education* **1954**, *31* (9), 446. DOI: 10.1021/ed031p446.

(69) Tasker, S. Z.; Standley, E. A.; Jamison, T. F. Recent advances in homogeneous nickel catalysis. *Nature* **2014**, *509*, 299, Review Article. DOI: 10.1038/nature13274.

(70) https://www.dailymetalprice.com/nickel.html (accessed 2023 6/11/2023).

(71) Ananikov, V. P. Nickel: The "Spirited Horse" of Transition Metal Catalysis. *ACS Catalysis* **2015**, *5* (3), 1964-1971. DOI: 10.1021/acscatal.5b00072.

(72) Zweig, J. E.; Kim, D. E.; Newhouse, T. R. Methods Utilizing First-Row Transition Metals in Natural Product Total Synthesis. *Chemical Reviews* **2017**, *117* (18), 11680-11752. DOI: 10.1021/acs.chemrev.6b00833.

(73) Trost, B. M.; Debien, L. Re-orienting coupling of organocuprates with propargyl electrophiles from SN2′ to SN2 with stereocontrol. *Chemical Science* **2016**, *7* (8), 4985-4989, 10.1039/C6SC01086E. DOI: 10.1039/C6SC01086E.

(74) Yoshida, M.; Ohno, S.; Shishido, K. Synthesis of Tetrasubstituted Furans by Palladium-Catalyzed Decarboxylative [3+2] Cyclization of Propargyl β-Keto Esters. *Chemistry – A European Journal* **2012**, *18* (6), 1604-1607. DOI: https://doi.org/10.1002/chem.201103246.

(75) Tsuji, J.; Watanabe, H.; Minami, I.; Shimizu, I. Novel palladium-catalyzed reactions of propargyl carbonates with carbonucleophiles under neutral conditions. *Journal of the American Chemical Society* **1985**, *107* (7), 2196-2198. DOI: 10.1021/ja00293a075.

(76) Zhang, G.; Song, Y.-K.; Zhang, F.; Xue, Z.-J.; Li, M.-Y.; Zhang, G.-S.; Zhu, B.-B.; Wei, J.; Li, C.; Feng, C.-G.; et al. Palladium-catalyzed allene synthesis enabled by β-hydrogen elimination from sp2-carbon. *Nature Communications* **2021**, *12* (1), 728. DOI: 10.1038/s41467-020-20740-w.

(77) Doni, E.; Mondal, B.; O'Sullivan, S.; Tuttle, T.; Murphy, J. A. Overturning Established Chemoselectivities: Selective Reduction of Arenes over Malonates and Cyanoacetates by Photoactivated Organic Electron Donors. *Journal of the American Chemical Society* **2013**, *135* (30), 10934-10937. DOI: 10.1021/ja4050168.

Chapter 6. Experimental Section

6.1 General Information

Nuclear magnetic resonance (NMR) spectra were measured on a Bruker at 400 MHz or 500 MHz. ^{1}H NMR spectra were calibrated from standard TMS (δ 0.0) or solvent resonance ($CDCl_3$: δ 7.27, MeOD: δ 3.31). ^{13}C NMR spectra were calibrated from solvent resonance ($CDCl_3$: δ 77.16, MeOD: δ 49.00). Structural assignments were made with additional information from gCOSY, gHSQC, and gHMBC experiments. High-resolution mass spectrometric analysis (HRMS) was measured on an Agilent Technologies 6530 Accurate-Mass QTOF LC/MS equipped with the Agilent Technologies 1200 series LC system. Infrared (IR) spectral analysis was performed on a Thermoscientific Everest ATR. Reactions monitored by thin layer chromatography (TLC) used TLC Silica gel 60 F_{254} and visualized under a 4-Watt 254/365 nm UV lamp. Flash column chromatography (FCC) (EtOAc/Hex or DCM/MeOH) was performed using a Biotage Isolera One Flash Chromatography instrument with a 25 g Biotage® Sfär Silica D-Duo 60 µm column, and with a 10 g Biotage® Sfär C18 D- Duo 100 Å 30 µm column for reverse phase FCC (0.1% TFA water/MeOH). A heating mantel was used as the heat source for transformations that required heating.

6.1.1 Materials

All materials were used as purchased from MilliporeSigma, Thermo Fisher Scientific, TCI, or Oakwood Chemical, unless otherwise noted. Tetrahydrofuran (THF) was purified by a column of activated alumina and 4 Å molecular sieves via Inert PurSolv Solvent System. Trimethylamine *N*-oxide (TMAO) was purified by dissolving in DMF and then vacuum distilling off DMF and water. This created a super saturated solution resulting in long needle-like white crystals which were then stored under rigorous anhydrous conditions with drierite and phosphorus pentoxide. Benzaldehyde

was purified by vacuum distillation before use. Solutions of lithium diisopropyl amine (LDA), sodium bis(trimethylsilyl)amide (NaHMDS), lithium bis(trimethylsilyl)amide (LiHMDS), *n*-butyl lithium (*n*-BuLi), *tert*-butyl lithium (*t*-BuLi), *sec*-butyl lithium (*sec*-BuLi) were titrated using salicylaldehyde phenylhydrazone before use. [1]

6.1.2 NMR Yield Calculation2

Unless otherwise noted, the crude reaction mixture was concentrated *in vacuo* and the 1,3,5 trimethoxybenzene standard was added to flask. An appropriate deuterated solvent (approx. 1 mL) was used to thoroughly mix and dissolve the crude reaction residue and standard to ensure homogeneity. An aliquot from this solution was then subjected to ^{1}H NMR analysis where the integration of the 1,3,5-trimethoxybenzene signal at δ 6.08 (s, 3H) was compared to the integration values of a well resolved signal corresponding to the product of interest. With this information, the following equations were used to calculate the NMR yield.

$$NMR\ yield = \frac{\left(\frac{N_p}{I_p} \Big/ \frac{N_s}{I_s}\right)}{1/n_s} = \left(\frac{N_p}{I_p} \Big/ \frac{N_s}{I_s}\right) \times \left(\frac{n_s}{1}\right)$$

$$\%\ NMR\ yield = \frac{NMR\ yield}{Theoretical\ yield} \times 100\%$$

- N_p= number of protons equal to the product signal
- I_p= integration of the product signal
- N_s= number of protons equal to standard signal at δ 6.08 = 3
- I_s= integration of standard signal at δ 6.08 = 3
- n_s = mmol of standard

Experimental Section: Chapter 1

General procedure for the preparation of silyl imines (106a-p) [3, 4]

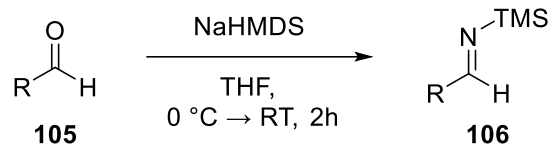

A solution of *p*-anisaldehyde (0.29 mL, 2.3 mmol, 1.0 equiv.) in dry THF (2.3 mL, 1.0 M) maintained under a positive pressure of nitrogen was stirred and cooled to 0 °C. A solution of 0.79 M NaHMDS (2.9 mL, 2.3 mmol, 1.0 equiv.) was added dropwise via syringe and the reaction mixture was allowed to warm up to room temperature over the course of two hours. ^{1}H NMR confirmed the formation of the silyl imine with the disappearance of the aldehyde proton around 10 ppm and the appearance of the imine proton at around 9 ppm.

General procedure for the preparation of silyl imines (106q-s)

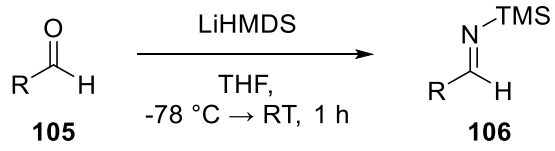

A solution of aldehyde (1.2 mmol, 1.0 equiv.) in dry THF (1.2 mL, 1.0 M) maintained under a positive pressure of nitrogen was stirred and cooled to -78 °C in a dry ice/acetone bath. A solution of 1.0 M LiHMDS (1.2 mL, 1.2 mmol, 1.0 equiv.) was added dropwise via syringe and the reaction mixture. After stirring for 30 min at -78 °C, the solution was allowed to warm up to room temperature and stir for an additional 30 min. ^{1}H NMR confirmed the formation of the silyl imine with the disappearance of the aldehyde proton around 10 ppm and the appearance of the imine proton at around 9 ppm.

General procedure for the preparation of imidazolidines (108)

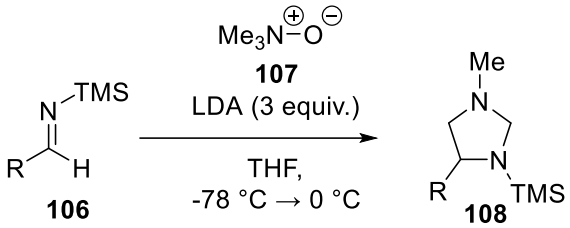

A solution of trimethylamine N-oxide (182 mg, 2.4 mmol, 1.0 equiv.) in dry THF (7.0 mL, 0.10 M) maintained under a positive pressure of nitrogen was stirred and cooled to -78°C. A solution of 1.7 M LDA (4.0 mL, 6.9 mmol, 3.0 equiv.) was added dropwise via syringe, followed by the slow addition of the crude 0.46 M silyl imine (4.0 mL, 2.3 mmol, 1.0 equiv.). LDA was titrated before use using salicylaldehyde phenylhydrazone. [1] The reaction was removed from the cold bath and allowed to stir and warm to room temperature for 2 h. The formation of the imidazolidine was confirmed by ^{1}H NMR and was taken onto the next step directly without further purification.

General procedure for the preparation of 1,2 diamines (109a-s)

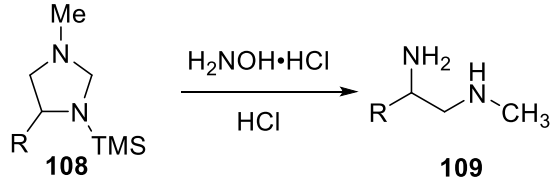

Under ambient conditions, hydroxylamine hydrochloride (850 mg, 12 mmol, 5.2 equiv.) was added to the crude reaction mixture of the imidazolidine along with 1.2 M HCl (0.20 mL, 0.01 M) The reaction vessel was equipped with a reflux condenser and the mixture was heated to 65 °C using a heating mantle for 12 h. The reaction was cooled to RT, acidified using 1.0 M HCl and washed with DCM (20 mL x 3), hexanes (x 2), and EtOAc (x 3). The aqueous layer was basified with 15% NaOH and the product extracted with DCM (20 mL x 3). The organic layers were combined, dried over $MgSO_4$, and concentrated under reduced pressure to afford pure 1,2 diamines unless otherwise noted. Product was isolated as a colorless oil. (94% yield, 405 mg, 2.2 mmol).

1-(4-methoxyphenyl)-*N*^{2}-methylethane-1,2-diamine (109a)

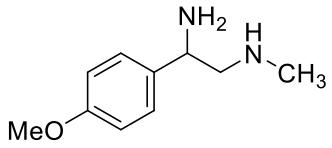

Silyl imine prepared according to the general procedure using *p*-anisaldehyde (0.29 mL, 2.3 mmol, 1.0 equiv.), 0.79 M NaHMDS (2.9 mL, 2.3 mmol, 1.0 equiv.), and THF (2.3 mL, 1.0 M). Silyl imine solution was used without further purification.

Diamine was prepared according to the general procedure using TMAO (182 mg, 2.4 mmol, 1.0 equiv.), 1.7 M LDA (4.0 mL, 6.9 mmol, 3.0 equiv.), crude 0.46 M silyl imine (4.0 mL, 2.3 mmol, 1.0 equiv.), THF (7.0 mL, 0.10 M), hydroxylamine hydrochloride (850 mg, 12 mmol, 5.2 equiv.) and 1.2 M HCl (0.20 mL, 0.01 M). Following aqueous work-up, no further purification was necessary. Product was isolated as a colorless oil. (94% yield, 405 mg, 2.2 mmol)

^{1}H NMR (400 MHz, $CDCl_3$) δ 7.26 (d, *J* = 8.7 Hz, 2H), 6.87 (d, *J* = 8.7 Hz, 2H), 4.03 (t, *J* = 6.7 Hz, 1H), 3.79 (s, 3H), 2.76 – 2.71 (m, 2H), 2.44 (s, 3H), 2.14 (br. s, 3H).

^{13}C NMR (101 MHz, $CDCl_3$) δ 158.8, 136.1, 127.5, 114.0, 59.4, 55.3, 54.3, 36.0.

IR: 2914, 2778, 1739, 1653, 1618, 1604, 1577, 1512, 1466, 1446, 1439, 1424, 1402, 1356, 1308, 1278, 1261, 1224, 1188, 1146, 1108, 1088, 1032, 1001, 970, 954, 940, 909, 883, 825, 808, 733, 715, 645, 569, 540, 507 cm^{-1}

HRMS (ESI) m/z: $[M+H]^+$ Calc'd for $C_{10}H_{17}N_2O$ 181.1336; Found 181.1340.

1-(3-methoxyphenyl)-*N*^{2}-methylethane-1,2-diamine (109b)

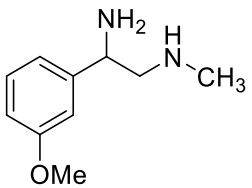

Silyl imine prepared according to the general procedure using *m*-anisaldehyde (0.29 mL, 2.4 mmol, 1.0 equiv.), 1.9 M NaHMDS (1.3 mL, 2.4 mmol, 1.0 equiv.), and THF (2.4 mL, 1.0 M). Silyl imine solution was used without further purification.

Diamine was prepared according to the general procedure using TMAO (180 mg, 2.4 mmol, 1.0 equiv.), 1.6 M LDA (4.5 mL, 7.2 mmol, 3.0 equiv.), crude 0.68 M silyl imine solution (3.5 mL, 2.4 mmol, 1.0 equiv.), THF (12 mL, 0.10 M), hydroxylamine hydrochloride (833 mg, 12 mmol, 5.0 equiv.) and 1.2 M HCl (0.2 mL, 0.01 M). Following aqueous work-up, no further purification was necessary. Product was isolated as a yellow oil. (76% yield, 328 mg, 1.8 mmol)

^{1}H NMR (400 MHz, $CDCl_3$) δ 7.26 (t, *J* = 7.7 Hz, 1H), 6.93 (s, 1H), 6.91 (d, *J* = 8.4 Hz, 1H), 6.80 (dd, *J* = 8.0, 2.6 Hz, 1H), 4.04 (dd, *J* = 7.8, 5.3 Hz, 1H), 3.81 (s, 3H), 2.81 – 2.70 (m, 2H), 2.44 (s, 3H), 1.88 (br. s, 3H).

^{13}C NMR (101 MHz, $CDCl_3$) δ 160.0, 146.3, 129.7, 118.8, 112.7, 112.1, 59.7, 55.4, 55.3, 36.8.

IR: 3290, 2937, 2836, 2793, 1668, 1599, 1584, 1486, 1464, 1453, 1435, 1377, 1347, 1317, 1254, 1152, 1112, 1078, 1040, 995, 855, 780, 740, 699, 629, 579, 564, 541 cm^{-1}

HRMS (ESI) m/z (z=2): [M+H+Na]+2 Calc'd for $C_{10}H_{17}N_2ONa$ 102.0614; Found 102.0615.

1-(2-methoxyphenyl)-*N*^{2}-methylethane-1,2-diamine (109c)

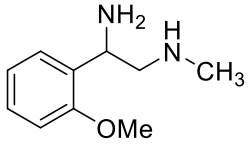

Silyl imine prepared according to the general procedure using *o*-anisaldehyde (328 mg, 2.4 mmol, 1.0 equiv.), 1.9 M NaHMDS (1.3 mL, 2.4 mmol, 1.0 equiv.), and THF (2.4 mL, 1.0 M). Silyl imine solution was used without further purification.

Diamine was prepared according to the general procedure using TMAO (193 g, 2.4 mmol, 1.0 equiv.), 1.9 M LDA (3.7 mL, 7.2 mmol, 3.0 equiv.), crude 0.60 M silyl imine (4.0 mL, 2.4 mmol,

1.0 equiv.), THF (12 mL, 0.10 M), hydroxylamine hydrochloride (834 g, 12 mmol, 5.0 equiv.) and 1.2 M HCl (0.20 mL, 0.01 M). Following aqueous work-up, no further purification was necessary. Product was isolated as a yellow oil. (93% yield, 396 mg, 2.2 mmol)

^{1}H NMR (400 MHz, $CDCl_3$) δ 7.31 (dd, *J* = 7.5, 1.7 Hz, 1H), 7.26 – 7.22 (m, 1H), 6.96 (td, *J* = 7.6, 6.3 Hz, 1H), 6.88 (dd, *J* = 8.2, 1.1 Hz, 1H), 4.34 (dd, *J* = 8.4, 4.8 Hz, 1H), 3.84 (s, 3H), 2.88 – 2.77 (m, 2H), 2.48 (s, 3H), 2.40 (br. s, 3H)

^{13}C NMR (101 MHz, $CDCl_3$) δ 157.0, 132.3, 128.2, 127.1, 120.8, 110.6, 57.4, 55.3, 50.2, 36.0.

IR: 3285, 2937, 2837, 2793, 1905, 1600, 1586, 1490, 1462, 1438, 1374, 1289, 1237, 1179, 1161, 1105, 1050, 1025, 932, 878, 810, 752, 703, 666, 617, 602, 579, 557, 542 cm^{-1}

HRMS (ESI) m/z: $[M+H_3O]^+$ Calc'd $C_{10}H_{19}N_2O_2$ 199.1441; Found 199.1437.

N^1-methyl-2-(2,3,4-trimethoxyphenyl)ethane-1,2-diamine (109d)

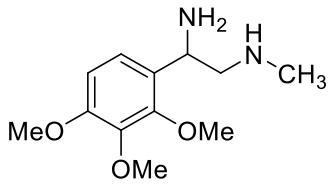

Silyl imine prepared according to the general procedure using 2,3,4-trimethoxybenzaldehyde (237 mg, 1.2 mmol, 1.0 equiv.), 1.9 M NaHMDS (0.63 mL, 1.2 mmol, 1.0 equiv.), and THF (1.2 mL, 1.0 M). Silyl imine solution was used without further purification.

Diamine was prepared according to the general procedure using TMAO (107 mg, 1.4 mmol, 1.4 equiv.), 1.8 M LDA (1.6 mL, 3.0 mmol, 3.0 equiv.), crude 0.67 M silyl imine (1.5 mL, 1.0 mmol, 1.0 equiv.), THF (10 mL, 0.10 M), hydroxylamine hydrochloride (354 g, 5.0 mmol, 5.0 equiv.) and 1.2 M HCl (0.10 mL, 0.01 M). Following aqueous work-up, no purification was necessary. Product was isolated as a yellow oil. (74% yield, 178mg, 0.74 mmol)

^{1}H NMR (400 MHz, $CDCl_3$) δ 7.02 (d, *J* = 8.7 Hz, 1H), 6.66 (d, *J* = 8.6 Hz, 1H), 4.28 (dd, *J* = 8.3, 4.9 Hz, 1H), 3.92 (s, 3H), 3.86 (s, 3H), 3.85 (s, 3H), 2.83 – 2.72 (m, 2H), 2.48 (s, 3H), 2.35 (br. s, 3H)

^{13}C NMR (126 MHz, $CDCl_3$) δ 153.0, 151.6, 142.2, 130.0, 121.3, 107.4, 61.3, 60.8, 58.4, 56.1, 49.7, 36.0.

IR: 3263, 2940, 2837, 1599, 1494, 1463, 1435, 1417, 1390, 1282, 1230, 1201, 1091, 1011, 964, 904, 853, 797, 728, 688, 666, 645, 602, 582, 574, 559, 539 cm^{-1}

HRMS (ESI) m/z: $[M+Na]^+$ Calc'd for $C_{12}H_{20}N_2O_3Na$ 263.1366; Found 263.1359.

1-(2,5-dimethoxyphenyl)-*N*^{2}-methylethane-1,2-diamine (109e)

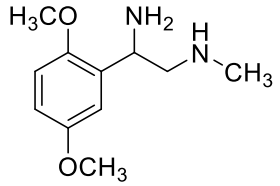

Silyl imine prepared according to the general procedure using 2,5-dimethoxybenzaldehyde (185 mg, 1.1 mmol, 1.0 equiv.), 1.2 M NaHMDS (1.0 mL, 1.2 mmol, 1.1 equiv.), and THF (1.1 mL, 1.0 M). Silyl imine solution was used without further purification.

Diamine was prepared according to the general procedure using TMAO (78 mg, 1.0 mmol, 1.0 equiv.), 2.7 M LDA (1.1 mL, 3.0 mmol, 3.0 equiv.), crude 0.5 M silyl imine (2 mL, 1.0 mmol, 1.0 equiv.), THF (7.0 mL, 0.10 M), hydroxylamine hydrochloride (416 mg, 6.0 mmol, 6.0 equiv.) and 1.2 M HCl Following aqueous work-up, no further purification was necessary. Product was isolated as a yellow oil. (80% yield, 168 mg, 0.80 mmol)

^{1}H NMR (400 MHz, $CDCl_3$) δ 6.93 (d, *J* = 3.1 Hz, 1H), 6.79 (d, *J* = 8.6 Hz, 1H), 6.73 (d, *J* = 8.7 Hz, 1H), 4.31 (t, 1H), 3.78 (s, 3H), 3.76 (s, 3H), 2.84 – 2.79 (m, 1H), 2.72 (dd, *J* = 11.6, 8.3 Hz, 1H), 2.45 (s, 3H), 2.03 (br. s, 3H).

^{13}C NMR (101 MHz, $CDCl_3$) δ 153.7, 151.1, 133.5, 113.4, 112.1, 111.5, 57.4, 55.8, 55.8, 50.2, 36.0.

IR: 2937, 2834, 2792, 1589, 1493, 1464, 1428, 1369, 1275, 1214, 1178, 1155, 1104, 1044, 1024, 871, 801, 732, 713, 603 cm^{-1}

HRMS (ESI) m/z: $[M+H_3O]^+$ Calc'd for $C_{11}H_{21}N_2O_3$ 229.1547; Found 229.1567.

N^1-methyl-2-phenylethane-1,2-diamine (109f)

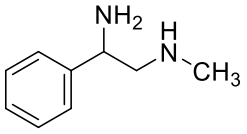

Silyl imine prepared according to the general procedure using benzaldehyde (0.10 mL, 1.0 mmol, 1.0 equiv.), 1.1 M NaHMDS (0.9 mL, 1.0 mmol, 1.0 equiv.), and THF (1.0 mL, 1.0 M). Silyl imine solution was used without further purification.

Diamine was prepared according to the general procedure using TMAO (34 mg, 0.40 mmol, 1.0 equiv.), 2.9 M LDA (0.41 mL, 1.2 mmol, 3.0 equiv.), crude 0.53 M silyl imine (0.80 mL, 0.40 mmol, 1.0 equiv.), THF (3.2 mL, 0.10 M), hydroxylamine hydrochloride (192 g, 2.0 mmol, 5.0 equiv.) and 1.2 M HCl (0.4 mL, 0.01 M). Following aqueous work-up, no further purification was necessary. Product was isolated as a yellow oil. (80% yield, 48 mg, 0.32 mmol). The spectrum is in agreement with previously reported. [5]

^{1}H NMR (400 MHz, $CDCl_3$) δ 7.33 – 7.30 (m, 4H), 7.28 – 7.22 (m, 1H), 4.06 – 4.02 (dd, J = 7.8, 5.4 Hz, 1H), 2.78 – 2.69 (m, 2H) 2.42 (s, 3H).

1-(3,5-dimethylphenyl)-N^2-methylethane-1,2-diamine (109g)

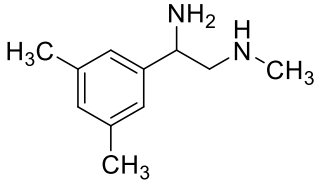

Silyl imine prepared according to the general procedure using 3,5-dimethylbenzaldehyde (0.16 mL, 1.2 mmol, 1.0 equiv.), 1.2 M NaHMDS (1.0 mL, 1.2 mmol, 1.0 equiv.), and THF (1.0 mL, 1.0 M). Silyl imine solution was used without further purification.

Diamine was prepared according to the general procedure using TMAO (80 mg, 1.0 mmol, 1.0 equiv.), 1.5 M LDA (2.0 mL, 3.0 mmol, 3.0 equiv.), crude 0.55 M silyl imine solution (1.8 mL, 1.0 mmol, 1.0 equiv.), THF (8.0 mL, 0.1 M), hydroxylamine hydrochloride (351 g, 5.0 mmol, 5.0 equiv.) and 1.2 M HCl (0.10 mL, 0.01 M). Following aqueous work-up, no further purification was necessary. Product was isolated as a yellow oil. (77% yield, 132 mg, 0.77 mmol)

^{1}H NMR (400 MHz, $CDCl_3$) δ 6.95 (s, 2H), 6.89 (s, 1H), 3.98 (t, 1H), 2.78 – 2.68 (m, 2H), 2.43 (s, 3H), 2.31 (s, 6H), 2.06 (br. s, 3H)

^{13}C NMR (101 MHz, $CDCl_3$) δ 144.5, 138.0, 128.8, 124.2, 59.8, 55.2, 36.3, 21.3.

IR: 3002, 2917, 2887, 2793, 2135, 1639, 1608, 1566, 1449, 1418, 1379, 1298, 1275, 1232, 1167, 1112, 1080, 1040, 975, 927, 909, 845, 806, 730, 705, 697, 634, 620 cm^{-1}

HRMS (ESI) m/z: $[M+CH_3OH_2]^+$ Calc'd for $C_{12}H_{23}N_2O$ 211.1805; Found 211.1819.

1-([1,1'-biphenyl]-4-yl)-*N*^{2}-methylethane-1,2-diamine (109h)

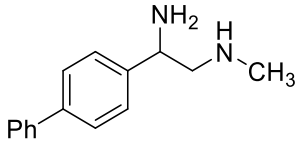

Silyl imine prepared according to the general procedure using [1,1'-biphenyl]-4-carbaldehyde (222 mg, 1.2 mmol, 1.0 equiv.), 1.9 M NaHMDS (0.63 mL, 1.2 mmol, 1.0 equiv.), and THF (1.2 mL, 1.0 M). Silyl imine solution was used without further purification.

Diamine was prepared according to the general procedure using TMAO (93 mg, 1.2 mmol, 1.0 equiv.), 0.86 M LDA (1.4 mL, 1.2 mmol, 3.0 equiv.), crude 0.68 M silyl imine solution (1.8 mL, 1.2 mmol, 1.0 equiv.), THF (7.0 mL, 0.10 M), hydroxylamine hydrochloride (418 mg, 6.0 mmol,

5.0 equiv.) and 1.2 M HCl (0.12 mL, 0.01M). Following aqueous work-up, no further purification was necessary. Product was isolated as a yellow oil. (88% yield, 233 mg, 1.0 mmol)

^{1}H NMR (400 MHz, $CDCl_3$) δ 7.58 – 7.54 (m, 4H), 7.43 – 7.38 (m, 4H), 7.31 (tt, *J* = 7.4, 1.3 Hz, 1H) 4.08 (dd, *J* = 7.9, 5.3 Hz, 1H), 2.82 – 2.71 (m, 2H), 2.44 (s, 3H), 1.86 (br. s, 3H)

^{13}C NMR (101 MHz, $CDCl_3$) δ 143.7, 140.8, 140.0, 128.7, 127.2, 127.2, 127.0, 126.9, 59.9, 55.0, 36.4.

IR: 3346, 3057, 3027, 2947, 2837, 2778, 1674, 1599, 1487, 1454, 1428, 1151, 1007, 839, 764 cm^{-1}

HRMS (ESI) m/z: $[M+H]^+$ Calc'd for $C_{15}H_{19}N_2$ 227.1543; Found 227.1548.

N^1-methyl-2-(naphthalen-2-yl)ethane-1,2-diamine (109i)

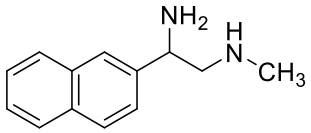

Silyl imine prepared according to the general procedure using 2-naphthaldehyde (391 mg, 2.5 mmol, 1.0 equiv.), 1.8 M NaHMDS (1.4 mL, 2.5 mmol, 1.0 equiv.), and THF (2.5 mL, 1.0 M). Silyl imine solution was used without further purification.

Diamine was prepared according to the general procedure using TMAO (184 mg, 2.4 mmol, 1.0 equiv.), 1.4 M LDA (5.2 mL, 7.2 mmol, 3.0 equiv.), crude 0.64 M silyl imine (3.8 mL, 2.4 mmol, 1.0 equiv.), THF (16 mL, 0.10 M), hydroxylamine hydrochloride (835 mg, 12 mmol, 5.0 equiv.) and 1.2 M HCl (0.24 mL, 0.01 M). Following aqueous work-up, no further purification was necessary. Product was isolated as a yellow oil, (71% yield, 341 mg, 1.8 mmol)

^{1}H NMR (400 MHz, $CDCl_3$) δ 7.85 – 7.81 (m, 4H), 7.50 – 7.46 (m, 3H), 4.25 (dd, *J* = 7.8, 5.3 Hz, 1H), 2.91 – 2.80 (m, 2H), 2.47 (s, 3H), 2.14 (br. s, 3H).

^{13}C NMR (101 MHz, $CDCl_3$) δ 142.1, 133.5, 133.0, 128.4, 127.9, 127.8, 126.3, 125.8, 125.1, 124.9, 59.8, 55.5, 36.5.

IR: 3275, 3053, 2931, 2845, 2790, 1633, 1601, 1507, 1447, 1365, 1270, 1125, 1018, 892, 856, 817, 744, 659, 540 cm^{-1}

HRMS (ESI) m/z: $[M+CH_3OH_2]^+$ Calc'd for $C_{14}H_{21}N_2O$ 233.1648; Found 233.1636.

***N*^{1},3,3-trimethylbutane-1,2-diamine (109j)**

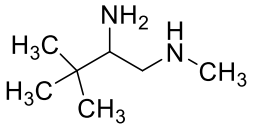

Silyl imine prepared according to the general procedure using pivaldehyde (0.13 mL, 1.2 mmol, 1.0 equiv.), 1.2 M NaHMDS (1.0 mL, 1.2 mmol, 1.0 equiv.), and THF (1.2 mL, 1.0 M). Silyl imine solution was used without further purification.

Diamine was prepared according to the general procedure using TMAO (76 mg, 1.0 mmol, 1.0 equiv.), 2.7 M LDA (1.1 mL, 3.0 mmol, 3.0 equiv.), crude 0.55 M silyl imine (2.0 mL, 1.0 mmol, 1.0 equiv.), THF (8.0 mL, 0.10 M), hydroxylamine hydrochloride (368 mg, 5.0 mmol, 5.0 equiv.) and 1.2 M HCl (0.10 mL, 0.01 M). Following aqueous work-up, product was purified by acidifying with 10% HCl until precipitate formed, removing solvent, and washing with cold DCM. Isolated as an off-white solid. (60% yield, 78 mg, 0.60 mmol)

^{1}H NMR (400 MHz, MeOD) δ 3.48 (dd, J = 35.6, 11.7 Hz, 2H), 3.25 (dd, J = 14.3, 9.0 Hz, 1H), 2.79 (br. s, 3H), 1.07 (s, 9H).

^{13}C NMR (101 MHz, MeOD) δ 59.3, 50.2, 34.7, 34.4, 26.4.

IR: 2965, 2692, 2384, 2131, 1591, 1519, 1474, 1408, 1380, 1350, 1125, 1037, 1012, 932, 810, 750, 553, 511, 460, 423 cm^{-1}

HRMS (ESI) m/z: $[M+H]^+$ Calc'd for $C_7H_{19}N_2$ 131.1543; Found 131.1553.

1-((3*r*,5*r*,7*r*)-adamantan-1-yl)-*N*^{2}-methylethane-1,2-diamine (109k)

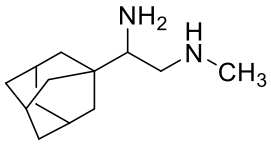

Silyl imine prepared according to the general procedure using adamantane-1-carbaldehyde (80 mg, 0.50 mmol, 1.0 equiv.), 1.0 M NaHMDS (0.50 mL, 0.50 mmol, 1.0 equiv.), and THF (0.50 mL, 1.0 M). Silyl imine solution was used without further purification.

Diamine was prepared according to the general procedure using TMAO (37.7 mg, 0.50 mmol, 1.3 equiv.), 1.5 M LDA (0.80 mL, 1.2 mmol, 3.0 equiv.), crude 0.50 M silyl imine (0.80 mL, 0.40 mmol, 1.0 equiv.), THF (4.0 mL, 0.10 M), hydroxylamine hydrochloride (150 mg, 2.2 mmol, 5.5 equiv.) and 1.2 M HCl (0.04 mL, 0.01M). Following aqueous work-up, no further purification was necessary. Product was isolated as a white powder. (72% yield, 60 mg, 0.28 mmol).

^{1}H NMR (400 MHz, CDCl3) δ 2.75 (dd, J = 10.9, 2.1 Hz, 1H), 2.43 (s, 3H), 2.34 – 2.24 (m, 2H), 1.96 (br. s, 3H), 1.72 – 1.58 (m, 8H), 1.52 (s, 7H).

^{13}C NMR (101 MHz, CDCl3) δ 60.0, 52.6, 38.6, 37.3, 36.4, 35.5, 28.5.

IR: 3366, 3314, 2900, 2846, 2679, 2464, 2190, 2063, 1591, 1449, 1363, 1344, 1316, 1299, 1250, 1184, 1139, 1123, 1099, 1037, 983, 937, 921, 894, 811, 771, 712, 632, 576, 563, 541 cm^{-1}

HRMS (ESI) m/z: $[M+Na]^+$ Calc'd for $C_{13}H_{24}N_2Na$ 231.1832; Found 231.1840.

2-((tert-butyldimethylsilyl)oxy)-3-methoxybenzaldehyde (SI-1)

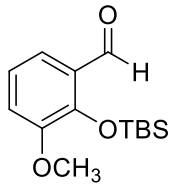

Prepared according to literature procedure. [6] An oven dried round bottom flask under positive nitrogen pressure was charged with *o*-vanillin (1.523 g, 10 mmol, 1.0 equiv.) and it was dissolved

in DCM (50 mL). 4-Dimethylaminopyridine (65 mg, 0.53 mmol, 0.053 equiv), and triethylamine (2.1 mL, 15 mmol, 1.5 equiv.) were added to the reaction and the mixture was cooled to 0°C. *tert*-Butyldimethylsilyl chloride (2.3601 g, 15 mmol, 1.5 equiv.) was added portionwaise and the reaction was allowed to warm up to RT. The reaction was monitored by TLC (1:1 Hex/EtOAc). Once complete the reactions mixture was poured into cold brine, extracted with DCM (x 3), dried over $MgSO_4$, and concentrated *in vacuo*. The residue was purified using FCC to afford a clear oil. (98% yield, 2.610 g, 9.8 mmol). R_f 0.95. The ^1H NMR is in agreement with that previously reported. [7]

^1H NMR (400 MHz, $CDCl_3$) δ 10.53 (s, 1H), 7.40 (dd, J = 7.9, 1.6 Hz, 1H), 7.17 – 6.83 (m, 2H), 3.85 (s, 3H), 1.01 (s, 9H), 0.23 (s, 6H).

1-(2-((tert-butyldimethylsilyl)oxy)-3-methoxyphenyl)-*N*^{2}-methylethane-1,2-diamine (109l)

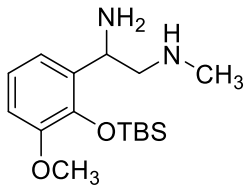

Silyl imine prepared according to the general procedure using 2-((tert-butyldimethylsilyl)oxy)-3-methoxybenzaldehyde (319 mg, 1.2 mmol, 1.0 equiv.), 1.0 M NaHMDS (1.2 mL, 1.2 mmol, 1.0 equiv.), and THF (1.2 mL, 1.0 M). Silyl imine solution was used without further purification.

Diamine was prepared according to the general procedure using TMAO (77 mg, 1.0 mmol, 1.0 equiv.), 1.5 M LDA (2.0 mL, 3.0 mmol, 3.0 equiv.), crude 0.50 M silyl imine (1.0 mmol, 1.0 equiv.), THF (8.0 mL, 0.10 M), hydroxylamine hydrochloride (349 mg, 5.0 mmol, 5.0 equiv.) and 1.2 M HCl (0.10 mL, 0.01 M). The standard aqueous work-up was followed with careful pH control. The solution was acidified to a pH and 4 and then basified to a pH of 10. No further purification was necessary. Product was isolated as a brown oil. (30% yield, 94 mg, 0.30 mmol)

^{1}H NMR (400 MHz, $CDCl_3$) δ 6.96 (dd, *J* = 7.8, 1.7 Hz, 1H), 6.91 (t, *J* = 7.8 Hz, 1H), 6.75 (dd, *J* = 7.9, 1.8 Hz, 1H), 4.51 (dd, *J* = 8.3, 4.4 Hz, 1H), 3.78 (s, 3H), 2.83 – 2.68 (m, 2H), 2.44 (s, 3H), 1.00 (s, 9H), 0.22 (s, 3H), 0.19 (s, 3H).

^{13}C NMR (101 MHz, $CDCl_3$) δ 149.7, 142.1, 135.8, 121.1, 118.1, 109.9, 57.9, 54.8, 48.2, 36.5, 26.2, 19.1, -3.5, -3.7.

IR: 2952, 2929, 2896, 2855, 2800, 1584, 1472, 1463, 1441, 1387, 1361, 1251, 1226, 1183, 1062, 1007, 907, 832, 810, 778, 733, 664, 610, 585, 574, 562, 551, 541, 531, 523 cm^{-1}

HRMS (ESI) m/z (z=2): $[M+2H]^{+2}$ Calc'd for $C_{16}H_{32}N_2O_2Si$ 156.1111; Found 156.1103.

4-((tert-butyldimethylsilyl)oxy)benzaldehyde (SI-2)

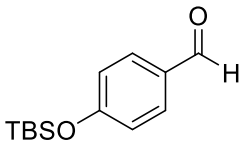

Prepared according to literature procedure. [6] 4-Hydroxybenzaldehye (610 mg, 5.0 mmol, 1.0 equiv.), DCM (30 mL), 4-dimethylaminopyridine (40 mg, 0.33 mmol, 0.066 equiv.), triethylamine (1.1 mL, 7.5 mmol, 1.5 equiv.) and *tert*-Butyldimethylsilyl chloride (1.090 g, 7.5 mmol, 1.5 equiv.) were used. The residue was purified by FCC, TLC conditions 1:1 Hex/EtOAc, R_f =0.95. (83% yield, 982 mg, 4.2 mmol). The ^{1}H NMR is in agreement with that previously reported. [8]

^{1}H NMR (400 MHz, $CDCl_3$) δ 9.90 (s, 1H), 7.80 (d, *J* = 8.7 Hz, 2H), 6.95 (d, *J* = 8. Hz, 2H), 1.00 (s, 9H), 0.26 (s, 6H).

1-(4-((*tert*-butyldimethylsilyl)oxy)phenyl)-*N*^{2}-methylethane-1,2-diamine (109m)

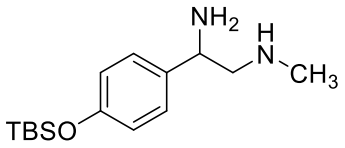

Silyl imine prepared according to the general procedure using 4-((tert-butyldimethylsilyl)oxy)benzaldehyde (595 mg, 2.4 mmol, 1.0 equiv.), 1.9 M NaHMDS (1.3 mL, 2.5 mmol, 1.0 equiv.), and THF (2.4 mL, 1M). Silyl imine solution was used without further purification.

Diamine was prepared according to the general procedure using TMAO (180 mg, 2.4 mmol, 1.0 equiv.), 1.6 M LDA (4.5 mL, 7.2 mmol, 3.0 equiv.), crude 0.66 M silyl imine (3.7 mL, 2.4 mmol, 1.0 equiv.), THF (16 mL, 0.10 M), hydroxylamine hydrochloride (840 mg, 12 mmol, 5.0 equiv.) and 1.2 M HCl (0.24 mL, 0.01 M). The standard aqueous work-up was followed with careful pH control. The solution was acidified to a pH and 4 and then basified to a pH of 10. No further purification was necessary. Product was isolated as a yellow oil. (77% yield, 518 mg, 1.8 mmol)

^{1}H NMR (400 MHz, $CDCl_3$) δ 7.16 (d, J = 8.5 Hz, 2H), 6.76 (d, J = 8.5 Hz, 2H), 4.02 (d, J = 7.6 Hz, 1H), 3.32 (br. s, 3H), 2.74 (dd, J = 6.8, 2.7 Hz, 2H), 2.41 (s, 3H), 0.94 (s, 9H), 0.15 (s, 6H).

^{13}C NMR (126 MHz, $CDCl_3$) δ 161.9, 134.8, 128.4, 127.5, 123.7, 120.3, 115.0, 36.0, 27.2, 25.8, 17.8, -4.5.

IR: 2951 2927 2882 2853 1593 1510 1470 1409 1361 1252 1238 1140 1072 1007 908 872 834 822 808 768 730 691 665 600 577 cm^{-1}

HRMS (ESI) m/z (z=2): $[M+2H]^{+2}$ Calc'd for $C_{15}H_{30}N_2OSi$ 141.1058; Found 141.1057.

1-(4-fluorophenyl)-*N*^{2}-methylethane-1,2-diamine (109n)

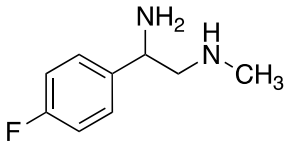

Silyl imine prepared according to the general procedure using 4-fluorobenzaldehyde (0.05 mL, 0.50 mmol, 1.0 equiv.), 0.86 M NaHMDS (0.58 mL, 0.50 mmol, 1.0 equiv.), and THF (0.50 mL, 1.0 M). Silyl imine solution was used without further purification.

Cycloadduct was prepared according to the general procedure using TMAO (41 mg, 0.54 mmol, 1.4 equiv.), 0.93 M LDA (0.86 mL, 0.8 mmol, 2.0 equiv.), crude 0.50 M silyl imine (0.80 mL, 0.40 mmol, 1.0 equiv.), THF (3.0 mL, 0.10 M). The reaction was quenched with water at 0 °C and the product was extracted with DCM (x 3). The organic layer was dried over $MgSO_4$, filtered and concentrated under reduced pressure. The residue was redissolved in THF (10 mL) and 1.0 M HCl (7.0 mL, 0.7 M). The procedure was then the same as the general method for forming 1,2-diamines. Following aqueous work-up, no further purification was necessary. Product was isolated as a colorless oil. (42% yield, 28 mg, 0.17 mmol)

^{1}H NMR (400 MHz, CDCl3) δ 7.34 (dd, J = 8.6, 5.4 Hz, 2H), 7.04 (t, J = 8.6 Hz, 2H), 4.07 (dd, J = 8.0, 5.1 Hz, 1H), 2.74 (m, 2H), 2.47 (s, 3H), 1.69 (br. s, 3H).

^{13}C NMR (101 MHz, CDCl3) δ 163.2, 160.8, 140.4, 140.4, 128.1, 128.0, 115.5, 115.3, 60.2, 54.8, 36.6.

IR: 3291, 3041, 2933, 2889, 2848, 2792, 2252, 2208, 2042, 1892, 1602, 1507, 1472, 1448, 1418, 1366, 1345, 1294, 1219, 1155, 1111, 1095, 1075, 1014, 832, 754, 719, 705, 652, 634, 625, 601, 559 cm^{-1}

HRMS (ESI) m/z: $[M+CH_3OH_2]^+$ Calc'd for $C_{10}H_{18}FN_2O$ 201.1398; Found 201.1391.

N^1-methyl-2-(4-(trifluoromethyl)phenyl)ethane-1,2-diamine (109o)

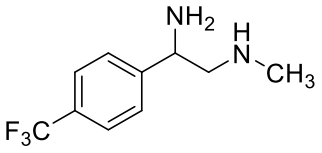

Silyl imine prepared according to the general procedure using 4-(trifluoromethyl)benzaldehyde (0.16 mL, 1.2 mmol, 1.0 equiv.), 1.9 M NaHMDS (0.63 mL, 1.2 mmol, 1.0 equiv.), and THF (1.2 mL, 1.0 M). Silyl imine solution was used without further purification.

Diamine was prepared according to the general procedure using TMAO (82 mg, 1 mmol, 1 equiv.), 1.9 M LDA (1.5 mL, 3.0 mmol, 3.0 equiv.), crude 0.66 M silyl imine (1.5 mL, 1.0 mmol, 1.0 equiv.), THF (10 mL, 0.10 M), hydroxylamine hydrochloride (377 mg, 5.0 mmol, 5.0 equiv.) and 1.2 M HCl (0.10 mL). Following aqueous work-up, no further purification was necessary. Product was isolated as a yellow oil. (32% yield, 71 mg, 0.28 mmol)

^{1}H NMR (400 MHz, $CDCl_3$) δ 7.60 (d, *J* = 8.7 Hz, 2H), 7.49 (d, *J* = 8.1 Hz, 2H), 4.17 (dd, *J* = 8.1, 5.0 Hz, 1H), 2.84 – 2.73 (m, 2H), 2.47 (s, 3H), 2.42 (br. s, 2H).

^{13}C NMR (101 MHz, CDCl3) δ 148.4 (s), 129.5 (q, *J* = 32.4 Hz), 128.2 (q, *J* = 272.7 Hz), 126.8 (s), 125.5 (q, *J* = 3.9 Hz), 122.8 (s), 120.1 (s), 59.4 (s), 54.8 (s), 36.1 (s).

IR: 3274, 2933, 2851, 2797, 2254, 2119, 1664, 1619, 1451, 1419, 1322, 1162, 1109, 1066, 1016, 955, 837, 735, 703, 652, 636, 605, 576, 561, 552, 530 cm^{-1}

HRMS (ESI) m/z: $[M+H_3O]^+$ Calc'd for $C_{10}H_{16}F_3N_2O$ 237.1209; Found 237.1204.

***N*^{1}-methyl-2-(3-(trifluoromethyl)phenyl)ethane-1,2-diamine (109p)**

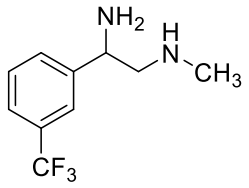

Silyl imine prepared according to the general procedure using 3-(trifluoromethyl)benzaldehyde (0.07 mL, 0.50 mmol, 1.0 equiv.), 1.8 M NaHMDS (0.29 mL, 0.50 mmol, 1.0 equiv.), and THF (0.5 mL, 1.0 M). Silyl imine solution was used without further purification.

Diamine was prepared according to the general procedure using TMAO (38 mg, 0.4 mmol, 1 equiv.), 1.4 M LDA (0.86 mL, 1.2 mmol, 3.0 equiv.), crude 0.63 M silyl imine (0.63 mL, 0.40 mmol, 1.0 equiv.), THF (3.0 mL, 0.10 M), hydroxylamine hydrochloride (140 mg, 2.0 mmol, 5.0

equiv.) and 1.2 M HCl (0.04 mL, 0.01 M). Following aqueous work-up, no further purification was necessary. Product was isolated as a yellow oil. (48% yield, 42 mg, 0.20 mmol)

^{1}H NMR (400 MHz, $CDCl_3$) δ 7.63 (ddp, *J* = 1.9, 1.3, 0.7 Hz, 1H), 7.60 – 7.51 (m, 2H), 7.49 – 7.44 (m, 1H), 4.17 (dd, *J* = 8.4, 4.8 Hz, 1H), 2.89 – 2.69 (m, 2H), 2.48 (s, 3H).

^{13}C NMR (101 MHz, $CDCl_3$) δ 145.5, 131.5 (q, *J* = 32.3 Hz), 130.1 (d, *J* = 1.0 Hz), 131.1, (d, *J* = 2.0 Hz), 129.1, 128.3 (q, *J* = 272.7 Hz), 124.4 (q, *J* = 4.04), 123.4 (d, *J* = 3.0 Hz), 123.4 (d, *J* = 4.0 Hz), 59.6, 54.9, 36.3.

IR: 3275, 2937, 2851, 2797, 1597, 1449, 1327, 1161, 1117, 1071, 1002, 899, 842, 802, 749, 703, 662, 621, 597, 560, 540, 528 cm^{-1}

HRMS (ESI) m/z: $[M+Na]^+$ $C_{10}H_{13}F_3N_2Na$ 241.0923; Found 241.0943.

***N*^{1}-methyl-2-(pyridin-2-yl)ethane-1,2-diamine (109q)**

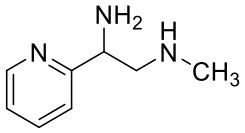

Silyl imine prepared according to the general procedure using picolinaldehyde (0.23 mL, 2.4 mmol, 1.0 equiv.), 1.5 M LiHMDS (2.4 mL, 2.4 mmol, 3.6 equiv.), and THF (2.4 mL, 1.0 M). Silyl imine solution was used without further purification.

Diamine was prepared according to the general procedure using TMAO (192 mg, 2.4 mmol, 1.0 equiv.), LDA (4.8 mL, 7.2 mmol, 3.0 equiv.), crude 0.50 M silyl imine (4.8 mL, 2.4 mmol, 1.0 equiv.), THF (10 mL, 0.10 M), hydroxylamine hydrochloride (840 mg, 12 mmol, 5.0 equiv.) and 1.2 M HCl (0.20 mL, 0.01%). No aqueous work-up was performed. Product was purified by reverse phase FCC, 0.1% TFA in water/MeOH. Isolated as an orange oil, (15% yield, 54 mg, 0.36 mmol)

^{1}H NMR (400 MHz, $CDCl_3$) δ 8.54 (d, *J* = 4.8 Hz, 1H), 7.70 (td, *J* = 7.7, 1.8 Hz, 1H), 7.34 (d, *J* = 7.8 Hz, 1H), 7.23 (ddd, *J* = 7.6, 4.8, 1.1 Hz, 1H), 5.38 (br. s, 3H), 4.33 (dd, *J* = 9.3, 4.3 Hz, 1H), 3.24 (dd, *J* = 12.2, 4.4 Hz, 1H), 3.10 (dd, *J* = 12.2, 9.4 Hz, 1H), 2.71 (s, 3H).

^{13}C NMR (101 MHz, $CDCl_3$) δ 160.5, 149.5, 137.4, 123.1, 121.8, 55.5, 53.5, 34.1.

IR: 3358, 3021, 2808, 1673, 1594, 1573, 1473, 1438, 1199, 1177, 1125, 1048, 997, 831, 799, 751, 720, 619, 597, 566, 545, 536 cm^{-1}

HRMS (ESI) m/z: $[M+H_3O]^+$ Calc'd for $C_8H_{16}N_3O$ 170.1288; Found 170.1295.

1-(furan-2-yl)-*N*^{2}-methylethane-1,2-diamine (109r)

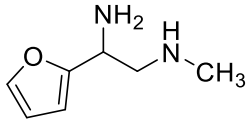

Silyl imine prepared according to the general procedure using furfural (0.22 mL, 2.6 mmol, 1.0 equiv.), 0.97 M LiHMDS (3.2 mL, 3.1 mmol, 1.2 equiv.), and THF (2.6 mL, 1.0 M). Silyl imine solution was used without further purification.

Diamine was prepared according to the general procedure using TMAO (184 mg, 2.4 mmol, 1.0 equiv.), 1.5 M LDA (4.8 mL, 7.2 mmol, 3.0 equiv.), crude 0.46 M silyl imine (2.4 mmol, 1.0 equiv.), THF (14 mL, 0.10 M), hydroxylamine hydrochloride (837 mg, 12 mmol, 5.0 equiv.) and 1.2 M HCl (0.24 mL, 0.01 M). No aqueous work-up was performed. Product was purified by reverse phase FCC, 0.1% TFA in water/MeOH. Isolated as an orange oil. (56% yield, 187 mg, 1.3 mmol)

^{1}H NMR (400 MHz, $CDCl_3$) δ 7.39 – 7.29 (m, 1H), 6.31 (dd, *J* = 3.3, 1.7 Hz, 1H), 6.19 – 6.11 (m, 1H), 4.06 (dd, *J* = 7.8, 5.1 Hz, 1H), 2.95 – 2.70 (m, 2H), 2.45 (s, 3H), 1.59 (s, 3H).

^{1}H NMR (400 MHz, $CDCl_3$) δ 7.34 (d, *J* = 0.9 Hz, 1H), 6.38 – 6.23 (m, 1H), 6.16 (d, *J* = 3.1 Hz, 1H), 4.06 (dd, *J* = 7.6, 5.2 Hz, 1H), 2.84 (ddd, *J* = 19.6, 11.8, 6.4 Hz, 2H), 2.45 (s, 3H), 1.5 (br. s, 3H).

^{13}C NMR (101 MHz, $CDCl_3$) δ 157.8, 141.6, 110.2, 104.9, 57.0, 49.4, 36.5.

IR: 3282, 2935, 2848, 2794, 1599, 1506, 1450, 1362, 1229, 1147, 1071, 1008, 912, 883, 863, 729, 620, 599, 558, 546, 539 cm^{-1}

HRMS (ESI) m/z: $[M+CH_3OH_2]^+$ Calc'd for $C_8H_{17}N_2O_2$ 173.1285; Found 173.1285.

***N*^{1}-methyl-2-(quinolin-4-yl)ethane-1,2-diamine (109s)**

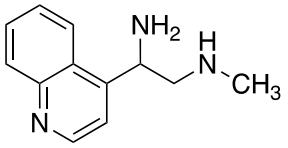

Silyl imine prepared according to the general procedure using 4-quinolinecarboxaldehyde (193 mg, 1.2 mmol, 1.0 equiv.), 1.0 M LiHMDS (1.2 mL, 1.2 mmol, 1.0 equiv.), and THF (1.2 mL, 1.0 M). Silyl imine solution was used without further purification.

Diamine was prepared according to the general procedure using TMAO (39.2 mg, 0.50 mmol, 1.0 equiv.), 0.75 M LDA (2.0 mL, 1.5 mmol, 3.0 equiv.), crude 0.50 M silyl imine (1.0 mL, 0.5 mmol, 1.0 equiv.), THF (3.0 mL, 0.10 M), 1.0M HCl (1.0 mL, 0.50 M). Following aqueous work-up, no further purification was necessary. Product was isolated as yellow oil. (76% yield, 77 mg, 0.38 mmol).

^{1}H NMR (400 MHz, $CDCl_3$) δ 8.90 (d, J = 4.5 Hz, 1H), 8.13 (d, J = 10.0 Hz, 1H), 8.10 (d, J = 10.0 Hz, 1H), 7.74 –7.68 (m, 1H), 7.61 – 7.54 (m, 2H), 4.91 (dd, J = 8.3, 3.8 Hz, 1H), 2.98 (dd, J = 12.0, 3.9 Hz, 1H), 2.77 (dd, J = 12.1, 8.3 Hz, 1H), 2.48 (s, 3H), 1.67 (br. s, 3H).

^{13}C NMR (101 MHz, $CDCl_3$) δ 150.4, 150.0, 148.3, 130.5, 129.1, 126.6, 126.3, 122.6, 117.6, 58.6, 50.1, 36.4.

IR: 3280, 3064, 2933, 2847, 2792, 2205, 1930, 1845, 1656, 1614, 1590, 1570, 1508, 1463, 1449, 1422, 1352, 1308, 1240, 1210, 1141, 1115, 1092, 1076, 1027, 953, 908, 869, 848, 814, 792, 759, 727, 642, .623, 599, 580, 556 cm^{-1}

HRMS (ESI) m/z: $[M+H]^+$ Calc'd for $C_{12}H_{16}N_3$ 202.1339; Found 202.1335.

Procedure for the mono-nosylation of 109a (113)

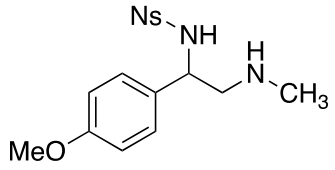

Under ambient conditions, a RBF flask was charged with **109a** (54 mg, 0.3 mmol, 1.0 equiv.), triethylamine (0.080 mL, 0.6 mmol, 2.0 equiv.) and DCM (3.0 mL, 0.1M). The solution was cooled to -78 °C while 2-nitrobenzenesulfonylchloride (66 mg, 0.3 mmol, 1.0 equiv.) was dissolved in DCM (0.5 mL) in a separate flask. The sulfonylchloride/DCM suspension was added dropwise to the **109a** solution, *via* syringe, over the course of 10 minutes at -78 °C. After addition, the solution was allowed to slowly warm to room temperature and was monitored by TLC until consumption of starting material. After 2h, the organic layer was washed with DI H_2O and the aqueous layers were rinsed with DCM (x2). The organic layers were combined, dried with $MgSO_4$, and concentrated *in vacu*. The compound was purified *via* flash column chromatography (5% MeOH in DCM) to afford a light yellow amorphous solid. (75% yield, 82 mg 0.23 mmol) (Rf = 0.60 in 10:1 DCM/MeOH)

^1H NMR (400 MHz, $CDCl_3$) δ 7.97 (dd, J = 7.2, 2.1 Hz, 1H), 7.69 (td, J = 7.0, 1.7 Hz, 2H), 7.62 (dd, J = 7.6, 1.9 Hz, 1H), 7.31 (d, J = 8.8 Hz, 2H), 6.89 (d, J = 8.7 Hz, 2H), 4.21 (dd, J = 8.9, 5.0 Hz, 1H), 3.82 (s, 3H), 3.52 (dd, J = 14.1, 8.9 Hz, 1H), 3.17 (dd, J = 14.1, 5.0 Hz, 1H), 2.89 (s, 3H), 1.67 (s, 2H).

^{13}C NMR (126 MHz, $CDCl_3$) δ 159.1, 148.3, 134.6, 133.6, 132.0, 131.6, 131.0, 127.8, 124.1, 114.1, 58.5, 55.3, 53.7, 35.8.

IR: 3378, 3095, 2913, 2838, 1611, 1586, 1541, 1511, 1464, 1440, 1372, 1343, 1303, 1246, 1160, 1124, 1059, 1030, 955, 852, 832, 769, 730, 701, 651, 638, 614, 575 cm^{-1}

HRMS (ESI) m/z: $[M+Na]^+$ Calc'd for $C_{16}H_{19}N_3O_5SNa$ 388.0938; Found 388.0970.

Procedure for the pivaloyl mono-functional of 109a (114)

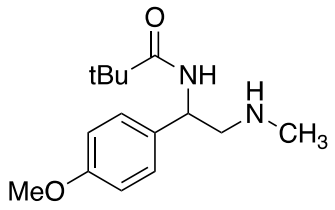

Under ambient conditions, a RBF flask was charged with **109a** (50 mg, 0.28 mmol, 1.0 equiv.), triethylamine (0.074 mL, 0.56 mmol, 2.0 equiv.) and DCM (2.8 mL, 0.1M). The solution was cooled to -78 °C while 2,2-dimethylpropanoyl chloride (pivaloyl chloride) (0.034 mL, 0.28 mmol, 1.0 equiv.) was dissolved in DCM (0.5 mL) in a separate flask. The pivaloyl chloride/DCM suspension was added dropwise to the **109a** solution, *via* syringe, over the course of 10 minutes at -78 °C. After addition, the solution was allowed to slowly warm to room temperature and was monitored by TLC until consumption of starting material. After 2h, the organic layer was washed with DI H_2O and the aqueous layers were rinsed with DCM (x2). The organic layers were combined, dried with $MgSO_4$, and concentrated *in vacu*. The compound was purified *via* flash column chromatography (35% MeOH in DCM) to afford a yellow oil. (60% yield, 44 mg, 0.17 mmol) (Rf = 0.45 in 10:1 DCM/MeOH)

^{1}H NMR (400 MHz, MeOD) δ 7.28 (d, J = 8.8 Hz, 2H), 6.92 (d, J = 8.7 Hz, 2H), 5.13 (dd, J = 8.9, 5.4 Hz, 1H), 3.79 (s, 3H), 3.13 (dd, J = 12.7, 9.1 Hz, 1H), 2.99 (dd, J = 12.7, 5.4 Hz, 1H), 2.51 (s, 3H), 1.22 (s, 9H).

^{13}C NMR (126 MHz, $CDCl_3$) δ 178.6, 159.0, 127.4, 114.2, 55.4, 55.3, 51.3, 38.8, 35.4, 27.6.

IR: 3332, 2958, 2871, 2837, 2802, 1888, 1639, 1613, 1586, 1511, 1480, 1463, 1399, 1366, 1302, 1276, 1246, 1214, 1178, 1118, 1032, 982, 912, 829, 730, 682, 645, 616, 575, 550, 542, 532 cm^{-1}

HRMS (ESI) m/z: $[M+Na]^+$ Calc'd for $C_{15}H_{24}N_2O_2Na$ 287.1730; Found 287.1748. **Procedure for the di-tosylation of 109a (115)**

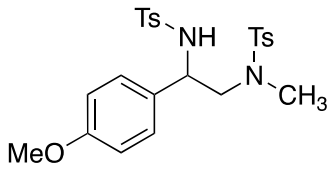

Under ambient conditions, a RBF flask was charged with **109a** (31mg, 0.17 mmol, 1.0 equiv.), diisopropylethylamine (0.073 mL, 0.43 mmol, 2.5 equiv.) and DCM (1.7 mL, 0.1M). *p*-Toluenesulfonylchloride (67 mg, 0.35 mmol, 2.05 equiv.) was added all at once and the solution was stirred at RT while being monitored by TLC until consumption of starting material. After 2h, the organic layer was washed with DI H_2O and the aqueous layers were rinsed with DCM (x2). The organic layers were combined, dried with $MgSO_4$, and concentrated *in vacu*. The compound was purified *via* flash column chromatography (30% EtOAc in hexanes) to afford a white solid. (96% yield, 78 mg 0.16 mmol) (Rf = 0.77 in 1:1 Hex/EtOAc)

^{1}H NMR (400 MHz, $CDCl_3$) δ 7.71 (d, J = 8.3 Hz, 2H), 7.60 (d, J = 8.3 Hz, 2H), 7.31 – 7.25 (m, 4H), 7.14 (d, J = 8.8 Hz, 2H), 6.79 (d, J = 8.7 Hz, 2H), 5.59 (d, J = 4.2 Hz, 1H), 4.33 (dt, J = 9.2, 4.4 Hz, 1H), 3.79 (s, 3H), 3.41 (dd, J = 14.4, 9.5 Hz, 1H), 2.70 (dd, J = 14.4, 4.8 Hz, 1H), 2.43 (s, 6H), 2.42 (s, 3H).

^{13}C NMR (126 MHz, $CDCl_3$) δ 159.4, 143.9, 143.2, 136.9, 134.0, 130.2, 129.9, 129.5, 128.1, 127.5, 127.3, 114.0, 55.7, 55.3, 55.0, 35.6, 21.6, 21.5.

IR: 3281, 2920, 2850, 1612, 1598, 1514, 1495, 1456, 1331, 1305, 1247, 1212, 1180, 1157, 1120, 1090, 1032, 944, 867, 831, 814, 780, 736, 720, 705, 666 cm^{-1}

HRMS (ESI) m/z (z=2): $[M+2H]^{+2}$ Calc'd for $C_{24}H_{30}N_2O_5S_2$ 245.0793; Found 245.0784.

Procedure for the mono-tosylation of 109a (116)

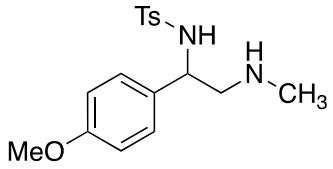

Under ambient conditions, a RBF flask was charged with 107a (33mg, 0.18 mmol, 1.0 equiv.), diisopropylethylamine (0.061 mL. 0.36 mmol, 2.0 equiv.) and DCM (3.4 mL, 0.1M). The solution was cooled to -78 °C while *p*-tolulenesulfonylchloride (34mg, 0.18 mmol 1.0 equiv.) was dissolved in DCM (0.5 mL) in a separate flask. The sulfonylchloride/DCM suspension was added dropwise to the 107a solution, *via* syringe, over the course of 10 minutes at -78 °C. After addition, the solution was allowed to slowly warm to room temperature and was monitored by TLC until consumption of starting material. After 2h, the organic layer was washed with DI H_2O and the aqueous layers were rinsed with DCM (x2). The organic layers were combined, dried with $MgSO_4$, and concentrated *in vacu*. The compound was purified *via* flash column chromatography (5% MeOH in DCM) to afford a white solid. (72% yield, 43 mg, 0.13 mmol.) (Rf = 0.54 in 10:1 DCM/MeOH)

^{1}H NMR (400 MHz, $CDCl_3$) δ 7.67 (d, J = 8.3 Hz, 2H), 7.31 (d, J = 8.6 Hz, 4H), 6.89 (d, J = 8.7 Hz, 2H), 4.18 (dd, J = 9.2, 4.5 Hz, 1H), 3.82 (s, 3H), 3.29 (dd, J = 13.4, 9.1 Hz, 1H), 2.81 (dd, J = 13.4, 4.5 Hz, 1H), 2.74 (s, 3H), 2.43 (s, 3H), 1.72 (br. s, 2H).

^{13}C NMR (101 MHz, $CDCl_3$) δ 159.1, 143.5, 134.7, 134.2, 129.7, 127.8, 127.5, 114.0, 58.9, 55.3, 53.7, 36.4, 21.5.

IR: 2921, 1739, 1611, 1512, 1456, 1338, 1304, 1247, 1217, 1180, 1160, 1119, 1089, 1033, 949, 833, 816, 775, 753, 720, 703, 653, 583 cm^{-1}

HRMS (ESI) m/z (z=2): $[M+2H]^{+2}$ Calc'd for $C_{17}H_{24}N_2O_3S$ 168.0748; Found 168.0735.

Synthesis of 4-(4-methoxyphenyl)-1-methyl-2-phenyl-4,5-dihydro-1*H*-imidazole (115/207) [9]

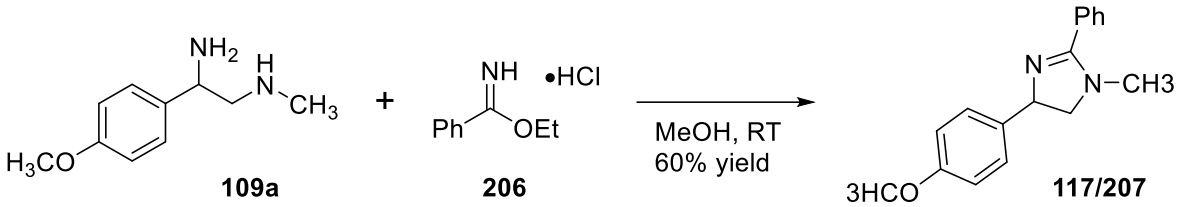

Diamine **109a** (323 mg, 1.8 mmol, 1.0 equiv.) was dissolved in 10 mL of methanol and ethyl benzimidate hydrochloride (415 mg, 2.2 mmol, 1.2 equiv.) was added. The reaction mixture was stirred at RT for 10 h and then volatiles were removed *in vacuo*. Residue was purified by flash column chromatography with a DCM/MeOH gradient to afford an off-white amorphous solid. (62% yield, 165 mg, 1.1 mmol). (Rf = 0.27 in 9:1 DCM/MeOH).

^{1}H NMR (400 MHz, $CDCl_3$) δ 7.74 (d, 2H), 7.54 (t, *J* = 7.5 Hz, 1H), 7.44 (t, *J* = 7.7 Hz, 2H), 7.27 (d, *J* = 8.6 Hz, 2H), 6.82 (d, *J* = 8.7 Hz, 2H), 5.26 (t, *J* = 10.0 Hz, 1H), 4.51 (t, *J* = 11.6 Hz, 1H), 3.72 (s, 3H), 3.69 (d, *J* = 8.3 Hz, 1H), 3.11 (s, 3H).

^{13}C NMR (126 MHz, $CDCl_3$) δ 165.7, 159.6, 133.4, 131.3, 129.5, 129.2, 127.7, 122.4, 114.5, 60.6, 58.3, 55.4, 34.9.

IR: 2836, 1603, 1560, 1514, 1491, 1445, 1376, 1246, 1178, 1095, 1027, 926, 832, 777, 725, 699, 616, 560, 545, 539 cm^{-1}

HRMS (ESI) m/z: $[M+H_3O]^+$ Calc'd for $C_{17}H_{21}N_2O_2$ 285.1598; Found 285.1575.

Synthesis of 4-(4-methoxyphenyl)-1-methylimidazolidin-2-one (118)

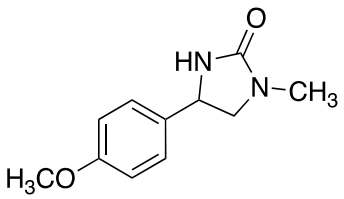

Under ambient conditions, a RBF flask was charged with **109a** (65 mg, 0.36 mmol, 1.0 equiv.), triethylamine (0.14 mL, 1.10 mmol, 3.0 equiv.) and DCM (1.80 mL, 0.2M). The solution was

cooled to 0 °C. Once cooled, triphosgene (128 mg, 0.43 mmol, 1.2 equiv.) was added all at once. After addition, the solution was allowed to slowly warm to room temperature and was monitored by TLC until consumption of starting materialz. After 1.5h, the solution was quenched with saturated sodium bicarbonate, and the aqueous layers were rinsed with DCM (x2). The organic layers were combined, dried with $MgSO_4$, and concentrated *in vacu*. The compound was purified *via* flash column chromatography (5% MeOH in DCM) to afford an off-white solid. (43% yield, 32 mg 0.15 mmol) (Rf = 0.69 in 10:1 DCM/MeOH)

^{1}H NMR (400 MHz, $CDCl_3$) δ 7.30 (d, J = 8.8 Hz, 2H), 6.92 (d, J = 8.8 Hz, 2H), 4.71 (t, J = 8.3 Hz, 2H), 3.83 (s, 3H), 3.75 (d, J = 8.9 Hz, 1H), 3.20 (d, J = 8.8 Hz, 1H), 2.84 (s, 3H).

^{13}C NMR (126 MHz, $CDCl_3$) δ 162.2, 159.5, 133.4, 127.4, 114.2, 56.3, 55.4, 53.2, 30.6.

IR: 3279, 2919, 2850, 2054, 1694, 1611, 1586, 1512, 1441, 1401, 1361, 1293, 1244, 1175, 1112, 1090, 1029, 954, 831, 813, 759, 662 cm^{-1}

HRMS (ESI) m/z (z=2): $[M+2H]^{+2}$ Calc'd for $C_{11}H_{16}N_2O_2$ 104.0600; Found 104.0591.

6.3. Experimental Section: Chapter 2

General procedure for the preparation of silyl imines (198)

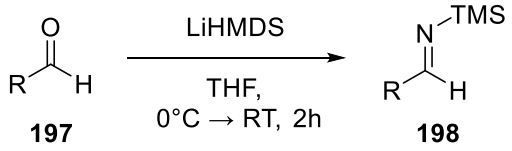

A solution of aldehyde (1.2 mmol, 1.0 equiv.) in dry THF (1.2 mL, 1.0 M) maintained under a positive pressure of nitrogen was stirred and cooled to -78 °C in a dry ice/acetone bath. A solution of 1.0 M LiHMDS (1.2 mL, 1.2 mmol, 1.0 equiv.) was added dropwise via syringe and the reaction mixture. After stirring for 30 min at -78 °C, the solution was allowed to warm up to room temperature and stir for an additional 30 min. ^{1}H NMR confirmed the formation of the silyl imine

with the disappearance of the aldehyde proton around 10 ppm and the appearance of the imine proton at around 9 ppm.

General procedure for the preparation of imidazolidines (199)

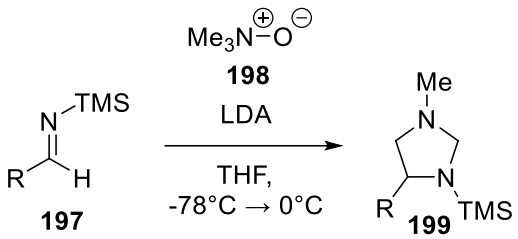

A solution of trimethylamine N-oxide (182 mg, 2.4 mmol, 1.0 equiv.) in dry THF (7.0 mL, 0.10 M) maintained under a positive pressure of nitrogen was stirred and cooled to -78°C. A solution of 1.7 M LDA (4.0 mL, 6.9 mmol, 3.0 equiv.) was added dropwise via syringe, followed by the slow addition of the crude 0.46 M silyl imine (4.0 mL, 2.3 mmol, 1.0 equiv.). LDA was titrated before use using salicylaldehyde phenylhydrazone. [1] The reaction was removed from the cold bath and allowed to stir and warm to room temperature for 2 h. The formation of the imidazolidine was confirmed by ^{1}H NMR and was taken onto the next step directly without further purification.

General procedure for the preparation of imidazolidines (200)

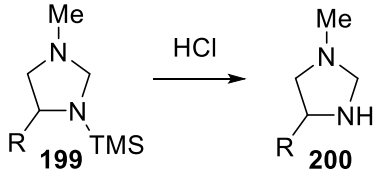

Volatiles were removed from the crude reaction mixture of the imidazolidine under reduced pressure. The residue was dissolved in THF (10 mL, 0.10 M)) and 1.0 M HCl (5 mL, 0.20 M) The reaction vessel was equipped with a reflux condenser and the mixture was heated to 65 °C for 12 h. The reaction was cooled to RT, transferred to a separatory funnel, and washed with DCM (20 mL x 3), hexanes (x 2), and EtOAc (x 3). The aqueous layer was basified with 15% NaOH and the product extracted with DCM (20 mL x 3). The organic layers were combined, dried over $MgSO_4$,

and concentrated under reduced pressure to afford pure 1,2 diamines unless otherwise noted. Product was isolated as an orange oil. (85% yield, 69 mg, 0.43 mmol).

Synthesis of 4-(1-methylimidazolidin-4-yl)quinoline 200a

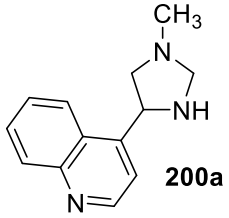

200a

Silyl imine prepared according to the general procedure using 4-quinoline carboxaldehyde (192 mg, 1.2 mmol, 1.0 equiv.), 1.0 M LiHMDS (1.2 mL, 1.2 mmol, 1 equiv.), and THF (1.2 mL, 1.0 M). Silyl imine solution was used without further purification.

Imidazolidine was prepared according to the general procedure using TMAO (39 mg, 0.52 mmol, 1.2 equiv.), 0.75 M LDA (2.0 mL, 1.5 mmol, 3.0 equiv.), crude 0.50 M silyl imine (1.0 mL, 0.50 mmol, 1.0 equiv.), THF (3.0 mL, 0.10 M), and 1.0 M HCl (1.0 mL, 0.01 M). Following aqueous work-up product was isolated as a brown oil. (78% yield, 83 mg, 0.39 mmol)

^{1}H NMR (400 MHz, Chloroform-*d*) δ 8.85 (d, *J* = 4.5 Hz, 1H), 8.14 – 8.06 (m, 1H), 7.94 – 7.88 (m, 1H), 7.76 (dd, *J* = 4.4, 1.0 Hz, 1H), 7.67 (ddd, *J* = 8.4, 6.7, 1.4 Hz, 1H), 7.52 (ddd, *J* = 8.3, 6.7, 1.3 Hz, 1H), 5.16 (t, *J* = 7.6 Hz, 1H), 3.92 (d, *J* = 7.4 Hz, 1H), 3.55 (dd, *J* = 9.7, 7.9 Hz, 1H), 3.44 (d, *J* = 7.4 Hz, 1H), 2.35 (s, 3H), 2.27 (dd, *J* = 9.7, 7.3 Hz, 1H).

^{13}C NMR (101 MHz, Chloroform-*d*) δ 150.89, 150.08, 148.33, 129.08, 126.52, 126.44, 123.21, 117.39, 72.74, 62.42, 57.02, 39.47.

IR: 3272, 3064, 3036, 2926, 2846, 2786, 2205, 1929,1839, 1592, 1569, 1508, 1485, 1462, 1421, 1391, 1362, 1337, 1300, 1238, 1223, 1167, 1150, 1094, 1073, 1029, 1002, 955, 907, 871, 853, 815, 792, 760, 727, 643, 612, 571, 566, 556 cm^{-1}

HRMS (ESI) m/z: $[M+H]^+$ Calc'd for $C_{13}H_{15}N_3$ 214.1339; Found 214.13422

Synthesis of 4-(1-methylimidazolidin-4-yl)pyridine 200b

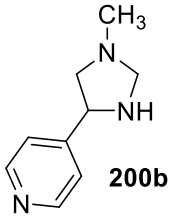

200b

Silyl imine prepared according to the general procedure using 4-pyridylcarboxaldehyde (0.10 mL, 1.1 mmol, 1.0 equiv.), 1.0 M LiHMDS (1.1 mL, 1.1 mmol, 1.0 equiv.), and THF (1.1 mL, 1.0 M). Silyl imine solution was used without further purification.

Imidazolidine was prepared according to the general procedure using TMAO (39 mg, 0.52 mmol, 1.2 equiv.), 0.75 M LDA (2.0 mL, 1.5 mmol, 3.0 equiv.), crude 0.50 M silyl imine (1.0 mL, 0.50 mmol, 1.0 equiv.), THF (3.0 mL, 0.10 M), and 1.0 M HCl (1.0 mL, 0.01 M). Following aqueous work-up, no further purification was necessary. Product was isolated as an orange oil. (85% yield, 69 mg, 0.43 mmol)

^{1}H NMR (400 MHz, $CDCl_3$) δ 8.53 (dd, J = 4.4, 1.5 Hz, 2H), 7.31 (dd, J = 6.1, 0.6 Hz, 2H), 4.48 (t, J = 7.6 Hz, 1H), 3.82 (d, J = 7.3 Hz, 1H), 3.44 (d, J = 7.3 Hz, 1H), 3.28 (dd, J = 9.6, 7.6 Hz, 1H), 2.38 (s, 3H), 2.34 (d, J = 2.1 Hz, 1H).

^{13}C NMR (101 MHz, $CDCl_3$) δ 153.3, 149.9, 121.5, 73.0, 62.4, 59.9, 39.4.

IR: 3255, 3027, 2941, 2847, 1788, 2251, 1941, 1666, 1597, 1557, 1491, 1451, 1411, 1363, 1308, 1219, 1151, 1125, 1063, 992, 895, 820, 732, 699, 668, 630, 622, 608, 584, 573 cm^{-1}

HRMS (ESI) m/z (z=2): $[M+2Na]^{+2}$ Calc'd for $C_9H_{13}N_3Na_2$ 104.5447; Found 104.5440.

Synthesis of 3-(1-methylimidazolidin-4-yl)pyridine 200c

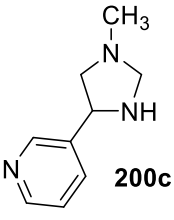

200c

Silyl imine prepared according to the general procedure using 3-pyridylcarboxaldehyde (0.1 mL, 1.1 mmol, 1.0 equiv.), 1.0 M LiHMDS (1.1 mL, 1.1 mmol, 1 equiv.), and THF (1.1 mL, 1.0 M). Silyl imine solution was used without further purification.

Imidazolidine was prepared according to the general procedure using TMAO (40 mg, 0.53 mmol, 1.1 equiv.), 0.96 M LDA (1.6 mL, 1.5 mmol, 3.0 equiv.), crude 0.50 M silyl imine (1.0 mL, 0.50 mmol, 1.0 equiv.), THF (3.0 mL, 0.10 M), and 1.0 M HCl (5 mL, 0.1 M). Following aqueous work-up product was isolated as a green oil. (32% yield, 30 mg, 0.16 mmol)

^{1}H NMR (400 MHz, Chloroform-*d*) δ 8.62 – 8.56 (m, 1H), 8.49 (dd, *J* = 4.8, 1.7 Hz, 1H), 7.75 (ddd, *J* = 7.9, 2.3, 1.6 Hz, 1H), 7.27 – 7.22 (m, 1H), 4.50 (t, *J* = 7.4 Hz, 1H), 3.78 (d, *J* = 7.3 Hz, 1H), 3.53 (d, *J* = 7.3 Hz, 1H), 3.23 (dd, *J* = 9.6, 7.6 Hz, 1H), 2.45 (dd, *J* = 9.5, 7.1 Hz, 2H), 2.40 (s, 3H), 2.29 – 2.17 (m, 1H).

^{13}C NMR (101 MHz, Chloroform-*d*) δ 148.67, 148.64, 139.65, 134.23, 123.61, 73.17, 62.88, 58.95, 39.56.

IR: 3260, 3030, 2925, 2845, 2784, 2478, 2251, 2177, 1936, 1648, 1591, 1577, 1476, 1452, 1428, 1362, 1311, 1235, 1151, 1126, 1103, 1042, 1025, 980, 964, 894, 843, 806, 714, 673, 630, 617, 602 ,592, 583, 566, 555 cm^{-1}

HRMS (ESI) m/z: $[M+H]^+$ Calc'd for $C_9H_{13}N_3$ 164.11822; Found 164.1204

Synthesis of 4-(furan-2-yl)-1-methylimidazolidine 200d

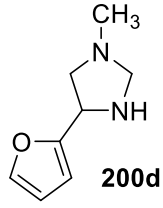

200d

Silyl imine prepared according to the general procedure using furfural (0.1 mL, 1.2 mmol, 1.0 equiv.), 1.0 M LiHMDS (1.5 mL, 1.5 mmol, 1.3 equiv.), and THF (1.2 mL, 1.0 M). Silyl imine solution was used without further purification.

Imidazolidine was prepared according to the general procedure using TMAO (83 mg, 1.1 mmol, 1.1 equiv.), 1.8 M LDA (1.6 mL, 3 mmol, 3.0 equiv.), crude 0.44 M silyl imine (2.3 mL, 1.0 mmol, 1.0 equiv.), THF (10 mL, 0.10 M), and 1.0 M HCl (5 mL, 0.2 M). Following aqueous work-up product was isolated as an off-white oil. (57% yield, 86 mg, 0.57 mmol)

^{1}H NMR (400 MHz, Chloroform-*d*) δ 7.37 (dd, *J* = 1.9, 0.9 Hz, 1H), 6.31 (dd, *J* = 3.2, 1.9 Hz, 1H), 6.21 (dt, *J* = 3.2, 0.8 Hz, 1H), 4.48 (ddd, *J* = 7.6, 6.5, 0.7 Hz, 1H), 3.60 (d, *J* = 0.9 Hz, 2H), 3.02 (dd, *J* = 9.6, 7.9 Hz, 1H), 2.74 (dd, *J* = 9.6, 6.6 Hz, 1H), 2.42 (s, 3H).

^{13}C NMR (101 MHz, Chloroform-*d*) δ 156.00, 142.16, 110.26, 105.85, 72.62, 59.37, 55.17, 39.79.

IR: 3280, 3112, 2941, 2844, 2788, 1738, 1671, 1601, 1506, 1451, 1362, 1227, 1150, 1073, 1008, 928, 883, 841, 806, 731, 630, 599 cm^{-1}

HRMS (ESI) m/z: $[M+H]^+$ Calc'd for $C_8H_{12}N_2O$ 153.10224; Found 153.10564

Synthesis of 4-([1,1'-biphenyl]-4-yl)-1-methyl-2-phenylimidazolidine (207).

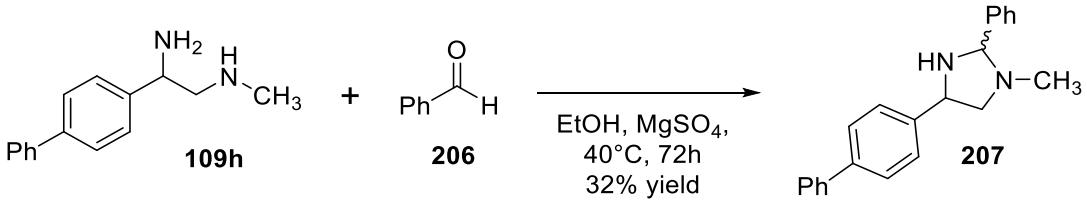

1-([1,1'-biphenyl]-4-yl)-N2-methylethane-1,2-diamine (205 mg, 0.9 mmol, 1 equiv.) was dissolved in EtOH (5 mL, 0.2 M) and stirred. Benzaldehyde (0.1 mL, 0.9 mmol, 1 equiv.) and $MgSO_4$ was added to the reaction flask and then the mixture was heated to 40 °C for 16 h. After

cooling to RT, the $MgSO_4$ was filtered out and the residue was purified by FCC. The product was isolated as a mixture of diastereomers in a 1:1.3 ratio. R_f = 0.26 in EtOAc (32 % yield, 91 mg, 0.29 mmol).

Major diastereomer: ^{1}H NMR (499 MHz, Chloroform-*d*) δ 7.68 – 7.51 (m, 15H [both diastereomers]), 7.51 – 7.31 (m, 12H [both diastereomers]), 4.86 – 4.73 (m, 1H), 4.24 (s, 1H), 3.85 – 3.67 (m, 1H), 2.51 (td, *J* = 9.4, 1.6 Hz, 1H), 2.28 (d, *J* = 1.7 Hz, 3H).

Minor diasteromer: ^{1}H NMR (499 MHz, Chloroform-*d*) δ 7.68 – 7.51 (m, 18H), 7.51 – 7.31 (m, 14H), 4.46 (dd, *J* = 8.8, 3.2 Hz, 1H), 4.15 (s, 1H), 3.45 (dd, *J* = 9.4, 3.1 Hz, 1H), 2.94 (t, *J* = 9.2 Hz, 1H), 2.30 (d, *J* = 1.6 Hz, 3H).

HRMS (ESI) m/z (z=2): $[M+2H]^{2+}$ Calc'd for $C_{11}H_{14}N_2O_2$ 158.0963; Found 158.0989.

6.4. Experimental Section Chapter 3

General procedure for the synthesis of 1-methyl-pyrrolidines

N-oxide (1 equiv.) was added to a dry and purged test tube under N_2 and dissolved in THF (0.1 M). In a separate dry and purged test tube a 1 M stock solution of stilbene (1 equiv.) in dry THF was prepared. The *N*-oxide solution was cooled to -78 °C via dry ice/acetone bath, and LDA (3 equiv.) was added dropwise. Then the stilbene solution was added dropwise and the reaction was removed from the cold bath. After three hours the reaction was quenched with water and the product was extracted with EtOAc (3 x's), dried over $MgSO_4$ and concentrated to afford the pyrrolidine product.

Synthesis of 1-methyl-3,4-diphenylpyrrolidine (297)

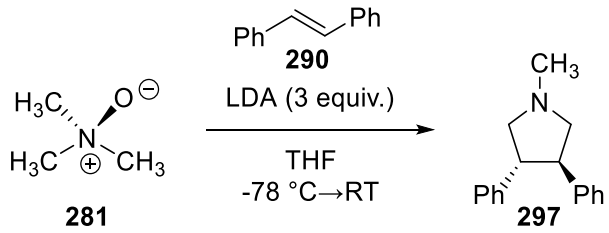

TMAO (15 mg, 0.2 mmol, 1 equiv.) was added to a dry and purged test tube under N_2 and dissolved in THF (2 mL, 0.1 M). In a separate dry and purged test tube a 1 M stock solution of *trans*-stilbene (183 mg, 1 mmol, 5 equiv.) in dry THF was prepared. The *N*-oxide solution was cooled to -78 °C via dry ice/acetone bath, and 1.9 M LDA (0.32 mL, 0.6 mmol, 3 equiv.) was added dropwise. Then the *trans*-stilbene solution (0.2 mL, 0.2 mmol, 1 equiv.) was added dropwise and the reaction was removed from the cold bath. After three hours the reaction was quenched with water and the product was extracted with EtOAc (3 x's), dried over $MgSO_4$ and concentrated to afford the pyrrolidine as an oil (95 % yield, 46 mg, 0.19 mmol). The ^{1}H NMR spectrum matched the reported spectrum. [10]

^{1}H NMR (400 MHz, Chloroform-*d*) δ 7.35 – 7.07 (m, 10H), 3.40 (td, *J* = 5.4, 2.3 Hz, 2H), 3.13 (ddd, *J* = 9.5, 5.9, 2.0 Hz, 2H), 2.87 (tt, *J* = 7.0, 2.0 Hz, 2H), 2.47 (s, 3H).

Synthesis of 1-methyl-3,4-diphenylpyrrolidine (297) with TMSOTf (300) implemented as an additive

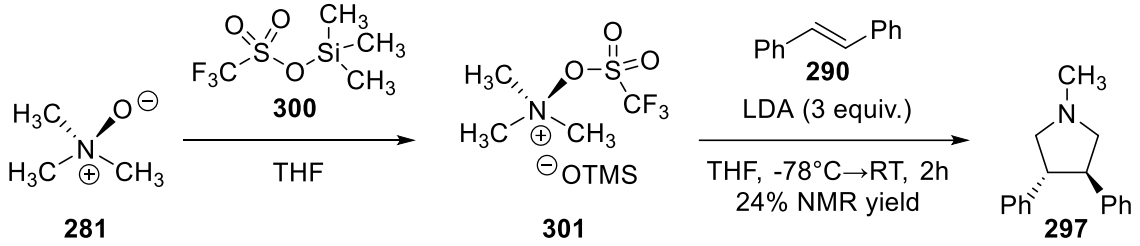

Dissolved *N*-oxide **287** (19 mg, 0.2 mmol, 1 equiv.) in dry THF and add TMSOTf (0.04 mL, 0.2 mmol). Let stir for 1 h and then cooled to -78 °C via dry ice/acetone bath, and 2.9 M LDA (0.21mL, 0.6 mmol, 3 equiv.) was added dropwise. Then the 1 M *trans*-stilbene solution (0.2 mL, 0.2 mmol, 1 equiv.) was added dropwise and the reaction was removed from the cold bath. After three hours the reaction was quenched with water and the product was extracted with EtOAc (3 x's), dried over $MgSO_4$ and concentrated. Product was analyzed by ^{1}H NMR and an NMR yield was obtained

of pyrrolidine **296**. NMR yield of product with TMSOTf was 24%; NMR yield of control reaction without additive was 67%.

6.5. Experimental Section Chapter 4

1-(tert-butyl)pyrrolidine (365)

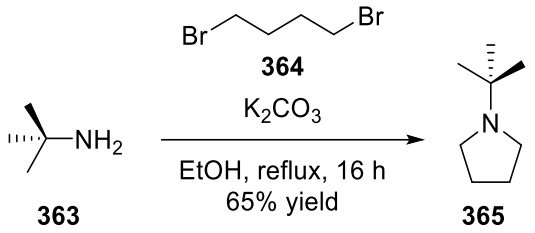

1,4-dibromo butane (2.4 mL, 20 mmol, 1.0 equiv.), *tert*-butyl amine (2.1 mL, 20 mmol, 1.0 equiv.), and potassium carbonate (2.782 g, 20 mmol, 1 equiv.) were added to a reaction flask and dissolved in EtOH (20 mL, 1.0 M). The reaction was heated to reflux for 16 h and the cooled to RT. The reaction was filtered and the filtrate was acidified with 1M HCl, and EtOH was removed *in vacuo*. The acid solution was transferred to a separatory funnel and washed with ether (3x's), and then basified with 1M NaOH and the product was extracted with ether (3 X's). The organic layer was dried over $MgSO_4$ and concentrated to afford the pyrrolidine as a yellow oil (65% yield, 1.601 g, 13 mmol). ^{1}H NMR matched the reported spectrum in the literature. [11]

Note: product is volatile

^{1}H NMR (400 MHz, Chloroform-*d*) δ 2.64 (tdd, *J* = 6.5, 3.0, 1.7 Hz, 4H), 1.83 – 1.75 (m, 4H), 1.11 (s, 9H).

Synthesis of 1-(tert-butyl)pyrrolidine 1-oxide (365)

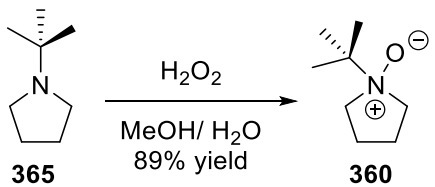

Tert-butyl pyrrolidine (636 mg, 5 mmol, 1 equiv,) was added to a reaction flask and dissolved in MeOH (2.5 mL, 2.0 M) and water (1.5 mL, 4.0 M). The solution was cooled to 0 °C using an ice bath, and H_2O_2 (1.5 mL, 15 mmol, 3.0 equiv.) was added dropwise. The reaction was warmed to RT and stirred for 12 h. The peroxide was quenched with MnO_2 and the reaction mixture was filtered over a celite plug. The filtrate was concentrated to half-volume, and the product was extracted with DCM (3x's), dried over $MgSO_4$ and concentrated to afford # as an off-white powder. (89% yield, 808 mg, 4.5 mmol).

^{1}H NMR (400 MHz, Chloroform-*d*) δ 3.48 – 3.31 (m, 2H), 3.31 – 3.15 (m, 2H), 2.56 – 2.35 (m, 2H), 1.98 – 1.78 (m, 2H), 1.45 (s, 9H).

^{13}C NMR (101 MHz, Chloroform-*d*) δ 70.20, 61.39, 25.12, 21.99.

IR: 3388, 3019, 2962, 1646, 1458, 1363, 1350, 1261, 1186, 1045, 990, 972, 926, 901, 819, 644, 549, 489, 415 cm^{-1}

General procedure for (1*R*,3*R*,4*S*)-7-(tert-butyl)-2,3-diphenyl-7-azabicyclo[2.2.1]heptane (362) synthesis

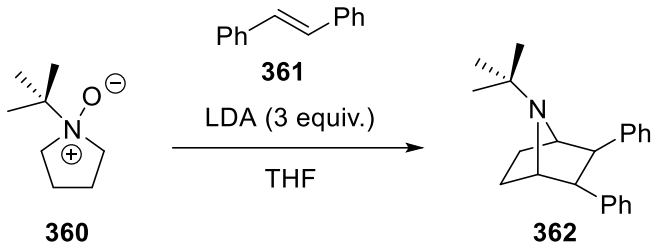

N-oxide was transferred from a 1M stock solution in DCM to a test tube and dried under vacuum. Stilbene was then added to the test tube and after purging, the reagents were dissolved in dry THF. The reaction was cooled to -78 °C with a dry ice/acetone bath and LDA was added dropwise. The reaction was allowed to warm slowly to RT over the course of 3 h. The reaction was quenched (water, ammonium chloride, or), extracted with EtOAc (3 x's), dried over $MgSO_4$, and concentrated. The residue was purifed by FCC.

(1*R*,3*R*,4*S*)-7-(tert-butyl)-2,3-diphenyl-7-azabicyclo[2.2.1]heptane (362)

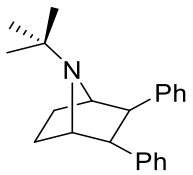

362

Tert-butyl *N*-oxo pyrrolidine (0.4 mL, 0.2 mmol, 1 equiv.) was transferred from a 1M stock solution in DCM to a test tube and dried under vacuum. *Trans*-stilbene (38 mg, 0.2 mmol, 1 equiv.) was then added to the test tube and after purging, the reagents were dissolved in dry THF (2 mL, 0.1 M). The reaction was cooled to -78 °C with a dry ice/acetone bath and 0.88 M LDA (0.68 mL, 0.6 mmol, 3 equiv.) was added dropwise. The reaction was allowed to warm slowly to RT over the course of 3 h. The reaction was quenched with saturated ammonium chloride solution, extracted with EtOAc (3 x's), dried over $MgSO_4$, and concentrated. The residue was purifed by FCC. Solvent conditions: 6:1 hexanes/EtOAc, R_f = 0.53 (56 % yield, 34 mg, 0.11 mmol).

^{1}H NMR (400 MHz, Chloroform-*d*) δ 7.62 – 7.50 (m, 2H), 7.33 – 7.20 (m, 6H), 7.20 – 7.10 (m, 2H), 3.96 – 3.88 (m, 1H), 3.61 (dt, *J* = 4.5, 1.1 Hz, 1H), 3.39 (t, *J* = 5.2 Hz, 1H), 2.74 (d, *J* = 6.1 Hz, 1H), 1.74 (dd, *J* = 12.1, 4.8 Hz, 1H), 1.57 – 1.42 (m, 3H), 1.19 (s, 9H).

^{13}C NMR (101 MHz, Chloroform-*d*) δ 147.88, 141.66, 128.42, 128.26, 128.14, 127.73, 126.01, 125.97, 64.14, 60.91, 59.42, 54.37, 51.78, 32.11, 30.35, 24.35.

IR: 3059, 3024, 2968, 2922, 2867, 1713, 1602, 1493, 1449, 1387, 1230, 1175, 1060, 1029, 751, 739, 697, 590, 530 cm^{-1}.

HRMS (ESI) m/z: $[M+H]^+$ Calc'd for $C_{22}H_{28}N^+$ 306.2216; Found 305.2263.

Synthesis of *N*-oxide adduct 365[12]

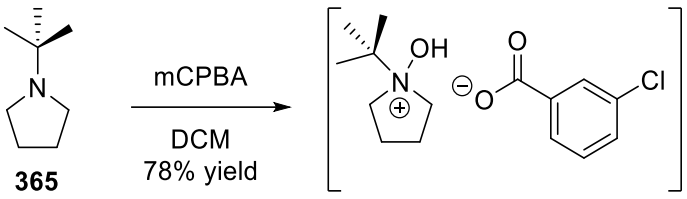

365 **366**

Tert-butyl pyrrolidine (2.137 g, 16.8 mmol, 1 equiv,) was added to a reaction flask and dissolved in DCM (24 mL, 0.7 M). The solution was cooled to 0 °C using an ice bath, and mCPBA (3.192 g, 18.5 mmol, 1.1 equiv.) was added portion wise. The reaction was stirred in the ice bath for 30 min. Basic alumina (8.000 g) was added to the reaction and the mixture stirred for 5 min, and filtered over a celite plug. The filtrate was concentrated, and the residue was redissolved in EtOAc and concentrated *in vacuo* (3x's) to afford **X** as a viscous orange oil (78% yield, 3.930 g, 13 mmol). ^{1}H NMR (400 MHz, Chloroform-*d*) δ 8.09 – 8.05 (m, 1H), 7.96 (dt, *J* = 7.6, 1.3 Hz, 1H), 7.43 (dddd, *J* = 8.0, 2.2, 1.2, 0.4 Hz, 1H), 7.36 – 7.29 (m, 1H), 4.24 – 4.01 (m, 2H), 3.57 – 3.32 (m, 2H), 2.76 – 2.44 (m, 2H), 2.19 – 1.91 (m, 2H), 1.58 (s, 9H).

6.6. Experimental Section Chapter 5

Synthesis of Diethyl 2-(2-iodobenzyl)malonate (449). [13]

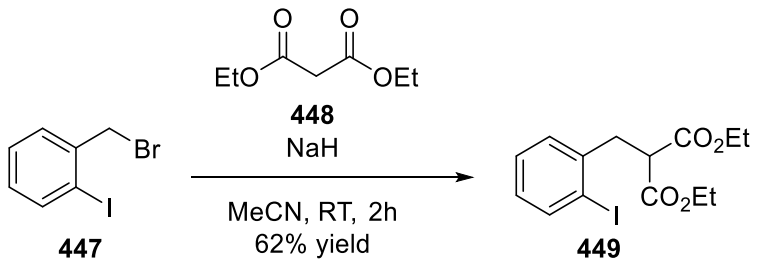

447 **449**

2-Iodobenzyl bromide (295 mg, 1 mmol) was dissolved in acetonitrile (2.5 mL) in a round bottom flask. Then diethyl malonate (0.18 mL, 1.2 mmol) followed by sodium hydride (61 mg, 1.3 mmol) were added to the flask. The resulting mixture stirred at room temperature for 2 h. The mixture was diluted, poured into 10 mL of saturated ammonium chloride solution, and extracted three times

with dichloromethane. The extract was dried, filtered, and concentrated. The product was purified via column chromatography and the structure confirmed by ^{1}H NMR.

^{1}H NMR (400 MHz, $CDCl_3$) δ 7.96 – 7.72 (m, 1H), 7.36 – 7.19 (m, 3H), 6.94 (ddd, *J* = 8.0, 5.5, 3.7 Hz, 1H), 4.32 – 4.05 (m, 4H), 3.85 (t, *J* = 7.8 Hz, 1H), 3.35 (d, *J* = 7.8 Hz, 2H), 1.36 – 1.14 (m, 6H).

Synthesis of Diethyl 2-(2-(3-hydroxypropynyl)benzyl)malonate (451). [13]

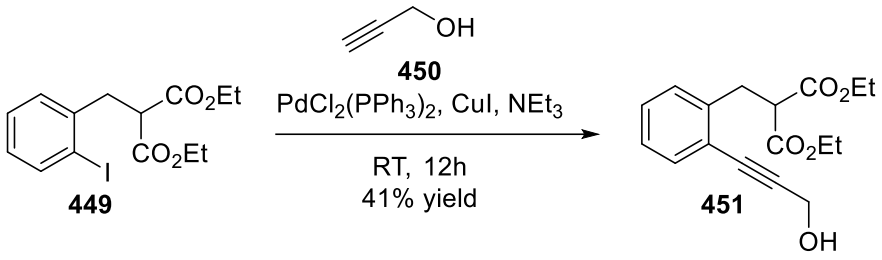

A dry round bottom flask was purged three times with nitrogen. **449** (0.74 mmol, 272 mg) was dissolved in DCM (3.7 mL) and added to the reaction flask followed by the addition of triethyl amine (0.31 mL, 2.2 mmol), propargyl alcohol (0.05 mL, 0.88 mmol) and $PdCl_2(PPh_3)_2$ (21 mg, 4 mol%). The reaction flask was purged three times with nitrogen and the reaction was left to stir for 5 minutes. Copper iodide (2 mg, 2 mol%) was added, the flask was purged three more times with nitrogen, and the reaction progress was monitored via TLC. Once the reaction was complete, the ammonium salt was filtered off and the solvent was removed. The product was purified using column chromatography and characterized via ^{1}H NMR.

^{1}H NMR (400 MHz, $CDCl_3$) δ 7.51 – 7.37 (m, 1H), 7.37 – 7.16 (m, 3H), 4.53 (s, 2H), 4.31 – 4.09 (m, 4H), 3.88 (t, *J* = 7.2 Hz, 1H), 3.38 (d, *J* = 7.2 Hz, 2H), 2.80 (s, 1H), 1.26 (dt, *J* = 11.3, 7.8 Hz, 7H).

Synthesis of Diethyl 2-(2-(3-((ethoxycarbonyl)oxy)propynyl)benzyl)malonate (371). [14]

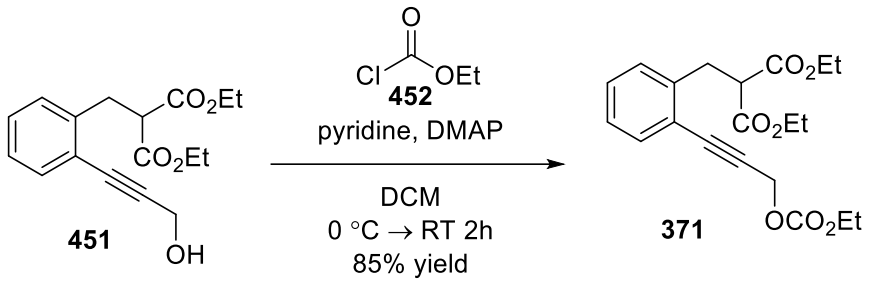

Compound **451** (92 mg, 0.3 mmol) was dissolved in DCM (1.5 mL) and added to a round bottom flask. Then pyridine (0.1 mL) and DMAP (7 mg, 0.06 mmol) were added and the reaction was placed in an ice bath. Once cooled to 0 °C, ethyl chloroformate (0.11 mL, 1.2 mmol) was added dropwise. The reaction was stirred at room temperature for 2 h. Then the reaction mixture was diluted with DCM and washed with saturated copper sulfate solution, water, dried over anhydrous sodium sulfate, and concentrated. The product was purified by column chromatography and characterized by ^{1}H NMR.

^{1}H NMR (400 MHz, $CDCl_3$) δ 7.43 (s, 1H), 7.23 (dd, J = 12.0, 10.5 Hz, 3H), 4.99 (s, 2H), 4.25 (q, J = 7.1 Hz, 2H), 4.15 (qd, J = 7.1, 4.1 Hz, 4H), 3.85 (t, J = 7.8 Hz, 1H), 3.35 (d, J = 7.8 Hz, 2H), 1.33 (t, J = 7.1 Hz, 3H), 1.21 (t, J = 7.1 Hz, 6H).

Synthesis of Diethyl 1-vinylidene-1,3-dihydro-*2H*-indene-2,2-dicarboxylate (4). [15]

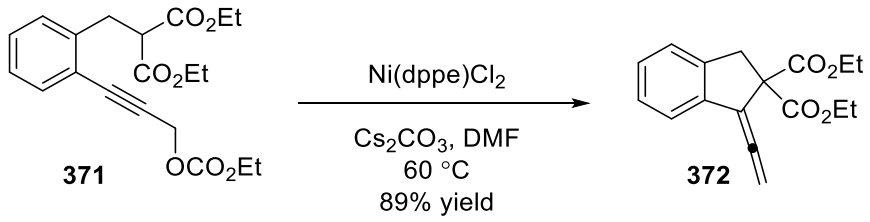

Compound **371** (93 mg, 0.26 mmol) was dissolved in DMF (2.6 mL) and added to a round bottom flask. Cesium carbonate (169 mg, 0.52 mmol) was added, the reaction was stirred for a minute, and then Ni(dppe)Cl_2 was added to the mixture. The reaction was heated to 60 °C and monitored by TLC. Once complete, the reaction was cooled to room temperature, quenched with water, and

the product was extracted with ethyl acetate three times. The organic layers were combined, washed with water and brine, dried over magnesium sulfate, and concentrated. The product was purified by column chromatography and characterized by ^{1}H NMR and ^{13}C NMR.

^{1}H NMR (400 MHz, $CDCl_3$) δ 7.34 – 7.15 (m, 4H), 5.42 (s, 2H), 4.38 – 4.15 (m, 4H), 3.74 (s, 2H), 1.34 – 1.22 (m, 6H).

^{13}C NMR (101 MHz, $CDCl_3$) δ 206.12 (s), 169.97 (s), 139.45 (s), 136.60 (s), 128.12 (s), 127.46 (s), 124.66 – 124.44 (m), 122.47 (d, *J* = 1.0 Hz), 107.47 (s), 82.60 (s), 77.42 (s), 77.11 (s), 76.79 (s), 62.28 (d, *J* = 0.9 Hz), 61.93 (s), 39.72 (s), 14.12 (s).

Synthesis of prop-2-yn-1-yl acetate (455) [16]

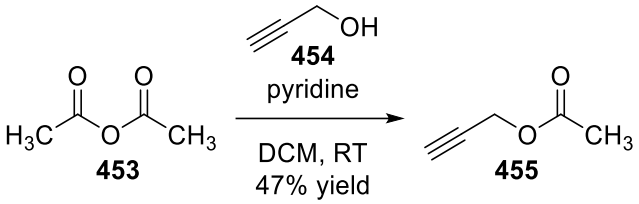

Under an inert atmosphere, a dried and purged reaction vessel was charged with propargyl alcohol (1.4 mL, 25 mmol, 1 equiv.) and triethylamine (3.8 mL, 27.5 mmol, 1.1 equiv.). The reagents were dissolved in DCM (50 mL, 0.5 M) and the reaction was cooled to 0 °C in an ice bath. Acetic anhydride (2.8 mL, 30 mmol, 1.2 equiv.) was added dropwise and the reaction was left to stir and slowly warm up to RT over 3 h. The reaction was then quenched with water, and washed with sodium bicarbonate. The organic layers were combined and washed with brine, dried over $MgSO_4$ and concentrated *in vacuo* to afford propargyl **455** (47% yield, 1.152 g, 11.8 mmol). ^{1}H NMR confirmed formation of the propargyl product and it matched the spectrum previously reported. [16]

^{1}H NMR (400 MHz, Chloroform-*d*) δ 4.61 (d, *J* = 2.5 Hz, 2H), 2.46 (td, *J* = 2.5, 0.5 Hz, 1H), 2.04 (s, 3H).

Synthesis of ethyl prop-2-yn-1-yl carbonate (457) [17]

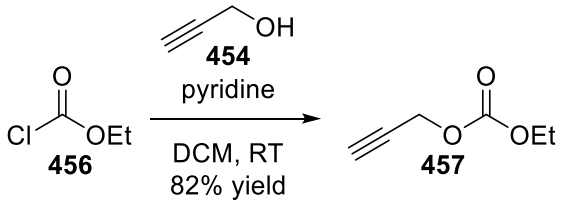

Under an inert atmosphere, a dried and purged reaction vessel was charged with propargyl alcohol (0.20 mL, 3.0 mmol, 1 equiv.) and pyridine (0.31 mL, 3.6 mmol, 1.2 equiv.). The reagents were dissolved in DCM (2 mL, 0.5 M) and the reaction was cooled in a 0 °C ice bath. Ethylchloroformate (0.34 mL, 3.6 mmol, 1.2 equiv.) was added dropwise and the reaction was left to stir and slowly warm up to RT over 3 h. The reaction was then quenched with water, and extracted with EtOAc (3 X's). The organic layers were combined and washed with brine, dried over $MgSO_4$ and concentrated *in vacuo* to afford propargyl **84** (82% yield, 285 mg, 2.8 mmol). ^{1}H NMR confirmed formation of the propargyl product and it matched the spectrum previously reported. [17]

^{1}H NMR (400 MHz, Chloroform-*d*) δ 4.57 (d, *J* = 2.5 Hz, 2H), 4.08 (q, *J* = 7.1 Hz, 2H), 2.45 (td, *J* = 2.4, 0.4 Hz, 1H), 1.17 (t, *J* = 7.2 Hz, 3H).

Synthesis tert-butyl prop-2-yn-1-yl carbonate (459) [18]

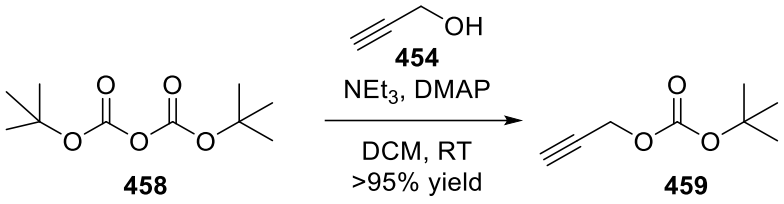

Propargyl alcohol (0.87 mL, 15 mmol, 1 equiv.) and triethylamine (2.7 mL, 19.5 mmol, 1.3 equiv.) were added to a reaction flash under positive N_2 pressure. DMAP was then added (18 mg, 0.15 mmol, 0.01 equiv), and the reagents were dissolved in dry DCM (38 mL, 0.4 M). The reaction was cooled in a 0 °C ice bath, and di-*tert*- butyl decarbonate (4.4 mL, 19.5 mmol, 1.3 equiv.) was added

dropwise. The reaction was stirred for 10 h and allowed to warm up to RT. The reaction was transferred to a separatory funnel and washed with 0.1 M HCl, then saturated sodium bicarbonate solution, followed by brine. The organic layer was dried over $MgSO_4$ and concentrated. The residue was purified over a silica plug (9:1 hexanes/EtOAc) to afford propargyl **459** (90% yield, 2.067 g, 13.5 mmol). ^{1}H NMR matched the reported spectrum. [18]

^{1}H NMR (400 MHz, Chloroform-*d*) δ 4.59 – 4.54 (m, 2H), 2.45 (dd, *J* = 2.7, 2.2 Hz, 1H), 1.40 (s, 9H).

Synthesis of 2-benzylmalononitrile (461)

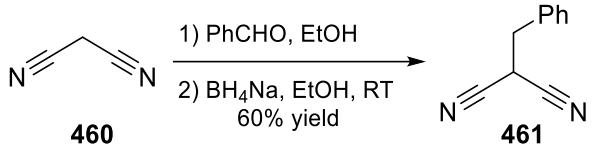

Malonitrile (0.272 g, 4 mmol) was dissolved in ethanol and combined with benzaldehyde (0.40 mL, 4 mmol) and allowed to stir overnight. The reaction was placed in an ice bath and cooled to 0°C. sodium borohydride (0.078 g, 2 mmol) was dissolved in ethanol and added to the reaction. The reaction was stirred vigorously for 15 minutes and then poured into water. DCM was added to the solution and the solution was quenched with 1M HCl. The organic layer was extracted twice using DCM. The layers were combined, dried over magnesium sulfate, and concentrated. The product was purified using flash chromatography and the solvent was removed in vacuo resulting in a white powder (0.35 g, 2.4 mmol, 60% yield). The obtained spectrum matches the known spectra. [19]

^{1}H NMR (400 MHz, $CDCl_3$) δ 7.45 – 7.38 (m, 3H), 7.36 – 7.31 (m, 2H), 3.92 (t, *J* = 7.0 Hz, 1H), 3.31 (d, *J* = 6.9 Hz, 2H).

Synthesis of diethyl 2-benzylmalonate (463) [20]

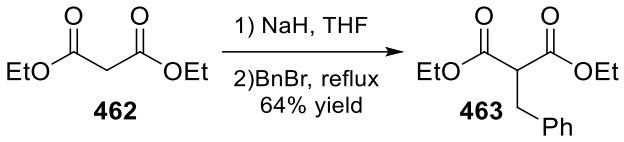

Ethyl malonate (1.57 mL, 10 mmol) and 20 mL THF were added to a dry round bottom flask. NaH (0.400 g, 10 mmol) was added and the mixture stirred at room temperature until gas production stopped. A reflux condenser was added and the reaction vessel was purged three times with nitrogen. Benzyl bromide was carefully added and the reaction mixture was heated to reflux for 8 hrs and just under for 18 hrs. The mixture was allowed to cool slowly to room temperature and was diluted with 40 mL diethyl ether. The solution was washed three times with water and dried over magnesium sulfate. The solvent was removed in vacuo and product was purified via distillation (64% yield, 1.601 g, 6.4 mmol). Resulting oil was characterized via ^{1}H NMR and the spectrum was in agreement with known spectra.[20]

^{1}H NMR (400 MHz, $CDCl_3$)- enol/keto mixture δ 7.37 – 7.08 (m, 5H), 4.17 (tdd, *J* = 15.0, 10.1, 4.8 Hz, 4H), 3.67 (t, *J* = 7.9 Hz, 1H), 3.24 (d, *J* = 7.7 Hz, 2H), 1.33 – 1.10 (m, 6H).

General procedure for nickel catalyzed reactions of ethyl propargyl carbonate and diethylbenzyl malonate. [15]

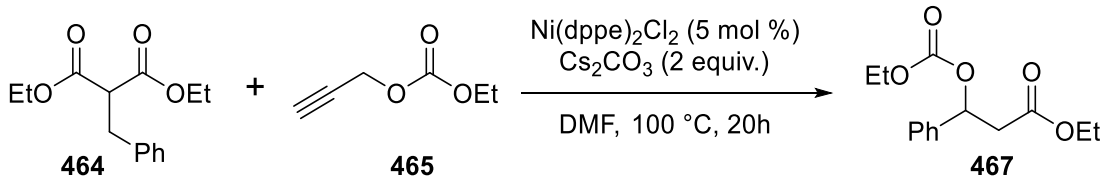

Ethyl propargyl carbonate (1 equiv.) and diethyl benzylmalonate (1 equiv.) were dissolved in DMF (0.1 M). Cesium carbonate (2 equiv.) was added to the mixture, and the reaction stirred for a minute. Ni(dppe)Cl_2 (5 mol%) was added to the reaction; it was heated to the desired temperature and stirred overnight. The reaction was cooled to room temperature. Once cool, the reaction was

quenched with water and extracted with ethyl acetate. The organic layers were combined, washed with water and brine, concentrated, and purified by flash column chromatography. The product was characterized by ^{1}H NMR, COSY, NOESY, ^{13}C NMR, DEPT 45, DEPT 90, IR, and ESI-MS.

Synthesis of ethyl 3-((ethoxycarbonyl)oxy)-3-phenylpropanoate (467)

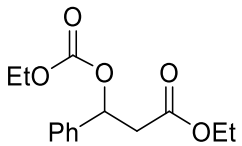

467

Ethyl propargyl carbonate (107 mg, 0.8 mmol, 1 equiv.) and diethyl benzylmalonate (0.2 mL, 0.8 mmol, 1 equiv.) were dissolved in DMF (0.1 M). Cesium carbonate (524 mg, 1.6 mmol, 2 equiv.) was added to the mixture, and the reaction stirred for a minute. Ni(dppe)Cl_2 (28 mg, 5 mol%) was added to the reaction; it was heated to 100 °C and stirred for 24 h. The reaction was cooled to room temperature. Once cool, the reaction was quenched with water and extracted with ethyl acetate. The organic layers were combined, washed with water and brine, concentrated, and purified by flash column chromatography.

^{1}H NMR (400 MHz, $CDCl_3$) δ 7.36 – 7.16 (m, 5H), 5.11 (dd, *J* = 8.5, 4.5 Hz, 1H), 4.18 (dq, *J* = 14.2, 7.1 Hz, 4H), 3.16 (ddd, *J* = 22.9, 14.3, 6.6 Hz, 2H), 1.37 – 1.17 (m, 6H).

^{13}C NMR (101 MHz, $CDCl_3$) δ 169.89 (s), 154.95 (s), 136.10 (s), 129.84 (s), 128.96 (s), 127.53 (s), 77.80 (s), 77.48 (s), 77.16 (s), 76.35 (s), 64.98 (s), 62.02 (s), 37.89 (s), 14.55 (d, *J* = 10.3 Hz).

IR: 2984, 2918, 1746, 1497, 1455, 1373, 1287, 1255, 1190, 1031, 789, 700 cm^{-1}

ESI MS m/z: $[M+Na]^+$ Calc'd for $C_{14}H_{18}NaO_5^+$ 289.1; Found 289.1

Synthesis of diethyl 2-benzyl-2-(prop-2-yn-1-yl)malonate (475) [21]

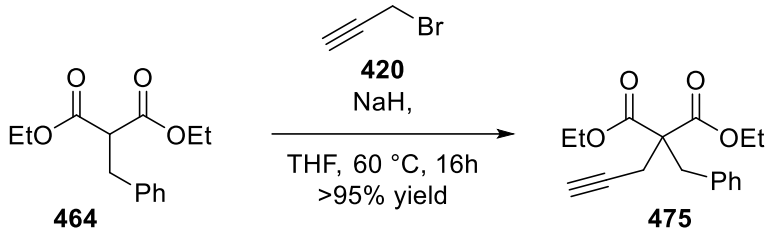

Under an inert N_2 atmosphere, a solution of diethyl benzylmalonate (0.24 mL, 1.0 mmol, 1 equiv.) in THF (0.35 mL) was added to a suspension of NaH (63 mg, 1.5 mmol, 1.5 equiv.) stirring at 0 °C. The reaction warmed to RT and was then added dropwise to a solution of propargyl bromide (0.11 mL, 1.2 mmol, 1.2 equiv.) heated to 65 °C and the reaction was stirred for 16 h. Once cooled to RT, the reaction was quenched with water and the product was extracted with EtOAc (3 x's). The organic layers were combined and washed with brine, dried over $MgSO_4$ and concentrated to afford ## as a clear oil (98% yield, 282 mg, 0.98 mmol). The ^{1}H NMR spectrum matched the reported literature. [21]

^{1}H NMR (400 MHz, Chloroform-*d*) δ 7.38 – 7.05 (m, 5H), 4.32 – 4.15 (m, 4H), 3.40 (s, 2H), 2.67 (d, *J* = 2.7 Hz, 2H), 2.15 (t, *J* = 2.7 Hz, 1H), 1.26 (td, *J* = 7.1, 2.4 Hz, 6H).

Synthesis of diethyl 2-benzyl-2-(propa-1,2-dien-1-yl)malonate (466)

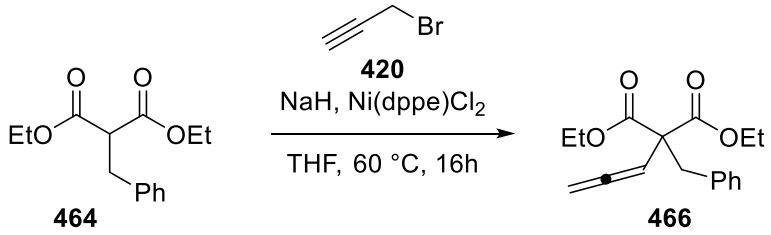

Under an inert N_2 atmosphere, diethyl benzylmalonate (0.34 mL, 3.0 mmol, 1 equiv.) was added to a suspension of NaH (92 mg, 3.8 mmol, 1.3 equiv.) in THF (6 mL) stirring at 0 °C. The reaction was left to stir and warm up to RT over 30 min.

In a separate reaction vessel under N_2, Ni(dppe)Cl_2 (80 mg, 0.15 mmol, 5 mol%) and propargyl bromide (0.72 mL, 3.0 mmol, 1 equiv.) were dissolved in THF (6 mL) and left to stir for 30 min. After that time, the diethylbenzylmalonate and sodium hydride solution was added to the propargyl solution portionwise over 30 min. The reaction was stirred for 16 h and then quenched with water and filtered through a celite plug. The filtrate was transferred to a separatory funnel and the product was extracted with EtOAc (3 x's). The organic layers were combined and washed with brine, dried over $MgSO_4$ and concentrated.

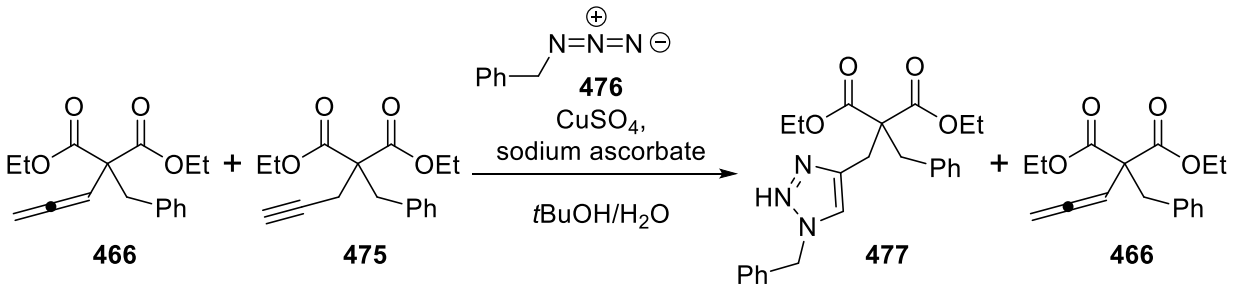

The crude mixture of products (716 mg) was added to a solution of benzyl azide (0.62 mL, 5.0 mmol, 2 equiv.) in *tert*-butanol (2.5 mL) and water (2.5 mL). The reaction mixture was stirred and copper (II) sulfate (98 mg, 0.37 mmol, 0.15 equiv.) and sodium ascorbate (152 mg, 0.74 mmol, 0.3 equiv) were added. The reaction stirred for 16 h, then was filtered through a celite plug. The solution was diluted with water and the product was extracted with EtOAc (3 x's). The organic layers were combined, washed with brine, dried over $MgSO_4$ and concentrated. The alkyne in the reaction mixture fully reacted and the allenic product **466** was isolated by FCC. Solvent conditions: 1% EtOAc in petroleum ether, product eluted in fractions 65-81. (13 % yield, 116 mg, 0.39 mmol).

^{1}H NMR (400 MHz, Chloroform-*d*) δ 7.28 – 7.13 (m, 5H), 5.62 (td, *J* = 6.8, 0.9 Hz, 1H), 4.94 (dd, *J* = 6.8, 1.0 Hz, 2H), 4.26 – 4.08 (m, 4H), 3.38 (s, 2H), 1.23 (td, *J* = 7.1, 0.9 Hz, 6H).

^{13}C NMR (101 MHz, Chloroform-*d*) δ 207.49, 169.78, 136.07, 130.29, 128.26, 127.07, 90.44, 61.82, 59.02, 40.68, 14.16.

IR: 2980, 2926, 1957, 1731, 1604, 1495, 1454, 1366, 1258, 1214, 1183, 1082, 1039, 856, 777, 742, 700, 562, 521, 464 cm^{-1}

HRMS (ESI) m/z: $[M+Na]^+$ Calc'd for $C_{17}H_{20}NaO_4^+$ 311.1254; Found 311.1261.

6.7 References

(1) Love, B. E.; Jones, E. G. The Use of Salicylaldehyde Phenylhydrazone as an Indicator for the Titration of Organometallic Reagents. *The Journal of Organic Chemistry* **1999**, *64* (10), 3755-3756. DOI: 10.1021/jo982433e.

(2) Borovika, A.; Tang, P.-I.; Klapman, S.; Nagorny, P. Thiophosphoramide-Based Cooperative Catalysts for Brønsted Acid Promoted Ionic Diels–Alder Reactions. *Angewandte Chemie International Edition* **2013**, *52* (50), 13424-13428. DOI: https://doi.org/10.1002/anie.201307133.

(3) Gennari, C.; Vulpetti, A.; Pain, G. Highly enantio- and diastereoselective boron aldol reactions of α-heterosubstituted thioacetates with aldehydes and silyl imines. *Tetrahedron* **1997**, *53* (16), 5909-5924. DOI: https://doi.org/10.1016/S0040-4020(97)00251-2.

(4) Georg, G. I.; Harriman, G. C. B.; Hepperle, M.; Clowers, J. S.; Vander Velde, D. G.; Himes, R. H. Synthesis, Conformational Analysis, and Biological Evaluation of Heteroaromatic Taxanes. *The Journal of Organic Chemistry* **1996**, *61* (8), 2664-2676. DOI: 10.1021/jo951961c.

(5) Borlinghaus, N.; Gergel, S.; Nestl, B. M. Biocatalytic Access to Piperazines from Diamines and Dicarbonyls. *ACS Catalysis* **2018**, *8* (4), 3727-3732. DOI: 10.1021/acscatal.8b00291.

(6) Chen, J.; Brown, D. P.; Wang, Y. J.; Chen, Z. S. New phenstatin-fatty acid conjugates: synthesis and evaluation. *Bioorg Med Chem Lett* **2013**, *23* (18), 5119-5122. DOI: 10.1016/j.bmcl.2013.07.025

(7) Xu, L.-W.; Li, L.; Bai, X.-F.; Song, T.; Deng, W.-H.; Wei, Y.-L.; Xia, C.-G. (EtO)3SiH-Promoted Palladium-Catalyzed Isomerization of Olefins: Convenient Synthesis of Internal Alkenes from Terminal Alkenes. *Synlett* **2013**, *25* (03), 417-422. DOI: 10.1055/s-0033-1340290.

(8) Kwong, C. K.-W.; Fu, M. Y.; Law, H. C.-H.; Toy, P. H. Isomerization of Electron-Poor Alkynes to the Corresponding (E,E)-1,3-Dienes Using a Bifunctional Polymeric Catalyst Bearing Triphenylphosphine and Phenol Groups. *Synlett* **2010**, *2010* (17), 2617-2620. DOI: 10.1055/s-0030-1258576.

(9) Karaali, N.; Aydin, S.; Baltas, N.; Mentese, E. Synthesis of novel tetra-substituted benzimidazole compounds containing certain heterostructures with antioxidant and anti-urease activities. *Journal of Heterocyclic Chemistry* **2020**, *57* (4), 1806-1815. DOI: https://doi.org/10.1002/jhet.3905.

(10) Roussi, G.; Beugelmans, R.; Chastanet, J.; Roussi, G. The [3+2] Cycloaddition Reaction of Nonstabilized Azomethine Ylide Generated from Trimetylmine N-Oxide to C=C, C=N, and C=S Bonds. *Heterocycles* **1987**, *26* (12), 3197-3202, Journal. DOI: 10.3987/r-1987-12-3197.

(11) Bottini, A. T.; Roberts, J. D. Nuclear Magnetic Resonance Spectra. Nitrogen Inversion Rates of N-Substituted Aziridines (Ethylenimines)1. *Journal of the American Chemical Society* **1958**, *80* (19), 5203-5208. DOI: 10.1021/ja01552a048.

(12) Bush, T. S.; Yap, G. P. A.; Chain, W. J. Transformation of N,N-Dimethylaniline N-Oxides into Diverse Tetrahydroquinoline Scaffolds via Formal Povarov Reactions. *Organic Letters* **2018**, *20* (17), 5406-5409. DOI: 10.1021/acs.orglett.8b02318.

(13) Bi, H.-P.; Guo, L.-N.; Duan, X.-H.; Gou, F.-R.; Huang, S.-H.; Liu, X.-Y.; Liang, Y.-M. Highly Regio- and Stereoselective Synthesis of Indene Derivatives via Electrophilic Cyclization. *Organic Letters* **2007**, *9* (3), 397-400. DOI: 10.1021/ol062683e.

(14) Bi, H.-P.; Liu, X.-Y.; Gou, F.-R.; Guo, L.-N.; Duan, X.-H.; Liang, Y.-M. Highly Regioselective Synthesis of Indene Derivatives Including an Allene Functional Group via Pd/C-Catalyzed Cyclization Reaction in Air. *Organic Letters* **2007**, *9* (18), 3527-3529. DOI: 10.1021/ol071385u.

(15) Gou, F.-R.; Bi, H.-P.; Guo, L.-N.; Guan, Z.-H.; Liu, X.-Y.; Liang, Y.-M. New Insight into Ni(II)-Catalyzed Cyclization Reactions of Propargylic Compounds with Soft Nucleophiles: Novel Indenes Formation. *The Journal of Organic Chemistry* **2008**, *73* (10), 3837-3841. DOI: 10.1021/jo800155a.

(16) Blencowe, A.; Qiao, G. G. Ring-Opening Metathesis Polymerization with the Second Generation Hoveyda–Grubbs Catalyst: An Efficient Approach toward High-Purity Functionalized Macrocyclic Oligo(cyclooctene)s. *Journal of the American Chemical Society* **2013**, *135* (15), 5717-5725. DOI: 10.1021/ja312418z.

(17) Nagase, Y.; Shirai, H.; Kaneko, M.; Shirakawa, E.; Tsuchimoto, T. Indium-catalyzed annulation of 3-aryl- and 3-heteroarylindoles with propargyl ethers: synthesis and photoluminescent properties of aryl- and heteroaryl[c]carbazoles. *Organic & Biomolecular Chemistry* **2013**, *11* (9), 1456-1459, 10.1039/C3OB27407A. DOI: 10.1039/C3OB27407A.

(18) Montgomery, T. D.; Rawal, V. H. Palladium-Catalyzed Modular Synthesis of Substituted Piperazines and Related Nitrogen Heterocycles. *Organic Letters* **2016**, *18* (4), 740-743. DOI: 10.1021/acs.orglett.5b03708.

(19) Tayyari, F. W., D.; Fanwick, P.; Sammelson, R. Monosubstituted Malononitriles: Efficient One-Pot Reductive Alkylations of Malononitrile with Aromatic Aldehydes. *Synthesis* **2008**, (2). DOI: 10.1055/s-2007-990945.

(20) Doni, E.; Mondal, B.; O'Sullivan, S.; Tuttle, T.; Murphy, J. A. Overturning Established Chemoselectivities: Selective Reduction of Arenes over Malonates and Cyanoacetates by

Photoactivated Organic Electron Donors. *Journal of the American Chemical Society* **2013**, *135* (30), 10934-10937. DOI: 10.1021/ja4050168.

(21) Doni, E.; Mondal, B.; O'Sullivan, S.; Tuttle, T.; Murphy, J. A. Overturning established chemoselectivities: selective reduction of arenes over malonates and cyanoacetates by photoactivated organic electron donors. *J Am Chem Soc* **2013**, *135* (30), 10934-10937. DOI: 10.1021/ja4050168

APPENDIX

^{1}H NMR, ^{13}C NMR, DEPT and 2D NMR

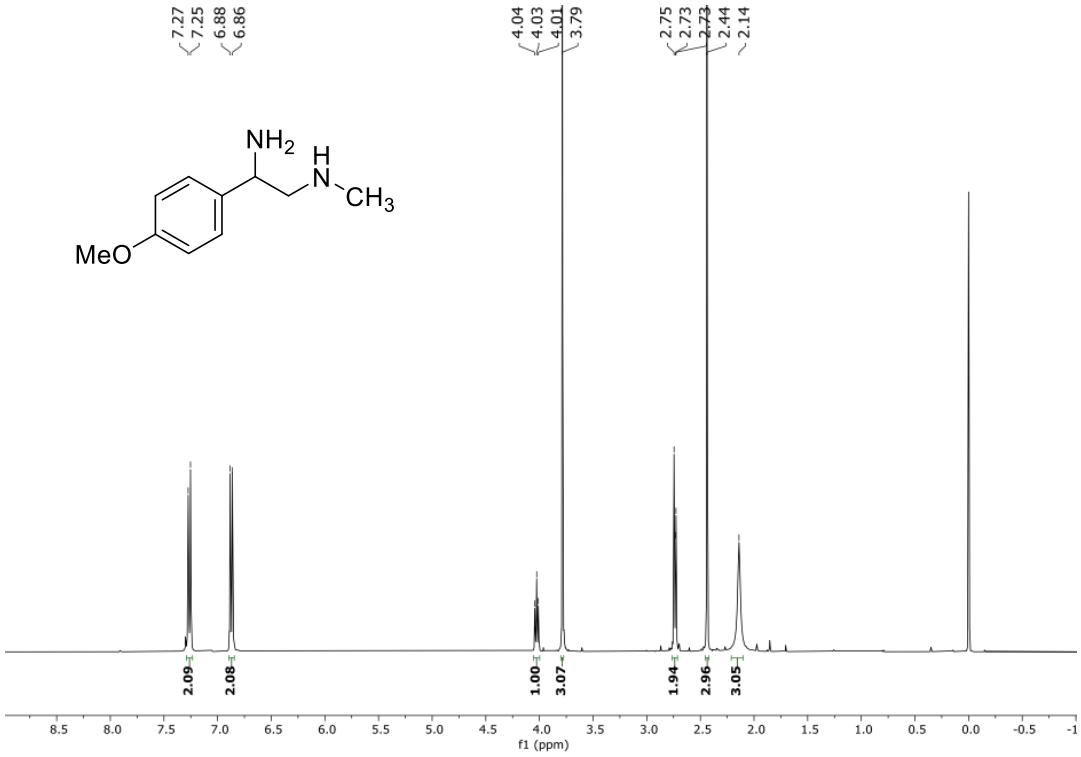

Figure 53. ^{1}H NMR spectrum of 109a (In $CDCl_3$, 400 MHz)

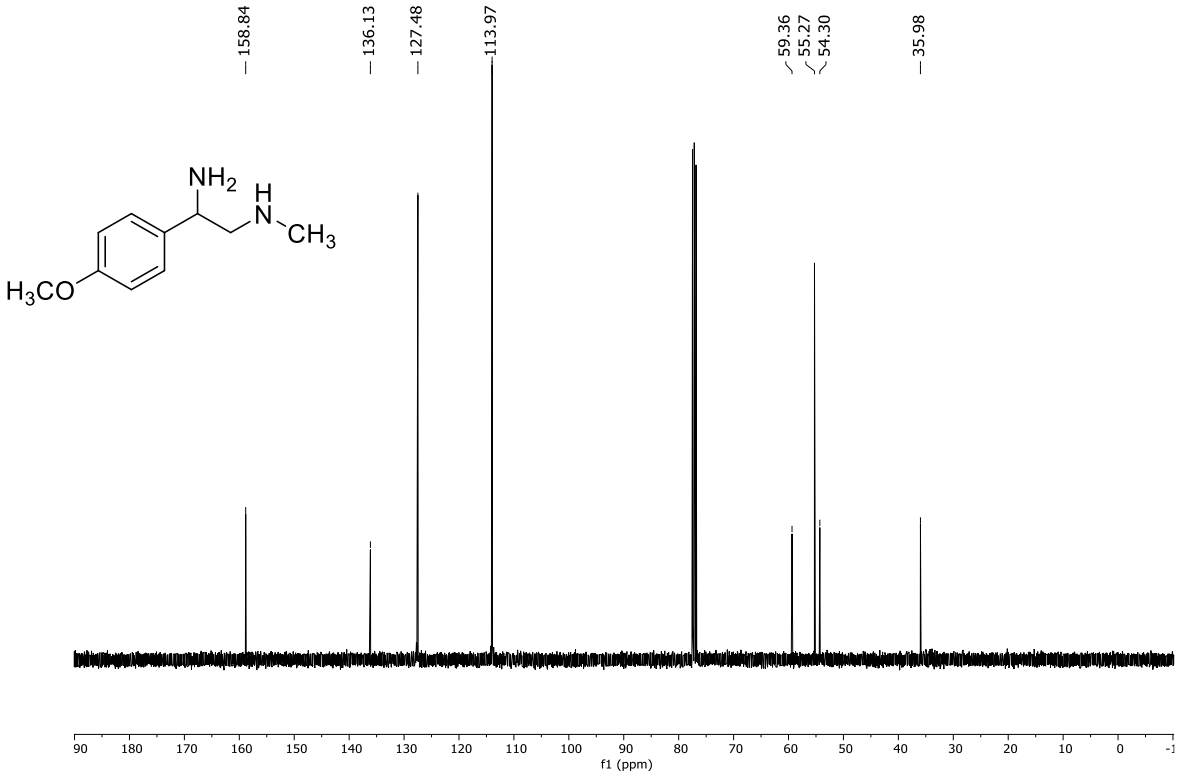

Figure 54. ^{13}C NMR spectrum of 109a (In $CDCl_3$)

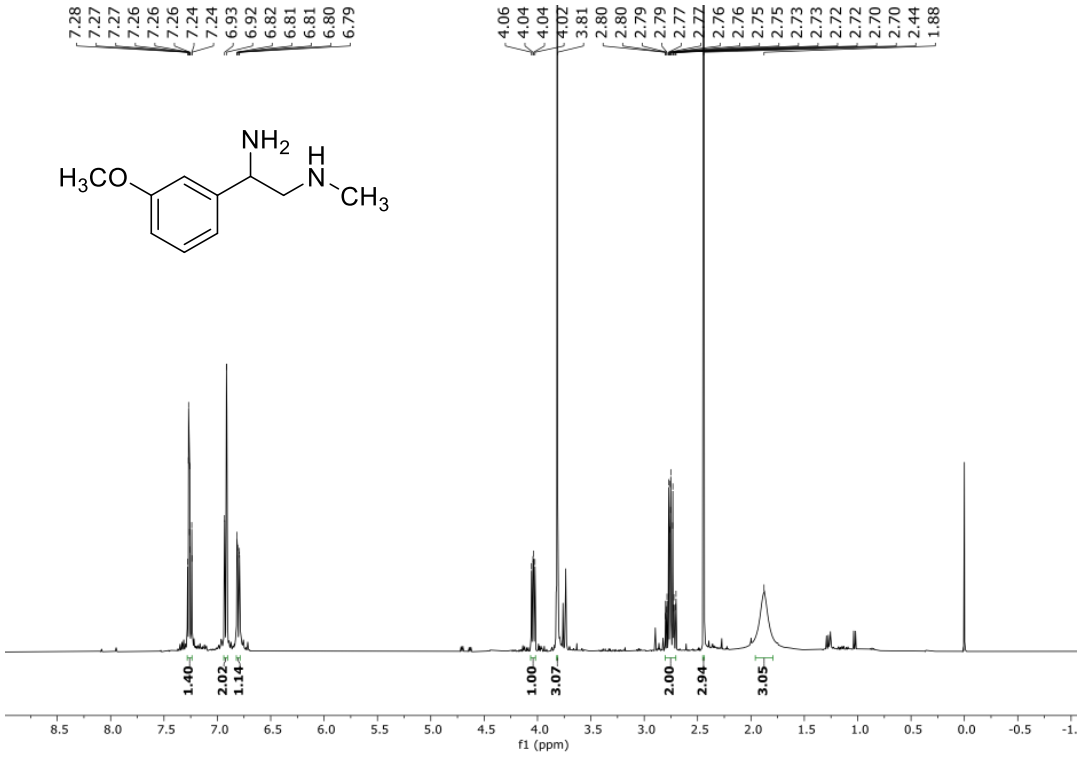

Figure 55. ^{1}H NMR spectrum of 109b (In $CDCl_3$, 400 MHz)

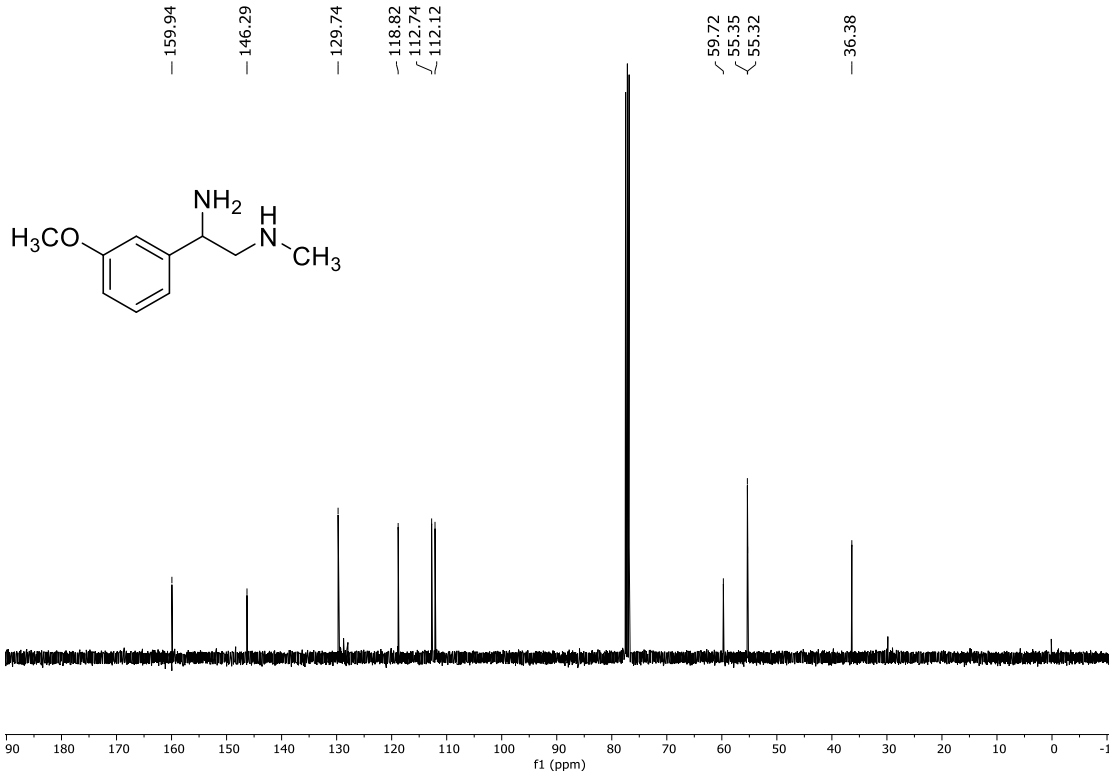

Figure 56.^{13}C NMR spectrum of 109b (In $CDCl_3$, 101 MHz)

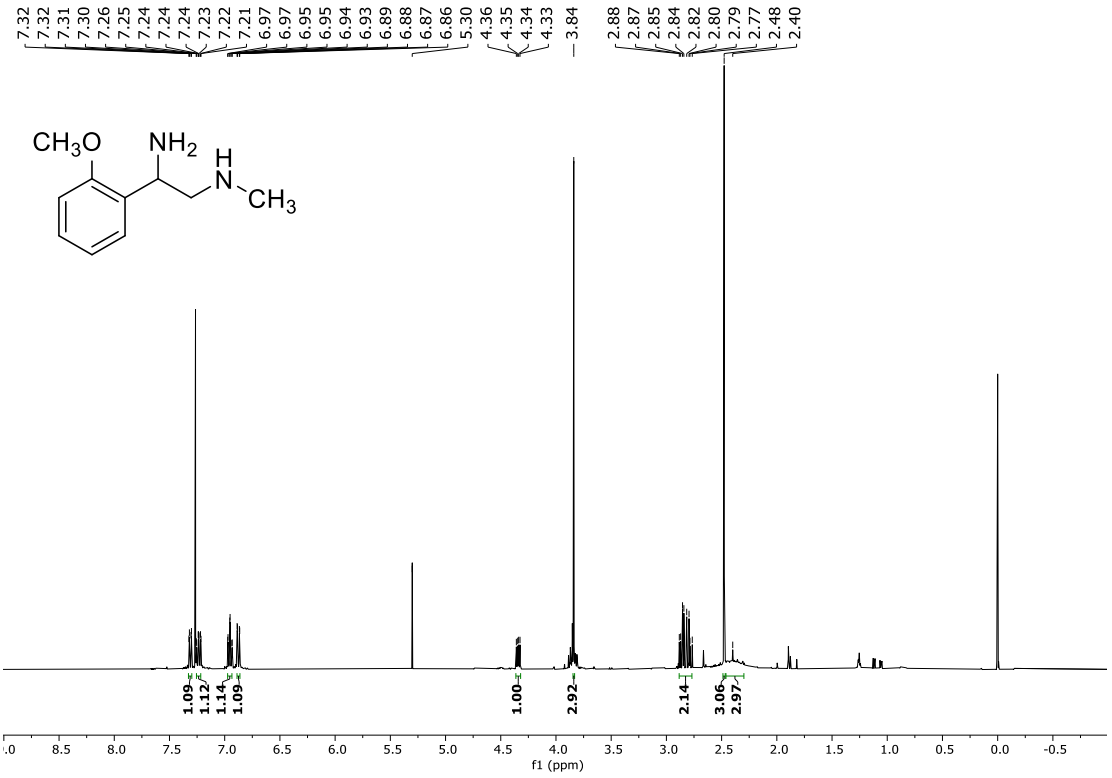

Figure 57. ^{1}H NMR spectrum of 109c (In $CDCl_3$, 400 MHz)

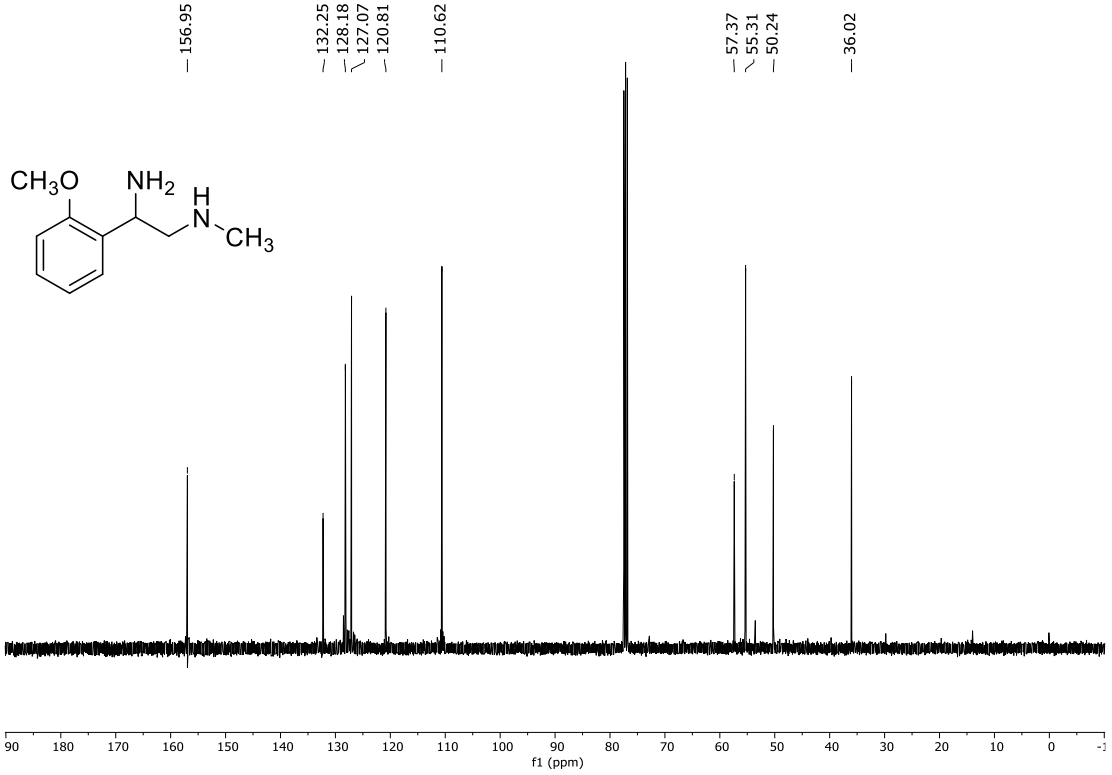

Figure 58. ^{13}C NMR spectrum of 109c (In $CDCl_3$, 101 MHz)

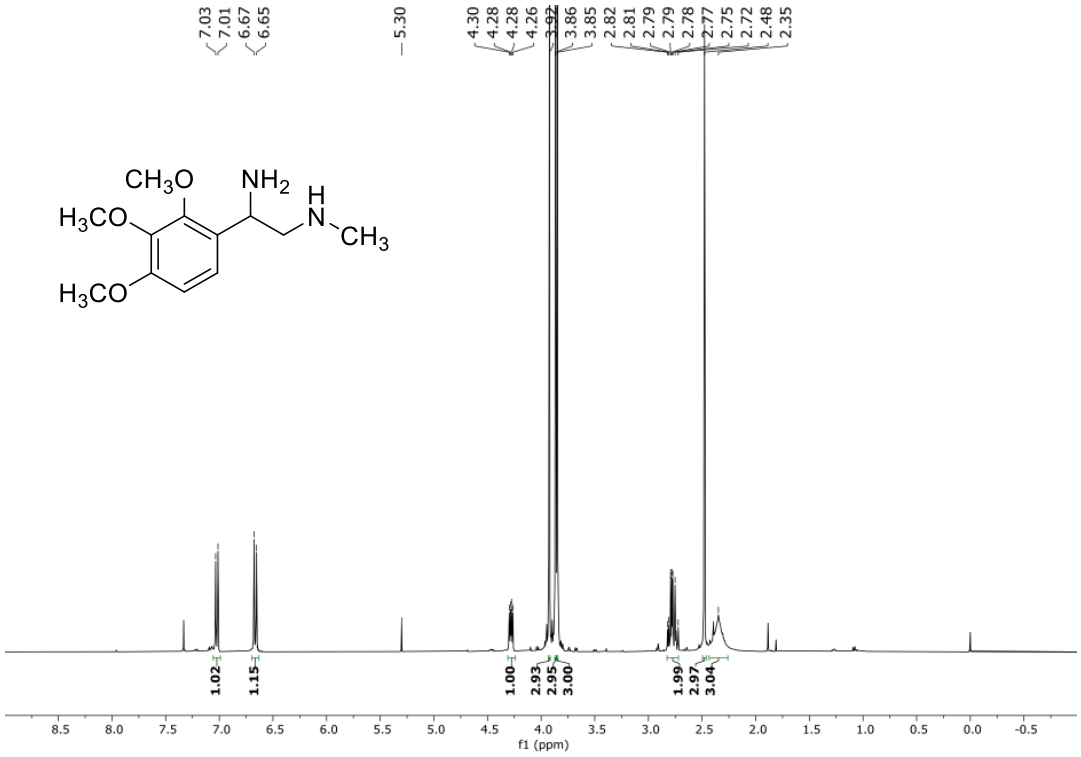

Figure 59. ^{1}H NMR spectrum of 109d (In $CDCl_3$, 400 MHz)

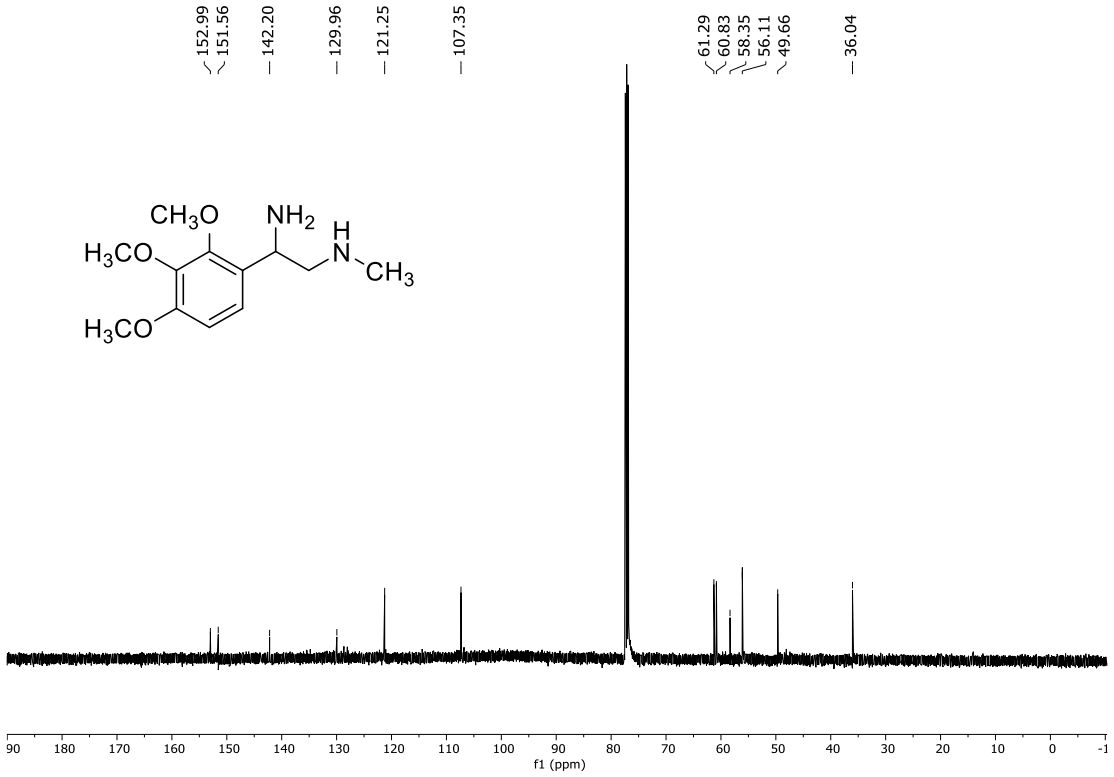

Figure 60. ^{13}C NMR spectrum of 109d (In $CDCl_3$, 126 MHz)

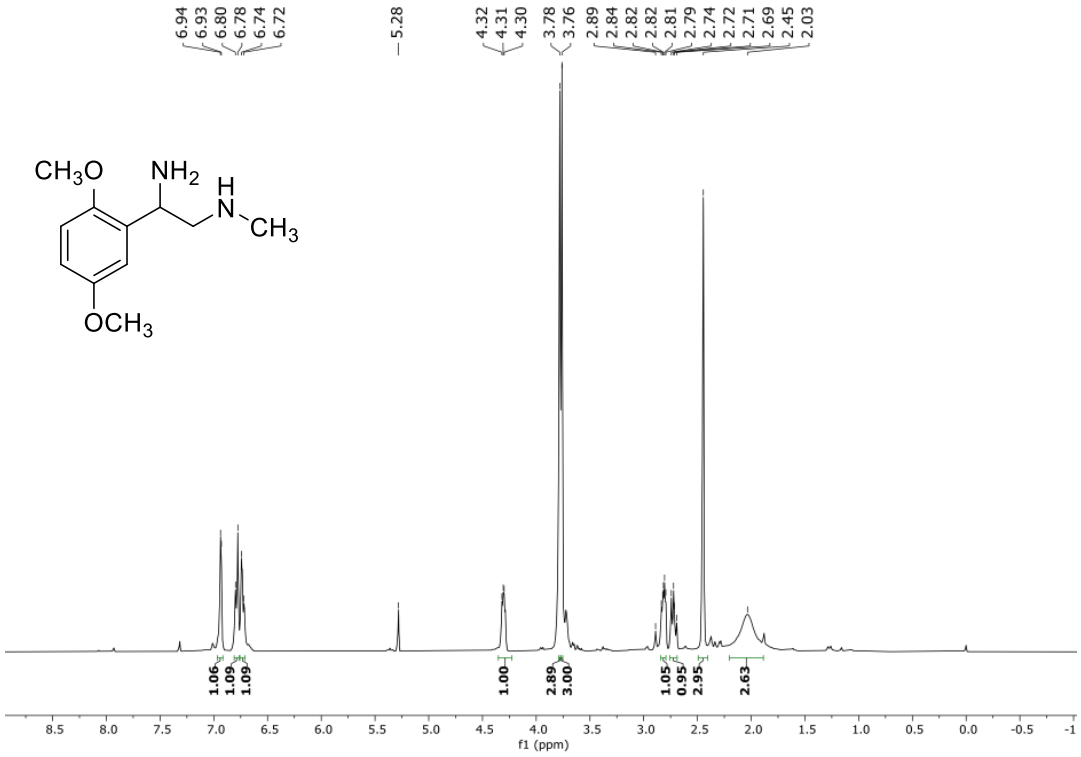

Figure 61. ^{1}H NMR spectrum of 109e (In $CDCl_3$, 400 MHz)

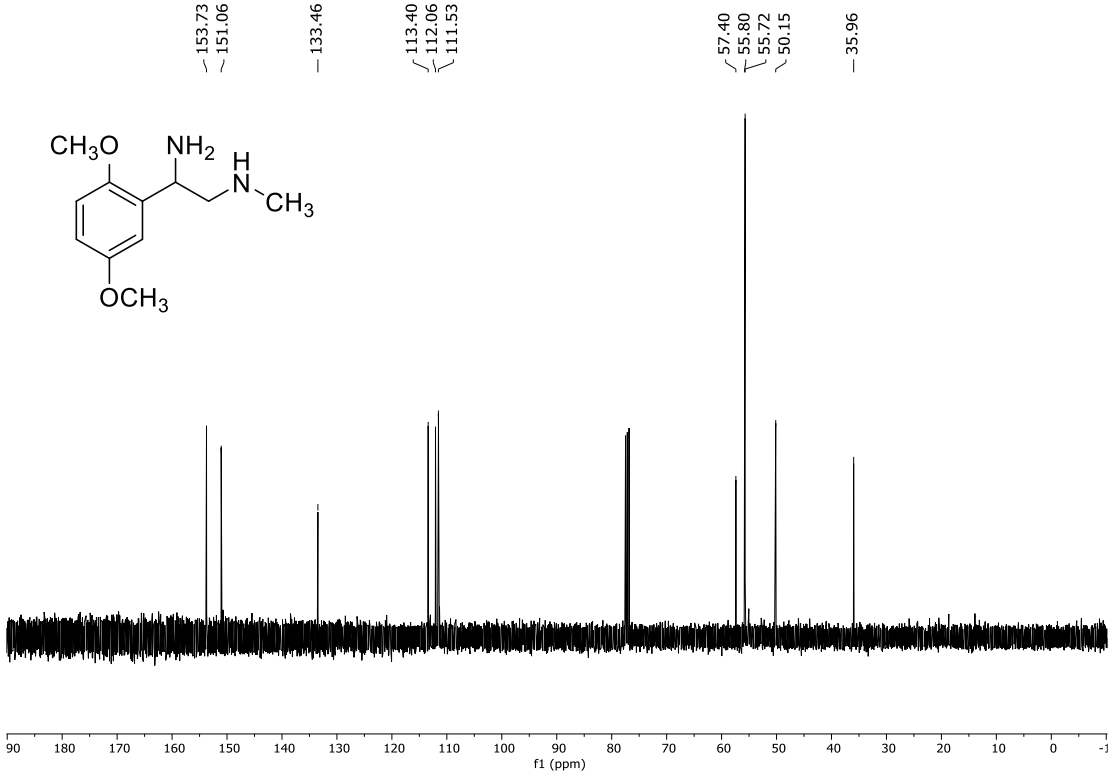

Figure 62. ^{13}C NMR spectrum of 109e (In $CDCl_3$, 101 MHz)

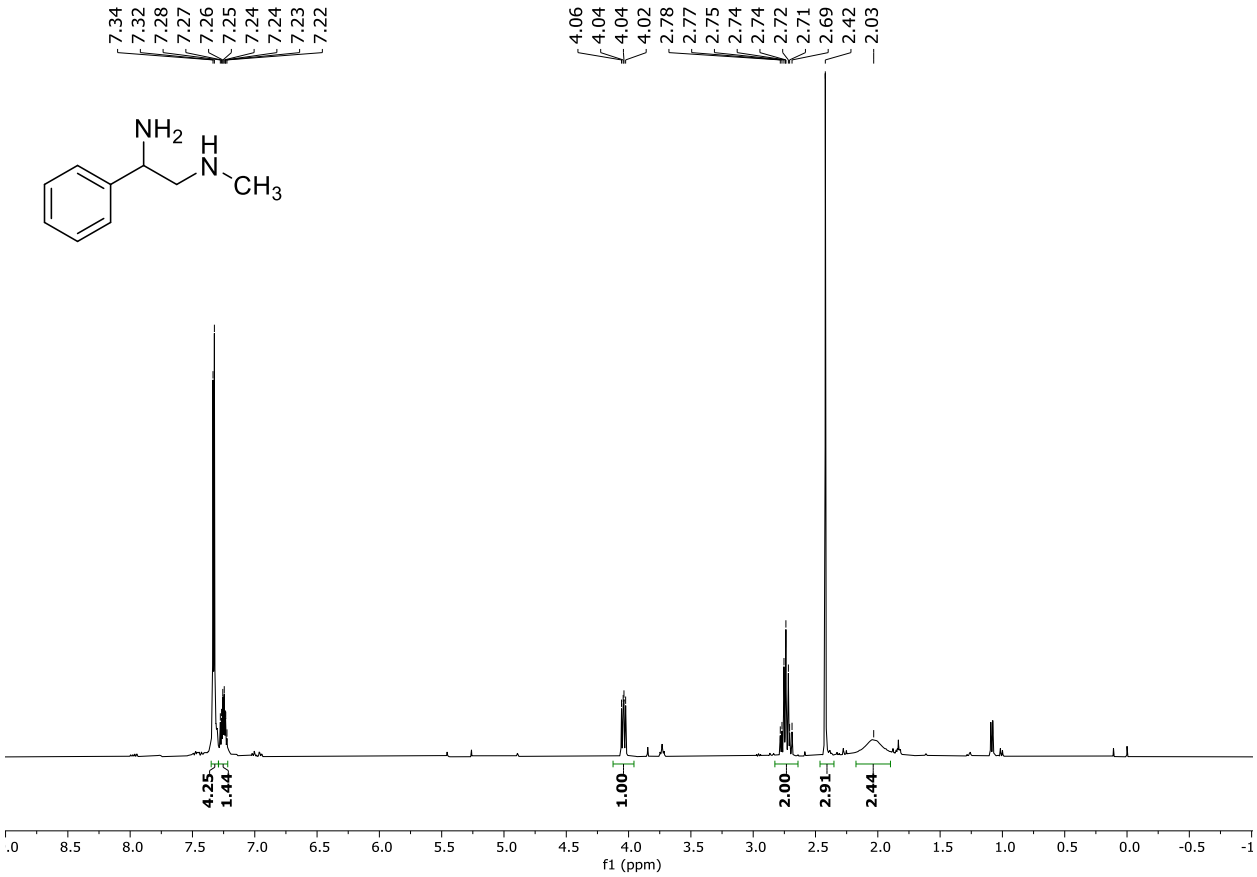

Figure 63. ^{1}H NMR spectrum of 109f(In $CDCl_3$, 400 MHz)

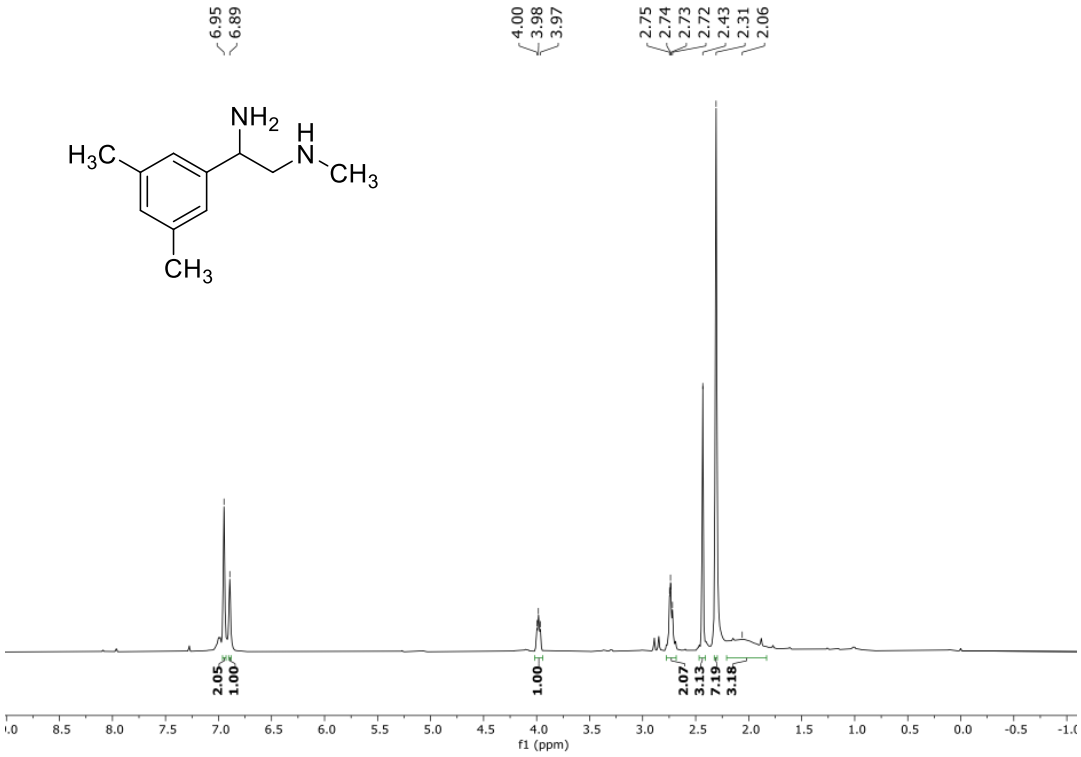

Figure 64. ^{1}H NMR spectrum of 109g (In $CDCl_3$, 400 MHz)

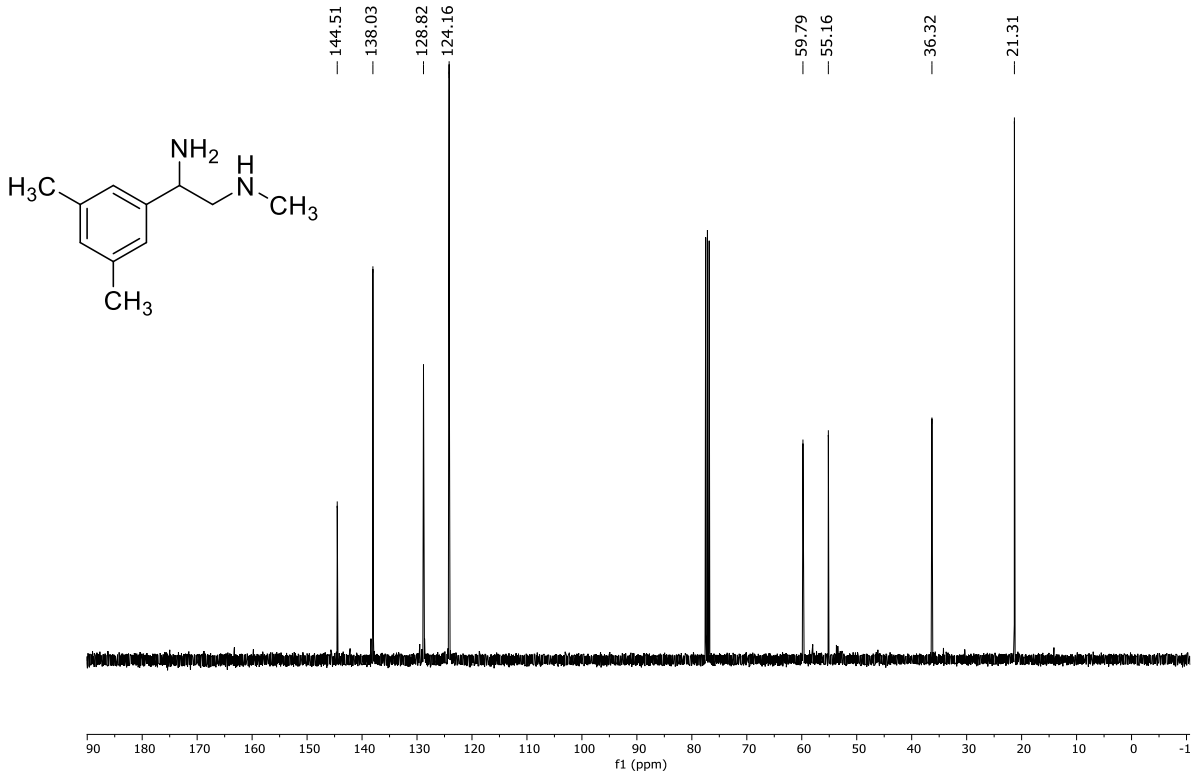

Figure 65. ^{13}C NMR spectrum of 109g (In $CDCl_3$, 101 MHz)

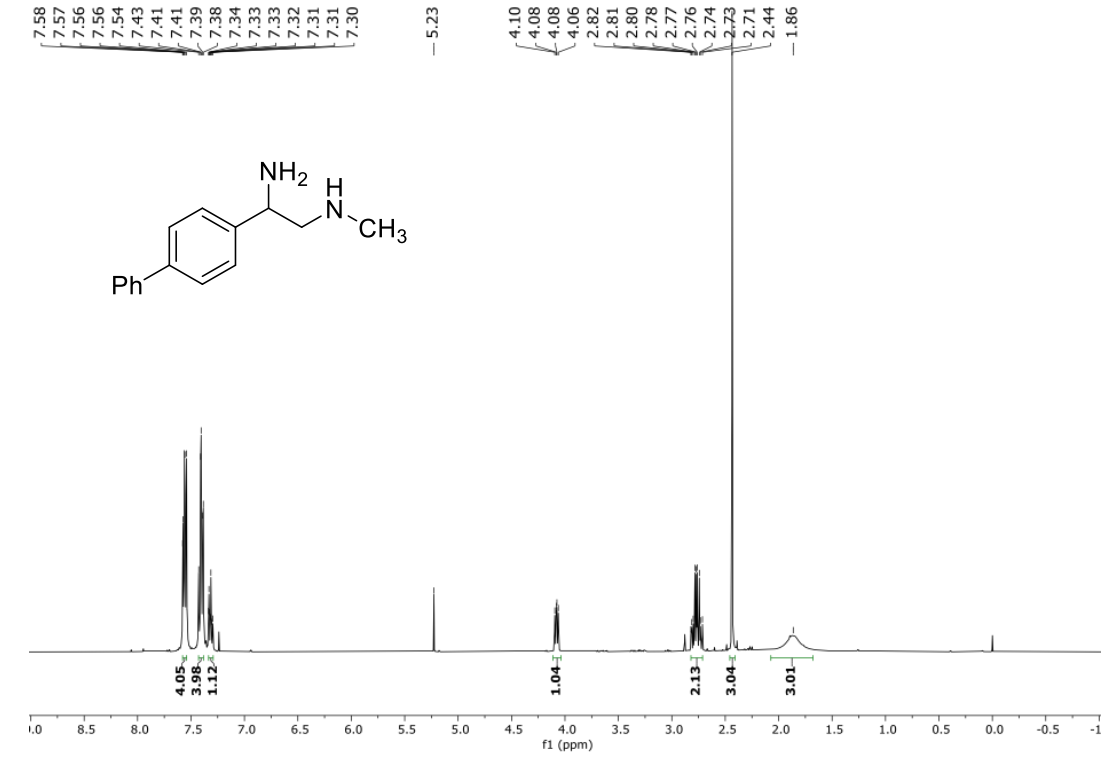

Figure 66. ^{1}H NMR spectrum of 109h (In $CDCl_3$, 400 MHz)

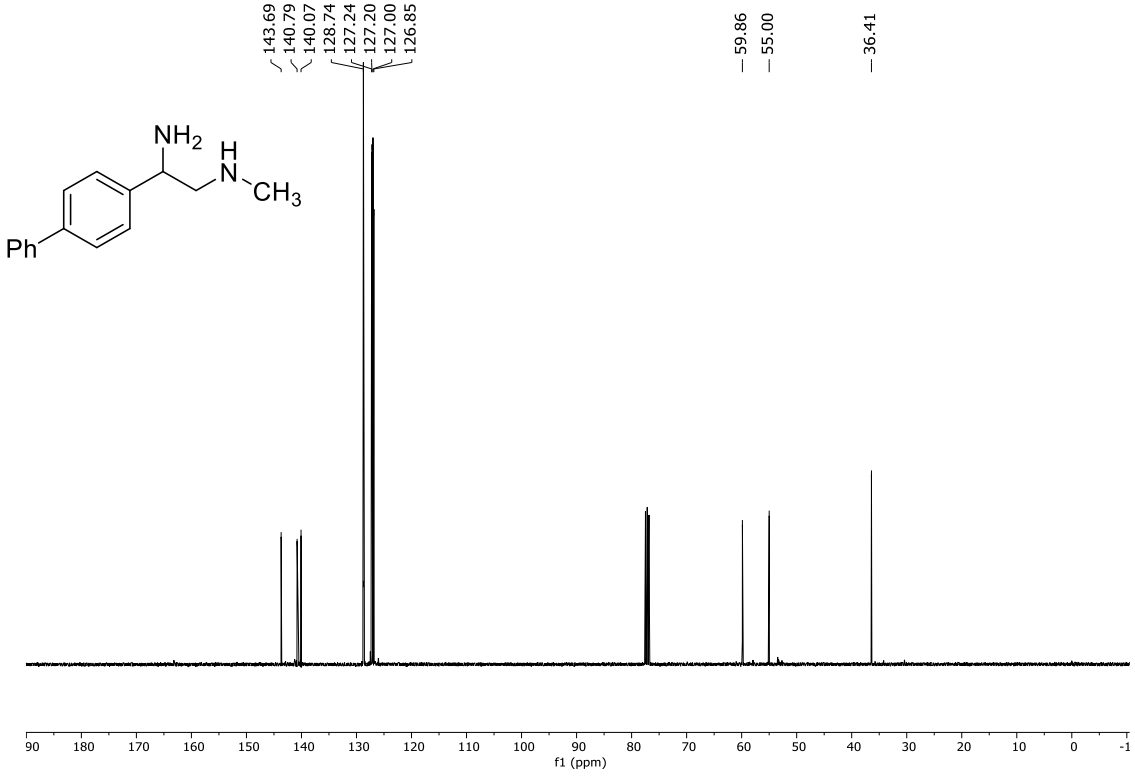

Figure 67. ^{13}C NMR spectrum of 109h (In $CDCl_3$, 101 MHz)

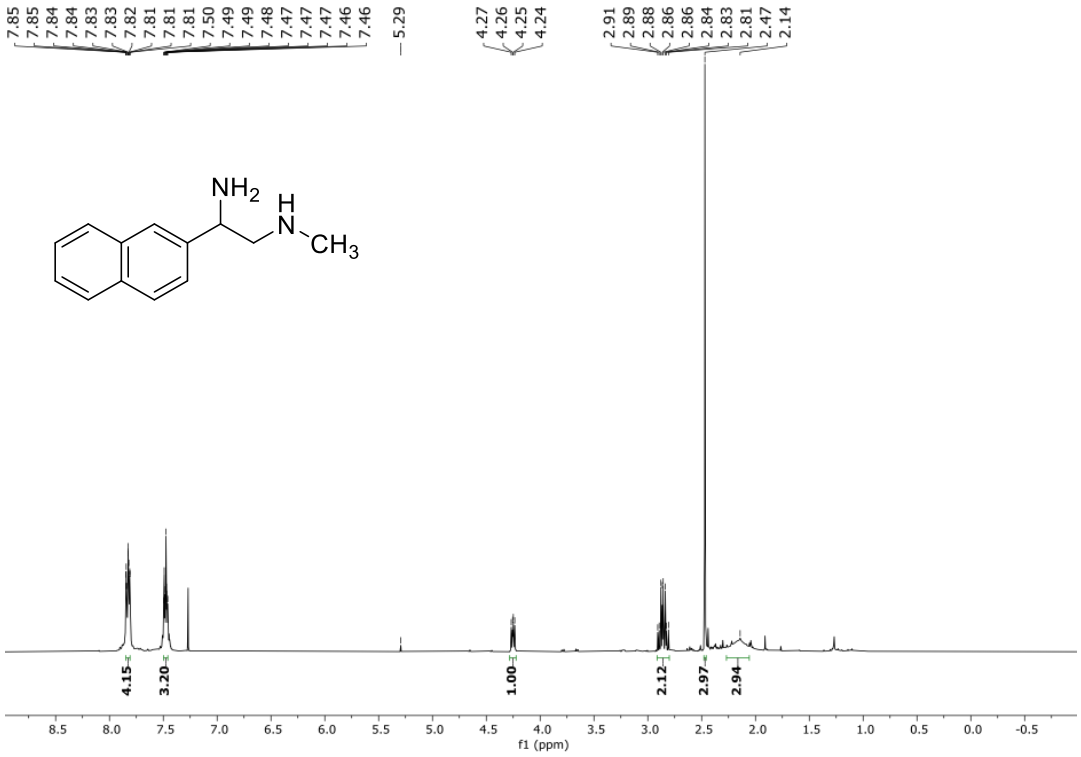

Figure 68. ^{1}H NMR spectrum of 109i (In $CDCl_3$, 400 MHz)

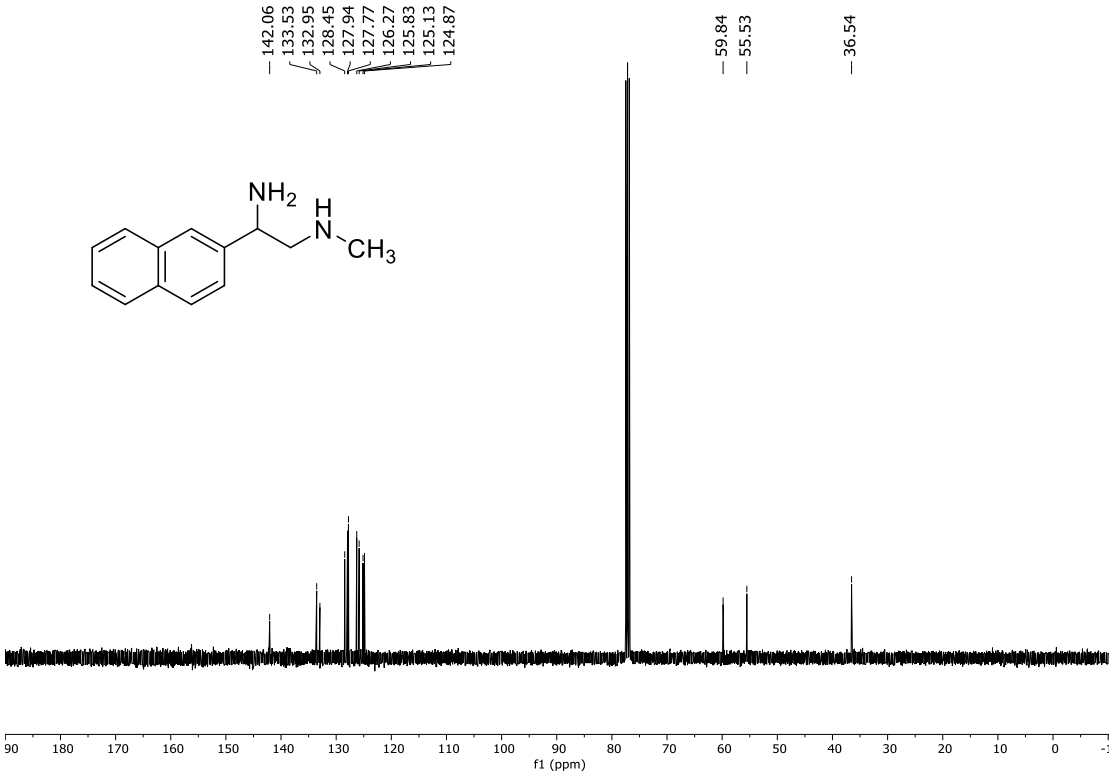

Figure 69. ^{13}C NMR spectrum of 109i (In $CDCl_3$, 101 MHz)

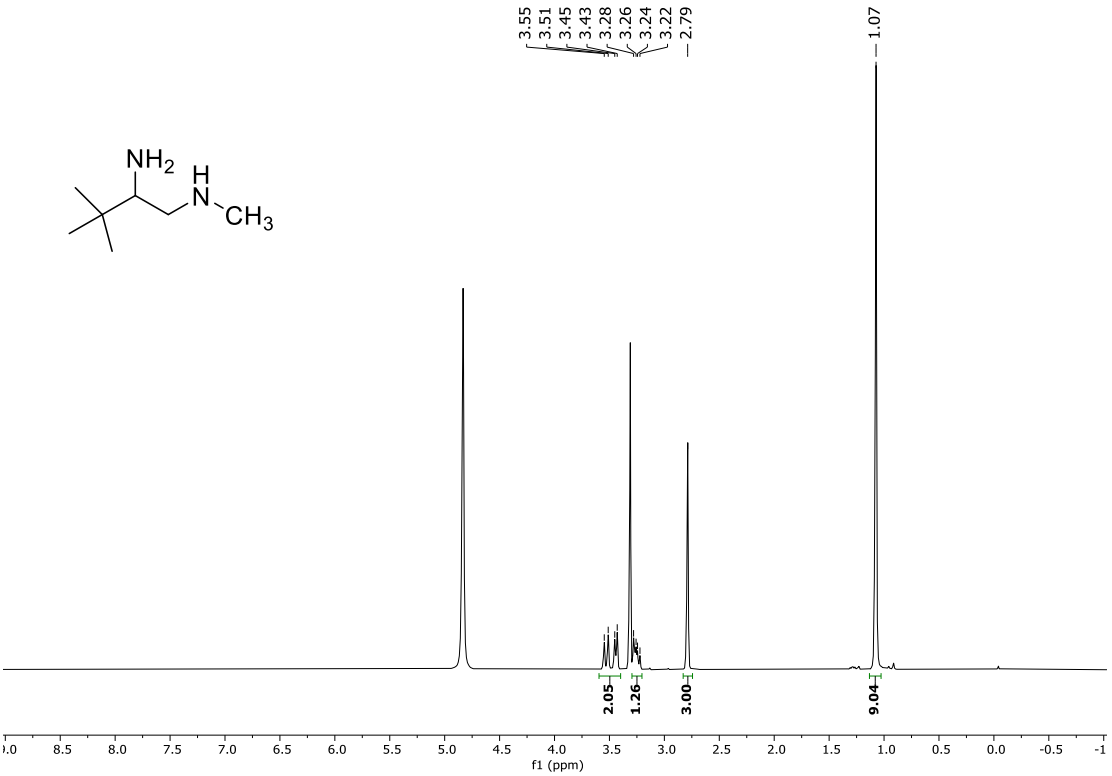

Figure 70. ^{1}H NMR spectrum of 109j (In MeOD, 400 MHz)

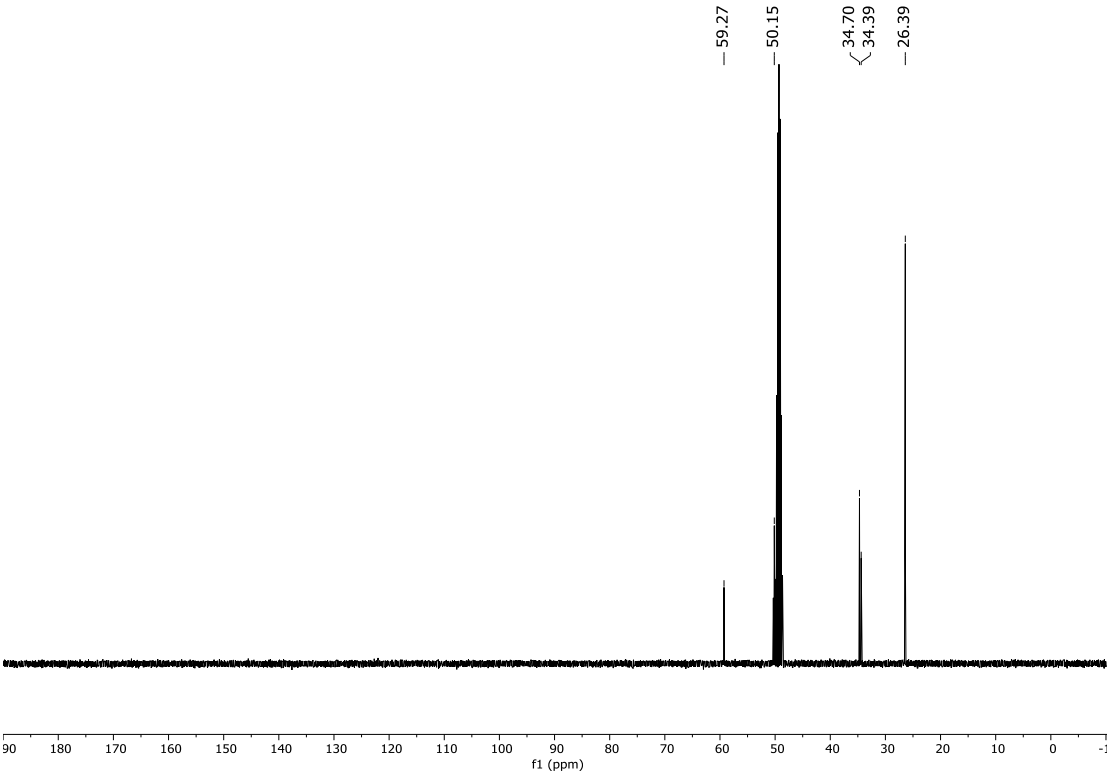

Figure 71. ^{13}C NMR spectrum of 109j (In MeOD, 101 MHz)

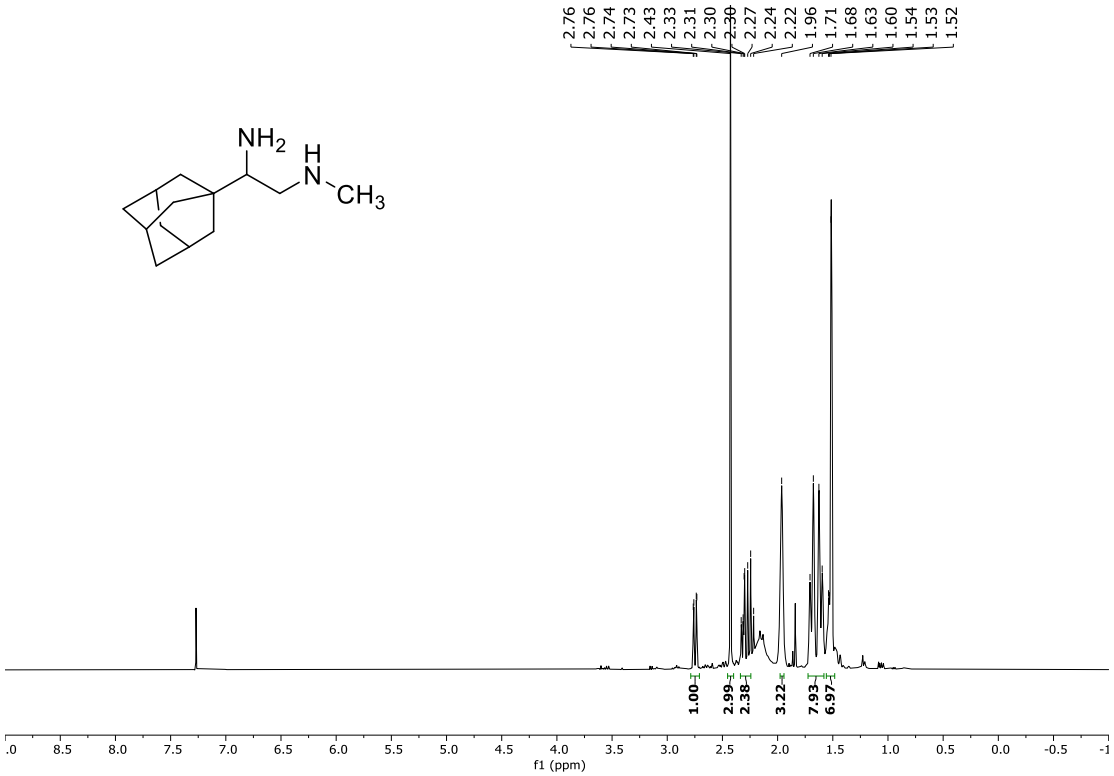

Figure 72. ^{1}H NMR spectrum of 109k (In $CDCl_3$, 400 MHz)

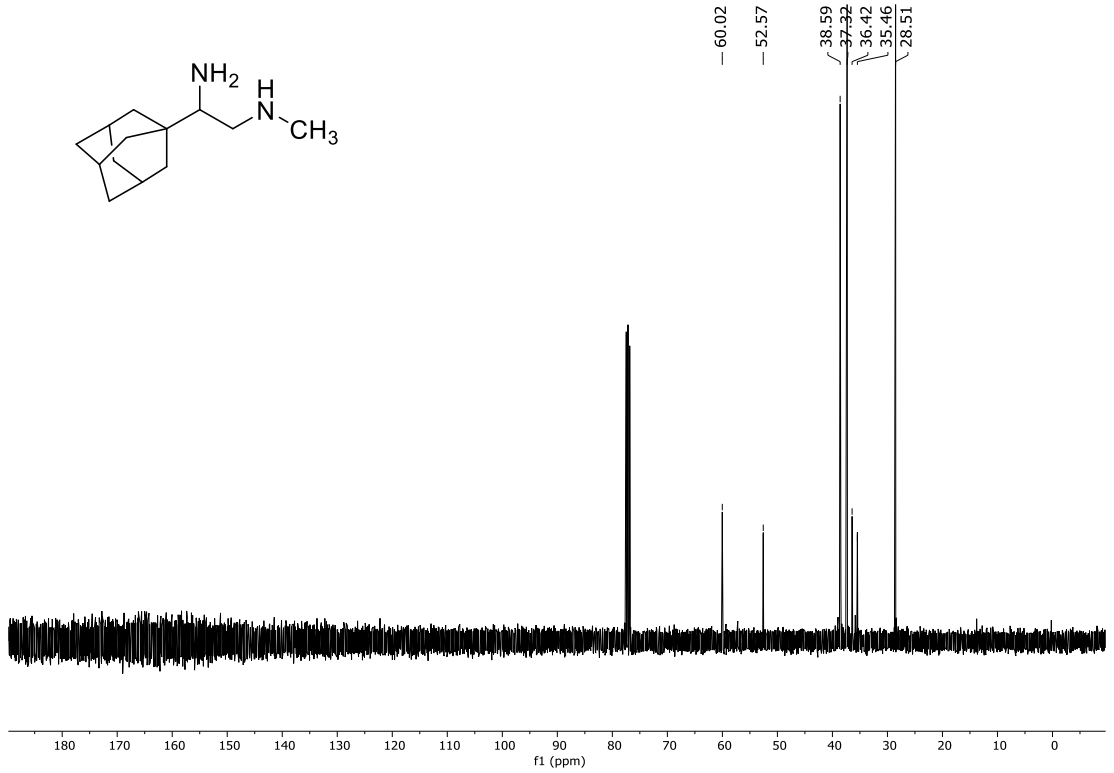

Figure 73. ^{13}C NMR spectrum of 109k (In $CDCl_3$, 101 MHz)

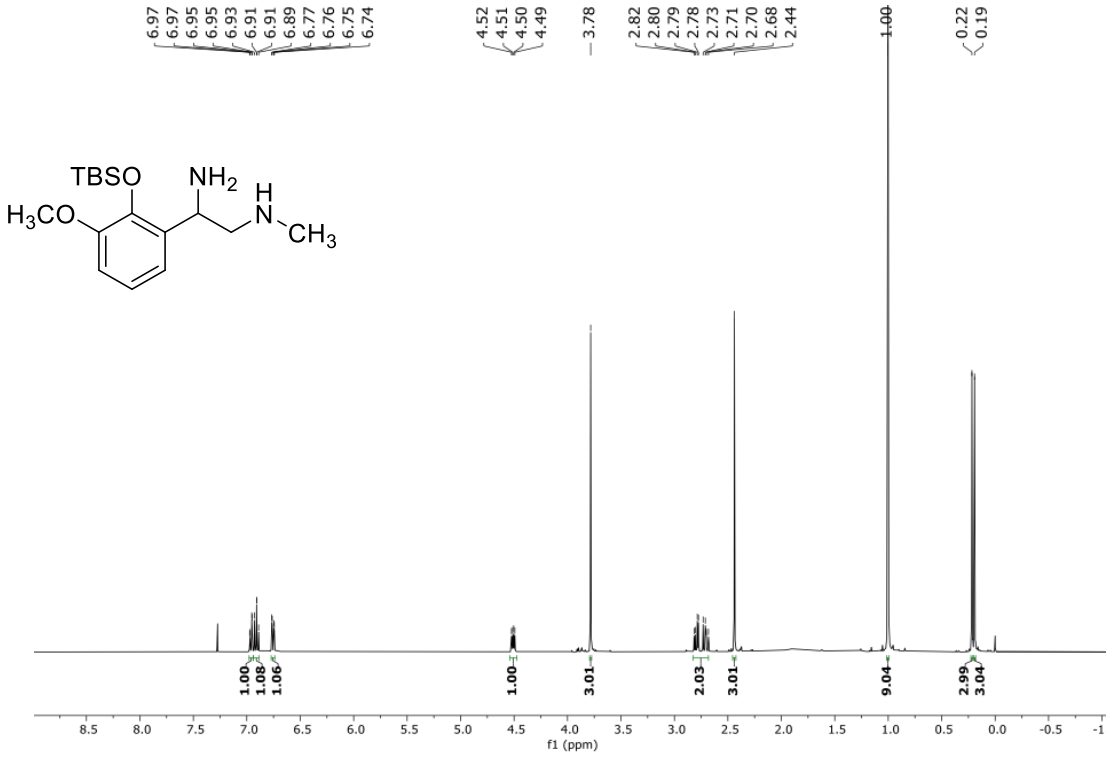

Figure 74. ^{1}H NMR spectrum of 109l (In $CDCl_3$, 400 MHz)

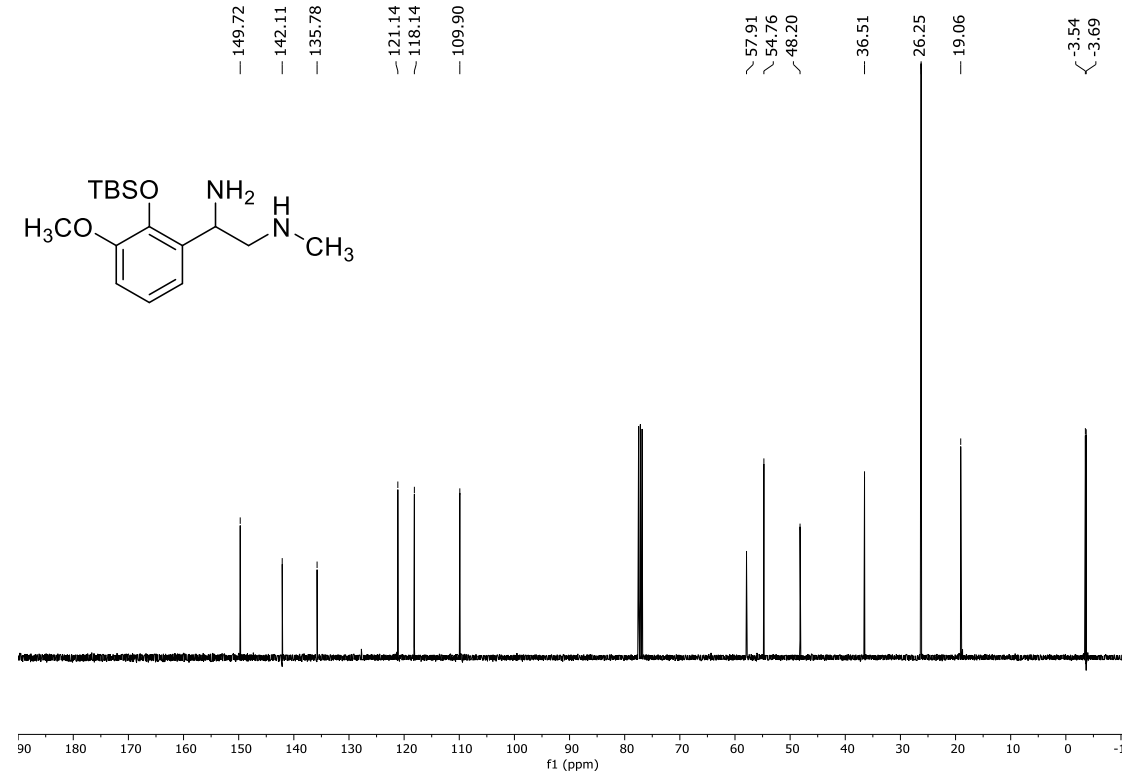

Figure 75. ^{13}C NMR spectrum of 109l (In $CDCl_3$, 101 MHz)

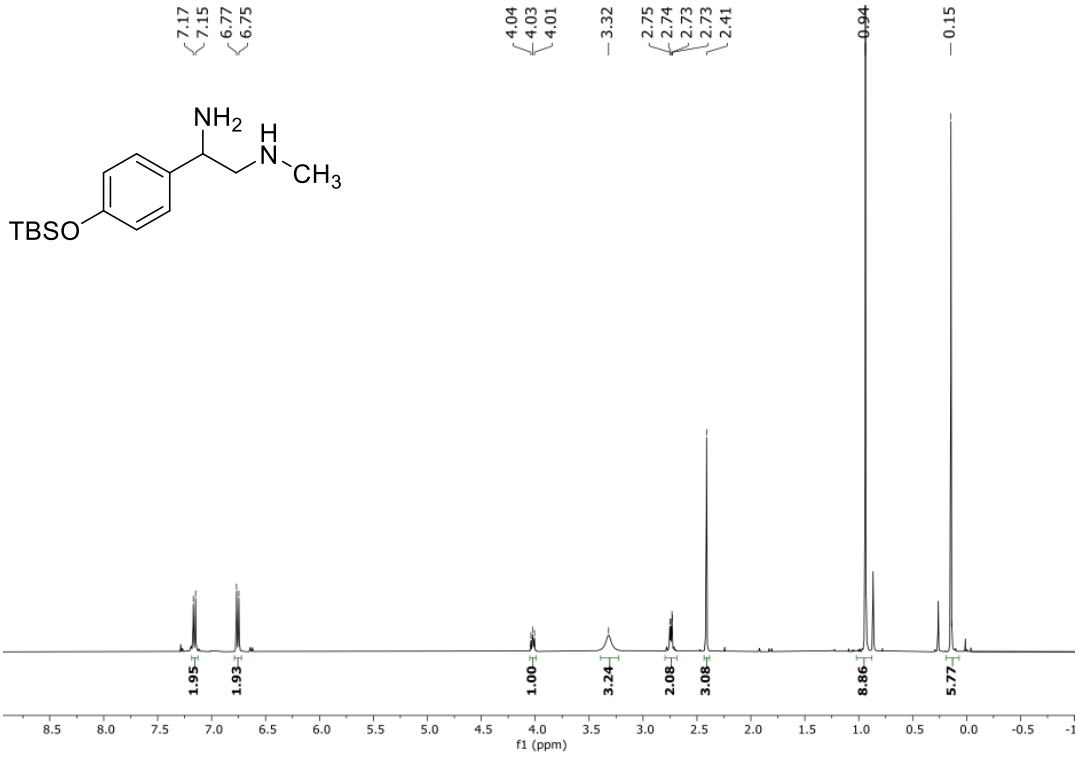

Figure 76. ^{1}H NMR spectrum of 109m (In $CDCl_3$, 400 MHz)

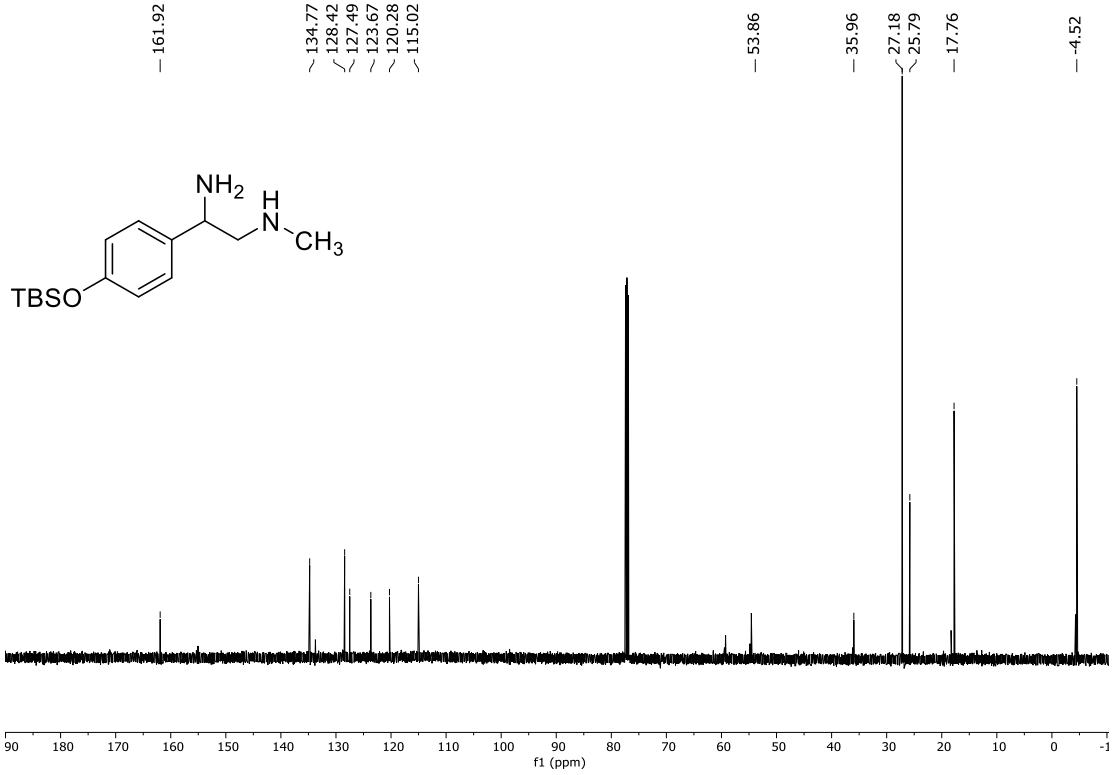

Figure 77. ^{13}C NMR spectrum of 109m (In $CDCl_3$, 126 MHz)

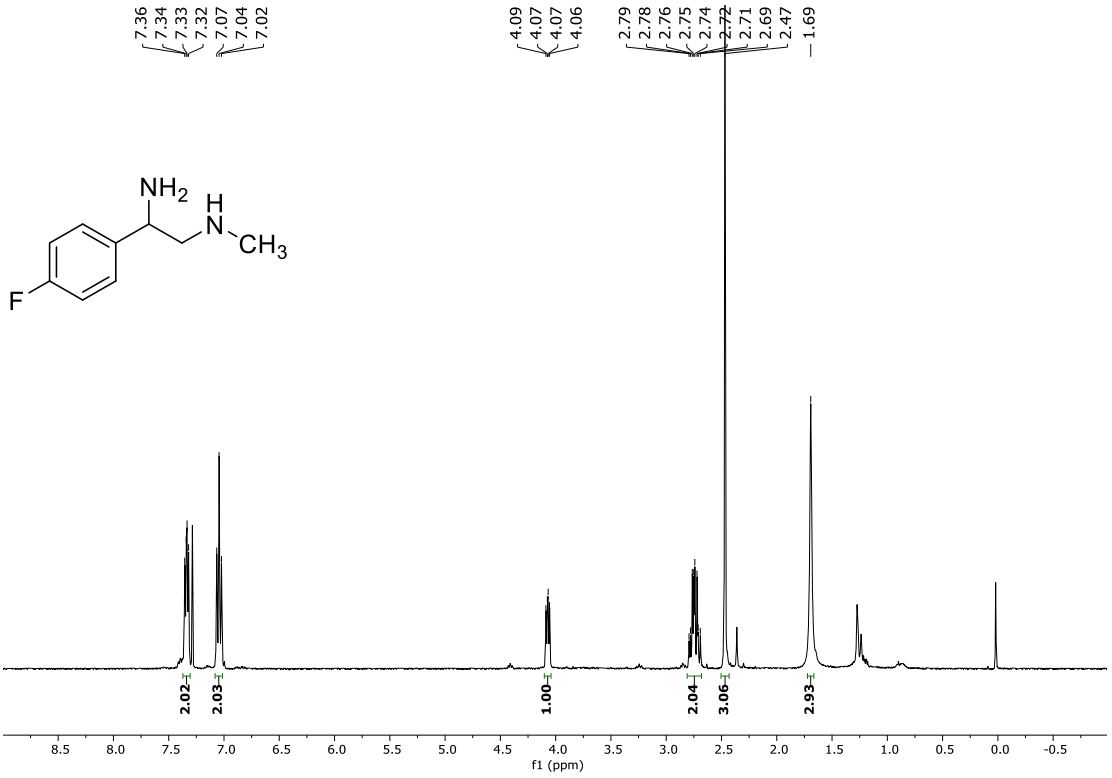

Figure 78. ^{1}H NMR spectrum of 109n (In $CDCl_3$, 400 MHz)

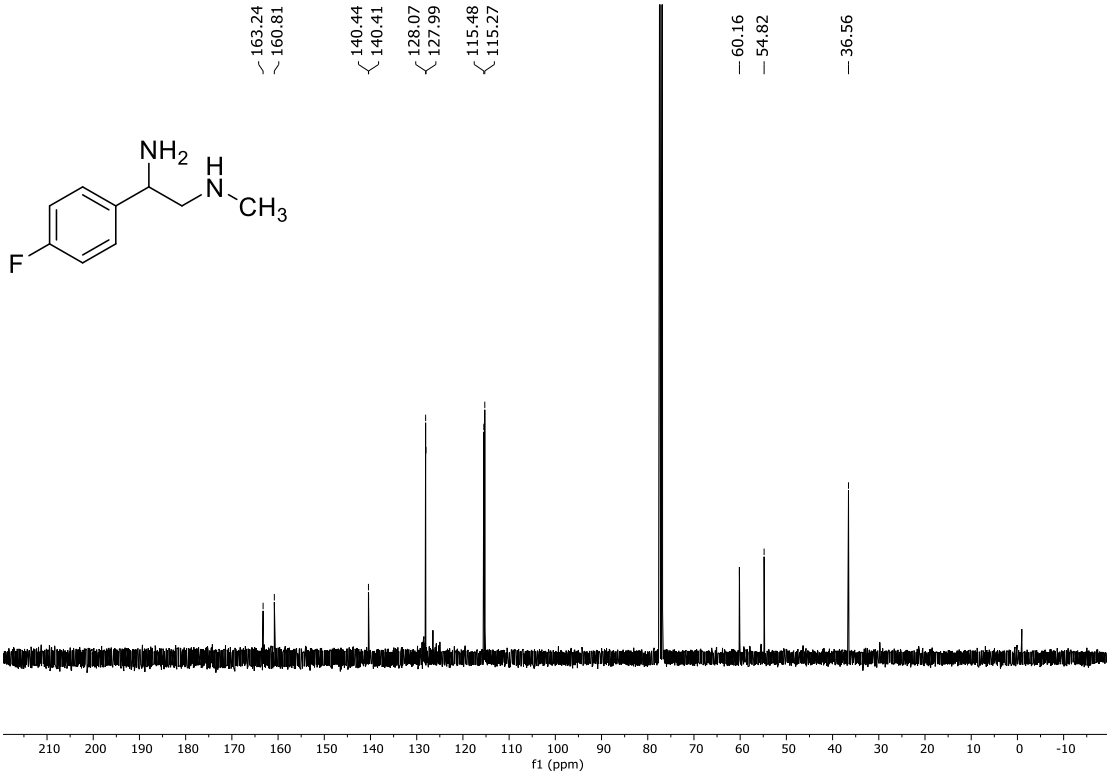

Figure 79. ^{13}C NMR spectrum of 109n (In $CDCl_3$, 101 MHz)

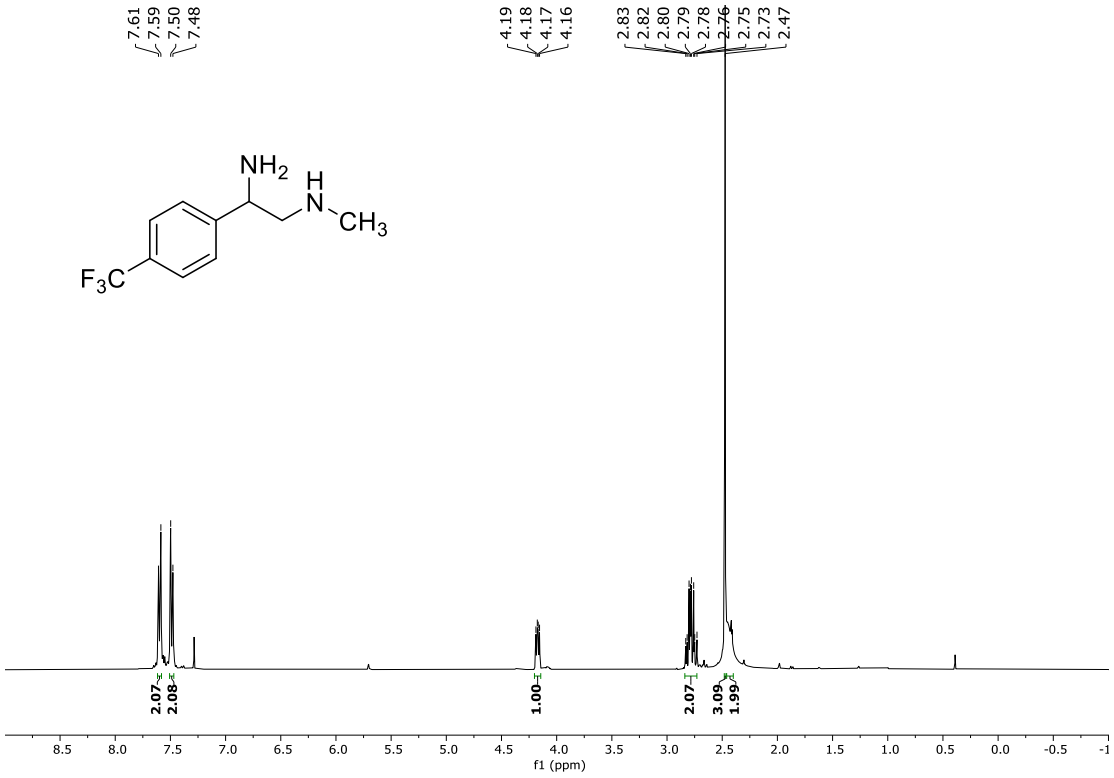

Figure 80. ^{1}H NMR spectrum of 109o (In $CDCl_3$, 400 MHz)

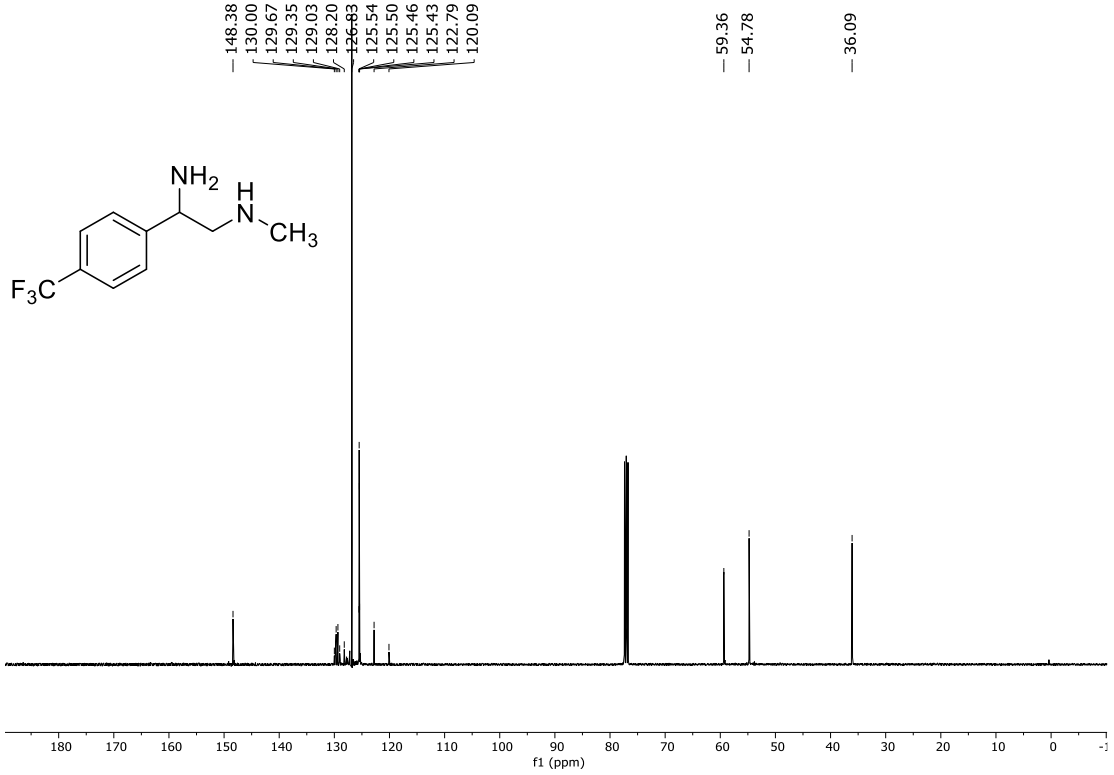

Figure 81. ^{13}C NMR spectrum of 109o (In $CDCl_3$, 101 MHz)

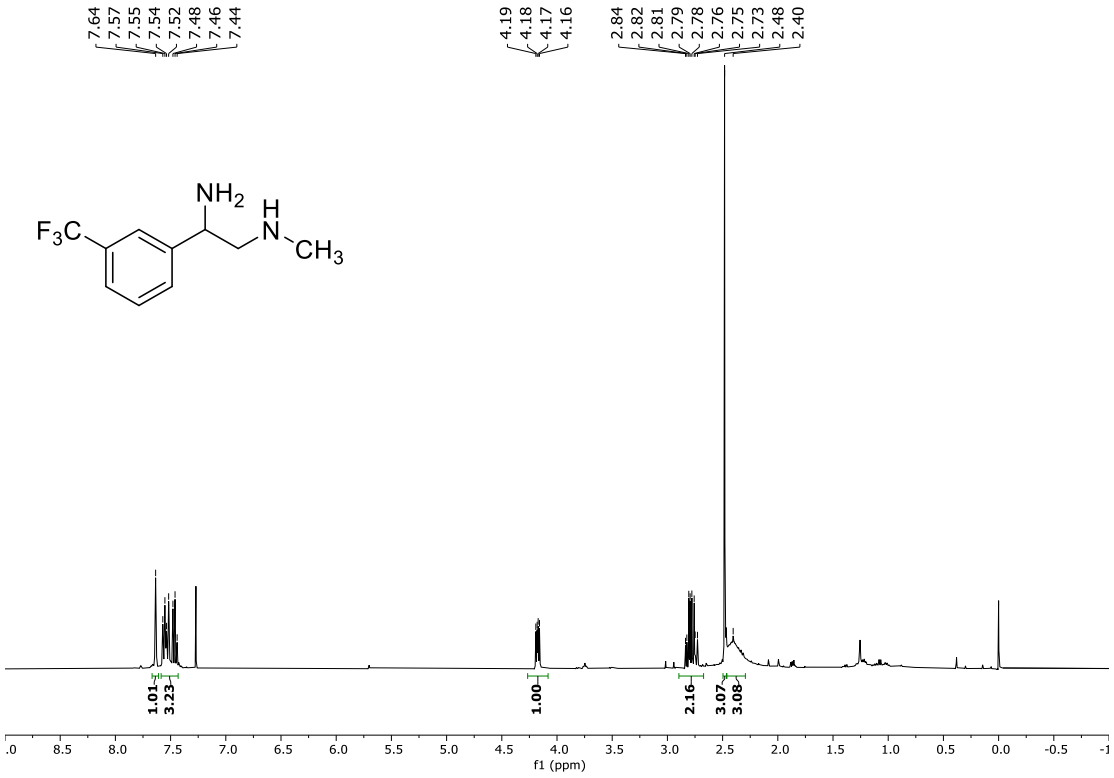

Figure 82. ^{1}H NMR spectrum of **109p** (In $CDCl_3$, 400 MHz)

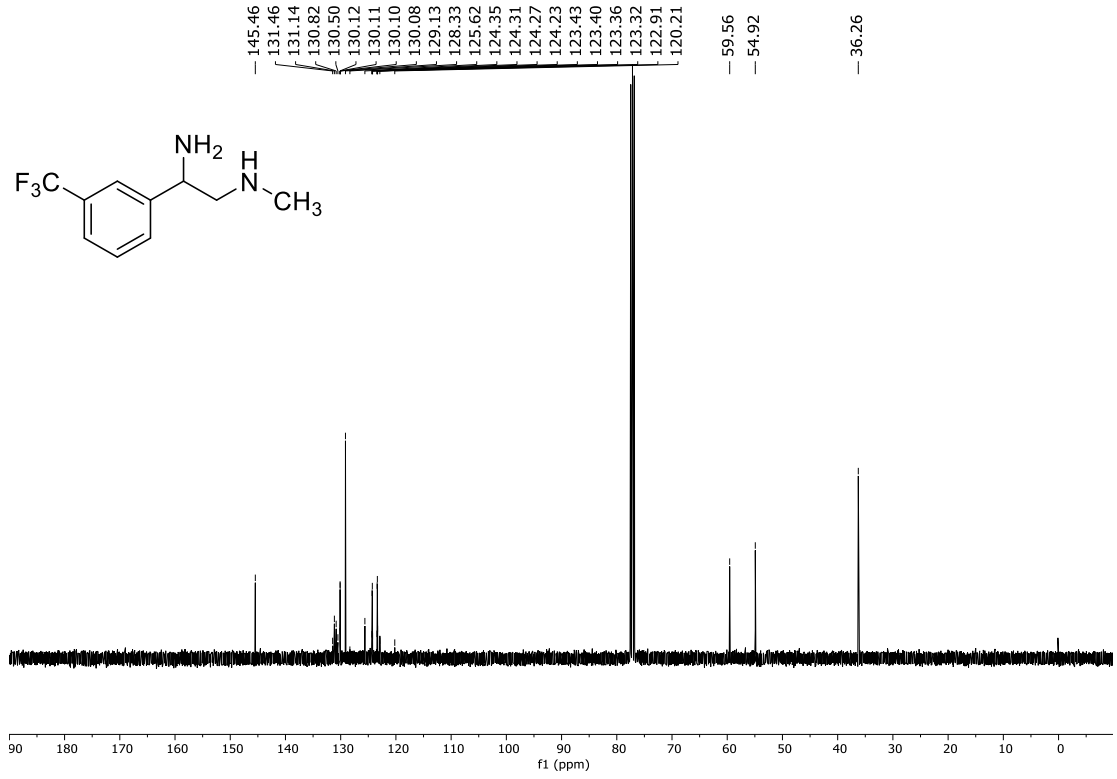

Figure 83. ^{13}C NMR spectrum of **109p** (In $CDCl_3$, 101 MHz)

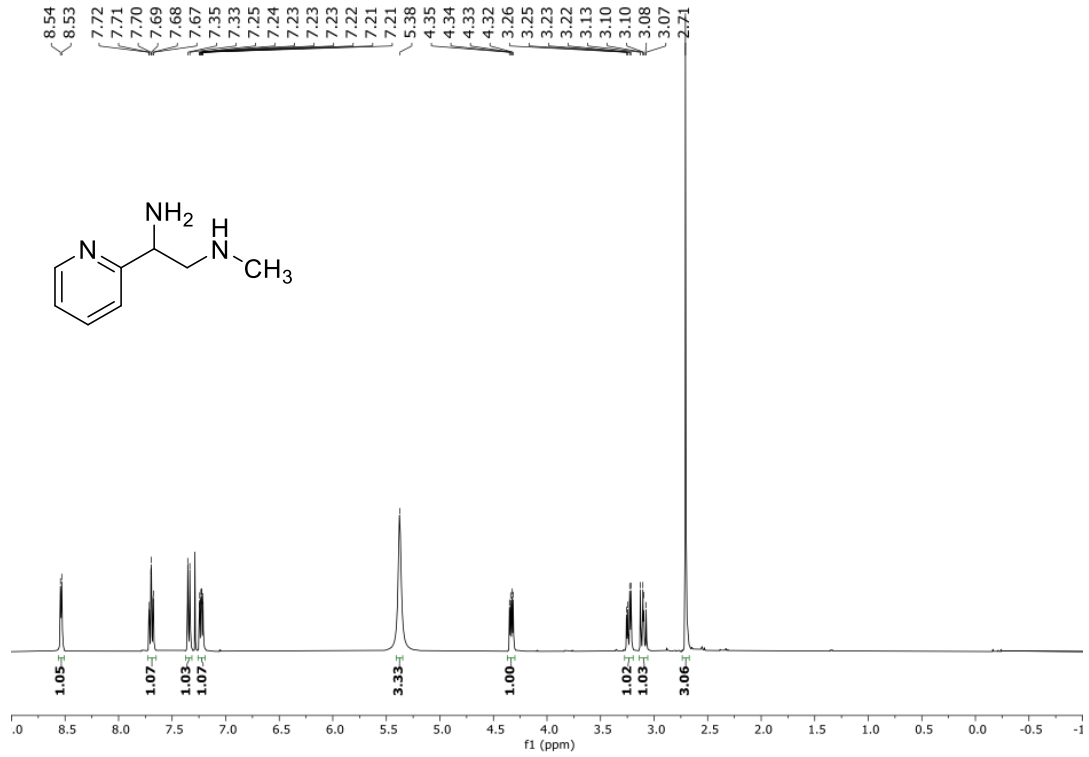

Figure 84. ^{1}H NMR spectrum of 109q (In $CDCl_3$, 400 MHz)

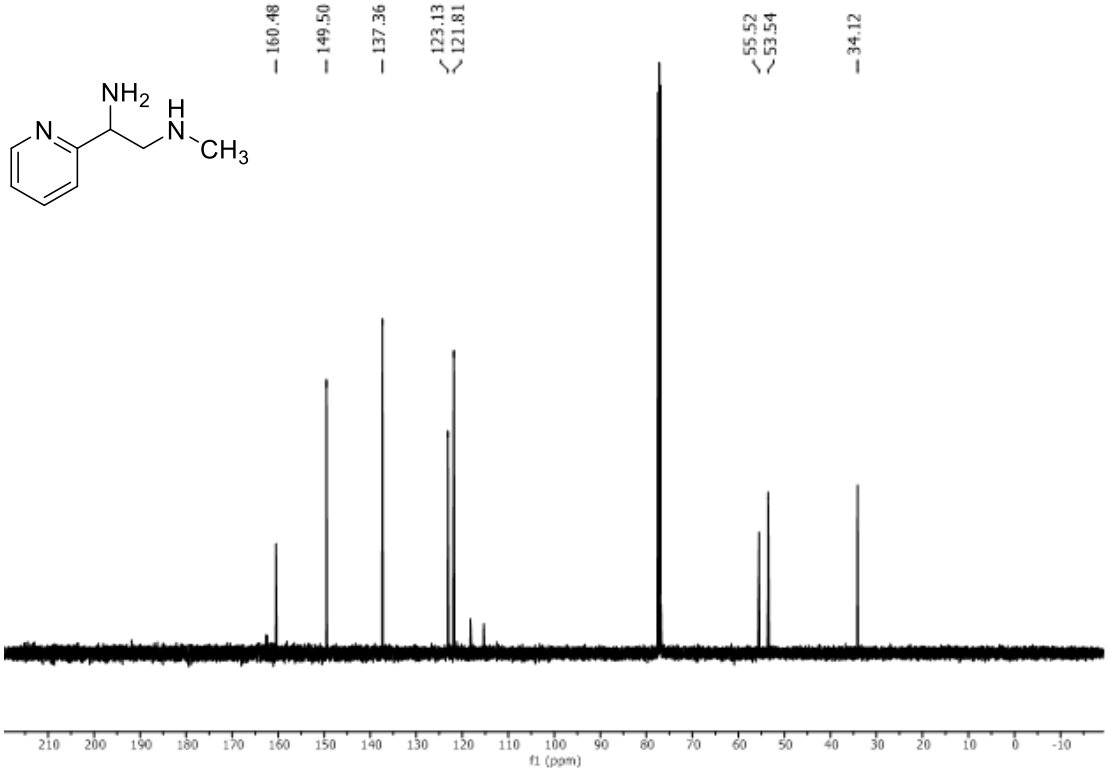

Figure 85. ^{13}C NMR spectrum of 109q (In $CDCl_3$, 101 MHz)

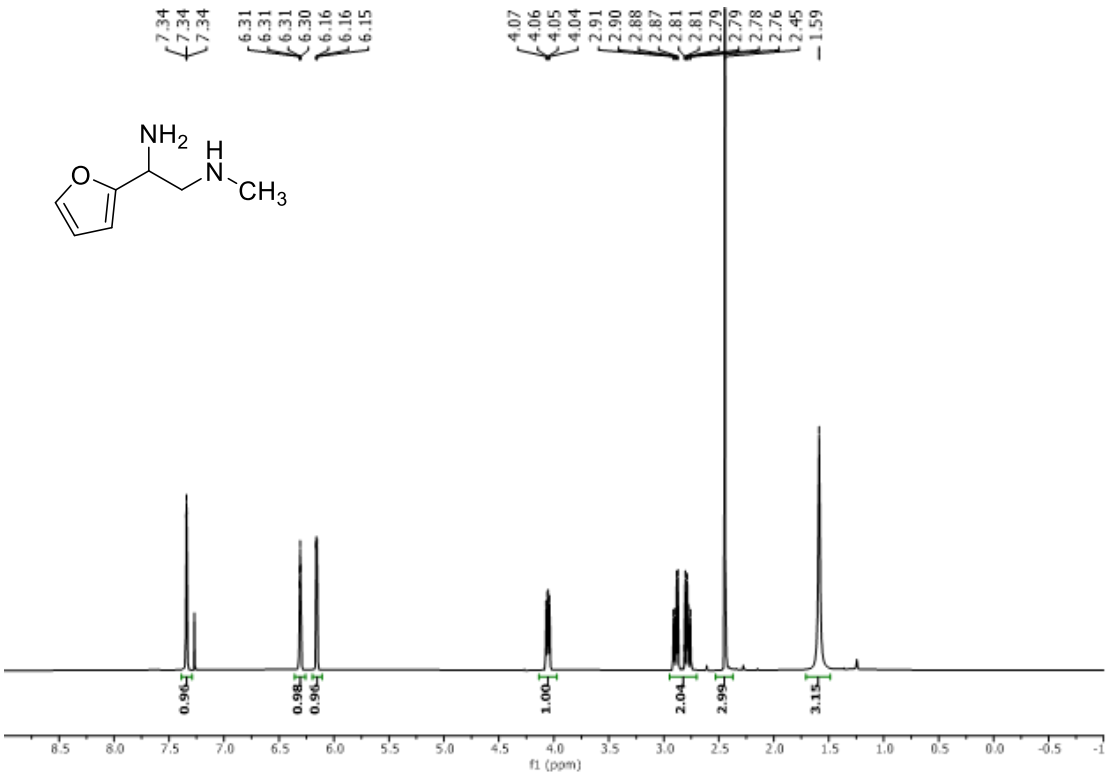

Figure 86. ^{1}H NMR spectrum of **109r** (In $CDCl_3$, 400 MHz)

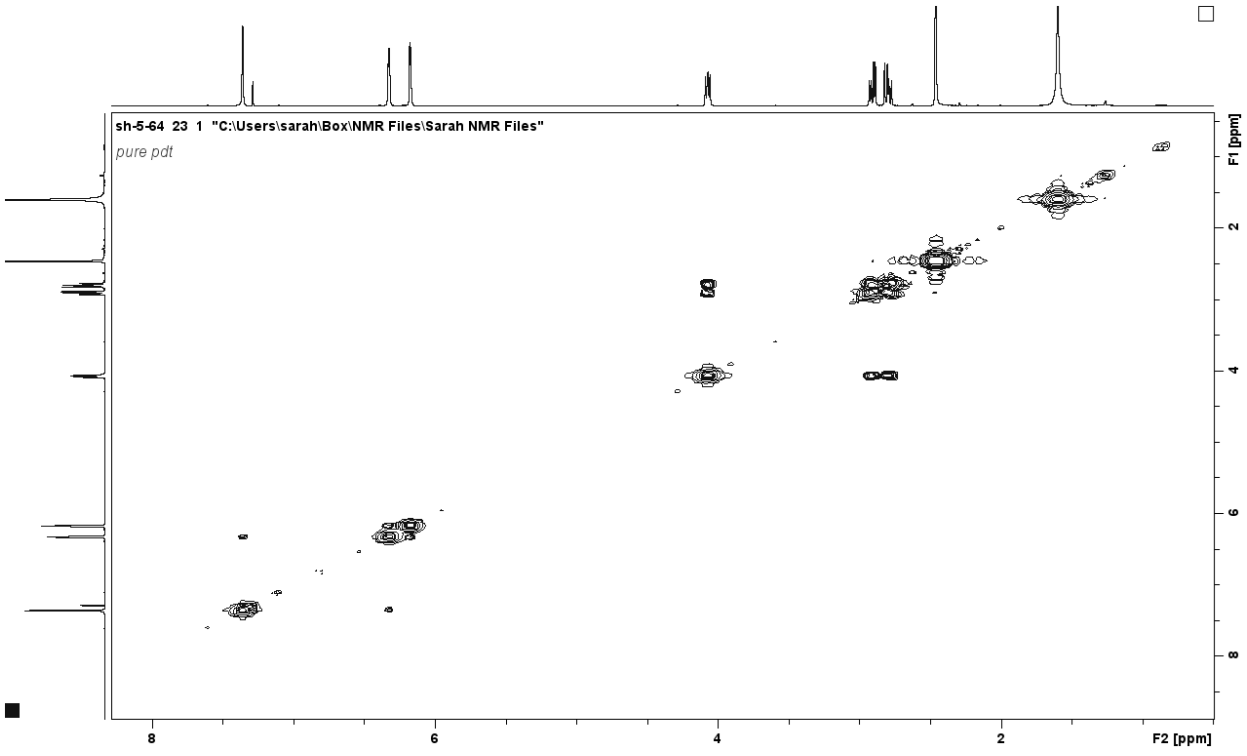

Figure 87. 2D COSY spectrum of 109r (In $CDCl_3$, 400 MHz)

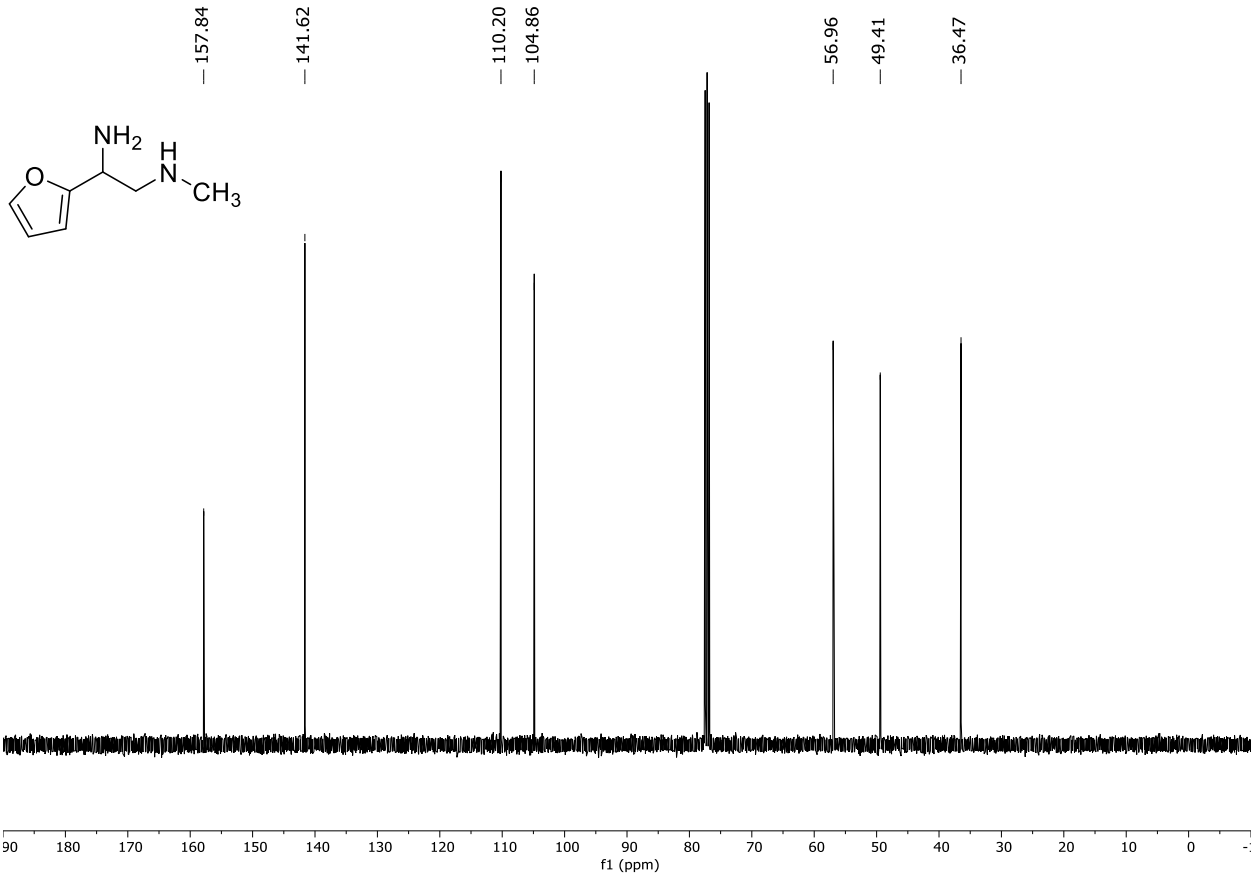

Figure 88. ^{13}C NMR spectrum of 109r (In $CDCl_3$, 101 MHz)

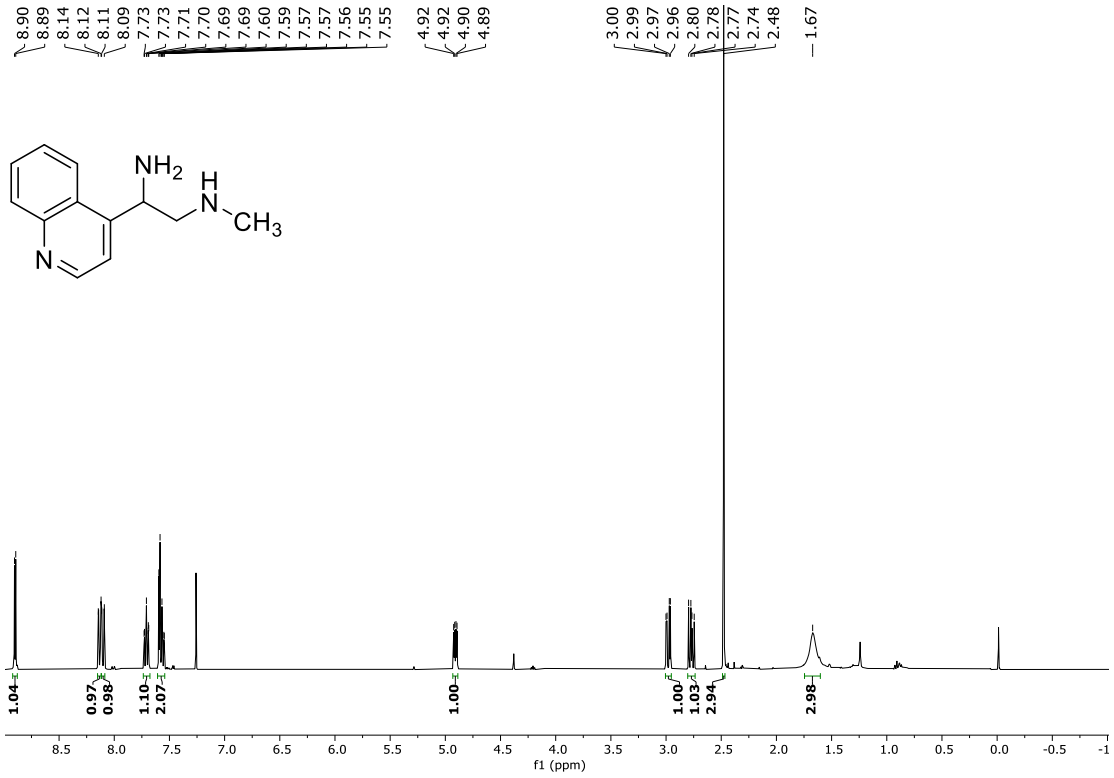

Figure 89. ^{1}H NMR spectrum of 109s (In $CDCl_3$, 400 MHz)

^{13}C NMR spectrum of **109s** (In $CDCl_3$, 101 MHz)

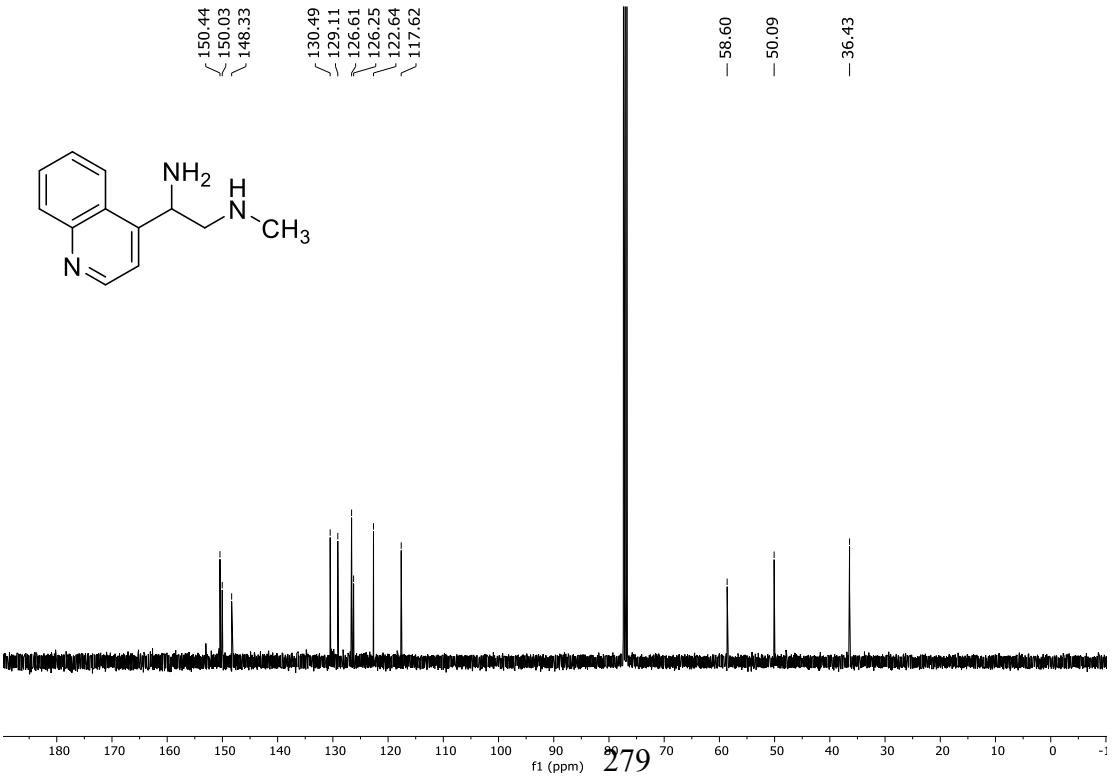

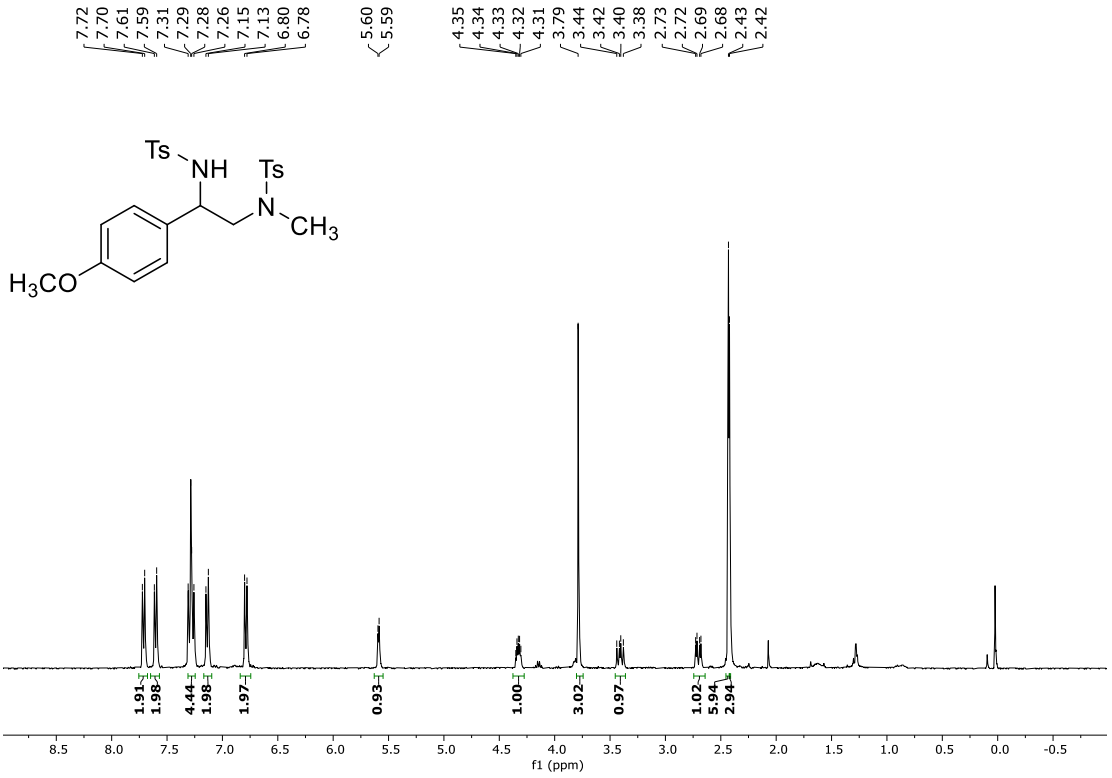

Figure 90. ^{1}H NMR spectrum of 115 (In $CDCl_3$, 400 MHz)

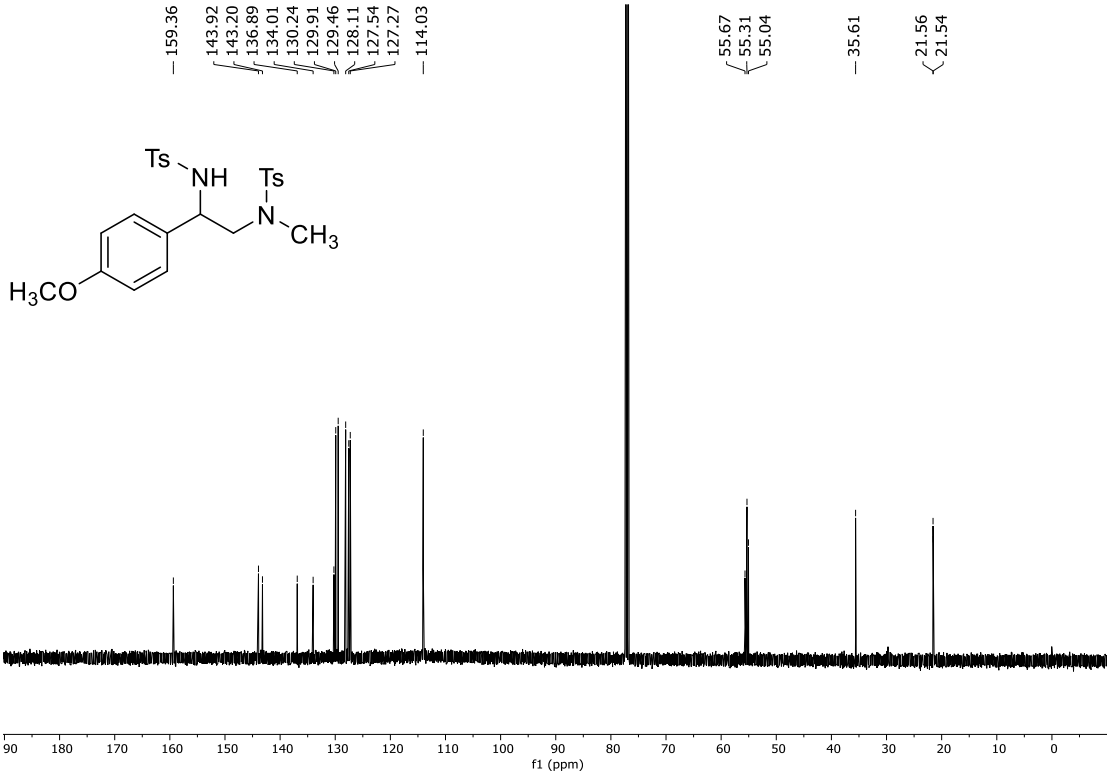

Figure 91. ^{13}C NMR spectrum of 115 (In $CDCl_3$, 126 MHz)

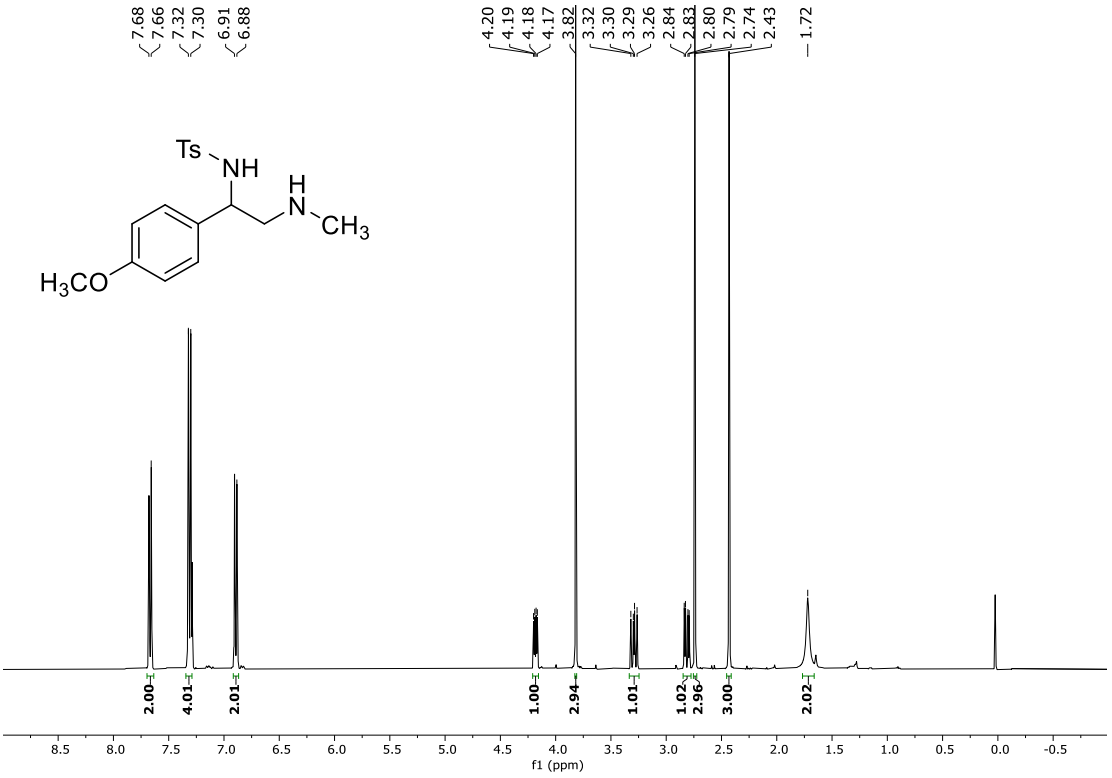

Figure 92. ^{1}H NMR spectrum of 114 (In $CDCl_3$, 400 MHz)

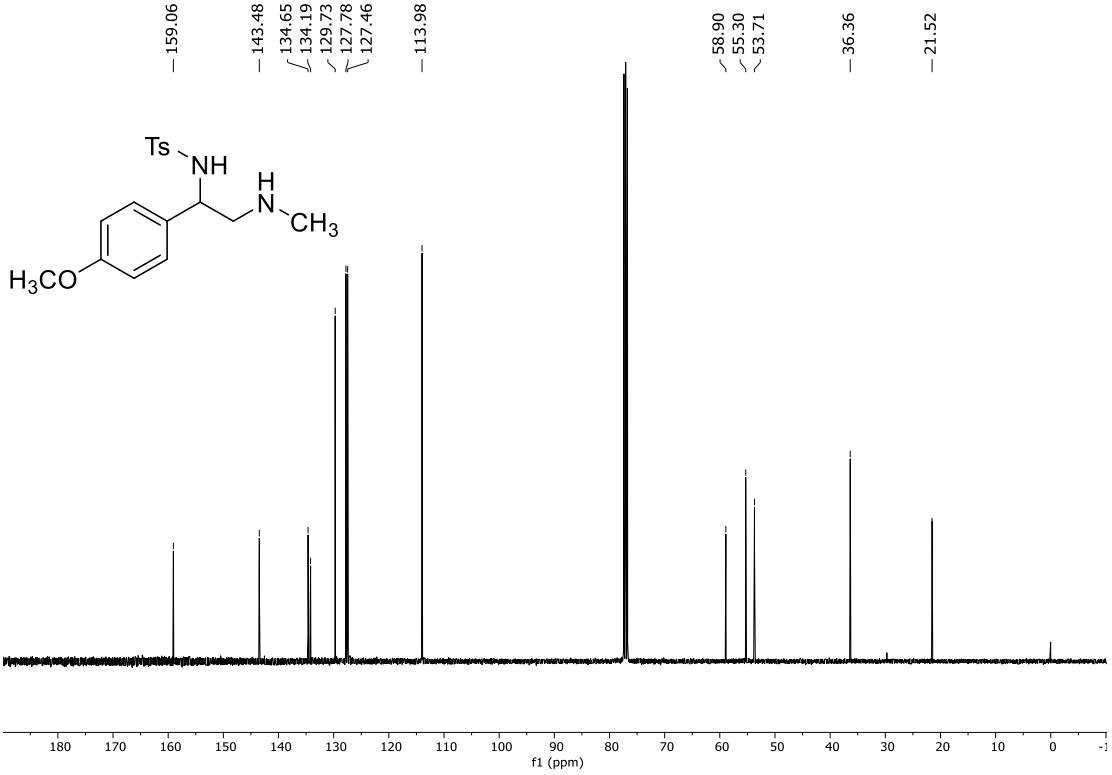

Figure 93. ^{13}C NMR spectrum of 114 (In $CDCl_3$, 101 MHz)

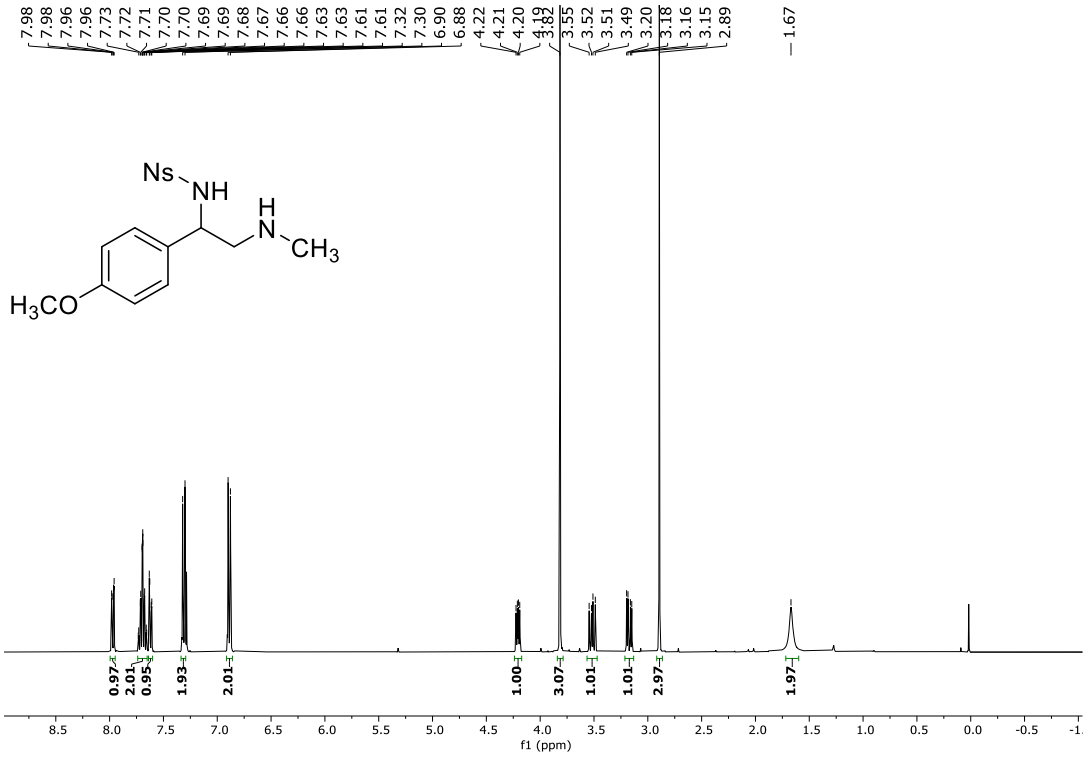

Figure 94. ^{1}H NMR spectrum of 113 (In $CDCl_3$, 400 MHz)

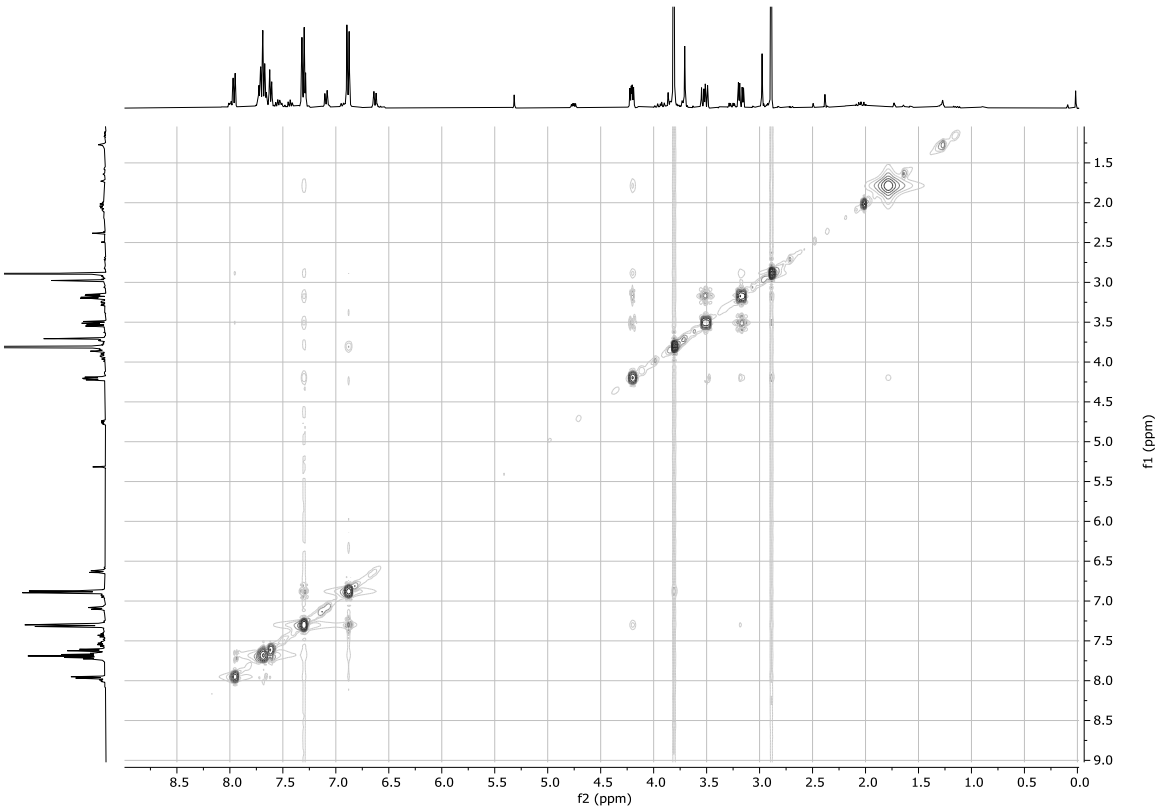

Figure 95. NOESY spectrum of 113 (In $CDCl_3$, 400 MHz)

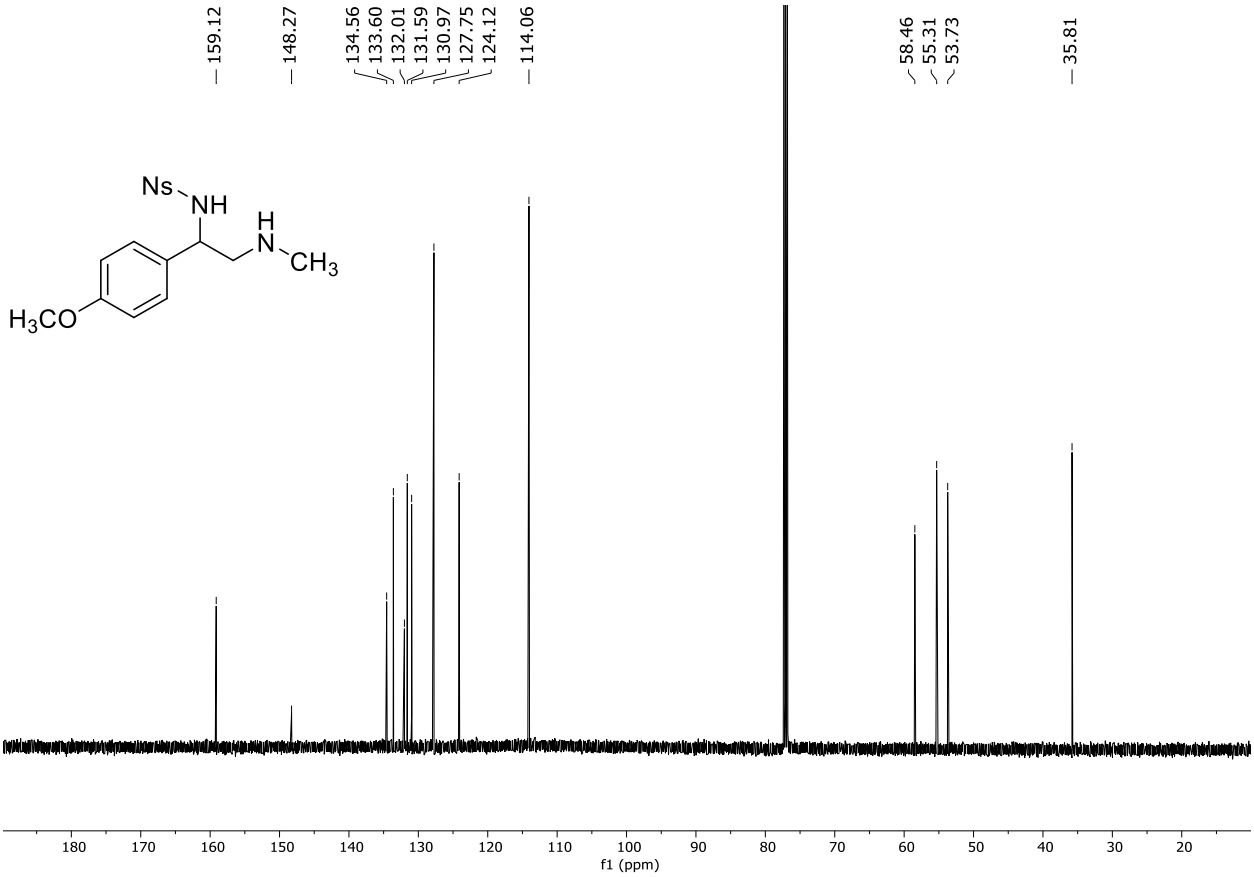

Figure 96. ^{13}C NMR spectrum of 113 (In $CDCl_3$, 126 MHz)

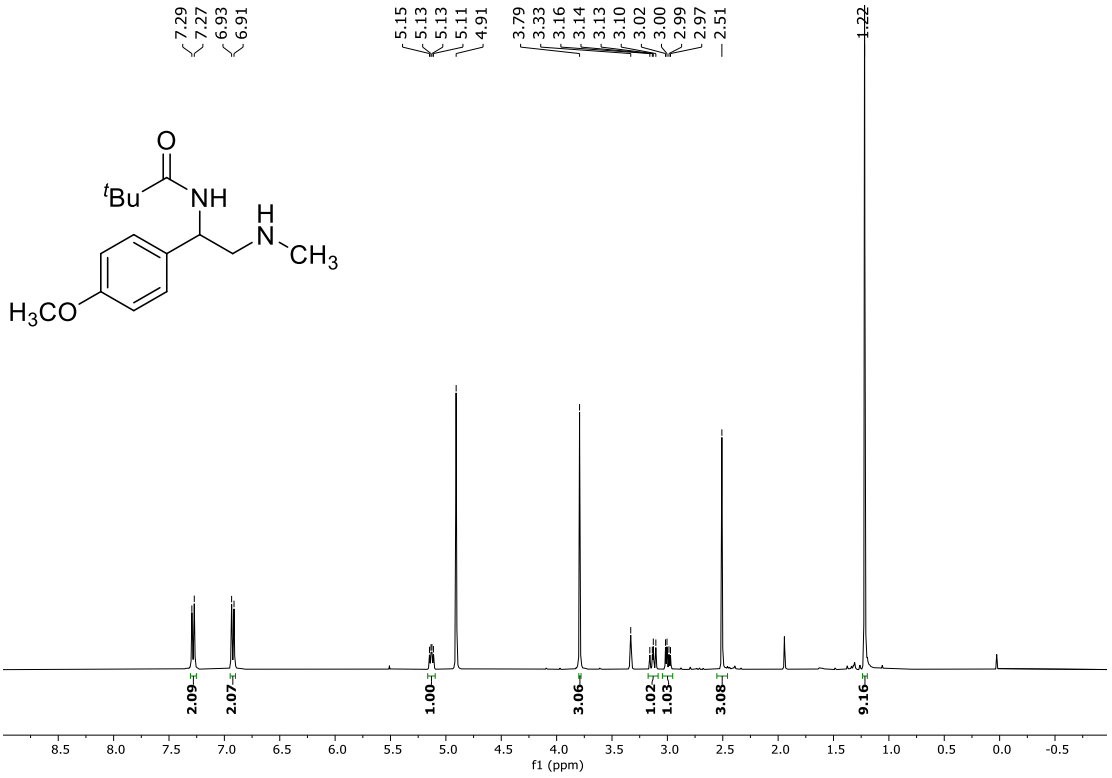

Figure 97. ^{1}H NMR spectrum of 112 (In MeOD, 400 MHz)

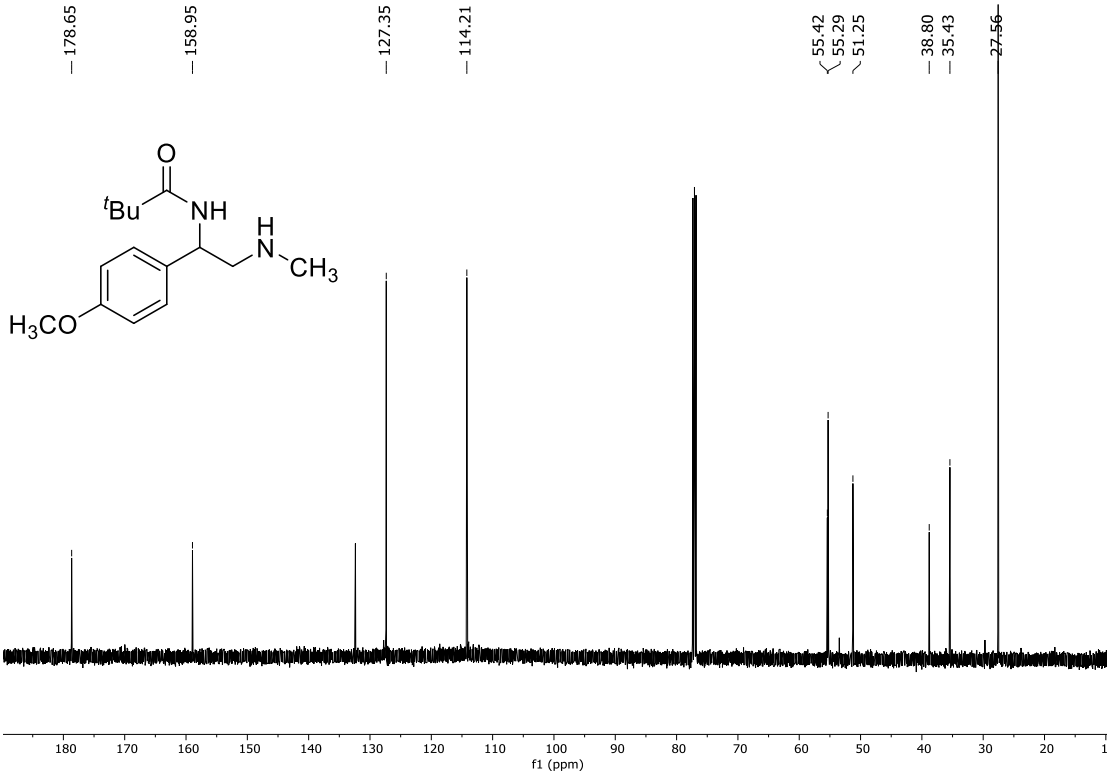

Figure 98. ^{13}C NMR spectrum of 112 (In $CDCl_3$, 126 MHz)

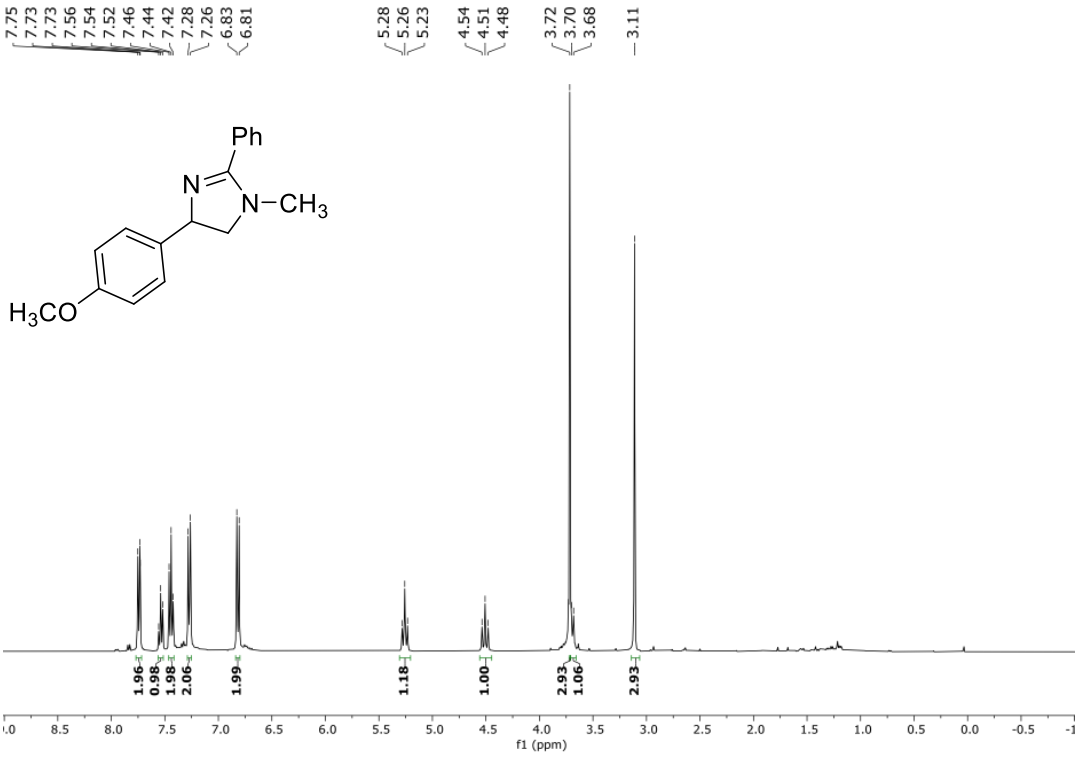

Figure 99. ^{1}H NMR spectrum of 117 (In $CDCl_3$, 400 MHz)

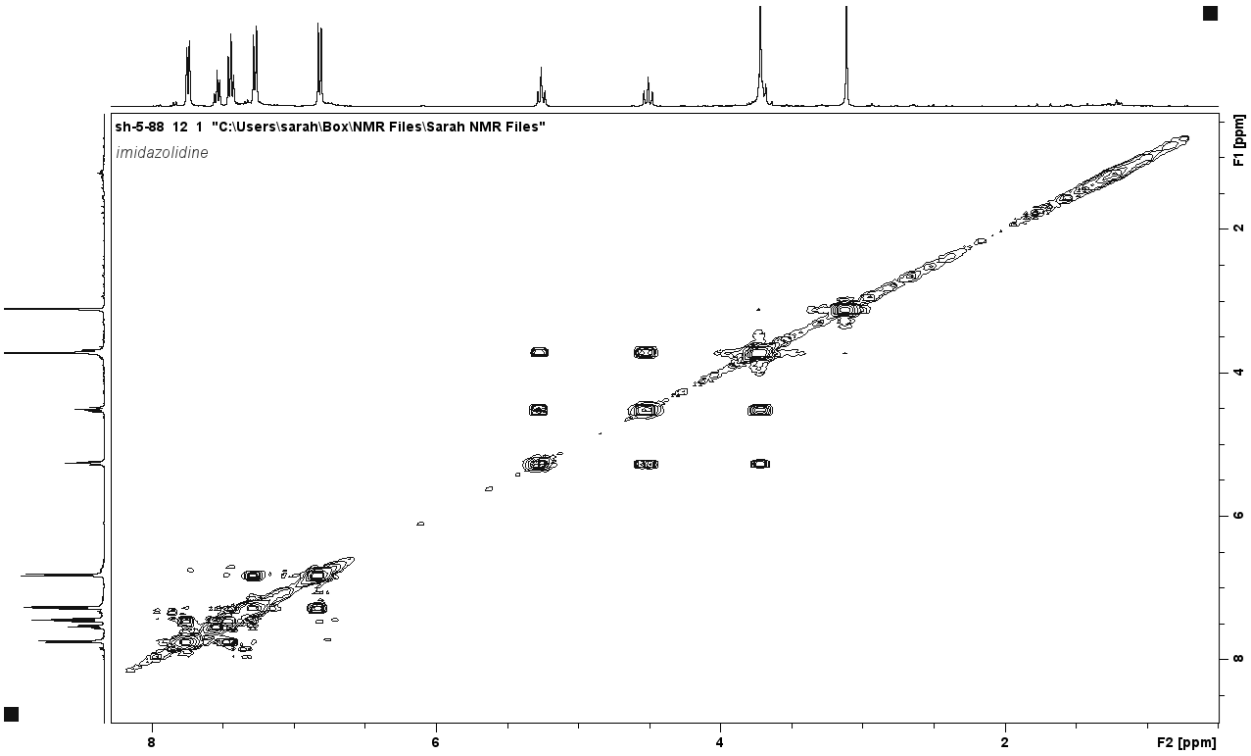

Figure 100. COSY spectrum of **117** (In $CDCl_3$, 400 MHz)

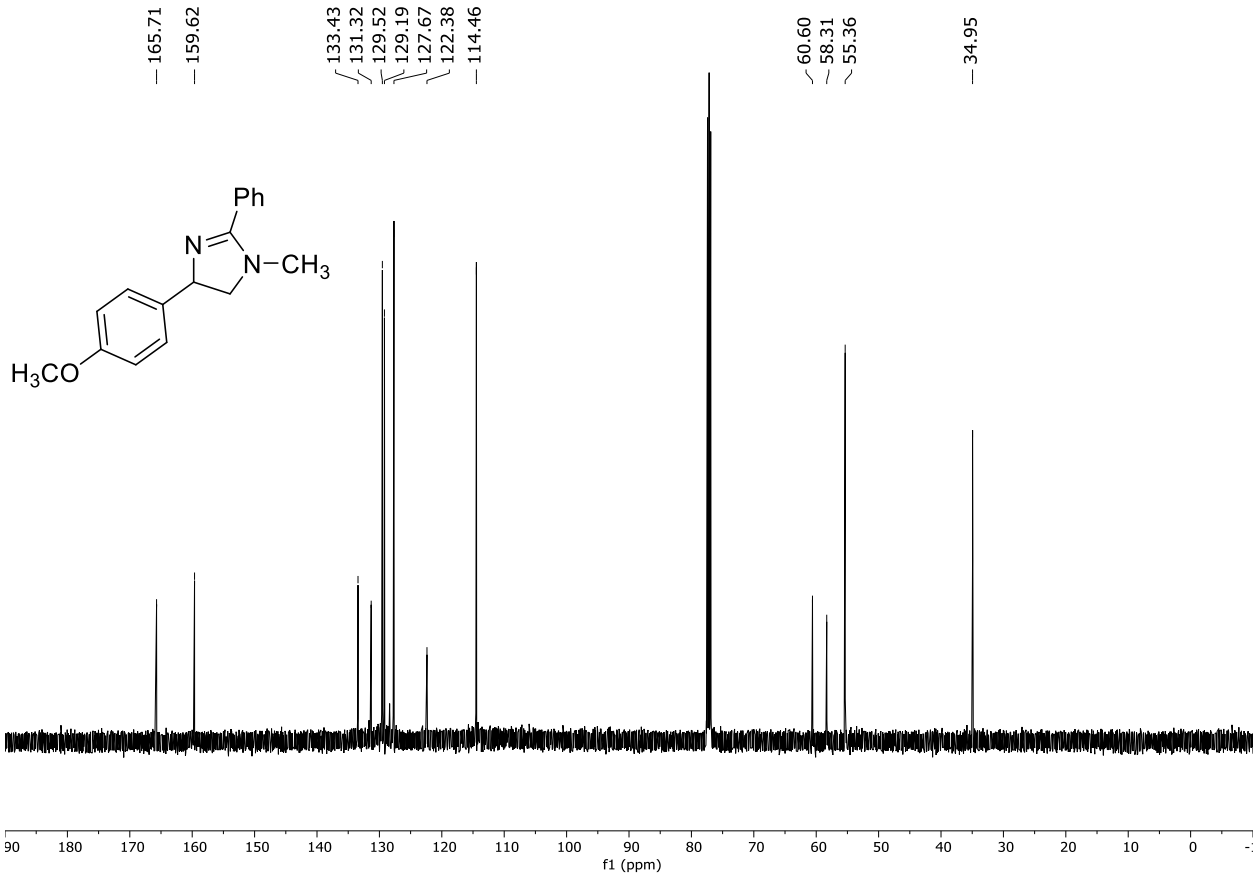

Figure 101. ^{13}C NMR spectrum of 117 (In $CDCl_3$, 126 MHz)

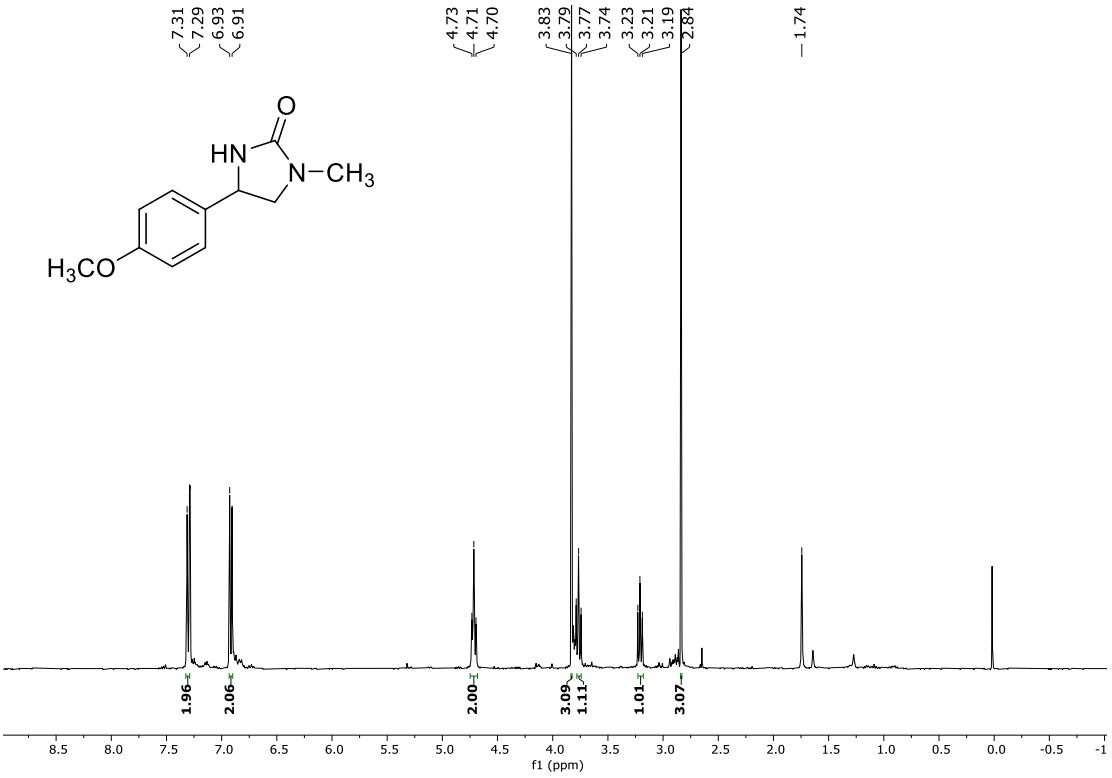

Figure 102. ^{1}H NMR spectrum of 118 (In $CDCl_3$, 400 MHz)

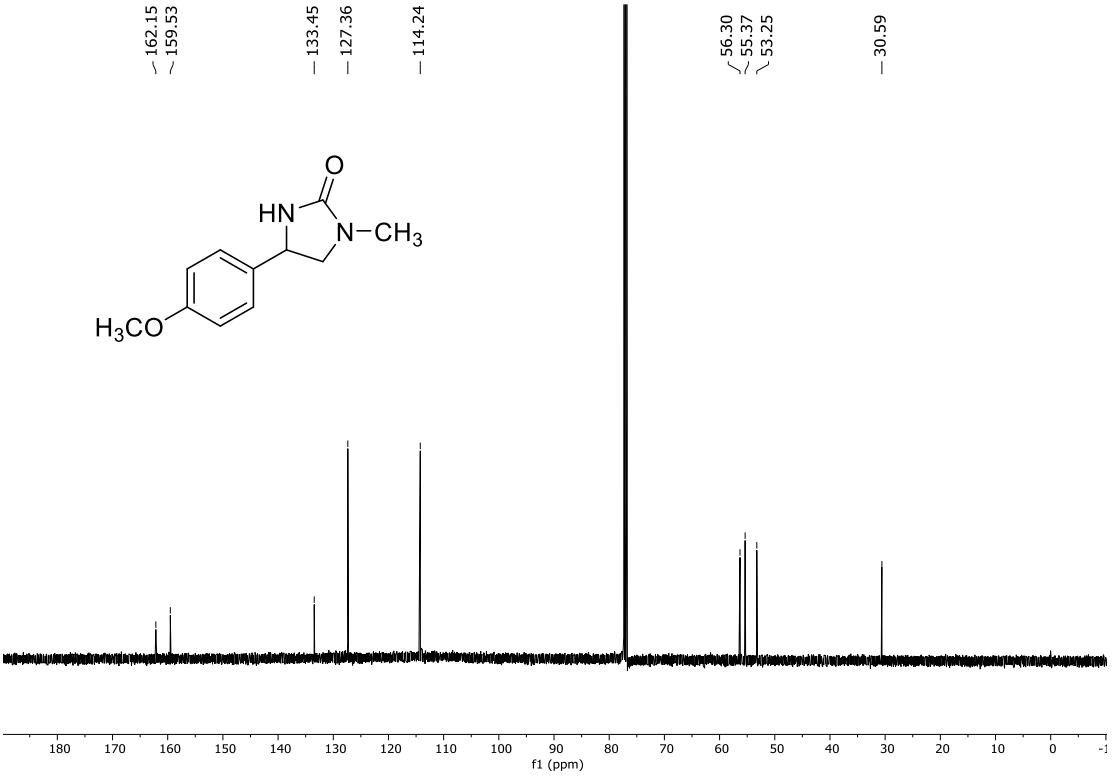

Figure 103. ^{13}C NMR spectrum of 118 (In $CDCl_3$, 126 MHz)

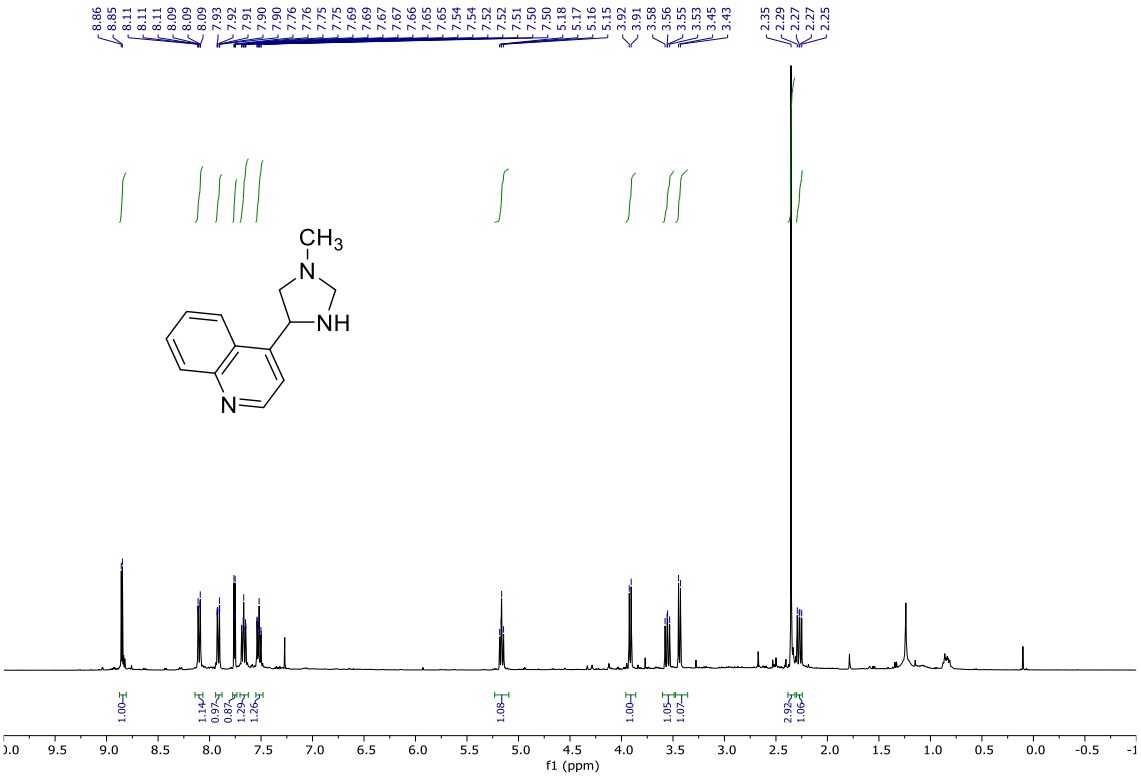

Figure 104. ^{1}H NMR spectrum of 200a (in $CDCl_3$, 400 MHz)

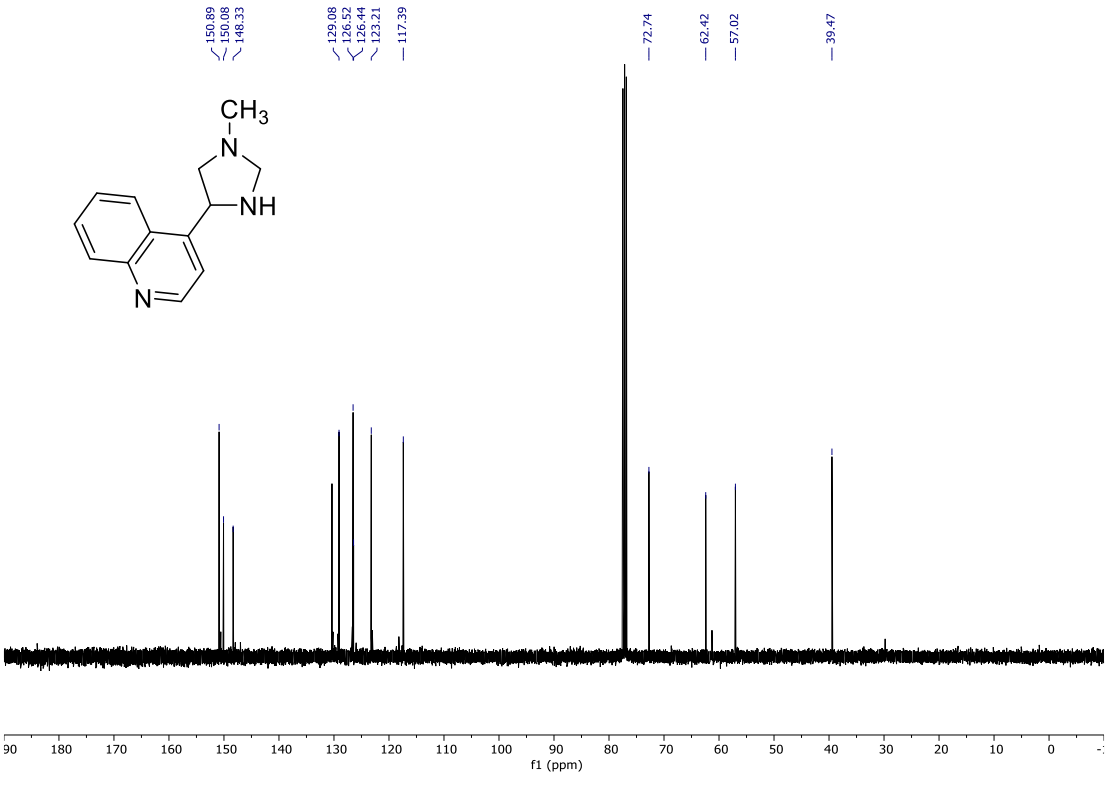

Figure 105. ^{13}C NMR spectrum of 200a (In $CDCl_3$, 101 MHz)

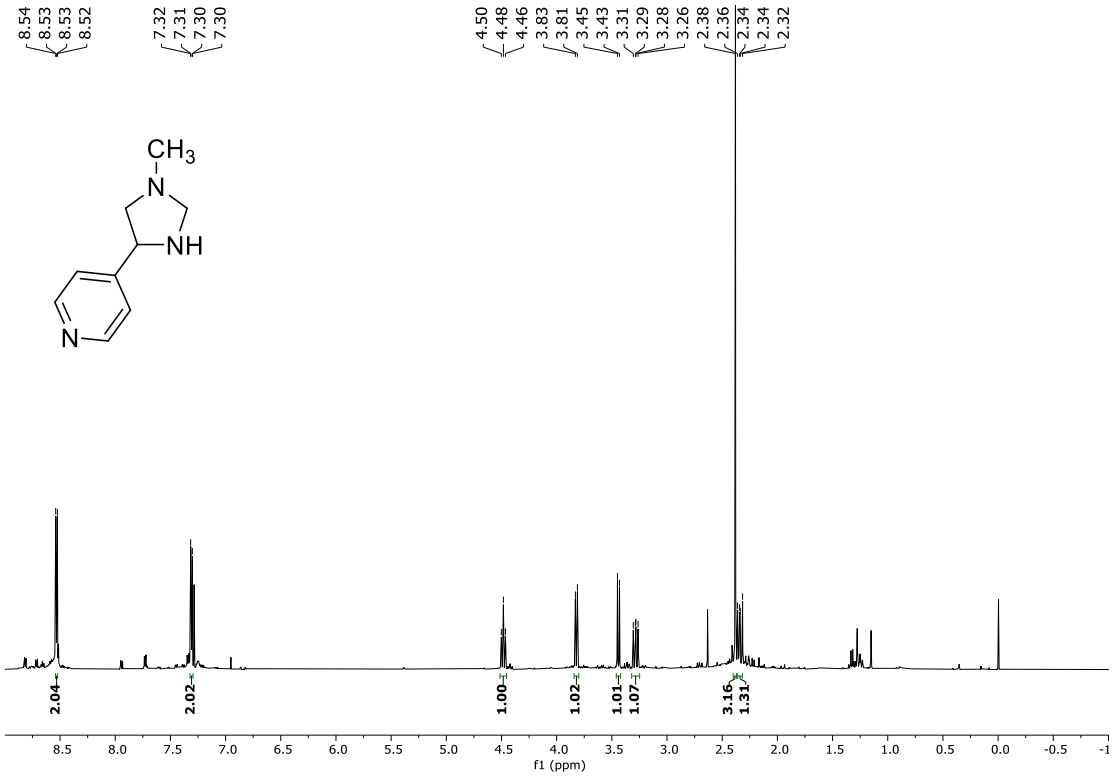

Figure 106. ^{1}H NMR spectrum of 200b (In $CDCl_3$, 400 MHz)

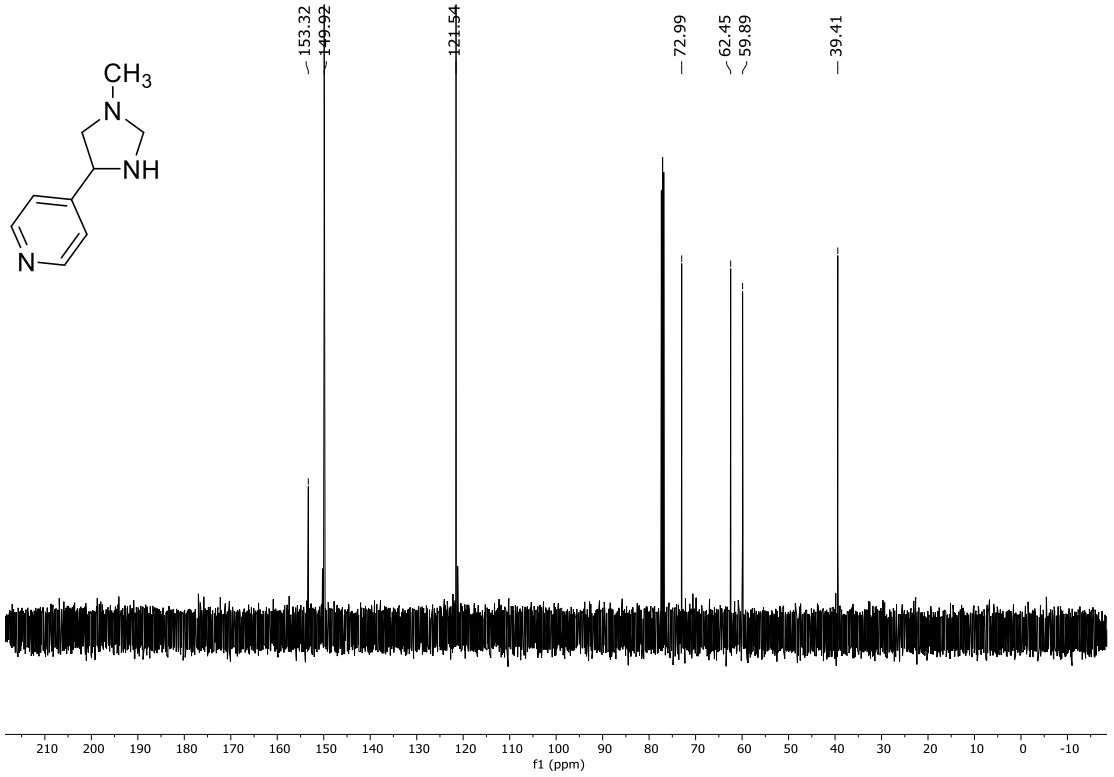

Figure 107. ^{13}C NMR spectrum of 200t (In $CDCl_3$, 101 MHz)

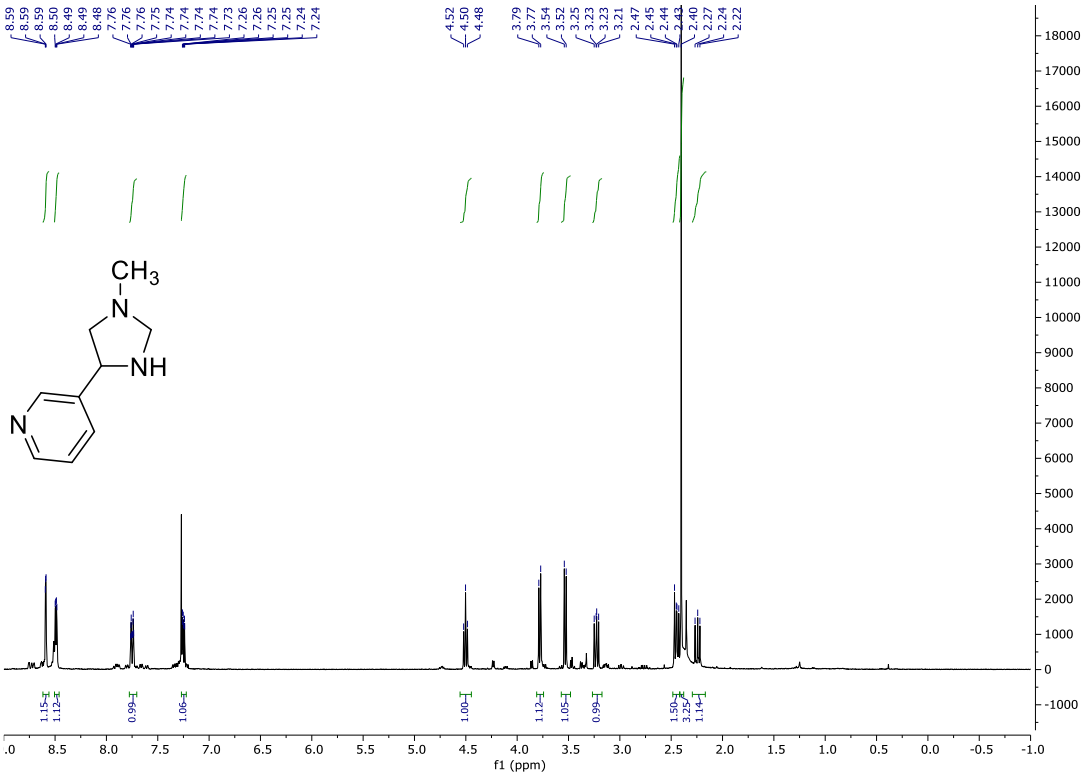

Figure 108. ^{1}H NMR spectrum of 200c (in $CDCl_3$, 400 MHz)

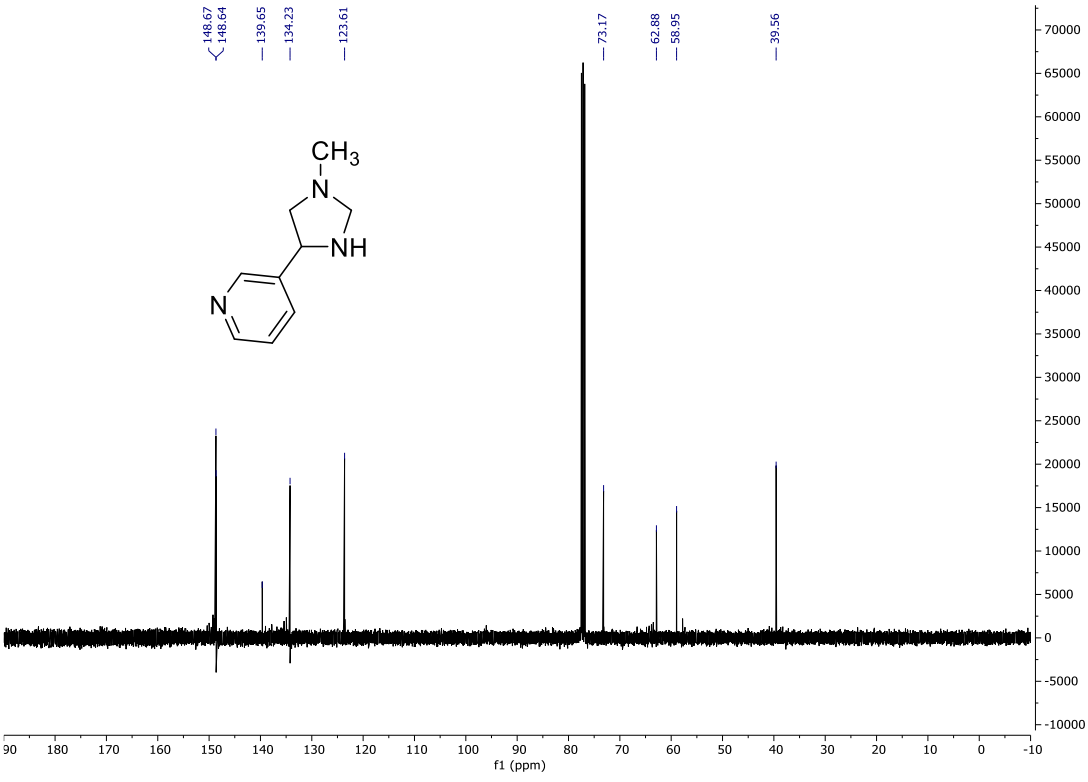

Figure 109.^{13}C NMR spectrum of 200c (In $CDCl_3$, 101 MHz)

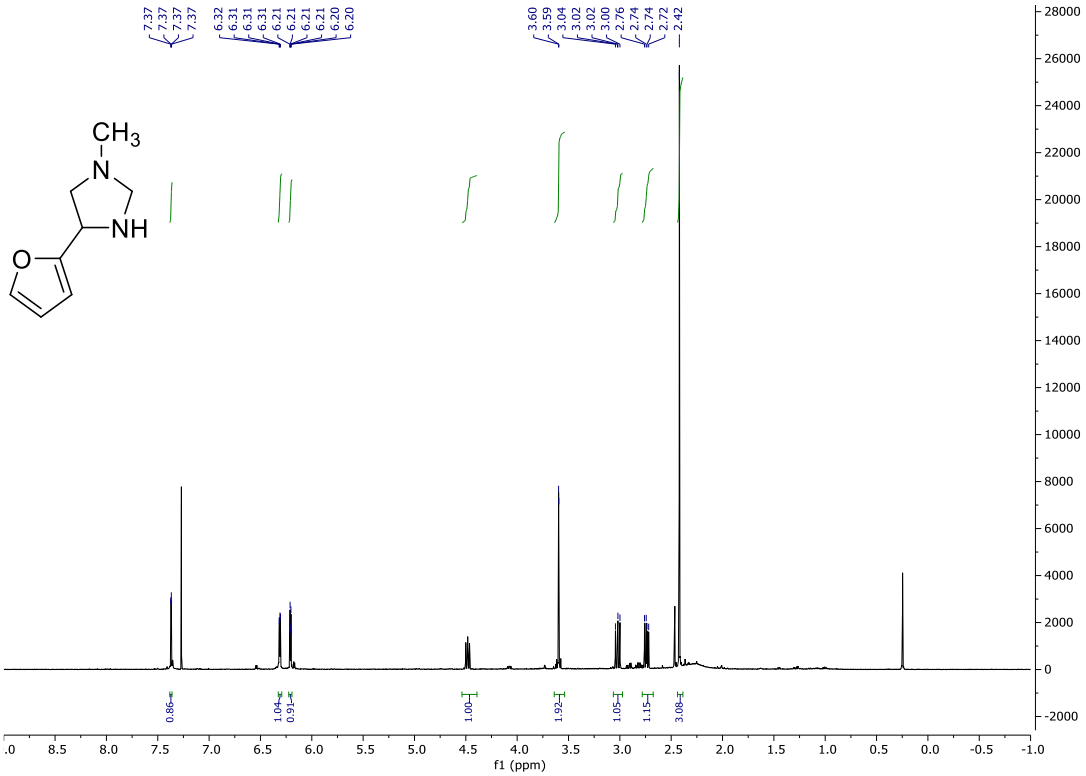

Figure 110. ^{1}H NMR spectrum of 200d (in $CDCl_3$, 400 MHz)

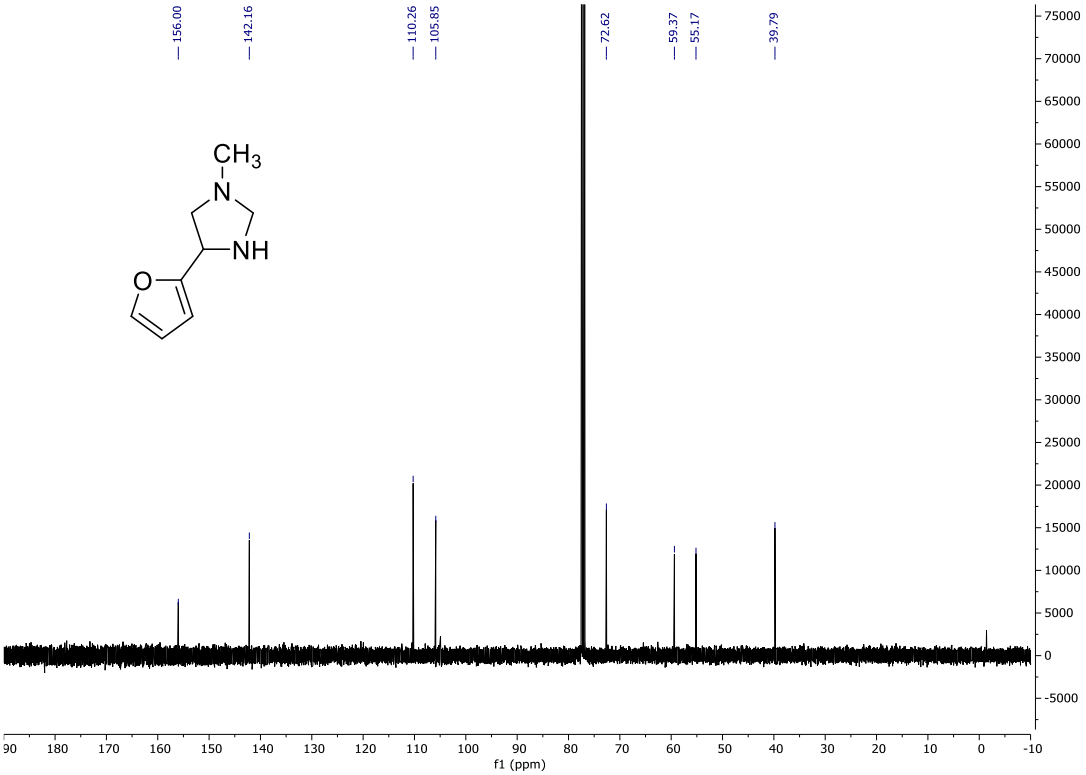

Figure 111. ^{13}C NMR spectrum of 200d (In $CDCl_3$, 101 MHz)

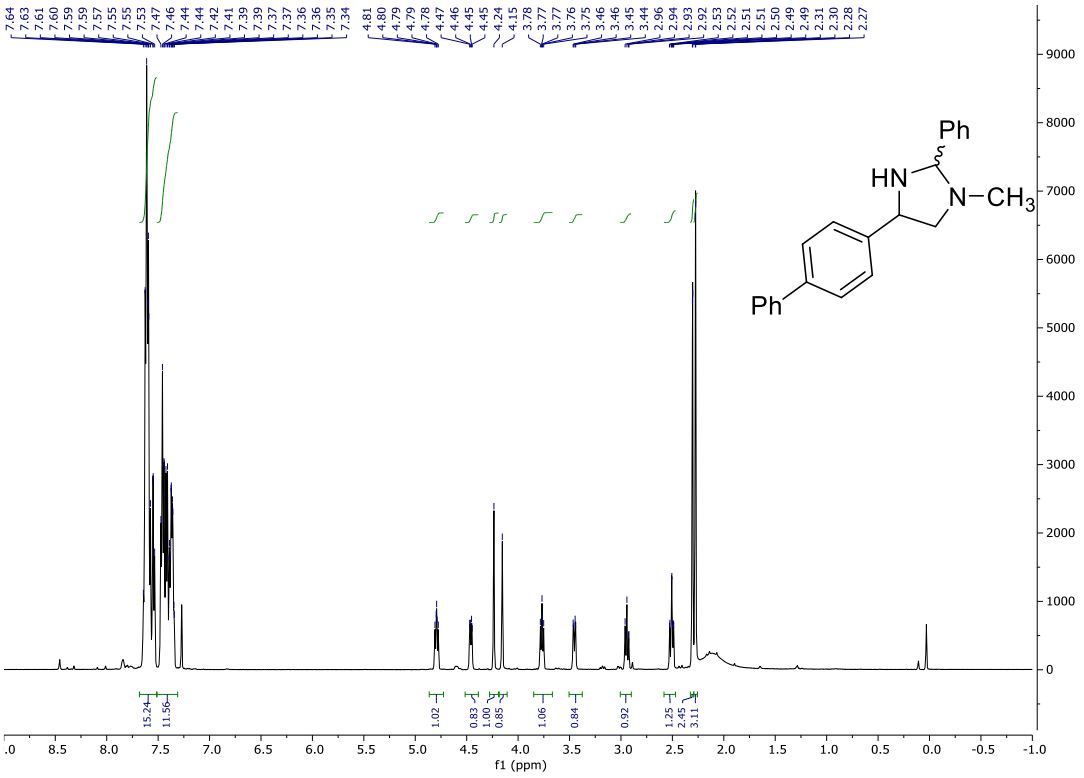

Figure 112. ^{1}H NMR spectrum of mixture of diastereomers of 207

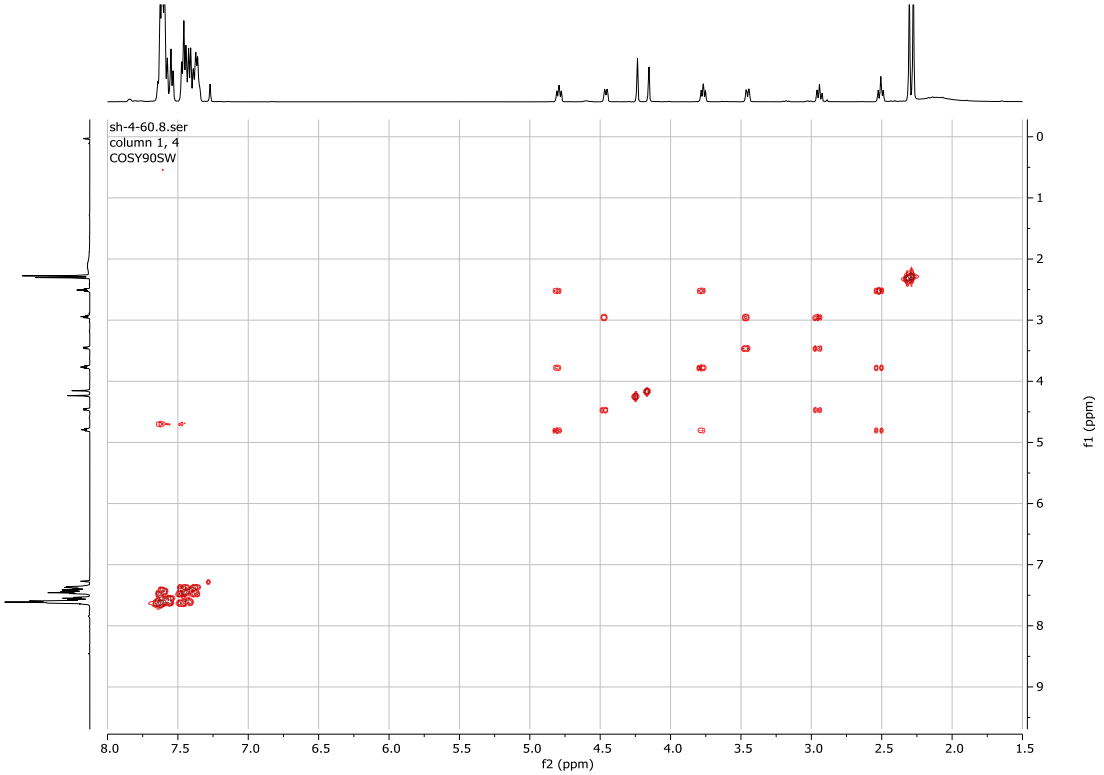

Figure 113. COSY of 207 diastereomer mixture

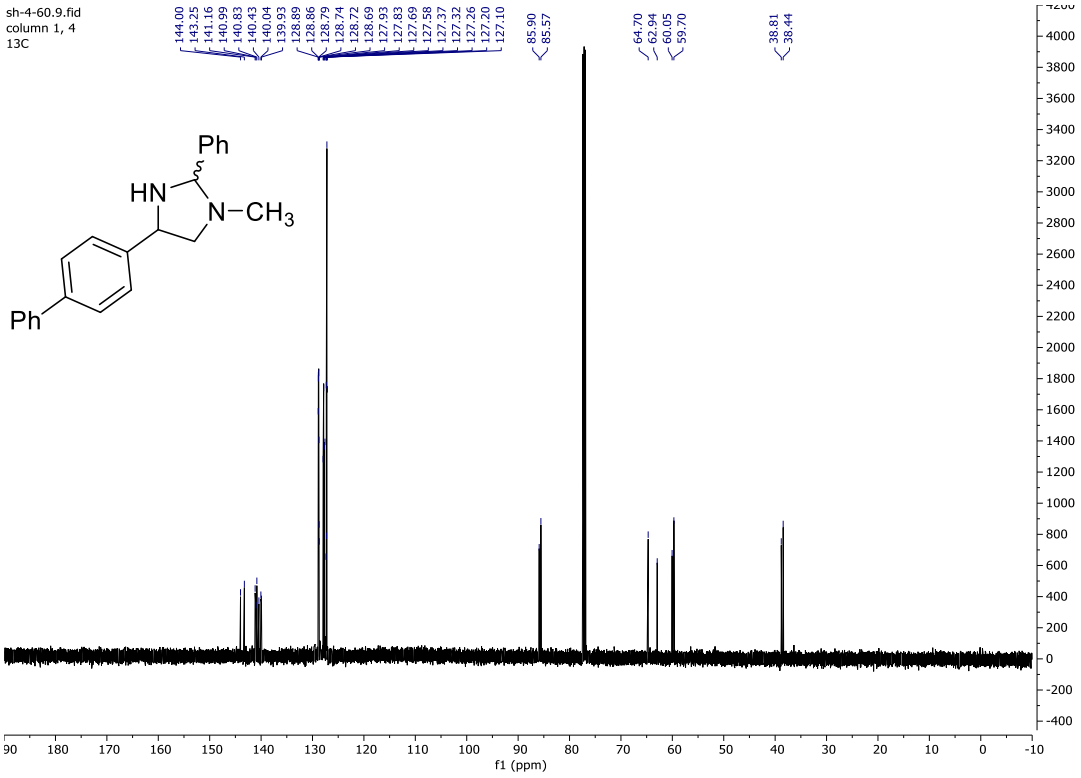

Figure 114. ^{13}C NMR for mixture of diastereomers of 207

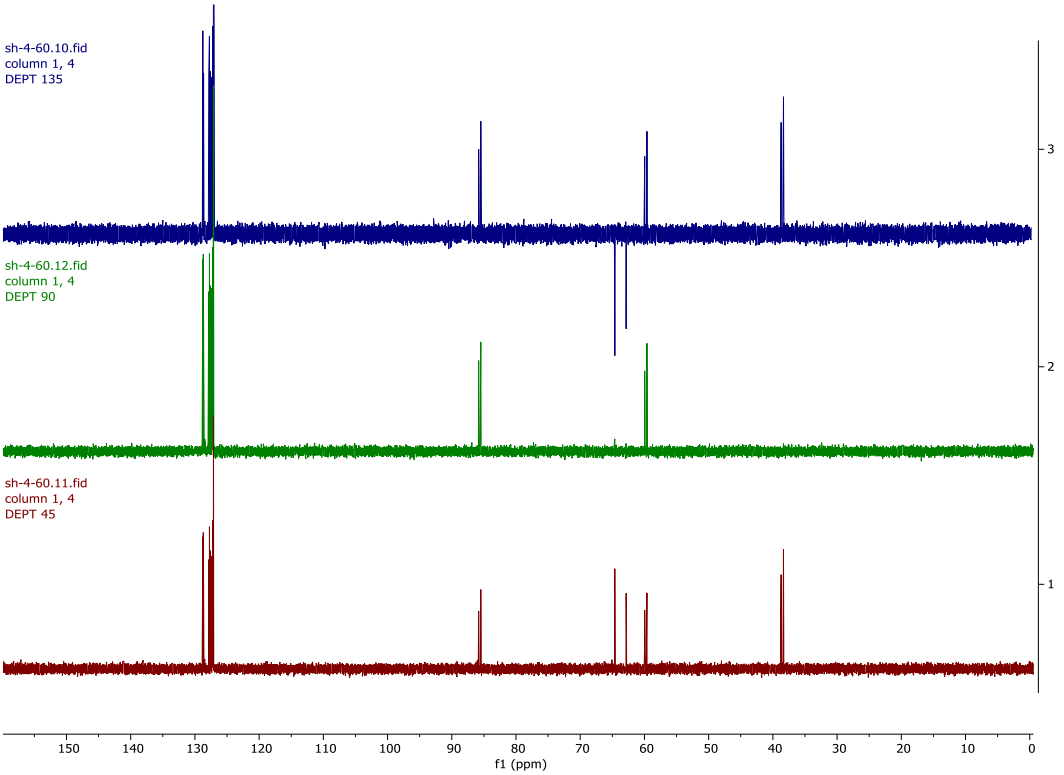

Figure 115. DEPT 135, 90, and 45 (top to bottom) of 207

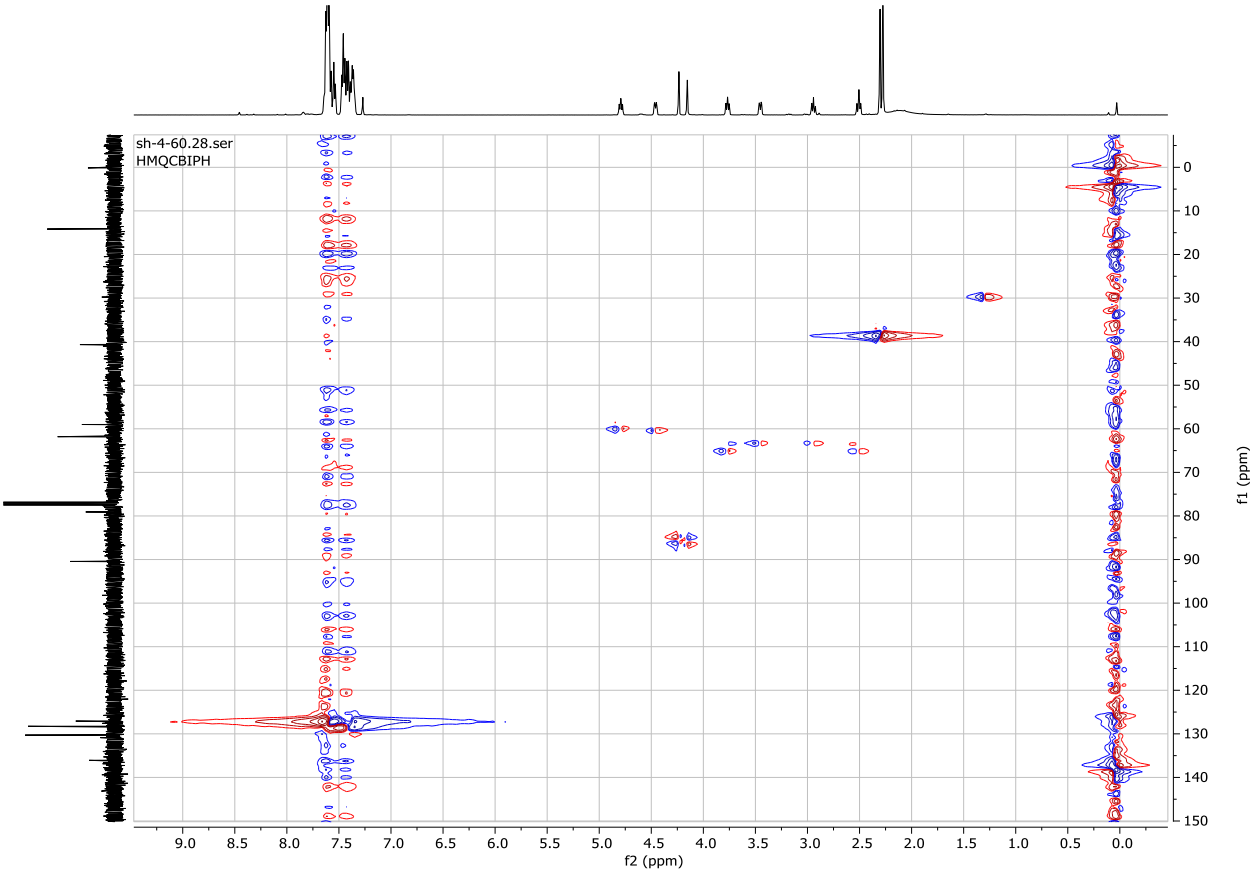

Figure 116. HSQC of 207 mixture

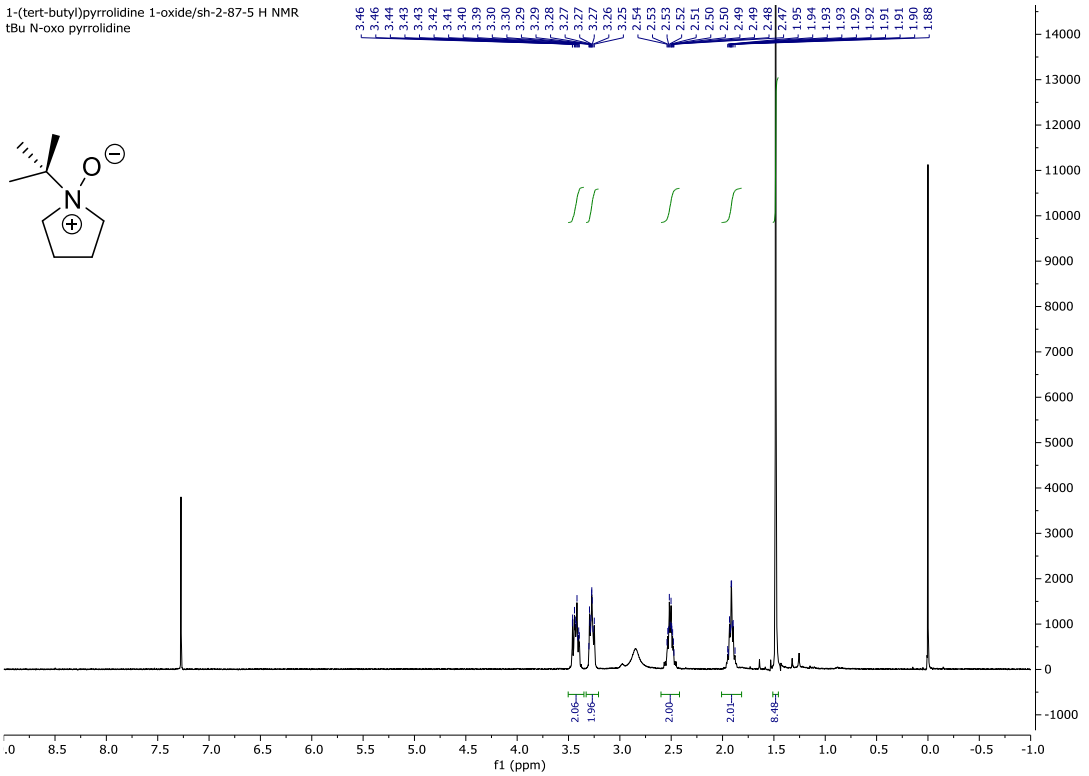

Figure 117. ^{1}HNMR spectrum of 360 (in $CDCl_3$, 400 MHz)

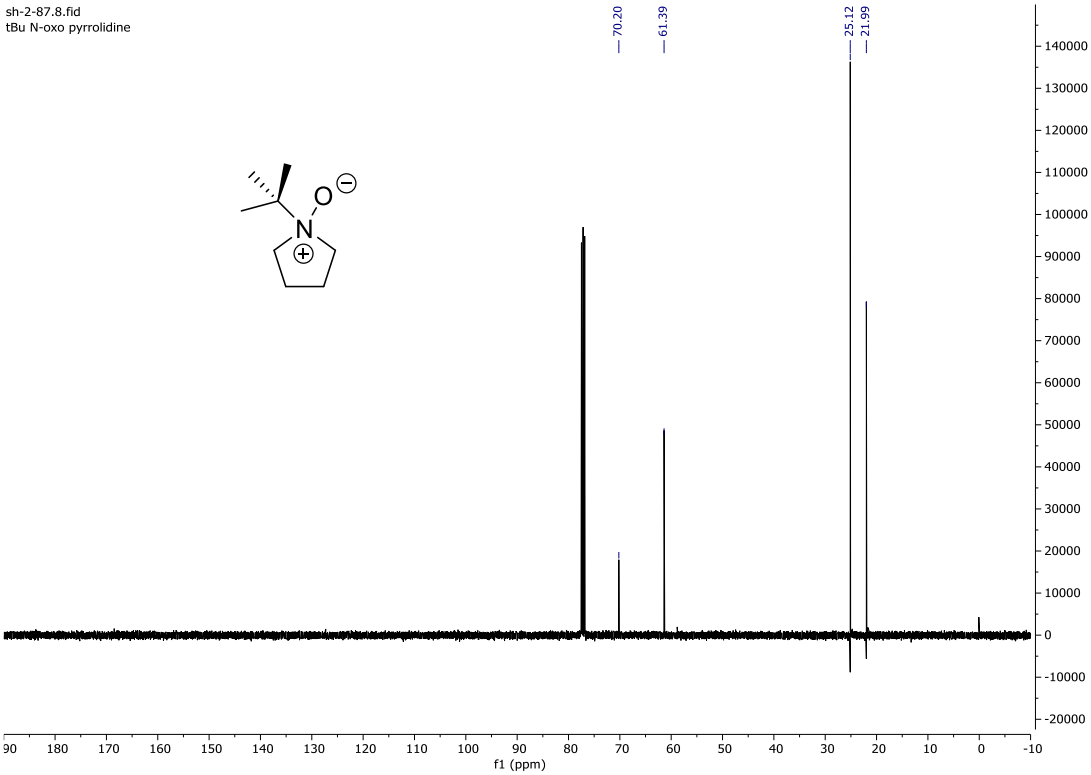

Figure 118. ^{13}C NMR spectrum of 360 (in $CDCl_3$, 101 MHz)

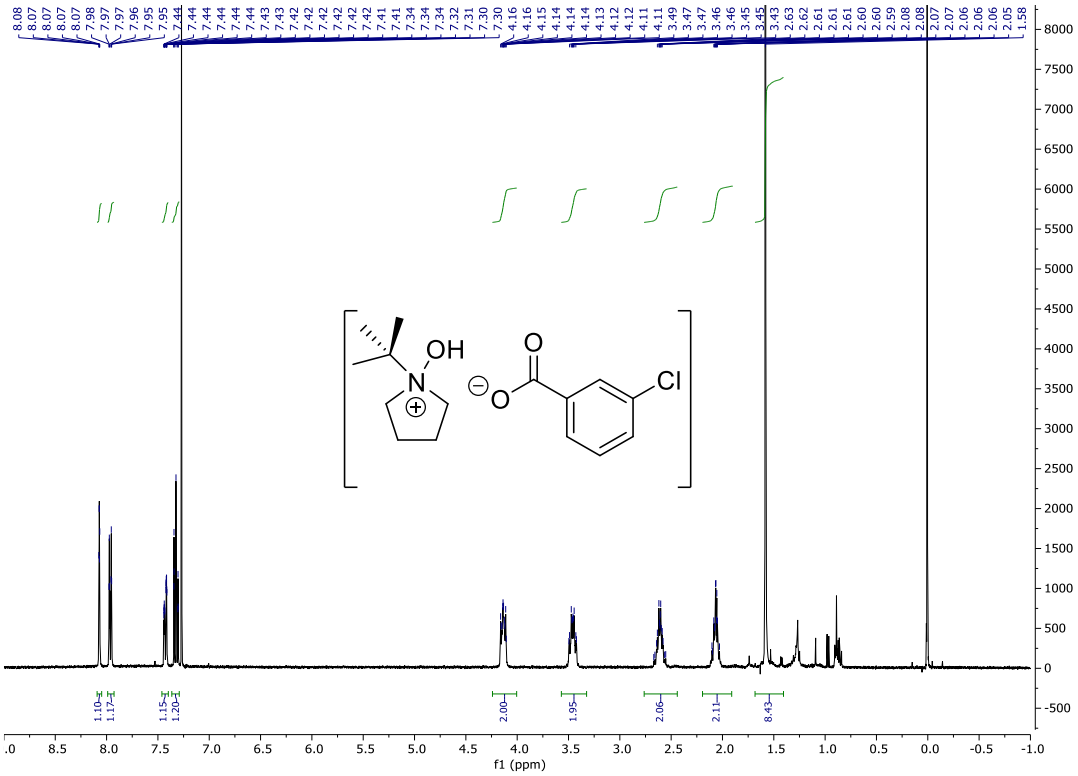

Figure 119. ^{1}H NMR spectrum of 366 (in $CDCl_3$, 400 MHz).

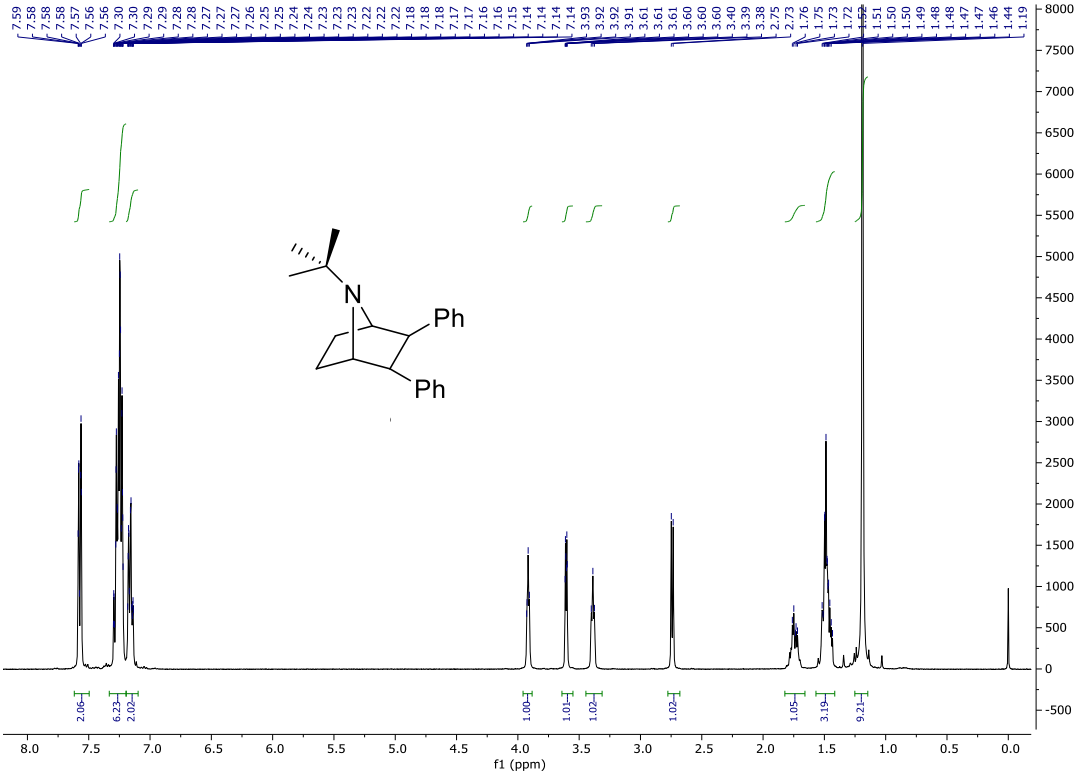

Figure 120. ^{1}H NMR spectrum of 362 (in $CDCl_3$ 400 MHz)

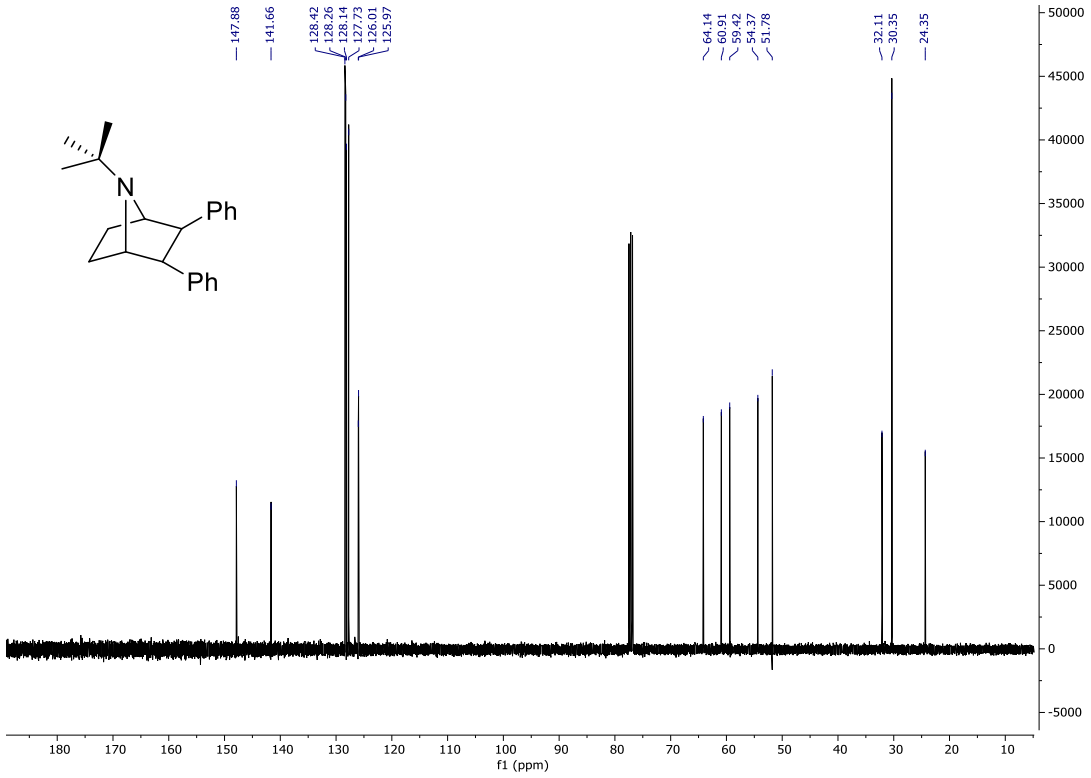

Figure 121. ^{13}C NMR spectrum of 362 (in $CDCl_3$, 101 MHz)

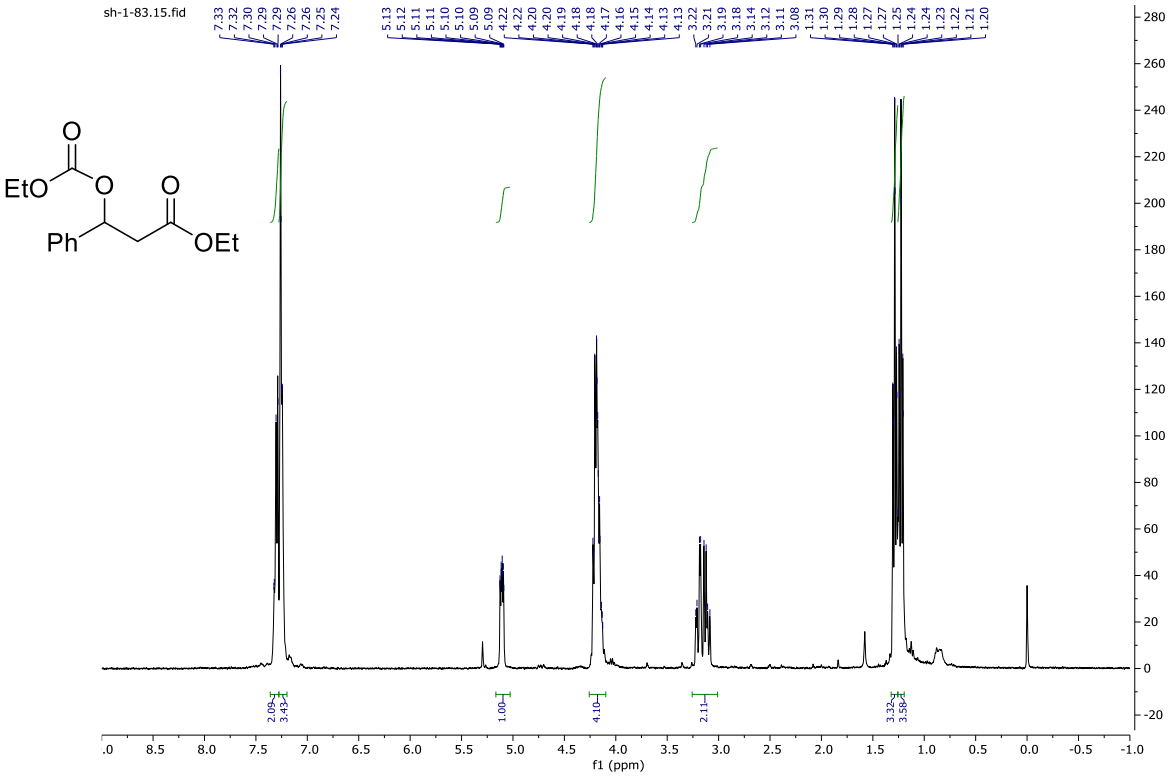

Figure 122. ^{1}H NMR spectrum of 467 (in $CDCl_3$, 400 MHz)

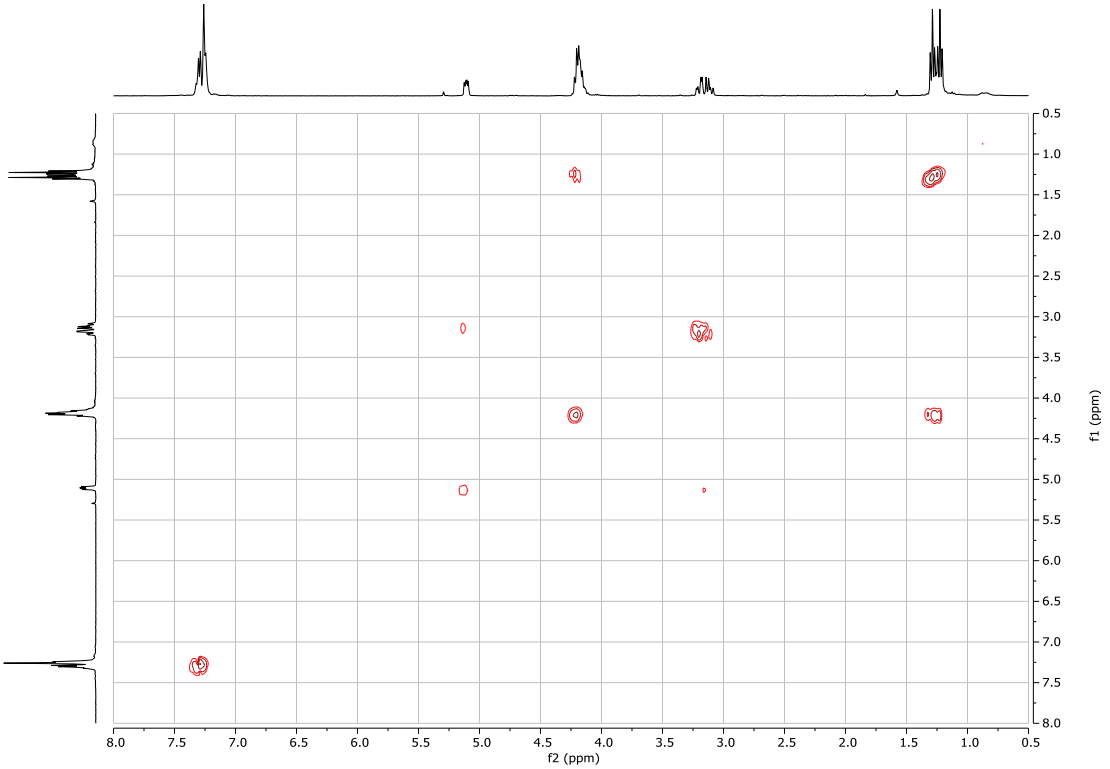

Figure 123. 2D COSY spectrum of 467

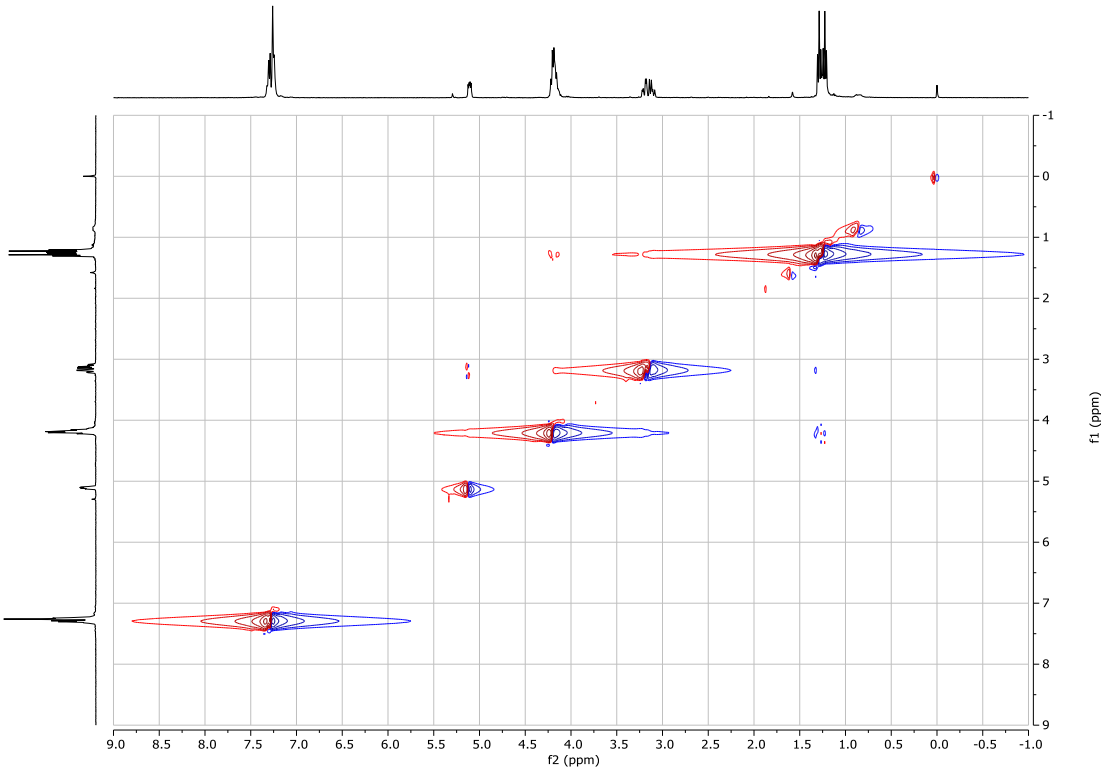

Figure 124. 2D NOESY spectrum of 467

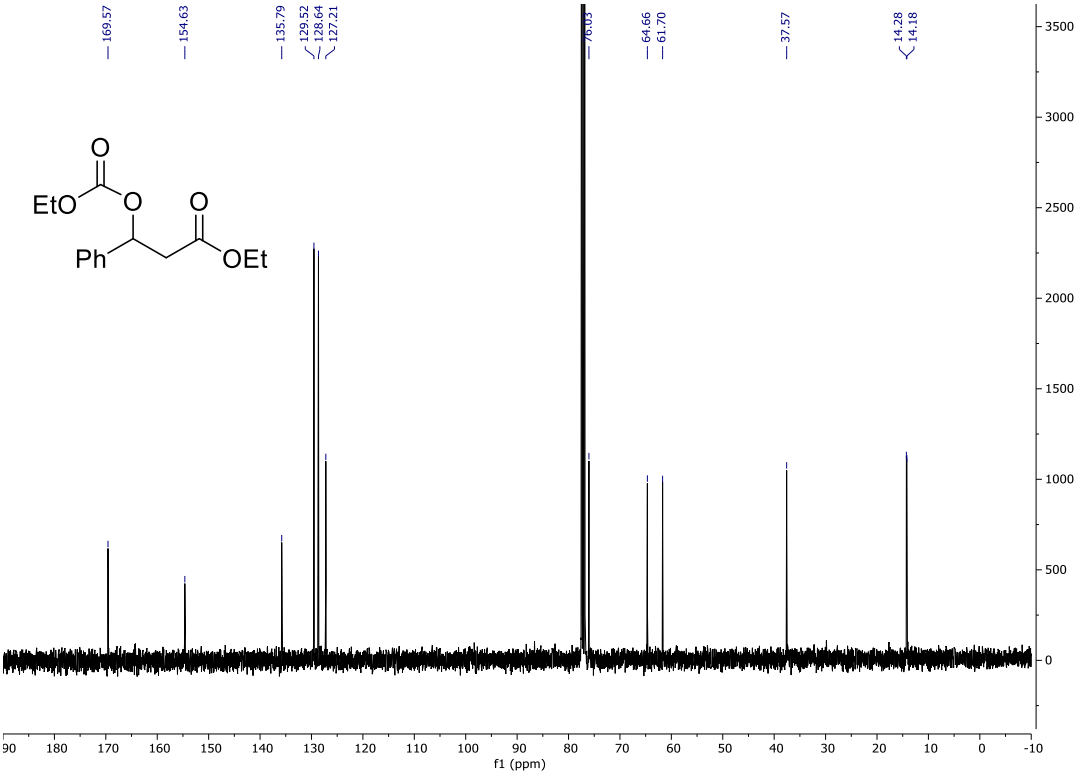

Figure 125. ^{13}C NMR spectrum of 467 (in $CDCl_3$, 101 MHz)

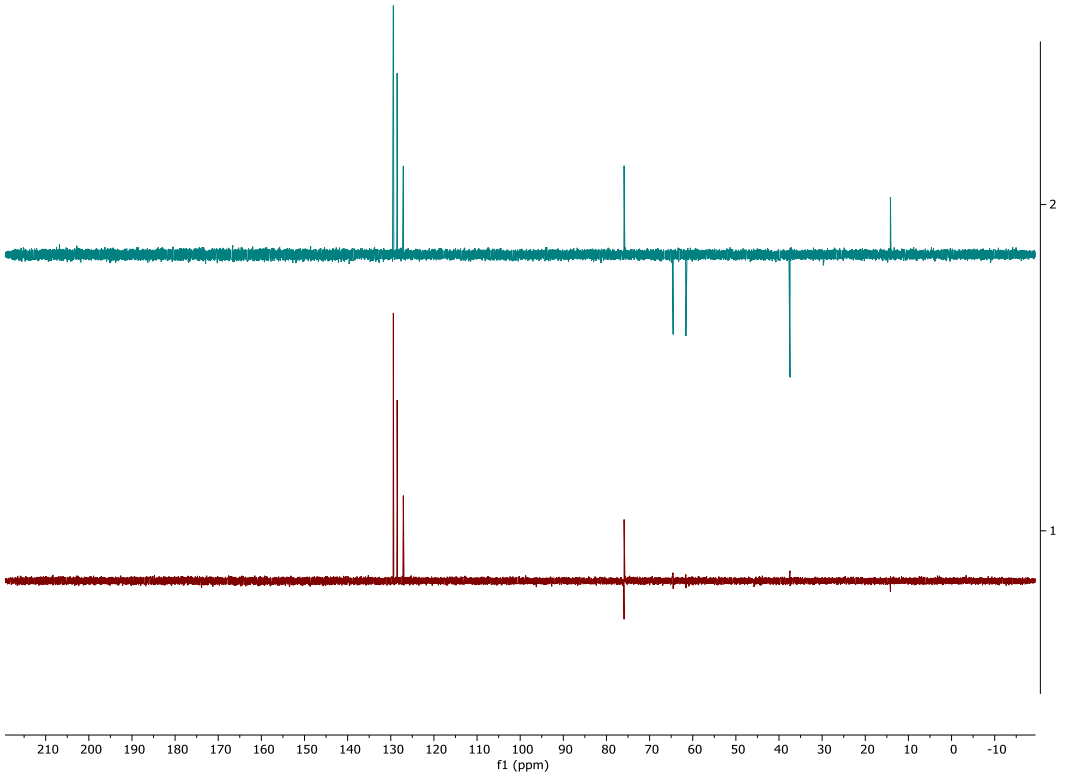

Figure 126. DEPT 135 (top), and DEPT 90 (bottom) spectra of 467

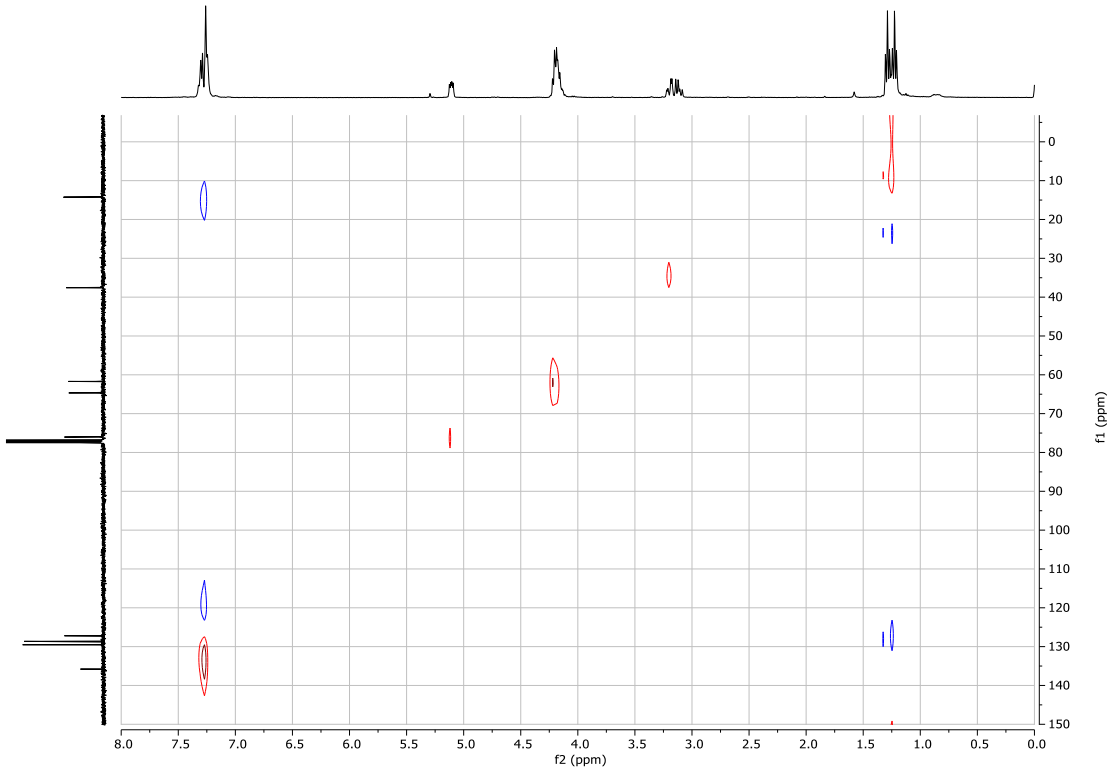

Figure 127. HSQC spectrum of 467

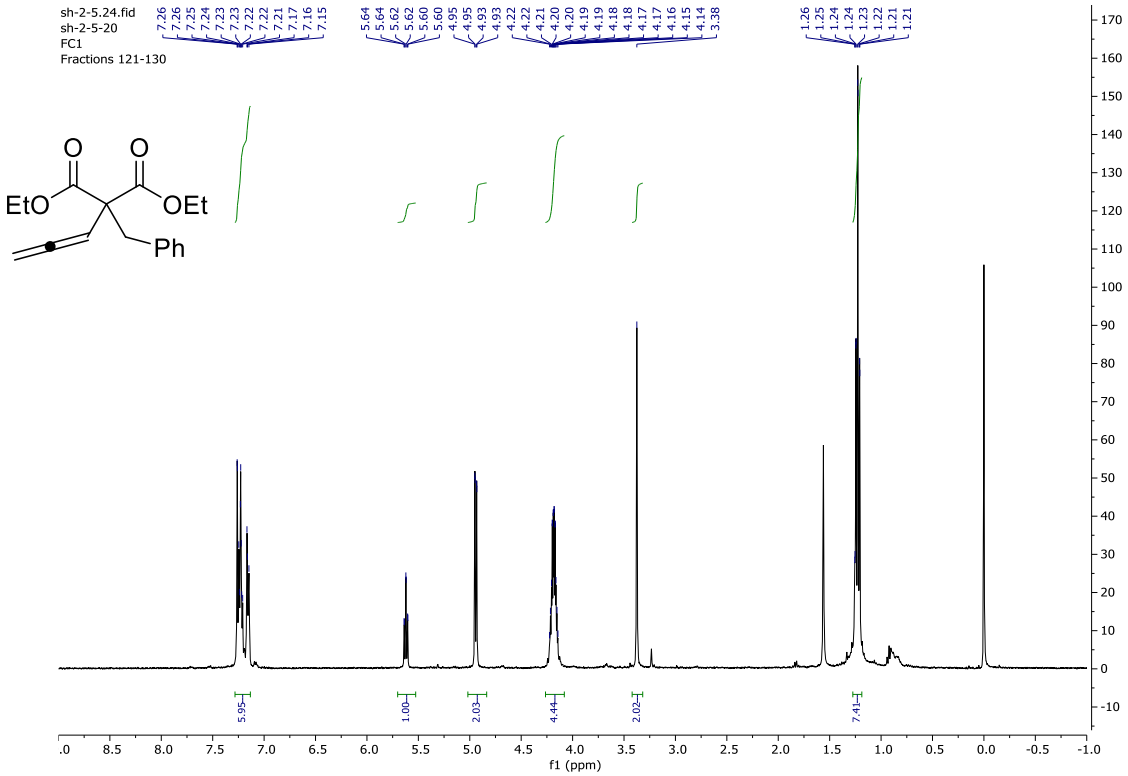

Figure 128. ^{1}H NMR spectrum of 466 (in $CDCl_3$, 400 MHz)

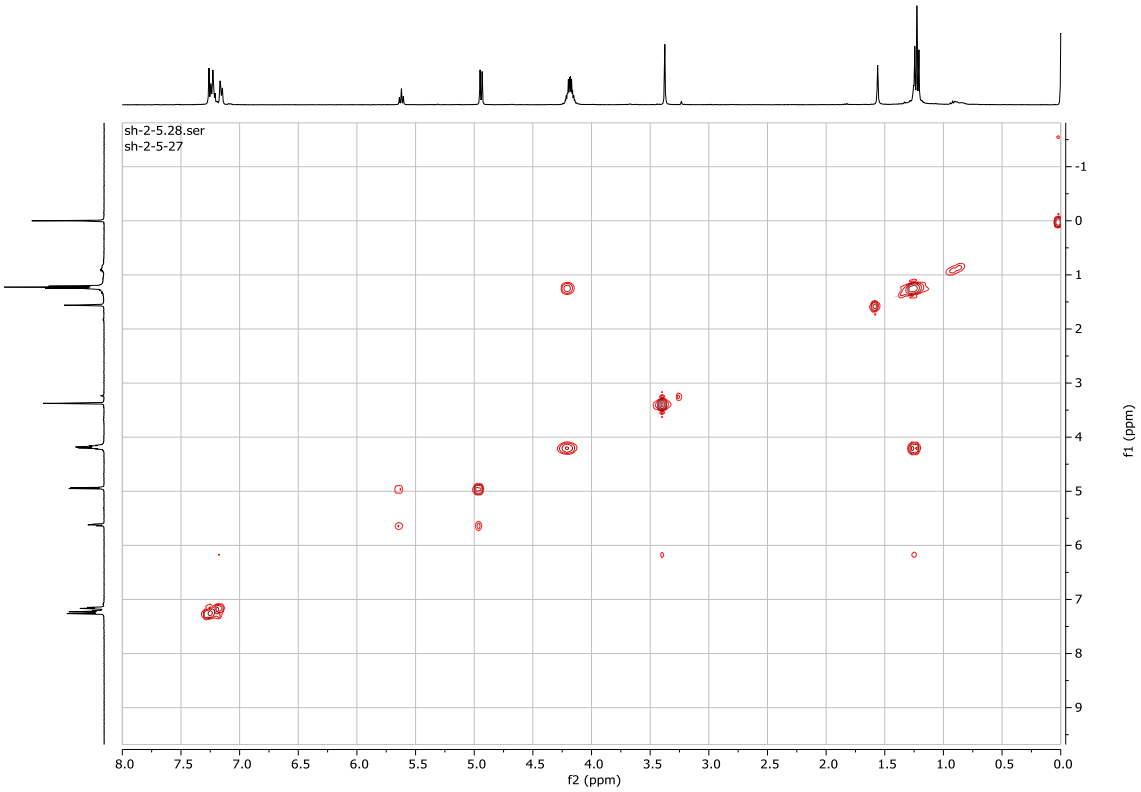

Figure 129. 2D COSY spectrum of 466

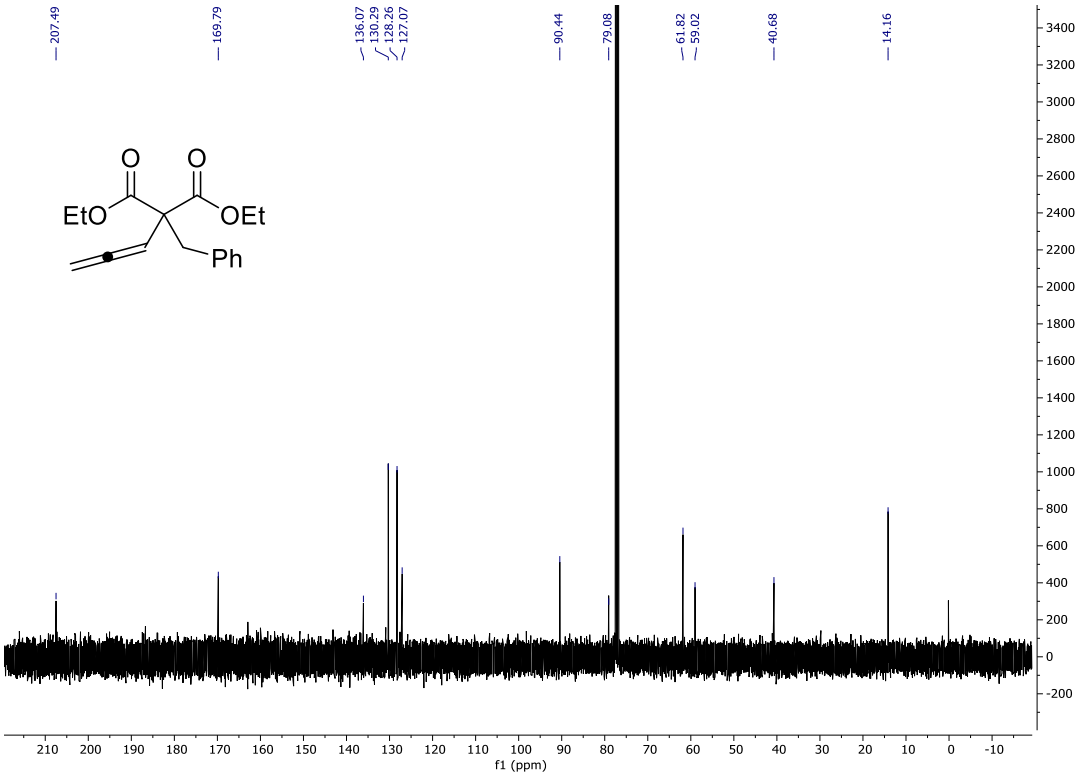

Figure 130. ^{13}C NMR spectrum of 466 (in $CDCl_3$, 101 Hz)

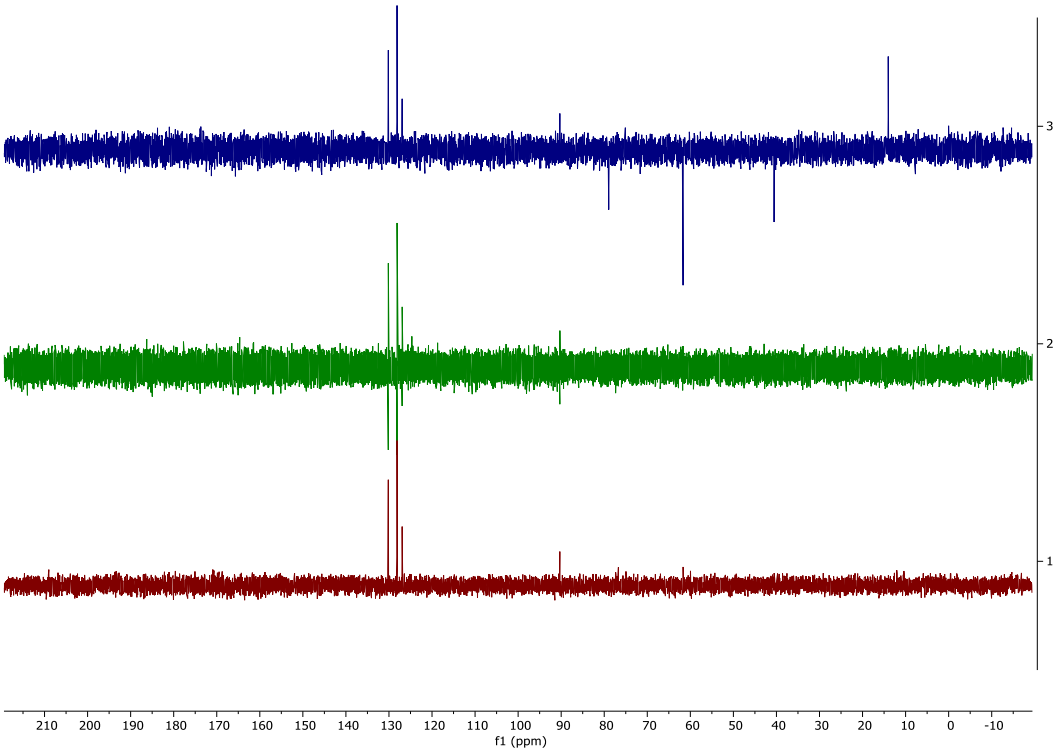

Figure 131. DEPT 135, 90, 45 (top to bottom) spectra of 466